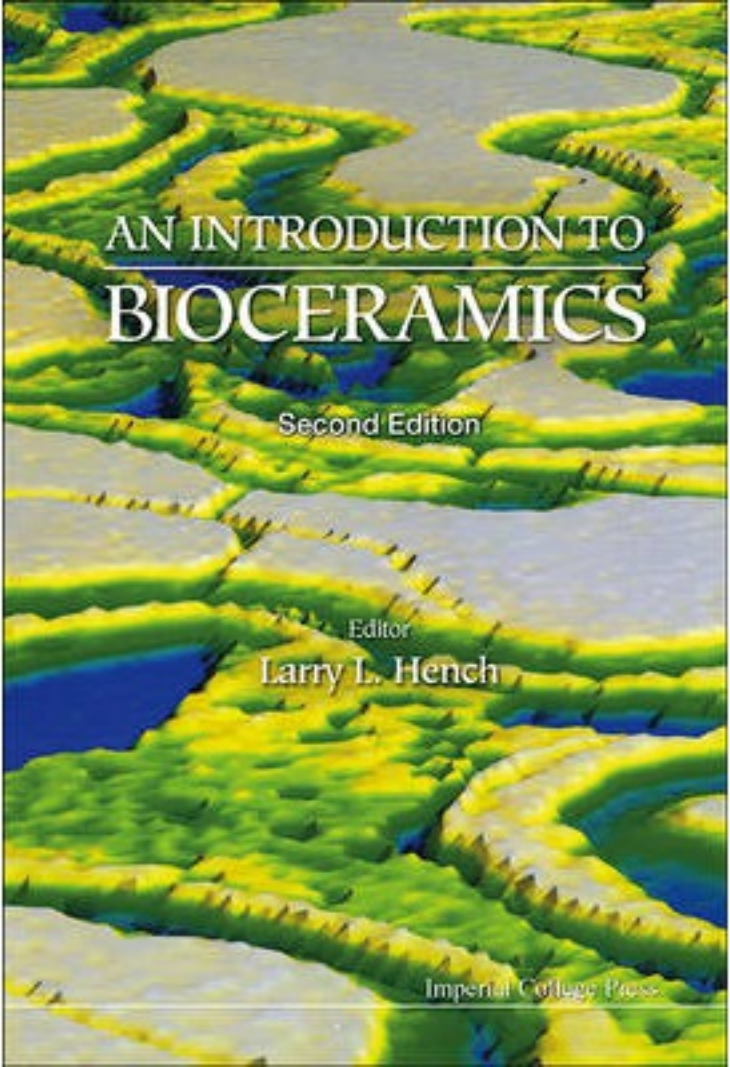
AN INTRODUCTION TO
BIOCERAMICS
Second Edition
Editor
Larry L. Hench
Imperial College Press

AN INTRODUCTION TO BIOCERAMICS

Second Edition

This page intentionally left blank

AN INTRODUCTION TO BIOCERAMICS

Second Edition

Editor

Larry L. Hench

University of Florida, USA

ICP

Imperial College Press

Published by

Imperial College Press
57 Shelton Street
Covent Garden
London WC2H 9HE

Distributed by

World Scientific Publishing Co. Pte. Ltd.

5 Toh Tuck Link, Singapore 596224

USA office: 27 Warren Street, Suite 401-402, Hackensack, NJ 07601

UK office: 57 Shelton Street, Covent Garden, London WC2H 9HE

British Library Cataloguing-in-Publication Data
A catalogue record for this book is available from the British Library.

AN INTRODUCTION TO BIOCERAMICS
Second Edition

ISBN 978-1-908977-15-1

Typeset by Stallion Press
Email: enquiries@stallionpress.com

Printed in Singapore

DEDICATIONS

Dedicated to Gerry Merwin (1947–1992) and Bill Hall (1922–1992), clinicians and scientists who pioneered use of new biomaterials.

A special dedication of this second edition is to Dr. June Wilson Hench, co-editor of the first edition, who made so many important discoveries in the field of bioactive glasses and pioneered the technological transformation from the laboratory to FDA-approved clinical products. Her lifetime of contributions to the field of Bioceramics, her mentorship of many students and her creativity is a legacy that will be never forgotten. June is greatly missed!

This volume is also dedicated to the memory and pioneering contributions of Professor Raquel LeGeros, co-author of Chapter 17, who passed away during the final stages of publication of the book. She will be remembered always for her warm and gentle leadership in the field of calcium phosphate bioceramics.

Cover Ackowledgement

Colour enhanced scanning electron micrograph (SEM) of bone regeneration (green and yellow areas) around S53P4 bioactive glass particle (grey areas). Photo courtesy of Dr. Heimo Ylanen, Abo Akademi University, Turku, Finland.

This page intentionally left blank

PREFACE

Since the 1970s, when it was first realized that the special properties of ceramic materials could be exploited to provide better materials for certain implant applications, the field has expanded enormously. Initial applications depended on the fact that smooth ceramic surfaces elicited very little tissue reaction and provided wear characteristics suitable for bearing surfaces. Resultant orthopedic use has enjoyed forty years' clinical success, notably in Europe.

Today, as well as the so-called inert "bioceramics", materials have been developed that have properties which allow their use where bonding to soft or hard tissues is needed, where controlled degradation is required, where loads are to be borne, where tissue is to be augmented, or where the special properties of ceramics can be allied with those of polymers or metals to provide implant materials with advantages over each.

In all of these applications, and many others described in this text, the tissue reactions to, and properties of, these bioceramics have been increasingly carefully studied so that they can be controlled and, more importantly, predicted. This is the information which must be understood before they are applied clinically.

Assessment of the growth of the field of bioactive ceramics in the first edition in 1993 showed that the number of presentations on that subject at the first World Biomaterials Congress in 1980 formed 6% of the program. By the time of the fourth such congress in 1992, that figure was 23% of the whole. In 1980 presentations came from 12 centers in 5 countries, in 1992 from 88 centers in 21 countries. Research is international and continues to expand worldwide, as indicated by the breadth of contribution in this second edition.

The breadth of bioceramics also continues to expand, as illustrated by the addition of 21 additional chapters in this second edition. Much of the expanded growth of subject matter is in the field of bioactive materials. Bioactive materials can be divided into two major areas: one contains bioactive glasses and glass-ceramics, which develop biological hydroxyapatite at their surfaces after implantation; and the other, contains calcium phosphate-based ceramics, which are usually developed from chemical precursors.

Materials from both groups have been used as powders and sometimes as solids in applications where mechanical requirements are low, and as composites and coatings where mechanical requirements are high. Some have been designed specifically for high strength applications. As the behavior of bioceramics in both short- and long-term applications has become increasingly predictable and reliable, their clinical application has increased, as indicted by the large number of clinical applications chapters presented in the second edition.

The growth of bioceramics as a field and as a vital component of the healthcare industry parallels the increasing need for affordable and improved healthcare for an increasingly large and aging population. The chapters presented in the second edition provide the latest understanding of this important field and provide the basis for creating the next generation of biomaterials.

Please note the following regarding the contents of this second edition. Several chapters of the first edition have been included without alteration. This is based upon my judgment as Editor that these are "classic" reviews of the field and merit inclusion "as is". Some other chapters, of equal importance, however, have been up-dated to include clinical results during the last twenty years in order to represent the growing clinical significance of the field of bioceramics. A few chapters have been greatly reduced in size because the content has not become clinically important. Because of their historical significance a short, edited version of the chapters has been included with key references. This decision has made it possible to keep within reasonable page limits for the second edition and still include a comprehensive up-dating of the field. I greatly appreciate these important new contributions from leaders of the field. I also hope that the authors of the chapters reduced in size will understand the rationale of my decision. Bioceramics has become one of the most important fields of the healthcare industry and I am pleased that this second edition represents this growing importance.

Larry L. Hench
Ft. Myers, FL
October 11, 2012

CONTENTS

AUTHOR INDEX

* Denotes affiliation from the first edition.
** Denotes current affiliation/affiliation of new authors to the second edition.

Editors

Hench, Larry L.
Chapters 1, 3, 4, 7, 8, 11, 22, 31, 34, 36, 37, 40, 41, 42
Advanced Materials Research Center, University of Florida, Gainesville, Florida, USA*
University of Florida, Gainesville, Florida and University of Central Florida, Florida, USA**

Wilson, June
Chapters 1, 6
Bioglass® Research Center, Advanced Materials Research Center, University of Florida, Gainesville, Florida, USA*

Authors

Andersson, Orjan
Chapters 3, 22
Abo Akademi, Turku, Finland*

Best, Serena M.
Chapter 18
University of Cambridge, Cambridge, UK**

Boccaccini, Aldo R.
Chapter 5
University of Erlangen, Germany**

Bonfield, William
Chapters 18, 27
IRC in Biomedical Materials Queen Mary and Westfield College London, London, UK*
University of Cambridge, Cambridge, UK**

Cama, Giuseppe
Chapter 40
King's College/Guy's Hospital, London, UK**

Dauskardt, Reinhold H.
Chapter 24
University of California, Berkeley, California, USA*

Day, Delbert E.
Chapter 29
University of Missouri, Missouri, USA*
University of Missouri Science and Technology, Rolla, Missouri, USA**

Day, Thomas E.
Chapter 29
University of Missouri, Missouri, USA.*
MoSci Corp., Rolla, Missouri, USA**

Deb, Sanjukta
Chapter 28
King's College/Guy's Hospital, London, UK**

de Groot, Klaas
Chapter 20
University of Leiden, the Netherlands*

Ducheyne, Paul
Chapter 26
University of Pennsylvania, Philadelphia, USA*

Dynan, William
Chapter 35
Medical College of Georgia, Augusta, Georgia, USA**

Frantzén, Janek
Chapter 12
Turku University, Turku, Finland*

Friederichs, Robert J.
Chapter 18
University of Cambridge, Cambridge, UK**

Gaisser, David M.
Chapter 11
NovaBone Products, Alachua, Florida, USA**

Gorustovich, Alejandro A.
Chapter 5
National Atomic Energy Commission CNEA Regional Noroeste, Argentina**

Greenspan, David C.
Chapters 31, 39
DSpinode Consulting, Gainesville, Florida, USA**

Gross, Ulrich M.
Chapter 15
University Hospital Steglitz, Free University of Berlin, Germany*

Happonen, Risto-Pekka
Chapter 6
Institute of Dentistry, University of Turku, Finland*

Haro Durand, Luis A.
Chapter 5
National Atomic Energy Commission CNEA Regional Noroeste, Argentina
National Research Council CONICET, A4408FTV, Argentina**

Höland, Wolfram
Chapters 16, 30
Otto-Schott-Institute for glass chemistry, Friedrich-Schiller-University Jena, Germany*
Ivoclar Vivadent AG, Principality of Liechtenstein**

Holmes, Ralph E.
Chapter 19
University of California at San Diego, USA*

Horowitz, Emanuel
Chapter 38
Johns Hopkins University, Baltimore, Maryland, USA*

Hulbert, Samuel F.
Chapter 2
Rose-Hulman Institute of Technology, Terre Haute, Indiana, USA*

Jones, Julian R.
Chapter 32
Imperial College London, London, UK**

Jung, Steven
Chapter 33
MoSci Corp., Rolla, Missouri, USA**

Klein, C.P.A.T.
Chapter 20
University of Leiden, the Netherlands*

Kokubo, Tadashi
Chapter 13, 23
Kyoto University, Japan*
Chubu University, Kasugai, Japan**

Lacefield, William R.
Chapter 21
University of Alabama at Birmingham School of Dentistry, Birmingham, Alabama, USA*

Li, Shuyi
Chapter 35
Medical College of Georgia, Augusta, Georgia, USA**

LeGeros, John P.
Chapter 17
New York University College of Dentistry, New York, USA.*

LeGeros, Raquel Z.
Chapter 17
New York University College of Dentistry, New York, USA*

Marcolongo, Michele
Chapter 26
University of Pennsylvania, Philadelphia, USA*

Mueller, Edward
Chapter 38
Food and Drug Administration Center for Devices and Radiological Health Rockville, USA*

Müller-Mai, Christian
Chapter 15
University Hospital Steglitz, Free University of Berlin, Germany*

Peitl, Oscar
Chapter 34
Universidade Federal de São Carlos, Brazil**

Rheinberger, Volker M.
Chapter 30
Ivoclar Vivadent AG, Principality of Liechtenstein**

Ritchie, Robert O.
Chapter 24
University of California, Berkeley, California, USA*

Robinson II, Paul
Chapters 9, 36
University of Florida, Gainesville, Florida, USA**

Roether, Judith A.
Chapter 5
University of Erlangen, Germany**

Schepers, Evert
Chapter 26
University of Leuven, Leuven, Belgium*

Schweiger, Marcel
Chapter 30
Ivoclar Vivadent AG, Principality of Liechtenstein**

Serbena, Francisco C.
Chapter 34
Federal University of San Carlos, San Carlos, Brazil**

Serkiz, Steven
Chapter 35
Medical College of Georgia, Augusta, Georgia, USA**

Shors, Edwin C.
Chapter 19
University of California at San Diego, USA*

Shute, Jonathan
Chapter 25
University of Florida, Gainesville, Florida, USA**

Thompson, Ian
Chapter 10
King's College/Guy's Hospital, London, UK**

Voigt, Christian
Chapter 15
University Hospital Steglitz, Free University of Berlin, Germany*

Vogel, Werner
Chapter 16
Otto-Schott-Institute for glass chemistry, Friedrich-Schiller-University Jena, Germany*

Wicks, George G.
Chapter 35
Savannah River National Laboratory, Aiken, South Carolina, USA**

Wolke, Joop G.C.
Chapter 20
University of Leiden, the Netherlands*

Yamaguchi, Seiji
Chapter 23
Chubu University, Kasugai, Japan**

Yamamuro, Takao
Chapter 14
Kyoto University, Japan*

Yli-Urpo, Antti
Chapter 6
Institute of Dentistry, University of Turku, Finland*

Zanotto, Edgar D.
Chapter 34
Federal University of San Carlos, San Carlos, Brazil**

Chapter 1

INTRODUCTION

Larry L. Hench and June Wilson

1.1. OVERVIEW

Thousands of years ago humans discovered that clay could be irreversibly transformed by fire into ceramic pottery. Ceramic pots stored grains for long periods of time with minimal deterioration. Impervious ceramic vessels held water and were resistant to fire, which allowed new forms of cooking. This discovery was a large factor in the transformation of human culture from nomadic hunters to agrarian settlers. This cultural revolution led to a great improvement in the quality and length of life.

During the last fifty years another revolution has occurred in the use of ceramics to improve the quality of life of humans. This revolution is the development of specially designed and fabricated ceramics for the repair and reconstruction of diseased, damaged or "worn out" parts of the body. Ceramics used for this purpose are called *bioceramics.* This book describes the principles involved in the use of ceramics in the body. Most clinical applications of bioceramics relate to the repair of the skeletal system, composed of bones, joints and teeth, and to augment both hard and soft tissues. Ceramics are also used to replace parts of the cardiovascular system, especially heart valves. Special formulations of glasses are also used therapeutically for the treatment of tumors.

Bioceramics are produced in a variety of forms and phases and serve many different functions in the repair of the body, which are summarized in Fig. 1.1 and Table 1.1. In many applications ceramics are used in the form of bulk materials of a specific shape, called *implants*, *prostheses*, or *prosthetic devices*. Bioceramics are also used to fill space while the natural repair processes restore function. In other situations the ceramic is used as a coating on a substrate, or as a second phase in a composite, combining the characteristics of both into a new material with enhanced mechanical and biochemical properties.

Bioceramics are made in many different phases. They can be single crystals (sapphire), polycrystalline (alumina or hydroxyapatite), glass (Bioglass®), glass-ceramics (A/W glass-ceramic) or composites (polyethylene-hydroxyapatite). The phase or phases used depend on the properties and function required. For example, single crystal sapphire is used as a dental implant because of its high strength. A/W glass-ceramic is used to replace vertebrae because it has high strength and

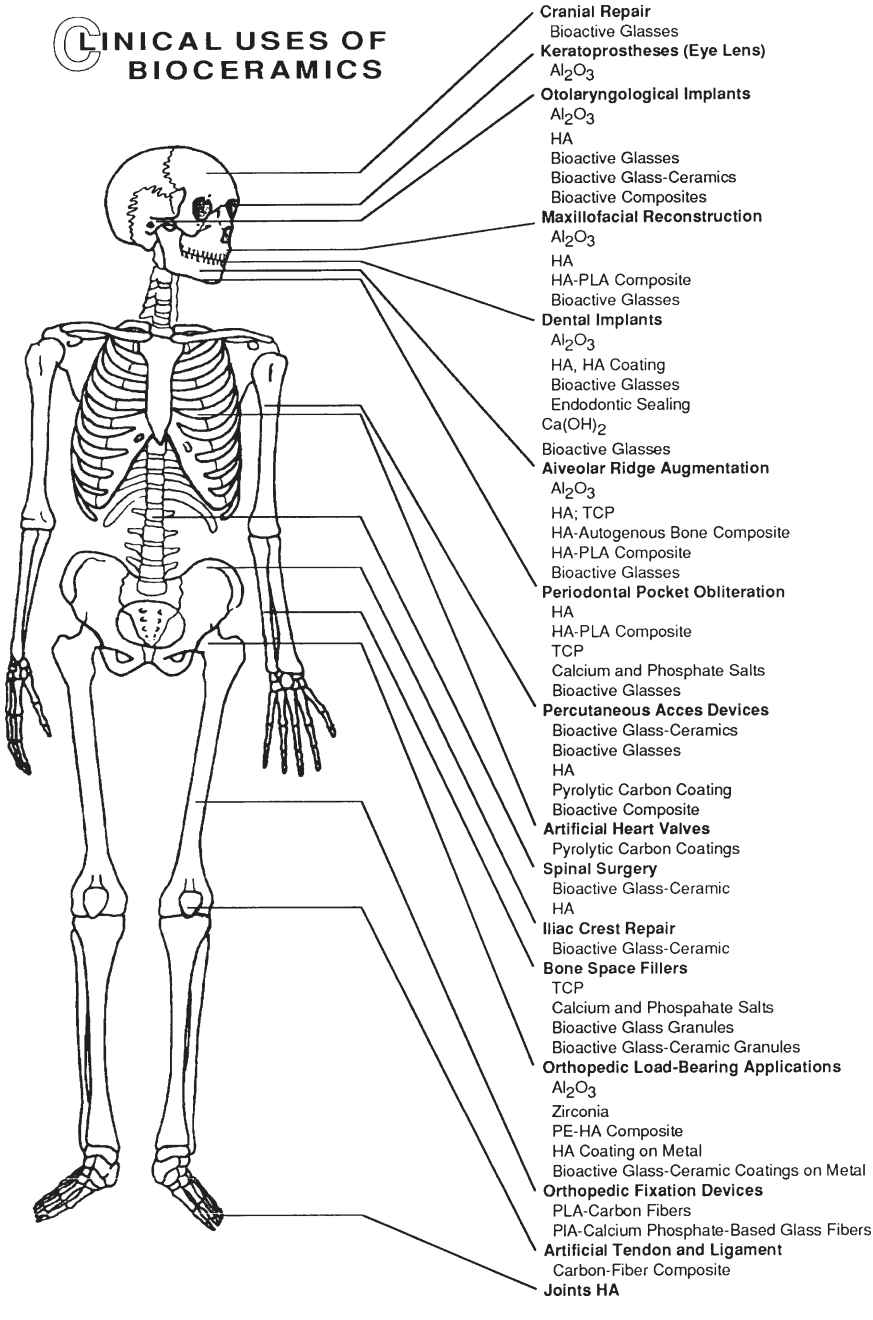

Fig. 1.1. Clinical uses of bioceramics.

Table 1.1. Form, Phase and Function of Bioceramics.

Form	Phase	Function
Powder	Polycrystalline, Glass	Space-filling, therapeutic treatment, regeneration of tissues
Coating	Polycrystalline, Glass Glass-Ceramic	Tissue bonding, thromboresistance, corrosion protection
Bulk	Single Crystal Polycrystalline, Glass Glass-Ceramic Composite (Multi-Phase)	Replacement and augmentation of tissue, replace functioning parts

bonds to bone. Bioactive glasses have low strength but bond rapidly to bone, so are used to augment the repair of boney defects.

Ceramics and glasses have been used for a long time outside the body for a variety of applications in the health care industry. Eye glasses, diagnostic instruments, chemical ware, thermometers, tissue culture flasks, chromatography columns, lasers, and fiber optics for endoscopy are commonplace products in the multi-billion dollar industry. Ceramics are widely used in dentistry as restorative materials: gold porcelain crowns, glass-filled ionomer cements, endodontic treatments, dentures etc. Such materials, called dental ceramics, are reviewed by Preston.[1] However, use of ceramics *inside* the body as implants is relatively new: alumina hip implants have been used for just over 40 years. (See Hulbert *et al.*, 1987, for a review of the history of bioceramics.[2])

This book is devoted to the use of ceramics as implants. Many compositions of ceramics have been tested for potential use in the body but few have reached human clinical application. Clinical success requires the simultaneous achievement of a stable interface with connective tissue and an appropriate, functional match of the mechanical behavior of the implant with the tissue to be replaced. Few materials satisfy this severe dual requirement for clinical use.

1.2. TYPES OF BIOCERAMICS–TISSUE INTERFACES

No material implanted in living tissues is inert; all materials elicit a response from the host tissue. The response occurs at the tissue–implant interface and depends upon many factors, listed in Table 1.2.

There are four general types of implant–tissue response, as summarized in Table 1.3. It is critical that any implant material avoids a toxic response that kills

Table 1.2. Factors affecting interfacial response.

Tissue Side	Implant Side
— Type of Tissue	— Composition of Implant
— Health of Tissue	— Phases in Implant
— Age of Tissue	— Phase Boundaries
— Blood Circulation in Tissue	— Surface Morphology
— Blood Circulation at Interface	— Surface Porosity
— Motion at Interface	— Chemical Reactions
— Closeness of Fit	— Closeness of Fit
— Mechanical Load	— Mechanical Load

Table 1.3. Implant–Tissue Interactions: Consequences.

Implant–Tissue Reaction	Consequence
Toxic	Tissue dies
Biologically nearly inert	Tissue forms a non-adherent fibrous capsule around the implant
Bioactive	Tissue forms an interfacial bond with the implant or regenerates natural tissues
Dissolution of implant	Tissue replaces implant

cells in the surrounding tissues or releases chemicals that can migrate within tissue fluids and cause systemic damage to the patient.[3] One of the main reasons for the interest in ceramic implants is their lack of toxicity.

The most common response of tissues to an implant is formation of a non-adherent fibrous capsule. The fibrous tissue is formed in order to "wall off" or isolate the implant from the host. It is a protective mechanism and with time can lead to complete encapsulation of an implant within the fibrous layer. Metals and most polymers produce this type of interfacial response; the cellular mechanisms which influence this response are described in a later section.

Biologically inactive, nearly inert ceramics, such as alumina or zirconia, also develop fibrous capsules at their interface. The thickness of the fibrous layer depends on the factors listed in Table 1.2. The chemical inertness of alumina and zirconia results in a very thin fibrous layer under optimal conditions (Fig. 1.2). More chemically reactive metallic implants elicit thicker interfacial layers. However, it is important to remember that the thickness of an interfacial fibrous layer also depends upon motion and fit at the interface, as well as the other factors indicated in Table 1.2.

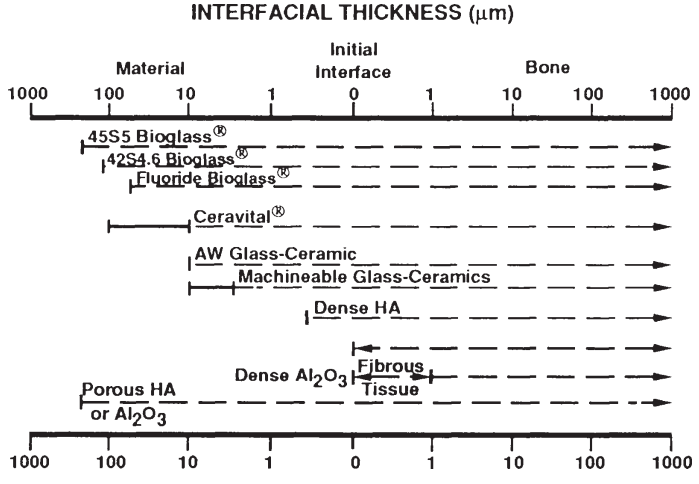

Figure 1.2. Comparison of interfacial thickness of reaction layer of bioactive implants or fibrous tissue of inactive bioceramics in bone. (Reprinted from L.L. Hench, 1991, Bioceramics: From Concept to Clinic, *J. Amer. Ceram. Soc.*, **74**, 1487–570, with permission.)

The third type of interfacial response, indicated in Table 1.3, is when a bond forms across the interface between implant and the tissue. This is termed a "bioactive" interface. The interfacial bond prevents motion between the two materials and mimics the type of interface that is formed when natural tissues repair themselves. This type of interface requires the material to have a controlled rate of chemical reactivity, as discussed in Chapters 3–6. An important characteristic of a bioactive interface is that it changes with time, as do natural tissues, which are in a state of dynamic equilibrium.

When the rate of change of a bioactive interface is sufficiently rapid the material "dissolves" or "resorbs" and is replaced by the surrounding tissues. Thus, a resorbable biomaterial must be of a composition that can be degraded chemically by body fluids or digested easily by macrophages (see below). The degradation products must be chemical compounds that are not toxic and can be easily disposed of without damage to cells.

1.3. TYPES OF BIOCERAMIC–TISSUE ATTACHMENTS

The mechanism of attachment of tissue to an implant is directly related to the tissue response at the implant interface. There are four types of bioceramics,

Table 1.4. Types of Tissue Attachment of Bioceramic Prostheses.

Type of Implant	Type of Attachment	Example
(1) Nearly inert	Mechanical interlock (Morphological Fixation)	Al_2O_3, Zirconia
(2) Porous	In-growth of tissues into pores (Biological Fixation)	Hydroxyapatite (HA) HA-coated; porous metals
(3) Bioactive	Interfacial bonding with tissues (Bioactive Fixation)	Bioactive glasses, Bioactive glass-ceramics, HA
(4) Resorbable	Replacement with tissues	Tri-calcium phosphate Bioactive glasses

each with a different type of tissue attachment, summarized in Table 1.4 with examples. The factors that influence the implant–tissue interfacial response listed in Table 1.2 also affects the type and stability of tissue attachment listed in Table 1.4.

The relative chemical activity of the different types of bioceramics is compared in Fig. 1.3. The relative reactivity shown in Fig. 1.3(a) correlates with the rate of formation of an interfacial bond of implants with bone (Fig. 1.3(b)). A type 1, nearly inert, implant does not form a bond with bone. A type 2, porous, implant forms a mechanical bond via in-growth of bone into the pores. A type 3, bioactive, implant forms a bond with bone via chemical reactions at the interface. A type 4, resorbable, implant is replaced by bone.

The relative level of reactivity of an implant also influences the thickness of the interfacial layer between the material and the tissue (Fig. 1.2). A type 1, nearly inert, implant forms a non-adherent fibrous layer at the interface. A chemically stable material like alumina elicits a very thin capsule. Consequently, when alumina or zirconia implants are implanted with a tight mechanical fit and movement does not occur at the interface they are clinically successful. However, if a type 1, nearly inert, implant is loaded such that interfacial movement occurs, the fibrous capsule can become several hundred micrometers thick and the implant loosens very quickly. Loosening invariably leads to clinical failure for a variety of reasons, which includes fracture of the implant or the bone adjacent to the implant.

Type 2, porous, ceramics and hydroxyapatite (HA) coatings on porous metals were developed to prevent loosening of implants. The growth of bone into surface porosity provides a large interfacial area between the implant and its host. This method of attachment is often called *biological fixation.* It is capable of withstanding more complex stress states than type 1 implants, which achieve only

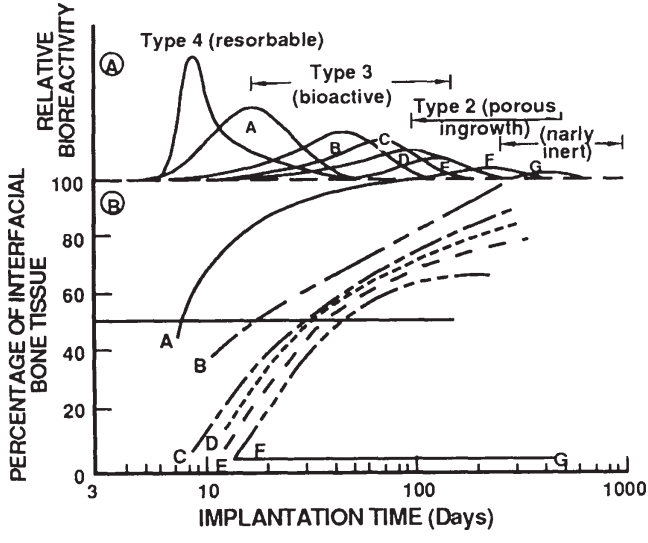

Figure 1.3. Bioactivity spectrum for various bioceramic implants: (a) relative rate of bioreactivity and (b) time dependence of formation of bone bonding at an implant interface ((A) 45S5 Bioglass®, (B) KGS Ceravital®, (C) 55S4.3 Bioglass®, (D) A/W glass-ceramic, (E) HA, (F) KGX Ceravital®, and (G) Al2O3-Si3N4). (Reprinted from L.L. Hench, 1991, Bioceramics: From Concept to Clinic, *J. Amer. Ceram. Soc.*, **74**, 1487–570, with permission.)

"morphological fixation". A limitation of type 2, porous, implants is the necessity for the pores to be at least 100 μm in diameter. This large pore size is needed so that capillaries can provide a blood supply to the ingrown connective tissues. Without blood and nutrition bone will die. Vascular tissue does not appear in pores <100 μm. Micro-movement at the interface of a porous implant can cut off capillaries, leading to tissue death, inflammation and destruction of interfacial stability.

When the porous implant is a metal, the large interfacial area can provide a focus for corrosion of the implant and loss of metal ions into the tissues, which may cause a variety of medical problems.[3] Coating a porous metal implant with a bioactive ceramic, such as HA, diminishes some of these limitations. The HA coating also speeds the rate of bone growth into the pores. The coatings often dissolve with time, which limits their effectiveness. The large size and volume fraction of porosity required for stable interfacial bone growth degrades the strength of the material. This limits the porous method of fixation to coatings or unloaded space fillers in tissues.

Resorbable implants (type 4 in Table 1.4) are designed to degrade gradually with time and be replaced with natural tissues. A very thin interfacial thickness, such as that shown in Fig. 1.2, is the final result. This approach is the optimal solution to the problems of interfacial stability. It leads to the regeneration of tissues instead of their replacement. The difficulty is meeting the requirements of strength and short-term mechanical performance of an implant while regeneration of tissues is occurring. The resorption rates must be matched to the repair rates of body tissues (Fig. 1.3), which vary greatly depending on the factors listed in Table 1.2. Some materials dissolve too rapidly and some too slowly. Large quantities of material must be handled by cells so the constituents of a resorbable implant must be metabolically acceptable. This is a severe limitation on the compositions that can be used.

Successful examples of resorbable implants include specially formulated polymers. Resorbable sutures composed of poly(lactic acid)-poly(glycolic acid) are metabolized to carbon dioxide and water. Thus, they function for a time to hold tissues together during wound healing then dissolve and disappear. Tricalcium phosphate (TCP) ceramics degrade to calcium and phosphate salts and can be used for space filling of bone.

Bioactive implants (type 3 in Table 1.4) offer another approach to achieve interfacial attachment. The concept of bioactive fixation is intermediate between resorbable and bio-inert behavior. A bioactive material undergoes chemical reactions in the body, but only at its surface. The surface reactions lead to bonding of tissues at the interface. Thus, a bioactive material is defined as: "a material that elicits a specific biological response at the interface of the material which results in the formation of a bond between the tissues and the material."

The bioactive concept has been expanded to include many bioactive materials with a wide range of bonding rates and thickness of interfacial bonding layers (Figs 1.2 and 1.3). They include bioactive glasses such as Bioglass®, bioactive glass-ceramics such as A/W glass-ceramic, dense synthetic HA, bioactive composites such as polyethylene-HA and bioactive coatings such as HA on porous titanium alloy. All of these materials form an interfacial bond with bone. The time dependence of bonding, the strength of the bond, the mechanism of bonding, the thickness of the bonding zone and the mechanical strength and fracture toughness differ for the various materials.

No bioactive material is optimal for all applications. It is essential to match the form, phases and properties of a bioactive implant with its rate of bonding and its function in the body (Table 1.1). Relatively small changes in composition can affect whether a bioceramic is nearly inert, resorbable or bioactive. These compositional effects are described in Chapter 3. It was discovered in 1981 that

certain bioactive glass compositions, such as 45S5 Bioglass®, will bond to soft connective tissues as well as bone. The compositions that bond to soft tissues have the highest rates of surface reaction of all the bioactive materials.

A common characteristic of all bioactive implants is the formation of a hydroxy-carbonate apatite (HCA) layer on their surface when implanted. The HCA phase is equivalent in composition and structure to the mineral phase of bone. The HCA layer grows as polycrystalline agglomerates. Collagen fibrils are incorporated within the agglomerates, thereby binding the inorganic implant surface to the organic constituents of tissues. Thus, the interface between a bioactive implant and bone is nearly identical to the naturally-occurring interfaces between bone and tendons and ligaments. The stress gradients across a bioactive interface are a closer match to natural stress gradients than those across the interface of type 1 or type 2 implants.

1.4. TISSUE RESPONSE TO IMPLANTS

To understand the way in which tissues respond to an implant it is necessary to understand the nature of the tissue at the interface and the significance of any alterations seen there. The significance of such changes will vary with the material and will be governed both by their severity and by their persistence; a transient change or a continuing one may both appear to be identical shortly after implantation.

The act of implantation evokes tissue changes from the surgery and the persistence and resolution of those changes may or may not be independent of the implant material and its properties. Some damage is inevitable on implantation in all but a few situations. Only when these materials are delivered by injection is the effect produced at a point distant from that at which it enters the body.

This introduction will discuss the inflammatory response, which is the tissue reaction to any form of damage. In this context damage may be due to surgery, material properties or mechanical damage due to wear particles. To understand the inflammatory response requires some knowledge of the normal tissue architecture and function and, in addition, certain frequently (and sometimes loosely) used terms will be defined.

Every organ in the body is made up from a combination, in varying proportions, of four tissue types:

1. Epithelium

Epithelial tissues cover and line organs throughout the body and can also secrete a wide variety of substances, either directly into the system through ducts or into the blood stream. Glands are made up of such secretory epithelium.

2. Muscle

Muscle tissue is found wherever movement is required. In the skeleton, muscle is under voluntary control; elsewhere, such as in the cardiovascular, digestive and respiratory systems, it is controlled biochemically.

3. Nervous tissue

Nervous tissue is specialized to transmit signals between the outside world, the brain and all of the body system.

4. Connective tissue

Connective tissue, the fourth group, is well named, since its constituent tissues connect and service all of the others. It includes blood supply to and from the organs. No organ in the body is without a connective tissue component and it is with connective tissue that the ceramic biomaterials, which are the subject of this book, interact.

For more information and details of the appearance of these tissue types see Ham or any similar histological textbook.[4]

An inflammatory response will always be present immediately after surgery while the damaged tissue, blood clot and bacteria introduced at that time are removed. The reddening and swelling which can be seen in inflammation mark the increase in blood supply (and its consequences) produced by the chemicals released by damaged tissues. In with the blood supply arrive the cells involved in the repair process. These include many cells, known as phagocytes for their ability to ingest, sometimes digest, and remove foreign material. It is the presence of these phagocytes at any time other than immediately post-implantation which can indicate problems with a material or an implant. All phagocytic cells begin life in the blood as one of the white cells or leucocytes (see Fig. 1.4).

The cells are distinguished by their size, shape and staining characteristics.[4] They migrate from the blood into the tissues to deal with foreign material. The most numerous are the neutrophils and a massive increase in their numbers signifies, amongst other things, infection, since they ingest bacteria. All of the granular cells have lobed nuclei and may be termed polymorphs or "PMN" for short. They may also be termed "microphages". The non-granular cells have round nuclei and different functions. The lymphocytes are the cells which produce antibodies and an increase in lymphocytes and certain of the granulocytes can indicate an allergic response. Monocytes in the blood are the source of the connective tissue phagocytes, the macrophages. Monocytes migrate from the circulation into the connective tissue (where they are re-named histiocytes) and when needed move through the connective tissue to ingest foreign material which is too large to be dealt with

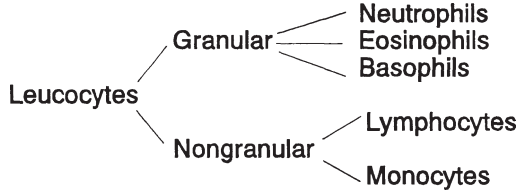

Figure 1.4. Classification of white blood cells.

by polymorphs. Where that material is tissue debris the enzymes secreted by macrophages are sufficient to digest the material with relatively little harm to the cell. However, when such debris is derived from an implant material or when the foreign body has attracted phagocytes because of its surface characteristics, the situation can be quite different. Not only may the cell be unable to digest the material, it may be killed by it and thus release the material to be repeatedly ingested in a vain attempt to eliminate it, at the same time accompanied by increasing amounts of dead macrophage tissue. The enzymes produced by these activated macrophages influence the fibroblasts, which produce the collagen to form the fibrous capsule around an implant. For as long as phagocytic activity continues the capsule will become thicker. When a particle, or more notably a surface, is of a size that it can not be encompassed by a macrophage acting alone, then the giant cell appears. Giant cells form when macrophages coalesce to produce a phagocyte large enough to deal with large particles or to attempt to deal with rough surfaces. However, the characteristics of giant cells are similar in many ways to those of macrophages. They do not themselves reproduce and the presence of giant cells at an interface some time after implantation can indicate a persistent stimulus.

Table 1.1 lists factors that can affect interfacial response and it should now be clear that all of these are mediated by the cells involved in the inflammatory response discussed above. Any defect on the tissue side produced by age or disease will affect it, any damage to implant or tissue as a consequence of roughness, porosity or relative movement will affect it, the loading in use will affect it and the nature of the material and chemical reactions will also affect it. Any material that in its intended use produces few, if any, of those factors which produce these tissue responses can be termed biocompatible.

A biocompatible material is one which possesses the ability to perform with an appropriate host response in a specific application. This definition, arrived at by consensus, emphasizes that biocompatibility is not lack of toxicity, but a requirement that a material performs appropriately.[5] It is essential to

recognize that every application of a material enforces different conditions and thus it may or may not be biocompatible in different applications.

The tissue response to nearly inert ceramics (type 1 implants) therefore is not dependant on chemistry so much as fit. If movement at the interface is minimal the phagocytic response will be transient and the thin capsule will be in place and quiescent shortly after implantation. With more chemically reactive materials, such as some metals, the reactive phase is extended and the capsule will therefore have more time to thicken before equilibrium is achieved. In the response to bioactive interfaces (type 3 implants), the capsule formation is minimal because of the removal of the influence of interfacial movement by the bonding mechanism. The reaction to resorbable implants (type 4) will persist until the components have been removed, for this type of reaction the materials' properties will be the controlling factor in tissue response. Where porous materials or rough surfaces (type 2 implants) are concerned, those which depend on mechanical interlock (with or without bioactivity) for the tissue reaction, all factors are important and the tissue reaction is the most complex. This is because almost all of the factors in Table 1.2 come into play, not only during the initial stabilization process but also during the long term. Because of the difficulty in achieving permanent stability within the pores under loaded conditions, breakdown within the pores is a potential problem and repair within the pores is difficult. These are a significant factor in development of these materials, which is further discussed in Chapters 19 and 32.

1.5. TYPES OF BONE AT BIOCERAMIC INTERFACES

Most bioceramic implants are in contact with bone. Thus, it is important to understand that there are various types of bone in the body. Bone is a living material, composed of cells and a blood supply encased in a strong, interwoven composite structure. There are three major components to the acellular structure of bone: collagen, which is flexible and very tough; hydroxycarbonate apatite, bone mineral, which is the reinforcing phase of the composite; and bone matrix or ground substance, which performs various cellular support functions. The three components are organized into a three-dimensional system that has maximum strength and toughness along the lines of applied stress. See Ham or Vaughn for a description of the growth and structure of bone and Revell for discussion of bone pathology.[4,6,7]

Two of the various types of bone are of most concern in the use of bioceramics. They are cancellous bone and cortical bone. Cancellous bone, also called trabecular or spongy bone, is less dense than cortical bone. It occurs across the ends of the long bones and is like a honeycomb in cross section. Because of

Table 1.5 Mechanical Properties of Skeletal Tissues.

Property	Cortical Bone	Cancellous Bone	Articular Cartilage	Tendon
Compressive Strength (MPa)	100–230[8, 9]	2–12[10]		
Flexural, Tensile Strength (MPA)	50–150[8, 9]	10–20[3]	10–40[11]	80–120[16]
Strain to Failure (%)	1–3[13]	5–7[13]	15–50[12]	10[16]
Young's (Tensile) Modulus (GPa)	7–30[8, 9, 13]	0.5–0.05[10, 13]	0.001–0.0[13]	1[13]
Fracture Toughness (K1c) (MPa m1/2)	2–12[9]			
Compressive Stiffness (N mm^{-1})			20–60[14]	
Compressive Creep Modulus (MPa)			4–15[15]	
Tensile Stiffness (MPa)			50–225[11]	

its lower density, cancellous bone has a lower modulus of elasticity and higher strain to failure than cortical bone (Table 1.5 and Fig. 1.5). Both types of bone have higher moduli of elasticity than soft connective tissues, such as tendons and ligaments (Table 1.5). The difference in stiffness (elastic modulus) between the various types of connective tissues ensures a smooth gradient in mechanical stress across a bone, between bones and between muscles and bones.

Bone at the interface with an implant is often structurally weak because of disease or ageing. Figure 1.6a shows the progressive loss of volume of bone with age. The decrease in bone area leads to a decrease in strength (Fig. 1.6b). See Revell for a discussion of the pathology of bone and the effects of age and disease on the structure and rate of repair of bone.[7]

The quality of bone at an implant–bone interface can deteriorate even further due to the presence of the implant or the method of fixation. Localized death of bone can occur, especially if bone cement, poly(methyl methacrylate) (PMMA), is used to provide mechanical attachment of the device. The local rise in temperature when the monomer cross-links to form the polymer is sufficient to kill bone cells to a depth of nearly a millimeter.

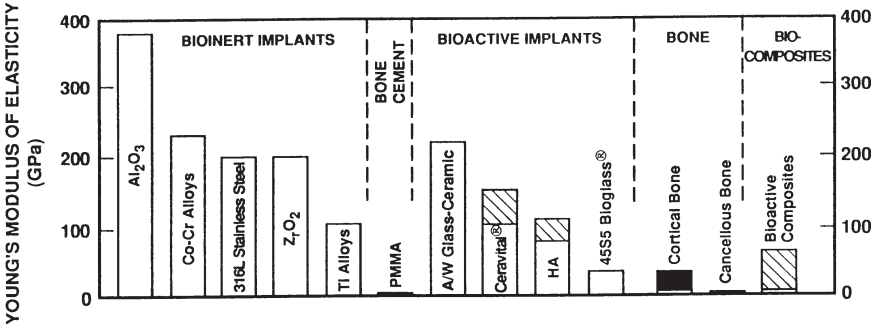

Figure 1.5. Modulus of elasticity (GPa) for prosthetic materials compared with bone.

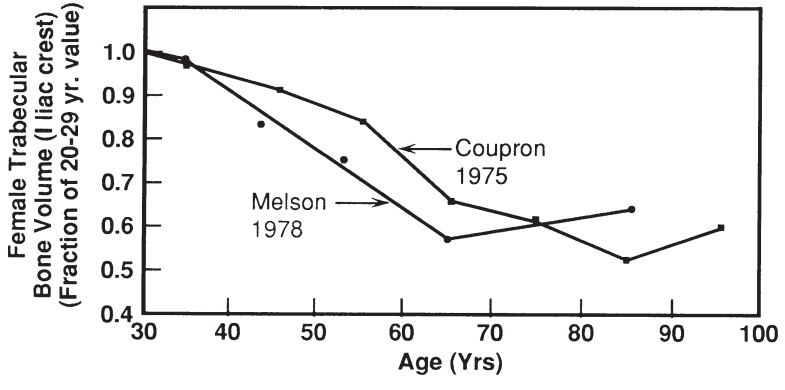

Figure 1.6a. Effect of age on female trabecular bone volume of the iliac crest.

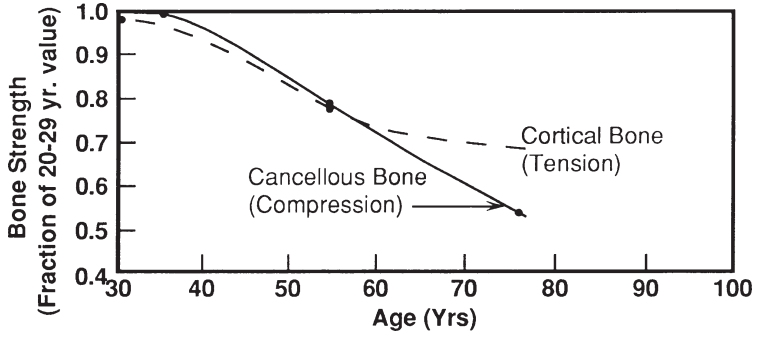

Figure 1.6b. Effect of age on strength of bone.

Another problem, called stress shielding, occurs when the implant prevents the bone from being properly loaded. The higher modulus of elasticity of the implant results in its carrying nearly all the load. Figure 1.5 compares the modulus of elasticity of the materials used for load bearing implants with the values of cortical bone and cancellous bone. The elastic modulus of cortical bone ranges between 7 and 25 GPa, depending upon age, location of the bone and direction of measurement (bone is anisotropic). This modulus is 10–50 times lower than that of alumina. Cancellous bone has a modulus that is several hundreds of times less than that of alumina.

The clinical problem arises because bone must be loaded in tension to remain healthy.[5–7] Stress shielding weakens bone in the region where the applied load is lowest or in compression. Bone that is unloaded or is loaded in compression will undergo a biological change that leads to bone resorbtion.[5–7]

The interface between a stress shielded bone and an implant deteriorates as the bone is weakened. Loosening and/or fracture of the bone, the interface, or the implant will result. The presence of wear debris that often occurs in artificial hip and knee joints accelerates the weakening of the stress-shielded bone, because the increased cellular activity involved in the removal of the foreign wear particles also attacks and destroys bone.[7] The combination of stress shielding, wear debris and motion at an interface is especially damaging and usually leads to failure.

Elimination of stress shielding is one of the primary motivations for the development of bioceramic composites, discussed in Chapters 25 and 26. The elastic modulus of a two-phase composite can be matched to that of bone, as shown in Fig. 1.5. If one of the phases is a bioactive material the composite can also form a bioactive bond with bone, thereby eliminating two of the primary causes for implant failure, interfacial loosening and stress shielding.

1.6. TYPES OF PROCESSING AND MICROSTRUCTURE OF BIOCERAMICS

Bioceramic materials can be classified into eight categories based upon processing method used and the microstructure produced; i.e., the distribution of phases developed in the material (Table 1.6). The differences in microstructure of the eight categories are primarily due to the different starting materials and thermal processing steps involved in making the materials. Chapter 37 discusses the sequence of processing steps used in making bioceramics and the characterization methods required to ensure reproducibility of properties of the final product.

Figure 1.7 summarizes the time–temperature profiles used in processing the ceramics listed in categories 1–6 in Table 1.6. The thermal processing of

Table 1.6. Ceramic processing methods

Type of Ceramic Processing	Example
1. Glass	45S5 Bioglass®
2. Cast or rapidly solidified polycrystalline ceramic	HA coating
3. Polycrystalline glass-ceramic	Ceravital®
4. Liquid-phase sintered (vitrified) ceramic	Glass-HA
5. Solid-state sintered ceramic	Alumina, zirconia
6. Hot pressed ceramic or glass-ceramic	A/W glass-ceramic
7. Sol-gel glass or ceramic	52S bioactive gel-glass
8. Multi-phase composite	PE-HA

sol-gel glasses and ceramics involves much lower temperatures and different types of processing methods, as shown below. Processing of composites differ for each type of composite, as discussed in Chapters 25 and 26.

For the reader unfamiliar with ceramic processing, some of the concepts relating thermal processes with microstructural development follow. For detailed treatment of the theory and practice of ceramic processing, consult Reed, Onoda and Hench or Kingery, Bowen and Uhlmann.[20–22]

The objective of ceramic processing is to make a specific form of the material that will perform a specific function (Table 1.1). This requires making a solid object, a coating or particulates (powders). There are two ways of making a specific shape: casting from the liquid state (types 1, 2, 3 in Table 1.6) or preforming the shape from fine-grained particulates followed by consolidation (types 4, 5, 6 in Table 1.6).

When a shape is made from powders it is called *forming*. The powders are usually mixed with water and an organic binder to achieve a plastic mass that can be cast, injected, extruded or pressed into a mold of the desired shape. The formed piece is called *green ware*. Subsequently, the temperature is raised to evaporate the water (*drying*) and the binder is burned out, resulting in *bisque ware*. At a much higher temperature the ware is densified during firing. After cooling to ambient temperature, one or more finishing steps may be applied, such as grinding and polishing, as illustrated in Fig. 37.1. The result is a finished product with desired properties. The properties depend upon the composition of the material, the phases developed during thermal processing and the microstructure of the material.

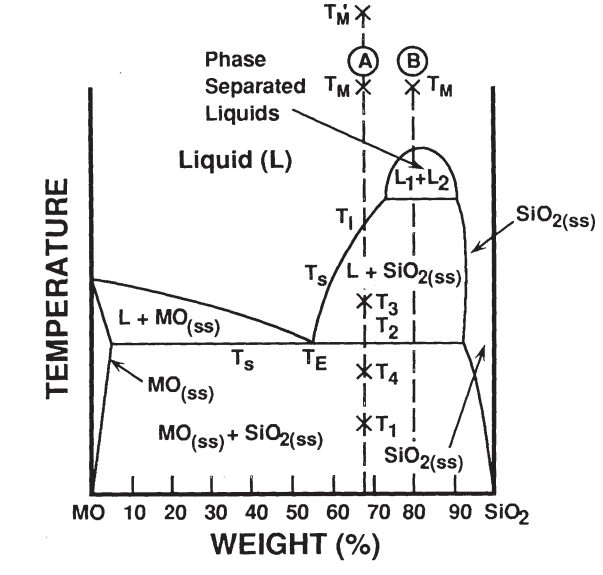

(a)

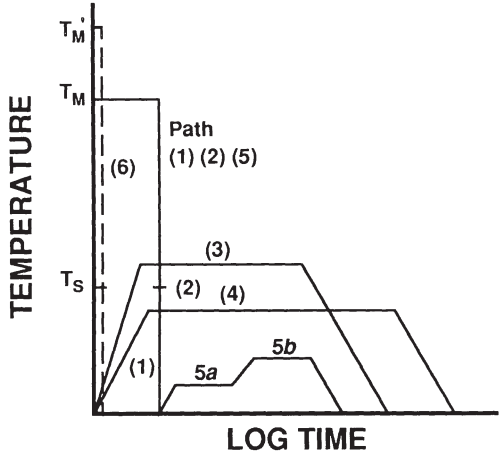

(b)

Figure 1.7. (a) composition A: microstructure: (1) glass; (2) cast polycrystalline (large-grained); (3) liquid-phase-sintered (vitrified); (4) solid-state sintered; (5) polycrystalline glass-ceramic; (6) polycrystalline coating from T_m. (b) composition B: (1) phase-separated glass. (2)–(5) same as (a). (ss) = solid solution, T_s = solidus line.

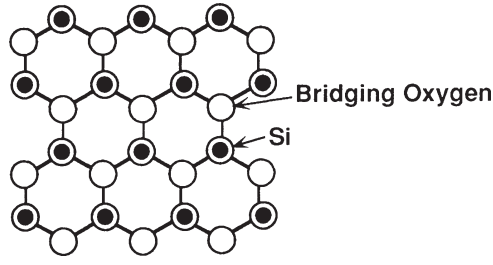

Figure 1.8a. Schematic structure of a crystalline silicate. All $Si(O_4)$ tetrahedra are bonded together by -Si-0-Si (siloxane) bonds.

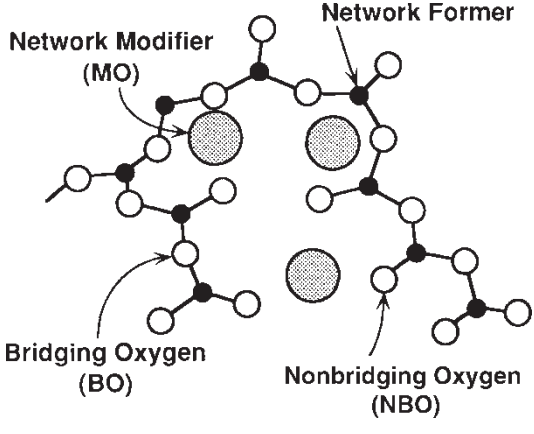

Figure 1.8b. Schematic structure of a random glass network composed of network modifiers (MO) and network formers (SiO_2). Some of the Si are bonded to each other by bridging oxygen (BO) bonds and others are coordinated with non-bridging oxygen (NBO) bonds to network modifying ions.

Phase equilibrium diagrams provide the basis for understanding the relationships between thermal processing schedules and the phases and microstructures produced.[23] Figure 1.7a is a binary phase equilibrium diagram consisting of SiO_2 (silica), a network-forming oxide, and some arbitrary network modifier oxide (MO). MO can be Na_2O, K_2O, CaO, MgO etc. Schematic structures of a glass, with a random network, and a crystal, with an ordered network, are shown in Fig. 1.8. There are two types of bonds in the glass or crystal network, bridging oxygen bonds between neighboring Si atoms, which hold the network together, and non-bridging oxygen bonds between Si and modifier atoms, which disrupt

the network. The biological behavior of glasses, glass ceramics and ceramics depends on the relative proportion of bridging oxygen bonds to non-bridging bonds in the phases of the material.

When a mixture of MO and SiO_2 is heated to the temperature T_M in Fig. 1.7a, the entire mass will melt and become liquid (L). The MO molecules break the Si-O-Si bonds of SiO_2 and lower the melting temperature, as shown in Fig. 1.7a. The liquid becomes homogeneous when held at this temperature for a sufficient length of time. In order to ensure homogeneity, melting is usually done several hundreds of degrees above T_M. In a very rapid process such as plasma spray coating of HA (Chapter 21), melting occurs but there is insufficient time for homogenization of the liquid. Selective evaporation of constituents of the melt can also occur; the higher the temperature the greater the probability of this happening, leading to an inhomogeneous product.

When the liquid is cast (paths 1, 2, 5), forming the shape of the object during the casting, either a glass or a polycrystalline microstructure will result. When the liquid is rapidly cooled onto a substrate (path 6) either a glass or a polycrystalline coating will be formed. A glass is produced when the composition contains a sufficient concentration of network formers and the cooling rate is sufficiently rapid (path 1 or 6). The viscosity of the melt increases greatly as it is cooled until, at T_1, glass transition point, the material is transformed into an amorphous solid; i.e., a glass.

If there are insufficient network formers or the cooling rate is too slow, a polycrystalline microstructure will result. The crystals begin growing from T_1 and below. Crystallization is complete when the temperature reaches T_2. The final material consists of the equilibrium crystal phases predicted by the phase diagram (path 2). However, the combination of lack of network formers and very rapid cooling, such as what occurs in plasma spray coating of hydroxyapatite, often produces a mixture of crystal phases which may or may not be equilibrium phases (see Chapters 17–21).[23]

When the MO and SiO_2 powders are first formed into the shape of the desired object and fired at a temperature T_3, liquid-phase-sintered structures will result (path 3). Before firing, the material will contain 10–40% porosity, depending on the forming process used. During heating a liquid begins to form at grain boundaries at the eutectic temperature, T_2. The liquid dissolves the interface, penetrates between the grains, fills the pores and draws the grains together by capillary attraction (Fig. 1.9a). These effects decrease the volume of the compact. Since the mass remains unchanged but only rearranged, the density increases. The liquid content and composition can be predicted from the phase diagram for

(A) Liquid-phase sintering

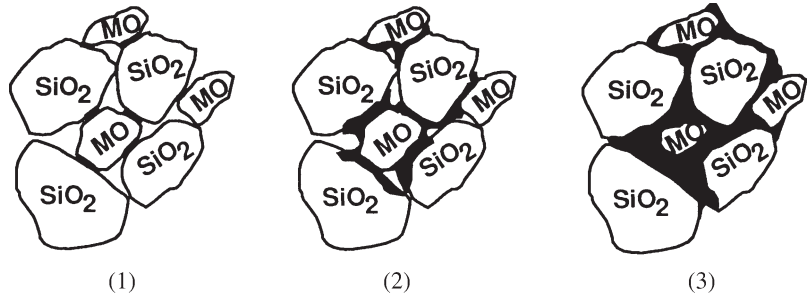

Figure 1.9a. Steps in liquid-phase sintering: (1) liquid begins to form at MO-SiO_2 grain boundaries at eutectic temperature (T_E); (2) liquid dissolves MO and SiO_2; (3) liquid fills the pores and pulls the grains together into a dense object.

(B) Solid-state sintering

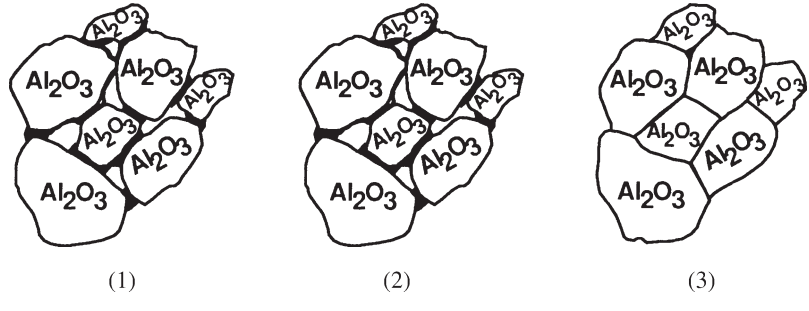

Figure 1.9b. Steps in solid-state sintering: (1) necks form at particle contacts by diffusion or creep; (2) necks grow to close pore channels and particles rearrange to eliminate pores; (3) pores are replaced by new grain boundaries.

long firing times. However, in most ceramic processing, liquid formation does not proceed to equilibrium due to the slowness of the reactions.

The microstructure resulting from liquid-phase sintering, or vitrification, as it is commonly called, consists of grains from the original powder compact surrounded by a liquid phase formed during firing at T_3. As the compact is cooled from T_3 to T_2 (the solidus temperature is T_8), the liquid phase crystallizes into a fine-grained matrix surrounding the original grains. If the liquid contains a sufficient concentration of network formers, the liquid will be quenched into a glassy matrix, which surrounds the original grains. Hot-pressing of ceramics or

glass-ceramics, such as A/W glass-ceramic, produces grain boundary reactions, densification and a final microstructure similar to that obtained by vitrification.

A powder compact can be densified without the presence of a liquid phase by a process called solid-state sintering. This is the process used to make medical-grade alumina and zirconia. Prevention of formation of grain boundary phases that are susceptible to grain boundary corrosion is the main advantage of solid-state sintering. In solid-state sintering, solid material is moved to areas of contact between particles. The driving force is reduction of surface energy gradients. A fully dense compact has no internal solid–vapor interfaces and therefore is lower energy than a porous material. Sintering occurs by thermal activation of molecules at the solid–pore interface; mechanisms include grain boundary diffusion, volume diffusion, surface diffusion, creep or various combinations depending upon the temperature, sintering atmosphere and composition of the material. Because long-range migration of atoms is necessary, solid-state sintering temperatures are usually greater than one-half of the melting point of the material: $T > TL/2$ (path 2).

During solid-state sintering the material moves to eliminate the pores and open channels that exist between the grains of the compact (Fig. 1.9b). As the pores and open channels are closed during heat treatment the crystals become tightly bonded together at their grain boundaries and the density, strength, toughness and corrosion resistance of the material increases greatly. The microstructure of a ceramic made by solid-state sintering consists of grains bonded together with a small amount of residual porosity.

The relative rate of densification during solid-state sintering is slower than that of liquid-phase sintering because material transport is slower in a solid than in a liquid. However, it is possible to solid-state sinter single component materials such as pure alumina, since liquid development is not necessary. Consequently, when optimal mechanical and chemical performance is required, as it is in prostheses, solid-state sintering becomes essential. Control of grain size during sintering is critical if properties are to be consistently superior. Excessive grain growth is always a potential hazard because of the high temperatures involved. Grain growth inhibitors can be used, but if they remain in grain boundaries they may degrade grain boundary resistance to body fluids. Optimization of medical-grade ceramics requires a systematic characterization effort, see Chapter 37.

Another class of microstructures is termed *glass-ceramics* because the object is formed as a glass but ends up as a polycrystalline ceramic. The transformation of the glass into a ceramic occurs in two steps. First, the glass is heat treated at a temperature in the range of 450–700 °C (path 5a) to produce a large concentration of nuclei from which crystals can grow. When sufficient nuclei are present to ensure that a fine-grained microstructure will be obtained, the

temperature of the object is raised to 600–900 °C, which promotes crystal growth (path 5b). Crystals grow from the nuclei until they impinge and 100% crystallization is achieved. The resulting microstructure is non-porous and fine-grained. The crystals are randomly oriented and can be very small and have a very uniform size distribution. The crystal phases may or may not correspond to the equilibrium crystal phases predicted by the phase diagram. When phase separation occurs, composition B in Fig. 1.7, a non-porous glass-in-glass microstructure, can be obtained. Use of these concepts makes it possible to produce a very broad range of glass-ceramics, as described in Chapters 16, 29 and 34.

1.7. SOL-GEL PROCESSING

Sol-gel processing is a chemically-based method for producing ceramics, glass, glass-ceramics and composites at much lower temperatures than the traditional processing methods described above. Brinker and Scherer, Hench and West and Hench describe the history, theory, processing details and applications of sol-gel processing.[24–26] The sol-gel method was used by Jarcho, and many others subsequently, to make hydroxyapatite ceramics.[27] The method has been recently used to make a new generation of bioactive gel-glasses[26–28] and offers promise for tailoring the composition of bioactive materials to match the requirements of specific applications, as discussed in Chapters 4, 5, 32 and 35.

Three methods can be used to make sol-gel materials:

Method 1: Gelation of colloidal powders
Method 2: Hypercritical drying
Method 3: Controlled hydrolysis and condensation of metal alkoxide precursors followed by drying at ambient pressure.

All three methods involve the creation of a three-dimensional, interconnected network, termed a *gel*, from a suspension of very small, colloidal particles, called a sol. Colloids are solid particles with diameters <100 nm. A sol is a dispersion of colloidal particles in a liquid. Milk is an example of a sol. A gel can be formed from an array of discrete colloidal particles by changing the pH of the sol (Method 1). The gel network can also be formed from the hydrolysis and condensation of liquid metal alkoxide precursors (Methods 2 and 3), illustrated in Fig. 1.10. An example of a metal alkoxide precursor used to provide the -Si-O-Si- network of bioactive gel-glasses is Si(OR)4, where R is CH3, C2H5, or C3H7. Other metal ions can also be used in addition to Si, such as, Ca, P, Ti etc.

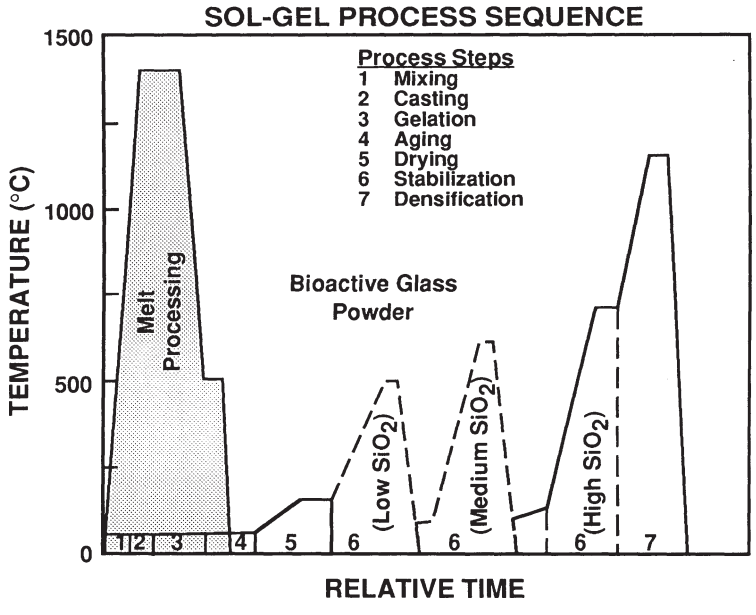

Figure 1.10. Processing steps in making bioactive gel glasses by the sol-gel method. Note lower temperatures compared with melt processing of a bioactive gel-glass with low silica content.

Seven steps are involved in making gel-glasses or ceramics by the sol-gel method. The first step, shown in Fig. 1.10, is mixing the precursors, which forms the low viscosity sol. As the network interconnects develop the viscosity increases greatly. Prior to completion of the network formation the sol can be applied as a coating, be pulled into a fiber, impregnated into a composite, formed into powders or cast into a mold with a precise shape and surface features (step 2). Gelation (step 3) occurs in the mold or on the surface of a substrate forming a solid object or a surface coating. Powders can be made with very highly controlled size distributions.

The three-dimensional gel network is completely filled with pore liquid. Aging (step 4) involves holding the gel in its pore liquid for several hours at 25–80 °C. This leads to localized solution and re-precipitation of the solid network, which increases the thickness of the inter-particle necks and the density and strength of the gel.

The pore liquid is removed during drying (step 5). Colloidal gels are easily dried since their pore size is large, > 100 nm. Alkoxide-based gels have very small pores (1–10 nm) and thus large capillary stresses can arise during drying.

Hypercritical drying at elevated temperature and pressure, above the pore liquid-solid critical point, avoids the solid–liquid interface and eliminates drying stresses (Method 2). Gels made by this method, called *aerogels*, have very low densities and strengths. They are used for optical applications but as yet have no biomaterial applications.

Gels dried under ambient temperature and relatively low temperatures are termed *xerogels* (Method 3). The generic term *gel* usually applies to a xerogel. Careful control of the hydrolysis and condensation rates in step 1 by use of acid or base catalysts is required to produce the very narrow pore size distributions in xerogels needed to reduce drying stress gradients. A gel is dried (step 5) when the physically adsorbed water is completely eliminated from the pores. This requires heating at controlled rates at temperatures of 120–180 °C. The surface area of gels made by Method 3 is very large, 200–800 m^2/g. The pore sizes can be varied from 1–12 nm.

Chemical stabilization of a dried gel, step 6 in Fig. 1.10, is necessary to control the environmental stability of the material. Thermal treatment in the range of 500–900 °C desorbs surface silanols (Si-OH) and eliminates 3-membered silica rings from the gel. These surface chemical features are important in controlling the rate of HCA formation on the gel-glasses and their bioactivity. Stabilization also increases the density, strength and hardness of the gels and converts the network to a glass with network properties similar to melt-derived glasses.

Densification of alkoxide-derived gel-glasses is completed in the range of 900–1150 °C depending upon composition. Gel-glasses with moderate (45–69%) SiO_2 content and high CaO-P205 content, for example, have all pores eliminated by the end of a 900 °C treatment, whereas gel-glasses with high Si content require 1000–1150 °C. Hydroxyls and adsorbed water must be removed from the gels prior to closure of pores or bloating and inhomogeneous microstructures will result. A very important advantage of the sol-gel process is the ability to control the surface chemistry of the material by these thermal treatments. See Chapter 32 for details.[26]

1.8. NEW DEVELOPMENTS

See References 30–33 for discussions of significant new developments in the field, especially clinical applications.

REFERENCES

1. Preston, J.D. (1988). Properties in Dental Ceramics, *Proc. IV Int. Symp. on Dental Materials*, pp. 153–165.

2. Hulbert, S.F., Bokros, J.C., Hench, L.L. *et al.* (1987). "Ceramics in Clinical Applications: Past, Present, and Future", in Vincenzini, P. (ed.), *High Tech Ceramics*, Elsevier, Amsterdam, pp. 189–213.
3. Black, J. (1984). Systemic Effects of Biomaterials, *Biomaterials*, **5**, 11–18.
4. Ham, A.W. (1969). *Histology*, J.B. Lippincott Co., Philadelphia, PA.
5. Williams, D. (ed.) (1990). *Concise Encyclopedia of Medical and Dental Materials*, Pergamon Press, Oxford.
6. Vaughn, J. (1981). *The Physiology of Bone*, Clarendon Press, Oxford.
7. Revell, P. (1986). *Pathology of Bone*, Springer-Verlag, Berlin & New York.
8. Evans, F.G. and King, A. (1961). *Biomedical Studies of the Musculoskeletal System*, Charles C. Thomas, Springfield, IL.
9. Bonfield, W. (1984). "Elasticity and Viscoelasticity of Cortical Bone", in Hastings, G.W. and Ducheyne, P. (eds), *Natural and Living Biomaterials*, CRC Press, Boca Raton, FL, pp. 43–60.
10. Van Audekercke, R. and Martens, M. (1984). "Mechanical Properties of Cancellous Bone", in Hastings, G.W. and Ducheyne, P. (eds), *Natural and Living Biomaterials*, CRC Press, Boca Raton, FL, pp. 89–98.
11. Kempson, G.E. (1982). Relationship Between the Tensile Properties of Articular Cartilage from the Human Knee and Age, *Ann. Rheum. Dis.*, **41**, 508–511.
12. Bader, D.L., Kempson, G.E., Barrett, A.J. *et al.* (1981). The Effects of Leukocyte Elastose on the Mechanical Properties of Adult Human Cartilage in Tension, *Biochim. et Biophys. Acta*, **677**, 103–108.
13. Black, J. (1988). *Orthopedic Biomaterials in Research and Practice*, Churchill Livingston, New York.
14. Bader, D.L., Kempson, G.E., Egan, J. *et al.* (1992). The Effects of Selective Matrix Degradation on the Short Term Compressive Properties of Adult Human Articular Cartilage, *Biochim. et Biophys. Acta*, **116**, 147–152.
15. Roberts, S., Weightman, B., Urban, J. *et al.* (1986). Mechanical and Biochemical Properties of Human Articular Cartilage in Osteoarthritic Femoral Heads and in Autopsy Specimens, *J. Bone Jt. Surg.*, **68B**, 278–288.
16. Butler, D.L., Grood, E.S., Noyes, F.R. *et al.* (1984). Effects of Structure and Strain Measurement Techniques on the Material Properties of Young Human Tendons and Fascia, *J. Biomech.*, **17**, 579–596.
17. Black, J. and Hastings, G. (eds) (1998). *Handbook of Biomaterial Properties*, Chapman and Hall, London.

18. Cowin, S.C. (ed.) (1989). *Bone Mechanics*, CRC Press, Boca Raton, FL.
19. Evans, G. and Yamada, H. (1970). *Strength of Biologicl Materials*, Williams and Wilkins, Baltimore, MD.
20. Reed, J. (1988). *Introduction to Ceramic Processing*, J. Wiley and Sons, Inc., New York.
21. Onoda, G. and Hench, L.L. (1978). *Ceramic Processing Before Firing*, J. Wiley and Sons, Inc., New York.
22. Kingery, W.D., Bowen, K. and Uhlmann, D.R. (1976). *Introduction to Ceramics*, J. Wiley and Sons, Inc., New York.
23. Bergeron, C.G. and Risbud, S.H. (1984). *Introduction to Phase Equilibria in Ceramics*, The American Ceramic Society, Columbus, OH.
24. Brinker, C.J. and Scherer, G.W. (1990). *Sol-Gel Science*, Academic Press, San Diego, CA.
25. Hench, L.L. and West, J.K. (1990). The Sol-Gel Process, *Chern. Rev.*, **90**, 33–72.
26. Hench, L.L. (1996). *SOL-GEL SILICA: Properties, Processing and Technology Transfer*, Elsevier, New York.
27. Jarcho, M. (1981). Calcium Phosphate Ceramics as Hard Tissue Prosthetics, *Clin. Orthop. Relat. Res.*, **157**, 259–278.
28. Li, R., Clark, A.E. and Hench, L.L. (1991). An Investigation of Bioactive Glass Powders by Sol-Gel Processing, *J. Appl. Biomaterials*, **2**, 231–239.
29. Li, R., Clark, A.E. and Hench, L.L. (1992). "Effects of Structure and Surface Area on Bioactive Powders by Sol-Gel Process", in Hench, L.L. and West, J.K. (eds), *Chemical Processing of Advanced Materials*, J. Wiley and Sons, Inc., New York, pp. 627–633.
30. Hench, L.L. (1991). From Concept to Clinic, *J. Amer. Ceram. Soc.*, **74**, 1487–1510.
31. Yamamuro, T., Hench, L.L. and Wilson, J. (eds) (1990). *Handbook on Bioactive Ceramics, Vol. I: Bioactive Glasses and Glass-Ceramics; Vol. II: Calcium Phosphate and Hydroxylapatite Ceramics*, CRC Press, Boca Raton, FL.
32. Hench, L.L. (1998). Bioceramics, *J. Amer. Ceram. Soc.*, **81**, 1705–1735.
33. Hench, L.L., Jones, J.R. and Fenn, M. (eds) (2011). *New Materials and Technologies for Healthcare*, Imperial College Press, London.

Chapter 2

THE USE OF ALUMINA AND ZIRCONIA IN SURGICAL IMPLANTS

Samuel F. Hulbert

2.1. INTRODUCTION

The use of ceramics in medicine has increased greatly during the past three decades.[1–10] All materials elicit a response from living tissues. Four types of responses are possible, as discussed in Chapter 1. The potential of ceramics as biomaterials relies upon their compatibility with the physiological environment. Bioceramics are compatible because they are composed of ions commonly found in the physiological environment (calcium, potassium, magnesium, sodium, etc.) and of ions showing limited toxicity to body tissue (zirconium and titanium). This chapter deals with the two nearly inert ceramics most used in surgical implants: alumina and zirconia.

Nearly inert bioceramics undergo little or no chemical change during long-term exposure to the physiological environment. Even in those cases where these bioceramics may undergo some long-term chemical or mechanical degradation, the concentration of degradation product in adjacent tissue is easily controlled by the body's natural regulatory mechanisms. Tissue response to immobilized inert bioceramics involves the formation of a very thin, several micrometers or less, fibrous membrane surrounding the implant material. Inert bioceramics may be attached to the physiological system through mechanical interlocking, by tissue ingrowth into undulating surfaces, or by cement fixation. The nearly inert ceramic most used for surgical implants is alumina.

2.2. ALUMINA CERAMICS AS IMPLANT MATERIALS

High-density, high purity (>99.5%) Al_2O_3 (alumina) is used in load-bearing hip prostheses and dental implants because of its combination of excellent corrosion resistance, good biocompatibility, high wear resistance and high strength. Although some dental implants are single-crystal sapphire, most Al_2O_3 devices

are very fine-grained polycrystalline α-Al_2O_3, produced by pressing and sintering at temperatures ranging from 1600–1800 °C, depending upon the properties of the raw material. A very small amount of MgO (<0.5%) is used as a grain growth inhibitor and is essential in order to achieve a fully dense sintered body with a fine grain microstructure. It is very important that the amount of SiO_2 and alkali oxides be below 0.1%, because they impede densification and promote grain growth. It is also essential that the amount of CaO be below 0.1% since its presence leads to a lowering of the static fatigue resistance.[11,12]

Strength, fatigue resistance, and fracture toughness of polycrystalline α-Al_2O_3 are a function of grain size and percentage of sintering aid, i.e., purity. Al_2O_3 with an average grain size of <4 μm and >99.7% purity exhibits good flexural strength and excellent compressive strength. These and other physical properties are summarized in Table 2.1 for a commercially available implant material, along with the International Standards Organization (ISO) requirements and the proposed new standards for alumina implants. Extensive testing has shown that alumina implants which meet or exceed ISO standards have excellent resistance to dynamic and static fatigue, and resist subcritical crack growth and impact failure.[4]

Other typical properties of commercially available alumina implant materials are listed in Table 2.2.

An increase in average grain size to >7 μm can decrease mechanical properties by about 20%. High concentration of sintering aids must be avoided because they remain in the grain boundaries and degrade fatigue resistance.

Table 2.1. Physical Characteristics of Al_2O_3 Bioceramics.

	Commercially Available High Alumina Ceramic Implants	**ISO Standard 6474**	**Proposed New ISO Standards**
Alumina content (% by weight)	>99.7	≥99.51	
$SiO_2 + Na_2O$%	<0.02	<0.1	
Density (g/cm3)	3.98	≥	≥3.94
Average grain size (μm)	3.6	<7	<4.5
Hardness (Vickers, HV)	2400	>2000	
Bending strength (MP) (after testing in Ringer's solution)	595	>400	>450

Table 2.2. Other Typical Properties of Commercially Available Alumina implants.

Surface finish Ra (μm)	0.02
Compressive strength (Mpa)	4000–4500
Young's modulus (Gpa)	380–420
Fracture toughness K_{1c} ($MN/m^{3/2}$)	4–6
Implant strength (Nc n/cm^2)	40–50

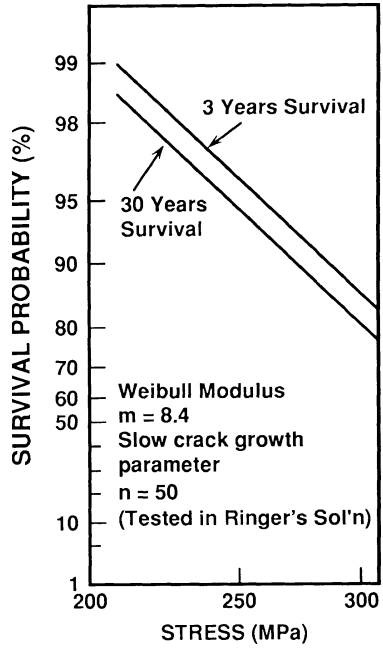

Figure 2.1. Stress-probability of time to fracture diagram for medical grade alumina in Ringer's Solution. (Based upon M.W. Real *et al.*[13])

Methods exist for lifetime predictions and statistical design of proof tests for load bearing ceramics. Applications of these techniques show that specific prosthesis load limits can be set for an Al_2O_3 device based upon the flexural strength of the material and its use environment.[12] Load bearing lifetimes of 30 years at 12,000 N loads or 200 Mpa stresses have been predicted.[11–13] Figure 2.1 is an applied stress-probability of time to failure (SPT) diagram for medical grade alumina, based upon Real *et al.*[13] It shows that for 30 years survival with failure of

no more than 1 in 100 components the maximum tensile stress that can be applied is limited to <200 Mpa. If stresses of 250 Mpa are applied to the ceramic component, within 3 years 4% of the implants are likely to fail and by 30 years 7% will probably fail. Use of SPT diagrams such as this, together with finite element analyses of local stress distributions, make it possible to design ceramic components that have very low probabilities of failure during the lifetime of the patient.

Results from aging and fatigue studies show that it is essential that Al_2O_3 implants be produced with the highest possible standards of quality assurance, especially if they are to be used as orthopedic prostheses in younger patients.

2.3. USE OF ALUMINA IN TOTAL HIP PROTHESES

Alumina ceramics are being used in hip and knee prostheses because of inertness, excellent biocompatibility, and high wear resistance. It is estimated that several million hip prostheses have been implanted, primarily with an alumina ball for the femoral head component, and that the number is growing by at least a 100,000 per year.[14] Figure 2.2 shows three femoral components of total hip prostheses with alumina balls. The main problem with present total hip systems, using ultrahigh molecular weight polyethylene as the articulating surface in the acetabulum, is loosening of the acetabular component caused by polyethylene wear debris. Numerous clinical studies indicate that using femoral heads of alumina ceramic bearing against alumina cup sockets reduces wear debris by a factor

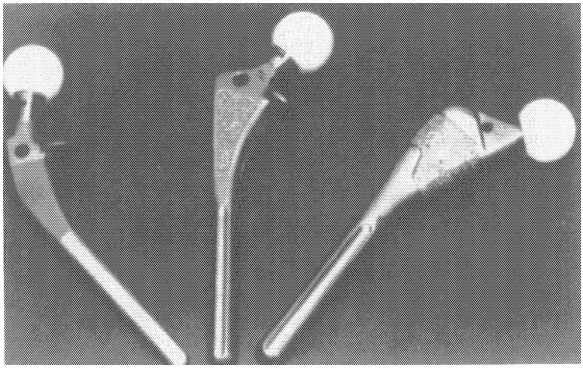

Figure 2.2. Medical-grade alumina used as femoral balls in total hip replacement. Note three alternative types of metallic stems used for morphological fixation. (Photography courtesy of J. Parr.) (Reprinted from Hench, L.L. (1991). Bioceramics: From Concept to Clinic, *J. Am. Ceram. Soc.*, **74**, 1487–1510, by permission of the American Ceramic Society.)

of ten or greater and by a factor of two or better when against ultrahigh molecular weight polyethylene (UHMWPE) cups.[3]

The first clinical use of a total hip prosthesis with an alumina head and alumina socket was reported by Boutin in 1971.[5] In 1981 he reported on 1,330 cases. There were four socket and six ball fractures, three stem fractures and seven incidents of severe wear.

Wear rates ranged from 5–9 μm per year. Dorlot *et al*. in 1986 reported wear rates of less than 1 μm per year. The average wear rate reported on 20 retrieved ceramic-on-ceramic total hip prostheses was 0.025 μm per year, which is far less than that observed with UHMWPE bearing on metal or ceramic heads.[15]

Winter, *et al*. reported on 10–14-year results using an alumina ball and alumina cup total hip placed in 100 patients between 1974 and 1979.[7] Twenty-three patients could not be reached for follow-up. Twenty-five patients had to have revision systems. There were eight ball fractures. Eighty percent of the 52 remaining prostheses were reported to have good clinical results.

Witvoet, *et al*. reported on 608 patients who received total hip prostheses consisting of a ceramic ball against a cemented alumina socket.[8] Overall probability of survival was 88% after eight years. The reason for failure was loosening at the cup–cement interface. Elastic modulus mismatch was assumed to be responsible for loosening. The survival rate of ceramic sockets was higher than with UHMWPE sockets in patients younger than 50 years of age.

In 1991, Sedel *et al*. reported on a ten-year clinical study of 187 cemented ceramic-to-ceramic total hip replacements.[9] The major cause of failure was aseptic loosening of the acetabular component (15 failures). Fracture of the socket and/or the femoral head occurred in five patients. All of the mechanical failures occurred in components manufactured prior to 1979. Development of alumina ceramic which met or exceeded ISO standards has reduced the number of mechanical failures and, in the case of the Sedel *et al.* study, completely eliminated mechanical failures. A ten-year survival rate of 82.6% was reported. The outer diameter of the acetabular component was a major variable influencing the results. The outer diameter of the acetabular components must be at least 50 mm. Another major factor was the age of the patient. Sedel *et al.* reported on alumina-to-alumina total hip prostheses involving 116 patients under 50 years of age, performed between April 1977 and August 1989.[10] The survival analysis gives a 98.5% probability of retaining the prosthesis for more than ten years.

A number of clinical studies have compared wear rates of socket components of UHMWPE against alumina balls versus metal balls. There is considerable variation of data, but in each case the wear rate for systems with metal balls is much higher than with alumina balls.

Oonishi *et al.* reported a study involving 956 total hip prostheses of alumina balls and UHMWPE cups performed between 1977 and 1988 and 117 prostheses involving metal heads and UHMWPE sockets performed between 1975 and 1981.[16] The amount of wear was measured by X-ray techniques. The wear rate for alumina–UHMWPE combinations was 0.098 mm per year and 0.245 mm per year for metal–UHMWPE combinations.

Ohashi *et al.* reported on 318 total hip prostheses done over a period of 13 years; 131 cases involved prostheses with metallic heads and 187 were prosthetics with alumina heads. UHMWPE acetabular components were used in all cases. The amount of wear was measured using X-ray techniques. The wear rate was 0.025 mm per year with alumina heads and 0.043 mm per year for metal heads.

Okumura reported a study conducted between 1981 and 1988, involving 105 total hip prostheses; 73 hips using an alumina ball, the rest using metal balls articulated against UHMWPE sockets.[18] Socket wear was measured using X-ray techniques. The observed socket wear with alumina balls was 0.08 mm per year while it was 0.14 mm per year with metal balls.

In 1991, Asada *et al*. compared the performance of a bipolar hip prosthesis with a Co-Cr-Mo alloy device in Beagle dogs.[19] They concluded that an alumina ceramic was the better articulating material. One of the most important properties of articulating components is the wear and friction behavior over an extended period of time. Comparative tests in hip joint simulators have demonstrated tribologic superiority of high-purity alumina ceramic systems compared with metal-to-metal and metal-to-UHMWPE combinations.

Dörre reports that 16 years of clinical experiences have shown low annual average wear rates for alumina/alumina surfaces, shown in Table 2.3.

In the case of alumina–UHMWPE articulating surfaces, the 20 μm refer to observations of explanted components and include only wear measurements. The 130 μm refers to penetration measurements between head and acetabular

Table 2.3. Average Annual Wear Rates of Articulating Surfaces in Total Hip Prosthesis.

Materials	**Wear Rate (μm/yr)**
Co-Cr-Mo Alloy/UHMWPE	200
Alumina/UHMWPE	20–130
Alumina/Alumina	2

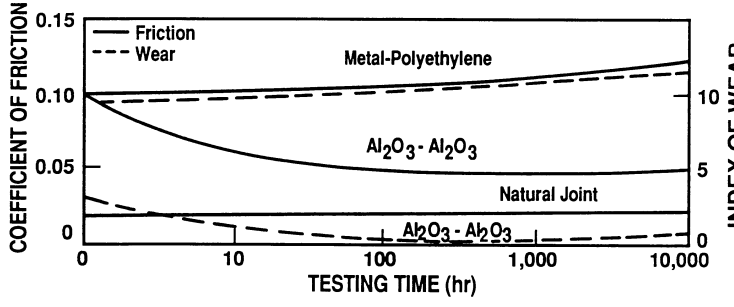

Figure 2.3. Time dependence of (-) coefficient of friction and (---) index of wear of alumina–alumina versus metal–PE hip joint (*in vitro* testing). (Reprinted from Hench, L.L. (1991). Bioceramics: From Concept to Clinic, *J. Am. Ceram. Soc.*, **74**, 1487–1510, by permission of the American Ceramic Society.)

components observed by means of radiographic analysis; it includes not only wear but also plastic flow. The long-term coefficient of friction of an alumina–alumina articulating surface decreases with time and approaches the value of a normal healthy joint, as illustrated in Fig. 2.3.

The outstanding frictional and wear properties of alumina ceramics are due to the materials' extremely low surface roughness and to their high surface energy, which results in the fast and strong adsorption of biological molecules. These layers of adsorbed molecules provide a liquid-like covering which limits the direct contact of the articulating solid surfaces. The high surface energy of alumina is demonstrated through contact angle measurements. With the single phase fine-grained structure of alumina, the surface roughness is lower than for carbide-containing biphasic Co-Cr-Mo-alloys. Any roughness on alumina is inverse (due to pull out of grains) instead of the protruding asperities encountered with the hard metal carbides (M_7C_3) present in some metal alloys. The concave surface that is not abrasive as opposed to abrasive metallic carbide protrusions that abrade the UHMWPE cup is a major contributing factor to the outstanding wear properties of alumina ceramics.

A very important prerequisite for the superior tribological behavior of alumina, particularly in the case of alumina/alumina articulation, is an extremely smooth polished surface with an average roughness of 0.01 µm and an extreme congruence of the sliding faces with a roundness deviation between 0.1 and 1 µm. The alumina ball and socket should be polished and used as a matched pair.

2.4. OTHER APPLICATIONS OF ALUMINA AS AN IMPLANT MATERIAL

Oonishi *et al.* developed and tested clinically total knee prostheses consisting of an Al_2O_3 femoral component with a tibial component of UHMWPE.[20]

Inoue *et al.* reported a clinical study involving 52 knee prostheses consisting of an Al_2O_3 femoral component bearing on a UHMWPE tibia component.[21] During the period of study, 1982–1988, there were no revision cases. *The Journal of Orthopaedic Ceramic Implants*,[22] published by the Japanese Society of Orthopaedic Ceramic Implants, contains 12 papers on total knee prostheses where one or both of the articulating surfaces were made of Al_2O_3.

Ceramic ankle joints, elbows, shoulders, wrists, fingers, as well as applications in ENT and ophthalmology and cranial surgery have been tested clinically with success equal to or better than other material systems, as reviewed in various articles.[1–3]

2.5. USE OF ZIRCONIA CERAMICS IN SURGICAL IMPLANTS

Medical grade alumina has outstanding biocompatibility and wear resistance. However, it exhibits moderate flexural strength and toughness. For this reason, the diameter of most alumina femoral head prostheses has been limited to 32 mm. Zirconia is also exceptionally inert in the physiological environment,[23,24] and zirconia ceramics have an advantage over alumina ceramics of higher fracture toughness and higher flexural strength and lower Young's modulus.[25]

Zirconia ceramics suggested for surgical implants fall into two basic types: tetragonal zirconia stabilized with yttria (TZP) and magnesium oxide partially stabilized zirconia (Mg-PCZ). Properties of zirconia are compared with alumina ceramic implant materials in Table 2.4.

Zirconia may be suitable for bearing surfaces in total hip prostheses. However, there are three major controversies regarding zirconia. One is the reported strength reduction with time in physiological fluids. The second is its wear properties, and third is the potential radioactivity of the material.

The deleterious martensitic transformation from tetragonal to monoclinic phase in yttria-doped zirconia due to aging in water and the accompanying reduction in toughness is well documented.[26] However, tests in simulated body fluids and in animals have shown only slight decreases in fracture strength and toughness.[27] The observed strength after two years is still much higher than the strength of alumina tested under similar conditions.

Table 2.4. Properties of Alumina Zirconia Ceramics Used in Surgical Implants.

Property	Unit	Al_2O_3	TZP	Mg-PSZ
Purity	%	>99.7	97	96.5
Y_2O_3/MgO	%	<0.3	3 mol	3.4 wt
Density	g/cm_3	3.98	6.05	5.72
Grain size (average)	µm	3.6	0.2–0.4	0.42
Bending strength	Mpa	595	1000	800
Compressive strength	Mpa	4250	2000	1850
Young's modulus	GPA	400	150	208
Hardness	HV	2400	1200	1120
Fracture toughness K_{1c}	$MN/m^{3/2}$	5	7	8

Streicher *et al*. reported on a detailed study of ceramic surfaces as wear partners for UHMWPE.[25] Investigation was carried out on five grades of alumina and zirconia in a pin-on-disc test against UHMWPE for suitability as articulating components for total joint prostheses. The tests showed a difference in surface quality between the various grades of ceramics. The UHMWPE wear rate caused by the ceramic counterfaces was the lowest for alumina and 20% less than in combination with Co-Cr-Mo-alloy. Zirconia ceramics yielded unfavorable wear and friction results.

The reason for the inferior tribological behavior of zirconia ceramics against the non-polar UHMWPE is not understood. Alumina and zirconia ceramics have similar roughness and wetting characteristics. The only major difference in their surface properties is that alumina ceramics are much harder.

Sudanese *et al*. evaluated zirconia wear resistance in a ceramic–ceramic coupling (ring on disc) test.[28] The wear rate of zirconia–zirconia couplings was 5,000 times that of alumina–alumina couplings. Zirconia ceramics should not be used for ceramic–ceramic articulating surfaces.

Zirconia is often accompanied by radioactive elements with a very long half-life, such as thorium and uranium. These elements are difficult and expensive to separate from zirconia. There are two types of radiation of concern in zirconia ceramics: gamma and alpha. The gamma radioactivity of alumina, zirconia and Co-Cr-alloy femoral head prostheses has been measured.[29] Alumina was found to have the lowest gamma radioactivity and zirconia and the Co-Cr-alloy were found to be approximately the same. The gamma radioactivity for the Co-Cr-alloy and

zirconia were found to be of the same order of magnitude as the national ambient radioactivity in France.[29]

The data suggest that the level of gamma radiation in commercially available zirconia bioceramics is not a major concern. However, significant amounts of alpha radiation have been observed with zirconia ceramics intended for surgical implants.[30]

Alpha particles, because of their high ionization capacity, destroy soft and hard tissue cells. The alpha emission observed from zirconia ceramic femoral head prostheses is a concern. Although the activity is small, questions concerning the long-term effects of alpha radiation emission from zirconia ceramics must be answered.

2.6. SUMMARY

Alumina and zirconia ceramics are both exceptionally biocompatible, due to their chemical stability in the physiological environment. Zirconia ceramics have a higher fracture strength, toughness and lower modulus of elasticity than alumina ceramics. The phenomena of slow crack growth, static and cyclic fracture, low toughness, stress corrosion, deterioration of toughness with time, and sensitivity to tensile stresses are all serious concerns for both ceramics in high load bearing applications. Both alumina and zirconia ceramics undergo slight reduction in fracture strength with time in the physiological environment. Alumina and zirconia bioceramics should be restricted to designs involving compressive loading or limited tensile loads.

The elastic modulus of nearly inert bioceramics is also a limitation on their use in the body. The Young's modulus (in GPa) of cancellous bone has a range from 0.05–0.5 depending on location and age; cortical bone ranges from 7–25. In contrast, medical grade alumina (> 99.7% Al2O3) has a Young's modulus of 380–420 GPa and partially stabilized zirconia has a value of 150–208 GPa. Thus, there is a modulus mismatch between cortical bone and an alumina implant in the range of 15–55X. The mismatch with cancellous bone is enormous, 760X–7600X.[3]

A consequence of a mismatch in elastic modulus is that a bioceramic implant will shield a bone from mechanical loading, allowing nearly all the mechanical load to be carried by the implant. Living bone must be under a certain amount of tensile load in order to remain healthy; if it is unloaded or is loaded in compression it will undergo biological changes which lead to resorption, weakening of the bone, and deterioration of the implant–bone interface.[3] The high modulus of elasticity of alumina and zirconia limit their effectiveness as load

bearing bone interface materials. Metal alloys suffer the same limitation. The high modulus of elasticity of alumina does not limit its ability to serve as an articulating surface.

Alumina is an excellent material for certain orthopedic applications, such as the ball in an artificial hip joint, because of its excellent biocompatability, low friction, high wear resistance, and high compressive strength. The tribological properties of alumina ceramics are far superior to zirconia ceramics. Alumina or alumina-articulating surfaces in total joint replacements have the best tribological properties (Table 2.5) and, even more important, the best clinical results.

2.7. LONG-TERM CLINICAL RESULTS

Over the last twenty years, the use of alumina in hip prosthesis has been well documented.[31] Clinical studies of the survivability of alumina implants has produced promising results.[31–34] Further studies investigated young patient populations[32] and the rate of wear of alumina versus other materials.[33] The longevity and means of failure have also been analyzed for many ceramic implants and much has been done to minimize the fracture rate of alumina implants in total hip arthroplasty (THA).[31–37] Squeaking and other small issues have also been documented and are some of the minor phenomena associated with use of ceramic implants.[38]

In 2010, Petsatodis *et al*. reported data on a 20-year clinical trial consisting of 100 patients who had in total 109 cementless alumina ceramic on ceramic primary THA.[31] The mean age of patients at the beginning of the study was 46 years old and 78 individuals of the initial patient population were available for the last follow-up at 20.8 years. The study was performed to measure the survivability of the implants in the individuals. The results of the study, measured with the Charnley modification of the Merle d'Aubigné-Postel scale,[31] were exceptional at the time of the last follow-up. Of the 78 individuals in the final

Table 2.5. Ranking of Articulating Surfaces for Total Joint Systems.

Superior	Al_2O_3 on Al_2O_3
Excellent	Al_2O_3 on UHMWPE
Good	Co-Cr-Mo on UHMWPE Ti-6Al-4V on UHMWPE
Poor	Metal on Metal

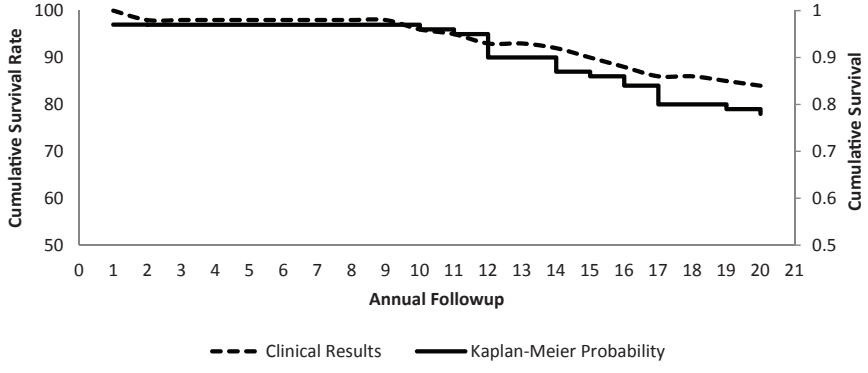

Figure 2.4. Clinical results of alumina in comparison to the calculated probability Kaplan–Meier model. (Based upon Petsatodis *et al*.[31])

follow-up, 68% reported excellent quality, 19% were good, 9% were fair, and 4% were in poor condition. "The cumulative rate of survival of the prostheses was 84.4% at 20.8 years."[31]

The cumulative survival rate from the clinical investigation published by Petsatodis *et al.* was compared with the Kaplan–Meier probability for survival in Fig. 2.4.[31] The results agreed closely with the calculated probability of survival. In another study by Petsatodis *et al*., which consisted of 220 patients with a mean follow-up of 13.7 years, there was a cumulative survival rate of 90.0%.[31] These results are of the same magnitude as the data shown in Fig 2.4.

For young individuals needing THA, the cause for implantation is usually more severe and survivability of implantation tends to be low. The results of a clinical study with alumina THA in individuals less than 30 years of age, published in 2008 by Nizard *et al.*, demonstrated poor results when compared to studies with older individuals.[32] The study investigated 101 patients who underwent THA with different past medical histories. The survivability of the patients was measured and then compared to their disease states. Of the initial 101 patients, 94 patients were available for follow-up. Failing to survive was defined as failure of either the acetabular or femoral components of the implant. At 10 years, 82.1% of implants had survived (72.4%–91.8% at 95% confidence interval), and at 15 years 72.4% of implants had survived (57.2%–87.6% at 95% confidence interval). The mean follow-up was 6.9 ± 4.7 years with a range of 1–26.5 years; there was a minimum follow-up of 1 year.

Analysis of the survival rate showed that some of the failures may be related to the disease state of the individuals prior to the THA and the method of cup and

stem fixation.[32] Comparison of the root disease states of the THA revealed differences in survivability. The rate of THA survivability was 64.9% at 8 years for patients with slipped capital femoral epiphysis, 65.5% at 14 years for patients with posttraumatic arthritis, and 85.7% at 15 years for individuals with osteonecrosis. For individuals in the study with osteonecrosis as a cause of THA, the survivability was of the same magnitude as that seen in older patients in Fig. 2.4.[31,32] The use of cemented stems and cups was the common method of fixation for THA of the patients in this study. The use of cement has been found to be potentially associated with separation of the lining with the acetabular cup; cementless cups and stems are now considered superior in quality for alumina THA. It is suggested that the use of cement in THA in this study was a contributing factor to the low survivability. "Improvements in the design and in the mode of fixation of this component should enhance the long-term results because very limited osteolysis was observed."[32]

Studies involving both young (for newer implant designs) and old patients are demonstrating relatively high survivability for alumina implants in THA.[31–35] Some of the factors involved in the longevity of THA are the wear of the liner that the femoral head rotates in and the strength of the implant to resist fracture. Measurement of wear is important because the release of certain materials into the body may result in undesirable effects and ruin the quality of the implant's functionality. Radiographic images are used to measure the depth of wear. The wear of the liner can then be compared by a multitude of means: the depth of the cup surface that has been worn or eroded; the volume of cup surface that is lost per year; or the cumulative volume of cup surface lost in total.[33]

The wear caused by alumina and other materials was documented in 2003 by Hernigou and Bahrami in a ten-year study with 136 patients.[33] Fifty-six of the patients had alumina femoral heads, 40 had zirconia heads, 20 had stainless-steel 32 mm heads, and 20 had stainless-steel 28 mm heads. All of the patients had polyethylene liners in the acetabular cup. The cumulative volume of wear of the polyethylene liner was compared between the alumina and zirconia and is seen in Fig. 2.5. A significant difference can be seen between the alumina and the zirconia over extended periods of time. The mean rate of wear (measured as linear penetration into a polyethylene liner) at five years was 0.040 mm/year for alumina, 0.072 mm/year for the stainless-steel 32 mm, 0.036 mm/year for the stainless-steel 28 mm, and 0.043 mm/year for the zirconia. At 12 years, the mean rate of wear was 0.071 mm/year for alumina, 0.192 mm/year for stainless-steel 32 mm, 0.134 mm/year for stainless-steel 28 mm, and 0.412 mm/year for zirconia.[33] The significant difference between the polyethylene lining wear rates, particularly of zirconia at 12 years, may be related to the thermal conductivities of the materials, changes in surface roughness over time, and crystal structure.[33]

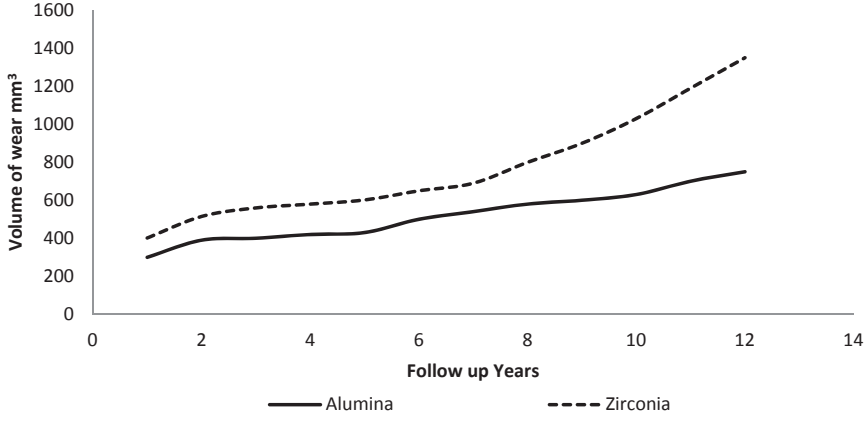

Figure 2.5. Time dependence of mean volume wear of polyethylene lining from alumina and zirconia femoral heads. (Based upon Hernigou *et al*.[67])

The rate of wear was also found to be greater in zirconia than alumina in another study, recorded in 2007 by Liang *et al*.[36] The study consisted of 103 patients with a total of 118 primary cemented THA in which 22 mm alumina or zirconia heads with titanium alloy femoral stems in polyethylene acetabular linings were used. The wear of the lining was measured with a mean follow-up of 5.4 years with a minimum follow-up of five years. The alumina heads had a mean rate of 0.078 ± 0.044 mm/year (range of 0.02–0.27 mm/year) of linear wear into the lining and the zirconia heads had a mean rate of 0.133 ± 0.073 mm/year (range of 0.01–0.40 mm/year) of linear wear into the lining. The study found that:

> [The] results after a minimum follow-up of 5 years showed that both the mean linear and volumetric wear rates were significantly greater in the zirconia group as compared with the alumina group.[36]

Material wear is often a factor in implants, but structural failure is one of the worst possible results for implantation longevity. Structural failure associated with implantation can be related to the structural geometry of the implant, the material of the implant, and other factors.[34,37] The use of poor quality alumina was found to be a cause for many of the previous fractures and failures seen in the past.[37] With newer materials, the percentage of ball fractures has become relatively low. In 1995, The American Hip and Knee Association performed a survey of 5,023 ceramic femoral heads and found that 11 had fractured.[37] In addition, three of the 11 failures were found to have been made

from a poor quality production method. More often, failure in THA is related to the acetabular cup or the femoral component that holds the head. A study submitted to the Food and Drug Administration (FDA) in 1997 described 1,717 failure cases and only 1% of the cases were related to failure of the femoral head. Other failures were from fracture of other components of the implant; 38% being related to the acetabular cup, and 18% were related to the femoral component and/or stem.[37]

Aside from wear and fracture, some minor issues have also been recorded during clinical trials. Certain patients experience squeaking or clicking from the implant during motion. Data from a clinical study published in 2011 by Schroder *et al*. surveyed 362 patients about sounds generated by their implant and 41 claimed they experienced noise that was audible to individuals other than themselves.[38] Patients claiming there was squeaking or that sound was audible did not correlate this with pain, and it did not reduce their quality of life. No relationship was found between implant wear and squeaking.[38]

2.7.1. Zirconia Clinical Results

Recent studies with zirconia have raised concern for many individuals about the quality of zirconia as a material for use in THA.[33,36,37,39] While the strength of zirconia is high, low survivability has led some physicians to abandon the use of zirconia in their practice.[33,39] The wear rates of zirconia have also been measured and compared with other materials and have shown poor wear characteristics.[33] In 1999, Allain *et al*. published a study of zirconia heads on polyethylene cups that included 100 patients, 78 of which were reviewed and 61 were analyzed in detail.[39] The mean follow-up was 5.8 years with a range of one to nine years. At the last follow-up of eight years, survivorship had reduced to 63% of patients. The yearly results in comparison to the Kaplan–Meier probability for this eight year analysis are seen in Fig. 2.6.

Studies on other uses for zirconia have also demonstrated poor results. A publication released in 2001, by Norton *et al*. revealed the results of 29 total hip replacements (THR) of zirconia heads with Hylemar linings in 26 patients.[40] At five years, the survival rate had dropped to below 40%. All patients in the study were below the age of 60, with a mean age of 49.2 years old. Much of the failure is thought to be related to the poor wear characteristics of Hylemar linings in combination with the wear characteristics associated with zirconia femoral heads. Norton *et al*. concluded "We feel that it is likely that all of those patients will require revision surgery within ten years."[40] This data suggests that Hylemar is a poor choice for use as a liner material when compared with polyethylene liners and zirconia femoral heads.

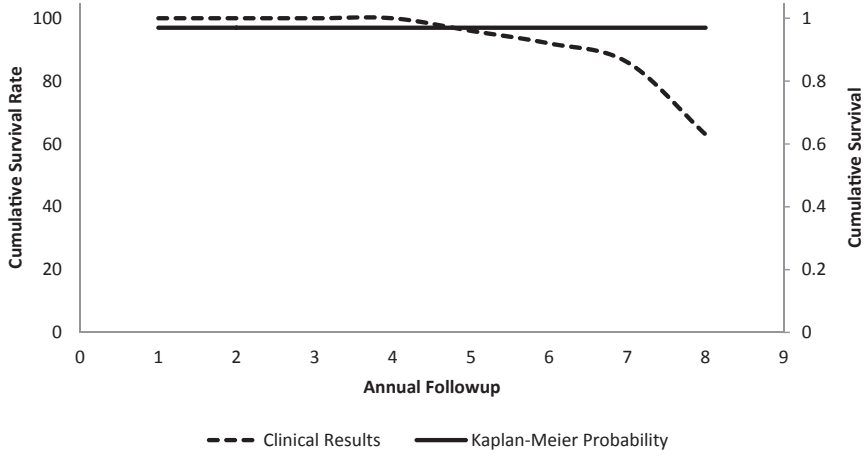

Figure 2.6. Mean volume wear of polyethylene lining from alumina, zirconia and stainless steel femoral heads. (Based upon Hernigou *et al*.[33])

2.8. OTHER MATERIALS AND MANUFACTURERS

Other materials aside from alumina and zirconia have also been used for THA, total knee replacement (TKR), THR, and other implantation procedures. Silicon nitride and surface coatings of diamond-like carbon are some newer materials that are starting to be tested.[37] Stainless steel and cobalt chrome alloy (CoCr) have commonly been used as implant metals for many past applications.[37] Ceramic composites have also been explored for use in certain implantation procedures. Zirconia toughened alumina (ZTA) and magnesium oxide partially stabilized zirconia (Mg-PSZ) are available for clinical investigation and yttria-stabilized tetragonal zirconia (Y-TZP) has been withdrawn from clinical trials.[37]

Breakdown of materials at the metal–ceramic interface has been shown to cause inflammation at the implantation site and in some cases has resulted in implant loosening.[37] Much data have been found to support the use of ceramics as an implant material. Metals have significantly less brittleness and thus are more resistant to fracture, but the wear and survivability of ceramics has been found to be more favorable in some clinical trials.[36] The use of different liners for the acetabular components of THA and THR is also critical in the resulting wear characteristics. Hylemar liners have shown poor wear results in studies;[40] alumina liners on alumina heads have shown excellent results (<5 ìm/year); carbon fiber UHMWPE has also shown great results with alumina heads (<4 ìm/year); normal UHMWPE has shown much higher wear rates: <100 ìm/year on Y-TZP and

Table 2.6. Manufacturers and Producers of Bioceramics and Other Materials.

Materials	Manufacturers of Parts or Entire Prosthesis
Alumina	Feldmühle Aktiengesellschaft, Kobe Steel Co Ltd , Metoxit, CeramTec, Kyocera, Ceraver and Morgan Matroc
Zirconia (Y-ZTP)	Kobe Steel Co Ltd, Desmarquest, Kyocera, Metoxit and Morgan Matroc
Zirconia (Mg-PSZ)	Xylon, Signal, Biopro
Silicon Nitride	Amedica
Cobalt Chrome	ThyssenKrupp
Surface Modifications and Coatings	
Diamond Like Carbon	Diamicron
Oxidized Zirconium	Smith and Nephew

alumina, and 200 ìm/year on CoCr; and Y-TZP heads on Y-TZP liners have shown detrimental results.[37]

A variety of different manufacturers are available for the production of implant materials. A table of different manufacturers for many of the materials in this chapter is seen in Table 2.6.

2.9. CONCLUSIONS

The use of ceramics as implants has increased over the last few decades. Alumina implants have shown excellent wear characteristics and survivability. Implants made of zirconia have demonstrated results that are less favorable and some clinics have reduced the use of zirconia-containing prostheses. For many procedures, alumina ceramic balls and UHMWPE liners and alumina ceramic on ceramic implants have shown the best results. While newer materials are still being tested, the current alumina bioceramics show sufficiently high survivability that it is difficult to demonstrate statistically significant improvements for new designs or materials since data out to 20 years is required. More data with longer-term studies is necessary for younger patient populations as this is still a significant problem. Additionally, further studies must also be performed to evaluate the importance of implant material with the disease state necessitating the implant.

REFERENCES

1. Hulbert, S.F., Bokros, J.C., Hench, L.L. *et al.* (1986). Ceramics in Clinical Applications, Past, Present and Future, *Proc. World Congress High Tech Ceramics Milan*, pp. 189–213.
2. Hench, L.L. (1991). Bioceramics: From Concept to Clinic, *J. Am. Ceram. Soc.*, **74**, 1487–1510.
3. Hench, L.L. (1998). Bioceramics, *J. Am. Ceram. Soc.*, **81**, 1705–1728.
4. Dorre, E. and Dawihl, W. (1980). "Ceramic Hip Endoprostheses", in Hastings, G.W. and Williams, D.F. (eds), *Mechanical Properties of Biomaterials*, J. Wiley and Sons, Inc., New York, pp. 113–127.
5. Boutin, P. (1981). T.H.R. Using Alumina-Alumina Sliding and a Metallic Stem: 1330 Cases and an 11-Year Follow-up, *Proc. Jap. Soc. Orthop. Ceram. Impl*, **1**, 11.
6. Doriot, J.M., Christel, P. and Meunier, A. (1988). Alumina Hip Prostheses: Long Term Behaviors, *Proc. 1st Int. Symp. Ceram. Med.,* pp. 236–301.
7. Winter, M., Griss, P., Scheller, G. *et al.* (1989). 10–14 Year Results of a Ceramic–Metal-Composite Hip Prostheses with a Cementless Socket, *Proc. 2nd Int. Symp. Ceram. Med.*, pp. 436–444.
8. Witvoet, J., Christel, P., Sedel, L. *et al.* (1988). Survivorship Analyses of Cemented Al_2O_3 Sockets, *Proc 1st Int. Symp. Ceram. Med.*, pp. 314–319.
9. Sedel, L., Meunier, A., Nizard, R.S. *et al.* (1991). "Ten Year Survivorship of Cemented Ceramic-Ceramic Total Hip Replacement", in Bonfield, W., Hastings, G.W. and Tanner, K.E. (eds), *Bioceramics, Vol. 4*, Butterworth-Heinemann Ltd, London, pp. 27–37.
10. Sedel, L., Christel, P., Meunier, A. *et al.* (1988). Alumina/Bone Interface — Experimental and Clinical Data, *Proc. 1st Int. Symp. Ceram. Med.*, pp. 262–271.
11. Ritter, Jr., J.E., Greenspan, D.C., Palmer, R.A. *et al.* (1979). Use of Fracture Mechanics Theory in Lifetime Predictions for Alumina and Bioglass coated Alumina, *J. Biomed. Mater. Res.*, **13**, 251–263.
12. Dorre, E., Dawihl, W., Krohn, V. *et al.* (1983). "Do Ceramic Components of Hip Joints Maintain their Strength in Human Bodies?", in Vinenzini, P. (ed.), *Ceramics in Surgery*, Elsevier, Amsterdam, pp. 61–72.
13. Real, M.W., Cooper, D.R., Morrell, R. *et al.* (1986). Mechanical Assessment of Biograde Alumina, *Journal de Physique, Colloque C1*, **47**, C11763–C11767.

14. Dorre, E. (1991). "Problems Concerning the Industrial Production of Alumina Ceramic Components for Hip Joint Prosthesis", in Ravaglioli, A. and Krajewski, A. (eds), *Bioceramics and the Human Body*, Elsevier, London and New York, pp. 454–460.
15. Dorlot, J.M., Christel, P., Sedel, L. *et al.* (1986). "Examination of Retrieved Hip-Prostheses: Wear of Alumina–Alumina Components", in Christel, P., Meunier, A. and Lee, A.J.C. (eds), *Biological and Biomechanical Performances of Biomaterials*, Elsevier, Amsterdam, pp. 495–500.
16. Oonishi, H., Igaki, H. and Takayama, Y. (1988). Comparison of Wear of UHMW Polyethylene Sliding Against Metal and Alumina in Total Hip Prostheses, *Proc. 1st Int. Symp. Ceram. Med.*, pp. 272–277.
17. Ohashi, T., Inoue, S., Kajikawa, K. *et al.* (1988). The Clinical Wear Rate of Acetabular Component Accompanied with Alumina Ceramic Head, *Proc. 1st Int. Symp. Ceram. Med.*, pp. 278–283.
18. Okumura, H., Yamamuro, T., Kumar, T. *et al.* (1988). Socket Wear in Total Hip Prosthesis with Alumina Ceramic Head, *Proc. 1st Int. Symp. Ceram. Med.*, pp. 284–289.
19. Asada, K., Yutani, Y., Sakamoto, H. *et al.* (1991). "Histological Study of Acetabular Clear Zone after Acetabular Reaming for Hip Arthroplasty using an Alumina Ceramic Endoprosthesis and a Metal One", in Bonfield, W., Hastings, G.W. and Tanner, K.E. (eds), *Bioceramics, Vol. 4*, Butterworth-Heinemann Ltd, pp. 47–54.
20. Oonishi, H., Okabe, N., Hamagchi, T. *et al.* (1982). Cementless Alumina Ceramic Total Knee Prosthesis, *Orthop. Ceram. Implan.*, **1**, 157–160.
21. Inoue, H., Yokoyama, Y., and Tanabe, G. (1988). Follow-Up Study of Alumina Ceramic Knee (KC-1 Type) Replacement, *Proc. 1st Int. Symp. Ceram. Med.*, pp. 301–307.
22. Ukon, Y., Oonishi, H., Murata, N. *et al.* (1986). Clinical Experience of KOM Type Cementless Alumina Ceramic Artificial Ankle Joint, *Orthop. Ceram. Implan.*, **6**, 125–129.
23. Garvie, R.C., Urban, D., Kennedy, D.R. *et al.* (1984). Biocompatibility of Magnesium Partially Stabilized Zirconia (Mg-PSZ Ceramics), *J. Mat. Sci.*, **19**, 3224.
24. Tateishi, T. and Yunoki, H. (1987). Research and Development of Advanced Biomaterials and Application to the Artificial Hip Joint, *Bull. Mech. Engr. Lab.*, **45**, 1–9.

25. Streicher, R.M., Semlitsch M, and Schon, R. (1991). Ceramic Surfaces as Wear Partners for Polyethylene, *Bioceramics,* **4**, 9–16.
26. Sato, T. and Shimada, M. (1985). Transformation of Yttria-Doped Zirconia Polycrystals by Annealing in Water, *J. Am. Ceram. Soc.*, **68**, 356–359.
27. Christel, P., Meunier, A., Heller, M. *et al.* (1989). Mechanical Properties and Short-Term *In Vivo* Evaluation of Yttrium-Oxide-Partially Stabilized Zirconia, *J. Biomed. Mat. Res.*, **23**, 45–61.
28. Sudanese, A., Toni, A., Cattaneo, G.L. *et al.* (1988). Alumina vs. Zirconium Oxide: A Comparative Wear Test, *Proc. 1st Int. Symp. Ceram. Med.*, pp. 237–240.
29. Cales, B. and Peille, C.N. (1988). Radioactive Properties of Ceramic Hip Joint Heads, *Proc. 1st Int. Symp. Ceram. Med.*, pp. 152–155.
30. Cieur, S., Heindl, R. and Robert, A. (1991). "Radioactivity of a Femoral Head of Zirconia Ceramics", in Jurgenson J.E. and Hulbert, S.F. (eds), *Bioceramics, Vol. 3*, Rose-Hulman Institute of Technology, Terre Haute, IN, pp. 367–371.
31. Petsatodis, G.E., Papadopoulos, P.P., Papavasiliou, K.A. *et al.* (2010). Primary Cementless Total Hip Arthroplasty with an Alumina Ceramic-on-Ceramic Bearing, *J. Bone Joint Surg. Br.*, **3**, 639–644.
32. Nizard, R., Pourreyron, D., Raould, A. *et al.* (2008). Alumina-on-Alumina Hip Arthroplasty in Patients Younger Than 30 Years Old, *J. Bone Joint Surg. Am.*, **466**, 317–323.
33. Hernigou, P. and Bahrami, T. (2003). Zirconia and Alumina Ceramics in Comparison with Stainless-Steel Heads, *J. Bone Joint Surg. Br.*, **85-B**, 504–509.
34. Koo, K., Ha, Y., Jung, W.H. *et al.* (2008). Isolated Fracture of the Ceramic Head After Third-Generation Alumina-on-Alumina Total Hip Arthroplasty, *J. Bone Joint Surg. Br.*, **90-A**, 329–336.
35. Kress, A.M., Schmidt, R., Holzwarth, U. *et al.* (2011). Excellent Results with Cementless Total Hip Arthroplasty and Alumina-on-Alumina Pairing: Minimum Ten-Year Follow-Up, *Int. Orthop. (SICOT)*, **35**, 195–200.
36. Liang, B., Kawanabe, K., Ise, K. *et al.* (2007). Polyethylene Wear Against Alumina and Zirconia Heads in Cemented Total Hip Arthroplasty, *J. Arthroplasty*, **22**, 251–257.
37. Rahaman, M.N., Yao, A., Bal, B.S. *et al.* (2007). Ceramics for Prosthetic Hip and Knee Joint Replacement, *J. Am. Ceram. Soc.*, **90**, 1965–1988.

38. Schroder, D., Bornstein, L., Bostrom, M.P.G. *et al.* (2011). Ceramic-on-Ceramic Total Hip Arthroplasty Incidence of Instability and Noise, *J. Bone Joint Surg. Am.*, **469**, 432–437.
39. Allain, J., Le Mouel, S., Goutallier, D. *et al.* (1999). Poor Eight-Year Survival of Cemented Zirconia-Polyethylene Total Hip Replacements, *J. Bone Joint Surg. Br.*, **81-B**, 835–842.
40. Norton, M.R., Yarlagadda, R. and Anderson, G.H. (2002). Catastrophic Failure of the Elite Plus Total Hip Replacement, with a Hylamer Acetabulum and Zirconia Ceramic Femoral Head, *J. Bone Joint Surg. Br.*, **84-B**, 631–635.

Chapter 3

BIOACTIVE GLASSES

Larry L. Hench and Orjan Andersson

3.1. INTRODUCTION

It was discovered by Hench and colleagues in 1969 that bone can bond chemically to certain glass compositions.[1] This group of glasses has become known as bioactive glasses, based upon the following definition: "*A bioactive material is one that elicits a specific biological response at the interface of the material which results in the formation of a bond between the tissues and the material.*"[2–5] Bioactive glasses have numerous applications in the repair and reconstruction of diseased and damaged tissue, especially hard tissue (bone). Clinical applications are discussed in reviews[3–5] and Chapters 6–12 and 30–34. One aspect that makes bioactive glasses different from other bioactive ceramics and glass-ceramics is the possibility of controlling a range of chemical properties and rate of bonding to tissues. The most reactive glass compositions develop a stable, bonded interface with soft tissues, as shown by Wilson.[6,7] It is possible to design glasses with properties specific to a particular clinical application. This is also possible with some glass-ceramics, but their heterogeneous microstructure restricts their versatility.

3.2. PROCESSING

Bioactive glasses are produced by conventional glass manufacturing methods (Chapter 1). Contamination of the glass must be avoided in order to retain the chemical reactivity of the material. Purity of raw materials must be assured. Analytical grade compounds are typically used for most components. Silica can be added in the form of high purity (flint quality) glass sand, since chemically prepared silicas are difficult to handle without adsorption of water and agglomeration. The choice of raw materials can affect the properties of the glass. Andersson has shown that the use of calcium phosphate compounds that contain crystal water result in glasses that crystallize more easily than if crystal water-free compounds are used.[8] This effect is due to the dissolution of OH ions in the glass structure and the associated decrease of viscosity. See Chapter 22 for a discussion

of the effects of viscosity on glass formation and crystallization. Preferential vaporization of fluxes will also affect glass viscosity and tendency to crystallize or phase separate, as well as alter the final glass composition.

Weighing, mixing, melting, homogenizing and forming of the glass must be done without introducing impurities or losing volatile constituents, such as Na_2O or P_2O_5. Melting is usually done in the range of 1300–1450 °C, depending on composition. The phase equilibrium diagram for the Na_2O-CaO-SiO_2 system shows a ternary eutectic very near the 45S5 glass composition (Table 3.1), which was the original basis for selecting this composition for investigation. There is a very steep liquidus as the composition increases in SiO_2 content, which greatly affects the melting and homogenization behavior of the glass. Only platinum or platinum alloy crucibles or glass melter should be used to avoid contamination of the melt.

Bulk specimens can be formed by casting or injection molding in graphite or steel molds. Annealing is crucial, 450–550 °C, because of the high coefficient of thermal expansion of the bioactive glass compositions. Each type of device must have its own annealing schedule established. Bioactive glasses are soft glasses and final shapes can be easily made by machining. Standard machine tools or dental handpieces can be used. Diamond-cutting tools are preferred with copious irrigation, although dry grinding is also possible. If a granulated or powdered material is required, the melt can be rapidly quenched in water or air before grinding and sieving into the desired particle sizes. The glass frit (see Chapter 37) should be rapidly dried to avoid corrosion while in contact with water. Other processing methods used for bioactive glass coatings are described in Chapter 22. Composites made with bioactive glasses are discussed in Chapter 25.

3.3. COMPOSITIONS

The base components in most bioactive glasses are SiO_2, Na_2O, CaO, and P_2O_5 (Table 3.1). The first, and most well-studied composition, termed Bioglass® 45S5 (Registered trademark University of Florida, Gainesville, FL), contains 45% SiO_2, 24.5% Na_2O, 24.4% CaO and 6% P_2O_5, all in weight percent.[1] The 45S5 composition in mole percent is given in Table 3.1, along with many other compositions investigated for surface reaction kinetics. Hench and coworkers have studied a series of glasses in this four-component system with a constant six weight percent P_2O_5 content. This work is summarized in the ternary SiO_2-Na_2O-CaO diagram shown in Fig. 3.1. The figure establishes the bioactive-bonding-boundary

Table 3.1. Glass Compositions by Mole %.

Designation	SiO_2	Na_2O	CaO	CaF_2	P_2O_5	B_2O_3	Al_2O_3
45S5.4F	46.1	24.4	16.2	10.8	2.6	0	0
45S5	46.1	24.4	26.9	0	2.6	0	0
#1(S63.5P6)	65.7	15.0	15.5	0	2.6	0.4	0.6
#9(S53P4)	53.9	22.6	21.8	0	1.7	0	0
#10(S45P7)	46.6	24.1	24.4	0	3.0	1.8	0
52S4.6	52.1	21.5	23.8	0	2.6	-	-
55S4.3	55.1	20.1	22.2	0	2.6	-	-
60S3.8	60.1	17.7	19.6	0	2.6	-	-
42SF	42.1	26.3	17.4	11.60	2.6	-	-
46SF	46.1	24.4	16.14	10.76	2.6	-	-
49SF	49.1	23.0	15.18	10.12	2.6	-	-
52SF	52.1	21.5	14.28	9.52	2.6	-	-
55SF	55.1	20.1	13.32	8.88	2.6	-	-
60SF	60.1	17.7	11.76	7.84	2.6	-	-
49S(gg)	50.	0	46.	0	4.	-	-
54S(gg)	55.	0	41.	0	4.	-	-
58S(gg)	60.	0	36.	0	4.	-	-
63S(gg)	65.	0	31.	0	4.	-	-
68S(gg)	70.	0	26.	0	4.	-	-
72S(gg)	75.	0	21.	0	4.	-	-
77S(gg)	80.	0	16.	0	4.	-	-
86S(gg)	90.	0	6.	0	4.	-	-

(gg) = gel-glass[9]

of compositions.[2–5] In region A the glasses are bioactive and bond to bone. In the middle of this area a smaller region is indicated (broken line), within which soft tissue bonding also occurs. Glasses in region B behave as nearly-inert materials and are encapsulated by non-adherent fibrous tissue when implanted. Compositions in

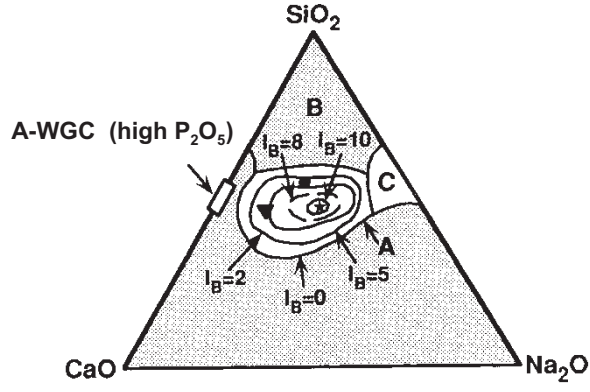

Figure 3.1. Compositional dependence (in weight percent) of bone bonding and soft-tissue bonding of bioactive glasses and glass-ceramics. All compositions in region A have a constant 6 weight percent of P_2O_5, A/W glass-ceramic has higher P_2O_5 content. Region E (soft-tissue bonding) is inside the dashed line, where $I_B > 8$. ((*) 45S5 Bioglass®, (▲) Ceravital®, (•) 55S4.3 Bioglass®, and (---) soft-tissue bonding; $I_B=100/t_{0.5bb}$.) (Reprinted from Hench, L.L. (1991). Bioceramics: From Concept to Clinic, *J. Amer. Ceram. Soc.*, **74**, pp. 1487–1570, with permission.)

region C are resorbed within 10 to 30 days in tissue. In region D the compositions are not technically practical and have not been implanted. The boundary between region A and C depends upon the ratio of surface area of the glass to the effective solution volume of the tissue, as well as the glass composition. Fine glass powders resorb more quickly than bulk implants.

Partial substitution of CaO by CaF_2 does not significantly alter the bone-bonding behavior. The fluoride additions, however, reduce the rate of dissolution and affect the location of the A–C boundary in Fig. 3.1. Substitutions of MgO for CaO or K_2O for Na_2O also have little effect on bone bonding. B_2O_3 and Al_2O_3 have also been used in bioactive glasses to modify processing schedules and rates of surface reaction.

Alumina is especially important in controlling glass surface durability and melting and forming characteristics. However, it is well established that Al_2O_3, in contrast to B_2O_3, can inhibit bone bonding. The amount of alumina that is tolerated depends on glass composition, but is generally in the order of 1.0–1.5 weight percent. More alumina can be added to a glass with a high reactivity (high bioactivity) than to a glass which reacts more slowly. The dimensions of the bone-bonding boundary (region A in Fig. 3.1) shrink as the percent of Al_2O_3 increases. Gross and coworkers have shown that the same effect occurs for other multivalent

cations, such as Ta_2O_5. Additions of more than 1.5–3% of multivalent ions usually make the glass inactive.[10]

In a multi-component system like the SiO_2–Na_2O–CaO–P_2O_5–B_2O_3–Al_2O_3 system, it is not possible to find a simple relationship between composition and tissue bonding that can be expressed in a two-dimensional diagram, such as Fig. 3.1. Andersson *et al*. described the *in vivo* behavior of glasses in this complex system with a phenomenological model developed by regression analysis.[8] The method predicts the *in vivo* behavior of glasses within certain compositional ranges. The prediction is based upon empirically-determined factors and makes it possible to select glasses for specific applications without having to test them in animals. This method of compositional optimization is described in Chapter 22. It works because glass is an amorphous material and most properties are additive, within certain compositional limits.

The role of phosphate in bioactive glasses is interesting. Early on it was assumed that P_2O_5 was required for a glass to be bioactive. However, it is now known that phosphate-free glasses, as well as glass-ceramics in which the phosphate is bound in a siable, relatively insoluble apatite phase, are bioactive. Kokubo and coworkers have shown that the minimal melt-derived glass compositional system for bioactivity is CaO–SiO_2, with a compositional limit of about 60 mole percent (Chapter 13). Li *et al*. have shown that gel-derived glasses in the Na_2O–CaO–SiO_2 are bioactive even up to 85 mole percent SiO_2 (Table 3.1).[9] This very broad range of bioactive compositions makes it possible to tailor the reactivity of the glasses for various applications, as discussed in Chapter 32. The role of phosphate in the glass appears only to aid in the nucleation of the calcium phosphate phase on the surface but is not a critical constituent because the surface will adsorb both calcium and phosphate ions from solution.

3.4. PROPERTIES

The primary advantage of bioactive glasses is their rapid rate of surface reaction, which leads to fast tissue bonding. Their primary disadvantage is mechanical weakness and low fracture toughness due to an amorphous two-dimensional glass network. The tensile bending strength of most of the compositions in Table 3.1 is in the range of 40–60 MPa, which make them unsuitable for load-bearing applications. Mechanical properties of bone are discussed in Chapter 1. For some applications low strength is offset by the glasses' low modulus of elasticity of 30–35 GPa. The importance of this value, which is close to that of cortical bone, is discussed in Chapter 1. The low strength does not influence

the utility of bioactive glasses as a coating, where interfacial strength between metal and the coating is the limiting factor. Low strength also has no effect on use of bioactive glasses as buried implants, in low-loaded or compressively loaded devices, in the form of powders or as the bioactive phase in composites. A new generation of highly bioactive glass-ceramics that also have high strength is described in Chapter 34.

3.5. REACTION KINETICS

The basis of the bone-bonding property of bioactive glasses is the chemical reactivity of the glass in body fluids. The surface chemical reactions result in the formation of a hydroxycarbonate apatite (HCA) layer to which bone can bond. Bonding occurs due to a sequence of reactions. See Hench *et al.*[5] for a detailed summary and extensive list of references. On immersion of a bioactive glass in an aqueous solution, three general processes occur: leaching, dissolution and precipitation. Leaching is characterized by release, usually by cation exchange with H^+ or H_3O^+ ions, of alkali or alkaline earth elements. Ion exchange is easy because these cations are not part of the glass network; they only modify the network by forming non-bridging oxygen bonds (Chapter 1). The release of network-modifying ions is rapid for glasses in the bioactive compositional region (Region A in Fig. 3.1). This ion exchange process leads to an increase in interfacial pH, to values >7.4.

Network dissolution occurs concurrently, by the breaking of –S–O–Si–O–Si– bonds through the action of hydroxyl (OH) ions. Breakdown of the network occurs locally and releases silica into solution in the form of silicic acid [$Si(OH)_4$]. The rate of dissolution of silica depends very much on glass composition. The dissolution rate decreases greatly for compositions of >60% SiO_2 because of the larger number of bridging oxygen bonds in the glass structure. The hydrated silica (SiOH) formed on the glass surface by these reactions undergoes rearrangement by polycondensation of neighboring silanols, resulting in a silica-rich gel layer.

In the precipitation reaction, calcium and phosphate ions released from the glass, together with those from the solution, form a calcia-phosphate-rich (CaP) layer on the surface. When formed *in vitro*, the CaP layer is mainly located on top of the silica gel, whereas *in vivo* it is formed within the gel layer. The calcium phosphate phase that accumulates in the gel surface is initially amorphous (a-CaP). It later crystallizes to an HCA structure by incorporating carbonate anions from solution within the a-CaP phase. The mechanism of nucleation and

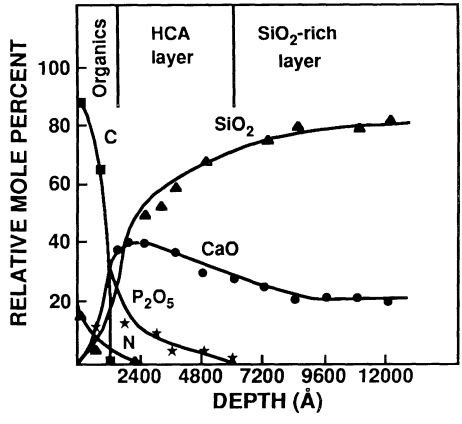

Figure 3.2. Bilayer films formed on 45S5 Bioglass® after 1 h in rat bone, *in vivo* (1 Å = 10^{-1} mm). (Reprinted from Hench, L.L. (1991). Bioceramics: From Concept to Clinic, *J. Amer. Ceram. Soc.*, **74**, 1487–1570, with permission.)

growth of the HCA layer appears to be the same *in vitro* and *in vivo*, and is accelerated by the presence of hydrated silica.

Figure 3.2 shows the CaP and silica-rich layers formed on a 45S5 bioactive glass within one hour of implantation in a rat bone. The implant was removed as the bonding sequence was beginning. The data were obtained using Auger electron spectroscopy (AES) combined with Ar ion milling. The analysis is of 50 Å "slices" of material, which combined together yields a compositional profile of the reaction interface. The silica-rich layer has formed to a thickness of more than 12,000 Å (>1 μm). The CaP layer is already 0.8 μm thick after one hour of reaction. Biological molecules are bonded within the bilayer to a depth of 0.1 μm, as indicated by the C and N signals in the outer layer of the surface. It is important to note that the mixed organic–inorganic bonding occurs within a region that has Si as well as Ca and P present.

Thus, the reactions on the implant side of the interface with a bioactive glass are:

Stage 1: Leaching and formation of silanols (SiOH)
Stage 2: Loss of soluble silica and formation of silanols
Stage 3: Polycondensation of silanols to form a hydrated silica gel
Stage 4: Formation of an amorphous calcium phosphate layer
Stage 5: Crystallization of a hydroxycarbonate apatite layer.

Table 3.2. Reaction Stages of a Bioactive Implant.

STAGE	
1	Rapid exchange of Na^+ or K^+ with H^+ or H_3O^+ from solution: $Si - O - Na^+ + H^+ + OH^- \rightarrow Si\text{-}OH^+ + Na^+ (solution) + OH^-$ This stage is usually controlled by diffusion and exhibits a $t^{-1/2}$ dependence.
2	Loss of soluble silica in the form of $Si(OH)_4$ to the solution, resulting from breaking of Si–O–Si bonds and formation of Si–OH (silanols) at the glass solution interface: $Si - O - Si + H_2O \rightarrow Si - OH + OH - Si$ This stage is usually controlled by interfacial reaction and exhibits a $t^{1.0}$ dependence.
3	Condensation and repolymerization of a SiO_2-rich layer on the surface depleted in alkalis and alkaline-earth cations: 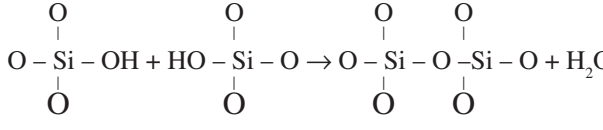
4	Migration of Ca^{2+} and PO_4^{3-} groups to the surface through the SiO_2-rich layer forming a $CaO–P_2O_5$–rich film on top of the SiO_2-rich layer, followed by growth of the amorphous $CaO–P_2O_5$-rich film by incorporation of soluble calcium and phosphates from solution.
5	Crystallization of the amorphous $CaO–P_2O_5$ film by incorporation of OH^-, CO_3^{2-}, or F^- anions from solution to form a mixed hydroxyl, carbonate, fluorapatite layer.

Table 3.2 summarizes these five reaction stages in more detail.[4,5] See the reference list for details of the experiments used to generate this reaction sequence.

For a bond with tissue to occur a layer of biologically active HCA must form. This appears to be the only common characteristic of all the known bioactive implants. The rate of tissue bonding appears to depend on the rate of HCA formation.

The kinetics of the reaction stages depend on the glass composition. Fourier transform infrared reflection (FTIR) spectroscopy can be used to determine the reaction rates and mechanism of all five stages of reaction. Figure 3.3 shows the FTIR spectra (using a diffuse reflection stage) of a 45S5 Bioglass® implant after 0, 1 and 2 hours in tris-buffer solution at 37 °C. The spectra are equivalent to those obtained using a simulated body fluid (see Chapter 37). The peak identifications are based upon previous assignments of IR spectra

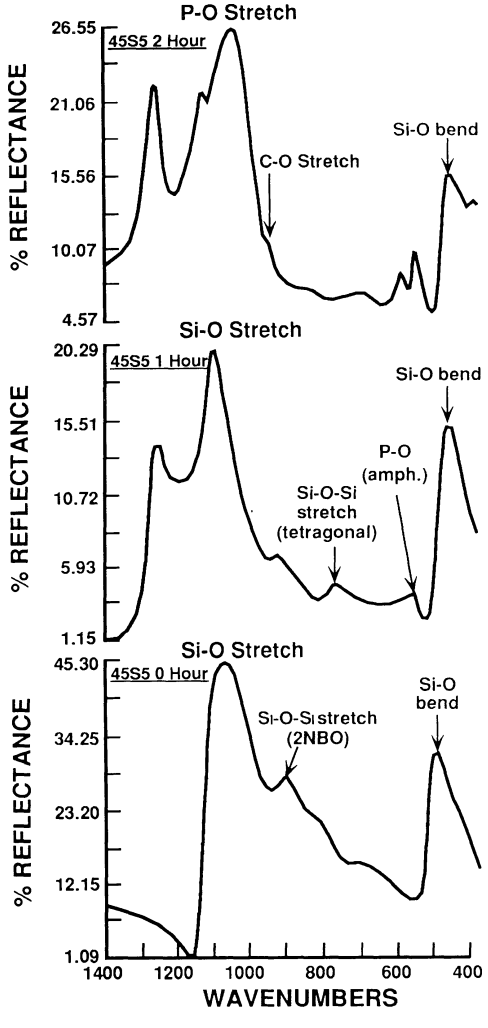

Figure 3.3. FTIR spectra of a 45S5 Bioglass® implant after 0, 1, and 2 h in TBS at 37 °C. (Reprinted from Hench, L.L. (1991). Bioceramics: From Concept to Clinic, *J. Amer. Ceram. Soc.*, **74**, 1487–1570, with permission.)

(see Chapter 17). The alkali-ion-hydronium ion exchange and network dissolution (Stages 1 and 2 in Table 3.2) rapidly reduces the intensity of the Si–O–Na and Si–O–Ca vibrational modes and replaces them with Si–OH bonds that have only one nonbridging oxygen (NBO) ion. Alkali content is depleted to a depth >0.5 μm

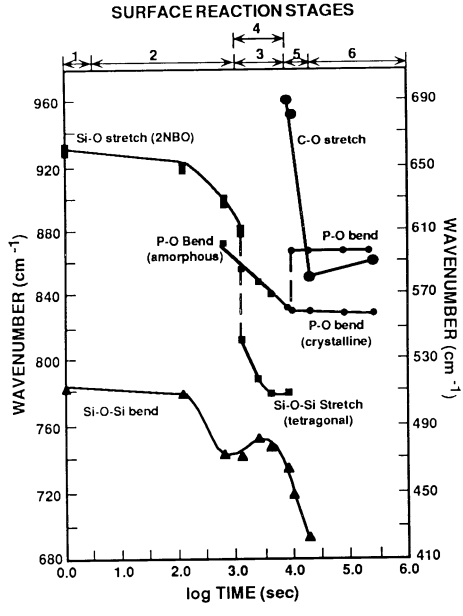

Figure 3.4. Time-dependent changes in IR vibrations of the surface of 45S5 Bioglass® implant in a 37°C TBS. (Reprinted from Hench, L.L. (1991). Bioceramics: From Concept to Clinic, *J. Amer. Ceram. Soc.*, **74**, 1487–1570, with permission.)

within a few minutes. Auger electron spectroscopy (AES) showed that by 2 minutes, alkali ion depletion occurred to depths >0.1 μm.[4,5]

As the Stage 1 and 2 reactions continue, the single Si–OH NBO modes are replaced by

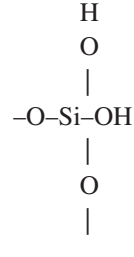

i.e., Si–2NBO stretching vibrations which are in the range of 930 cm^{-1}, decreasing to 880 cm^{-1}. By 20 minutes, the Si–2NBO vibrations are largely replaced by a new mode assigned to the Si–O–Si bond vibration between two adjacent SiO_4 tetrahedra (Fig. 3.4).

This new vibrational mode corresponds to the formation of the silica-gel layer by the Stage 3 (Table 3.2) polycondensation reaction between neighboring surface silanols. This mode decreases in frequency until it is hidden after one hour by the growing CaP-layer.

As early as ten minutes, a P–O bending vibration associated with formation of an amorphous CaP layer appears. This is due to precipitation from solution (Stage 4 in Table 3.2). Clark *et al*. showed (using AES) that by two minutes Ca and P enrichment occurred on the glass surface to a depth of approximately 20 nm. Ogino *et al*. showed (with AES) that by one hour the CaP layer grew to 200 nm in thickness.[11]

Within 40 minutes (Fig. 3.4) the P–O bonding vibration is strong and exhibits a continually decreasing frequency as the CaP-rich layer builds. At about 1.5 ± 0.2 h, the P–O bending vibration associated with the amorphous calcium phosphate layer is replaced by two P–O modes (Fig. 3.3) assigned to crystalline apatite. Concurrent with the onset of apatite crystallization (Stage 5 in Table 3.2) is the appearance of a C–O vibrational mode associated with the incorporation of carbonate anions in the apatite crystal lattice, as discussed by LeGeros and LeGeros in Chapter 17. The crystals are nucleated and grow as HCA, the same phase as biological HCA formed in mineralizing tissues. The reason for the equivalence is the similarity of nucleating mechanisms and physiological growth conditions.

The C–O mode decreases in wave number as the HCA layer grows. By ten hours the HCA layer has grown to 4 μm in thickness, which is sufficient to dominate the FTIR spectra and mask most of the vibrational modes of the silica-gel layer or the bulk-glass substrate. By 100 hours the polycrystalline HCA layer is thick enough to yield X-ray diffraction (XRD) results, as discussed in Chapter 37. The primary 26 and 33 2Θ peaks of HCA are visible with considerable line broadening. By two weeks the FTIR spectra show three P-O vibrational modes and the XRD data are equivalent to biological HCA grown *in vivo.*

Thus, the bioactive glass implant surface provides a substrate that is favorable for the rapid nucleation and growth of biologically-equivalent HCA (Stage 5 in Table 3.2). Differences in the *in vivo* behavior of various glass compositions are due to the differences in the rate of Stage 5, HCA formation. Table 3.3 summarizes a series of investigations of the effects of glass composition and solution composition on the kinetics of reaction Stages 1–5. The sequence of surface reactions is independent of solution composition.[4,5] However, the presence of Ca and P in a simulated body fluid (SBF) solution accelerates to a small extent the repolymerization of silica (Stage 3) and formation of the amorphous calcium-phosphate

Table 3.3. Time for Onset of Reaction Stages 1, 2, 3, 4 and 5 for Bioactive Glasses.

Time (min) in tris buffer															
Composition	**1**	**2**	**10**	**20**	**40**	**60**	**90**	**120**	**150**	**360**	**720**	**1440**	**3600**	**4320**	**12000**
45S5.4F(2)	1+2		3+4					5							
45S5 (old) (2)	1+2				3+4			5							
45S5 (new)	1+2		3+4					5							
Composition #1 (S63.5P6)	NO SPECTRAL CHANGES NOTED														
Composition #9 (S53P4)	1+2						3			4				5	
Composition #10 (2) (S45P7)	1+2			3+4					5						
42SF	1+2		3+4						5						
46SF	1+2		3+4					5							
49SF	1+2		3+4					5							
52SF	1+2		3+4						5						
*55*SF		1+2					3+4						5		
60SF				1+2						3					4
49S(Gel-Glass)			5												
54S(Gel-Glass)			5												
58S(Gel-Glass)			5												
63S(Gel-Glass)					1-5										
68S(Gel-Glass)					1-5										
72S(Gel-Glass)					1-5										
77S(Gel-Glass)												5			
86S(Gel-Glass)															5

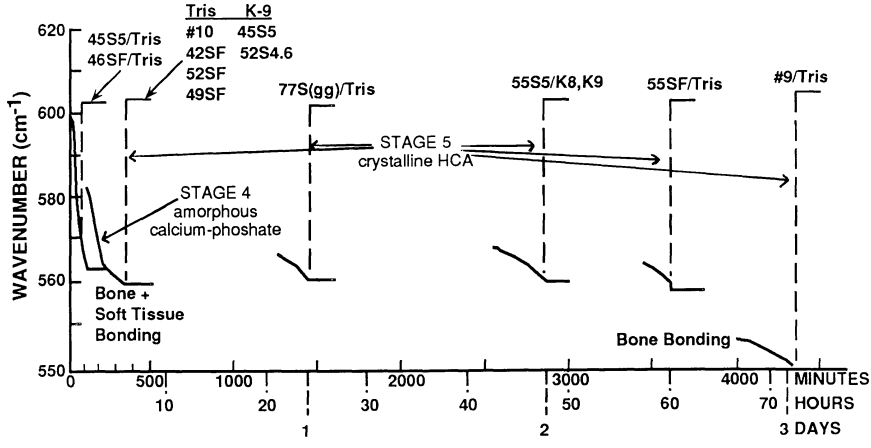

Figure 3.5. Effect of glass composition on time for onset of crystallization of hydroxy-carbonate apatite (HCA) on the surface in TRIS buffer or simulated body fluid (K-9) solutions.

(a-CaP) layer (Stage 4). The major effect of solution composition is on the crystallization of HCA (Stage 5). Figure 3.5 shows that the process of HCA crystallization is the same for the various glasses and the tris-buffer or SBF solution K-9, the only difference is the rate of crystallization. The rate of crystallization increases to a small extent in Ca- and P- containing SBF solutions (in 90 minutes rather than 120 minutes). However, Mg ions in SBF slow down formation of the a-CaP layer and greatly retard crystallization of HCA on the glass surface.

Table 3.3 and Fig. 3.5 show that most of the effects of glass composition are on the time required for HCA crystallization. This finding makes it possible to summarize the relationship between surface reaction rates of bioactive glasses and their *in vivo* behavior. Figure 3.6 shows the critical compositional relationship between *in vitro* and *in vivo* kinetics. For glasses with up to about 53 mole percent Si, HCA crystallization occurs very rapidly on the glass surface, within two hours. These compositions develop a rapid bond with bone and also form an adherent, interdigitating collagen bond with the soft tissues. Glasses with Si content between 53 and 58 mole percent SiO_2 require two to three days to form both the a-CaP layer and to crystallize HCA. Such glass compositions are bioactive, but they bond only to bone. When implanted in soft tissues, the fibrous capsule formed around them is parallel to the interface and is non-adherent. Compositions with >60% SiO_2 do not form a crystalline HCA layer even after four weeks in SBF. An amorphous calcium-phosphate layer forms but it does not

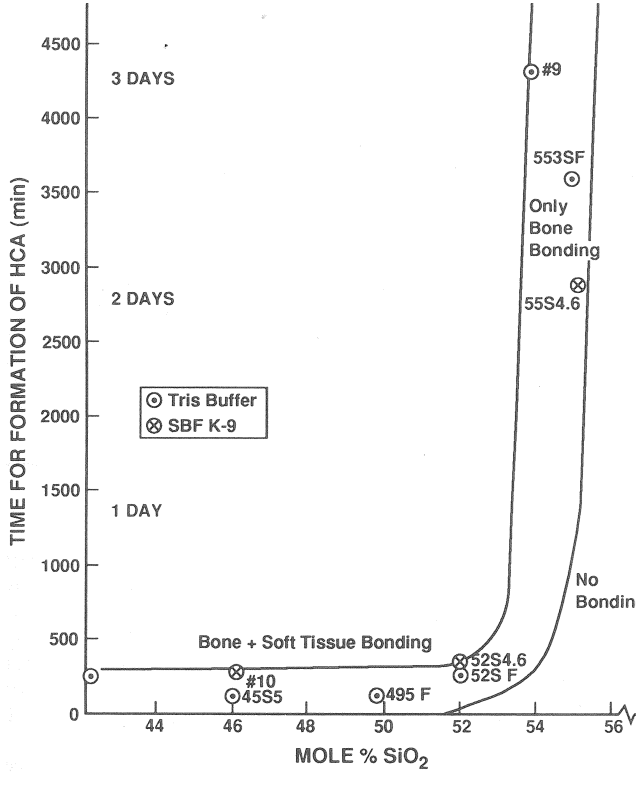

Figure 3.6. Effect of bioactive glass composition on *in vitro* reaction kinetics and *in vivo* tissue response.

crystallize to HCA. Such glasses are not bioactive and bond neither to bone nor soft tissues.

The *in vitro* kinetics studies described above were conducted in well specified conditions with the ratio of glass surface area (SA) to solution volume (V) fixed at 0.1 cm^{-1}. Changing the SA/V ratio changes the reaction kinetics. The SA/V ratio relevant to an implant is very difficult to estimate. It depends not only on the surface area of the implant and the size of the cavity into which it is placed but also on tightness of fit, blood flow, metabolic rate of the tissues, inflammation etc. Thus, the kinetics obtained from *in vitro* analyses are only an estimate of the reaction rates *in vivo.* However, the compositional effects observed *in vitro* appear to be equivalent *in vivo.*

3.6. TISSUE BONDING

The five reaction stages that occur on the material side of the interface do not depend on the presence of tissues. They occur in distilled water, tris-buffer solutions or simulated body fluids. Bonding to tissues requires an additional series of reactions. Chapters 4 and 5 present new findings that explain many of the biological reactions on the tissue side of the bioactive glass–tissue interface. The sequence of events associated with formation of a bond with tissues is:

Stage 6: Adsorption of biological moieties in the SiO_2-HCA layer
Stage 7: Action of macrophages
Stage 8: Attachment of stem cells
Stage 9: Differentiation of stem cells
Stage 10: Generation of matrix
Stage 11: Mineralization of matrix.

Rapid growth of HCA agglomerates on a bioactive glass surface incorporates collagen fibrils *in vitro* (Fig. 3.7) without the presence of cells, enzymes or biological growth factors. The crystals appear to form around the collagen fibrils and form bonds with them on an ultrastructural level, similar to what has been observed by transmission electron microscopy of bone bonded to bioactive glass.[1] The same bonding process of collagen incorporation within the growing gel layer has been observed in soft tissues by Wilson (Figs 3.8 and 3.9).[6,7] Thus, Stage 6 appears to be well established with respect to collagen. Chapter 4 summarizes biological steps 7–10.

Within a week mineralizing bone appears at the interface of the more reactive bioactive glasses (Stage 11). By four weeks the interface is completely bonded to bone without any intervening fibrous tissues. The time sequence of bone formation on bioactive glasses is reviewed in detail elsewhere.[3–5]

Figure 3.10 shows a scanning electron micrograph of a cross section of a bioactive glass (S46PO) after eight weeks in rabbit tibia. In the back-scatter mode it is easy to distinguish the characteristic silica-rich (dark) and calcium phosphate-rich (bright) layers. The composition of the glass is SiO_2, 46.0; Na_2O, 26.0; CaO, 25.0; P_2O_5, 0.0; B_2O, 2.0 and Al_2O_3, 1.0 weight percent. Since the glass does not originally contain phosphate it is clearly seen that phosphate is absorbed and that calcium phosphate forms mainly within the silica-rich layer. This emphasizes the role of the silica structure in inducing the HCA formation.

The most important criterion for tissue bonding is the mechanical resistance of the tissue–implant interface. There is no consensus on the best test

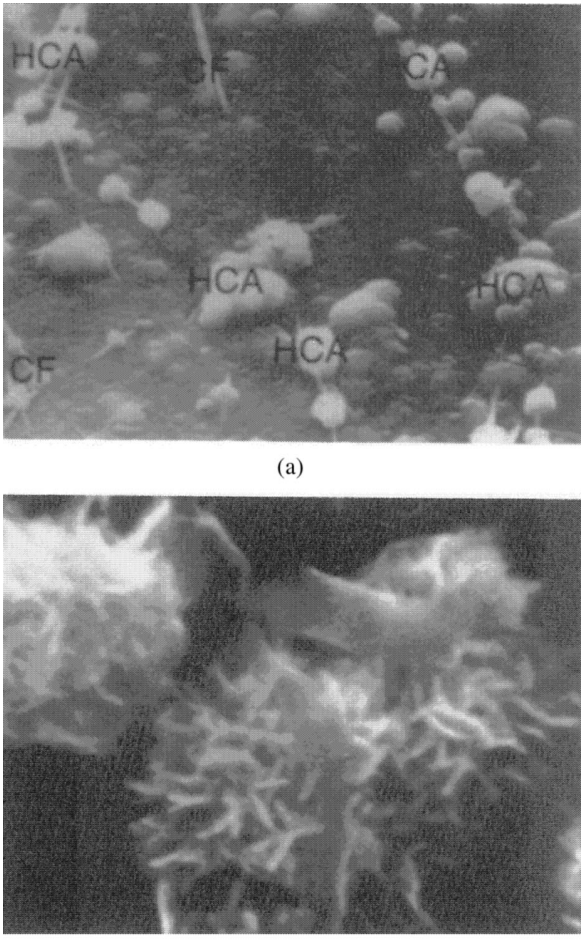

Figure 3.7. (a) SEM micrograph of collagen fibrils incorporated within the HCA layer growing on a 45S5 Bioglass® substrate *in vitro.* (b) Close-up (11,300X) of the HCA crystals bonding to a collagen fibril. (Photographs courtesy of C. Pantano.)

method to determine interfacial adherence of bioactive implants. Studies by the Florida group of bone bonding to bioactive glasses and glass-ceramics, primarily 45S5 composition, showed very high interfacial strength values using a variety of mechanical test methods.[11] Most of the studies involved loaded prostheses, such as segmental bone replacements (Fig. 3.11) or femoral head prostheses. In most

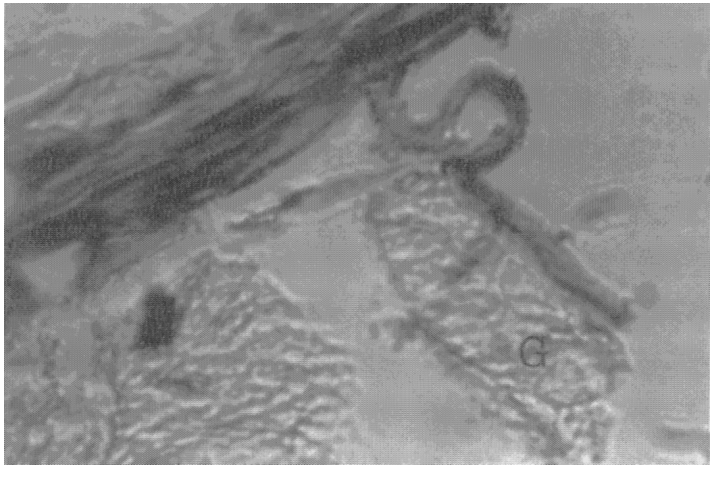

Figure 3.8. Peeling of collagen, which remains adherent to the 4SSS bioactive-glass (G) decalcified section. (Original magnification 250 X.)

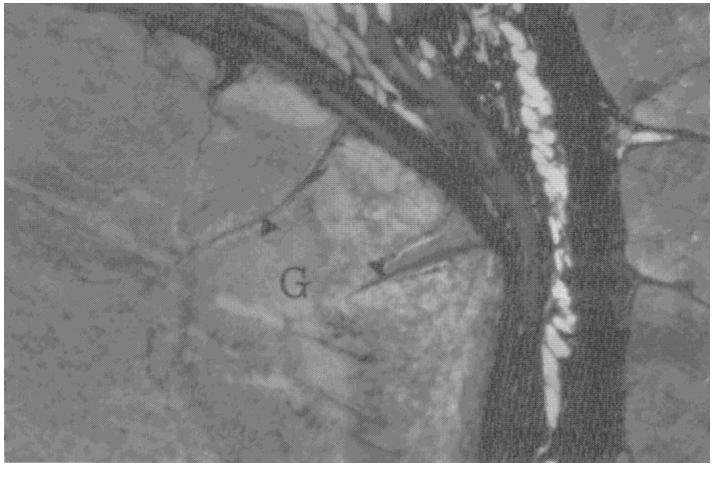

Figure 3.9. Collagen fibers (•) in cracks on the 45SS bioactive-glass surface (G) undecalcified section. (Original magnification 100 X.)

studies the interface did not fail, fracture occurred either in the implant, such as shown in Fig. 3.11, or in the bone, distal to the implant.

Various push-out or pull-out tests have also been reported for bioactive glasses and glass-ceramics. Chapters 13 and 14 discuss the method used by the

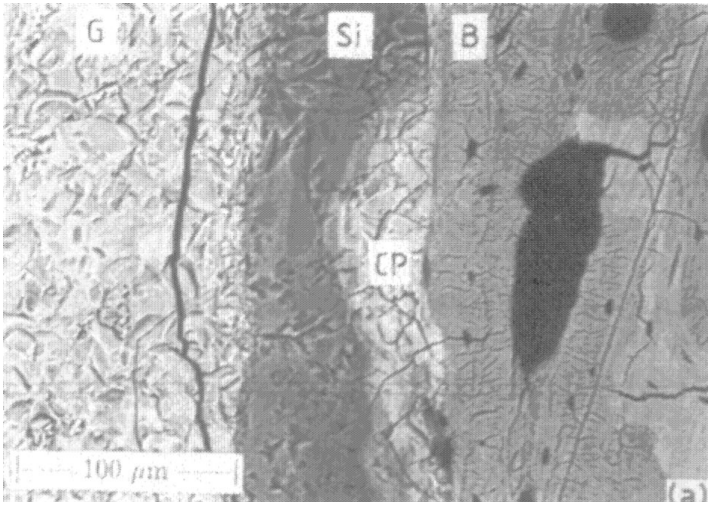

Figure 3.10. Scanning electron micrograph of a cross section of a phosphate-free bioactive glass (S46PO) after eight weeks in rabbit tibia. G = bulk glass; Si = Si-rich layer; CP = Ca, P-rich layer; B = bone.

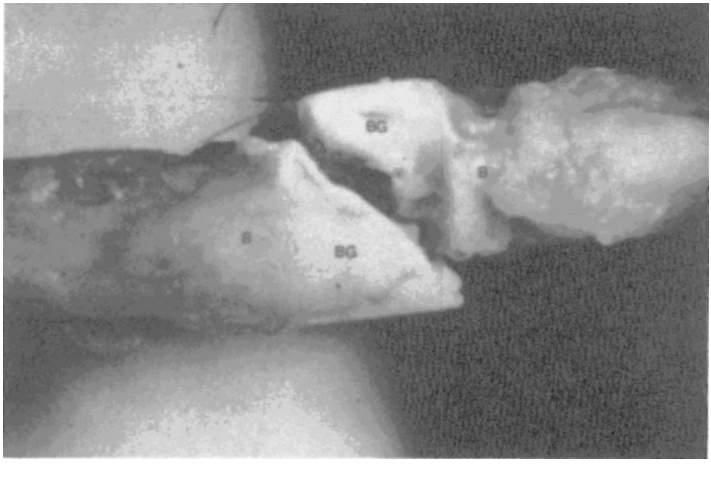

Figure 3.11. Fracture of (BG) 45S5 Bioglass®-ceramic segmental bone replace in monkey due to impact torsional loading. Note (B) bonded interface. (Photograph courtesy G. Piotrowski.) (Reprinted from Hench, L.L. (1991). Bioceramics: From Concept to Clinic, *J. Amer. Ceram. Soc.*, **74**, 1487–1570, with permission.)

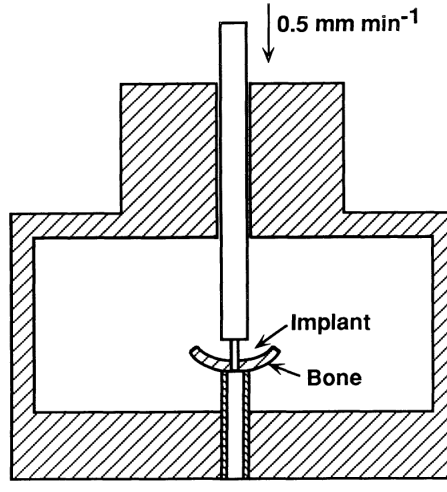

Figure 3.12. Schematic illustration of a specimen in the push-out test fixture.

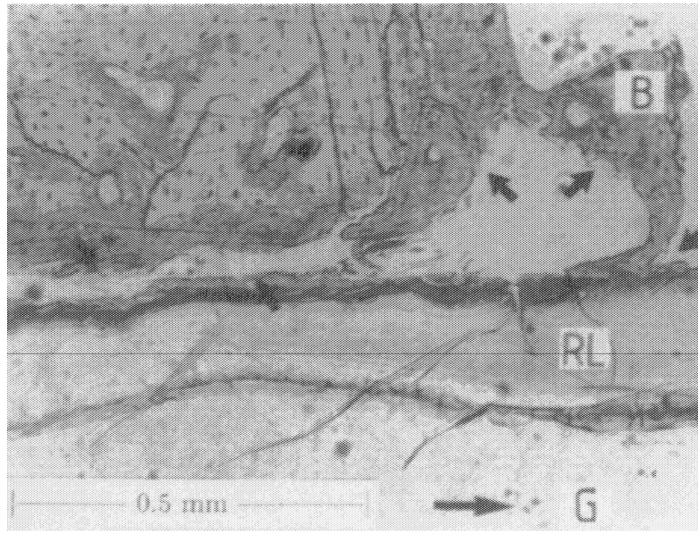

Figure 3.13. Optical micrograph of a cross section of glass S46PO after push-out. B = bone; RL = reaction layer; G = bulk glass. Direction of loading is indicated by long arrow and fracture line by short arrows.

Kyoto group. The push-out test method used by Andersson and colleagues in Finland is illustrated in Fig. 3.12.[11]

The conical implant is pushed out of the rabbit tibia at a cross-head speed of 0.5 mm/min. Prior to testing, the bone covering the base of the cone is removed by grinding. The base of the cone is also slightly ground in this process and a flat supporting surface is produced. The conical shape reduces the contribution from the surface roughness. It is difficult to measure the contact area since the bone grows along the surface of the implant and may be present only as a very thin layer. If the glass is sectioned along its axis after the test it is possible to estimate the thickness. With this method interfacial strength values of 15–25 MPa have been obtained for a number of bioactive glasses. For an inert glass the same test gave a value of 0.5 MPa or less, for glasses just outside the bioactivity border values of 2–3 MPa, and for smooth titanium 2 MPa. Thus, non-bonding biocompatible glasses behave as titanium. When testing bioactive glasses, it is observed that the fracture line in some areas is within the silica-rich layer and in others within bone. Figure 3.13 shows a cross section of glass S46PO after the push out. It is clear that bone has adhered to the glass and fracture has occurred within the bone.

3.7. RATE OF BONDING

The rate of development of the interfacial bond between an implant and bone can be referred to as the level of bioactivity. Hench introduced an index of bioactivity as a measure of this.[3–5] The index is given by $I_B = (100/t_{0.5bb})$, where $t_{0.5bb}$ is the time for more than 50% of the surface to be bonded to bone. In the ternary diagram for the compositional dependence of the bioactivity, iso-I_B contours have been indicated (Fig. 3.1). Thus, the closer to the bioactivity boundary a glass is, the slower the rate of bonding. When the constant 6 weight percent P_2O_5 content is that in Fig. 3.1, I_B goes toward zero as the SiO_2 content is raised close to 60%. Bioactive implants with intermediate I_B values do not develop a stable bond with soft tissue. The broken line in Fig. 3.1 indicates the region within which the I_B values are sufficiently high for soft tissue bonding.

The thickness of the bonding zone is roughly proportional to the I_B value and the failure strength of a bioactive bond appears to be inversely proportional to the thickness of the zone. Thus, a very high I_B value gives a thick bonding zone and low shear strength. Depending on whether rapid bonding or high shear strength is preferred, different compositions are optimal.

REFERENCES

1. Hench, L.L., Splinter, R.J., Allen, W.C. *et al.* (1972). Bonding Mechanisms at the Interface of Ceramic Prosthetic Materials, *J. Biomed. Maters. Res.*, **2**, 117–141.
2. Hench, L.L. and Wilson, J.W. (1991). Surface-Active Biomaterials, *Science*, **226**, 630–636.
3. Hench, L.L. (1991). Bioceramics: From Concept to Clinic, *J. Amer. Ceram. Soc.*, **74**, 1487–1510.
4. Hench, L.L. (1998). Bioceramics, *J. Amer. Ceram. Soc.*, **81**, 1705–1735.
5. Hench, L.L., Hench, J.W. and Greenspan, D.C. (2004). Bioglass: A Short History and Bibliography, *J. Aust. Ceram. Soc.*, **40**, 1–42.
6. Wilson, J., Pigott, G.H., Schoen, F.J. *et al.* (1981). Toxicology and Biocompatibility of Bioglass, *J. Biomed. Mater. Res.*, **15**, 805–817.
7. Wilson, J. and Nolletti, D. (1986). "Bonding of Soft Tissues to Bioglass", in Christel, P., Meunier, A. and Lee, A.J.C. (eds), *Biological and Biomechanical Performance of Biomaterials*, Elsevier, Amsterdam, pp. 99–104.
8. Andersson, O.H. (1990). *The Bioactivity of Silicate Glass* (PhD Thesis, Dept. of Chemical Engineering, Abo Akademi, Finland).
9. Li, R., Clark, A.E., Hench, L.L. (1991). An Investigation of Bioactive Glass Powders by Sol-Gel Processing, *J. Appl. Biomaterials*, **2**, 231–239.
10. Gross, U. and Strunz, V. (1985). The Interface of Various Glasses and Glass-Ceramics with a Bony Implantation Bed, *J. Biomed. Mater. Res.*, **19**, 251–271.
11. Hench, L.L., Paschall, H.A., Allen, W.C. *et al.* (1975). Interfacial Behavior of Ceramic Implants, *National Bureau of Standards Special Publication*, **415**, 19–35.
12. Andersson, O.H., Liu, G., Kangasniemi, K. *et al.* (1992). Evaluation of the Acceptance of Glass in Bone, *J. Maters. Sci. Maters. in Med.*, **3**, 145–150.

Chapter 4

BIOACTIVE GLASSES: GENE ACTIVATION

Larry L. Hench

4.1. INTRODUCTION

First-generation biomaterials, including metals, such as stainless steel and titanium, bio-polymers, such as poly(methyl methacrylate), and bioceramics, such as alumina and zirconia, were designed to be as inert as possible in order to minimize the thickness of interfacial scar tissue, as discussed in Chapter 1. These bioinert materials are still the most commonly used biomaterials. Bioactive glasses have provided an alternative type of material and biomaterial–tissue interface from the 1970s onwards, termed second generation bioactive materials. Bioactive materials are capable of bonding implants to tissues without the formation of interfacial scar tissue. Examples of bioactive materials include bioactive glasses (e.g. 45S5 Bioglass®), synthetic hydroxyapaptite (HA), and bioactive glass-ceramics (e.g. A/W glass-ceramic, Cerabone), all discussed in this book. Resorbable materials, such as poly(lactic acid) and poly(glycolic acid) and tri-calcium phosphate (TCP), were developed in the 1970s and 1980s and are another category of second-generation biomaterials. Biodegradable polymers are used as resorbable sutures, for example. Details of the characteristics of bioactive materials are presented in numerous reviews and textbooks.[1–5]

4.2. THIRD-GENERATION BIOMATERIALS

During the last decade, the concepts of bioactive materials and resorbable biomaterials have converged into a new, third-generation of biomaterials; bioactive materials are being made resorbable, and resorbable polymers are being made bioactive.[6] Molecular modifications of resorbable polymers and bioactive composite systems elicit specific interactions with cell integrins and thereby direct cell proliferation, differentiation, and extracellular matrix production and organization. Third-generation bioactive glasses, composites, hybrid materials, and macroporous foams are being designed to activate genes that stimulate

regeneration of living tissues. This chapter reviews the discovery that controlled release of biologically active Ca and Si species released from bioactive glasses leads to the up-regulation and activation of seven families of genes in osteoprogenitor cells that give rise to rapid bone regeneration. This finding offers the possibility of creating a new generation of gene activating biomaterials designed specially for tissue engineering (TE) and *in situ* regeneration of tissues.[6]

Two alternative routes of repair are now available with the use of third-generation, molecularly tailored biomaterials.

4.2.1. Tissue Engineering

The aim of this strategy is to seed progenitor cells onto biologically active resorbable scaffolds, such as those described in Chapter 32. The cells are grown outside the body, become differentiated, and produce an extracellular matrix, forming a TE construct, which is then implanted into patients to replace diseased or damaged tissues. With time the scaffolds are resorbed and replaced by host tissues that include a viable blood supply and nerves. The living TE constructs adapt to the physiological environment and should provide long-lasting repair.[7,8]

4.2.2. *In Situ* Tissue Regeneration

This approach involves the use of biomaterials in the form of powders, solutions, doped microparticles, porous granules, or scaffolds to stimulate local tissue repair directly, inside the body.[8] Bioactive materials release chemicals in the form of ionic dissolution products, or growth factors such as bone morphogenic protein (BMP), at controlled rates, by diffusion or network breakdown, which activate the cells in contact with the stimuli. The cells produce additional growth factors that in turn stimulate multiple generations of growing cells to self-assemble into the tissues *in situ* along the biochemical and biomechanical gradients that are present. NovaBone®, Perioglas® and NovaMin® products are all third-generation bioactive glass products based upon 45S5 Bioglass®.[8]

4.3. BIOACTIVE GLASSES: 45S5 BIOGLASS®

The grandfather composition of bioactive glasses was discovered in 1969.[1,9] It is called 45S5 Bioglass®. The glass composition is 45% SiO_2, 24.5% Na_2O, 24.5% CaO, 6% P_2O_5 (in weight %). The glass was first tested in a rat

femoral implant model and was shown to bond strongly to bone within six weeks. This finding was the basis of the first paper published in 1971 in the Journal of Biomedical Materials Research, which summarized the *in vivo* results and the *in vitro* tests that provided an explanation for the interfacial bonding of the implant to bone.[9] The *in vitro* tests showed that the 45S5 Bioglass® composition developed a hydroxycarbonate apatite (HCA) layer in test solutions that did not contain calcium or phosphate ions. The surface phase of HCA that was formed *in vitro* was equivalent to the interfacial HCA crystals observed *in vivo* by Dr. T.K. Greenlee's transmission electron micrographs of the bonded interface.[1,9] The HCA crystals were bonded to layers of collagen fibrils produced at the interface by osteoblasts. The chemical bonding of the HCA layer to collagen created the strongly bonded interface between glass and bone.[1,9,10]

A key review article that summarizes the mechanisms of bone–Bioglass® bonding was published in 1982: "Adhesion to Bone" by L.L. Hench and A.E. Clark.[10] The paper documents in Part A the time sequence of bonding of Bioglass® in rat femur and tibia. In Part B, the bonding of Bioglass® implants to the femur in canine and monkey bones is summarized. Part C reviews the data of bonding of mandibular and maxillary bone of primates and swine to Bioglass® implants. All species exhibited stable bone bonded implants. Bonding occurred rapidly, regardless of species, within weeks of implantation.[10]

4.4. BIOGLASS®–BONE BOND STRENGTH

One of the most difficult topics studied in the first decade of Bioglass® experiments was determining the strength of the bond to bone. Eight different biomechanical test models were developed. A quantitative evaluation of interfacial shear strength in rat and monkey models showed that the strength of the interfacial bond between Bioglass® and cortical bone was equal to or greater than the strength of the host bone.[11] Weinstein, Klawitter and Cook published a key paper describing the biomechanics of the bonded interface between bone and Bioglass®.[12]

4.5. BIOGLASS® SURFACE REACTIONS

Bone bonding occurs as a result of a rapid sequence of chemical reactions on the surface of the Bioglass® implant when inserted into living tissues. New analytical techniques, such as cryogenic Auger electron spectroscopy, analytical

scanning transmission electron microscopy, cryogenic electron microprobe analysis, and the application of Fourier transform infrared reflection spectroscopy (FTIR), were developed, which made it possible to determine the kinetics of the surface reactions with great precision. The 11 surface and cellular reaction stages are described in Chapter 3 and a series of papers describe the kinetics studies.[13–16] Slow resorption of the glass surface releases soluble ionic species and creates a high surface area hydrated silica gel due to a condensation reaction between neighboring Si-OH groups.

Nucleation of a crystalline HCA layer follows. Controlled release of soluble Si and Ca species is especially important. Recent molecular biology studies, discussed below, show that the Si species and Ca ions at specific concentrations are responsible for the genetic response to the bioactive glasses and lead to rapid growth of new bone. The mechanism for the HCA layer bonding to bone involves protein adsorption and cell attachment. The result is growth of new bone with an architecture and biomechanical properties equivalent to normal bone.[10,17,18]

4.6. CLASSES OF BIOACTIVITY

Bioactive materials used for either tissue replacement or tissue regeneration must possess controlled chemical release kinetics that synchronize with the sequence of cellular changes occurring in natural wound repair.[1,10,14–16] If dissolution rates are too rapid, the ionic concentrations are too high to be effective. If the rates are too slow, the concentrations are too low to stimulate cellular proliferation and differentiation. Large differences in rates of *in vivo* bone regeneration and extent of bone repair, documented in papers by Oonishi *et al.*[17] and Wheeler *et al*.,[18] indicate that there are two classes of bioactive materials.[14,15] Class A bioactivity leads to both osteoconduction and osteostimulation as a consequence of rapid reactions on the bioactive glass surface. The surface reactions involve ionic dissolution of critical concentrations of soluble Si and P species and Ca and Na ions that give rise to both intracellular and extracellular responses at the interface of the glass with its physiological environment. Class B bioactivity occurs when only osteoconduction is present, i.e. bone migrates along an interface. This limited tissue response is due to slower surface reactions and minimal ionic release. Only extracellular responses occur at the interface of Class B bioactive tissue interfaces.[1,16] Differences between Class A and B bioactive materials are summarized in several sources.[1,14–16] The clinical consequences of these differences is more rapid bone growth and more bone in a graft site for Class A bioactive materials, as discussed later in this chapter in Sections 4.9–4.11 on clinical applications.

4.7. BIOACTIVE CONTROL OF GENES AND THE OSTEOBLAST CELL CYCLE

For many years it was assumed that formation of a biologically active HCA surface reaction layer was the critical requirement for bioactive behavior.[1,14–16] However, studies from 2000 to 2003 showed formation of a surface HCA layer to be useful but not the critical stage of reaction for bone regeneration. The controlled rates of release of ionic dissolution products, especially critical concentrations of soluble Si species and calcium ions, is the critical requirement for osteoproduction, now called osteostimulation, as first described by June Wilson and Sam Low.[19]

In order for new bone to form it is essential for osteoprogenitor cells (adult stem cells) to undergo cell division (mitosis). The osteoprogenitor cells that are present must receive the correct chemical stimuli from their local environment, which then instructs them to enter the active segments of the cell cycle. Numerous papers document the critical importance of local chemical environment on osteoblast cell growth *in vitro* and *in vivo*.[1,20–25] Figure 4.1 shows the osteoblast progenitor cell cycle. Resting cells are in the G_0 phase. Every new cell cycle begins after a cell has completed the preceding mitosis. If the local chemical environment is suitable, and following a critical period of growth in the G_1 phase, the cell enters the S phase when DNA synthesis begins and leads to duplication of all the chromosomes in the nucleus. During a second growth phase, G_2, the cell prepares to undergo division and checks its replication accuracy using DNA repair enzymes.

Details of the feedback controls and cell cycle checkpoints have been described.[20–23] If the local chemical environment does not lead to completion of the G_1 phase or the G_2 phase then the cell proceeds to programmed cell death, apoptosis. Bioinert materials or Class B bioactive materials do not produce the local chemical environment to enable the few osteoprogenitor cells present to pass through these cell cycle checkpoints. Only Class A bioactive materials produce rapid new bone formation *in vivo*, e.g. osteostimulation.[17–28] Approximately 17–20 $\mu g ml^{-1}$ of soluble silica and 88–100 $\mu g ml^{-1}$ of soluble Ca ions are required for the interfacial environment to be osteogenic. The ions are provided by controlled dissolution of a bulk implant or the 45S5 Bioglass® particles in a particulate such as NovaBone® or Perioglas®.

Molecular biology studies by Xynos *et al*. in Professor Dame Julia Polak's group at Imperial College London showed that the bioactive shift of osteoblast cell cycle is under genetic control.[24,25] Within a few hours of exposure of human primary osteoblasts to the soluble chemical extracts of 45S5 Bioglass®, several

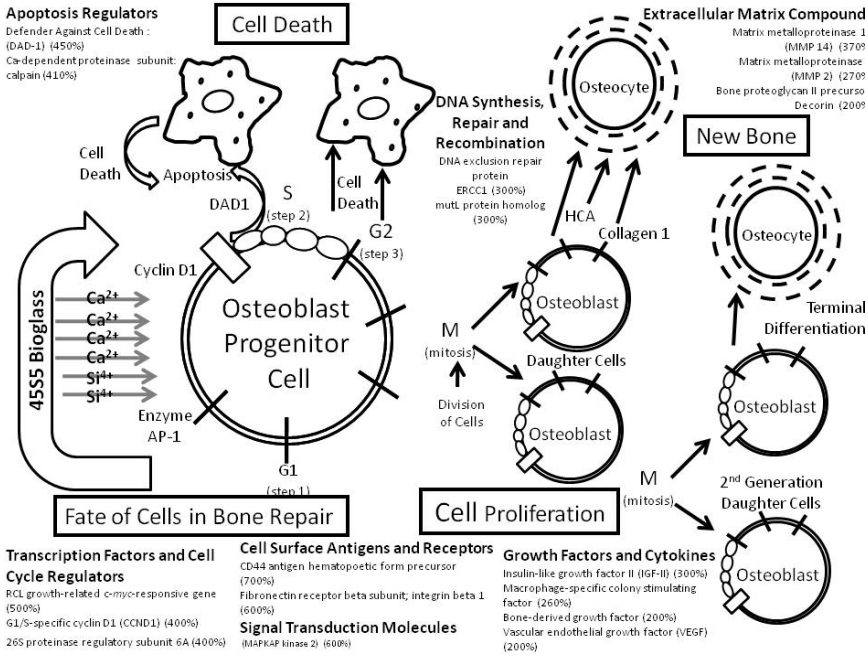

Figure 4.1. Schematic of osteoblast progenitor cell cycle leading to: 1) programmed cell death (apoptosis); 2) mitosis and cell proliferation; or 3) terminal cell differentiation towards an osteocyte.

families of genes are activated, including genes encoding nuclear transcription factors and potent growth factors, especially IGF-II, along with IGF binding proteins and proteases that cleave IGF-II from their binding proteins.[23] There is a 200–500% increase in the expression of these genes over those of the control cultures.[23–25] Activation of several immediate early response genes and synthesis of growth factors is likely to modulate the cell cycle response of osteoblasts to bioactive glasses. These findings indicate that Class A bioactive glasses enhance new bone formation (osteogenesis) through a direct control over genes that regulate cell cycle induction and progression. Bioactive induction of the transcription of extracellular matrix components and their secretion and self-organization into a mineralized matrix appears to be responsible for the rapid formation and growth of bone nodules and differentiation of the mature osteocyte phenotype in the presence of Class A bioactive materials such as 45S5 Bioglass® and sol-gel derived bioactive gel glasses of compositions 58S (60 mol% SiO_2, 36 mol% CaO, 4 mol% P_2O_5) and 70S30C (70 mol% SiO_2, 30 mol% CaO), tested by Bielby *et al.*[26]

Several studies have confirmed the results of the early Xynos *et al.* findings and extended the generality to include several types of precursor cells and differing sources of ionic stimuli.[27,28] Gene array analyses of five different *in vitro* models using five different sources of inorganic ions provide the experimental evidence for a genetic theory of osteogenic stimulation.[25] All seven experiments showed enhanced proliferation and differentiation of osteoblasts towards a mature, mineralizing phenotype, without the presence of any added bone growth proteins such as dexamethasone or BMP.[22] Shifts in osteoblast cell cycles were observed as early as six hours, with elimination (by apoptosis) of cells incapable of differentiation. The remaining cells exhibited enhanced synthesis and mitosis. The cells quickly committed to generation of extracellular matrix (ECM) proteins and mineralization of the matrix.[28] Gene array analyses at 48 hours showed early up-regulation or activation of seven families of genes that favored both proliferation and differentiation of the mature osteoblast phenotypes, including: transcription factors and cell cycle regulators (six with increases of 200–500%); apoptosis regulators (three at 160–450% increases); DNA synthesis, repair and recombination (four at 200–300%); growth factors (four at 200–300%, including IGF-I1 and VEG F); cell surface antigens and receptors (four at 200–700%, especially CD44); signal transduction molecules (three at 200–600%); and ECM compounds (five at 200–370%).

A summary of the seven families of genes activated or up-regulated from the experiments is given in Table 4.1.

4.8. DESIGN CONCEPTS FOR GENETIC CONTROL OF BONE REGENERATION

Two developments make it possible to design a new generation of biomaterials that can control gene expression *in vitro* and *in vivo*. The first is the enhanced understanding of the role of controlled release of ionic dissolution products from bioactive glasses in controlling the molecular biology of osteoprogenitor cells, as reviewed above. The second is use of sol-gel processing of bioactive glasses to achieve additional control of the rates of ionic release of biologically active stimuli.

Compositions and textures of sol-gel derived glasses can be varied over wide ranges and thereby be used to control the rates and concentrations of soluble Si and Ca species in the physiological solutions. Details of sol-gel processing of bioactive gel-glasses, textural analyses and bioactivity studies are presented in prior publications.[29,30] Sol-gel processing makes it possible to produce

hierarchical microstructures with nanometer scale pores in the solid webs of 3D scaffolds, while creating an interconnected pore network with greater than 100 μm passages between macropores of 200–600 μm in diameter. Chapter 32 discusses these materials and hierarchical scaffolds in detail. Gough *et al.* demonstrated that such bioactive 3D scaffolds support osteoblast growth and induced differentiation of the cells without use of supplementary organic growth factors.[28,31]

The Beilby *et al.* investigations[26] were especially significant because the cell source was embryonic stem (ES) cells. Soluble Si and Ca species released from 58S sol-gel derived glasses stimulated gene expression in the murine ES cells characteristic of a mature phenotype in primary osteoblasts. The osteogenic effect of the bioactive gel-glass extracts was dose dependent. The conclusion was that the bioactive gel-glass material was capable of stimulating differentiation of ES cells toward a lineage with therapeutic potential in TE. Christodoulou *et al.* extended even further the scientific basis of the genetic effect of the dissolution products of 58S gel-glasses on osteogenesis, which were added to cultures of primary osteoblasts derived from human fetal long bone explants cultures (hFOBs).[27] The over 200% up-regulation of gp130 and MAPK3 and down-regulation of IGF-1 were confirmed by real-time RT-PCR analysis. These data suggest that 58S ionic dissolution products possibly mediate the bioactive effect of the gel-glass through components of the IGF system and MAPK signaling pathways. The results from human fetal osteoblasts confirm many of the findings reviewed above and shown in Table 4.1 using primary human osteoblast cultures derived from excised femoral heads of elderly patients, and thereby demonstrate the generality of the findings of genetic stimulation by the ionic dissolution products of bioactive glasses and gel-glasses.

The implications of the above studies are that it is now feasible to design the dissolution rates and architecture of bioactive, resorbable inorganic scaffolds to achieve specific biological effects *in vivo* that synchronize with the progenitor cell population present *in situ*. This offers, for the first time, the potential to design biomaterials for specific patients and their clinical needs.

4.9. THIRD-GENERATION BIOACTIVE GLASS CLINICAL PRODUCTS

Second-generation Bioglass® implants performed well when replacing diseased or missing hard tissue.[28] The discovery that Bioglass® could stimulate osteoblasts to produce more bone tissue earlier than other synthetic biomaterials led to the innovative concept of *osteostimulation*, the basis for third-generation

Table 4.1. Families of Genes in Primary Human Osteoblasts Activated or Up-Regulated by Ionic Dissolution Products of Bioactive Glasses.[27]

Transcription Factors and Cell Cycle Regulators	**Activation (%)**
RCL growth-related c-*myc*-responsive gene	500
G1/S-specific cyclin D1 (CCND1)	400
26S proteinase regulatory subunit 6A	400
Cyclin-dependent kinase inhibitor 1 (CDKN1A)	350
cAMP-dependent transcription factor ATF-4	240
Cyclin K	200
DNA Synthesis, Repair, and Recombination	**Up-regulation (%)**
DNA exclusion repair protein ERCC!	300
mutL protein homolog	300
High-mobility-group protein (HMG-1)	230
Replication factor C 38-kDa subunit (RFC38)	200
Apoptosis Regulators	**Up-regulation (%)**
Defender against cell death 1 (DAD-1)	450
Ca-dependent proteinase small (regulatory) subunit; calpain	410
Deoxyribonuclease II (Dnase II)	160
Growth Factors and Cytokines	**Activation (%)**
Insulin-like growth factor II (IGF-II)	300
Macrophage-specific colony stimulating factor (CSF1; MCSF)	260
Bone-derived growth factor	200
Vascular endothelial growth factor precursor (VEGF)	200
Cell Surface Antigens and Receptors	**Activation (%)**
CD44 antigen hematopoetic form precursor	700
Fibronectin receptor beta subunit; integrin beta 1	600
N-sam; fibroblast growth factor receptor-1 precursor	300
Vascular cell adhesion protein-1 precursor (V-CAM1)	200
Signal Transduction Molecules	**Activation (%)**
MAP kinase-activated protein kinase 2 (MAPKAP kinase 2)	600
Dual specificity nitrogen-activated protein kinase 2	200
ADP-ribosylation factor 1	200
Extracellular Matrix Compounds	**Activation (%)**
Matrix metalloproteinase 14 precursor (MMP 14)	370
Matrix metalloproteinase 2 (MMP 2)	270
Metalloproteinase 1 inhibitor precursor (TIMP 1)	220
TIMP 2 (MI)	220
Bone proteoglycan II precursor; decorin	200

biomaterials. Development of third-generation Bioglass® products focussed on using particles rather than monolithic shapes. The products are manufactured and used under the trademarks PerioGlas® and NovaBone®. Chapter 40 summarizes the process for technology transfer and the timeline for development of clinical products based upon 45S5 Bioglass®.

The first NovaBone® particulate material cleared for sale in the U.S. was PerioGlas®, which was cleared via the 510(k) process in December, 1993. In 1995, PerioGlas® obtained a CE mark and marketing of the product began in Europe. The initial indication for the product was to restore bone loss resulting from periodontal disease in infrabony defects. In 1996, additional indications for use were cleared by FDA, including use in tooth extraction sites and for alveolar ridge augmentation.[29]

During a 25-year clinical history, PerioGlas® has demonstrated excellent clinical results with virtually no adverse reactions to the product. Numerous clinical studies have demonstrated the efficacy of the product in multiple uses. A historical review lists many of these clinical studies can be found Saravanapavan *et al*., 2003.[30] Chapter 9 summarizes the successful clinical results.

Building on the successes of PerioGlas® in the market, a Bioglass® particulate for orthopedic bone grafting was introduced into the European market in 1999, under the trade name NovaBone®. Early studies by Wilson and Low in a canine model showed effective bone regeneration with uses of 45S5 Bioglass® particulate.[19] Other animal models followed in various laboratories worldwide.[31] The product was cleared for general orthopedic bone grafting in non-load bearing sites in February, 2000. To date, PerioGlas® and NovaBone® products are sold in over 35 countries, and the manufacturer (NovaBone Products LLC, FL, USA) reports that the product has been used in more than 1,000,000 surgeries. Table 4.2 lists the various medical and dental products used clinically.

4.10. SYNTHETIC BIOACTIVE GLASS BONE GRAFT OR AUTOGRAFT?

A publication in the *Journal of Pediatric Orthopaedics* by Ilharreborde *et al*. in 2008 illustrates the value of 45S5 Bioglass® (NovaBone®) as an alternative to use of autografts.[32] At the present time, iliac crest autograft is considered to be the gold standard material for spinal fusion, as discussed in Chapter 10. However, it is well known that there are limitations to the use of autografts, such as additional operative time, increased loss of blood, morbidity, length of time of healing of the second operative site and pain in the donor site. Chapter 10

Table 4.2. Clinical Medical and Dental Products Based upon 45S5 Bioglass.

Orthopedics
Trauma
Long bone fracture (acute and/or comminuted); alone and with internal fixation
Femoral non-union repair
Tibial plateau fracture
Arthroplasty
Filler around implants (acetabular reconstruction)
Impaction grafting
General
Filling of bone after cyst/tumor removal
Spine Fusion
Interbody fusion (cervical, thoracolumbar, lumbar)
Posterolateral fusion
Adolescent idiopathic scoliosis
Cranial–Facial
Cranioplasty
Facial reconstruction
General oral/dental defects
Extraction sites
Ridge augmentation
Sinus elevation
Cystectomies
Osteotomies
Periodontal Repair
Dental–Maxillofacial–ENT
Toothpaste and treatments for dentinal hypersensitivity
Pulp capping
Sinus obliteration
Repair of orbital floor fracture
Endosseous ridge maintenance implants
Middle ear ossicular replacements (Douek MED)

compares the use of autografts compared with synthetic graft materials in oral and maxillofacial reconstructive surgery. The aim of the Ilharreborde *et al*. study was to compare bioactive glass (NovaBone®) with iliac graft autograft as bone substitutes in the treatment of thoracic adolescent idiopathic scoliosis (AIS). Eighty-eight consecutive patients underwent posterior spinal fusion for progressive AIS, with 40 patients implanted with autograft and 48 patients receiving NovaBone® particulate. A minimum two-year follow-up was required, with medical data and radiographs analyzed retrospectively and compared statistically. The results showed that the Bioglass® particulate was as effective as iliac crest graft in achieving fusion and maintenance of correction in the AIS patients. Fewer complications were seen in the Bioglass® group. Thus, the authors concluded, "Bioactive glass can be proposed in the treatment of AIS, avoiding the morbidity of iliac crest harvesting."[32]

4.11. SYNTHETIC BIOACTIVE GLASS OR CALCIUM PHOSPHATE BONE GRAFT?

Another example of use of NovaBone® bioactive glass particulate as a synthetic bone graft is in lumbar spinal fusions. A spinal surgical group performed 88 cases of lumbar spinal fusion, with all cases consisting of intervertebral body arthrodesis, the majority of which were also combined with postererolatral fusion.[33] All cases used pedicale screws and rods for stabilization. Direct comparison with Vitoss® tri-calcium phosphate (TCP) were made in 26 of the postreolateral fusion cases, with NovaBone® implanted on the left side and Vitoss® on the right side. The results based upon CT myelograms at six months showed 100% interbody fusion for patients grafted with NovaBone® particulate. In addition to the interbody fusion, there was also postereolateral fusion for 50% of the NovaBone® grafts within six months. In contrast, only 11% of the patients achieved postlateral fusion in the Vitoss® TCP sites by six months. Direct review of grafted sites during re-entry supported the observation that there was greater bone formation at the NovaBone® grafted sites than for Vitoss® sites.[33]

4.12. SUMMARY AND IMPLICATIONS FOR THE FUTURE

A cellular and molecular basis for development of third-generation biomaterials provides the scientific foundation for molecular design of scaffolds for TE and for *in situ* tissue regeneration and repair, with minimally invasive surgery. The economic advantages of these new approaches may aid in solving the

problems of caring for an aging population. It should be feasible to design a new generation of gene-activating biomaterials tailored for specific patients and disease states. The results suggest that bioactive stimuli may be used to activate genes in a preventive treatment to maintain the health of tissues as they age. Only a few years ago this concept would have seemed unimaginable. But we need to remember that only 43 years ago the concept of a material that would not be rejected by living tissues also seemed unimaginable. The socio-economic benefits of a new approach to regenerative repair of the body are just beginning to be realized.

REFERENCES

1. Hench, L.L., Wilson, J. and Greenspan, D.C. (2004). Bioglass: A Short History and Bibliography, *J. Aust. Ceram. Soc.*, **40**, 1–42.
2. Ratner, B.D., Hoffman, A.S., Schoen, F.J. *et al.* (2004). *Biomaterials Science: An Introduction to Materials in Medicine, 2nd edition*, Academic Press, New York.
3. Park, J.B. and Lake, R.S. (1990). *Biomaterials: An Introduction*, Plenum, New York.
4. Hench, L.L. and Wilson, J. (eds) (1996). *Clinical Performance of Skeletal Prostheses*, Chapman and Hall, London.
5. Hench, L.L. (1991). Bioceramics: From Concept to Clinic, *J. Am. Ceram. Soc*., **74**, 1487–1510.
6. Hench, L.L. and Polak, J.M. (2002). Third-Generation Biomedical Materials, *Science*, **295**, 1014–1017.
7. Place, E.S., Evans, N.D. and Stevens, M.M. (2009). Complexity in Biomaterials and Other Challenges in the Translation of Tissue Engineering, *Nat. Mater.*, **8**, 457–470.
8. Hench, L.L., Jones, J.R. and Fenn, M.B. (eds) (2011). *New Materials and Technologies for Healthcare,* Imperial College Press, London.
9. Hench, L.L., Splinter, R.J., Greenlee, T.K. *et al.* (1971). Bonding Mechanisms at the Interface of Ceramic Prosthetic Materials, *J. Biomed. Mater. Res. Symp.*, **2**, 117–141.
10. Hench, L.L. and Clark, A.E. (1982). "Adhesion to Bone", in Williams, D.F. and Winters, G.D. (eds), *Biocompatibility of Orthopaedic Implants*, *Vol. II*, CRC Press, Boca Raton, FL, Chapter 6.

11. Piotrowski, G., Hench, L.L., Allen W.C. *et al.* (1975). Mechanical Studies of the Bone-Bioglass Interfacial Bond, *J. Biomed. Mater. Res. Symp.*, **9**, 47–61.
12. Weinstein, A.M., Klawitter, J.J. and Cook, S.D. (1980). Implant-Bone Interface Characteristics of Bioglass Dental Implants, *J. Biomed. Mater. Res.*, **14**, 23–29.
13. Hench, L.L. (1981). "Stability of Ceramics in the Physiological Environment", in Williams, D.F. (ed.), *Fundamental Aspects of Biocompatibility*, *Vol. I*, CRC Press, Boca Raton, FL. pp. 67–85.
14. Hench, L.L. and West, J.K. (1996). Biological Applications of Bioactive Glasses, *Life Chem. Rep.*, **13**, 187–241.
15. Hench, L.L. (1998). Bioceramics, *J. Am. Ceram. Soc.*, **81**, 1705–1728.
16. Hench, L.L. and Wilson, J. (eds) (1993). *An Introduction to Bioceramics*, World Scientific Publishing, Singapore.
17. Oonishi, H., Hench, L.L., Wilson, J. *et al.* (2000). Quantitative Comparison of Bone Growth Behaviour in Granules in Bioglass®, A-W Glass Ceramic, and Hydroxyapatite, *J. Biomed. Mater. Res.*, **51**, 37–46.
18. Wheeler, D.L., Eschbach, E.J., Hoellrich, R.G. *et al.* (2000). Assessment of Resorbable Bioactive Material for Grafting of Critical-Size Cancellous Defects, *J. Orthop. Res.*, **18**, 140–148.
19. Wilson, J. and Low, S.B. (1992). Bioactive Ceramics for Periodontal Treatment: Comparative Studies, *J. Appl. Biomater.*, **3**, 123–129.
20. Hench, L.L., Polak, J.M., Xynos, I.D. *et al.* (2000). Bioactive Materials to Control Cell Cycle, *Mater. Res. Innovat.*, **3**, 313–323.
21. Xynos, I.D., Hukkanen, M.V.J., Batten, J.J. *et al.* (2000). Bioglass® 45S5 Stimulates Osteoblast Turnover and Enhances Bone Formation *In Vitro*: Implications and Applications for Bone Tissue Engineering, *Calcif. Tiss. Int.*, **67**, 321–329.
22. Hench, L.L., Day, D.E., Holand, W. *et al.* (2010). Glass and Medicine, *Int. J. Appl. Glass Sci.*, **1**, 104–117.
23. Xynos, I.D., Edgar, A.J, Buttery, L.D. *et al.* (2000). Ionic Dissolution Products of Bioactive Glass Increase Proliferation of Human Osteoblasts and Induced Insulin-Like Growth Factor II mRNA Expression and Protein Synthesis, *Biochem. Biophys. Res. Comm*., **276**, 461–465.
24. Xynos, I.D., Edgar, A.J, Buttery, L.D. *et al.* (2001). Gene Expression Profiling of Human Osteoblasts Following Treatment with the Ionic Dissolution Products of Bioglass® 45S5 Dissolution, *J. Biomed. Mater. Res*., **55**, 151–157.

25. Hench, L.L. (2003). Glass and Genes: The 2001 W.E.S. Turner Memorial Lecture, *Glass Technology*, **44**, 1–10.
26. Bielby, R.C., Christodoulou, I.S., Pryce, R.S. *et al.* (2004). Time and Concentration-Dependant Effects of Dissolution Products of 58S Sol-Gel Bioactive Glass on Proliferation and Differentiation of Murine and Human Osteoblasts, *Tissue Eng.*, **10**, 1018–1026.
27. Christodoulou, I., Buttery, L.D.K., Saravanapavan, P. *et al.* (2005). Characterization of Human Fetal Osteoblasts by Microarray Analysis Following Stimulation with 58S Bioactive Gel-Glass Ionic Dissolution Products, *J. Biomed. Mater. Res.*, **77B**, 431–446.
28. Jones, J.R., Tsigkou, O., Coates, E.E. *et al.* (2007). Extracellular Matrix Formation and Mineralization on a Phosphate-Free Porous Bioactive Glass Scaffold Using Primary Human Osteoblast (HOB) cells, *Biomaterials*, **28**, 1653–1663.
29. Hench, L.L. and West, J.K. (1990). The Sol-Gel Process, *Chem. Rev.*, **90**, 33–72.
30. Saravanapavan, P., Jones, J.R. and Hench, L.L. (2003). Bioactivity of Gel-Glass Powders in the CaO-SiO_2 System: A Comparison with Ternary (CaO-P_2O_5-SiO_2) and Quaternary Glasses (SiO_2-CaO-P_2O5-Na_2O), *J. Biomed. Mater. Res.*, **66A**, 110–119.
31. Gough, J.E., Jones, J.R. and Hench, L.L. (2004). Nodule Formation and Mineralisation of Human Primary Osteoblasts Cultured on a Porous Bioactive Glass Scaffold, *Biomaterials*, **25**, 2039–2046.
32. Ilharreborde, B., Morel, E., Fitoussi, F. *et al.* (2008). Bioactive Glass as a Bone Substitute for Spinal Fusion in Adolescent Idiopathic Scoliosis: A Comparative Study with Iliac Crest Autograft, *J. Ped. Orthoped.*, **28**, 347–351.
33. Thomas, D.J., Griffiths, H.J. and Perrin, J.C. (2010). The Use of a Calcium Phosphosilicate in Lower Lumbar Spinal Fusion, *Clincal Report from the Department of Orthopedic Surgery, Sewickly Hospital at Pittsburgh, PA* NovaBone Products, Jacksonville, FL.

Chapter 5

ANGIOGENIC POTENTIAL OF BIOACTIVE GLASSES

Alejandro A. Gorustovich, Luis A. Haro Durand, Judith A. Roether and Aldo R. Boccaccini

5.1. INTRODUCTION

Enhancement of the angiogenic potential of implantable tissue scaffolds is the focus of considerable research efforts in tissue engineering (TE) strategies.[1–3] Angiogenesis, the formation of new blood vessels from the endothelium of the existing vasculature, plays a pivotal role in TE and wound healing. During wound repair, microvascular endothelial cells migrate into the blood clot; they proliferate and form new blood vessels. This complex process is regulated at the molecular level by growth factors, ECM proteins, membrane receptors and signalling molecules that tightly modulate the formation of new blood vessels (Fig. 5.1).[4] This process, called neovascularisation, contributes to the success of regenerating and growing new tissue, because blood vessels bring oxygen, nutrients and growth factors as well as serve as a route for inflammatory cells and precursor cells to reach to the highly metabolically active regenerating tissue. If TE scaffolds have the ability to induce neovascularisation, the viability of native or transplanted cells within scaffolds will be increased, which will enhance the possibility of engineering larger volumes of new tissues. Several approaches are being proposed to induce rapid vascular in-growth, such as gene and/or protein delivery of angiogenic growth factors and *ex vivo* culturing of scaffolds with endothelial cells alone or in combination with other cell types.[3,5]

An increasing number of investigations in the bone TE field demonstrate that bioactive silicate glasses may improve vascularisation and bone regeneration in both healthy and highly compromised experimental models of bone healing.[6] Bioactive silicate glass of composition (in weight percentage (wt%)) 45% SiO_2, 24.5% Na_2O, 24.5% CaO and 6% P_2O_5 (45S5 Bioglass®) was the first man-made inorganic material developed to bond to bone.[7] Several other types of silicate glasses, based on that original silicate composition, have been developed over the years; the goal has been the improvement of degradation behaviour, mechanical properties or processibility. In this context, the

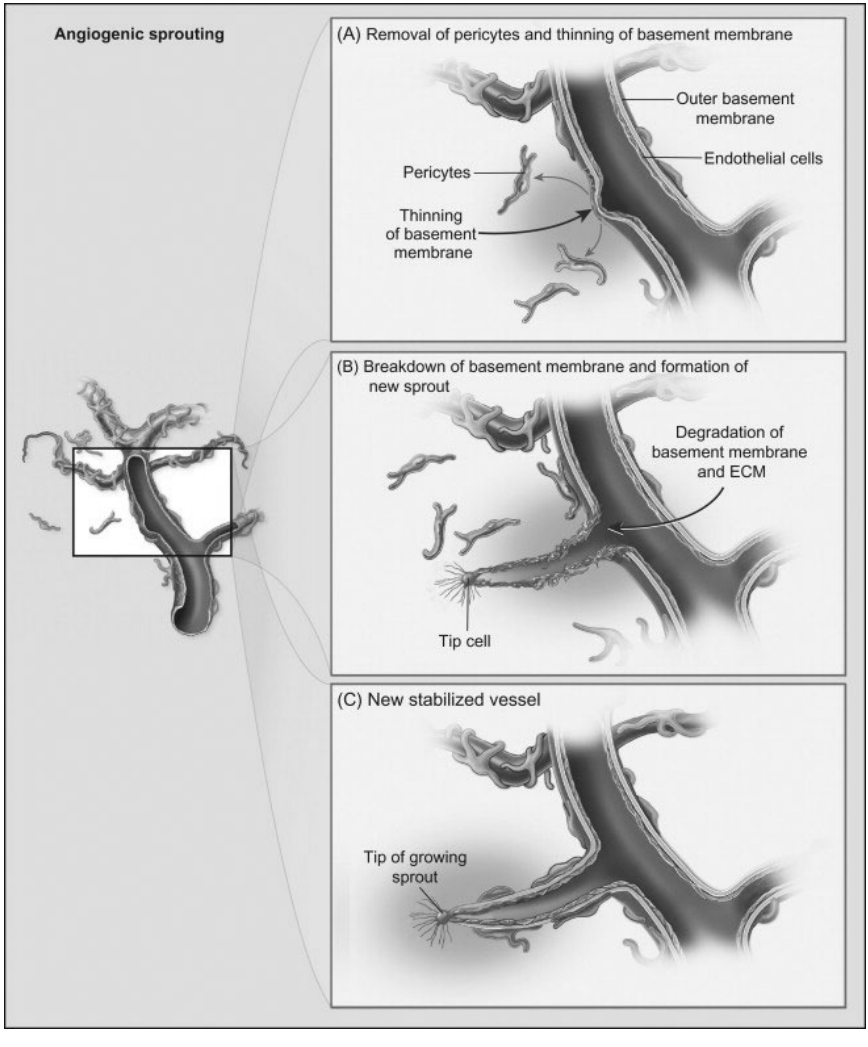

Figure 5.1. Schematic diagram showing new vessel formation via the sprouting of endothelial cells from a pre-existing vessel. (A) Initially, the formation of a new vessel requires removal of associated mural cells (pericytes). (B) Then, endothelial cells degrade the extracellular matrix (ECM), migrate into the perivascular space, proliferate and align themselves into patent blood vessels (C). (Reproduced from Reference 4 with permission from Elsevier.)

chemical composition of bioactive glasses can be varied (within certain limits) to tailor their rate of dissolution in the biological environment. It is possible to design glasses with degradation properties and bioreactivity specific to a

particular TE application.[7] In addition, bioactive glasses are suitable starting materials to develop glass-ceramics and composites, e.g. combining bioactive glasses with biopolymers.[8] As indicated above, there is experimental evidence to be briefly reviewed in this chapter and discussed extensively elsewhere,[6] considering both *in vitro* and *in vivo* studies, that bioactive glasses can serve as angiogenic agent to induce increased vascularisation when incorporated in bone TE constructs.

Table 5.1. *In Vitro* Studies Showing the Angiogenic Indicators Stimulated in Response to Bioactive Glasses.

Biological Response	Material	Reference
Enhanced mitogenic stimulation of endothelial cells	Bioactive glass coated cell culture plates	9, 10
	Alginate beads containing 0.1% (w/v) 45S5 Bioglass® particles	11
	0.6, 1.2 and 6 mg 45S5 Bioglass®-loaded collagen sponges	12
	Slabs of 5% ZnO (wt%)-doped 45S5 bioactive glass	13
	3D porous scaffolds made from poly (lactide-*co*-glycolide) with approximately 0.5 mg 45S5 Bioglass® particle coating	14
	3D porous scaffolds made from 45S5 bioactive glass	15
	Ionic dissolution products from 2% B_2O_3 (wt%)-doped 45S5 bioactive glass	16
Enhanced migratory and spreading capacity of endothelial cells	Ionic dissolution products from 2% B_2O_3 (wt%)-doped 45S5 bioactive glass	16
	SiO_2-CaO bioactive glass nanospheres	17
Increased formation of endothelial tubules	Bioactive glass coated cell culture plates	9
	1.2 mg 45S5 Bioglass®-loaded collagen sponges	12
Increased secretion of pro-angiogenic cytokines (i.e. VEGF, bFGF, IL-6)	Bioactive glass coated cell culture plates	9, 10, 18
	Bioactive glass/alginate beds	11
	PLGA/Bioactive glass composite disks	19
	Bioactive glass/PLGA porous microspheres	20
	PDLLA/Bioactive glass composite films	21
	Collagen/Bioactive glass scaffolds	12
	Ionic dissolution products from 2% B_2O_3 (wt%)-doped 45S5 bioactive glass	16

5.2. *IN VITRO* EVIDENCE

As summarised in Table 5.1, several cell biology *in vitro* investigations have shown that bioactive glass in particulate form, especially the composition 45S5 Bioglass®, as well as bioactive glass filled composites stimulate endothelial cell proliferation, migration and endothelial tubules formation.[9–17] Moreover, previous cell culture studies have demonstrated that bioactive glasses stimulate a significant increase in secretion of pro-angiogenic cytokines, such as vascular endothelial growth factor (VEGF) and basic fibroblast growth factor (bFGF) from fibroblasts[9–12] and interleukin-6 (IL-6) from endothelial cells.[16]

5.3. *IN VIVO* EVIDENCE

Previous *in vivo* studies have evaluated the effect of the incorporation of relatively small quantities of 45S5 Bioglass® (in particulate form) into scaffolds on the angiogenic response in both soft connective and bone tissues, as reviewed elsewhere.[6] In an early investigation in this field, a biodegradable polyglycolic acid (PGA) composite mesh coated with Bioglass® particles was implanted subcutaneously into rats.[9] It was shown that the composite scaffolds became infiltrated by a significantly higher number of blood vessels when compared with uncoated control scaffolds.[9] Related *in vivo* experiments showed that approximately 0.5 mg of 45S5 Bioglass® particles coated on a VEGF-releasing PLGA porous scaffold were capable of enhancing neovascularisation in a critical-sized cranial bone defect in rats.[14] In addition, greater neovascularisation and bone regeneration were found in irradiated critical-sized calvarial defects filled with collagen sponges loaded with 1.2 mg of Bioglass® in comparison to controls at two weeks post-implantation in rats.[22] More recently, the angiogenic properties of micron-sized (m-BG) and nano-sized (n-BG) 45S5 bioactive glass filled poly (D,L lactide)(PDLLA) composites were investigated in a rat model.[21] After eight weeks of implantation, m-BG and n-BG containing scaffolds were well-infiltrated with newly formed tissue and demonstrated higher vascularisation and percentage blood vessel to tissue than neat PDLLA scaffolds (Fig. 5.2).[21]

Employing the quail embryo chorioallantoic membrane as the experimental model, the authors have obtained preliminary data showing that there is a significant effect of the ionic dissolution products (IDPs) from 45S5 Bioglass® containing 2 wt% B_2O_3 (45S5.2B) on angiogenesis.[16] We evidenced that 45S5.2B IDPs have pro-angiogenic potential, as confirmed by increased endogenous expression levels of integrin $\alpha_v\beta_3$, a marker of angiogenic vascular tissue, 48 h after treatment and by a higher number of blood vessels as early as five days after treatment.[16]

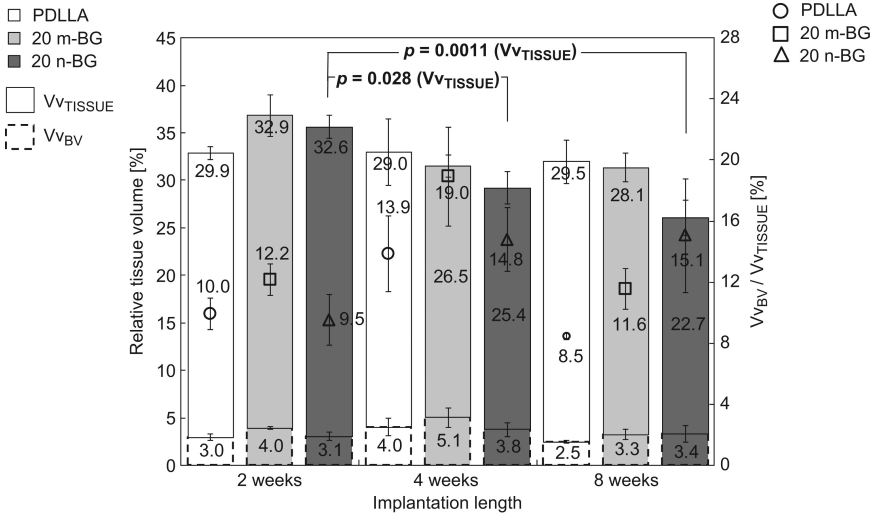

Figure 5.2. Effect of implantation length on *de novo* tissue growth and vascularisation of PDLLA-based composite scaffolds developed by Gerhardt *et al*.[21] The relative tissue volumes (Vv_{TISSUE} and Vv_{BV}) and the percentage of blood vessel to tissue are shown as means (n = 3; error bars: S.E.M). Data are shown for neat PDLLA, PDLLA/n-BG (20 wt%) and PDLLA/m-BG (20 wt%) composites. (Reproduced from Reference 21 with permission of Elsevier Inc.)

In addition to 45S5 Bioglass®, bioactive glasses and silicate glass-ceramics of other compositions are under investigation for their ability to promote angiogenesis.[23] In a recent study,[24] borate bioactive glass scaffolds (13–93B3) seeded with rat bone marrow-derived MSCs or doped with 0.4 wt% Cu, or a combination of both (MSCs + 0.4 wt% Cu), were reported to produce a significant increase in blood vessels after six-week subcutaneous implantation in rats, compared to the as-prepared 13–93B3 scaffolds.

5.4. CONCLUSIONS AND OUTLOOK

The application of bioactive glasses in bone TE scaffolds is widely beneficial, considering the investigated angiogenic potential of these materials, summarised in this chapter, in addition to their well-known osteogenic and bioactive potential, discussed in Chapters 3 and 4. *In vitro* studies have demonstrated increases in the concentration of angiogenic indicators through both direct and indirect contact of cells with 45S5 Bioglass® particles or with their

ionic dissolution products. Moreover, *in vivo* studies have confirmed the ability of certain bioactive glasses to stimulate neovascularisation. Given the well-established stimulatory effects of the dissolution products of bioactive glasses on cell behaviour in the context of bone regeneration,[25] further research should investigate the specific influence of relevant ions released from bioactive glasses and their relative concentrations on angiogenesis. In addition, correlation between scaffold morphology and neovascularisation remains an area for future investigation, including the effect of porosity, pore size, interconnectivity and pore orientation. In the field of composite scaffolds, the availability of bioactive glass nanoparticles and their successful incorporation in biodegradable polymers[26] provides an opportunity to assess the effect of enhanced surface bioreactivity and degradation rate, exhibited by nanoparticles, on angiogenesis and neovascularisation.

REFERENCES

1. Lovett, M., Lee, K., Edwards, A. *et al.* (2009). Vascularisation Strategies for Tissue Engineering, *Tissue Eng. Part B Rev.*, **15**, 353–370.
2. Phelps, E.A., Garcia, A.J. (2009). Update on Therapeutic Vascularisation Strategies, *Regen. Med.*, **4**, 65–80.
3. Das, A., Botchwey, E. (2011). Evaluation of Angiogenesis and Osteogenesis, *Tissue Eng. Part B Rev.*, **17**, 403–414.
4. Cleaver, O., Krieg, P.A. (2010). "Vascular development", in Rosenthal, N. and Harvey, R.P. (eds), *Heart Development and Regeneration*, Elsevier, New York, pp. 487–528.
5. Ghanaati, S., Unger, R.E., Webber, M.J. *et al.* (2011). Scaffold Vascularisation *In Vivo* Driven by Primary Human Osteoblasts in Concert with Host Inflammatory Cells, *Biomaterials*, **32**, 8150–8160.
6. Gorustovich, A., Roether, J.A. and Boccaccini, A.R. (2010). Effect of Bioactive Glasses on Angiogenesis: A Review Of *In-Vitro* and *In-Vivo* Evidences, *Tissue Eng. Part B Rev.*, **16**, 199–207.
7. Hench, L.L. (2009). Genetic Design of Bioactive Glass, *J. Eur. Ceram. Soc.*, **29**, 1257–1265.
8. Rezwan, K., Chen, Q.Z., Blaker, J.J. *et al.* (2006). Biodegradable and Bioactive Porous Polymer/Inorganic Composite Scaffolds for Bone Tissue Engineering, *Biomaterials*, **27**, 3413–3431.

9. Day, R.M., Boccaccini, A.R., Shurey, S. *et al.* (2004). Assessment of Polyglycolic Acid Mesh and Bioactive Glass for Soft-Tissue Engineering Scaffolds, *Biomaterials*, **25**, 5857–5866.
10. Day, R.M. (2005). Bioactive Glass Stimulates the Secretion of Angiogenic Growth Factors and Angiogenesis *In Vitro*, *Tissue Eng.*, **11**, 768–777.
11. Keshaw, H., Forbes, A. and Day, R.M. (2005). Release of Angiogenic Growth Factors from Cells Encapsulated in Alginate Beads with Bioactive Glass, *Biomaterials*, **26**, 4171–4179.
12. Leu, A. and Leach, J.K. (2008). Proangiogenic Potential of a Collagen/Bioactive Glass Substrate, *Pharm. Res.*, **25**, 1222–1229.
13. Aina, V., Malavasi, G., Fiorio Pla, A. *et al.* (2009). Zinc-Containing Bioactive Glasses: Surface Reactivity and Behaviour towards Endotelial Cells, *Acta Biomater*., **5**, 1211–1222.
14. Leach, J.K., Kaigler, D., Wang, Z. *et al.* (2006). Coating of VEGF-Releasing Scaffolds with Bioactive Glass for Angiogenesis and Bone Regeneration, *Biomaterials*, **27**, 3249–3255.
15. Deb, S., Mandegaran, R. and Di Silvio, L. (2010). A Porous Scaffold for Bone Tissue Engineering/45S5 Bioglass Derived Porous Scaffolds for Co-Culturing Osteoblasts and Endothelial Cells, *J. Mater. Sci. Mater. Med.*, **21**, 893–905.
16. Haro Durand, L., Vargas, G., Gongora, A. *et al.* (2011). Increased Angiogenesis Elicited by Boron-Containing Bioactive Glass, *Regen. Med.*, **6**(Suppl. 2), 263.
17. Hong, Z., Luz, G.M., Hampel, P.J. *et al.* (2010). Mono-Dispersed Bioactive Glass Nanospheres: Preparation and Effects on Biomechanics of Mammalian Cells, *J. Biomed. Mater. Res. A.*, **95**, 747–754.
18. Moosvi, S.R. and Day, R.M. (2009). Bioactive Glass Modulation of Intestinal Epithelial Cell Restitution, *Acta Biomater.*, **5**, 76–83.
19. Day, R.M., Maquet, V., Boccaccini, A.R. *et al.* (2005). *In Vitro* and *In Vivo* Analysis of Macroporous Biodegradable Poly(D,L-lactide-co-glycolide) Scaffolds Containing Bioactive Glass, *J. Biomed. Mater. Res.*, **75A**, 778–787.
20. Keshaw, H., Georgiou, G., Blaker, J.J. *et al.* (2009). Assessment of Polymer/Bioactive Glass-Composite Microporous Spheres for Tissue Regeneration Applications, *Tissue Eng. Part A*, **15**, 1451–1461.
21. Gerhardt, L.C., Widdows, K.L., Erol, M.M. *et al.* (2011). The Pro-Angiogenic Properties of Multi-Functional Bioactive Glass Composite Scaffolds, *Biomaterials*, **32**, 4096–4108.

22. Leu, A., Stieger, S.M., Dayton, P. *et al.* (2009). Angiogenic Response to Bioactive Glass Promotes Bone Healing in an Irradiated Calvarial Defect, *Tissue Eng. Part A*, **15**, 877–883.
23. Zhai, W., Lu, H., Chen, L. *et al.* (2011). Silicate Bioceramics Induce Angiogenesis During Bone Regeneration, *Acta Biomater.*, **8**, 341–349.
24. Rahaman, M.N., Day, D.E., Bal, B.S. *et al.* (2011). Bioactive Glass in Tissue Engineering, *Acta Biomater*, **7**, 2355–2373.
25. Hoppe, A., Güldal, N.S. and Boccaccini, A.R. (2011). A Review of the Biological Response to Ionic Dissolution Products from Bioactive Glasses and Glass-Ceramics, *Biomaterials*, **32**, 2757–2774.
26. Boccaccini, A.R., Erol, M., Stark, W.J. *et al.* (2010). Polymer/Bioactive Glass Nanocomposites for Biomedical Applications: A Review, *Comp. Sci. Technol.*, **70**, 1764–1776.

Chapter 6

BIOACTIVE GLASSES: CLINICAL APPLICATIONS — HISTORICAL

June Wilson, Antti Yli-Urpo and Risto-Pekka Happonen

6.1. INTRODUCTION

When it was first proposed that glass might be used as an implant material the concept was slow to find acceptance. The properties of glasses were, after all, well known. They are brittle, generally fragile and could easily be broken or fractured accidentally, generating particles or pieces which could migrate and which were expected to damage tissues and blood vessels. Glass could be cast or molded but could not be easily drilled or carved by any but expert hands.

The bioactive materials, which were glasses, had, however, other valuable properties. They would develop at their surfaces, when in contact with body fluids and tissues, a reactive layer which, because of its gel-like structure, provided a compliant interface between bulk glass and tissue. It was found that the 45S5 formulation of Bioglass® (registered U.S. Trademark, University of Florida, Gainesville, FL, USA, 32611) and related compositions did not break-up when drilled with standard surgical drilling equipment. The glass was relatively soft and extremely suitable for microsurgical drilling techniques, opening up its use in certain otolaryngological applications (Fig. 6.1), as discussed in Chapter 7. However, it could never be certain that particles would not appear after implantation of a solid device if it were to become damaged in some way, and exhaustive tests were done to find out what the effect of "ground glass" of this nature might be in tissues. Fortunately, the constituent chemicals, silicon, sodium, oxygen, calcium and phosphorous, are all found in the body and, at the concentrations derived from an implant, did not disturb the adjacent tissues. Particles could be ingested by phagocytic cells, those cells found in blood and tissues which are programmed to pick up and digest all unusual particles, and did not affect the viability or behavior of those cells. Particles could be injected into the bloodstream and come to rest in the capillary bed, but did not cause any emboli or detectable effect on blood flow. Many other tests showed that these bioactive glasses in solid or particulate form were not toxic to any of the tissues or systems with which they were in contact.[1] They were shown to bond to osseous tissues and

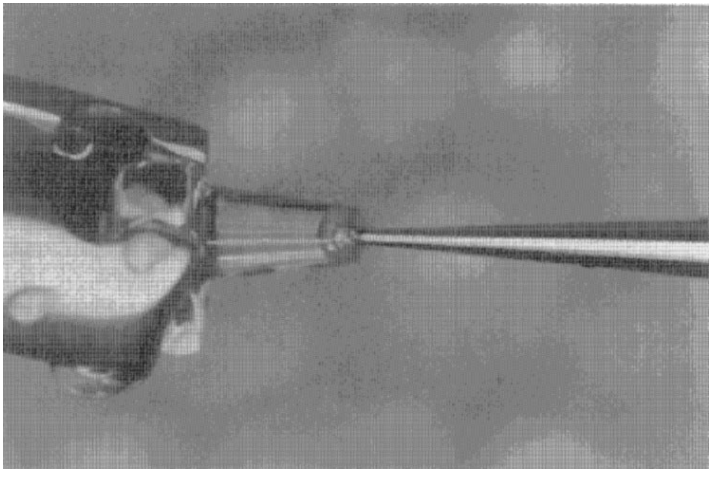

Figure 6.1. The stem of a Bioglass® middle ear prosthesis is being drilled to fit over the stapes. The facet is approximately 0.5 mm wide.

to soft tissues through a compliant interface and these special properties defined the clinical applications for which they were first used.[1]

Compositions of Bioglass®, notably 45S5, and the glass designated #9 (S53P4) from Finland have been tested in many medical and dental applications. See Chapter 3 for the chemical compositions of these glasses and the mechanisms of bonding to tissues. Applications have required several different forms of the material:

1. Solid shapes.
2. Particulates of various size ranges.
3. Particulates combined with autologous bone particles.
4. Particulates delivered via an injectable system.

Results of clinical applications are discussed in Chapters 7–12 and 30–34.

6.2. SOLID SHAPES

The glasses can be fabricated by casting into shaped implants for specific purposes where mechanical strength is of secondary importance.[2]

The first successful use of 45S5 Bioglass® was as a replacement for the ossicles in the middle ear, as a treatment for the conductive hearing loss which

develops when the sound waves impinging on the tympanic membrane do not reach the oval window in the inner ear (Chapter 7). Conduction loss in the middle ear can result from trauma, chronic infection or be due to congenital abnormality. Replacement of one or more of the ossicles can restore the continuity of the conducting system. Materials previously used have included polymers, both porous and solid, and metals of various types. These nearly inert biomaterials engender a fibrous tissue reaction which effectively holds the implant in place. Scar tissue around an implant, however, will dampen rather than transfer sound waves, and implants which promote scar tissue become gradually less efficient. The major mode of failure is extrusion through the tympanic membrane. When metal or plastic implants are in continuous contact with the soft tissue of the eardrum they wear through and are lost through the hole. These two problems, immobilization by a means other than fibrous tissue and prevention of extrusion, are solved by the special properties of 45S5 Bioglass®, which bonds to both hard and soft tissues.[1,3] A bone bond can be achieved with the remainder of the stapes if it can be retained to protect the connection at the oval window. A collagenous bond mimicking the normal connection between ossicles can also be achieved if necessary (see Chapter 3). Most importantly, the soft tissue bond between the implant and the tympanic membrane eliminates the movement at that interface, which leads to extrusion. Success has been achieved by 45S5 Bioglass® devices even after a previously damaged tympanic membrane has been repaired with a skin or muscle graft. A typical device is shown in Fig. 6.2. The stem of the implant may be

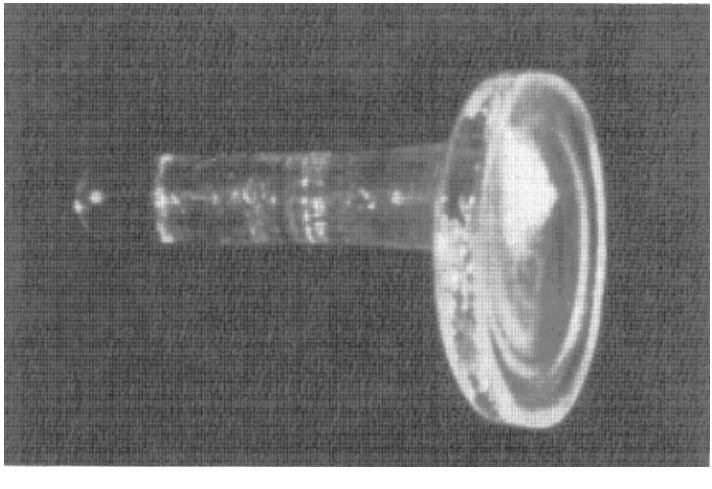

Figure 6.2. A Bioglass® middle ear device.

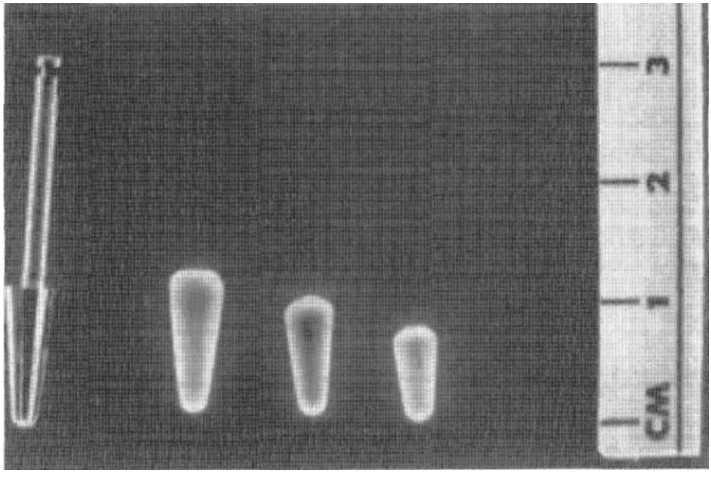

Figure 6.3. Endosseous ridge maintenance devices (ERMI) and matching dental burr.

shortened and shaped to fit the individual patient. These and similar devices have been in clinical use for many years (Chapter 7).

In oral surgery, cone-shaped devices made from 45S5 Bioglass® have been used to fill the defect in the jaw which is created when a tooth is removed (Fig. 6.3).[4–6] Chapter 8 describes this clinical application. Removal of one or more teeth produces changes in the jaw bone which are followed by gradual bone loss, so that the normal shape of the bone which supports healthy teeth changes to a narrow "knife edge" ridge with reduced height, which cannot comfortably support dentures. Without some means of preventing this bone loss, denture wearers are often destined to suffer increasing discomfort from ill-fitting dentures and in many cases may eventually become unable to wear dentures at all. These devices have now been in use for almost a decade and those made from bioactive glass have proven to be more successful than others which have been tried (Chapter 8).

In Finland, an innovative use of solid, cast bioactive glass implants has been used in the treatment of facial injuries in which the bone which supports the eye is damaged. Such "blow out fractures" of the orbit have been treated by the insertion of a curved implant of bioactive glass to restore the floor of the orbit (Fig. 6.4).[7,8] A series of curved plates is cast and the most suitable one is selected by the surgeon at the operation. Chapter 10 summarizes maxillofacial repair using 45S5 Bioglass® implants. Chapter 12 describes the use of the Finnish bioactive glass composition S53P4 in various types of spinal surgeries.

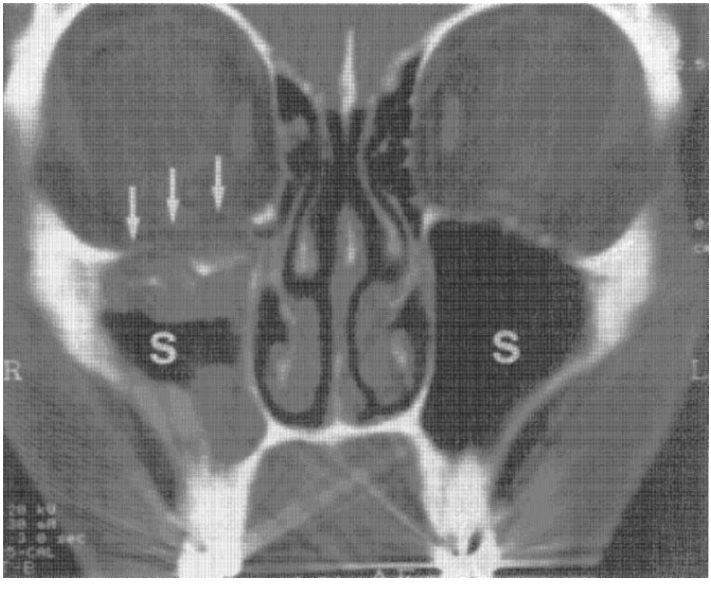

Figure 6.4(a). Computer tomography (CT) of a 23-year old man demonstrates blow-out fracture of the right orbital floor (arrows) with herniation of orbital tissues into the maxillary sinus (S).

Another use with potential for wide application is that of providing a soft tissue seal for an implant which passes through the skin. Electrodes, which are an essential part of an extracochlear implant, developed at the University of London to treat profound deafness, must be connected both to the cochlea (or inner ear) and to the complex electronics on the outside. Any material that passes through the skin and subcutaneous tissues without an effective seal can provide a channel along which bacteria, which are always present on the skin, can move to cause infection. This is particularly dangerous in any positioning close to the brain because of potentially fatal meningitis. The anchors containing the electrodes in this implant are coated with 45S5 Bioglass® and are implanted in the cranium. The implant is placed so that part is in bone, where the Bioglass® provides a bond to immobilize it. The part which passes through the skin bonds to the soft tissues and provides the essential seal. The soft tissue bond is protected from damage due to movement by the bone bond and relatively thin layer of soft tissue overlying it. Such implants have been in place for several years with no significant problems.[4,5]

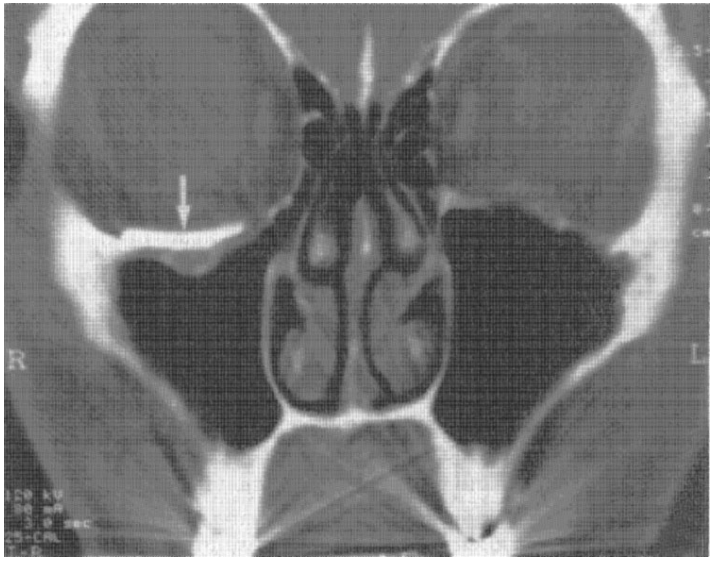

Figure 6.4(b). CT scan of the same patient taken four months after correction of the fracture using a curved bioactive glass (S53P4) implant (arrow). (Courtesy of Dr. Kalle Aitasalo, Department of Otolaryngology, University Central Hospital of Turku, Turku, Finland.)

6.3. PARTICULATES OF VARIOUS SIZE RANGES

Bioactive glass in the form of particulate has found application in the treatment of periodontal disease.[9] In this condition the area of gum, and eventually bone, which surrounds the teeth becomes infected and in consequence the attachment of soft tissue which seals and supports the teeth is broken and infection reaches the bone, which is then destroyed (Fig. 6.5). As these supporting structures break down, the teeth are lost. More teeth are lost due to periodontal disease than for any other reason. The condition is treated by combinations of surgery and antibiotics, but it is essential to replace lost bone and soft tissue connections if teeth are to be saved. Bioactive glasses have been shown to be effective for this use. In animal studies it was shown that bone and soft tissue connections were restored to a level close to that of normal teeth when a bioactive glass (45S5 Bioglass®) which could bond to hard and soft tissues was used. Results were much better than with hydroxylapatite materials previously used.[9] These findings have been confirmed in clinical trials. Clinical use of this 45S5 Bioglass® product (PerioGlas®) is summarized in Chapter 9.

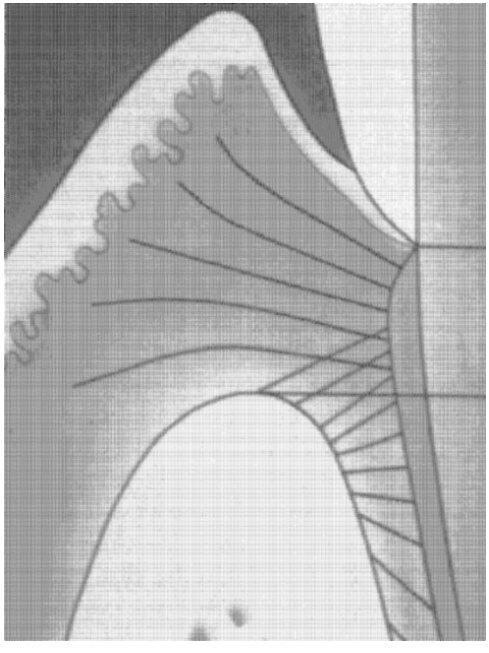

Figure 6.5(a). The normal structure of the periodontium, with insertion of the fibers of the periodontal ligament above the alveolar bone.

Another application which is being developed using 45S5 Bioglass® particulate is for the treatment of patients with paralysis of one of the vocal cords. Such patients typically have had surgery, which may be for many different reasons, in which the nerve to the cord is cut. Sounds are produced when the vocal cords on each side of the larynx, which form a V shaped opening through which air is breathed, come together and vibrate as air is expelled from the lungs and passes over them. If one or both cords cannot move, proper sound production cannot occur because air escapes and the voice is "breathy". In addition, the normal vocal cords protect the airway from aspiration of fluids and infection. Any treatment which can move the paralyzed cord close to the functional one so that closure can occur is effective in restoring voice and preventing infection. Such a treatment can be obtained by placing particulate Bioglass® behind the paralyzed cord. The material remains bonded in the soft tissues, producing an augmentation which displaces the paralyzed cord to where it can function. The augmentation is more effective than that produced by an injectable material of PTFE, which has been used for this purpose,

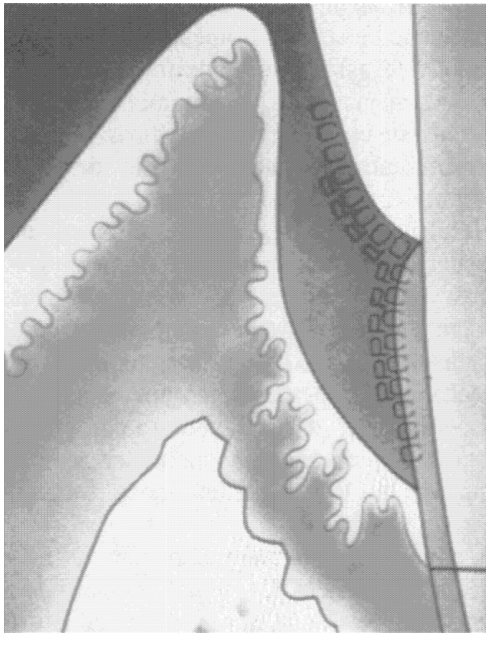

Figure 6.5(b). The changes due to periodontitis. The fibers have been disrupted and the bone eroded. A successful treatment for this condition must restore the periodontal ligament as well as augment the alveolar bone. (Figures courtesy of Dr. Samuel B. Low, Department of Periodontology, College of Dentistry, University of Florida, Gainesville, Florida.)

because of the bonding to soft tissue which occurs and retains the bioactive glass at the site. The augmentation is due to the retained glass and not the granulomatous reaction to an inert polymer, which can disappear with migration of polymer beads from the site. Such migration has produced embolism distant from the site, which has been damaging. There are no such emboli after administration of particulate Bioglass®. Attempts to detect emboli have included light microscopy of adjacent tissues, drainage and other lymph nodes as well as chemical analysis of tissues in which emboli might conceivably be found. No sign, either direct or indirect, of migration of Bioglass® particles has been found, and this, combined with specific administration of particulates *in vivo* and *in vitro* during toxicity testing, show that migration and embolism are not a problem.[1]

6.4. PARTICULATES WITH AUTOLOGOUS BONE

The success of particulate material in restoring bone in the periodontal area, where the surgical site preparation releases bone fragments and associated growth factors to combine with the bioactive glass, has led to a series of investigations in which the glass has been mixed with autologous bone before implanting.[6] The best material for restoring lost or damaged bone for reconstructive and cosmetic reasons is undoubtedly fresh autologous bone, which carries none of the potential problems of rejection or viral contamination that are of concern when banked or freeze-dried bone are used. See Chapter 10 for details. Such bone can be harvested locally or from a site such as the iliac crest and it is the "gold standard" for bone grafts. However, it is rarely available in large quantities and removal may leave a compromised ilium, which may itself then need treatment. In addition, there is significant morbidity associated with this procedure. Applications in which available autologous bone fragments are extended by mixing with bioactive glass are used in maxillofacial reconstruction (Chapter 10). Granules, powders and small blocks of glasses 45S5 and S53P4 have been combined, using a layering technique with available bone in patients with bone defects resulting from bone cysts and tumor removal. Patients with chronic frontal sinus infections, chronic pansinusitis and mucocele have been successfully treated in this way. A particular advantage seems to be the flexibility within the system, using blocks, powder, granules and bone as needed and as available. Successful results have been achieved in patients with conditions that have been considered intractable. For many reconstructive purposes, the mechanical properties of the bone used are secondary in importance to the implant's ability to fill space and be stable. Some applications exist in which improvement in mechanical properties as well as volume is desirable. One such application is the reconstruction of the lower jaw, or mandible, after tumor removal or post-traumatic injury. For details see Chapter 10. The restored mandible must be both aesthetically pleasing and be able to support the stress of chewing. Microsurgical techniques have been developed which permit successful movement of a piece of bone, together with a blood supply. The bone chosen is usually rib, but sometimes it is the fibula, and the aesthetic requirement of a reconstructed mandible can be met. Unfortunately such bone is rarely strong enough or big enough to satisfy mechanical requirements. In experiments using 45S5 Bioglass® particulates combined with autologous bone fragments in dogs, ribs have been augmented to up to ten times their original cross-sectional dimension. This increase in bone volume will supply more satisfactory mechanical properties when bone augmented in this way is used in load bearing situations.

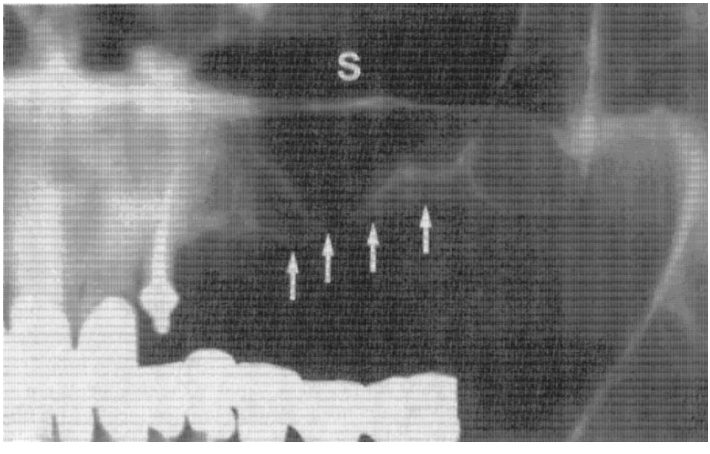

Figure 6.6(a). Radiograph of a 69-year old woman shows that the amount of bone in the area of left maxillary sinus (S) is insufficient (arrows) to support dental implants. A sinus lift operation using a mixture of bioactive glass granules and autologous bone chips was made to achieve more bone on the floor of the maxillary sinus. Implants were inserted eight months after the sinus lift operation.

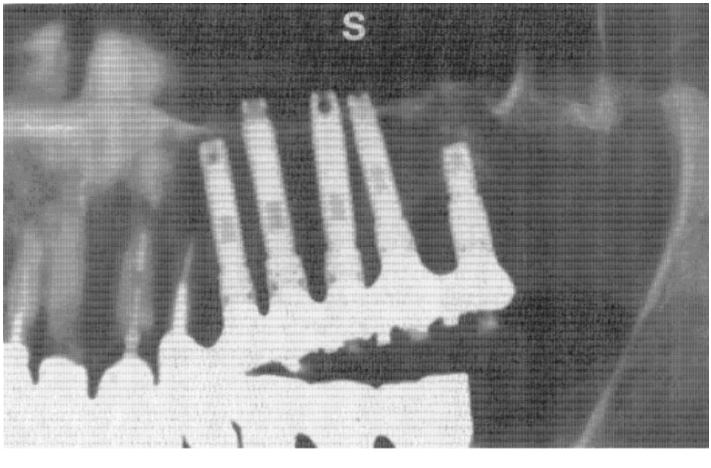

Figure 6.6(b). Radiograph of the same area six months after insertion of implants of S53P4 bioactive glass shows considerable increase in the amount of bone on the floor of the maxillary sinus. Note good osseointegration of the fixtures. (Courtesy of Dr. Juha Peltola, Department of Oral Diseases, University Central Hospital of l'urku, Turku, Finland.)

However, this will require careful long-term follow-up studies since all bone (autologous, freeze dried or augmented) remodels under use conditions and the final remodeling will not take place until some time after transplantation.

A mixture of bioactive glass granules and autologous bone chips has also been used in situations where the amount of bone is insufficient for dental implants to be inserted. This is a rather common problem in posterior parts of the upper jaw (or maxilla), where, as a result of resorption of the alveolar crest, only a thin bone plate many be found in the floor or maxillary sinus. In such situations the mixture is grafted to the floor of the maxillary sinus, around fixtures projecting into the sinus. Results of this so called "sinus lift" operation are promising (Fig. 6.6).

Hench, Hench and Greenspan review numerous publications of this application.[6] Various orthopedic applications are presented in Chapters 11 and 12. Potential applications in tissue engineering are given in Chapter 32. New approaches to prevent tooth pain sensitivity and dental cavity preparation using 45S5 Bioglass® powders are presented in Chapters 30 and 31, respectively.

6.5. PARTICULATES BY INJECTION

A final group of applications are those which depend on the soft tissue adhesion of these materials and which are facilitated by the ability to introduce them by injection. For such applications, the interrelationships between particle size and shape, characteristics of the vehicle and needle size and length provide many problems which need to be solved before bioactive glasses may be used in this way. When these problems can be overcome and the bioactive glass particles placed as required the treatments are effective. Preclinical experiments in animals have concentrated on the treatment of two urological conditions which occur in children and some adults.[6]

The principle of tissue augmentation is the same as described for the movement of vocal cords, which is to augment specific areas of soft tissue safely (and as far as possible) permanently in a controlled fashion. In patients with incontinence due to decreased urethral resistance, such as those with spina bifida and bladder exstrophy, effective treatment results from tissue augmentation periurethrally, which increases urethral resistance. Such treatment with a suspension of PTFE has been effective, but for reasons already given, a replacement material is needed. When tested in an animal model, marked increases in urethral resistance were achieved and were maintained up to three months. The treatment is expected to be equally effective in children and clinical trials await the development of a satisfactory combination of materials and delivery system.

A second condition, ureteral reflux, is also amenable to treatment by specific localized areas of soft tissue augmentation. In this condition there is a failure of the mechanism which normally prevents a back flow (or reflux) of urine from the bladder to the ureter. Such reflux allows bacteria, found normally in the bladder, to reach the kidneys, causing pyelonephritis and associated kidney damage. If reflux cannot be prevented, treatment must include a lifetime of antibiotic therapy, which is undesirable. If the soft tissues beneath the ureter, at the point where it enters the bladder, can be augmented, the reflux can be controlled. Preclinical experiments in animals have shown that this is feasible. However, clinical application requires that injection be made via an endoscope to avoid open surgery, particularly since the injection may need to be repeated if the effect is found to be insufficient or transitory. Clinical trials again await the development of a satisfactory combination of materials and delivery system. Hench, Hench and Greenspan summarize these studies with references.[6]

6.6. SUMMARY

Bioactive glass materials are available in a range of compositions and implant shapes which are able to bond to soft tissues and/or bone. These materials vary in their reactivity and speed of bonding and in the ability of the bone to provide mechanical strength. They have been successfully applied as solids and particulates and may be combined with other materials, both natural and synthetic, to provide treatment for many disparate clinical conditions.

REFERENCES

1. Wilson, J., Pigott, G.H., Schoen, F.J. *et al.* (1981). Toxicology and Biocompatibility of Bioglasses®, *J. Biomed. Mater. Res.*, **15**, 805–817.
2. Wilson, J., Merwin, G.E. and Hench, L.L. (1985). Machining Bioglass® Implants, *SAMPE Journal*, **21**, 6–8.
3. Wilson, J. and Nolletti, D. (1990). "Bonding of Soft Tissues to Bioglass®", in Yamamuro, T., Hench, L.L. and Wilson, J. (eds), *Handbook of Bioactive Ceramics, Vol. I, Bioactive Glasses and Glass-Ceramics*, CRC Press, Boca Raton, FL, pp. 283–302.
4. Stanley, H.R., Hall, M.B., Colaizzi, F. *et al.* (1987). Residual Alveolar Ridge Maintenance with a New Endosseous Implant Material, *J. Prosthetic Dentistry*, **58**, 607–613.

5. Hench, L.L. (1998). Bioceramics, *J. Am. Ceram. Soc.*, **81**, 1705–1728.
6. Hench, L.L, Hench, J.W. and Greenspan, D.C. (2004). Bioglass: A Short History and Bibliography, *J. Aust. Ceram. Soc.*, **40**, 1–42.
7. Wilson, J. and Merwin, G.E. (1988). Biomaterials for Facial Bone Augmentation: Comparative Studies, *J. Applied Biomaterials*, **22**, 159–177.
8. Thompson, I. (2011). "Clinical Applications of Bioactive Glasses for Maxillo-Facial Repair", in Hench, L., Jones, J.R. and Fenn, M.B. (eds), *New Materials and Technologies for Healthcare*, Imperial College Press, London, pp. 77–96.
9. Wilson, J. and Low, S.B. (1992). Bioactive Ceramics for Periodontal Treatment: Comparative Studies in the Patus Monkey, *J. Applied Biomaterials*, **3**, 123–129.

Chapter 7

CLINICAL APPLICATIONS OF BIOACTIVE GLASSES: ENT

Larry L. Hench

7.1. INTRODUCTION

The discovery of the composition of 45S5 bioactive glass (Bioglass®) in 1969 and the surface reaction mechanisms that result in the formation of a chemical bond with living tissues is described in Chapter 3.[1–3] For many years it was assumed that only bone would form a bond to bioactive materials, including bioactive glasses, glass-ceramics and calcium-phosphate based bioceramics, as discussed in Chapters 3–20.[1–3] However, a seminal paper by Wilson *et al.* in 1981 proved that soft connective tissues could also form a bond to 45S5 Bioglass®.[4] Dr. Wilson continued the investigation of the interfacial interaction of soft tissues and established, in a key paper with David Nolleti, the compositional dependence of the bonding of bioactive glasses to soft tissues.[5] This paper showed that only glass compositions with sufficiently rapid surface reaction rates would form a soft tissue bond. The rapidly growing silica-rich surface layer nucleates growth of a thicker hydroxylcarbonate apatite (HCA) layer that chemically bonds to collagen fibrils produced by fibroblasts at the implant–tissue interface. The thickness of the bonding layers increase with time, as reviewed in Chapter 8. The thickness after several months is several hundred micrometers, equivalent to natural junctions between hard and soft tissues, such as tendons, ligaments and bone or the periodontal ligament and teeth. The capability of both hard and soft tissue bonding is of special relevance to this chapter. The thickness of the bonding layer between ossicles and the tympanic membrane (TM (ear drum)) are duplicated by the 45S5 Bioglass® implant.[5–7] The soft tissue bonding glasses are restricted to glass compositions in the middle of the bioactive boundary described in Chapter 3. These compositions of bioactive glass that exhibit both bone and soft tissue bonding are termed Class A bioactive materials.[1–5] When the glass composition exceeds 52% by weight of SiO_2 the glass will bond to bone but not to soft tissues, and are termed Class B bioactive materials. This finding of stable strong interfacial bonding to soft tissues as well as bone provided the basis for the clinical use of Bioglass® in ossicular replacement, reconstruction of other ear, nose and throat (ENT) defects and also for implants to maintain the alveolar ridge of edentulous patients (Chapter 8).

7.2. CLINICAL NEED

Conductive hearing loss occurs when the pathway of acoustic transmission between the TM and the oval window is broken.[8,9] This can happen as the consequence of numerous pathological conditions, such as the dissolution of ossicles due to chronic middle ear infections (*otitis media*). The bacterial or viral infections can spread to the mastoid bone of the middle ear (*mastoiditis*). This is a severe condition that often requires surgical intervention which may involve removal of some or all of the auditory bones. Other conditions include the development of a *cholesteatoma*, which is a formation of cholesterol crystals in the middle ear that exert pressure on the surrounding tissues, including the ossicles, leading to damage of the bones. Many patients exhibit a combination of the above diseases and require surgery. Treatment to restore hearing requires restoration of the ossicular chain between the TM and the oval window. Lobel describes several of the types of devices used to replace missing ossicles.[9] Clinical success depends upon many factors and may be measured as improvement in hearing, change in the speech reception threshold, the air-bone gap and the pure tone average, discussed in reviews.[8–9] The major cause of failure is extrusion of the device used to replace all or parts of the ossicular chain through the tympanic membrane. A conference acknowledged that Wullstein was the first surgeon to recognize that alloplastic materials could be used to restore hearing in ENT patients with a destroyed stapes superstructure,[10] leading to worldwide acceptance, especially following work by Shea that pioneered the use of polyethylene devices for middle ear prostheses.[10] The early work was reviewed in an international meeting in 1983 with the conclusion that "The short-term results with all alloplastic materials were usually excellent but the implants tended to extrude with time when they were in contact with the eardrum".[10]

7.3. ALTERNATIVE OSSICULAR PROSTHESES

An extensive review by Lobel describes the numerous types of materials and device designs used to restore the ossicular chain.[9] For many years homografts and autografts were considered the best available material for repair or replacement of ossicles. However, concerns over availability of graft material from cadavers and transmission of diseases that can affect the neurological system, such as prions, have led to use of allografts. Polyethylene (PE) devices used with and without cartilage between the implant and the TM have been the most popular.[9,10] Hydroxyapatite (HA), Ceravital® bioactive glass-ceramic and alumina implants have also been used for this application. Short-term success of

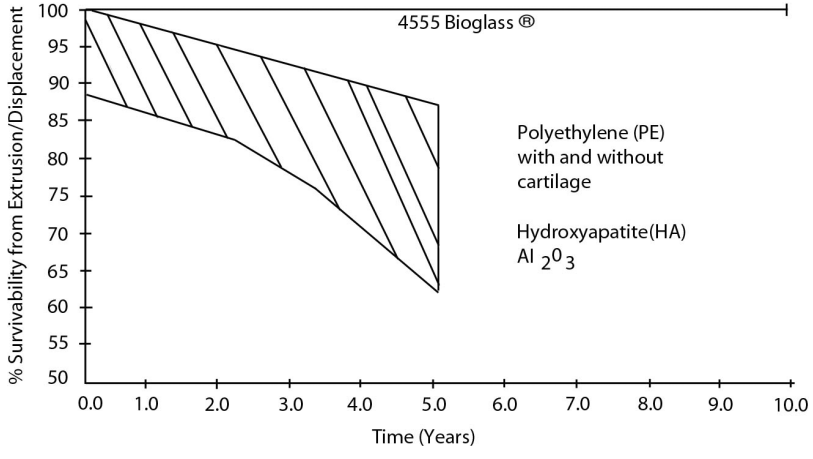

Figure 7.1. Survivability of various middle ear prostheses devices based upon loss by extrusion or displacement.

restoration of hearing was often achieved; however, it was rare to obtain long-term (>10 years) retention of ossicular replacement devices. Figure 7.1 summarizes the series of clinical results reviewed by Lobel.[9] Although various criteria for performance were reported in the review, the most significant is survivability of the implant from extrusion, the ordinate of Figure 7.1. The data show that survivability decreases greatly after three years post-implantation for either the bioinert (PE) or Class B (HA, Ceravital®) implants, becoming as great as 40% extrusion by five years. Extrusion of the device through the TM remains the primary cause of long-term failure.

7.4. FIRST BIOGLASS® CLINICAL PRODUCT: REPLACEMENT OF OSSICULAR BONES

The first Bioglass® clinical product cleared for marketing in the United States was a device used to treat conductive hearing loss by replacing the bones of the middle ear.[3] The device was called the "Bioglass® Ossicular Reconstruction Prosthesis", and trademarked "MEP®". The device was cleared via the 510(k) process in January 1985. It was a solid, cast Bioglass® structure that acted to conduct sound from the tympanic membrane to the cochlea. The advantage of the MEP® over other devices in use at the time was its ability to bond with soft tissue (tympanic membrane) as well as bone tissue. Tests of interfacial stability between Bioglass® implants and components of the ossicular chain were conducted in mice

by Merwin and Wilson at the University of Florida ENT department.[7] Successful bonding of small Bioglass® fibres to the stapes and the TM[11] were demonstrated, leading to ethical committee approval of clinical trials at the University of Florida.[8] The success of the early University of Florida trials[8] and evidence of bonding to the TM to prevent extrusion led surgeon Ellis Douek, head of ENT at Guy's Hospital in London, to start clinical trials as well. The results of ten-year follow-up of both clinical trials are presented in Wilson, Douek and Rust.[12] The most important finding was that no implant was lost by extrusion at any time during the ten years. Good quality of hearing was maintained in all of the patients examined that had intact implants. The study found that a few of the earliest implants had fractured at some time post implantation. The source of fracture was ascertained to be due to either microcracks developed from machining the implant to fit securely into the implant site or failure at post-stem junctions. These problems were alleviated in later devices by using a more robust and simpler design of the Bioglass® device, trademarked the Douek MED®. Use of the micromachining techniques reported by Merwin *et al.*[13] also prevents mechanical failure of the device post-implantation. The new design led to a follow-up trial of 22 patients that has been treated by Ellis Douek since 1992, with all of the patients having hearing improvement and no implant extrusions or fractures at the time of reporting.[12] Details of long-term follow-up of the University of Florida patients are in the paper by Rust *et al.*[14]

Other uses in head and neck surgery of bioactive glasses are described in the historical review and bibliography in Hench, Hench and Greenspan[3] and in Chapter 10.

7.5. RECONSTRUCTION OF THE POSTERIOR CANAL WALL

As mentioned above, *mastoiditis* is a severe condition caused by infection that often requires surgery.[15] Acute cases must have reconstruction of the attic and posterior canal to restore a proper anatomic configuration and function. The goal of the reconstruction is to create an aerated mastoid cavity which is contiguous with the tympanic cavity. Many materials have been utilized for reconstruction over the years, including a variety of autologous and synthetic options; the most popular being autologous elastic cartilage from the concha, widely considered to be the standard technique in attic and posterior canal wall reconstruction.[15] However, a limitation of this procedure is the need for second site surgery, with associated prolonged operative time and potential added morbidity.

Bioactive glass is likely to be the most suitable synthetic substitutes for conchal cartilage due to the ability to bond to both soft and hard tissues[1–7] and

produce an antimicrobial effect.[16] Prior studies in otology have tested 45S5 Bioglass® for ossicular and canal wall reconstruction.[14] A recent paper by Abramovich *et al.* has compared the effectiveness of bioactive glass implants with conchal cartilage in reconstructing the attic and posterior canal wall following tympanomastoidectomy.[15] A first cohort of 12 patients underwent attic and posterior canal wall reconstruction with autogenous conchal cartilage at St Mary's Hospital, London. A second cohort of 12 patients underwent reconstruction at St Mary's with prefabricated Bioglass® devices custom made by Dr. Ian Thompson at Guy's Hospital, London.

The results reported by Abramovich *et al.*[15] were:

> By one year postoperatively, both reconstructive graft materials showed good epithelialisation, no granulation, no infection, no ear canal stenosis and no extrusion. At operative second-looks, Bioglass particularly showed good tissue bonding, including both neovascularisation and connective tissue integration. Overall clinical outcome was equivalent for both materials. Both graft materials showed no statistically significant difference in post-operative hearing levels.

7.6. CONCLUSION

Bonding of Class A bioactive glasses to both bone and soft connective tissues, such as the tympanic membrane, make it possible to reconstruct components of the ear, nose and throat system and achieve long-term clinical results without extrusion of the implants.

REFERENCES

1. Hench, L.L. (1991). Bioceramics: From Concept to Clinic, *J. Amer. Ceram. Soc.*, **74**, 1487–1510.
2. Hench, L.L. (2004). Bioceramics, *J. Amer. Ceram. Soc.*, **81**, 1705–1735.
3. Hench, L.L., Hench, J.W. and Greenspan, D.C. (2004). Bioglass: A Short History and Bibliography, *J. Aust. Ceram. Soc.*, **40**, 1–42.
4. Wilson, J., Pigott, G.H., Schoen, F.J. *et al.* (1981). Toxicology and Biocompatibility of Bioglass, *J. Biomed. Mater. Res.*, **15**, 805–817.
5. Wilson, J. and Nolletti, D. (1986). "Bonding of Soft Tissues to Bioglass", in Christel, P., Meunier, A. and Lee, A.J.C. (eds), *Biological and Biomechanical Performance of Biomaterials*, Elsevier, Amsterdam, pp. 99–104.

6. Wilson, J. and Noletti, D. (1990). "Bonding of Soft Tissues to Bioglass®", in Yamamuro, T., Hench, L.L. and Wilson, J. (eds), *Handbook of Bioactive Ceramics Vol.1: Bioactive Glasses and Glass-Ceramics*, CRC Press, Boca Raton, FL, pp. 283–302.
7. Merwin, G.E., Atkins, J.S., Wilson, J. *et al.* (1982). Comparison of Ossicular Replacement Materials in a Mouse Ear Model, *Otolaryngol. Head Neck Surg.*, **90**, 461–469.
8. Merwin, G.E. (1990). "Review of Bioactive Materials for Otologic and Maxillofacial Applications", in Yamamuro, T., Hench, L.L. and Wilson, J. (eds), *Handbook of Bioactive Ceramics, Vol. I*, CRC Press, Boca Raton, FL, pp. 323–328.
9. Lobel, K. (1996). "Ossicular Replacement Prostheses", in Hench, L.L. and Wilson, J. (eds), *Clinical Performance of Skeletal Prostheses*, Chapman and Hall, London, pp. 214–236.
10. Grote, J.J. (ed.) (1984). *Biomaterials in Otology*, Martinus Nijhoff, Boston, MA.
11. Wilson, J., Atkins, J.S., Merwin, G.E. *et al.* (1985). Histopathological Evaluation of Interaction between Tympanic Membrane and Implant Materials, *Trans. Soc. Biomat.*, **8**, 195.
12. Wilson, J., Douek, E. and Rust, K. (1995). Bioglass® Middle Ear Devices: Ten Year Clinical Results, *Bioceramics*, **8**, 239–245.
13. Wilson, J., Merwin, G.E. and Hench, L.L. (1985). Machining Bioglass® Implants, *SAMPE Journal*, **21**, 6–8.
14. Rust, K.R., Singleton, G.T., Wilson, J. *et al.* (1996). Bioglass® Middle Ear Prosthesis: Long-Term Results, *Am. J. Otol.*, **17**, 371–374.
15. Abramovich, S., Hannan, S.A., Huins, C.T. *et. al.* (2008). Prospective Cohort Comparison of Bioactive Glass Implants and Conchal Cartilage in Reconstruction of the Attic and Posterior Canal Wall Following Tympanomastoidectomy, *Clin. Otolaryngol*., **33**, 553–559.
16. Wilson, A. and Newman, H. (2002). Particulate Bioglass Reduces the Viability of Bacterial Biofilms Formed on its Surface in an *In Vitro* Model, *Clin. Oral Implan. Res.*, **13**, 53–58.

Chapter 8

CLINICAL APPLICATIONS OF BIOACTIVE GLASSES: ENDOSSEOUS RIDGE MAINTENANCE

Larry L. Hench

8.1. INTRODUCTION

In 1984 it was estimated that nearly 10% of the US population, approximately 20 million, had all or most of their teeth missing, i.e. were edentulous. Many of these individuals were wearing dentures but 70% were dissatisfied with them.[1] A major source of the dissatisfaction was the continuous resorption of the alveolar ridges that support the denture. Alveolar ridge bone loss not only reduces stability of dentures but also contributes to a progressive deterioration of oral health and systemic health problems.[2] These complications are severe in elderly patients, especially those that have been edentulous for many years. Ridge resorption can progress so rapidly after tooth extraction that dentures cannot be worn for more than a short period of time before a reline or rebase is necessary. This is expensive and time consuming and may be impractical for many elderly patients on limited incomes. Often, resorption is severe enough that there is insufficient alveolar bone remaining for any denture retention. Consequently, extreme alveolar bone resorption is termed "a major disease entity" for the elderly.[2] The rapidly-increasing world population, combined with increased life expectancy, leads to a projected population of edentulous people in the range of 100–200 million by 2020. Thus, there is great need for a rapid, technically simple, inexpensive and effective means of maintaining the structure and stability of alveolar ridges following tooth extraction.

Loss of natural teeth quickly initiates a remodelling of the bone of the residual alveolar ridge.[1] The contour of the alveolar bone undergoes continuous change according to the degree of stress applied. The total amount of bone resorbed and the rate of resorption differ for each individual and can vary greatly in the same individual at different times.[1] Ridge resorption occurs most rapidly in the first 6–24 months after extraction. However, in some people resorption continues to remove large amounts of bone until death.[1] The resorption rate of the mandible is typically four times the rate of the maxillae.[2]

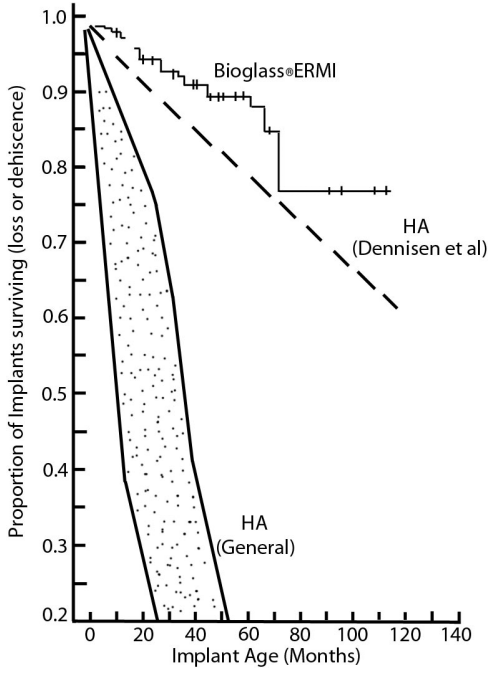

Figure 8.1. Survivability of alveolar ridge maintenance implants. See Stanley *et al.* for sources of clinical data represented in the graphs.[2]

8.2. THE IDEAL TOOTH REPLACEMENT

Various techniques have been tried to preserve or rebuild the edentulous alveolar ridge, most with limited success.[1,2] Since loss of natural tooth roots is the basic cause of loss of the alveolar ridge, the most logical biological approach to solving this problem is to replace natural tooth roots with artificial implants, as suggested and tried by Dennisen and colleagues.[3] Results of the early studies using synthetic hydroxylapatite (HA) ceramic cones to replace tooth roots were favourable.[3] However, subsequent studies in other clinics with similar HA ceramic cones resulted in much lower clinical success, as shown in Fig. 8.1, which is based upon data analyses of eight clinical studies.[2] Analysis of the cause of failure of the HA cones has led to a set of design criteria for an ideal tooth root replacement, first proposed by Stanley *et al*. in 1996[2] and expanded for this chapter as Table 8.1.

Table 8.1. Requirements for an Ideal Tooth Replacement Implant.

1) No evidence of early resorption of the implant material
2) Acceptable strength to fill the space without crushing under masticatory forces
3) Strong attachment to hard tissues at the implant–bone interface
4) Strong attachment to soft connective tissues at gingival interface
5) Normal distribution of forces to the alveolar bone
6) No adverse host reactions
7) Inexpensive
8) Easy to place in the tooth root socket with minimal socket preparation
9) Available in multiple sizes to match dimensions of the tooth root socket
10) Easy to sterilize
11) Easy to re-contour, when necessary

8.3. CLINICAL FINDINGS OF HA CONE IMPLANTS

Figure 8.1 summarizes the wide range of success and failure of HA cones based upon eight clinical studies reviewed by Stanley *et al*.[2] Their analysis of the HA failures suggests that numerous variables affected the clinical performance. These include: fit of the implant in the tooth root socket; technique of implantation; shape of the implant; contouring of the implant at time of surgery; primary closure; length of healing period prior to fitting of dentures; condition of the alveolar ridge at time of surgery and oral hygiene. They also concluded that:

> the concept of prevention of alveolar ridge resorption is valid for implants that remain in place. However, loss of HA implants by loosening or exfoliation is too high to justify general clinical use.[2]

8.4. BIOGLASS® ENDOSSEOUS RIDGE MAINTENANCE IMPLANTS (ERMIs)

The discovery of bone bonding[4] and soft tissue bonding[5] of 45S5 Bioglass® provided a new approach to satisfying all 11 criteria for an ideal tooth replacement material listed in Table 8.1. Until 1981 it was assumed that only bony tissues would form a bond to bioactive materials. A paper by Wilson *et al.* proved that soft connective tissues could also form a bond to 45S5 Bioglass®.[5] See Chapter 3 for a discussion of the composition and bonding mechanisms of 45S5 Bioglass®. This is one of the most important papers

in the history of Bioglass® technology and clinical product development for two reasons. The discovery of soft tissue bonding is one, as discussed in Chapter 3. The second is the extensive documentation in the paper of the results of more than 20 *in vitro* and *in vivo* tests that establish the safety of use of bulk as well as particulate forms of Bioglass® implants. This compendium of data provided the basis for ethical committee approval of the use of Bioglass® in clinical trials at the University of Florida, as discussed below.

Wilson continued investigation of the interfacial interaction of soft tissues and established, in a key paper with David Nolleti, the compositional dependence of the bonding of bioactive glasses to soft tissues.[6] Only glass compositions that exhibit rapid surface reaction rates form a soft tissue bond. These glasses are restricted to the compositions in the middle of the bioactive boundary, shown in Chapter 3. Details of the surface reactions are also discussed in several review articles.[7–9] When the glass composition exceeds 52% by weight of SiO_2 the glass will bond to bone but not to soft tissues. This finding provided the basis for clinical use of Bioglass® in ossicular replacement (Chapter 7) and also for implants to maintain the alveolar ridge of edentulous patients, the subject of this chapter.

By the mid 1980s sufficient animal data had been accumulated that safety of use of bioactive glasses as prostheses seemed assured.[5,10,11] Ethical permission was obtained from the J. Hillis Miller Health Center at the University of Florida to commence clinical trials of endosseous ridge maintenance implants for preservation of the alveolar ridge, and these trials began in the College of Dentistry under direction of Dr Harold Stanley, Professor and Chairman of Oral Medicine, and Drs A.E. Clark and Matt Hall. Successful results from these trials[12] led to application for regulatory approval by the FDA for commercial use of Bioglass® prostheses. See Chapters 38 and 39 for a discussion of the pathways for regulatory approval and Chapter 40 for the technology transfer steps that lead to a commercial product.

The second Bioglass® device to be placed into the US market was the Endosseous Ridge Maintenance Implant (ERMI®), which was cleared via the 510(k) process in November 1988.[7] The device was intended to support labial and lingual plates in natural tooth roots and to provide a more stable ridge for denture construction following tooth extraction. The devices were simple cones of 45S5 Bioglass® that were placed into fresh tooth extraction sites. They bonded to the bone tissue and proved to be extremely stable, with much lower failure rates than other materials that had been used for that same purpose. A number of clinical studies supported the regulatory clearance and have been published as reviewed previously.[2,7]

8.5. FEATURES OF 45S5 BIOGLASS® RELEVANT TO AN IDEAL TOOTH ROOT REPLACEMENT

There are several characteristics of 45S5 Bioglass® that satisfy some of the most critical requirements of an ideal tooth root replacement listed in Table 8.1.

1) The bioactive material bonds rapidly to both cortical and cancellous bone.
2) The material forms an adherent bond with the collagen of soft connective tissues.
3) It develops an inorganic interfacial reaction zone of 200–300 μm thickness composed of an elastically compliant hydrated silica gel layer and a hydroxylcarbonate apatite (HCA) layer bonded to tissues. The inorganic bonding zone mimics the thickness and mechanical properties of the periodontal membrane.
4) It stimulates proliferation of bone due to activation of bone progenitor stem cells which leads to interfacial bonding within a few weeks of implantation and regeneration of bone to fill spaces between the implant and living tissue.
5) The chemically bonded interface between the implant and host bone transfers stress to maintain the health of the bone and prevent resorption.

8.6. CLINICAL RESULTS OF 45S5 BIOGLASS® ERMIs

Figure 8.1 summarizes the results of a series of clinical studies published by Stanley *et al*. during the period 1986–1994.[1,2,13] Long-term follow-up of 20 of the original 29 patients consisted of 12 males and 8 females, with a mean age at the time of surgery of 42.3 years (range 24–76 years).[13] Originally a total of 168 implants were placed in these patients; 14 received complete maxillary/mandibular dentures and 6 received the combination of a complete maxillary denture and a mandibular removal partial denture. After an average post-implant period of 51.13 months (range 36–71 months) a total of 21 (12.5%) implants had been lost (average 30.9 months) and 13 (7.7%) had been recontoured (average 17.0 months, range 4–64 months). Of 83 cones placed in the maxilla, three (5.3%) of 57 in anterior sites and three (17.6%) of 17 in posterior sites were lost. Of 85 placed in the mandible, 9 (17.3%) of 52 were lost from anterior sites and 4 (12.1%) of 33 from posterior sites.

Generally, the anterior mandible has the highest implant survival rate and the posterior maxilla the lowest survival rate, success usually declining when implants are placed in more porous bone. In the 20 recalled patients, the order of

success of the implants was: maxillary anterior implants had the highest success rate; second were mandibular posterior implants; third the maxillary posterior implants; and least successful were the mandibular anterior implants.

Requirements of recontouring of the implants and relining of the dentures are summarized in previous reviews. The average time interval for a reline of the maxillary complete denture in patients with a removable mandibular partial denture was shorter (10.9 months) than the average interval for reline in patients with two complete dentures (14.4 months). Early use of dentures to slow the rate of resorption after ERMI implantation did not seem to be important. The initial early rate of alveolar ridge resorption, which takes the remaining bone down to the level of the implanted cones, continues, regardless of the time placement of dentures. The results of Figure 8.1 show that 45S5 Bioglass® ERMIs will probably succeed in any location, provided there is sufficient bone present and they are placed deeply enough to provide interfacial stability and dentures are placed after sufficient healing time of the soft tissues.[1,2,13]

8.7. FACTORS FOR CLINICAL SUCCESS

Differences in clinical methods as well as variables in the implant materials and designs are responsible for the large difference in clinical success of Bioglass® cones versus the general failure of HA cones in edentulous patients. The most important differences are summarized here, based upon analysis and reviews by Stanley.[1,2,13]

1) Bioglass® cone implants were placed deep in the ridge, 2 mm below the crestal bone, to maximize bone–implant contact, leading to a tight fit that was immobile. This deep placement also avoided any need to recontour the implant itself. Placing the implants below the crestal protected them from permucosal dehiscence due to bone resorption and pressure mobilization induced by removable prostheses.
2) Special dental burs were developed that matched the shape and dimensions of the cone implants.
3) The burs were used at low speeds of <2000 rpm with copious irrigation to prepare the bone bed for the implant immediately post-extraction. This protocol thereby minimized trauma to the implant site and preserved a bone bed with sufficient number of osteoprogenitor cells to rapidly regenerate bone. See Chapter 3 for details of the steps and requirements for bone regeneration in the presence of Class A bioactive implants such as 45S5 Bioglass®.

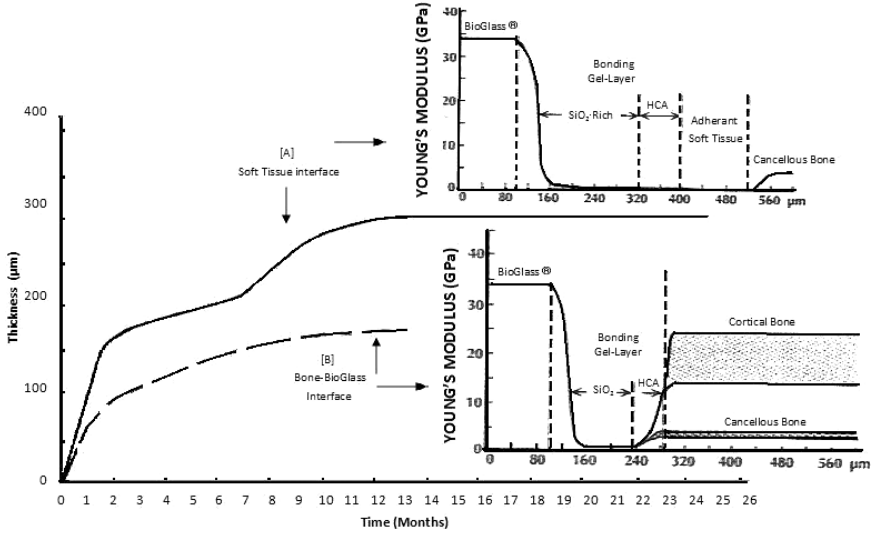

Figure 8.2. Development of reaction layers on Bioglass® ERMI ridge maintenance implants for (A) soft tissue interface and (B) bone interface. Inserts are the calculated elastic modulus gradients of the (A) implant–soft tissue interface and (B) bone–implant interface. The figure is based upon results of Wilson *et al.* and Weinstein *et al.*[14,15]

4) The ERMI implant system consisted of a set of 12 conical implants with rounded tops and 4 burs. The range of sizes of the implants made it possible to match implant to dimensions of the tooth socket and thereby ensure a close fit with minimal site preparation.
5) Use of a primary mucosal closure by suturing.
6) Delay of placement of dentures for at least six weeks to allow implant–tissue bonding to occur without disturbance of the bioactive interface.

Rapid formation of the interfacial bonding layers and fast regeneration of new bone at the implant–bone interface makes the Bioglass® implant stable and ensures proper stress transfer to the alveolar bone to prevent onset of resorption. A study in dogs conducted by Wilson *et al*. using the same implants, burs and protocol as for humans made it possible to achieve a quantitative histomorphometric analysis of the hard and soft tissue bonding interfaces of the ERMIs.[14] Within three months the bonding had stabilized for both hard and soft tissues. The soft tissue was bonded by collagen fibres interdigitated in a 150–400 µm thick bonding gel layer composed of biological HCA and an

underlying silica-rich gel layer that began to form on the implants within minutes of implantation (Fig. 8.2A). The thickness of the soft tissue bonding layer was nearly 50% thicker than the bonding zone between bone and the implant, shown in Fig. 8.2B. The thickness of both bone and soft tissue interfaces was stable after about seven months, as shown in Fig. 8.2.[14]

The elastic compliance (stiffness) of this bonding zone and the favourable stress transfer resulting from the bonding of collagen fibrils is likely to be related to the short- and long-term success of the 45S5 Bioglass® ERMIs.[15] In contrast, synthetic bioceramic HA implants bond much more slowly and form a bond only to bone with a thickness of bone–implant bond of less than 1 μm. This thin bonding interface results in a much greater, factor of 400, gradient of elastic modulus between the living and non-living materials. The unnatural gradient in elastic modulus results in large stress gradients to the bone[15] and stimulates resorption and failures, such as shown in Fig. 8.1.

8.8. CONCLUSIONS

The long-term success of 45S5 Bioglass® endosseous ridge maintenance implants (ERMIs) are attributed to rapid bonding to both bone and soft connective tissues that lead to a stable implant in the tooth root bed. All the conditions of an ideal implant for prevention of alveolar ridge resorption are met by the 45S5 Bioglass® ERMI system.

REFERENCES

1. Stanley, H.R. (1995). "Alveolar Ridge Maintenance Using Endosseously Placed Bioglass (45S5) Cones", in Wise, D.L. *et al*. (eds), *Encyclopedic Handbook of Biomaterials and Bioengineering; Part B: Applications Vol. 2*, Marcel Dekker Inc, New York, pp. 1559–1616.
2. Stanley, H.R., Clark, A.E. and Hench, L.L. (1995). "Alveolar Ridge Maintenance Implants", in Hench, L.L. and Wilson, J. (eds), *Clinical Performance of Skeletal Prostheses*, Chapman and Hall, London, pp. 255–270.
3. Denissen, H.W., Walk, W. and Veldhuis, A.A.H. (1989). Eleven-Year Study of Hydroxyapatite Implants, *J. Prosthet. Dent.*, **61,** 706–712.
4. Hench, L.L., Splinter, R.J., Greenlee, T.K. *et al.* (1971). Bonding Mechanisms at the Interface of Ceramic Prosthetic Materials, *J. Biomed. Mater. Res.*, **2**, 117–141.

5. Wilson, J., Pigott, G.H., Schoen, F.J. *et al.* (1981). Toxicology and Biocompatibility of Bioglasses®, *J. Biomed. Mater. Res.*, **15**, 805–817.
6. Wilson, J. and Noletti, D. (1990). "Bonding of Soft Tissues to Bioglass®", in Yamamuro, T., Hench, L.L. and Wilson, J. (eds), *Handbook of Bioactive Ceramics Vol. 1: Bioactive Glasses and Glass-Ceramics*, CRC Press, Boca Raton, FL, pp. 283–302.
7. Hench, L.L., Hench, J.W. and Greenspan, D.C. (2004). Bioglass: A Short History and Bibliography, *J. Aust. Ceram. Soc.*, **40**, 1–42.
8. Hench, L.L. (1991). Bioceramics: From Concept to Clinic, *J. Am. Ceram. Soc*., **74**, 1487–1510.
9. Hench, L.L. (1998). Bioceramics, *J. Am. Ceram. Soc.*, **81**, 1705–1728.
10. Hench, L.L. and Clark, A.E. (1982). "Adhesion to Bone", in Williams, D.F. and Winter, G.D. (eds), *Biocompatibility of Orthopaedic Implants*, CRC Press. Boca Raton, FL, pp. 212–245.
11. Stanley, H.R., Hench, L.L., Bennett, Jr., C.G. *et al.* (1981). The Implantation of Natural Tooth Form Bioglass® in Baboons — Long Term Results, *J. Oral Implant.*, **2**, 26–36.
12. Hall, M.B., Stanley, H.R., King, C. *et al.* Early Clinical Trials of 45S5 Bioglass® for Endosseous Ridge Maintenance with a New Endosseous Implant Material, *J. Prosthet. Dent.*, **58**, 607–613.
13. Stanley, H.R., Hall, B., Clark, A.E. *et al.* (1997). Using 45S5 Bioglass® Cones as Endosseous Ridge Maintenance Implants to Prevent Alveolar Ridge Resorption: A 5-Year Evaluation, *Int. J. Oral Maxillofac. Implants*, **12**, 95–105.
14. Wilson, J., Clark, A.E., Hall, M. *et al.* (1993). Tissue Response to Bioglass® Endosseous Ridge Maintenance Implants, *J. Oral Implantology*, **XIX**, 295–302.
15. Weinstein, A.M., Klawitter, J.J. and Cook, S.D. (1980). Implant–Bone Interface Characteristics of Bioglass Dental Implants, *J. Biomed. Mater. Res.*, **14**, 23–29.

Chapter 9

CLINICAL APPLICATIONS OF BIOACTIVE GLASSES: PERIODONTAL REPAIR

Paul Robinson II

9.1. INTRODUCTION

Periodontal disease (PD) affects the supporting structures of the teeth. Five to twenty per cent of all populations suffer from severe stages of generalized PD, while a majority of adults are affected by mild to moderate PD.[1] PD is believed to stem from a host response or the accumulation of bacteria on the gums and teeth, which can lead to subsequent degradation of the surrounding bone. Deposits of bacteria reside within films of plaque which can degrade the gum forming *pockets* around the teeth, thereby exposing deeper bony structure and increasing the risk of inflammation and infection. A number of factors that can exacerbate PD include poor nutrition, smoking, poor dental hygiene, accumulation of hard tarter deposits (*calculus*), low hereditary resistance and complications arising from diseases such as diabetes. This chapter will present the general structure of teeth, the common treatments for PD and the application of bioactive materials for the regeneration of dental tissues.

9.2. DENTAL TISSUE STRUCTURE

The hard tissue of the tooth is comprised of three calcified connective tissues (Fig. 9.1). The main body of the tooth — the *dentin* — is protected by hard *enamel* that protrudes above the gum line. The remaining dentin sits within the bony socket below the gum line and is encased by the *dental cementum*. Categorically, the enamel and dentin form the *anatomical crown*, while the subgingival dentin and dental cementum constitute the *anatomical root*. Within the dentin is the pulp cavity containing loose connective tissue, blood vessels and nerve fibers.

Apart from the structure of the tooth are four common sub-gingival tissues affected by periodontal disease: (1) the gingivae, (2) the periodontal ligament, (3) the dental cementum lining at the tooth roots and (4) the alveolar bone.[1–4]

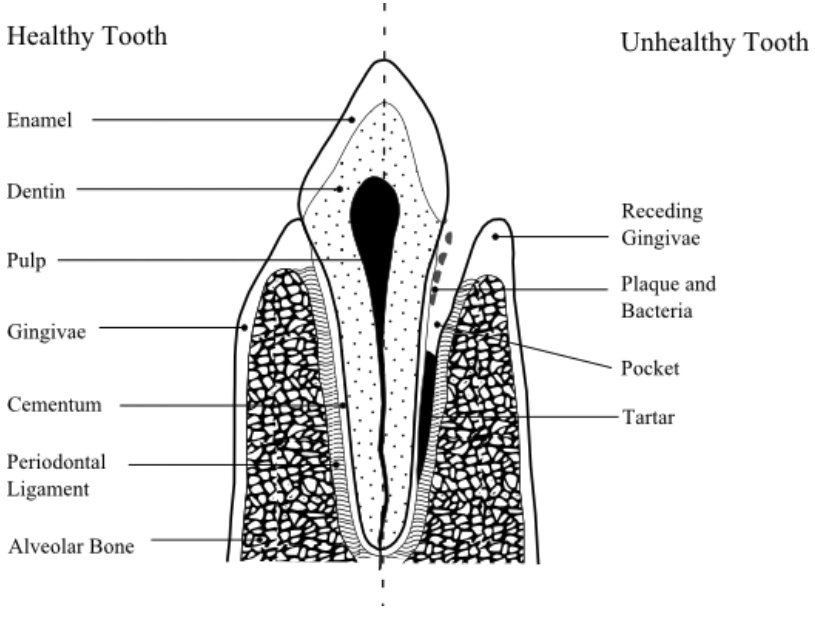

Figure 9.1. Tooth structure illustrating components of a healthy tooth (left) compared to unhealthy symptoms of PD (right). The anatomical crown includes supra-gingival structures, i.e. enamel and dentin; the anatomical root involves all other sub-gingival structures.

1. Gingivae: a fibrous tissue that attaches to the tooth by a specialized tissue lining called the *functional epithelium*, which seals the interface between the soft and hard tissues.
2. Dental cementum: this thin mineralized tissue of ectomesenchymal origin covers the roots of teeth. The dental cementum supports the attached tooth by anchoring embedded collagen fibers of the periodontal ligament.
3. Periodontal ligament: this highly vascularized and fibrous connective tissue of collagen fiber bundles surrounds and attaches the roots of teeth with the supporting alveolar bone socket. The periodontal ligament bears most of the mechanical forces that occur during normal oral activity. Since the turnover rate of the periodontal ligament is high, it can be used to detect frequent remodeling or suggest PD.
4. Alveolar bone: the alveolar bone socket (*alveolus*) comprises compact bone. The periodontal ligament inserts into it and supports the tooth. The alveolar bone can resorb following tooth extraction or remodel during regular mechanical loading.

9.3. PERIODONTAL DISEASES

Periodontal diseases affect adolescents and adults. The most severe cases of PD are observed in adults after the age of 30. Dentists classify at least three types of PD (Fig. 9.1)[1]:

- Gingivitis: gingivitis is an inflammatory response aggravated by hormonal, disease or drug-related stimuli, but it is most commonly associated with the accumulation of plaque around the teeth. Symptoms include swollen gums that easily bleed and it is observed both in youths and adults. As these symptoms indicate an early stage of PD, this disease is not commonly found in the bone and the symptoms are often reversible in younger patients.
- Periodontitis (*pyorrhea*): periodontitis is the most common form of PD. Bacterial plaque mineralizes and extends down into tooth root. With time, the gums reduce in health as tissues gradually recede from the tooth forming pockets 1–3 mm deep. As plaque proceeds below the gum line, bacterial toxins combine with the body's immune responses and gradually break down supporting alveolar bone and connective tissue. Symptoms include hypersensitivity to temperature gradients and to fluid flow through tubule structures located within the dentin. Unlike less severe cases of PD, periodontitis requires treatment to stop progression and to prevent further degradation of the periodontal ligament and superficial alveolar bone.[1] Related treatments will be further discussed in the next section.
- Periodontosis: periodontosis is a rare form of PD found in adolescents and young adults. Although a patient suffering from periodontosis may experience little inflammation or discomfort, X-rays can reveal destruction of the molars and upper incisors.

9.4. TREATMENTS, SURGERY AND REGENERATION

A series of treatments are available to reduce or repair the effects of PD. These treatments range from moderate medical intervention to more invasive surgical procedures. The primary treatment recommended by most dentists aims to prevent bacteria buildup. Patients can independently reverse early forms of PD by regular brushing and flossing while maintaining a healthy, nutritional diet. A secondary treatment is a form of deep gingival cleaning offered by a dental hygienist called *scaling* and *root planing*. Scaling involves scraping calculus buildup from the tooth surface. Root planing removes rough surfaces of the tooth root to reduce bacteria that contribute to disease. A tertiary measure of treatment

Table 9.1. Treatments of Periodontal Disease (PD).

Medication	Application
Antimicrobial mouthrinse	Prescription mouthrinse containing antimicrobial chlorhexidine
Antibiotic gel	A gel containing antibiotic doxycycline placed in pockets for slow release following scaling and root planing.
Antibiotic microspheres	Particles containing minocycline for slow release.
Enzyme suppressant	Low dosage doxycycline to restrain the immune response and limit enzymatic breakdown of tissues.
Oral antibiotics	For short-term treatment of acute local infection.

involves medication to reduce risk of infection. Table 9.1 illustrates medications placed in the pockets following scaling and root planing to control bacteria and reduce pocket size.[4]

For severe cases of PD, surgical procedures may be required, including deeper cleaning or bone repair. If inflammation and pockets persist following sufficient root planing, the periodontist may decide to perform *flap surgery*, where the gums are retracted to remove tartar below the gum line. In order to reduce bacterial affinity, the teeth are afterwards cleaned and smoothed with fillings. The gums are then sutured closely against the teeth.

Long-term accumulation of tartar can lead to degradation of the alveolus, which can lead to permanent tooth loss. In the event of bone loss, a periodontist may perform surgical procedures to help regenerate bone. Regeneration of periodontal tissue requires coordinated restoration of new alveolar bone, the periodontal ligament and the dental cementum bonding the two tissues. Regeneration of bone for advanced cases of PD include the following surgical treatments:[5,6]

1. guided tissue regeneration
2. bioactive molecules
3. bone graft materials.

In *guided tissue regeneration*, a membrane is inserted between the gingivae and the bone. The mesh is often made of either biocompatible polytetraflouroethylene (PTFE) or bioresorbable materials such as polylactic acid (PLA), PLA with polyglycolic acid (PGA) and bovine collagen membranes to reduce second surgeries. The

inserted mesh creates a space that inhibits gum tissue migration into the region where bone is desired to grow, allowing repopulation of progenitor cells for bone and periodontal ligament tissue growth. The primary functions of wound stability and space maintenance vary with surgical technique, however. Consequently, the membranes used in guided tissue regeneration often yield inconsistent and poor mechanical performance between patients.[5]

Bioactive molecules are growth factors that have been used to genetically induce bone regeneration, e.g. bone morphogenic proteins. Such molecules have been used in conjunction with a supporting allograft to improve overall regeneration. See a review by Hughes *et al*. on several bioactive molecules used in PD treatment to coat materials for induction of new bone formation.[5]

Bone grafts offer an opportunity to repair bony defects by bioresorbable materials that are osteoconductive or osteostimulatve. Osteoconductive grafts bond to bone and facilitate growth along the bone–implant interface. Osteostimulative grafts induce new bone formation by recruiting undifferentiated mesenchymal cells that differentiate into osteoblasts. Autogenous bone extracted from the local oral site or the iliac crest can serve as an adequate osteostimulative graft, but such autografts are not widely used due to complications arising from second site morbidity and pain. An alternative is a xenograft of freeze-dried bovine tissue, which is osteoconductive. Unfortunately, xenografts can pose potential risks of prion exposure, disease transmission or immunorejection. Synthetic alternatives (allografts) include polymers for hard tissue replacement and a range of resorbable bioactive glasses and glass-ceramics. The particulate form of 45S5 Bioglass® offers regenerative options for osseous treatment of PD without the biological complications associated with implanting auto- and xenografts. See Chapter 10 for a discussion of the relative merits and limitations of various types of bone grafting materials.

9.5. TISSUE REGENERATION OF BONE DAMAGED BY PERIODONTAL DISEASE

In situ tissue regeneration involves the use of biomaterials in the form of powders, solutions or doped microparticles to stimulate local tissue repair.[5,6] Bioactive materials release chemicals in the form of ionic dissolution products at controlled rates by diffusion or network breakdown that activate the cells in contact with the stimuli.[7–9] The cells produce additional growth factors, such as vascular endothelial growth factor (VEGF), that in turn stimulate multiple generations of growing cells to self-assemble into the vascularized tissues *in situ* along the biochemical

and biomechanical gradients that are present. Chapter 4 discusses the biological mechanisms of bone regeneration and the role of osteogenic stimuli released from bioactive glasses. A normal 3D architecture of regenerated bone is created by the osteoblasts when the cells are exposed to a release of critical concentrations of the soluble ionic constituents of the bioactive glass. Approximately 17–20 ppm of soluble Si and 88–100 ppm of soluble Ca ions are required. The ions are provided by controlled dissolution of a bioactive glass substrate. Thus, the role of the bioactive glass is primarily to release the critical concentrations of biologically-active ions at the rate needed for cell differentiation and growth under genetic control (see Chapter 4).[7–9]

9.6. THIRD-GENERATION CLINICAL PRODUCTS

While the second generation Bioglass® materials performed well in replacing diseased or missing hard tissue, such as use in maintenance of the alveolar ridge for edentulous patients discussed in Chapter 8, the discovery that 45S5 Bioglass® could positively affect osteoblasts by stimulating them to produce more bone tissue earlier than other synthetic biomaterials has led to much broader clinical applications,[7–10] especially in the prevention of the loss of teeth from periodontal disease. To take advantage of the property of osteostimulation, and the need to regenerate diseased or missing tissues in a range of sizes of bone defects, the development of third-generation Bioglass® products focused on using particles rather than monolithic shapes. The first 45S5 Bioglass® particulate material cleared for sale in the U.S. was PerioGlas®, which was cleared via the 510(k) process in December, 1993. In 1995, PerioGlas® obtained a CE mark and marketing of the product began in Europe. The initial indication for the product was to restore bone loss resulting from PD in infra-bony defects. In 1996, additional indications for use were cleared by FDA, including use in tooth extraction sites and for alveolar ridge augmentation.

The first paper to describe potential use of 45S5 Bioglass® particulate in repair of periodontal defects was published in 1987 by Dr. June Wilson and Professor Sam Low, Department of Periodontology, and colleagues at the University of Florida.[8] Detailed studies of the monkey model followed in 1992 and 1994.[9,10] Schepers *et al*. reported similar findings in a different animal model.[11] Other related studies are in included in the reference list.[12,13]

Over a 20-year clinical history, PerioGlas® has demonstrated excellent clinical results with virtually no adverse reactions to the product. Numerous clinical studies have demonstrated the efficacy of the synthetic graft in multiple uses. Table 9.2 summarizes selected clinical studies of PD treatment using bioactive glasses over the last

Table 9.2. Studies of 45S5 Bioglass® (PerioGlas®) in the Treatment of PD.

Author	Year	
Yukna, R.	2001	PerioGlas® treatment of mandibular class II furcations compared similarly with the gold standard ePTFE barrier treatment among 27 patients. Applying PerioGlas® was found to offer a more simple surgical technique.[26]
Mengel, R.	2003	A 12-month clinical study indicates improvements of clinical parameters using bioactive glass and bioabsorbable membranes. This study suggests the efficacy of bioactive glass with other regenerative treatments for 12 patients with aggressive PD.[27]
Sculean, A.	2005	A one-year study indicates reduction in PD using combinations of bioactive glass with enamel matrix protein derivative (EMD). No statistical improvement was observed compared to using EMD alone.[28]
Mengel, R.	2006	A five-year study of radiological evidence in 16 patients indicates significantly high reduction of aggressive PD using bioactive glass graft to fill intrabony defects.[29]
Gatti, A.	2006	Three cases of dental defect treatment using PerioGlas® indicate successful healing and loading after two years.[30]
AboElsaad, N.	2009	A study of combined soft-laser irradiation and PerioGlas® implantation in 20 patients showed accelerated defect-filling over bioactive glass alone after three months; no difference was discernible after six months.[31]
Leknes, K.	2009	A 12-month clinical study showed significant clinical attachment levels using bioactive glass filler material compared to enamel matrix derivative for 13 patients with proximal intrabony periodontal defects.[32]
Felipe, M.	2009	Six dogs with intrabony periodontal defects were treated with small (300–355 μm) and large (90–710 μm) bioactive glass particles. Tests with smaller particles for this application confirmed evidence from similar studies showing faster resorption and bone substitution.[33]
Mistry, S.	2011	A 12-month assessment of endosseous dental implants for 31 patients indicated bioactive glass-coated titanium implants had comparable osteointegration and performance to common HA-coated implants.[34]
Subbiah, R.	2011	A three, six and nine month evaluation for eight patients treated with PerioGlas® suggested improved bone-fill over flap debridement technique alone.[35]
Sohrabi, K.	2011	A literature review compares several controlled clinical studies and confirm that bioactive glass treatment yields significant improvement of key clinical parameters.[36]

decade, comparing parameters of measured pocket/probing depth, clinical tooth attachment levels and radiographic evaluation.[14–36] To date, PerioGlas® is sold in over 35 countries, and the manufacturer estimates that the product has been used in several million surgeries (data on file at NovaBone Corporation, Alachua, FL).

Other dental and maxillofacial applications include pulp capping,[37,38] sinus obliteration[39,40] and repair of orbital floor fracture.[41,42]

9.7. CONCLUSION

In summary, teeth consist of several tissue structures, all of which can be affected by PD. In severe cases, surgical repair of osseous defects is required. Techniques for osseous repair include guided tissue regeneration, bioactive molecules and resorbable bioactive materials such as commercially available PerioGlas®. The osteostimulative properties of PerioGlas® have aided in the repair of PD for millions of patients.

REFERENCES

1. Research, Science and Therapy Committee Report. (2005). Epidemiology of Periodontal Diseases, *J. Periodontol.*, **76**, 1406–1419.
2. Gray, H. (1977). *Gray's Anatomy*, Crown Publishers Inc., New York.
3. Cormack, D. and Ham, A. (1987). *Ham's Histology*, J.B. Lippincott Company, Philadelphia, PA.
4. Anon. (2011). *Periodonal (Gum) Disease: Causes, Symptoms and Treatments*, National Institutes of Health, pp. 1–14.
5. Hughes, F., Ghuman, M. and Talal, A. (2010). Periodontal Regeneration: A Challenge for the Tissue Engineer?, *Proc Inst Mechanical Engineers, Part H: Journal of Engineering in Medicine*, pp. 1345–1358.
6. Reynolds, M., Aichelmann-Reidy, M. and Branch-Mays, G. (2010). Regeneration of Periodontal Tissue: Bone Replacement Grafts, *Dent. Clin. North Am.*, **54**, 55–71.
7. Hench, L., Polak, J., Xynos, I. *et al.* (2000). Bioactive Materials to Control Cell Cycle, *Mater. Res. Innov.*, **3**, 313–323.
8. Wilson, J., Low, S., Fetner, A. *et al.* (1987). Bioactive Materials for Periodontal Treatment: A Comparative Study, *Biomater. Clin. Appl.*, **8**, 223–228.

9. Wilson, J. and Low, S. (1992). Bioactive Ceramics for Periodontal Treatment: Comparative Studies in the Patus Monkey, *J. Appl. Biomater.*, **3**, 123–129.
10. Fetner, A., Hartigan, M. and Low, S. (1994). *Periodontal Repair Using PerioGlas in Nonhuman Primates: Clinical and Histologic Observations,* Compendium, Newtown, PA, **15**, 932–935.
11. Schepers, E, Clercq, M., Ducheyne, P. *et al.* (2008). Bioactive Glass Particulate Material as a Filler for Bone Lesions, *J. Oral Rehabil.*, **18**, 439–452.
12. Karatzas, S., Zavras, A., Greenspan, D. *et al.* (1999). Histologic Observations of Periodontal Wound Healing After Treatment with PerioGlas in Nonhuman Primates, *Int. J. Periodont. Rest.*, **19**, 489–499.
13. Greenspan, D. (1999). Bioactive Ceramic Implant Materials, *Curr. Opin. Solid St. M.*, **4**, 389–393.
14. Wilson, J., Clark, A., Douek, E. *et al.* (1994). Clinical Applications of Bioglass Implants, *Bioceramics*, **7**, 415–422.
15. Shapoff, C., Alexander, D. and Clark, A. (1997). Clinical Use of a Bioactive Glass Particulate in the Treatment of Human Osseous Defects, *Compend. Contin. Educ. Dent.*, **18**, 352–363.
16. Low, S., King, C. and Krieger, J. (1997). An Evaluation of Bioactive Ceramic in the Treatment of Periodontal Osseous Defects, *Int. J. Periodont. Rest.*, **17**, 358–367.
17. Lovelace, T., Mellonig, J. T., Meffert, R. M. *et al.* (1998). Clinical Evaluation of Bioactive Glass in the Treatment of Periodontal Osseous Defects in Humans, *J. Periodontol.*, **69**, 1027–1035.
18. Anderegg, C., Alexander, D. and Freidman, M. (1999). A Bioactive Glass Particulate in the Treatment of Molar Furcation Invasions, *J. Periodontol.*, **70**, 384–387.
19. Norton, M. and Wilson, J. (2001). Bone Augmentation with Bioactive Ceramics before Insertion of Endosseous Dental Implants: Histories and Human Histology on Seventeen Consecutive Cases, *Key Eng. Mat.*, **192–195**, 869–872.
20. Sculean, A., Berakdar, M., Arweiler, N. *et al.* (2000). Treatment of Intrabony Defects with Enamel Matrix Proteins and a Bioactive Glass Particulate: A Report on Ten Cases, *Regenerative Parodontaltherapie*, **3**, 231–240.
21. Barbe, G., Sculean, A. and Chiantella, G. (2001). Vertical Reconstruction of Horizontal Periodontal Defects using a Bioactive Glass: A Case Report with

a 36 Months Follow-Up, *Journal de Parodontologie et D Implantologie Orale*, **20**, 51–60.

22. Park, J., Suh, J.J., Choi, S.H. *et al.* (2001). Effects of Pretreatment Clinical Parameters on Bioactive Glass Implantation in Intrabony Periodontal Defects, *J. Periodontol.*, **72**, 730–740.
23. Norton, M. and Wilson, J. (2002). Dental Implants Placed in Extraction Sites Implanted with Bioactive Glass: Human Histology and Clinical Outcome, *Int. J. Oral Max. Impl.*, **17**, 249–257.
24. Sculean, A., Barbé, G., Chiantella, G.C. *et al.* (2002). Clinical Evaluation of an Enamel Matrix Protein Derivative Combined with a Bioactive Glass for the Treatment of Intrabony Periodontal Defects in Humans, *J. Periodontol.*, **73**, 401–408.
25. Froum, S., Weinberg, M. and Tarnow, D. (1998). Comparison of Bioactive Glass Synthetic Bone Graft Particles and Open Debridement in the Treatment of Human Periodontal Defects. A Clinical Study, *J. Periodontol.*, **69**, 698–709.
26. Yukna, R., Evans, G., Aichelmann-Reidy, M. *et al.* (2001). Clinical Comparison of Bioactive Glass Bone Replacement Graft Material and Expanded Polytetrafluoroethylene Barrier Membrane in Treating Human Mandibular Molar Class II Furcations, *J. Periodontol.*, **72**, 125–133.
27. Mengel, R., Soffner, M. and Flores-de-Jacoby, L. (2003). Bioabsorbable Membrane and Bioactive Glass in the Treatment of Intrabony Defects in Patients with Generalized Aggressive Periodontitis: Results of a 12-Month Clinical and Radiological Study, *J. Periodontol.*, **74**, 899–908.
28. Sculean, A., Pietruska, M., Schwarz, F. *et al.* (2005). Healing of Human Intrabony Defects Following Regenerative Periodontal Therapy with an Enamel Matrix Protein Derivative Alone or Combined with a Bioactive Glass. A Controlled Clinical Study, *J. Clin. Periodontol.*, **32**, 111–117.
29. Mengel, R., Schreiber, D. and Flores-de-Jacoby, L. (2006). Bioabsorbable Membrane and Bioactive Glass in the Treatment of Intrabony Defects in Patients with Generalized Aggressive Periodontitis: Results of a 5-Year Clinical and Radiological Study, *J. Periodontol.*, **77**, 1781–1787.
30. Gatti, A., Simonetti, L., Monari, E. *et al.* (2006). Bone Augmentation with Bioactive Glass in Three Cases of Dental Implant Placement, *J. Biomater. Appl.*, **20**, 325–339.

31. AboElsaad, N., Soory, M., Gadalla, L. M. *et al.* (2009). Effect of Soft Laser and Bioactive Glass on Bone Regeneration in the Treatment of Infra-Bony Defects (A Clinical Study), *Lasers Med. Sci.*, **24**, 387–395.
32. Leknes, K., Andersen, K., Bøe, O. *et al.* (2009). Enamel Matrix Derivative Versus Bioactive Ceramic Filler in the Treatment of Intrabony Defects: 12-Month Results, *J. Periodontol.*, **80**, 219–227.
33. Felipe, M., Andreade, F.A., Novaes, A.B. *et al.* (2009). Potential of Bioactive Glass Particles of Different Size Ranges to Affect Bone Formation in Interproximal Periodontal Defects in Dogs, *J. Periodontol.*, **80**, 808–815.
34. Mistry, S., Kundu, D., Datta, S. *et al.* (2011). Comparison of Bioactive Glass Coated and Hydroxyapatite Coated Titanium Dental Implants in the Human Jaw Bone, *Aust. Dent. J.*, **56**, 68–75.
35. Subbaiah, R. and Thomas, B. (2011). Efficacy of a Bioactive Alloplast, in the Treatment of Human Periodontal Osseous Defects — A Clinical Study, *Med. Oral Patol. Oral Cir. Bucal*, **16**, e239–e244.
36. Sohrabi, K., Saraiya, V., Laage, T.A. *et al.* (2011). An Evaluation of Bioactive Glass in the Treatment of Periodontal Defects: A Meta-Analysis of Randomized Controlled Clinical Trials, *J. Periodontol.*, **84**, 453–464.
37. Oguntebi, B., Clark, A. and Wilson, J. (1993). Pulp Capping with Bioglass® and Autologous Demineralized Dentin in Miniature Swine, *J. Dent. Res.*, **72**, 484–489.
38. Stanley, H. and Clark, A. (2001). Pulp Capping with a Modified Bioglass Formula (# A68-modified), *Am. J. Dent.*, **14**, 227–232.
39. Aitasalo, K. and Suonpää, J. (1997). Behaviour of Bioactive Glass (S53P4) in Human Frontal Sinus Obliteration, *Bioceramics*, **10**, 429–432.
40. Peltola, M. (2001). Clinical Followup Method for Frontal Sinus Obliteration with Bioactive Glass S53P4, *J. Biomed. Mater. Res.*, **58**, 54–60.
41. Kinnunen, I., Aitasalo, K., Pollonen, M. *et al.* (2000). Reconstruction of Orbital Floor Fractures Using Bioactive Glass, *J. Craniomaxillofac. Surg.*, **28**, 229–234.
42. Aitasalo, K., Kinnunen, I., Palmgren, J. *et al.* (2001). Repair of Orbital Floor Fractures with Bioactive Glass Implants, *J. Oral Maxillofac. Surg.*, **59**, 1390–1396.

Chapter 10

CLINICAL APPLICATIONS OF BIOACTIVE GLASSES: MAXILLOFACIAL REPAIR

Ian Thompson

10.1. INTRODUCTION

This chapter summarizes use of bioactive glasses that are being clinically applied in the reconstruction and regeneration of bone following maxillofacial surgery.

10.2. CLINICAL REQUIREMENTS

The first decision a surgeon must make when determining a treatment plan for a patient requiring a bone graft is to select the source of the graft material. Options are:

- Autogenous: use of bone from the patient's own skeleton *(autograft)*
- Allogenic: use of bone donated from a human source *(allograft)*
- Xenogenic: use of bone obtained from another species *(xenograft)*
- Alloplastic: use of a synthetic graft material *(synthetic graft)*

10.3. AUTOGRAFTS

Autogenous bone, used as an autograft, is regarded as the gold standard due to its characteristic of being both osteoconductive (provides a surface along which bone cells migrate) and osteoinductive (stimulates undifferentiated stem cells to change their phenotype to that of bone cells). In other word, they can regenerate bone naturally. However, autografts have two drawbacks: donor site morbidity and unpredictable rates of resorption due to biomechanical factors. In order to overcome donor site problems many surgeons have used allogenic bone from bone banks, with potential concerns of immunorejection and disease transmission.

10.4. ALLOGENIC BONE GRAFTS

The work by Urist *et al.* led to a clinically safe allogenic bone for bone banks.[1] The resultant material was called antigen-extracted autodigested allogenic bone, or so called AAA bone. This system allows the bone to be antigen low whilst maintaining high levels of morphogenetic proteins.[1] Recent papers suggest that AAA bone has variable osteoinductive characteristics and often may only exhibit osteoconductive properties. The reduction of osteoinduction is due to the sterilization process that removes or denatures the bone morphogenetic proteins.[2,3] The AAA bone process is also described as demineralized freeze-dried bone (DFDB). The use of xenografts as DFDB materials has led to a commercial xenogenic product formed from a bovine source, Bio-Oss®. Both allogenic and xenogenic bone are commercially available but are expensive, have minimal osteoinductive properties and both are generally regarded as osteoconductors.[2–5] They are used sparingly in our surgeries due to the possible infection risk by the transfer of latent virus or prion particles, e.g. HIV or CJD. The relative merits of different graft materials and their variability of performance in graft sites are discussed in a recent work by the author.[6]

10.5. LIMITATIONS OF AUTOGENEOUS BONE GRAFTS

Although autografts are the ideal source of bone for surgical repair there are many donor site problems, including: blood loss; potential for infection; pain at the site of the donor graft for extensive period of time; loss of mobility, as muscles are removed from the donor site, particularly with iliac crest sites; nerve damage, particularly with mandibular and iliac crest donor sites; and damage due to pneumothorax, specifically with ribs as donor sites.

10.6. SOURCE OF AUTOGENEOUS BONE FOR GRAFTING

The options for source of autograft material from a patient and other surgical factors include:

- Sites to harvest the new bone are typically the iliac crest (anterior or posterior), ribs, calvarium, mandible (chin or ramus)
- Cancellous or cortical bone
- Membranous or endochondral bone (embryonic origin) e.g. hip and rib are endochondral, the mandible and calvarium are membranous bone
- Fixation method (screw or suture, metal or polymer).

The donor site is usually the iliac crest of the pelvis. Another implant (usually synthetic) is needed to fill the space and recovery time can be lengthy and painful. Rapid resorption of the transplanted bone can occur because its structure is that of pelvic bone, not that of the defect site, and therefore osteoclasts may resorb it. Each of the above grafting alternatives has positive and negative effects on healing rates and ultimate clinical outcome of the bone graft. Despite the above concerns, autografts are regarded as the better option for bone grafts when compared with the various xenografts and allografts cited above. All autograft procedures require a donor site to harvest the bone graft, which results in pain and discomfort for the patient, an increased risk of infection, a second surgical team and increased costs associated with all aspects of the operation. Thus, any bone grafting procedure has room for improvement, with much recent effort being given to alloplastic, synthetic materials.

10.7. NEED AND CRITERIA FOR ALLOPLASTIC BONE GRAFTS

The need for alternatives to autogeneous bone in grafting large defects has led to development of alloplastic, man-made, synthetic graft materials, as reviewed by Thompson.[6] Alloplastic materials are designed to provide a base for new bone to grow on, providing a rapid return of function. The goal is to inhibit fibrous (scar) tissue growing into a site where bone formation is desirable, e.g. at the proposed implant site.

These studies have led to a set of design criteria for alloplastic bone grafting materials, listed in Table 10.1.

Synthetic hydroxyapatite ($Ca_{10}(PO_4)_6OH_2$) particles and blocks have been routinely used as alveolar ridge augmentation materials (see Chapters 17–19). They are popular because HA has a similar composition to the apatite in bone and is osteoconductive. However, there have been a number of problems with synthetic HA grafts: particle misplacement, postoperative particle migration into undesirable areas, implant flattening and excessive postoperative ridge width.[7–9] A further clinical problem noted has been nerve dysaesthesia, a change in the ability of the nerve to conduct the impulse, which may result in a "pins and needles" sensation or numbness. The dysaesthesia has been attributed to particles moving into the mental foramen and pressurizing the nerve.[10] In an attempt to stop particle migration, a number of binding agents have been used in conjunction with the alloplastic materials: plaster of Paris, collagen, and fibrin. Another

Table 10.1. Set of Design Criteria for Alloplastic Bone Grafting Materials.

An alloplastic bone graft material should:

- Provide an osteoconductive surface.
- Be entirely resorbable within 6–12 months.
- Be dimensionally stable in a bony defect.
- Be dimensionally stable while it is resorbing.
- Be compatible (as should its resorption products) with the host tissues.
- Stimulate formation of new bone with an architecture equivalent to the bone being replaced.

The following features are also required of alloplastic bone graft material:

- Ease of application.
- Able to be sterilized.
- Possible use as a carrier system for an osteoinductive medium.

There are a number of alloplastic materials clinically used in maxillofacial reconstructions:

- Dense HA, porous HA, in particles or solid blocks.
- Bioactive glass.
- Collagen meshes.
- Resorbable polymers.

experimental approach has been to use degradable tubes filled with particulate HA. The results in 12 patients show that the tubes become "clinically solid" within 8–16 weeks.[11] It is stated that "the ridges are desirable for denture construction. Although the augmentation becomes clinically solid, it is doubtful if the HA is interdispersed with actual bone." [12]

Due to these variable results, the decision in our clinic at Guy's Hospital was made to *not* use HA-based materials for maxillofacial reconstruction in the clinical trials summarized below. The material chosen for the clinical trials was bioactive glass because this bioactive material meets all of the design criteria listed in Table 10.1.

10.8. APPLICATIONS OF BIOACTIVE ALLOPLASTIC (SYNTHETIC) POWDERS

A range of bioactive glass powders have been used in clinical practice for over 20 years with good clinical success (see Chapters 6–12). The "grandfather" bioactive glass is the original 45S5 (46.1 mol% SiO_2, 24.4 mol% Na_2O, 26.9 mol% CaO, and 2.6 mol% P_2O_5) composition, marketed as PerioGlas® and NovaBone® by NovaBone Corp. (Alachua, FL, Table 10.2).

The change in chemical composition of the alloplastic material gives rise to differing rates of osteostimulation and mechanical properties, typically the higher the silica content the slower the dissolution of the glass structure once implanted into the body, and the resultant lower level of bioactivity and osteostimulation. The most bioactive composition, 45S5 Bioglass®, releases a critical concentration of ionic dissolution products as it resorbs. The biologically-active soluble silica and calcia ions result in up-regulation of seven families of genes in osteoprogenitor cells and gives rise to rapid bone regeneration.[13]

The sites for application of particulate bioactive glass are numerous, from simply filling extracted tooth sockets, thereby alleviating alveolar ridge resorbtion (Chapter 8), to use in the reconstruction of complex orthopedic fractures and spinal fusion (Chapters 11, 12).[14] However, the particulate systems lack dimensional stability when applied as a large volume of powder when first placed into the surgical site. Therefore, the powders are typically used in intra bony cavities, as the "containing" walls of the cavity reduce migration of the glass particles around the local surgical site due to blood flow and patient locomotion. Histology has shown the glass particles form a biological bond to collagen fibers within 24 hours (Chapters 3, 4, 6, 9). After this initial interaction of glass surface and collagen fibers the particulate material becomes very stable; there is no evidence of migration of glass particles after formation of the initial biological bond.

Table 10.2. 45S5 Bioglass® Properties Compared with Human Bone.[14,15]

Material	Density (g/cm^3)	Hardness (Vickers, HV)	Bending Strength (MPa)	Fracture Toughness (K_{1C})(MPa $m^{1/2}$)	Young's Modulus (GPa)
Cortical Bone	1.6–2.1	—	50–150*	2–12	7–30
Cancellous Bone	1.0	—	10–20	0.1	0.05–0.5
Bioglass® (45S5)	2.6572	458 ± 9.4	42 (Tensile)	0.6	35

*strength depends upon direction and rate of loading and source of bone.

A number of composite and paste systems have been developed to minimize the movement of the glass particles within the surgical site.[15] The above applications have been approved by governmental regulatory bodies, based upon a comprehensive series of *in vitro* and *in vivo* tests. An important *in vivo* test is the Oonishi model.[16,17] This test is relatively inexpensive and can be used to quantify comparison of rates of osteoregeneration of differing materials. This model was used by the author to quantify bone growth response to several alloplastic materials systems.[16–18] Positive results from these *in vivo* studies provided basis for ethical committee approval to conduct the clinical trials described herein.

10.9. THE OONISHI MODEL (A critical size defect in the rabbit femoral condyle)

Holes 6 mm in diameter are drilled bilaterally in the femoral condyles of mature rabbits. Immediately afterward, granules of the alloplastic material to be tested are placed in sufficient amounts to fill the holes in the femoral condyles. Five femoral condyles are used for each time period. For a detailed investigation nine time periods are studied, 2, 3, and 5 days and 1, 2 , 3, 6, 12, and 24 weeks. A less costly preliminary comparison of materials can be done by reducing time periods to 1, 2, 3, and 6 weeks. Most key differences between materials show within 1–6 weeks. Following euthanasia, non-decalcified specimens of the femoral condyles are observed by light microscopy and backscattered scanning electron microscopic (SEM) imaging. Rates of bone in-growth from the periphery of the defect to the interior are measured quantitatively using image processing. Details are given in the pioneering references where the Oonishi Model is used to compare various bioactive materials.[16,17] These studies show that an extensive network of bone bridges form rapidly between bioactive glass particles. The architecture of bone that results is equivalent to that of normal trabecular bone present in the femoral condyles.[17] The mechanical properties of the regenerated bone are also equivalent, as shown by Wheeler *et al.* using the Oonishi Model.[19]

10.10. CLINICAL CASES

10.10.1. Bioactive Glass Alloplastic Bone Grafts for Maxillofacial Reconstruction

One of the more common applications of bioactive glass is the filling of cystic cavities in mandibles. Cystic cavities as large as 15 cm^3 are frequently

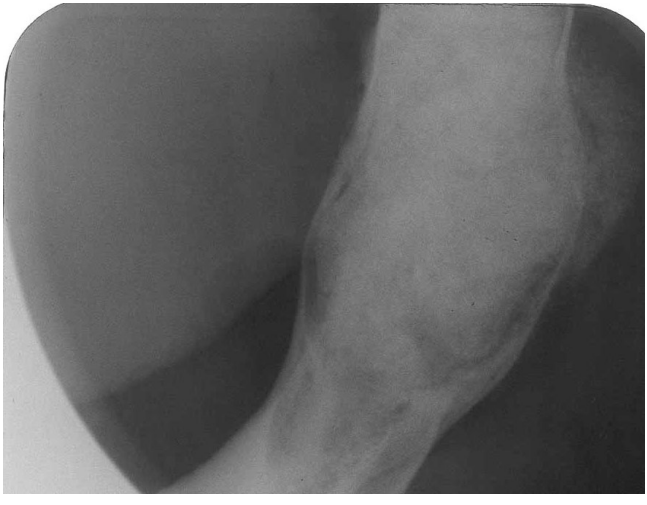

Figure 10.1. Postoperative X-ray, cystic activity has deformed the mandible.

filled with bone chips harvested from the iliac crest plus some additional bone graft substitute material such as 45S5 Bioglass® bioactive glass. The surgical steps used to fill a cystic cavity are described in Thompson.[6]

The immediate postoperative X-ray shows how the cyst has deformed the macroscopic shape of the mandible (Fig. 10.1). After six months of healing the mandible has regained its natural anatomic shape and begun to regenerate the internal trabecular structure (Fig. 10.2).

Clinical comparisons of bioactive glass with or without autogenous bone in similar cases to that described above has shown that there is no reduction in healing time when only the alloplastic material is used. Thus, grafting clinical sites with only bioactive glass particles does not require additional autogenous bone to heal a bony defect. This is an important finding, since it eliminates problems of second site morbidity, cost, time, and pain. The positive findings of successful use of bioactive glass particulate alone in a graft site indicates that if there is a sufficient supply of blood then there will be a cascade of healing inductive factors such as TGF-β delivered to the site,[13] thereby eliminating the need for bone morphogenetic proteins and other inductive factors being released from an autogenous bone graft. These clinical conclusions are consistent with the *in vitro* findings of gene up-regulation of osteoprogenitor cells induced by bioactive glasses (Chapter 4) and the angiogenic potential of bioactive glasses (Chapter 5).

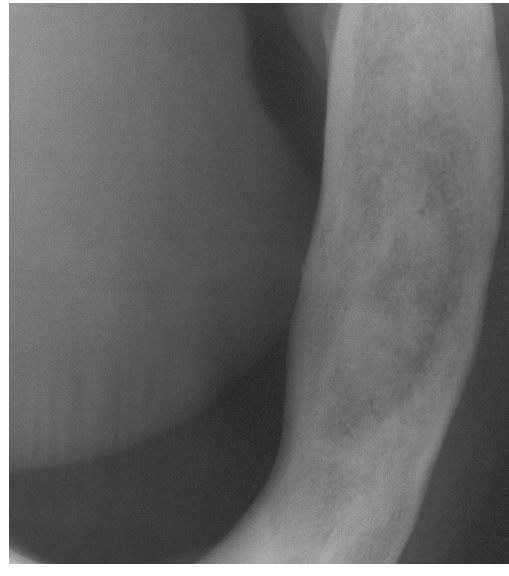

Figure 10.2. Six months post operative X-ray, remodeling of mandible.

10.11. CLINICAL APPLICATIONS

10.11.1. Monolithic Bioactive Glass Implants Combined with Bioactive Alloplastic Powders

Bulk pieces of bioactive glass have been clinically successful when used as middle ear prosthesis, where they were used to replace the small bones (ossicles) in the middle ear to restore hearing (Chapter 7), dental ridge maintenance implants (Chapter 8) and in non-load bearing facial skeletal reconstruction (Chapter 6).

Clinicians have generally moved away from using bulk bioactive glass implants due to the difficulty in altering the shape of the implant to fit the patient during surgery. Recently, the work of the author at Guy's Hospital London has shown that prefabrication of bulk bioactive glass implants using computer tomography (CT) scans to create accurate molds has led to a good clinical outcome and makes the implants much easier for surgeons to implant without modification of the device. The CT scans of the patient provide 3D images of the defect site. The images can be used as data input into computer aided design (CAD) files that can be used to machine-custom molds for the casting of the

Bioglass®. The dimensional accuracy leads to improved contact between the implant and host tissue, resulting in more rapid site stability post surgery. There is also less surgical trauma to the patient when the implant is custom made to fit the surgical site.

10.11.2. Case History

The following describes a patient who suffered an orbital floor trauma due to a road traffic accident. The resulting hypoglobus left the patient with blurred vision, which will increase to permanent blindness if not relieved. Initial attempts to use an autogeneous bone graft from the iliac crest failed as the material resorbed away after six months. Porous polyethylene was considered to be an infection risk, due to the clinician's previous experiences. Local ethical permission was granted to cast a bioactive glass implant from rapid prototyped molds. Figure 10.3 shows the CT data of the affected site and the unaffected site, note the change in orbital floor height and contour. Using CT data a dimensionally-accurate mold was created, which allowed the implant

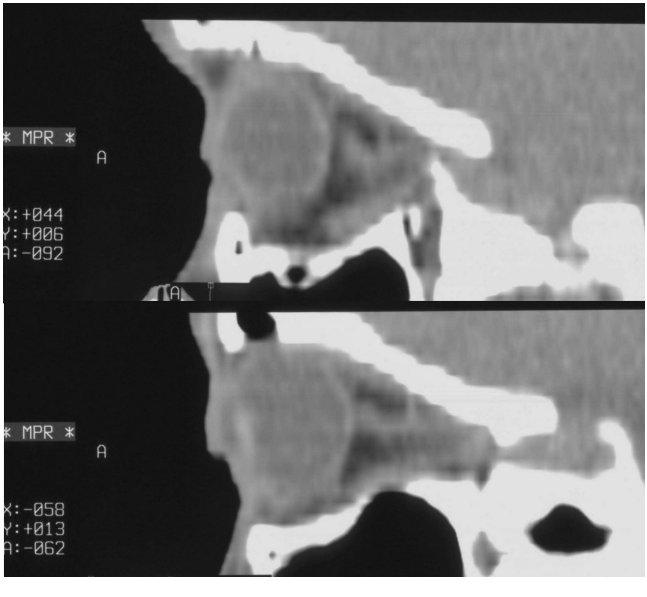

Figure 10.3. Top: collapsed orbital floor, globe has fallen back into skull so kinking optic nerve. Bottom: normal orbital floor.

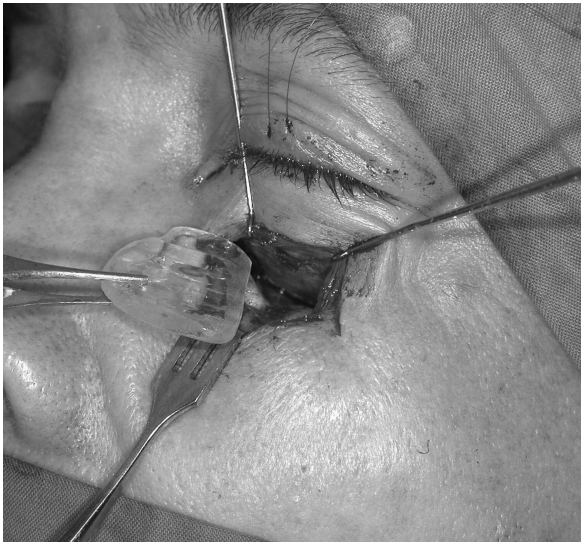

Figure 10.4. Placement of bioactive glass monolith in surgical site.

to be cast with sufficient contour to mimic the correct orbital floor anatomy. The molten 45S5 glass implant was cast and subsequently annealed to remove any thermal stresses. Samples were taken for mechanical and bioactivity testing.

The surgical site was opened and the implant positioned on top of the collapsed orbital floor (Fig. 10.4). Powdered bioactive glass was used to pack around the implant to improve the contact between the collapsed bony orbital floor and the implant's lower surface. The implant was secured into the site with degradable sutures. A postoperative X-ray shows the location of the glass implant and the regained symmetry between the left and right orbital floor positions (Fig. 10.5). A five-year follow up showed the patient regained full movement of the eye and lost all complications from blurred vision. The patient is happy with the aesthetic look of his face due to correction of the hypoglobus.

This case is part of a 30-patient trial at Kings College/Guy's Hospital. The trial's findings show zero postoperative infection and zero loss of implants from migration or any other factors. The patients are happy with the regained function of their damaged orbital floors, and with correction of their facial symmetries.

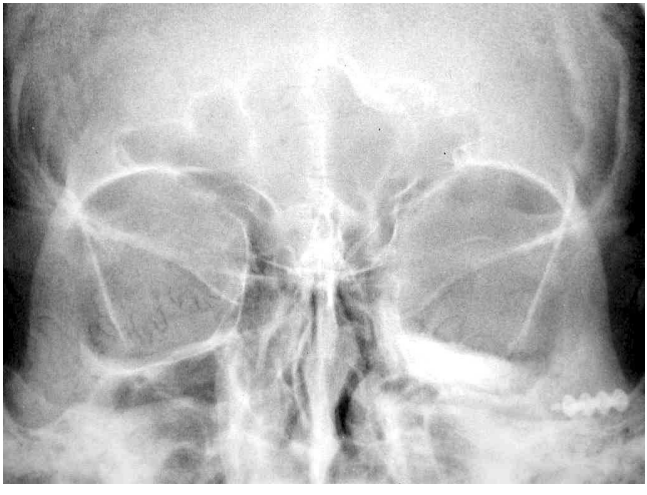

Figure 10.5. Postoperative X-ray, showing bioactive glass implant. Note the new orbital floor height is symmetrical to unaffected side.

10.12. CONCLUSION

Bioactive glass is an effective bone graft substitute material when used as a particulate. Published clinical data and success of our cases reinforce evidence that bioactive glass is more than just an osteoconductive material. Its use in a range of clinical applications has only been compromised when the glass is over-packed into a site, making it difficult for in-growing bone to colonize the mass of glass particulate. The glass has a number of applications when cast as a block or monolithic shape and is particularly effective when used in combination with particulate grafts. Use of CT scans to create highly dimensionally accurate molds for casting bulk bioactive glass implants make it possible to achieve rapid surgical reconstruction of large-scale defects. Particulate bioactive glass particles used in conjunction with accurate castings are especially effective clinically; they lower costs and time in surgery, minimize pain and trauma to the patient, and ensure long-term stability of the repaired surgical site.

REFERENCES

1. Urist, M.R., Mikulski, A. and Boyd, S.D. (1975). A Chemosterilized Antigen Extracted Autodigested Alloimplant for Bone Banks, *Arch. Surg.*, **110**, 416–427.

2. Sennerby, L. and Lundgren, S. (1998). "Histologic Aspects of Stimultaneous Implant and Graft Placement", in Jensen, O.T. (ed.), *The Sinus Bone Graft*, Quintessence Publishing, Chicago, pp. 95–105.
3. Aspenberg, P., Kalebo, P. and Alberktsson, T. (1988). Rapid Bone Healing Delay by Bone Matrix Implantation, *Int. J. Oral Maxillofac. Impl.*, **3**, 123–127.
4. Oberg, S. and Rosenquist, J.B. (1994). Bone Healing After Implantation of Hydroxyapatite Granules and Blocks (Interpore 200®) Combined with Autolyzed Antigen Extracted Allogenic Bone and Fibrin Glue, *Int. J. Oral. Maxillofac. Surg.*, **23**, 110–114.
5. Hollinger, J.O., Schmitz, J.P., Mark, D.E. *et al.* (1990). Osseous Wound Healing with Xenogenic Bone Implants with a Biodegradable Carrier, *Surgery*, **107**, 50–54.
6. Thompson, I. (2011). "Clinical Applications of Bioactive Glasses for Maxillo-Facial Repair", in Hench, L.L., Jones, J.R. and Fenn, M.B. (eds), *New Materials and Technologies for Healthcare*, Imperial College Press, London, pp. 77–96.
7. Silverberg, M., Singh, M., Gans, B. *et al.* (1986). Polyglycolic Acid Mesh Contained Hydroxylapatite for Augmentation of Bone in the Rat, *Proc 9th Int. Conf. Oral Maxillofac. Surg.*, pp. 145–152.
8. Gongloff, R.K., Montgomery, C.K., Lee, R. *et al*. (1986). Collagen Tubes: Role in Subperiosteal Contour Augmentation, *Int. J. Oral. Maxillo. Surg*., **15**, 669–674.
9. Barsan, R.E. and Kent, J.N. (1985). Hydroxylapatite Reconstruction of Alveolar Ridge Deficiency with an Open Technique – A Preliminary Report, *Oral Surg*., **59**, 113–119.
10. Gongloff, R.K. (1988). Use of Collagen Tube Contained Implants of Particulate Hydroxyapatite for Ridge Augmentation, *J. Oral Maxillofac. Surg*., **46**, 641–647.
11, Collins, T.A. (1989). Use of Collagen Tubes Containing Particulate Hydroxlapatite for Augmentation of the Edentulous Atrophic Maxilla: A Preliminary Report, *J. Oral Maxillofac. Surg*., **47**, 137–141.
12. Blonk, M.S., Kent, J.N., Ardoin, R.C. *et al*. (1987). Mandibular Augmentation in Dogs with Hydroxylapatite Combined with Demineralized Bone, *J. Oral Maxillofac. Surg*., **45**, 414–420.
13. Hench, L.L., Xynos, I.D., Edgar, A.J. *et al.* (2002). Gene Activating Glasses, *J. Inorg. Mater.*, **17**, 897–909.

14. Thompson, I. and Hench, L. (2000). "Medical Application of Composites", in Kelly, A. and Zweben, C. (eds), *Comprehensive Composite Materials Vol. 6*, Elsevier, Amsterdam, pp. 727–753.
15. Thompson, I. and Hench, L. (1998). Mechanical Properties of Bioactive Glasses, Glass-Ceramics and Composites, *Proc Inst Mech Engrs*, Vol. 212 part H, pp. 127–136.
16. Oonishi, H., Hench, L.L. Wilson, J. *et al.* (1999). Comparative Bone Growth Behaviour in Granules of Bioceramic Materials of Various Sizes, *J. Biomed Mater Res*, **44**, 31–43.
17. Oonishi, H., Hench, L.L., Wilson, J. *et al.* (2000). Quantitative Comparison of Bone Growth Behaviour in Granules in Bioglass®, A-W Glass Ceramic, and Hydroxyapatite, *J. Biomed. Mater. Res.*, **51**, 37–46.
18. Chan, C.,Thompson, I., Robinson, P. *et al.* (2002). Evaluation of a Bioglass® — Dextran Composite as a Bone Graft Substitute, *J. Oral Maxillofac. Surg*., **31**, 73–77.
19. Wheeler, D.L., Eschbach, E.J., Hoellrich, R.G. *et al.* (2000). Assessment of Resorbable Bioactive Material for Grafting of Critical-Size Cancellous Defects, *J. Orthop. Res*., **18**, 140–148.

Chapter 11

CLINICAL APPLICATIONS OF BIOACTIVE GLASS: ORTHOPAEDICS

David M. Gaisser and Larry L. Hench

11.1. INTRODUCTION

Numerous animal studies at the University of Florida during 1969–1982 established the scientific basis for use of 45S5 Bioglass® in repair of orthopaedic defects. A key review article that summarizes the answers to questions regarding the strength and stability of the bone and time to develop a bone–Bioglass® implant bond was published in 1982 by Hench and Clark.[1] In Part A, the paper documents the time sequence of bonding of Bioglass® in rat femur and tibia, based upon ten references.[1,2] In Part B, bonding of Bioglass® implants to the femur in canine and monkey bones is summarized in five citations.[1,2] Part C reviews the data of bonding of mandibular and maxillary bone of primates and swine to Bioglass® implants with five citations.[1,2] These publications established that bone–Bioglass® bonds occurred in all the animal species tested. The rate of bond formation was slightly longer in larger species. A stable bone-bonded implant in the anterior region of the mandible of a baboon after four years of functional use is presented in this paper, one of the longest *in vivo* primate studies published. All of these early animal studies used bulk implants.

The discovery of osteoproduction (now termed osteostimulation) by Wilson and Low in the Patus monkey model of periodontal disease revolutionized the approach to bone repair with Bioglass®.[3] The emphasis shifted from use of bulk implants to *replace* bone to the use of Bioglass® particulate to stimulate *regeneration* of bone. The process of osteostimulation is under genetic control, as reviewed in Chapter 4. Building on the clinical success of PerioGlas®, the 45S5 Bioglass® particulate used in oral and maxillofacial indications (Chapter 9), a Bioglass® particulate for orthopaedic bone grafting was introduced into the European market in 1999, initially under the trade name OsteoGlas® and subsequently as NovaBone®. Studies by June Wilson *et al*. in a canine model showed effective bone regeneration with uses of 45S5 Bioglass® particulate.[4] Other animal models followed in various laboratories worldwide, as reviewed by Hench with 15 citations.[2] The NovaBone® product was cleared by the FDA for general orthopaedic bone grafting in non load-bearing sites in July, 2002.

Table 11.1. Orthopaedic Products, Based Upon 45S5 Bioglass®.

Trauma	
	Long bone fracture (acute and/or comminuted); alone and with internal fixation
	Femoral nonunion repair
	Tibial plateau fracture
Arthroplasty	
	Filler around implants (acetabular reconstruction)
	Impaction grafting
Spine Fusion	
	Interbody fusion (cervical, thoracolumbar, lumbar)
	Posterolateral fusion
	Adolescent idiopathic scoliosis
General	
	Filling of bone after cyst or tumour removal

11.2. RANGE OF CLINICAL APPLICATIONS

An increasing range of orthopaedic applications for NovaBone® synthetic bone graft have been reported during the last decade. Table 11.1 lists many of them. This chapter reviews some case histories and a clinical trial that compares 45S5 Bioglass® synthetic graft with autogeneous bone grafts.

11.3. COMPARATIVE STUDIES OF REGENERATIVE BIOACTIVE GLASS

The osteoblast lineage cell culture results reviewed in Chapter 4 showed that osteogenesis was enhanced when the progenitor cells were exposed to either Bioglass® ionic dissolution products or Bioglass® particulate. These findings correlated with the quantitative studies of Bioglass® particulate compared with calcium-phosphate synthetic bone grafts in the Oonishi femoral condyle critical-sized defect model.[5] Both cell culture and animal studies correlate with favourable clinical results using the same bioactive material, 45S5 Bioglass®.[6–12]

Clinical studies that compare the success of autogeneous bone grafts versus grafts of the gene-activating glasses show equivalent rates of bone regeneration and fewer side effects with the bioactive glasses.[12] Iliac crest autograft is currently the gold standard for spinal fusion. However, there are disadvantages of an autogeneous graft, including increased blood loss, increased operative time,

Table 11.2. Conclusions from 45S5 Bioglass® Spinal Fusion Clinical Study.[12]

[1]	Bioglass is as effective as iliac crest graft to achieve fusion and maintain correction in AIS.
[2]	Fewer complications were seen in the bioactive glass group of patients.
[3]	The morbidity of iliac crest harvesting can be avoided by use of bioactive glass in spinal fusion.

second site morbidity, and pain, as reviewed in Chapter 10. A comparative study of bioactive glass (45S5 Bioglass®) versus iliac crest autograft for spinal fusion in adolescent idiopathic scoliosis (AIS) has been reported for a group of 88 consecutive patients.[12] Forty patients received iliac crest autograft and 48 received Bioglass® with a minimum of two-year follow-up. The results showed fewer infections (2% vs 5%) and fewer mechanical failures (2% vs 7.5%) in the Bioglass® group. Loss of correction of the main thoracic curve was also less for the Bioglass® group (11% vs 15.5%). The conclusions of this retrospective clinical study are summarized in Table 11.2.[12]

These are important conclusions for the 21st-century challenge of achieving affordable healthcare for the aged. Elimination of the need for second site (iliac crest) surgery in elderly patients that require spinal fusion means less exposure to anaesthesia and potential for infection. It also avoids pain and healing of the second site. Similar clinical findings have shown that rapid bone regeneration occurs when 45S5 Bioglass® is used as a synthetic bone graft in revision surgery for failed total hip prostheses, as described below.

11.4. CASE HISTORIES

Early orthopaedic studies evaluated the use of bioactive glass as an autograft extender for lumbar spine fusion. Since then, the material has been used either alone or as a graft extender in a variety of indications, including lumbar fusion, cervical spine fusion, acute long bone fractures and the treatment of nonunions, as well as for use in revision surgery.

11.4.1. Autograft Extender in Posterior Lumbar Fusion

Figure 11.1 demonstrates the use of a 45S5 bioactive glass particulate (NovaBone®) as an autograft extender in posterior lumbar fusion following diagnosis of degenerative spondylolisthesis and stenosis. Following bilateral hemilaminectomy and foraminotomy at L4–L5, the local transverse processes and

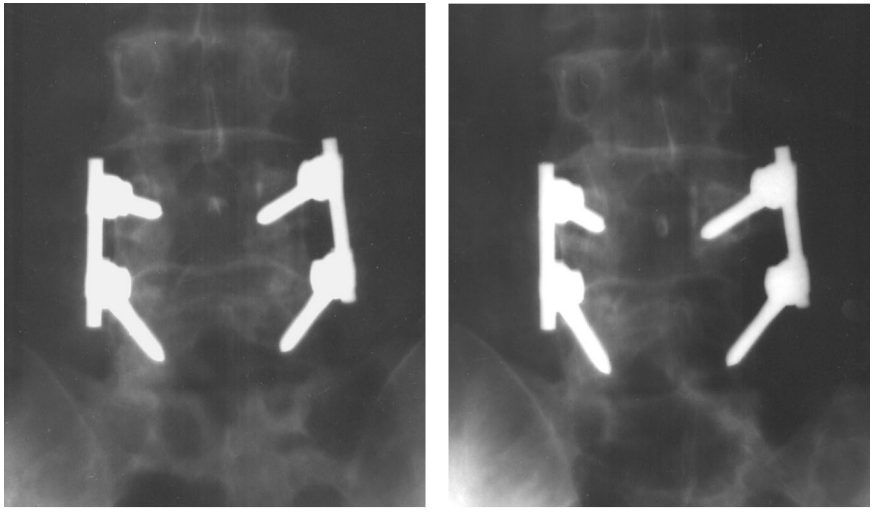

(a) (b)

Figure 11.1. Use of a bioactive glass particulate as an autograft extender in posterior lumbar fusion. The left side was grafted with a 50/50 mixture of NovaBone® with autogeneous bone and the right side with 100% autogeneous bone. (a) Two months; (b) six months.

facet joints were decorticated, followed by grafting with a 50:50 mixture of bioactive glass and autogenous iliac crest bone on the left and autograft alone on the right. At two months, both left and right fusion masses can be seen. At six months, solid fusion is observed, with no differences between the graft types. Thus, the results are equivalent to the conclusions of the comparative clinical study reviewed above.[12]

11.4.2. Treatment of a Femoral Nonunion

In Fig. 11.2, bioactive glass particulate (NovaBone®) was used in the treatment of a femoral nonunion of 14 months duration. After several attempts at treatment, a femoral nail was placed in an effort to stabilize the fracture. However, the patient subsequently fell and the nail was forced proximally and bent at the nonunion site. The nail was removed and replaced with an intramedullary rod. The nonunion was debrided and grafted with bioactive glass particulate mixed with autogenous bone. Postoperatively, the new rod is seen in place and the graft

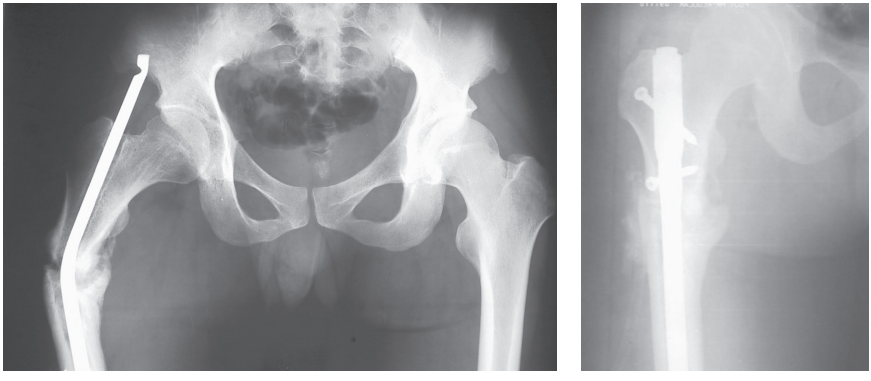

(a) (b)

Figure 11.2. Use of bioactive glass particulate (NovaBone®) in treatment of a femoral nonunion. (a) Patient shows intramedullary rod and graft in site of nonunion. (b) At six months, the fracture line has disappeared and the nonunion has healed.

mass observed. At six months, the fracture line has disappeared and the former nonunion has healed.

11.4.3. Revision Arthroplasty

Figure 11.3 shows the use of bioactive glass particulate in revision arthroplasty. Following aseptic loosening, a hip implant of 15 years duration was removed and replaced. The all-polyethylene acetabular component was removed and the site prepared for grafting. The acetabular graft area is visible on the post-operative radiograph as an area of increased radio-opacity behind the non-cemented cup, associated with a visible up-fracture of the medial acetabular wall. By six months, the graft area has remodelled to an appearance more similar to that of the surrounding bone.

11.4.4. Treatment of an Acute Spiral Fracture

Figure 11.4 demonstrates graft material use in the treatment of an acute spiral fracture of the humerus following a motor vehicle accident. An open reduction of the fracture was performed and the fracture site grafted with 10 cc of bioactive glass particulate (NovaBone®). An external fixator was placed to achieve mechanical stabilization. At six months, the fracture site had fully healed without complication and the fixator had been removed.

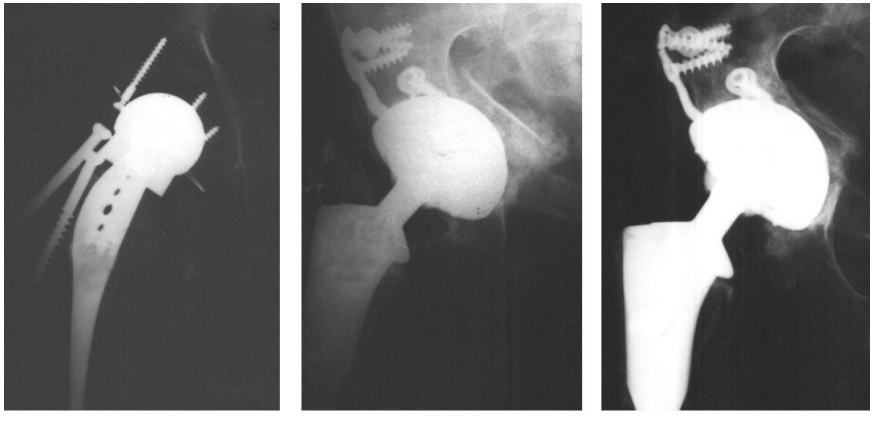

(a) (b) (c)

Figure 11.3. Use of bioactive glass particulate in revision arthroplasty. (a) Preoperative radiograph of failed hip arthroplasty. (b) Immediate postoperative view, with visible graft area visible behind acetabular component. (c) At six months, bone remodelling behind acetabular component is observed.

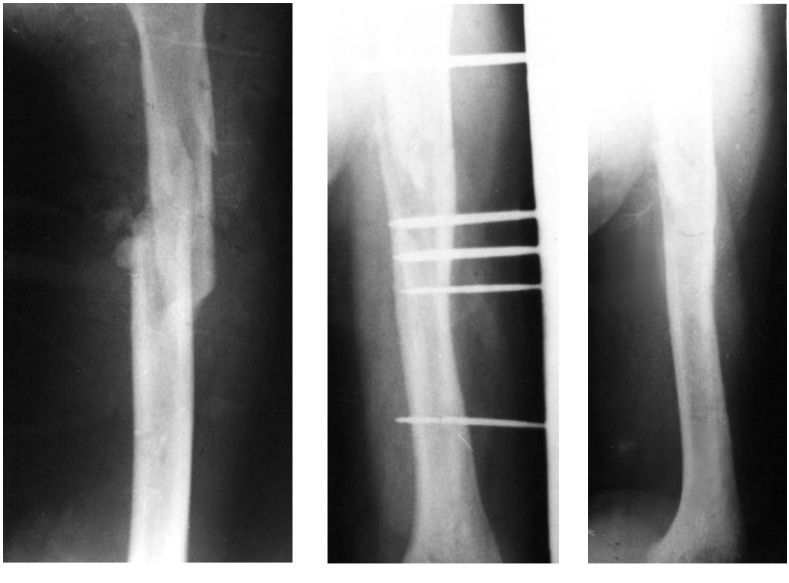

(a) (b) (c)

Figure 11.4. NovaBone® graft material used to treat an acute spiral fracture of the humerus. (a) Preoperative. (b) Immediate postoperative. (c) Six months after grafting, the site has fused and the external fixator has been removed.

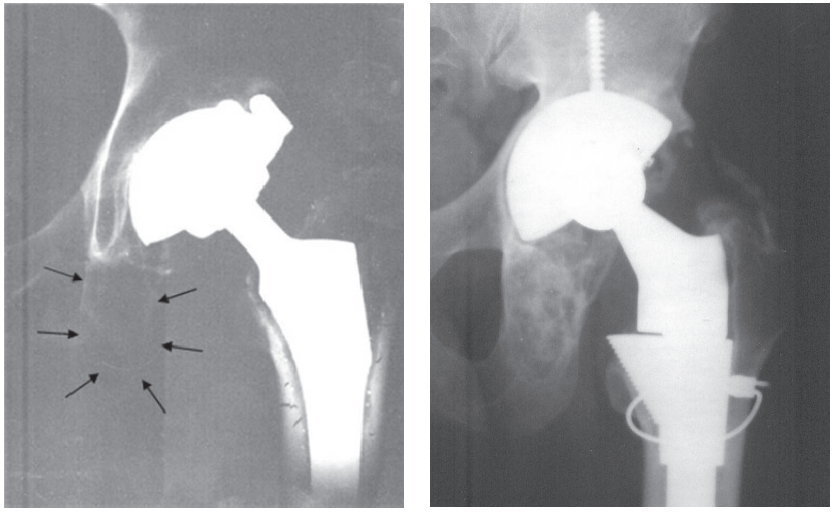

(a) (b)

Figure 11.5. Bioactive glass grafting of a unicameral cyst in the ischium. (a) Preoperative radiograph. The arrows indicate the site of cyst. (b) Three years post-implantation and revision arthroplasty, site has healed with no cyst recurrence.

11.4.5. Bone Graft Prior to Revision hip Arthroplasty

Figure 11.5 shows a large unicameral cyst in the ischium of a patient prior to revision hip arthroplasty due to implant loosening. The existing hardware was removed and replaced, and the cyst was debrided. The residual cavity then was grafted with a 50:50 mixture of autogenous bone and bioactive glass (NovaBone®). Three years after implantation, the graft site is stable with no recurrence of the cyst, the site is being filled with dense bony tissue.

11.5. CONCLUSION

More than a decade of use of 45S5 Bioglass® (NovaBone®) synthetic graft material in a wide range of orthopaedic cases has demonstrated that rapid bone regeneration is achieved when the synthetic is used either as a graft extender with autogeneous bone or by itself. Use of the synthetic graft can minimize the need for second site surgery to obtain autogeneous bone in elderly patients or in cases where the quality of bone has been compromised by various factors, such as osteoporosis.

REFERENCES

1. Hench, L.L. and Clark, A.E. (1982). "Adhesion to Bone", in Williams, D.F. and Winter, G.D. (eds), *Biocompatibility of Orthopaedic Implants*, **6**, CRC Press. Boca Raton, FL.
2. Hench, L.L., Hench, J.W. and Greenspan, D.C. (2004). Bioglass: A Short History and Bibliography, *J. Aust. Ceram. Soc.*, **40**, 1–42.
3. Wilson, J. and Low, S.B. (1992). Bioactive Ceramics for Periodontal Treatment: Comparative Studies in the Patus Monkey, *J. Appl. Biomaterials*, **3**, 123–169.
4. Wilson, J., Yu, L.T. and Beale, B.S. (1992). Bone Augmentation Using Bioglass® Particulates in Dogs: Pilot Study, *Bioceramics*, **5**, 139–146.
5. Oonishi, H., Kutshitani, S., Yasukawa, E. *et al.* (1997). Particulate Bioglass® Compared with Hydroxyapatite as a Bone Graft Substitute, *J. Clin. Ortho. Res.*, **334**, 316–325.
6. Shapoff, C.A., Alexander, D.C. and Clark, A.E. (1997). Clinical Use of a Bioactive Glass Particulate in the Treatment of Human Osseous Defects, *Compendium Contin. Educ. Dent*., **18**, 352–363.
7. Lovelace, T.B., Mellonig, J.T., Meffert, R.M. *et al.* (1998). Clinical Evaluation of Bioactive Glass in the Treatment of Periodontal Osseous Defects in Humans, *J. Periodontol.*, **69**, 1027–1035.
8. Park, J.S., Suh, J.J., Choi, S.H. *et al.* (2001). Effects of Pre-Treatment Clinical Parameters on Bioactive Glass Implantation in Intrabony Periodontal Defects, *J. Periodontal.*, **72**, 730–740.
9. Aitasalo, K., Kinnunen, I., Palmgren, J. *et al.* (2001). Repair of Orbital Floor Fractures with Bioactive Glass Implants, *J. Oral Maxillofac. Surg.*, **59**, 1390–1395.
10. Yukna, R.A., Evans, G.H., Aichelmann-Reidy, M.B. *et al.* (2001). Clinical Comparison of Bioactive Glass Bone Replacement Graft Material and Expanded Polytetrafluoroethylene Barrier Membrane in Treating Human Mandibular Molar Class II Furcations, *J. Periodontol.*, **72**, 125–133.
11. Mengel, R., Soffner, M., Flores-de-Jacoby, L. (2003). Bioabsorbable Membrane and Bioactive Glass in the Treatment of Intrabony Defects in Patients with Generalized Aggressive Periodontitis: Results of a 12-Month Clinical and Radiological Study, *J. Periodontol.*, **74**, 899–908.
12. Ilharreborde, B.E., Morel, F., Fitoussi, A. *et al.* (2008). Bioactive Glass as a Bone Substitute for Spinal Fusion in Adolescent Idiopathic Scoliosis: A Comparative Study with Iliac Crest Autograft, *J. Pediatr. Orthop.*, **28**, 347–351.

Chapter 12

BIOACTIVE GLASS IN SPINAL REPAIR

Janek Frantzén

12.1. INTRODUCTION

Spine surgery is one of the fastest growing areas in the field of surgery. An annual growth is estimated to be 6%, reaching US $2.3 billion in revenues for biologics used in spine surgery by the year 2015.[1] The trend in modern spine surgery evolves towards minimally-invasive procedures that result in faster recovery for the patient and less injury to surrounding tissues. Common for most spinal fusion procedures is the need to build bone in an extraosseal environment. The gold standard has been the patient's own bone (autograft), harvested from the iliac crest, providing a scaffold and osteogenic factors that are needed for fusion of the vertebra. This additional procedure is associated with a prolonged operation time, increased blood loss and causes additional postoperative pain beyond the time that the spine heals.[2,3] See Chapter 10 for a discussion of the pros and cons of autografts versus synthetic bone grafts.

Many spine procedures use hardware such as titanium, polyether-etherketone (PEEK) or composite implants.[4,5,6] In addition to mal-unions, one of the main concerns for spine surgeons is to avoid postoperative infection. All infections require long antibiotic treatment and deep infections need reoperations for debridement and, in a majority of cases, the removal of the implanted hardware, causing a high incidence of long-term morbidity to the patient.[7,8]

An optimal bone graft substitute would address all these concerns by having osteoconductive, ostostimulative and bioactive bone bonding properties. A bone graft substitute that supports angiogenesis, possesses antibacterial properties that protect implants used in surgery and also enhances wound healing and bone regeneration would have a great impact on the clinical result.

12.2. SPINAL FUSION

The degeneration of the spine is a multifactorial process. Degenerative spondylolisthesis is a common cause of lower back pain and radiculopathy in adults older than 40 years.[9] Secondary changes such as facet hypertrophy and thickening of the ligamentum flavum lead to spinal stenosis and cause neurogenic

claudication. If conservative treatment fails, surgery with decompression, restoration of the intervertebral space and fusion is justified. Acquired diseases such as infection, tumors or scoliosis often require fusion of affected segments of the spine as part of the treatment. A majority of spine fractures can be treated conservatively with braces and physiotherapy. Unstable spine burst fractures with neurological deficits require prompt surgery in order to decompress the neural elements and realign the vertebra.[10]

Surgical fusion of the spine requires an instrumented spondylodesis with posterior transpedicular screw fixation, where the screws are interconnected to rods on each side of the spine. Additional stability can be achieved by combining intercorporal spacers, expandable corpectomy devices and various plating systems, depending on the pathology. Autogenous bone is harvested from the iliac crest or bone material from the decompressive procedure is used to fill spacers or posterolaterally at the fusion sites between the transverse processes. Meticulous preparation by decortification of the fusion site is imperative in order to achieve an extraosseal fusion, regardless of the type of bone graft material used.

Potential options for bone graft substitutes are platelet gels, demineralized bone matrices, synthetic bone grafts and bone morphogenetic proteins. Recently, safety concerns have been raised in the use of bone morphogenetic proteins.[11] The options mentioned above have shown promising preclinical data but still lack sufficient clinical data demonstrating efficacy in lumbar fusion.[12]

12.3. BIOACTIVE GLASS IN SPINE SURGERY: BACKGROUND

The unique bone bonding of bioactive glass is well-established.[13,14] Formation of a SiO_2 and calcium-phosphate-rich layer is the result of leaching of ions, dissolution and precipitation, described in Chapters 3 and 4. The antibacterial properties are attributed to an increased osmotic pressure caused by the ions leaching from the surface of the glass. The surface reaction leading to the production of sodium hydroxide leads to an increase in the pH, initially contributing to the antibacterial effect of bioactive glass. The early results showed bacteriostatic effects in experimental and clinical otorhinological use.[15] Furthermore, bioactive glass has been shown *in vitro* to have effective bacterial growth-inhibiting properties toward 17 anaerobic bacteria,[16] and bactericidal effects on 29 clinically important aerobic bacteria.[17] In addition, preclinical studies have shown that the bioactive glass surface is not only conductive but also osteoproductive in promoting migration, replication and differentiation of osteogenic cells and their matrix production.[18] The cellular response in defects filled with bioactive glass granules

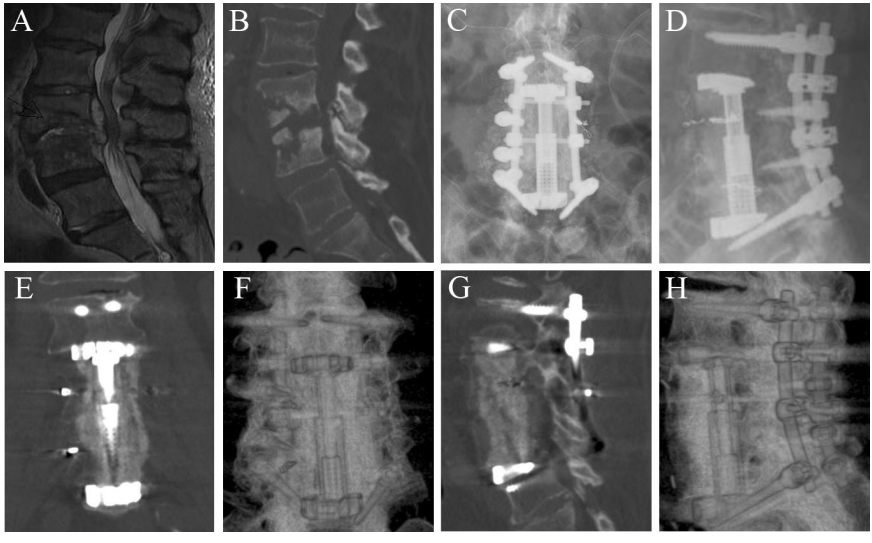

Figure 12.1. 75-year old female suffered from severe back pain. Spondylodiscitis was verified on MRI. She had received broad antibiotics for more than two years. *Mycobacterium tuberculosis* was identified by PCR from pus that was drained from the psoas abscesses during surgery. Antibiotic treatment was then directed towards this pathogen.

A. Preoperative sagittal T2 weighted MRI showing spondylodiscitis at L3–L4 and an epidural abscess.

B. Preoperative sagittal CT reconstruction shows the destruction of L3 and L4 vertebral bodies.

C–D. Postoperative AP and lateral X-ray after posterior decompression L2–L4, spondylodesis L2–L5, lumbotomy, canalisation of paravertebral abscess, resection of vertebraes L3 and L4 and anterior reconstruction using an expandable, vertebral body replacement device and 32 cc of S53P4 bioactive glass.

E–H. Two-year postoperative CT and 3D MIP reconstructions showing solid fusion and that the patient had fully recovered.

was characterized by continuous overexpression of type III collagen and osteogenic mesenchymal cells, prior to their differentiation to osteoblasts, organized as a dense periosteum-like layer on the surface the bioactive glass granules.

The first clinical publication on the use of bioactive glass (S53P4) in the treatment of osteomyelitis in the lower extremities and spine showed that it was effective as a one-stage procedure, with a favorable outcome in 10 out of 11 patients lasting for a mean of 24 months (range 10–38 months).[19] See Fig. 12.1 for an example of the procedure.

There are only a few publications to date on the use of bioactive glass in instrumented spine surgery. In lumbar fusions using a HA-BAG composite (Chitra-HABg) as graft material, a high resorption rate and a poor consolidation was reported in 95% of the BAG composite cases. The Chitra-HABg used in this study which had to be terminated early contained 80% HA and 20% of a BAG (composition unknown). The outcome of that study was excellent on the autograft side.[20]

An apatite-wollastonite containing bioactive glass-ceramic (A/W glass-ceramic), developed at the Kyoto University in 1982, was used in 14 patients undergoing lumbar fusion. Seven out of 11 patients followed for 18 months showed subtotal/total fusion and at two-year follow-up the remaining six patients were all in this category. References and various surgical applications of the A/W glass-ceramic in many thousands of cases in Japan are discussed in Chapter 14 by Professor T. Yamamuro.

A combination of bioactive glass 45S5 Bioglass® (Novabone®) and autograft bone has been compared with autograft bone alone in the treatment of 88 patients with adolescent idiopathic scoliosis, resulting in similar results to those obtained using autograft alone.[21] The loss of correction of the main thoracic curve was slightly less for the bioactive glass group. Moreover, the blood loss and the complication rate were also significantly lower for the bioactive glass group.[21]

12.4. BIOACTIVE GLASS IN SPINE SURGERY: TURKU UNIVERSITY

Bioactive glasses of a composition modified from the original 45S5 composition were investigated at Turku University during the 1980s. Preclinical animal tests showed strong interfacial bonding with bone. In an experimental rabbit model for spine fusion there was no significant difference between bioactive glass granules and autograft in new bone formation at the 12 week time point.[22] Details are presented in Chapter 3, including the chemical formula that contains 53% SiO_2. The designation of the bioactive glass is S53P4. In our prospective long-term study for the use of bioactive glass S53P4 (BonAlive®) in degenerative spondylolisthesis of the lumbar spine and unstable burst fractures, we reported the clinical and radiological findings. In the degenerative group standard instrumented lumbar fusion was performed and a mean of 25 g (20–40 g) of S53P4 bioactive glass granules and autograft was placed on each posterolateral fusion bed in 20 patients during 1996–1998. Seventeen patients participated in the whole 11-year follow-up, two died of unrelated causes and one was lost to follow-up.

A solid bony fusion was seen on CT scans on the side of autogenous bone in all patients and on the side of bioactive glass in 12 out of 17 patients. The fusion rate of all 41 fusion sites for bioactive glass was 88% at the levels L4/5 and L5/S1. The mean visual analogue scales (VAS) for back pain at 11-year follow-up was 3.5 (range 0 to 8) compared to the preoperative value of 7.3 (range 4 to 9). The mean Oswestry disability index (ODI) at the follow-up was 21 (range 0 to 52) compared with the preoperative score of 49 (range 32 to 64). The overall subjective satisfaction was better for 15 patients at the 11-year follow-up than before the operation.[23] Figure 12.2 illustrates this clinical application.

In the trauma group two patients had incomplete spinal cord injuries classified as Frankel C; the others were neurologically intact. Fractures were reduced and fixed using USS® instrumentation and a mean of 23 g (10–35 g) bioactive glass S53P4, and autograft was placed on each posterolateral fusion bed. Ten patients participated in the ten-year follow-up. Three patients had died from unrelated causes and three patients did not want to participate for personal reasons. No additional operations or hardware removals had been performed after the primary operation. A solid bony fusion was seen with CT in all patients on the side of autogenous bone. On the side where bioactive glass was used a solid bony fusion was observed in five patients and a partial fusion in five patients. This resulted in a fusion-rate of 71% for BAG; 15 fused segments out of 21 in total. The mean ODI was excellent, 12 (range 0–46). The mean VAS for radicular and back pain was 1 (range 0–4). All patients had returned to their jobs. At the time of the ten-year follow-up, five of the ten patients were retired on the basis of their age, none because of their medical condition.[24] Good clinical and radiological results have also been observed clinically using bioactive glass S53P4 mixed equally with autograft in a two-year follow-up (unpublished results). Figure 12.3 illustrates this clinical application of bioactive glass.

12.5. TREATMENT OF VERTEBRAL FRACTURES

Vertebral fracture incidence increases exponentially after the age of 50, affecting 30–50% of women and 20–30% of men during their life.[25] Such fractures cause severe back pain, disability and impairment, leading to a raised mortality rate extending beyond the first year after the fracture.[26] Vertebroplasty, i.e. injection of poly(methyl methacrylate) (PMMA), is the common treatment for vertebral compression fractures non-responsive to conservative care. This treatment provides effective, immediate pain relief, but the material has received criticism for its properties. In a recent prospective randomized FDA-IDE trial,

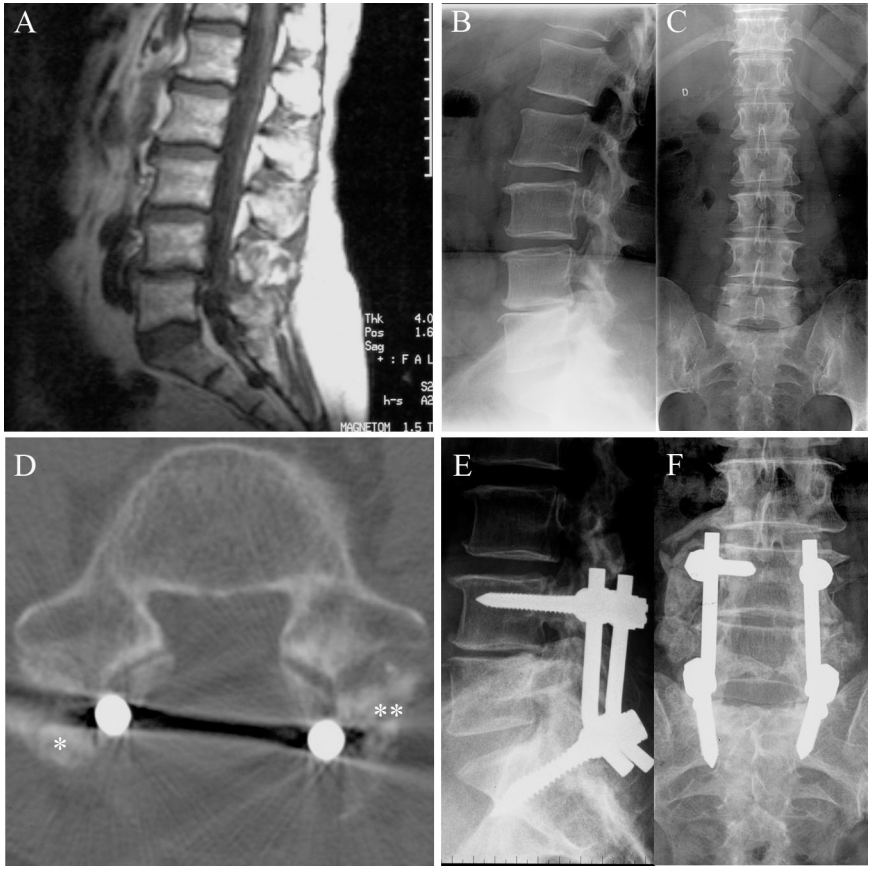

Figure 12.2. The patient is a 76-year old female treated for a L4/5 degenerative spondylolslisthesis with instability symptoms and radicular pain in the lower extremities.

A. Preoperative T1 weighted sagittal MRI shows disc degeneration at L4/5 and segmental stenosis.

B. Lateral X-ray image shows loss of disc height and traction spurs at L4/5 and a 4 mm L5 antelithesis in neutral standing position.

C. AP plain X-ray shows straight posture and no signs of scoliosis preoperatively.

D. One-year postoperative axial CT image at level of L4 shows a solid fusion on both the (*)autograft and on the (**)BG side.

E–F. Plain X-ray images show strong fusion on the autograft side and bridging ostephytes from L3.

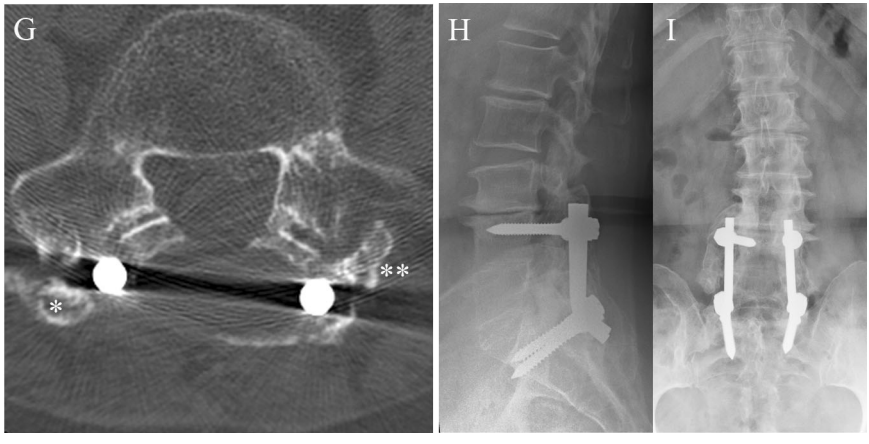

Figure 12.2. (*Continued*)

G. 11.5 year postoperative axial CT image at level of L4 shows a solid fusion on both the (*)autograft and on the (**)BG side.

H–I. Plain X-ray images show severe loss of disc height at adjacent level L3/4 with prominent anterior osteophytes and slight degenerative retrolisthesis of L3. Shown in AP view, L3 is fused to L4 on the right side and a slight degenerative scoliosis is observed above the fusion.

investigators compared the treatment results of 162 patients receiving Cortoss to 94 patients receiving PMMA for vertebroplasty injection.[27] Cortoss consists of 33% di-functional methacrylates (bis-GMA, TEGDMA, bis-EMA) that form a highly cross-linked three-dimensional polymer, reinforced with 67% radio-opaque and bioactive glass ceramic particles. Its mechanical properties closely match those of bone in compression. Non-inferiority of Cortoss relative to PMMA was observed, with Cortoss-treated patients experiencing significant pain relief at three months (p=0.0395) and better maintenance or improvement in function at 24 months (p=0.0299). Incidence of serious device-related adverse events was 4.3% in both groups, none were life-threatening.

12.6. FUTURE ASPECTS

Preliminary results suggest that bioactive glass S53P4 can be considered a good, effective and usable material for the treatment of osteomyelitis, still warranting long-term follow-up. Bioactive glass as a bone graft extender can be considered as a good alternative in degenerative and trauma spine surgery. From

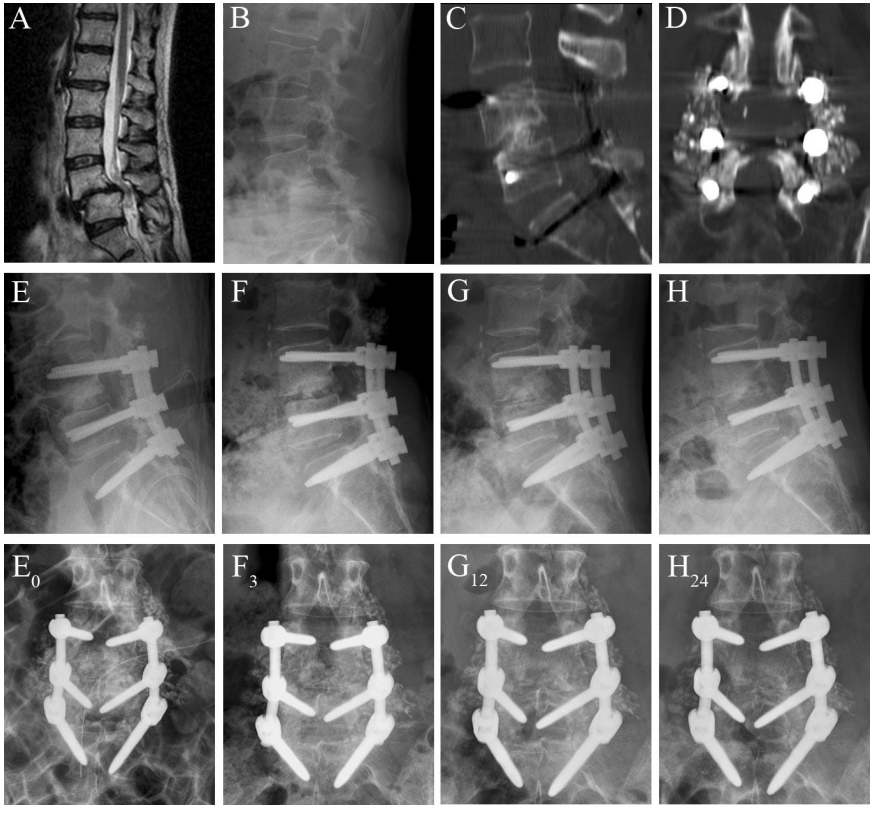

Figure 12.3. 51-year old female with predominantly low-back pain for several years, severe for six months, radicular pain and a mild peroneal palsy. Neurogenic claudication at 30 m and an antropoid gait. She was treated by a transpedicular fusion L4-S1, decompression and a reduction combined with an intercorporal fusion L4-L5 using autograft and 8 cc of S53P4 bioactive glass. She returned to her work as a nurse four-months postoperatively. At the 24-month postoperative control the subjective outcome was excellent, ODI was 1/45(2,2%). (Courtesy of Dr. Juho Rantakokko, Turku University Hospital.)

A. T2 weighted sagittal MRI showing a 15 mm L4/5 high-grade degenerative slip and severe spinal stenosis and Modic I end-plate changes.

B. Functional X-ray in forward bending showed an increase of the slip.

C–D. Postoperative sagittal and coronal reconstruction confirming the reduction and autograft and bioactive glass covering the transverse processes L4, L5 and sacrum.

E–H. Postoperative lateral X-rays 0, 3, 12 and 24 months postoperatively confirms the intact posture and fusion building intercorporally between L4–L5.

E_0–H_{24}. Postoperative AP X-rays 0, 3, 12 and 24 months postoperatively shows the development over time of a solid fusion L4-S1.

a socio-economic point of view one needs to take into account when using autografts the longer operation time required for harvesting bone, risk of infection and postoperative hematoma, resulting in a potentially increased sick leave when evaluating the cost of treatment. Local hospital bone banks are getting more centralized, opening an opportunity for increased use of synthetic bone substitute materials. The clinical use of bioactive glass as a bulk implant has been limited due to its structural weakness. The modulus of elasticity is high but due to the amorphous structure it is brittle. This makes a weight-bearing construct difficult to develop for spine surgery. Methods such as rapid prototyping and unidirectional freezing of suspensions have resulted in the creation of porous bioactive glass scaffolds with compressive strength and elastic modulus, which are comparable to, or approach the values for, human cortical bone.[28,29,30] These scaffolds have potential applications in the regeneration of load-bearing bones.[31]

12.7. CONCLUSION

One has to remember that the patient is always in focus and the surgeon's primary task is to provide the best care available for the patient. Bone graft substitutes offer promise for the future but they have to be safe, effective and affordable. In the end it all comes down to Hippocrates' quote: "As to diseases, make a habit of two things — to help, or at least, to do no harm."

REFERENCES

1. William Blair & Company, L.L.C., Industry Report, January 6, 2011.
2. Robertson, P.A. and Wray, A.C. (2001). Natural History of Posterior Iliac Crest Bone Graft Donation for Spinal Surgery: A Prospective Analysis of Morbidity, *Spine*, **26**, 1473–1476.
3. Banwart, J.C., Asher, M.A. and Hassanein, R.S. (1995). Iliac Crest Cone Graft Harvest Donor Site Morbidity: A Statistical Evaluation, *Spine*, **20**, 1055–1060.
4. Aebi, M., Etter, C., Kehl, T. *et al.* (1987). Stabilization of the Lower Thoracic and Lumbar Spine with the Internal Spinal Skeletal Fixation System. Indications, Techniques, and First Results of Treatment, *Spine*, **12**, 544–551.
5. Dickman, C.A., Fessler, R.G., MacMillan, M. *et al.* (1992). Transpedicular Screw-Rod Fixation of the Lumbar Spine: Operative Technique and Outcome in 104 Cases, *J. Neurosurg*., **77**, 860–870.

6. Ponnappan, R.K., Serhan, H., Zarda, B. *et al.* (2009). Biomechanical Evaluation and Comparison of Polyetheretherketone Rod System to Traditional Titanium Rod Fixation, *Spine*, **9**, 263–267.
7. Stambough, J.L. and Beringer, D. (1992). Postoperative Wound Infections Complicating Adult Spine Surgery, *J. Spinal. Disord.*, **5**, 277–285.
8. Labler, L., Keel, M., Trentz, O. *et al.* (2006). Wound Conditioning by Vacuum Assisted Closure (V.A.C.) in Postoperative Infections after Dorsal Spine Surgery, *Eur. Spine. J.*, **15**, 1388–1396.
9. Booth, K.C., Bridwell, K.H., Eisenberg, B.A. *et al.* (1999). Minimum 5-year Results of Degenerative Spondylolisthesis Treated with Decompression and Instrumented Posterior Fusion, *Spine*, **24**, 1721–1727.
10. Stambough, J.L. (1997). Posterior Instrumentation for Thoracolumbar Trauma, *Clin. Orthop. Rel. Res*., **335**, 73–88.
11. Carragee, E.J., Hurwitz, E.L. and Weiner, B.K. (2011). A Critical Review of Recombinant Human Bone Morphogenetic Protein-2 Trials in Spinal Surgery: Emerging Safety Concerns and Lessons Learned, *Spine*, **11**, 471–491.
12. Rihn, J.A., Kirkpatrick, K. and Albert, T.J. (2010). Graft Options in Posterolateral and Posterior Interbody Lumbar Fusion, *Spine*, **35**, 1629–1639.
13. Hench, L., Splinter, R., Allen, J. *et al.* (1971). Bonding Mechanisms at the Interface of Ceramic Prosthetic Materials, *J. Biomed. Mater. Res.*, **5**, 117–141.
14. Hench, L.L. (1991). Bioceramics: From Concept to Clinics, *J. Am. Ceram. Soc*., **74**, 1487–1510.
15. Stoor, P., Söderling, E. and Salonen, J.I. (1998). Antibacterial Effects of a Bioactive Glass Paste on Oral Microorganisms, *Acta. Odontol. Scand*., **56**, 161–165.
16. Leppäranta, O., Vaahtio, M., Peltola, T. *et al.* (2008). Antibacterial Effect of Bioactive Glasses on Clinically Important Anaerobic Bacteria *In Vitro*, *J. Mater. Sci. Mate. Med.*, **19**, 547–551.
17. Munukka, E., Leppäranta, O., Korkeamäki, M. *et al.* (2008). Bactericidal Effects of Bioactive Glasses on Clinically Important Aerobic Bacteria, *J. Mater. Sci. Mater. Med.*, **19**, 27–32.
18. Virolainen, P., Heikkilä, J., Yli-Urpo, A. *et al.* (1997). Histomorphometric and Molecular Biologic Comparison of Bioactive Glass Granules and

Autogenous Bone Grafts in Augmentation of Bone Defect Healing, *J. Biomed. Mater. Res*., **36**, 9–17.

19. Lindfors, N., Hyvönen, P., Nyyssönen, M. *et al.* (2010). Bioactive Glass S53P4 as Bone Graft Substitute in Treatment of Osteomyelitis, *Bone*, **47**, 212–218.
20. Acharya, N.K., Kumar, R.J., Varma, H.K. *et al.* (2008). Hydroxyapatite-Bioactive Glass Ceramic Composite as a Stand-alone Graft Substitute for Posterolateral Fusion of Lumbar Spine: A Prospective, Matched, and Controlled Study, *J. Spinal. Disord. Tech.*, **21**, 106–111.
21. Ilharreborde, B., Morel, E., Fitoussi, F. *et al*. (2008). Bioactive Glass as a Bone Substitute for Spinal Fusion in Adolescent Idiopathic Scoliosis: A Comparative Study with Iliac Crest Autograft, *J. Ped. Orthop*., **28**, 347–351.
22. Lindfors, N.C. and Aho, A.J. (2000). Tissue Response to Bioactive Glass and Autogenous Bone in the Rabbit Spine, *Eur. Spine. J*., **9**, 30–35.
23. Frantzén, J., Rantakokko, J., Aro, H.T. *et al.* (2011). Instrumented Spondylodesis in Degenerative Spondylolisthesis with Bioactive Glass and Autologous Bone: A Prospective 11-Year Follow-Up, *J. Spinal. Disord. Tech.*, **24**, 455–461.
24. Rantakokko, J., Frantzén, J.P., Heinänen, J. *et al.* (2012). Posterolateral Spondylodesis Using Bioactive Glass S53P4 and Autogenous Bone in Instrumented Unstable Lumbar Spine Burst Fractures: A Prospective 10-year Follow-Up Study, *Scand. J. Surg.*, **101**, 66–71.
25. Kanis, J.A. and McCloskey, E.V. (1992). Epidemiology of Vertebral Osteoporosis, *Bone*, **13**, 1–10.
26. Center, J.R., Nguyen, T.V., Schneider, D. *et al.* (1999). Mortality after All Major Types of Osteoporotic Fracture in Men and Women: An Observational Study, *Lancet*, **13**, 878–882.
27. Bae, H., Hatten, H.P. Jr, Linovitz, R. *et al.* (2012). A Prospective Randomized FDA-IDE Trial Comparing Cortoss, to PMMA for Vertebroplasty: A Comparative Effectiveness Research Study with 24-Months Follow-Up, *Spine*, **7**, 544–550.
28. Rahaman, M.N., Day, D.E., Bal, B.S. *et al.* (2011). Bioactive Glass in Tissue Engineering, *Acta. Biomater.*, **7**, 2355–2373.
29. Fu, Q., Rahaman, M.N., Bal, B.S. *et al.* (2010). Preparation and *In Vitro* Evaluation of Bioactive Glass (13–93) Scaffolds with Oriented Microstructures for Repair and Regeneration of Load-Bearing Bones, *J. Biomed. Mater. Res.*, **93**, 1380–1390.

30. Huang, T.S., Rahaman, M.N., Doiphode, N.D. *et al.* (2011). Porous and Strong Bioactive Glass (13–93) Scaffolds Prepared by Freeze Extrusion Fabrication, *J. Mater. Sci. Mater. Med.*, **22**, 515–523.
31. Xia, W. and Chang, J. (2010). Bioactive Glass Scaffold with Similar Structure and Mechanical Properties of Cancellous Bone, *J. Biomed. Mater. Res. B Appl. Biomater.*, **95**, 449–455.

Chapter 13

A/W GLASS-CERAMIC: PROCESSING AND PROPERTIES

Tadashi Kokubo

13.1. COMPOSITION AND PROCESSING

Glass can be converted by heat treatment into glass-crystal composites containing various kinds of crystalline phases with controlled sizes and contents. The resultant glass-ceramic can exhibit superior properties to the parent glass and to sintered crystalline ceramics. Generally, monophase bioactive ceramics such as Bioglass®-type glasses and sintered hydroxyapatite (HA) do not show as high a mechanical strength as human cortical bone. Natural bone is a composite in which an assembly of HA small crystal particles is effectively reinforced by organic collagen fibers. Kokubo *et al*. attempted to prepare a similar composite by a process of crystallization of glass in 1982. In this attempt, β-wollastonite ($CaO \cdot SiO_2$), consisting of a silicate chain structure, was chosen as the reinforcing phase.[1]

A parent glass in the pseudoternary system $3CaO \cdot P_2O_5$-$CaO \cdot SiO_2$-$MgO \cdot CaO \cdot 2SiO_2$ was prepared by the conventional melt-quenching method. When the glass in a bulk form was heated up to 1,050°C at a rate of 5°C/min, fine grained oxyapatite and fibrous β-wollastonite precipitated. Large cracks were, however, formed in the middle part of the crystallized product, because the wollastonite precipitated only from the outer surfaces of the glass.[2] In the next preparation the parent glass was crushed into a fine powder 5 μm in average size, pressed into the desired form and then subjected to the same heat treatment. The cracks were eliminated, but a small number of micropores remained in the intergranular spaces of the glass powders because the apatite and wollastonite precipitated before complete densification.[3] A small amount of CaF_2 was added to the composition of the parent glass, and glass powder of the composition MgO 4.6, CaO 44.7, SiO_2 34.0, P_2O_5 6.2 and CaF_2 0.5 weight percentage (wt%) was subjected to the same treatment. As a result, the glass powders were fully densified at about 830°C, and then the oxyfluoroapatite ($Ca_{10}(PO_4)_6(O,F_2)$) and wollastonite precipitated successively at 870 and 900°C respectively, to give a crack- and pore-free dense and homogeneous glass-ceramic.[2]

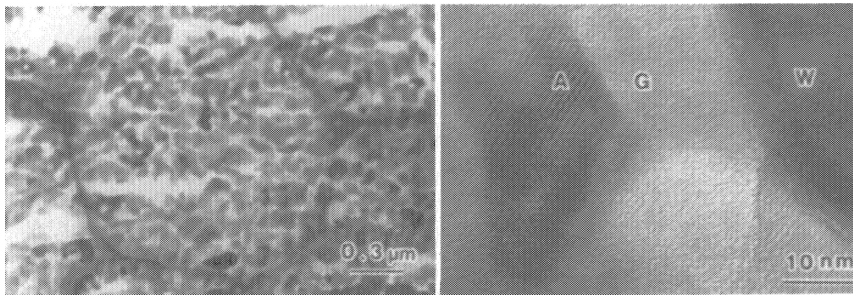

Figure 13.1. Transmission electron micrograph of A/W: glass-ceramic; A: apatite; W: wollastonite; G: glassy phase.

Figure 13.1 shows a transmission electron micrograph of the resultant glass-ceramic. In this case, the wollastonite did not take the fibrous form. Both the apatite and wollastonite were homogeneously dispersed in a glassy matrix, taking the shape of a rice grain 50 to 100 nm in size. According to powder X-ray diffraction, the contents of apatite, wollastonite and residual glassy phase were 38, 34 and 28 wt%, respectively, and the composition of the residual glassy phase was estimated to be MgO 16.6, CaO 24.2 and SiO_2 59.2 wt%.[3,4] This glass-ceramic was named A/W after the names of the crystalline phases and is called Cerabone® A/W commercially.

13.2. MECHANICAL PROPERTIES

A/W glass-ceramic can easily be machined into various shapes, even into screws, by diamond tools. Figure 13.2 shows A/W glass-ceramic shaped into artificial vertebrae, intervertebral spacers, spinous process spacers and iliac spacers. Some physical properties of the glass-ceramic are shown in Table 13.1. The bending strength (215 MPa) of this glass-ceramic is almost twice that (115 MPa) of dense sintered HA and even higher than that (160 MPa) of human cortical bone in an air environment. The parent glass G and the glass-ceramic A, precipitating only the apatite, have bending strengths of 72 and 88 MPa, respectively. It is evident that the high bending strength of A/W glass-ceramic is due to the precipitation of the wollastonite as well as apatite. A/W glass-ceramic has a fracture toughness of 2.0 $MPa \cdot m^{1/2}$ whereas glass G and the glass-ceramic A have only 0.8 and 1.2 $MPa \cdot m^{1/2}$, respectively. This means that the high bending strength of A/W glass-ceramic is attributed to its high fracture toughness. A/W glass-ceramic has a fracture surface energy of 15.9 Jm^{-2}, whereas glass G and glass-ceramic

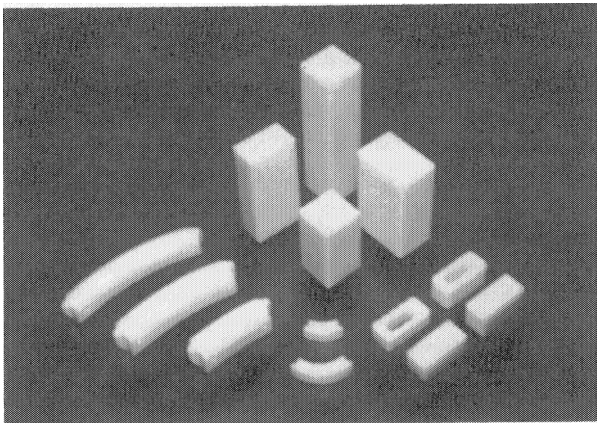

Figure 13.2. Iliac spacers (left), artificial vertebrae (middle top), spinal spacers (middle bottom) and intervertebral spacers (right).

Table 13.1. Physical Properties of A/W Glass-Ceramic.

Density (g/cm^3)	3.07
Bending Strength (MPa)	215
Compressive Strength (MPa)	1080
Young's Modulus (GPa)	118
Vickers Hardness (HV)	680
Fracture Toughness (MPa$^{1/2}$)	2.0
Slow Crack Growth (n)	33

A have only 3.3 and 6.4 Jm^{-2}, respectively. The high fracture toughness of A/W glass-ceramic is attributable to the high fracture surface energy. Glass G and glass-ceramic A show a fairly smooth fracture surface, whereas A/W glass-ceramic has a roughened fracture surface, as shown in Fig. 13.3. This means that the wollastonite effectively prevents straight propagation of the cracks, causing them to turn or branch out.[5] It is notable that the wollastonite exhibits such a reinforcing effect, even though it is not in a fibrous form.

When loaded in an aqueous body environment, this glass-ceramic shows a decrease in mechanical strength, i.e. fatigue, by slow crack growth due to stress corrosion, similar to other ceramics. The magnitude of its fatigue is, however, much lower than those of glass G and glass-ceramic A.[6] The decrease in

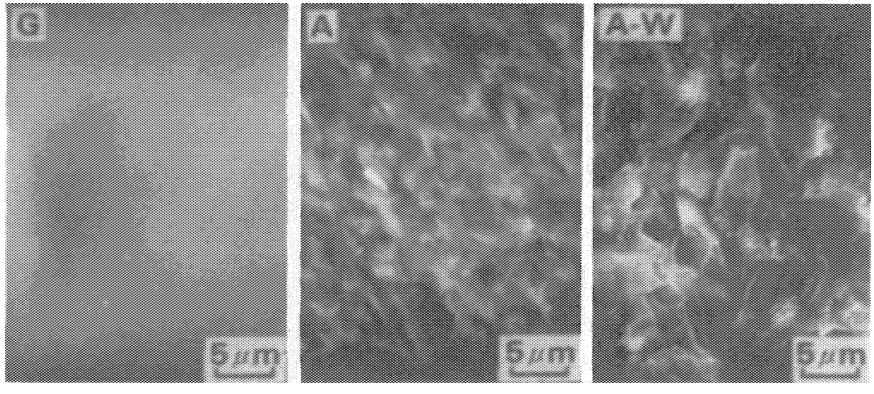

Figure 13.3. Scanning electron micrographs of fracture surfaces of glass G, glass-ceramic A and A/W glass-ceramic.

Table 13.2. Ion Concentrations of Simulated Body Fluid (SBF) and Human Blood Plasma.

	Ion Concentration (mM)							
	Na^+	K^+	Ca^{2+}	Mg^{2+}	cr	HCO^{3-}	HPO^{l-}	sol^-
SBF	142	5	2.5	1.5	147.8	4.2	1	0
Human Plasma*	142	5	2.5	1.5	103	27	1	0.5

Chemical Anatomy, Physiology and Pathology of Extracellular Fluid, 6 ed., Harvard University Press, Cambridge, MA.

bending strength of A/W glass-ceramic with decreasing stress rate in a simulated body fluid with ion concentrations nearly equal to those of the human blood plasma of pH 7.25 at 36.5°C (Table 13.2) is much lower than those of glass G and glass-ceramic A (Fig. 13.4). The parameter, n, of slow crack growth, which is derived from the dependence of the bending strength upon the stressing rate, is 33 for A/W glass-ceramic, whereas it is 9 and 18 for glass G and glass-ceramic A, respectively. When a bending stress of 65 MPa is continuously applied in the body, A/W glass-ceramic should withstand it for over ten years, whereas glass G, glass-ceramic A, and dense sintered HA would survive only one minute. The magnitude of the fatigue of A/W glass-ceramic can be further decreased by a surface modification such as Zr^+ ion implantation.[7] Animal experiments have shown that A/W glass-ceramic maintains its high mechanical strength for long periods *in vivo*.[8]

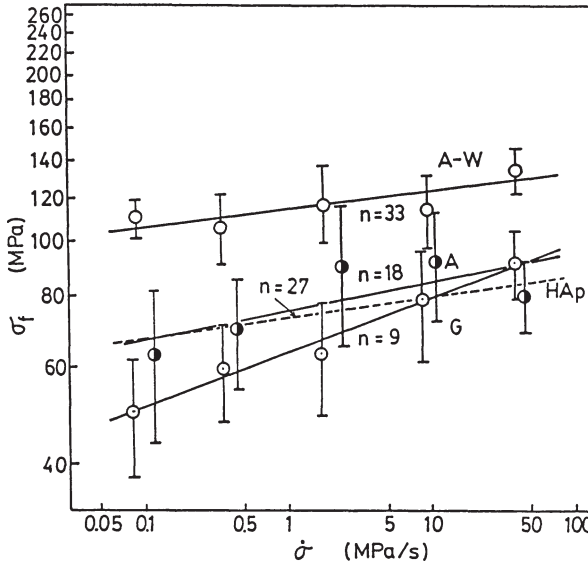

Figure 13.4. Dependence of bending strength (σ_f) of glass G, glass ceramic A, A/W glass-ceramic and dense sintered HA in the simulated body fluid at 36.5°C upon stressing rate ($\sigma\bullet$).

13.3. SURFACE CHEMISTRY

A/W glass-ceramic is so tightly bonded to the living bone that the fracture under tensile stress does not usually occur at the interface between the glass-ceramic and bone, but within the bone. Its bioactivity is much higher than that of sintered HA. For example, its granular particles are covered with newly grown bone on up to 90% of their surfaces within four weeks in rat tibia, whereas those of the sintered HA are only 60% covered even after 16 weeks, as shown in Fig. 13.5.[9] Thus high bioactivity of A/W glass-ceramic is attributed to a specific surface property.

When A/W glass-ceramic is implanted into a bone defect, it forms a thin layer, rich in Ca and P, on its surface and bonds to the surrounding bone through this layer, as shown in Fig. 13.6.[10] This CaP-rich layer is identified as a layer of an apatite by X-ray microdiffraction, as shown in Fig. 13.7.[11] With transmission electron microscopy, A/W glass-ceramic is seen closely connected to the living bone through this apatite layer, without a distinct boundary, as shown in Fig. 13.8.[12]

The same type of apatite layer is formed on the surface of A/W glass-ceramic even in a simulated body fluid with ion concentrations nearly equal to those of human blood plasma (Table 13.2), as shown in Fig. 13.9. According to

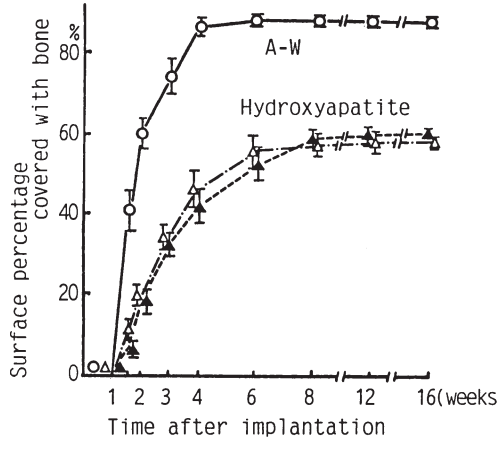

Figure 13.5. Surface area of A/W glass ceramic and two kinds of commercial sintered HA covered with newly grown bone as a function of time after implantation.

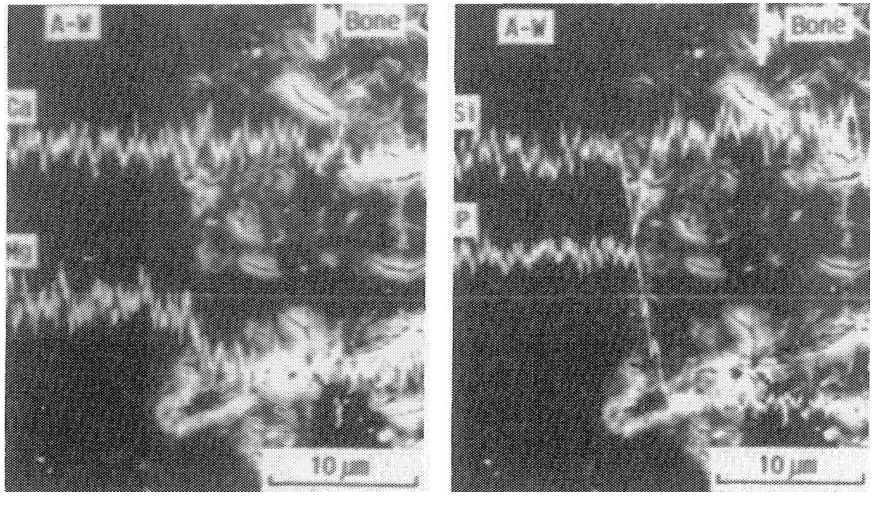

Figure 13.6. Electron probe X-ray microanalysis of the interface of A/W glass-ceramic in rabbit tibia.

thin-film X-ray diffraction and Fourier transform infrared reflection spectroscopy of the surfaces of A/W glass-ceramic soaked in simulated body fluid, the surface apatite layer consists of a carbonate-containing HA with small crystallite and/or defective structure.[13]

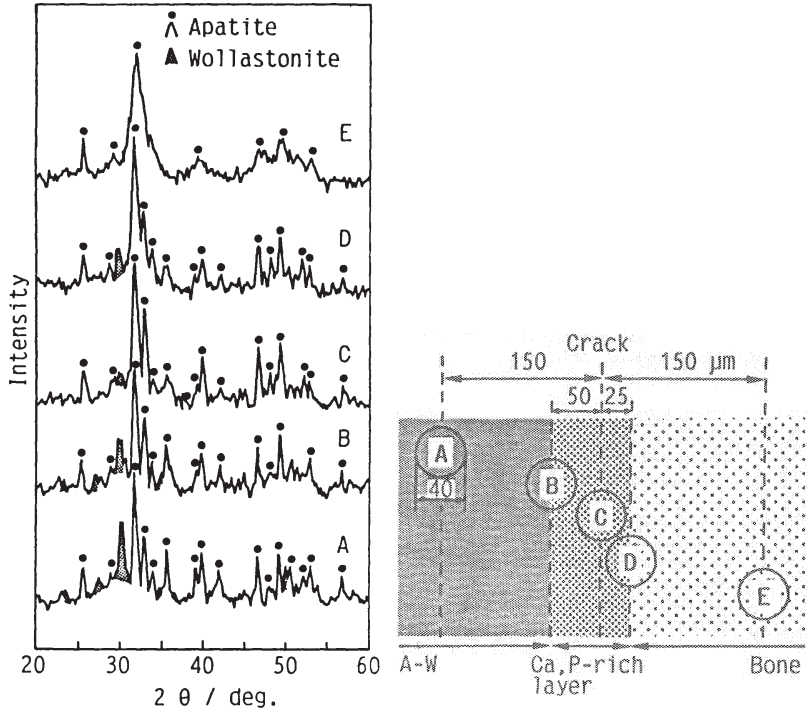

Figure 13.7. X-ray microdiffraction of the interface of A/W glass-ceramic to the bone of sheep vertebra.

The compositional and structural characteristics of this apatite are similar to those of the apatite in the natural bone. It is expected that a bone-producing cell (osteoblast) would proliferate preferentially over fibroblasts on the surface of the apatite layer. Consequently, fibrous tissue, which usually forms around foreign material, is not formed around A/W glass-ceramic, and the surrounding bone can grow directly on the surface apatite layer. When this occurs, a tight chemical bond forms between the surface apatite and the bone apatite, in order to reduce the interfacial energy. This is confirmed by the observation that a pair of A/W glass-ceramic samples which were implanted, soaked in the simulated body fluid,[14] or implanted subcutaneously into rats,[15] were then so tightly bonded together through a mutual apatite layer that they could not be separated. This suggests that the bone-like apatite layer which is formed on the surface of A/W glass-ceramic in the body plays an essential role in forming the chemical bond of the glass-ceramic to the bone. The same type of CaP-rich layer or apatite layer has been

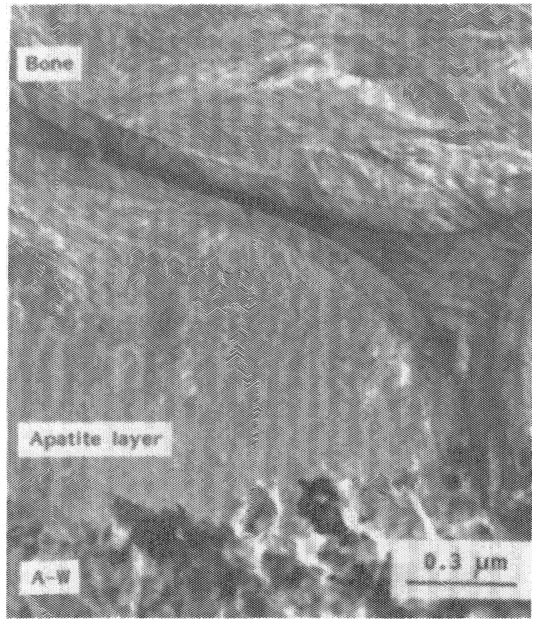

Figure 13.8. Transmission electron micrograph of the interface of A/W glass-ceramic in rat tibia.

observed also in Bioglass®-type glasses,[16] Ceravital®-type glass-ceramic,[17] and sintered HA,[18] but not for non-bioactive glasses[19] or glass-ceramics.[20] The bone-like apatite layer plays an essential role in forming the chemical bond of all bioactive materials which bond to bone. The higher bioactivity of A/W glass-ceramic than that of sintered HA might be attributed to the higher rate of formation of the apatite layer on A/W glass-ceramic.[18]

The human body fluid is already supersaturated with respect to apatite under normal conditions.[21] Therefore, once apatite nuclei have formed, they can spontaneously grow. A/W glass-ceramic releases appreciable amounts of calcium and silicate ions into the simulated body fluid.[4] It is probable that these ions promote apatite nucleation on the surface of A/W glass-ceramics. In order to study this mechanism in more detail, the compositional dependence of apatite formation on the surface of glasses in the simple ternary system $CaO\text{-}SiO_2\text{-}P_2O_5$ was investigated in simulated body fluid. It was found that only $CaO{\cdot}SiO_2$-based glasses formed the apatite layer on their surfaces within 30 days, whereas the $CaO \cdot P_2O_5$-based glasses did not. This behavior is in contrast to the conventional expectation, at least within the glass-forming compositional region, as shown in

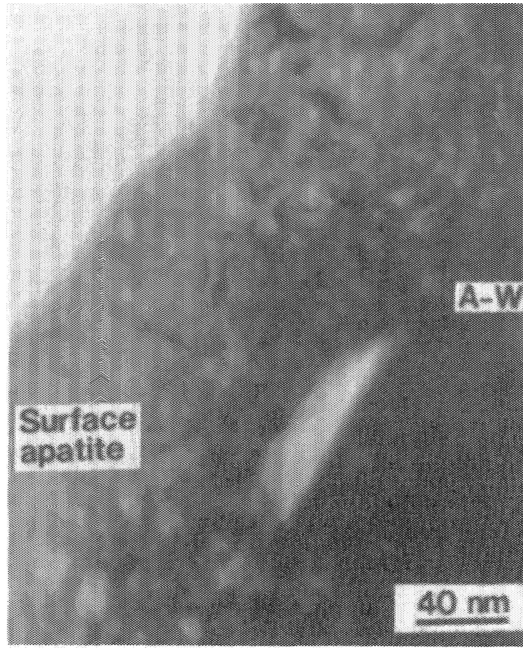

Figure 13.9. Transmission electron micrograph of a cross section of A/W glass-ceramic soaked in simulated body fluid.

Fig. 13.10.[22] Even P_2O_5-free $CaO \cdot SiO_2$ binary glasses formed the apatite layer *in vitro* as well as *in vivo*.[23] The $CaO \cdot SiO_2$-based glasses release an appreciable amount of calcium, whereas the $CaO \cdot P_2O_5$-based glasses release phosphates. Both types of ions increase the ionic activity product of the apatite in the surrounding fluid. The magnitude of the increase is almost equal between the $CaO \cdot SiO_2$-based glasses and the $CaO \cdot P_2O_5$-based glasses, as shown in Fig. 13.11.[24] In spite of this, only the $CaO \cdot SiO_2$-based glasses formed the apatite layer which decreased the ionic activity product of the fluid.

This behavior is due to a peculiar surface structure of the $CaO \cdot SiO_2$-based glasses which provides favorable sites for apatite nucleation. The $CaO \cdot SiO_2$-based glasses form a silica hydrogel layer prior to the formation of the apatite layer.[23, 24] It is probable that this hydrated silica induces apatite nucleation. This is confirmed by the observation that a pure silica gel, prepared by the sol-gel method, formed bone-like apatite on it when soaked in simulated body fluid at pH 7.4, as shown in Fig. 13.12.[25] Such apatite formation was observed neither on the surface of silica glass nor on that of a crystalline quartz silica. This suggests

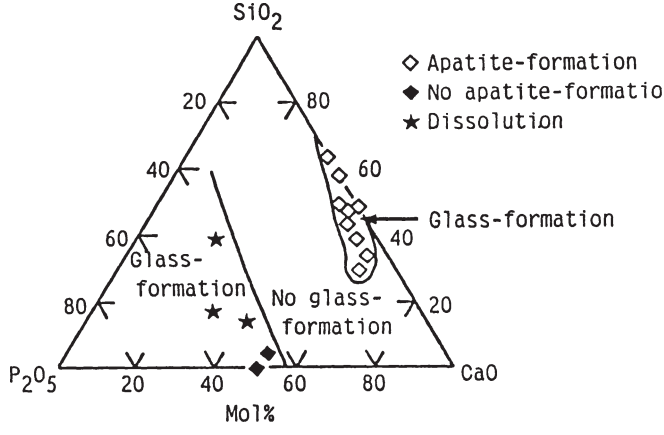

Figure 13.10. Compositional dependence of apatite formation on glasses in the system $CaO\text{-}SiO_2\text{-}P_2O_5$ in simulated body fluid (soaking time: 30 days).

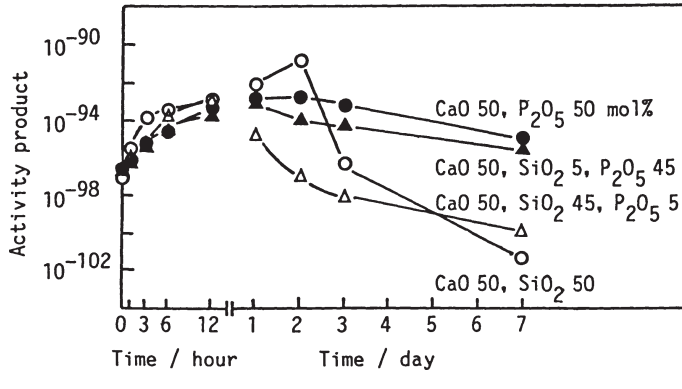

Figure 13.11. Variation of the ionic activity product of the apatite in simulated body fluid with the immersion of $CaO–SiO_2–P_2O_5$ glasses.

that a certain kind of silanol group, abundant on the surface of the silica gel, is responsible for the apatite nucleation.

13.4. SUMMARY

The mechanism of apatite formation on the surfaces of $CaO \cdot SiO_2$-based glasses and glass-ceramics, including A/W glass-ceramic, in the body can be interpreted as follows. The calcium ion dissolved from the glasses and

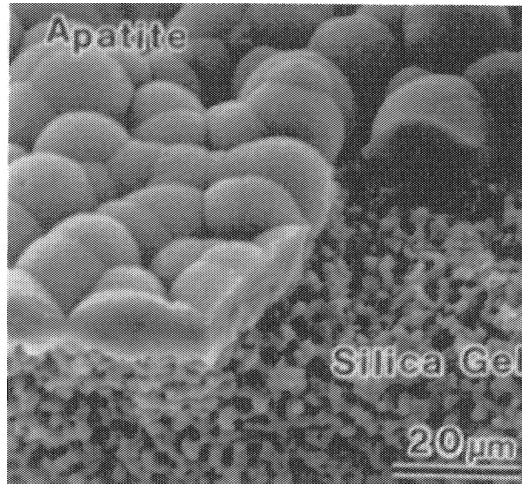

Figure 13.12. Apatite formation on a pure silica gel in simulated body fluid of pH 7.4.

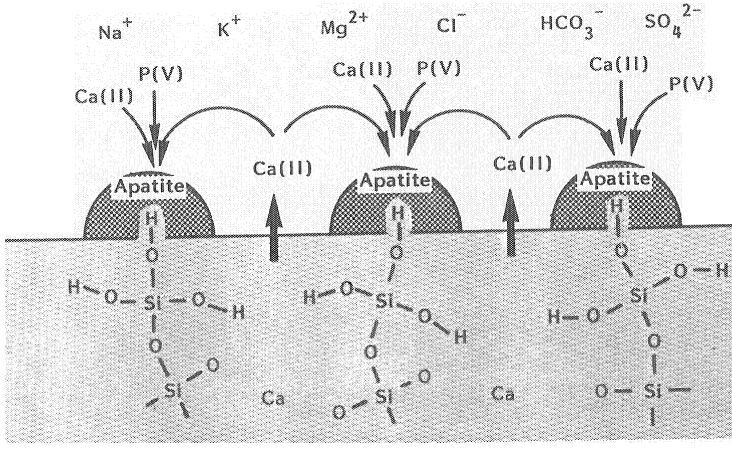

Figure 13.13. Schematic representation of the mechanism of apatite formation on the surfaces of $CaO \cdot SiO_2$-based glasses and glass-ceramics in the body.

glass-ceramics increases the ion activity product of the apatite in the surrounding body fluid, and the hydrated silica on the surfaces of the glasses and glass-ceramics provides favorable sites for apatite nucleation, as shown in Fig. 13.13. Consequently, the apatite nuclei are rapidly formed on their surfaces. Once the

apatite nuclei are formed, they spontaneously grow by consuming calcium and phosphate ions from the surrounding body fluid. In the case of A/W glass-ceramic, although the presence of the silica gel layer on its surface could not be detected even under the high resolution transmission electron micrographs (see Figs 13.8 and 13.9), the dissolution of an appreciable amount of the silicate ion from the glass-ceramic into the simulated body fluid indicates the formation of a large number of silanol groups at the surface of the glass-ceramic in the body.

If the explanation of the mechanism of the apatite formation described above is valid, it is expected that the bone-like apatite layer could be formed on the surfaces of various kinds of materials including metals, ceramics and organic polymers by the following biomimetic method at ordinary temperature and pressure.[26] When a material as a substrate is placed on or in granular particles of a $CaO \cdot SiO_2$-based glass soaked in the simulated body fluid for a certain period, as shown in Fig. 13.14, a large number of apatite nuclei can be formed on the surface of the substrate, as well as on the surfaces of the glass particles, by the calcium and silicate ions dissolved from the glass particles. When the substrate is then soaked in another solution supersaturated with respect to the apatite, the apatite nuclei grow spontaneously *in situ* on the substrate by consuming the calcium and phosphate ions from the surrounding solution to form the apatite layer.[27]

A dense and uniform layer of bone-like apatite was formed on various kinds of materials, including stainless steel, titanium metal, platinum, gold, silicon, carbon, alumina, zirconia, polymethylmethacrylate, polyethylene, polyethylene terephthalate (PET), and polyethersulfone (PES), by this method, as shown in Fig. 13.15.[26,27] The thickness of the apatite layer continued to increase with increased soaking time in the second solution, as shown in Fig. 13.16. The rate of growth of the apatite layer increased with increasing temperature (Fig. 13.16) and the degree of the supersaturation of the second solution.[28]

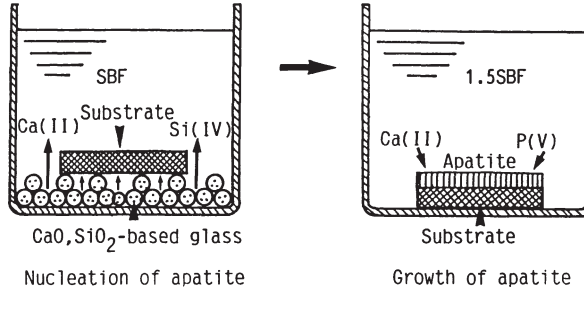

Figure 13.14. Apatite formation on various substrates.

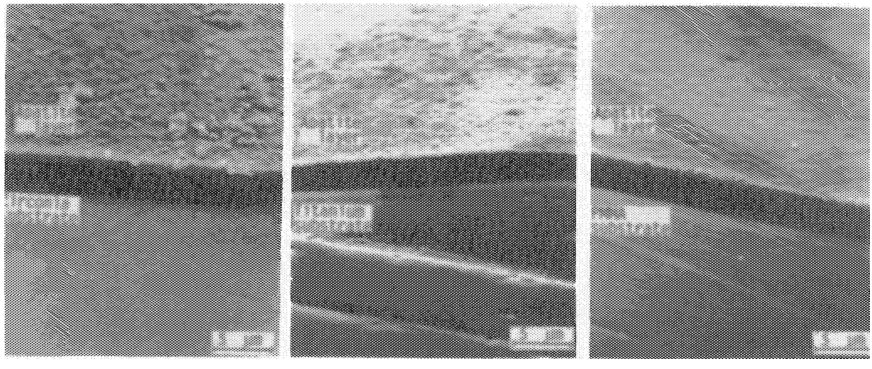

Figure 13.15. Apatite layer formed on various substrates.

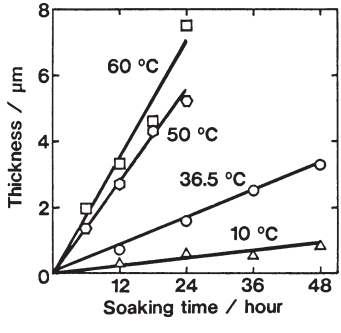

Figure 13.16. The thickness of the apatite layer as a function of soaking time in a solution with ion concentrations 1.5 times those of simulated body, fluid at various temperatures.

The rate of growth in the solution with ion concentrations 1.5 times of the simulated body fluid at 60°C was 7 μm/day. The adhesive force of the apatite layer thus formed to the substrate varied with the time and roughness of the substrate. PET and PES showed remarkably high adhesive strength to the apatite layer among the examined polymers. Figure 13.17 shows the bone-like apatite layer coated on fine fibers of a cloth of PET. This apatite–polymer composite can be bent sharply without peeling off the apatite layer. This type of composite may be useful for fabricating highly bioactive artificial bone with mechanical properties close to those of the natural bone; not only fracture strength and fracture toughness, but also elastic modulus. In addition, this type of organic polymer coated with apatite is expected to show high compatibility even with soft tissues.

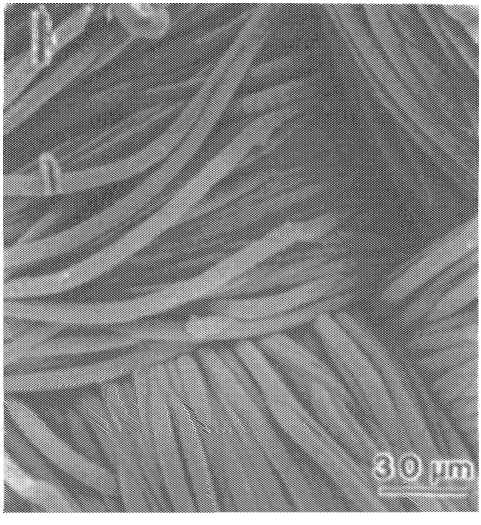

Figure 13.17. Apatite layer coated on fine fibers of a cloth of PET.

The fundamental understanding of the mechanism of the apatite formation on A/W glass-ceramic in the body described above also provides the way for developing other kinds of high performance bioactive materials, such as self-setting bioactive materials, useful as bone fillers and drug delivery system[29,30] and ferrimagnetic bioactive materials useful as thermoseeds for hyperthermia treatment of cancer.[31,32]

REFERENCES

1. Kokubo, T., Shigematsu, M., Y. Nagashima, Y. *et al.* (1982). Apatite- and Wollastonite-Containing Glass-Ceramics for Prosthetic Application, *Bull. Inst. Chem. Res.*, **60**, 260–268.
2. Kokubo, T., Ito, S., Sakka, S. *et al.* (1986). Formation of a High-Strength Bioactive Glass-Ceramic in the System MgO-CaO-SiO_2-P_2O_5, *J. Mater. Sci.*, **21**, 536–540.
3. Kokubo, T., Nagashima, Y. and Tashiro, M. (1982). Preparation of Apatite Containing Glass-Ceramics by Sintering and Crystallization of Glass Powders, *Yogyo-Kyokai-Shi*, **90**, 151.

4. Kokubo, T., Kushitani, H., Ohtsuki, C. *et al.* (1992). Chemical Reaction of Bioactive Glass and Glass-Ceramics with a Simulated Body Fluid, *Mater. Med.*, **3**, 79–83.
5. Kokubo, T., Ito, S., Shigematsu, M. *et al.* (1985). Mechanical Properties of a New Type of Apatite-Containing Glass-Ceramic for Prosthetic Application, *J. Mater. Sci*., **20**, 2001–2004.
6. Kokubo, T., Ito, S., Shigematsu, M. *et al.* (1987). Fatigue and Life Time of Bioactive Glass-Ceramic A-W Containing Apatite and Wollastonite, *J. Mater. Sci*., **22**, 4067–4070.
7. Takaoka, G.H., Tanaka, R., Usui, H. *et al.* (1992). "Surface Modification of Bioactive Ceramic (Artificial Bone) by Ion Implantation", in Cima, L.G. and Ron, E.S. (eds), *Tissue-Inducing Biomaterials*, Materials Research Society, Pittsburgh, PA, pp. 23–28.
8. Kitsugi, T., Yamamuro, T., Nakamura, T. *et al.* (1987). Aging Test and Dynamic Fatigue Test of Apatite-Wollastonite Containing Glass-Ceramics and Dense Hydroxyapatite, *J. Biomed. Mater. Res.*, **21**, 467–484.
9. Ono, K., Yamamuro, T., Nakamura, T. *et al.* (1990). Quantitative Study on Osteoconduction of Apatite-Wollastonite Containing Glass-Ceramic Granules, Hydroxyapatite Granules, and Alumina Granules, *Biomaterials*, **11**, 265–271.
10. Kitsugi, T., Nakamura, T., Yamamuro, T. *et al.* (1987). SEM-EPMA Observation of Three Types of Apatite-Containing Glass-Ceramics Implanted in Bone: The Variance of a Ca-P-rich Layer, *J. Biomed. Mater. Res.*, **21**, 1255–1271.
11. Kokubo, T., Ohtsuki, C., Kotani, S. *et al.* (1990). "Surface Structure of Bioactive Glass-Ceramic A-W Implanted into Sheep and Human Vertebra", in Heimke, G. (ed.), *Bioceramics, Vol. 2*, German Ceramic Society, Cologne, pp. 105–112.
12. Neo, M., Kotani, S., Fujita, Y. *et al.* (1992). Difference of Bone-Bonding Mechanism between Surface-Active Ceramics and Reasonable Ceramics: A Study by Scanning and Transmission Electron Microscopy, *J. Biomed. Mater. Res.*, **26**, 255–267.
13. Kokubo, T., Ito, S., Huang, Z. *et al.* (1987). Ca, P-rich Layer Formed on High-Strength Bioactive Glass-Ceramic A-W, *J. Biomed. Mater. Res.*, **24**, 331–343.

14. Kokubo, T., Hayashi, T., Sakka, S. *et al.* (1987). Bonding Between Bioactive Glasses, Glass-Ceramics or Ceramics in a Simulated Body Fluid, *Yogyo-Kyokai-Shi*, **95**, 785–791.
15. Kitsugi, T., Yamamuro, T., Nakamura, T. *et al.* (1987). Bonding Behavior Between Two Bioactive Ceramics *In Vivo*, *J. Biomed. Mater. Res.*, **21**, 1109–1123.
16. Hench, L.L. and Clark, A.E. (1981). "Adhesion to Bone", in Williams, D.F. (ed.), *Fundamental Aspects of Biocompatibility, Vol. 1*, CRC Press Boca Raton, FL, pp. 67–85.
17. Otsuki, C., Kushitani, H., Kokubo, T. *et al.* (1991). Apatite Formation on the Surface of Ceravital-Type Glass-Ceramic in the Body, *J. Biomed. Mater. Res.*, **25**, 1363–1370.
18. Kokubo, T., Kushitani, H., Ebisawa, Y. *et al.* (1989). "Apatite Formation on Bioactive Ceramics in Body Environment", in Oonishi, H., Aoki, H. and Sawai, K. (eds.), *Bioceramics, Vol. 1*, Ishiyaku EuroAmerica, Tokyo, pp. 157–162.
19. Kitsugi, T., Yamamuro, T., Nakamura, T. *et al.* (1989). Bone Bonding Behavior of $MgO–CaO–SiO_2–P_2O_5–CaF_2$ Glass (Mother Glass of A-W Glass-Ceramics), *J. Biomed. Mater. Res.*, **23**, 631–648.
20. Kitsugi, T., Yamamuro, T., Nakamura, T. *et al.* (1989). The Bonding of Glass Ceramics to Bone, *Int. Orthop. (SICOT)*, **13**, 199–206.
21. Neuman, W. and Neuman, M. (1958). The Chemical Dynamics of Bone Mineral, *Arthritis Rheum.*, **1**, 473–474.
22. Ohtsuki, C., Kokubo, T., Takatsuka, K. *et al.* (1991). Composition Dependence of Bioactivity of Glasses in the System $CaO-SiO_2-P_2O_5$: Its *In Vitro* evaluation, *J. Ceram. Soc.*, **99**, 1–6.
23. Ohura, K., Nakamura, T., Yamamuro, T. *et al.* (1991). Bone-Bonding Ability of P_2O_5-Free $CaO·SiO_2$ Glasses, *J. Biomed. Mater. Res.*, **25**, 357–365.
24. Ohtsuki, C., Kokubo, T. and Yamamuro, T. (1992). Mechanism of Apatite Formation on $CaO-SiO_2-P_2O_5$ Glasses in a Simulated Body Fluid, *J. Non-Crystal. Solids*, **143**, 84–92.
25. Li, P., Ohtsuki, C., Kokubo, T. *et al.* (1992). Apatite Formation Induced by Silica Gel in a Simulated Body Fluid, *J. Am. Ceram. Soc.*, **75,** 2094–2097.
26. Abe, Y., Kokubo, T. and Yamamuro, T. (1990). Apatite Coating on Ceramics, Metals and Polymers Utilizing a Biological Process, *J. Mater. Sci-Mater. M.*, **1**, 233–238.

27. Kokubo, T., Hata, K., Nakamura, T. *et al.* (1991). "Apatite Formation on Ceramics, Metals and Polymers Induced by a CaO, SiO_2-Based Glass in a Simulated Body Fluid", in Bonfield, W., Hastings, G.W. and Tunner, K.E. (eds), *Bioceramics, Vol. 4*, Butterworth-Heinemann, Guildford, pp. 113–120.
28. Kokubo, T., Hata, K., Nakamura, T. *et al.* (1992). Growth of Bone-Like Apatite Layer on Various Materials in Simulated Body Fluids, *Transactions of Fourth World Biomaterials Congress*, Berlin, p. 67.
29. Kokubo, T., Yoshihara, S., Nishimura, N. *et al.* (1991). Bioactive Bone Cement Based on CaO-SiO_2-P_2O_5 Glass, *J. Am. Ceram. Soc.*, **74**, 1739–1741.
30. Nishimura, N., Yamamuro, T., Taguchi, Y. *et al.* (1991). A New Bioactive Bone Cement: Its Histological and Mechanical Characterization, *J. Applied Biomater.*, **2**, 219–229.
31. Kokubo, T., Ebisawa, Y., Sugimoto, Y. *et al.* (1992). "Preparation of Bioactive and Ferromagnetic Glass Ceramic for Hyperthermia", in Hulbert, J.E. and Hulbert, S.F. (eds), *Bioceramics, Vol. 3*, Rose-Hulman Institute of Technology, Terre Haute, pp. 213–233.
32. Ikenaga, M., Ohura, K., Nakamura, T. *et al.* (1991). "Hyperthermic Treatment of Experimental Bone Tumor with a Bioactive Ferromagnetic Glass-Ceramic", in Bonfield, W., Hastings, G.W. and Tanner, K.E. (eds), *Bioceramics, Vol. 4*, Butterworth-Heinemann, Guildford, pp. 255–262.

Chapter 14

A/W GLASS-CERAMIC: CLINICAL APPLICATIONS

Takao Yamamuro

14.1. INTRODUCTION

There are many kinds of ceramics currently available for the repair of extensive lesions or defects in bones and joints. Bioglass®, Ceravital®, and synthetic hydroxyapatite (HA)[1] develop a strong chemical bond with bone *in vivo*. Mechanical strengths exceeding that of the human cortical bone are not reached, however, except for dense A/W glass-ceramic. As described earlier, A/W glass-ceramic is capable of binding strongly to living bone in a few weeks and has a mechanical strength significantly higher than that of human cortical bone (Chapter 13). Since 1983, we have used A/W glass-ceramic in the spine and hip surgery of patients with extensive lesions or bone defects, and the results were quite satisfactory, as summarized below.

14.1.1. Bonding of A/W Glass-Ceramic to Bone

The bonding ability of A/W glass-ceramic to bone was evaluated using rabbit tibial bones, and the load to failure was measured and compared with that of other bioactive ceramics. In the first experiment,[2] each bioactive ceramic was shaped into a rectangular plate (2 mm × 10 mm × 15 mm), surfaces were polished by No. 1500 SiC paper, and they were placed in an ethanol-filled ultrasonic cleaner for 20 min. The tibial proximal metaphyses were exposed subperiosteally, a 15 mm long hole penetrating the medial and lateral cortex was made using a dental burr parallel to the longitudinal axis of the tibia, and a ceramic plate was implanted into each hole. Each experimental group comprised of 4–8 rabbits, which were killed 2, 4, 8, and 25 weeks post-implantation. A segment of the tibia containing a ceramic implant was excised and the bone dissected as shown in Fig. 14.1A. After dissection, the bone on either side of the implant was not directly connected with the other but was joined only through the intervening implant, Fig. 14.1B. Each segment was held with a hook connected to an

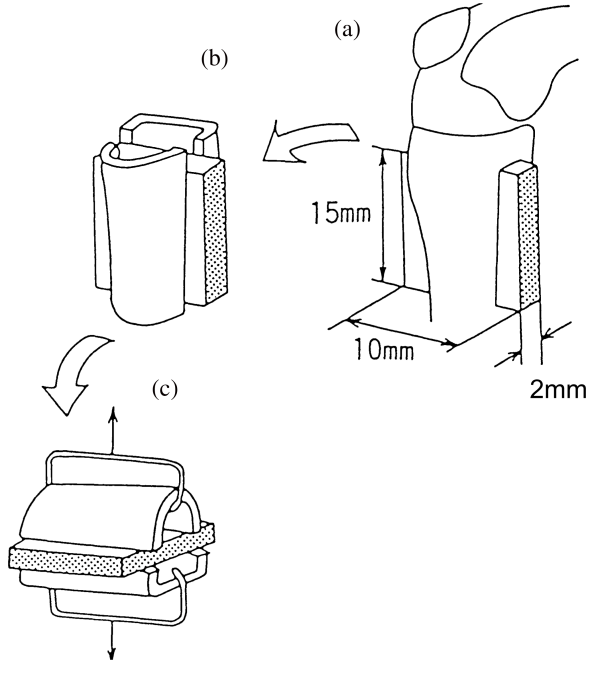

Figure 14.1. Diagram of detaching test system.

Instron-type testing machine. The implant was placed horizontally and pulled in the opposite direction at a cross-head speed of 3.5 cm/min (Fig. 14.1C). The load at which the implant, the bone, or the interface was broken was designated as the failure load. The failure load 8 and 25 weeks after implantation is shown in Table 14.1. A/W glass-ceramic showed tight bonding to bone comparable with synthetic dense HA, and in 25 weeks its load was 70% of that of bone. The breaking of the bond occurred mostly in the bone in A/W glass-ceramic groups, while it occurred mostly in the ceramic in HA groups, but not at the bonded interface in either group. The bonded interface was observed by contact microradiography and SEM after being ground to about 80 μm thick. Histological examination revealed that A/W glass-ceramic bonded directly to the bone tissue (Fig. 14.2), as did synthetic HA by forming a CaP-rich layer at the interface.[3]

In the second experiment,[4] the bonding of A/W glass-ceramic to the surface of cortical bone, the proximal metaphyseal cortex of rabbit tibia was exposed subperiosteally and an implant made of A/W glass-ceramic was fixed on the surface of cortex with a metal screw (Fig. 14.3). The rabbits were killed 2, 4, 8,

Table 14.1. Failure Loads Obtained by Detaching Test.

Ceramics	Mean ± S.D. (kg)	
	8 Weeks	24 Weeks
		24 Weeks
Alumina	0.18 ± 0.018	
Bioglass®	2.75 ± 1.8	
Ceravital®	5.51 ± 1.48	4.35 ± 1.45
Dense HA	6.57 ± 1.36	7.77 ± 1.91
A/W Glass-Ceramic	7.44 ± 1.91	8.19 ± 3.6

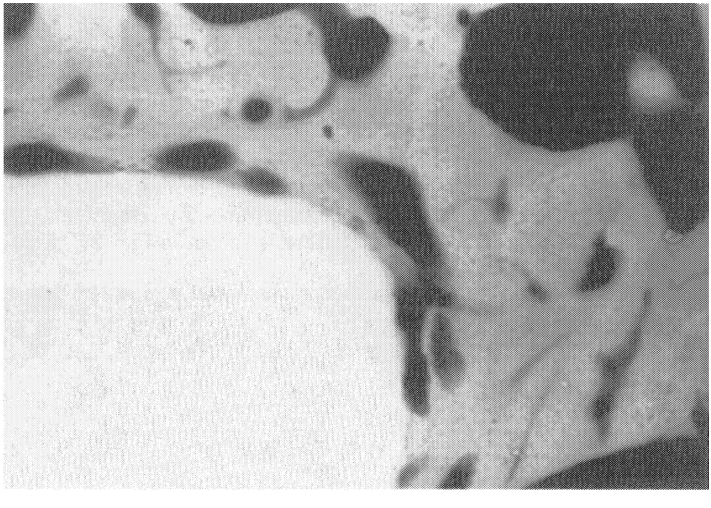

Figure 14.2. A/W glass-ceramic bonded to bone.

and 25 weeks after the implantation. Each experimental group comprised of 5–6 animals. After removing the metal screw, the bone segment was excised and the bone covering the margin of the implant was completely removed. The implant and the piece of bone were held by hooks which were connected to an Instron-type testing machine. The implant was pulled perpendicularly to the base of the implant in contact with bone cortex, at a cross-head speed of 3.5 cm/min, and the load required to detach the implant from the bone or to break the bone was measured. All the A/W glass-ceramic implants were detached from the surface of bone cortex, leaving bone attached to the implants after 4, 8, and 25 weeks after

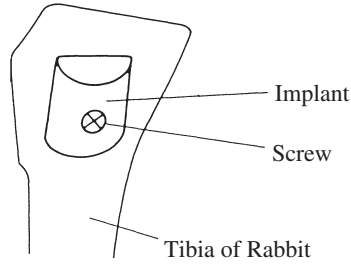

Figure 14.3. Fixation of implant.

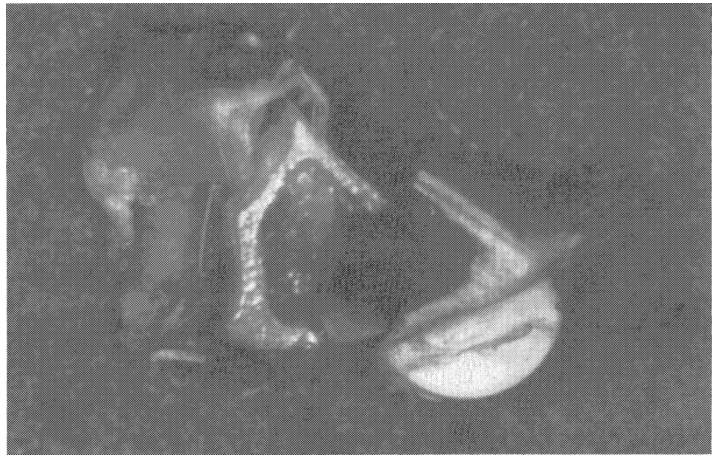

Figure 14.4. Implant and bone after detachment test. The bone has broken.

implantation. The fracture occurred within the bone in most instances, and the A/W glass-ceramic implants did not break (Fig. 14.4). Figure 14.5 shows that the tensile strength of bonding between the A/W glass-ceramic implant and the surface of bone cortex increased remarkably four weeks after the implantation and was almost maximal by eight weeks. The histological appearance at the interface is shown in Fig. 14.2.

It has been confirmed mechanically and histologically that implants made of A/W glass-ceramic bond firmly to living bone in a few weeks and the implants do not deteriorate *in vivo*.[5,6] *In vitro* studies suggest that A/W glass-ceramic bonds to bone in a shorter time than synthetic HA, presumably because it contains a glassy phase, which releases more Ca ions in the early post-implantation stage

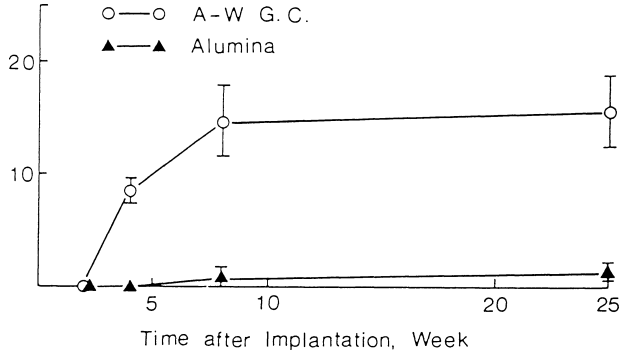

Figure 14.5. Tensile strength in kg/cm^2 (vertical axis) against implant time in weeks (horizontal axis).

than HA, and releases silicate ions, which may initiate crystallization of biological apatites working as their nuclei on the surface of the implant (Chapter 13).

14.2. ANIMAL STUDIES

14.2.1. Intercalary Replacement of a Segment of the Long Bone with an A/W Glass-Ceramic Implant in Animals

Intercalary replacement of the shafts of rabbit tibiae with A/W glass-ceramic implants was performed under weight-bearing conditions to determine whether this glass ceramic is useful as a material for load-bearing prostheses.[8] A 16 mm segment of the middle of the shaft of each rabbit tibia was resected and the defect was replaced with a hollow cylindrical implant. The implant was 9 mm in diameter and 15 mm long, and had a central hole with a diameter of 3.05 mm. It was fixed to the tibia by intramedullary nailing using a 3 mm Kirschner wire. A cast was applied from thigh to toe for six weeks after operation, and the animals afterwards allowed free movement. There were four groups each comprising eight rabbits. Two groups, one group with A/W glass-ceramic implants and the other with alumina ceramic implants, were killed 12 weeks after implantation. Two other similar groups were killed 25 weeks after implantation. The Kirschner wire was removed, the segment of the tibia that contained the implant was excised, and the proximal and distal bones were pulled apart with a tension-tester at a cross-head speed of 3.5 cm/min.

The load to failure of specimens that contained the A/W glass-ceramic implant increased with time, 19.8 ± 7.06 Newtons after 12 weeks of implantation

to 126.4 ± 32.54 Newtons after 25 weeks of implantation, while the failure loads with alumina ceramic implants at the same implantation period were 0 and 19.6 ± 13.92 Newtons, respectively. No glass-ceramic implants broke during the tension testing. Histological observation of the interface between the implant and bone revealed that the gaps which had been observed at the interface immediately after operation were filled with woven bone tissue in the 12 week specimens with an A/W glass-ceramic implant. On the other hand, in specimens containing an alumina ceramic implant, gaps were always filled with a thin layer of fibrous tissue. On the basis of mechanical strength and the performance of the bone–implant interface, prostheses fabricated from A/W glass-ceramic should be usable under load-bearing conditions.

14.2.2. Replacement of the Vertebrae of Sheep with an A/W Glass-Ceramic Prosthesis

Ten castrated male sheep weighing from 40 to 60 kg underwent replacement of the third and fourth lumbar vertebrae with vertebral prostheses made of A/W glass-ceramic, without bone graft.[9] Under general anesthesia, the lumbar vertebrae were approached retroperitoneally. The intervertebral disc between the two lumbar vertebrae was removed with about half of the vertebral bodies above and below. The bone defect thus produced was then filled with a vertebral prosthesis. The prosthesis was cylindrical, 15 mm in length and 10 mm in diameter in two animals, and 30 mm × 12 mm in eight animals. In the former group, the prostheses were implanted without any fixation. In the latter group, the prostheses were securely fixed with Zielke's instrumentation. The animals were immobilized for two days postoperatively with a specially-made body brace, and they were allowed free movement thereafter. They were killed at various times 3–27 months postoperatively. After removing the Zielke's instrumentation, the vertebrae containing A/W glass-ceramic prostheses were prepared for microscopic, contact micrographic, SEM, and EPMA observations.

In the two cases in which 15 mm long prostheses were implanted and animals killed 24 months and 27 months after operation respectively, bone bonding between the prostheses and the two vertebrae was observed by radiography and contact microradiography. The prostheses were bonded directly to the trabeculae of the cancellous bone, and even at the sites where trabeculae were lacking, irregularly shaped new bone of about 12 μm in thickness was observed, covering the prosthesis surface. In other animals, which received a 30 mm long implant, direct bonding of the prosthesis to both vertebrae was observed in two cases and bonding to one vertebra only in one case. SEM-EPMA and X-ray

microdiffraction analysis of the interface, whether bonded or not, always showed a CaP-rich layer on the surface of the prosthesis. This layer was confirmed as apatite by crystallographic analysis. From this study, together with previous studies using rabbit tibia,[2–4,8] we presumed that failure of bonding of the prostheses to the vertebrae might be due to a failure of fixation rather than chemical inactivity of the prosthetic surface, and this was later confirmed with clinical experience where a very firm fixation method was employed.

14.3. CLINICAL APPLICATIONS

14.3.1. Replacement of the Vertebrae with A/W Glass-Ceramic Vertebral Prostheses in Clinical Cases

In the past, when the vertebral column was extensively damaged by tumors or trauma, its reconstruction had been attempted by the use of autogenous bone and allograft in combination with metals, PMMA bone cement, or alumina ceramic. However, autogenous bone and allograft have certain limits in their availability, and the long-term durability of non-bone-bonding implants is not always satisfactory due to loosening and dislocation. To make a strong, bone-bonding vertebral anaplerosis, we prepared vertebral prostheses made of A/W glass-ceramic for clinical use. The prosthesis is in many different sizes so that the surgeon is able to choose the appropriate one in the operating theater (Fig. 14.6).

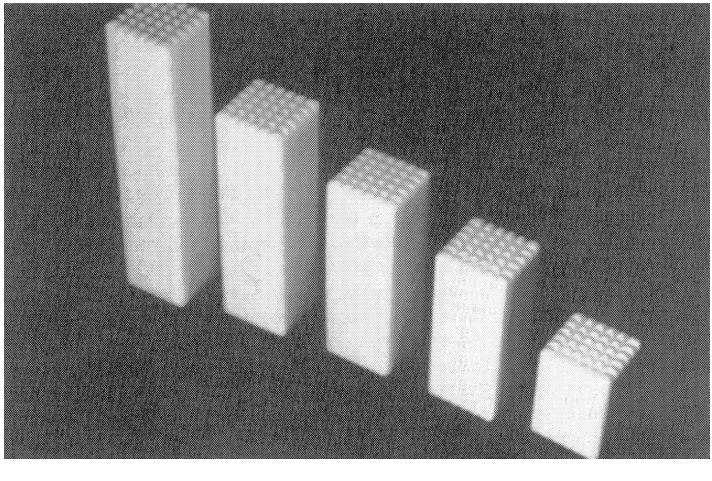

Figure 14.6. Selection of A/W vertebral prosthetic devices.

In 1983, the first replacement operation of thoracic vertebra using an A/W glass ceramic prosthesis was performed at Kyoto University Hospital in a 50 year old female patient who developed breast cancer metastasis in the tenth thoracic vertebra, associated with mild paraplegia.[10] During the operation, through a thoracotomy, total excision of the tenth thoracic vertebra and partial excision of the vertebrae above and below were performed, and a vertebral prosthesis was securely implanted in the bone defect, combined with some autogenous bone graft. The patient survived without recurrence of the tumor in the operated site, although she developed another metastatic lesion in a lumbar vertebra six years postoperatively which was then also replaced with prosthesis (Fig. 14.7).

The A/W glass-ceramic vertebral prosthesis was used in 70 clinical cases during the period 1983–1990 at Kyoto University and Hokkaido University. The age distribution of the patients ranged from 22–79 years with an average of 51–55 years. There were 39 males and 31 females. Among them, 19 cases were metastatic tumors, 30 were burst fractures, 15 were compression fractures, and others were lumbar instabilities due to spondylolysis, spondylolisthesis, or intervertebral disc hernia. Among 19 cases of metastatic tumors that underwent a vertebral prosthetic replacement, there were 12 different malignant tumors. Some patients, such as those with malignant melanoma, osteosarcoma, and lung cancer, died within a few months postoperatively. Many others survived for longer than three years, particularly those with breast cancer, renal cancer, thyroid cancer, and prostate cancer, who tended to survive for longer than five years. It is important to be able to provide patients with a pain-free and non-paralyzed life to make their

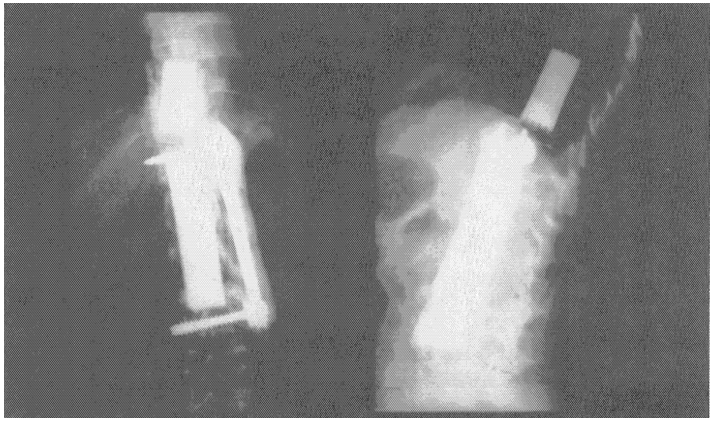

Figure 14.7. Radiograph of vertebral prosthesis, six years and six months postoperation.

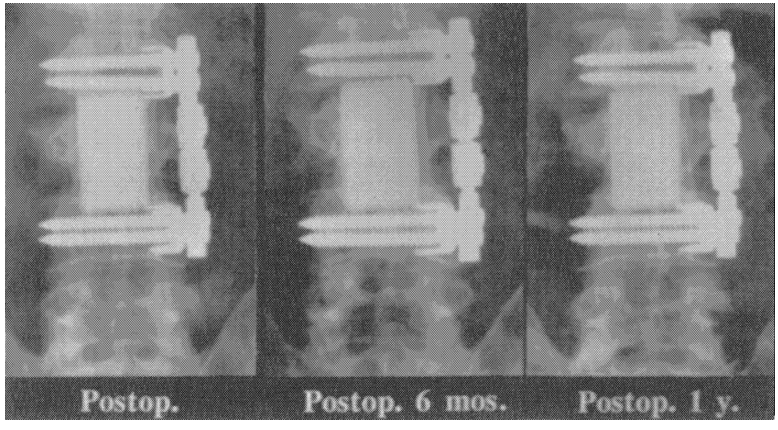

Figure 14.8. Radiographs of patient with burst fracture of lumbar vertebra (L3).

remaining, limited life time valuable. This prosthetic replacement operation seems particularly indicated for patients with vertebral metastases of slow growing malignant tumors.

In cases of burst fracture of the thoracic and lumbar vertebrae with paraplegia, the vertebral prosthetic replacement after decompression of the spinal cord always gives satisfactory results, although more-or-less paralysis may remain, depending on the preoperative severity and duration of spinal cord compression. The patient illustrated in Fig. 14.8 sustained burst fracture of the third lumbar vertebra with mild paraplegia after falling from a height. Anterior decompression of the spinal cord and reconstruction of the spinal column were performed shortly after the injury by the use of a 4 cm long vertebral prosthesis, which was firmly fixed with a Kaneda device. The patient recovered completely from paraplegia. In cases of compression fracture of the thoracic and lumbar vertebra with paraplegia, the vertebral prosthetic replacement of the fractured vertebral body always gives good results, although posterior decompression and spinal instrumentation with Luque's rods may be indicated in some cases before anterior vertebral replacement. In any case, late collapse of the replaced spinal segments, which can occur when autogenous or allogenic bone is used, was prevented by the use of an A/W glass-ceramic vertebral prosthesis (Fig. 14.9).

An A/W glass-ceramic vertebral spacer was used in six cases of lumbar instability for the purpose of posterior lumber interbody fusion fixed with Steffee's device (Fig. 14.10). In all cases, solid fixation and stability of the lumbar vertebrae had been achieved by laminectomy and posterior interbody fusion with vertebral spacers (Fig. 14.11). Based on nine years of clinical experiences with

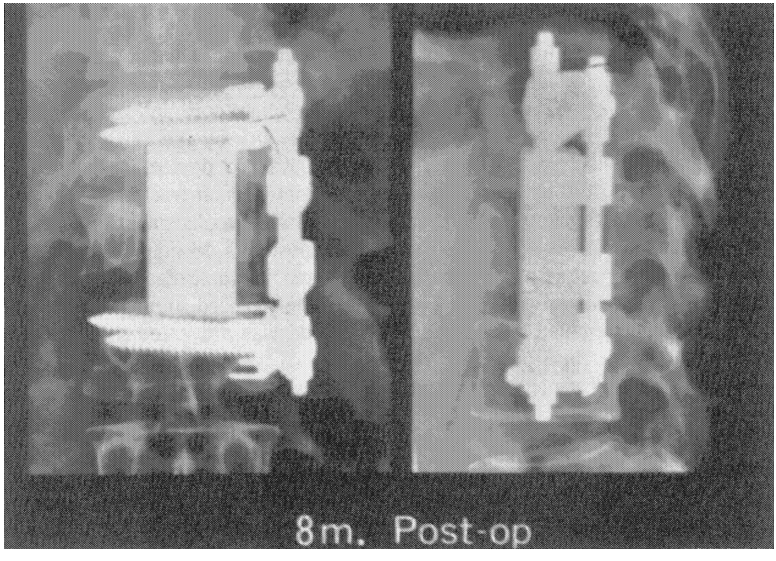

Figure 14.9. Radiograph of patient with fracture of lumbar vertebra (Ll).

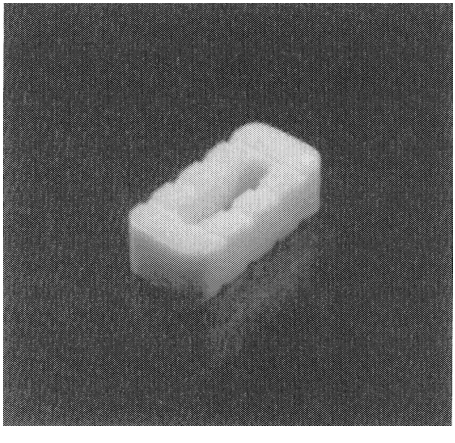

Figure 14.10. A/W glass-ceramic vertebral spacer.

the A/W glass-ceramic vertebral prosthesis,[11] we concluded that this vertebral prosthesis is useful for the reconstruction of the spinal column which had been severely destroyed by tumors, trauma, or degenerative diseases, provided a very firm fixation of the prosthesis to the adjacent bone is accomplished by the use of various spinal instrumentations in addition to autogenous bone grafting.

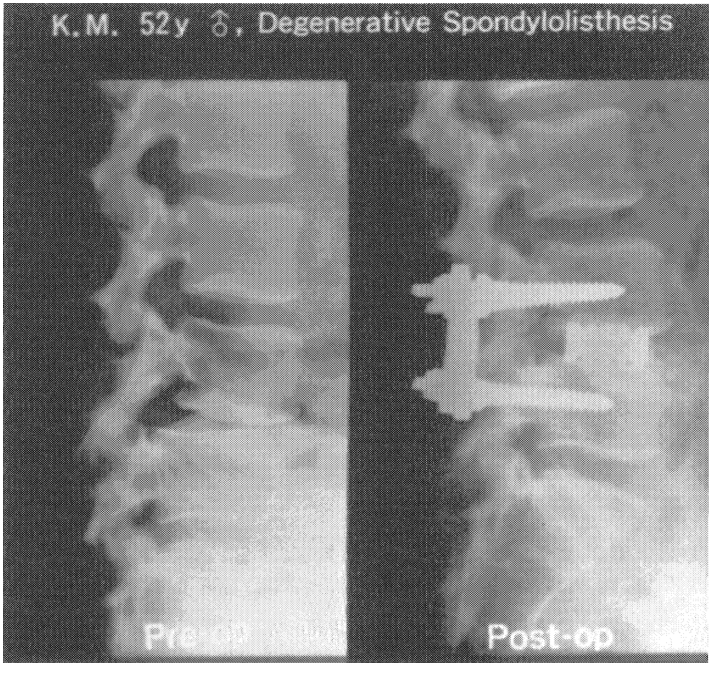

Figure 14.11. Radiograph showing A/W glass-ceramic used to treat lumbar instability.

14.3.2. Reconstruction of the Iliac Crest with an A/W Glass-Ceramic Prosthesis

In surgery of the spine, skeletal tumors, and skeletal trauma, large autogenous bone grafts are often taken from the iliac crest. Taking such bone grafts from the iliac crest not only distorts the shape of the remaining ilium, but produces other complications, such as tenderness, discomfort, pain on walking, fracture of the rest of the iliac crest, paresthesia, and abdominal herniations. To prevent such complications and fill bone defects, iliac crest prostheses of various sizes were fabricated from A/W glass-ceramic and used in 113 cases between 1989 and 1990 (Fig. 14.12). The age of the patients ranged from 14–75 years (average 42.5 years), and the length of the bone defects ranged from 15–70 cm (average 43 cm). Results obtained one to two years after the operation were excellent in 97% of the patients, there was no spontaneous pain in 96%, no tenderness in 91%, and no foreign body feeling in 96%. Overall, patients' satisfaction was excellent or good in 100% of the cases. Early fixation and ultimate stability were excellent in 94 and 96%, respectively. New bone formation around the iliac crest

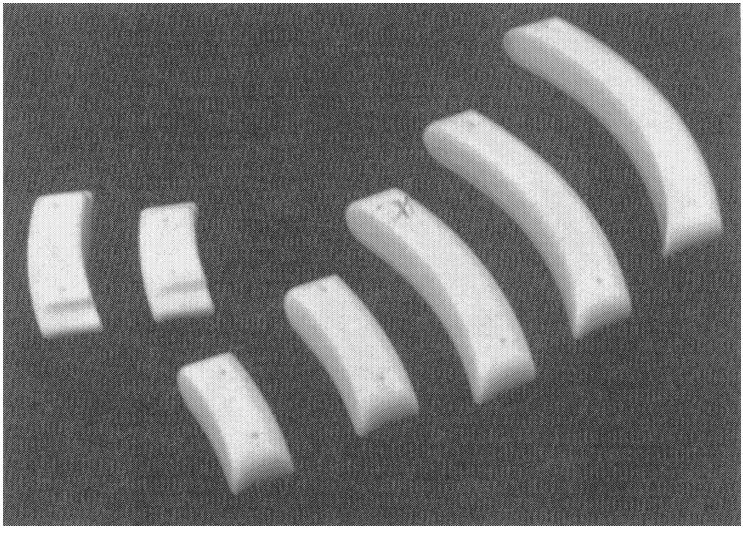

Figure 14.12. A range of A/W glass-ceramic iliac crest prostheses.

prostheses progressed steadily, and one year following the operation good new bone formation was observed in 90% of the patients. In half the cases, there was no radiological clear zone on either side of the prosthesis (Fig. 14.13).[12]

14.3.3. A/W Glass-Ceramic Granules as a Bone Defect Filler

Bone defects remaining after the excision of bone tumors are usually filled with either autogenous bone or allograft. However, sufficient amounts of autogenous bone and allograft are not always available. In cases of aseptic loosening of hip prostheses combined with large bone loss, a large amount of autogenous or allogenic bone is required. In such cases, we used A/W glass-ceramic granules in combination with autogenous cancellous bone and fibrin glue as bone substitute. In our animal experiments,[13] A/W glass-ceramic-fibrin mixture showed significantly better osteoconduction and acceleration of the bone-repairing process than A/W glass-ceramic granules. A/W glass-ceramic granules mixed with autogenous cancellous bone and fibrin glue are recommended to fill this type of bone defect. The case illustrated in Fig. 14.14 was revised due to aseptic loosening of a Charnley hip prosthesis which had been inserted 15 years previously. At the revision operation, 45 g of A/W glass-ceramic granules was used, mixed with autogenous bone and fibrin glue. Loosening of the stem of hip prostheses has been

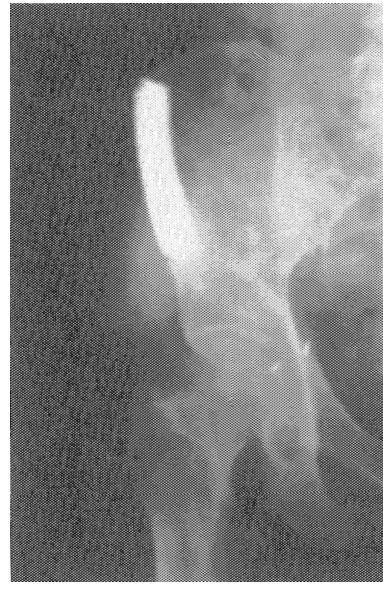

Figure 14.13. Radiograph of an iliac crest prosthesis after one year.

revised by the use of a long stem in combination with A/W glass-ceramic granules mixed with autogenous bone and fibrin glue.

From 1989 until 1993, we used A/W glass-ceramic granules in 32 cases of revision surgery of hip prostheses. The age of the patients at the time of revision surgery ranged from 30–76 years (average 60 years). Retrieved prostheses varied in type. In seven cases, only the socket of the prosthesis was retrieved. The amount of A/W glass-ceramic granules used at the operation ranged from 10–75 g, with an average of 31 g. The results of the revision operations using A/W glass-ceramic granules have been satisfactory.

14.4. CASE HISTORIES

See Hench for colored illustrations of many of the devices and cases described herein.[14]

14.4.1. Vertebral Prostheses

During the period 1983–1994, when the author retired from Kyoto University, the vertebral prosthesis made of A/W glass-ceramic (AW-GC) had

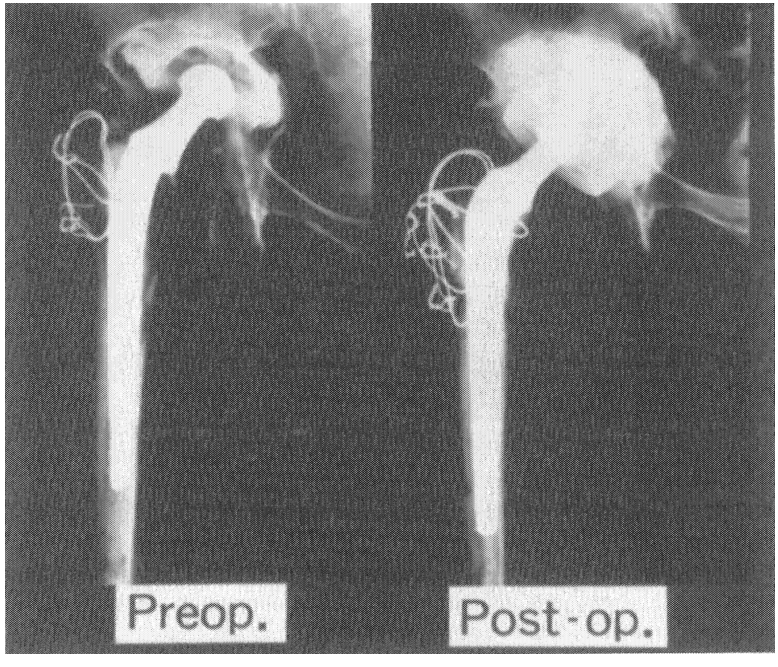

Figure 14.14. Radiographs of a hip prosthesis revision in a 55 year old female patient.

been used in 1,070 cases in Japan. The device was used to treat bone tumors, burst fracture, and fracture dislocation of the spine. By 2010, the AW-GC vertebral prosthesis had been used to treat approximately 3,000 cases. There have been no serious complications reported, such as loosening, collapse, or breakage of the prosthesis. Figure 14.15 illustrates the progressive growth of bone around an AW-GC vertebral prosthesis.

14.4.2. Intervertebral Spacers

During the period 1989–1994, intervertebral spacers made of AW-GC were used for 1,005 lumbar spine fusion cases. The number of cases by 2010 had reached approximately 5,000. The AW-GC spacer has an osteoconductive effect, as shown by radiological follow-up studies. No case has shown late narrowing of the intervertebral space that is often observed when bone autograft or allograft is used for the interbody fusion. Figure 14.16 shows a clinical case of use of AW-GC intervertebral spacers.

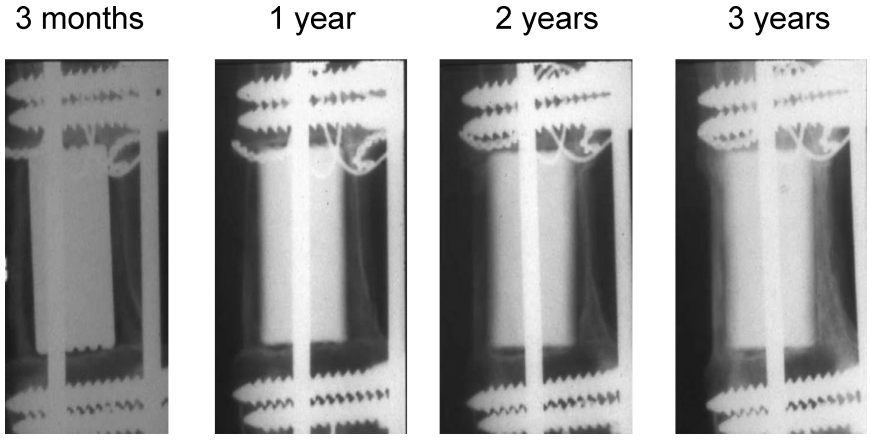

Figure 14.15. Time course of radiological changes around an AW-GC vertebral prosthesis observed in a young female. The patient was treated for a metastasis of alveolar soft part sarcoma in L3 vertebra, which was removed prior to implantation of AW-GC. No recurrence has been observed for 20 years, with the bone trabeculae around the prosthesis becoming thicker with time.

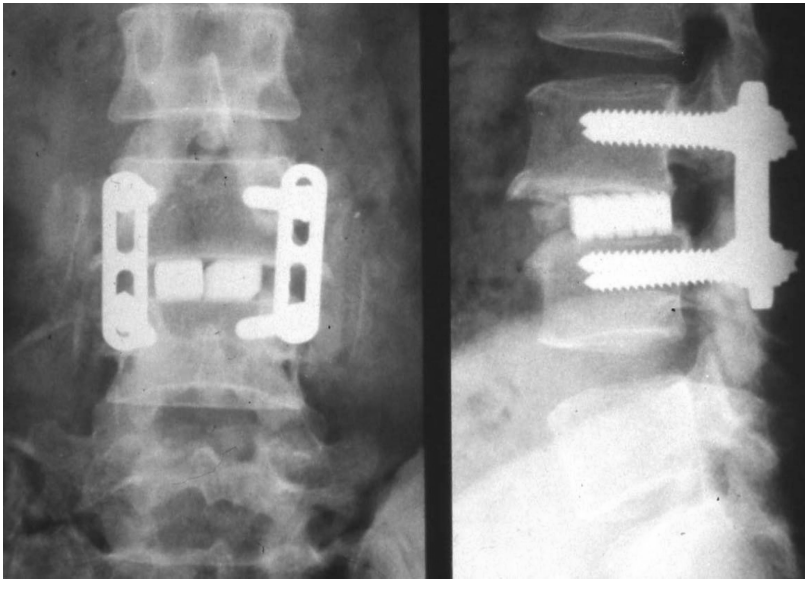

Figure 14.16. Intervertebral spacers of AW-GC used to treat a 40 year old patient with isthmic spondylolisthesis, causing severe low back pain and neuralgia in the leg. The spacers had an osteoconductive effect.

14.4.3. Laminoplasty Spacer

Laminoplasty spacers were made of AW-GC to be used for laminoplastic enlargement in cases of multiple spinal canal stenoses of the cervical spine. Typically four to five laminae are enlarged and bone defects remaining in each lamina are filled with the spacer, which is fixed to the spinous process with threads. In most cases, bone bonding of the spacer was observed on CT images within six months after surgery, resulting in excellent stability of the spacer. The advantages of using the AW-GC spacer in laminoplastic enlargement are that: no surgical intervention for harvesting an autograft is required, and late collapse of the implant never occurs, as can be the case with autograft. During the period 1988–1994, the AW-GC laminoplasty spacer was used in 778 cases in Japan. By 2010 the number had reached 12,000 cases. This operation is considered to be the best indicated for myelopathy caused by multi-level spinal canal stenosis of the cervical spine. Figure 14.17 illustrates use of the AW-GC laminoplasty spacer in a 75 year old male with tetraplegia.

14.4.4. Iliac Crest Prosthesis

Harvesting of autograft from the iliac crest is often necessary. The large bone defect remaining following the removal of the bone can create various cosmetic and neurological problems, especially chronic pain. Iliac crest prostheses

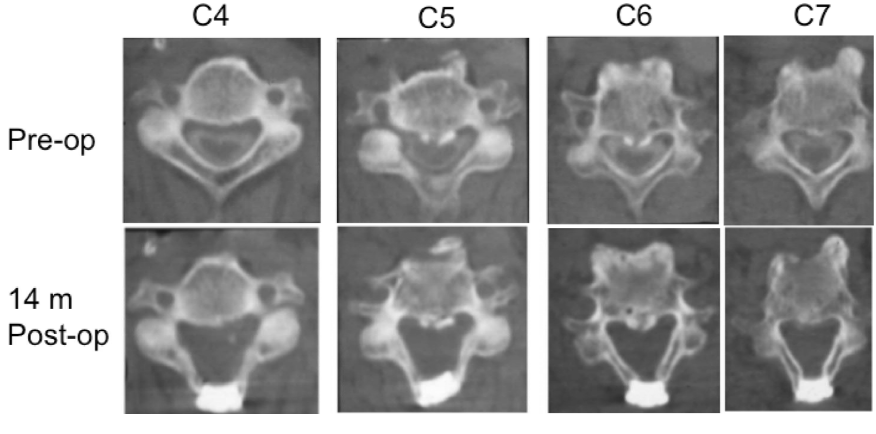

Figure 14.17. AW-GC used as laminoplasty spacer to enlarge the spinal canal for treatment of a 75 year old male suffering from tetraplegia due to ossification of the posterior longitudinal ligament from C4 to C7. All of the spacer has united to the adjacent laminae by 14 months postoperation.

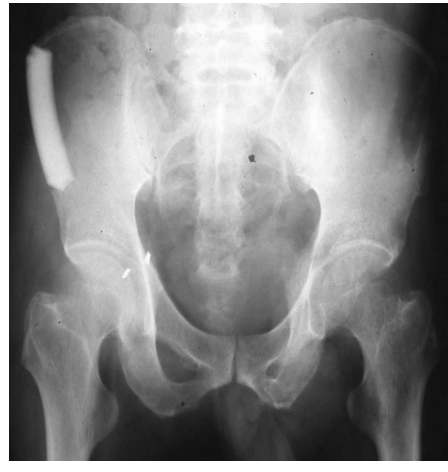

Figure 14.18. Replacement of a large bone defect in the iliac crest with an AW-GC prosthesis after harvest of an autograft.

made of AW-GC were used to fill the bone defect in 4,113 cases during the period 1987–1994. By 2010 the number of cases reached approximately 20,000. It is reported that 97% of the patients are satisfied with the iliac crest prosthesis. Figure 14.18 shows a typical clinical case using AW-GC as iliac crest prosthesis.

14.4.5. Bone Defect Spacers

Removal of large bone tumors developed in weight-bearing locations of long bones requires a strong, tough bone-bonding material to replace the lost bone. AW-GC large bone spacers have been used to fulfill this need. Clinical results after four years show satisfactory weight-bearing and function of the long bone. These findings show that AW-GC can be used clinically as a bone substitute in locations where synthetic HA implants cannot be used.

14.5. CONCLUSION

Twenty-seven years of clinical use of bioactive apatite-wollastonite glass-ceramic (AW-GC) in many thousands of patients has demonstrated excellent success. The concept of bioactive bone-bonding of orthopedic prostheses has revolutionized the long-term treatment of many ailments.

REFERENCES

1. Jarcho, M., Kay, J.F., Gumaer, K.I. *et al.* (1977). Tissue, Cellular and Subcellular Events at a Bone-Ceramic Hydroxyapatite Interface, *J. Bioeng.*, **1**, 79–91.
2. Nakamura, T., Yamamuro, T., Higashi, S. *et al.* (1985). A New Glass Ceramic for Bone Replacement: Evaluation of its Bonding to Bone Tissue, *J. Biomed. Mater. Res.*, **19**, 685–698.
3. Kitsugi, T., Yamamuro, T., Nakamura, T. *et al.* (1989). The Bonding of Glass Ceramics to Bone, *Int. Orthop.*, **13**, 199–206.
4. Yoshii, S., Kakutani, Y., Yamamuro, T. *et al.* (1988). Strength of Bonding Between A/W Glass-Ceramic and the Surface of Bone Cortex, *J. Biomed. Mater. Res.*, **22**, 327–338.
5. Kitsugi, T., Yamamuro, T., Nakamura, T. *et al.* (1987). Aging Test and Dynamic Fatigue Test of Apatite-Wollastonite-Containing Glass-Ceramics and Dense Hydroxyapatite, *J. Biomed. Mater. Res.*, **21**, 467–484.
6. Kokubo, T., Ito, S., Shigematsu, M. *et al.* (1987). Fatigue and Life-Time of Bioactive Glass-Ceramic A/W Containing Apatite and Wollastonite, *J. Mater. Sci.*, **22**, 4067–4070.
7. Ebisawa, Y., Kokubo, T., Ohura, K. *et al.* (1990). Bioactivity of $CaO.SiO_2$ Based Glasses: *In Vitro* Evaluation, *J. Mater. Sci. Mater. Med.*, **1**, 239–244.
8. Kitsugi, T., Yamamuro, T. and Kokubo, T. (1988). Bonding Behavior of a Glass-Ceramic Containing Apatite and Wollastonite in Segmental Replacement of the Rabbit Tibia Under Load-Bearing Conditions, *J. Bone Joint Surg.*, **71**, 264–272.
9. Yamamuro, T., Shikata, J., Okumura, H. *et al.* (1990). Replacement of the Lumbar Vertebrae of Sheep with Ceramic Prostheses, *J. Bone Joint Surg.*, **72**, 889–893.
10. Yamamuro, T., Nakamura, T., Higashi, S. *et al.* (1984). "Artificial Bone For Use As A Bone Prosthesis", in Atsumi, K., Maekawa, M. and Ota, K. (eds), *Progress in Artificial Organs-1983*, ISAO Press, Cleveland, OH, pp. 810–814.
11. Yamamuro, T. (1990). "Replacement of the Spine with Bioactive Glass-Ceramic prostheses", in Yamamuro, T., Hench, L.L. and Wilson, J. (eds), *Handbook of Bioactive Ceramics, Vol. 1*, CRC Press, Boca Raton, FL, pp. 345–352.

12. Yamamuro, T. (1990). "Reconstruction of the Iliac Crest With Bioactive Glass-Ceramic Prostheses", in Yamamuro, T., Hench, L.L. and Wilson, J. (eds), *Handbook of Bioactive Ceramics, Vol. 1*, CRC Press, Boca Raton, FL, pp. 335–342.
13. Ono, K., Yamamuro, T., Nakamura, T. *et al.* (1998). Apatite-Wollastonite Containing Glass-Ceramic Fibrin Mixture as a Bone Defect Filler, *J. Biomed. Mater. Res.*, **22**, 869–885.
14. Hench, L.L. (1998). Bioceramics, *J. Am. Ceram. Soc.*, **81**, 1705–1728.

Chapter 15

CERAVITAL® BIOACTIVE GLASS-CERAMICS

Ulrich M. Gross, Christian Müller-Mai and Christian Voigt

Editor's Note: *This chapter is an abbreviated version of Chapter 7 of the first edition of An Introduciton to Bioceramics. Ceravital® was a short-lived bioactive glass-ceramic used for only a few years in middle ear prostheses. Structural failures occurred due to attack of the crystal-glass phase boundaries in the material. A short summary of the pioneering studies by Professor Ulrich Gross and colleagues at the Free University of Berlin document the important effects of various metallic constituents in the glass-ceramics on the mineralization and bonding of bone and especially the role of matrix vessels. References to this historical work follow.*

15.1. SUMMARY

Shortly after L.L. Hench published his paper titled "Bonding Mechanisms at the Interface of Ceramic Prosthetic Materials"[1] in 1971, by which a new era of concepts, developments and products in the field of biomaterials was induced, E. Pfeil and H. Bromer used this information to design new glasses and glass-ceramic compositions.[2] They coined the term "Ceravital", which means a number of different compositions of glasses and glass-ceramics and not only one product. These new materials were optimistically considered to be applicable for load-bearing conditions to replace bones and teeth.[3] However, the mechanical properties were not compatible with this aim. Furthermore, it was shown that the surface reactivity, which is the leading force for the bone-bonding mechanism, is operative at areas of the implant surface where soft tissue is interfacing and provides a *milieu* for dissolution of the material and activation of mononuclear and multinuclear resorbing cells. The experimental data indicated that the long-term stability of the material was endangered by this process. Other compositions were designed to decrease the solubility of the glasses and glass-ceramics (Table 15.1).[4–6] *In vitro* experiments showed that this approach was successful and that the solubility of the material could be adjusted to various conditions, from high to

Table 15.1. Composition of Bone-Bonding Glass-Ceramic KG Cera, Mina 13 and Non-Bonding Glass-Ceramic KGy-213, M8/1 in Weight Percent.

	KG Cera	Mina 13	KGy213	MS/1
SiO_2	46.2	46	38	50
$Ca(PO_2)z$	25.5	16	13.5	7.1
CaO	20.2	33	31	—
Na_2O	4.8	0	4	5
MgO	2.9	5		
K_2O	0.4		—	—
$A1_2O_3$		—	7	1.5
TazOs	—	—	5.5	—
TiO_2	—		1	
BzO_3			—	4
$Al(PO_3h)$	—	—	—	2.4
SrO		—	—	20
LazO3	—			6
Gd_2O_3	—	—	—	4

low solubilities, by the addition of metal oxides to the melt. However, *in vivo* investigations demonstrated that these new materials containing metal oxides inhibited development, maturation and especially mineralization of the bone matrix adjacent to the implant interface. Mechanisms of inhibition of mineralization were studied and the role of matrix vesicles in the promotion of mineral deposition analyzed.[7,8] There were several approaches to improve the biomechanical properties of the materials, including enameling[9] and making composites.[10] None were successful for clinical use. The only field in which glass-ceramic Ceravital® implants were clinically applied was to replace the ossicular chain in the middle ear, where the loads are minimal and the mechanical properties of the material are sufficient.[11] However, Ceravital® is no longer in clinical use for this application.

15.2. TISSUE–CERAVITAL® RESPONSE

At approximately six days, a bone regeneration phase starts, due to the first mineralized foci in the extracellular matrix which are observable in the light microscope (LM). Young trabeculae are observed, which continue to mineralize

and grow wider. In the case of KG Cera, some trabeculae attach to parts of the implant surface and a thin bony lamella additionally forms on the implant surface between the attaching trabeculae. Histomorphometry already yields approximately 10% bone-contact to KG Cera implants at seven days after implantation. In the transmission electron microscope (TEM) the bonding zone is an electron-dense seam which is known to develop on surface-reactive bone-bonding glass-ceramics.

More collagen is incorporated in the outer part of the bonding zone at later stages and may represent the beginning of primary bone. In the case of glasses and glass-ceramics this bonding layer consists of Si-rich and CaP-rich parts which provide a chemical bonding of the implant to bone.[1]

In the case of non-bonding implants the situation at the interface is completely different.[4–13] On the whole implant surface there is no evidence for mineralization, i.e. there is a seam of non-mineralized extracellular matrix on the implant surface in the LM and there are no attaching layers of collagen-fibers showing different stages of mineralization in the TEM. Instead of mineralization, large multinucleated cells of about 50 µm in length and more were found attaching to the surface. This indicates that the difference in the healing around non-bonding and bone-bonding glass-ceramic implants occurred between the second phase (formation of granulation tissue) and third phase (formation of bone tissue) of wound healing.

Bone-bonding and non-bonding specimens prepared for scanning electron microscopic (SEM) evaluation showed trabecular structures fixing the implants within the marrow cavity. The amount of trabeculae was higher for the bone-bonding material KG Cera.[7] TEM studies demonstrated that the insertion of bone-bonding and non-bonding glass-ceramic implants affected the mineralization process differently. The production of matrix vesicles was changed in an implant-dependent, and time-dependent manner, which might alter the calcification of osteoid differently. Total matrix vessel (MV) numbers around KG Cera and KGy-213 showed significant higher values ($p < 0.05$) around the bone-bonding material KG Cera when compared to the non-bonding material KGy-213. This clearly demonstrates that more MVs were produced around the bonding material. The significant higher value of MV per area of non-calcified extracellular matrix (ECM) points to the possibility that the capacity of osteoblasts to produce MV is reduced around the metal oxide containing non-bonding implants. These results led to the suggestion that mineralization around non-bonding implants leads to inhibited tissue maturation, whereas bone-bonding implants seem to promote primary calcification via an increased number of matrix vesicles.

Additionally, the matrix vesicle distance to the calcifying front was lower in the case of the non-bonding material KGy-213 at three days and significantly statistically lower at six days after implantation when compared to the bone-bonding material. This suggests that the ECM is not as mature in the KGy-213 material as in KG Cera. These results point to an affected osteoblastic function in the case of the non-bonding material where less extracellular matrix was produced. The data led to the conclusion that the negative effect of non-bonding implants might be on the growth of calcifying fronts. To achieve bone-bonding, the surface solubility is of utmost importance. Up to a certain level, a higher solubility results in increased bioactivity. In a previous study, it was shown that up to 1.6% Al_2O_3 can be tolerated without diminishing bone-bonding behavior. The percentage of metal ions can be slightly higher if the surface solubility is increased up to a defined maximum.

15.3. REMODELING

This phase starts at approximately 14 days, when tissues typical of the organ, i.e. mineralized bone or bone marrow, are produced and last for a life-time. This phase comprises of the replacement of trabecular bone by lamellar bone or bone marrow. The remodeled tissue will be adapted to the local needs, e.g. mechanical load.

15.3.1. The Material Response

The surfaces of glass-ceramic implants show degradation phenomena which are dependent on the chemical composition of the bulk material as well as on the tissue in contact with the surface. When bone-bonding occurs the surface is protected and stabilized against further degradative processes. Other tissues, e.g. soft tissue, allow ongoing degradation by various processes. Most obvious changes occur in bonding glass-ceramics, which show changes in surface morphology in the SEM and TEM. The ceramic phase of the implant is partially liberated as early as three days after implantation. The process continues until the ceramic phase is almost totally liberated approximately 28 days after implantation. Leaching phenomena start at the phase transition between glass and ceramic phases.[12] Such processes are enhanced on glow discharged (GD)-sterilized KG Cera implants, which show changes at three days, which were seen on autoclaved implants as early as 14 and more days after implantation, with zones displaying partially or totally freed ceramic particles. Leaching leads additionally to the liberation of the ceramic phase to loss of small implant particles which are then incorporated by

cells, such as macrophages and osteoblast-like cells.[13] A direct bioresorption of bulk materials seems also to be possible. It was shown that osteoblast-like cells were able to phagocytose dense hydroxyapatite implants.[13] Such cells were also observed on the KG Cera glass-ceramic with loose implant particles in the cytoplasm. Ruffled borders were not observed. However, it seems possible that these cells are able to increase the degradation by lowering the pH underneath their cellular membrane, which in turn increases the implant solubility.

Non-bonding implants with reduced solubility due to the addition of metal oxides to the bulk material do not show evidence of leaching phenomena up to 14 days after implantation. At this stage macrophages can be observed with incorporated particles of implant origin. Similar observations were made when comparing surfaces of autoclaved and GD-sterilized implants.

15.4. CONCLUSIONS

In vivo studies with different species showed that the cellular response to the glass-ceramics depends on the amount of metal oxides being released and influencing negatively the cellular function and the development and maturation of the ECM. There were two major groups: bone-bonding and non-bonding glass-ceramics. The non-bonding materials contained metallic elements that inhibited bone formation at the tissue–material interface.

REFERENCES

1. Hench, L.L., Splinter, R.J., Allen, W.C. *et al.* (1971). Bonding Mechanisms at the Interface of Ceramic Prosthetic Materials, *J. Biomed. Mater. Res. Symp.*, **2**, 117–141.
2. Bromer, H., Pfeil, E. and Kas, H.H. (1973). German Patent, 2,326,100.
3. Blencke, B.A., Bromer, H., Pfeil, E. *et al.* (1973). Implantate aus Glaskeramik in der Knochenchirurgie (Tierexperimentelle Untersuchungen), *Langenbecks Arch. Klin. Chir. Suppl. Chir. Forum*, **94**, 116–119.
4. Gross, U.M. and Strunz, V. (1980). The Anchoring of Glass Ceramics of Different Solubility in the Femur of the Rat, *J. Biomed. Mater. Res.*, **14**, 607–618.
5. Gross, U., Brandes, J., Strunz, V. *et al.* (1981). The Ultrastructure of the Interface Between a Glass Ceramic and Bone, *J. Biomed. Mater. Res.*, **15**, 291–305.

6. Gross, U.M. and Strunz, V. (1985). Interface of Various Glasses and Glass Ceramics in a Bony Implantation Bed, *J. Biomed. Mater. Res.*, **19**, 251–271.
7. Müller-Mai, C., Amir, D., Wendland, H. *et al.* (1990). The Effect of Glass-Ceramic Implants on Matrix Vesicle Calcification After Two Weeks of Rat Tibial Bone Healing, *J. Biomed. Mater. Res.*, **24**, 1571–1584.
8. Müller-Mai, C.M., Amir, D., Schwartz, Z. *et al.* (1991). Ultrastructural Histomorphometry of Extracellular Matrix Vesicles in Primary Calcification Around Bone-Bonding and Non-Bonding Glass-Ceramics, *Cells & Materials*, **1**, 341–352.
9. Zeiler, G., Strunz, V. and Gross, U. (1986). "Bone Implant Surfaces with Coatings Containing Surface-Reactive Particles", in Kossowsky, R. and Kossowsky, N. (eds), *Material Sciences and Implant Orthopedic Surgery*, NATO ASI Series, Martinus Nijhoff Publ., Dordrecht, pp. 249–259.
10. Müller-Mai, C., Schmitz, H.J, Strunz, V. *et al.* (1989). Tissues at the Surface of the New Composite Material Titanium/Glass-Ceramic for Replacement of Bone and Teeth, *J. Biomed. Mat. Res.*, **23**, 1149–1168.
11. Reck, R. (1984). Bioactive Glass-Ceramics in Ear Surgery: Animal Studies and Clinical Results, *Laryngoscope*, **94**, Suppl. 33, 1–54.
12. Müller-Mai, C., Voigt, C., Knarse, W. *et al.* (1991). The Early Host and Material Response of Bone-Bonding and Non-Bonding Glass-Ceramic Implants as Revealed by Scanning Electron Microscopy and Histochemistry, *Biomaterials*, **12**, 865–871.
13. Müller-Mai, C.M., Voigt, C. and Gross, U.M. (1990). Incorporation and Degradation of Hydroxyapatite Implants of Different Surface Roughness and Surface Structure in Bone, *Scanning Microsc.*, **4**, 613–624.

Chapter 16

MACHINABLE AND PHOSPHATE GLASS-CERAMICS

Wolfram Höland and Werner Vogel

16.1. INTRODUCTION

The development of new materials for bone implants and substitutes in man has gained major importance over the past 20 years. In addition to metals, alumina, and organic polymers, glasses and glass-ceramics have come especially to the fore. These new implant materials are biocompatible, and may have bioactive properties. They are not regarded as foreign bodies and encapsulated by fibrotic tissue; instead, direct bonding takes place. The special combinations of properties required for medical indications can be adjusted and varied in glasses and glass-ceramics.

Glass-ceramics consist of at least one glassy and at least one crystalline phase. The processing to develop a glass-ceramic is characterized by a formation of a base glass and an additional heat treatment of the glass. During this heat-treatment process, nucleation and crystallization has to be controlled to form the crystals in the base glass (Chapter 1).

Biomaterials for bone substitution are called bioactive if a stable bond to the bone is formed. Hench *et al*.[1] showed that Bioglass® can bond to bone in animals. The interface reactions between Bioglass® and bone, the formation of different Ca-, P-, and SiO_2-rich layers, the dependence on the composition of the implant, the environment, and reaction time were studied.[2] It was shown that the preferred bonding of bone and biomaterial (glass-ceramic or sintered ceramic) can be achieved if the biomaterial contains apatite crystals in the basic material[3–5] or develops an apatite layer. Mica crystals will permit predictable mechanical machining properties.[6] We believe that for a material to be machinable and bioactive, it should contain both mica and apatite crystals and we have developed glass-ceramics for medicine derived from different base glasses.[7–9]

16.2. COMPOSITONS AND PROCESSING

BIOVERIT I is a mica-apatite glass-ceramic with a chemical composition from the SiO_2-(Al_2O_3)-MgO-Na_2O-K_2O-F-CaO-P_2O_5 base glass system. These

glasses are from the silico-phosphate type. The key to the development of BIOVERIT I was to form a phase-separated base glass consisting of three glassy phases and to control the nucleation and crystallization by heat treating the glass. BIOVERIT II glass-ceramic contains mica as the main crystal phase and secondary crystals, e.g. cordierite crystals.

The base glass is derived from the SiO_2-Al_2O_3-MgO-Na_2O-K_2O-F system, called silicate glasses. The base glass is phase separated into two glassy phases and micas were formed during heat treatment of the glass. Because of the high mica content, BIOVERIT I and II are machinable glass-ceramics.

The chemical composition of BIOVERIT III glass-ceramic is characterized by glasses from the CaO-Al_2O_3-P_2O_5-Na_2O (ZrO_2-FeO/Fe_2O_3) system, so called "invert" glasses of a phosphate type. In comparison to BIOVERIT I and II, the base glass of BIOVERIT III does not show phase separation. Apatite, $AlPO_4$ crystals, and other phosphate crystals grow via a special process in the base glass during heat treatment.[10,11]

Machinable mica-based glass-ceramics were developed for technical applications by Beall *et al*.[12] The composition of the base glasses are characterized by the alkali-fluoroboro-silicate system. Grossman[13] formed special tetrasilicic-mica in alkali-fluorosilicate glasses. The glass-ceramic implants known as Dicor® have been used for dental restorations. Typical chemical compositions of BIOVERIT-type glass-ceramics are shown in Tables 16.1–16.3, with the range of possible chemical compositions given. Example 1 of BIOVERIT I (Table 16.1) is a mica-apatite glass-ceramic with special fluorophlogopite mica crystals (Na/K $Mg_3(AlSi_3O_{10})F_2$). Example 2 demonstrates a mica-apatite glass-ceramic with

Table 16.1. Composition of BIOVERIT I.

	Weight Percent		
	Composition Range	**Example 1**	**Example 2**
SiO_2	29.5–50	30.5	38.7
MgO	6–28	14.8	27.7
CaO	13–28	14.4	10.4
Na_2O/K_2O	5.5–9.5	2.3/5.8	0/6.8
Al_2O_3	0–19.5	15.9	1.4
F	2.5–7	4.9	4.9
P_2O_5	8–18	11.4	8.2
TiO_2	additions	—	1.9

Table 16.2. Composition of BIOVERIT II.

	Weight Percent	
	Composition Range	**Example 1**
SiO_2	43–50	44.5
Al_2O_3	26–30	29.9
MgO	11–15	11.8
Na_2O/K_2O	7–10.5	4.4/4.9
F	3.3–4.8	4.2
Cl	0.01–0.6	0.1
CaO	0.1–3	0.2
P_2O_5	0.15	0.2

Table 16.3. Composition of BIOVERIT III.

	Weight Percentage
	Composition
P_2O_5	45–55
Al_2O_3	6–18
CaO	13–19
Na_2O	11–18
$MeO/Me_2O_3/MeO_2$ (MnO,CoO,NiO,FeO, Fe_2O_3,Cr_2O_3 ,ZrO_2)	1.5–10

tetrasilicic mica crystals. The formation of these crystals was possible by heat treating the base glass compositions at temperatures between 610 and 1050°C. The controlled crystallization takes place via phase separation of the base glass.[7–9]

BIOVERIT II (Table 16.2) is a glass-ceramic consisting of a new type of curved mica of fluorophlogopite-type. A second crystal phase has also been precipitated in the glass. The basis for the nucleation and crystallization is also the phase separation of the glasses which has been caused by Na_2O-, K_2O- and F-additions to the glass.

BIOVERIT III is a pure phosphate glass which does not contain silica. During the development of BIOVERIT III as a biomaterial, a new way for the

control of the crystallization in phosphate glasses was found.[10] It starts from phosphate invert glasses of the P_2O_5-Al_2O_3-CaO-Na_2O system, the structure of which is formed only by mono- and diphosphate units. Doping with a suitable nucleation agent, e.g. iron oxide or ZrO_2, leads to a supersaturation of the glass with this component in a certain concentration range. This supersaturation is reduced by a subsequent thermal treatment, which results in the precipitation of a primary crystal phase in the glass. In this case this phase may be an Na-Ca-Fe-phosphate of the varulite-type. Crystal nuclei have developed which initiate the precipitation of the actual main crystal phase apatite, $AlPO_4$, in various modifications and specific complex phosphate structures.

The BIOVERIT III glass-ceramic, which is SiO_2-free and is bioactive (i.e. the material can bond to living bone), is a material containing the following phases: apatite, $AlPO_4$, (berlinite), and complex phosphate structures.[11]

16.3. PROPERTIES

Characteristic properties of BIOVERIT I, II, and III are shown in Tables 16.4–16.6. It is possible to control the properties by the chemical composition and the content of the crystals in the glass matrix.

BIOVERIT I and II are machinable glass-ceramics; these biomaterials are workable with standard metal tools and instruments. They can also be easily modified during surgical procedures. The workability of the biomaterial depends on the mica content as well as the morphology of the glass-ceramic, e.g. a glass-ceramic with high mica content has excellent machinability, thus the workability of BIOVERIT II is better than that of BIOVERIT I. The content of the crystals

Table 16.4. Properties of BIOVERIT I Glass-Ceramic.

Density	2.8	g/cm^3
Linear thermal expansion coefficient (20–400°C)	$8–12 \cdot 10^{-6}$	m/mK
Bending strength	140–180	MPa
Fracture toughness, K_{1C}	1.2–2.1	$MPa \cdot m^{1/2}$
Young's modulus	70–88	GPa
Compressive strength	500	MPa
Vickers hardness, HV 10	5000	MPa
Hydrolytic class (DIN 12111)	2–3	

Table 16.5. Properties of BIOVERIT II Glass-Ceramic.

Density	2.5	g/cm^3
Linear thermal expansion coefficient (20–400°C)	$7.5 \cdot 10^{-6}$	m/mK
Bending strength	90–140	Mpa
Fracture toughness, K_{1C}	1.2–1.8	$MPa \cdot m^{1/2}$
Young's modulus	70	GPa
Compressive strength	150	MPa
Vickers hardness	up to 8000	Mpa
Hydrolytic class (DIN 12111)	1–2	
Roughness (after polishing)	0.1	μm

Table 16.6. Properties of BIOVERIT III Glass-Ceramic.

Density	2.7–2.9	g/cm^3
Linear thermal expansion coefficient (20–400°C)	$14–18.10^{-6}$	m/mK
Bending strength	60–90	MPa
Fracture toughness, K_{1C}	0.6	$MPa \cdot m^{1/2}$
Young's modulus	45	GPa
Hydrolytic class (DIN 12111)	2–3	

within the glass-ceramic is also responsible for the translucency of the material. A higher content of crystals gives a lower translucency than a lower crystal content. Color can be controlled by adding special pigments, namely the oxides NiO, Cr_2O_3, MnO_2, FeO, Fe_2O_3, and others in small amounts to the base glass of the glass ceramic.

The translucency and color of the materials are important in dental applications. Mechanical properties, such as bending strength and fracture toughness, of BIOVERIT I and II allow them to be used as biomaterials for bone substitution (Tables 16.4 and 16.5).

The mechanical properties of BIOVERIT III (primarily bending strength) are lower than those of mica glass-ceramics. But their thermal properties make them suitable for the preparation of composites with certain metals, especially the Co-Cr-Mo alloys widely used in implantology. All these glass-ceramics (BIOVERIT I, II, III) have good chemical properties (hydrolytic stability).

16.4. SURFACE CHEMISTRY

Electron microscopic investigations show the surface of the BIOVERIT glass-ceramics at a high magnification. BIOVERIT I (Fig. 16.1) contains apatite crystals with a diameter of about 1–2 μm and large mica crystals embedded in the glassy matrix.

BIOVERIT II (Fig. 16.2) shows a special type of curved mica crystal. This type of crystal does not exist in nature; it is only formed in glasses. The mica crystals are spherical in shape and the cordierite crystals are precipitated between the mica platelets.

The crystals of apatite and $AlPO_4$-type of BIOVERIT III are shown in Fig. 16.3. It was also possible to precipitate berlinite-type $AlPO_4$-crystals, which show piezoelectric properties. Other complex phosphate crystals can grow in the glass-ceramics.

Reactions on the surface of the biomaterials are studied *in vitro.* Glass-ceramic BIOVERIT I was kept for one week in Ringer's solution. Figure 16.4b

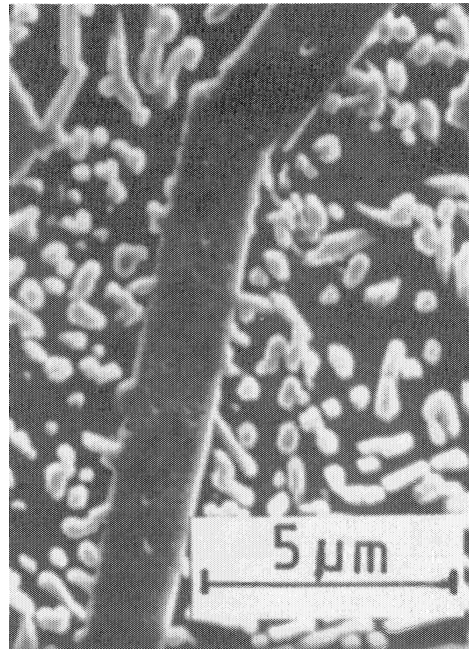

Figure 16.1. Scanning electron micrograph (SEM) of BIOVERIT I. Mica (phlogopite) and apatite crystals were precipitated in the glass matrix (surface hydrofluoric acid (HF) etched).

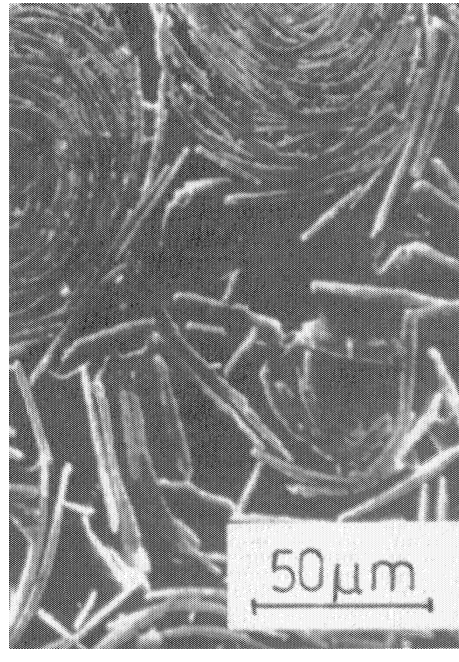

Figure 16.2. SEM of BIOVERIT II. Curved mica crystals of phlogopite-type and cordierite crystals grown in the glass matrix (HF etched).

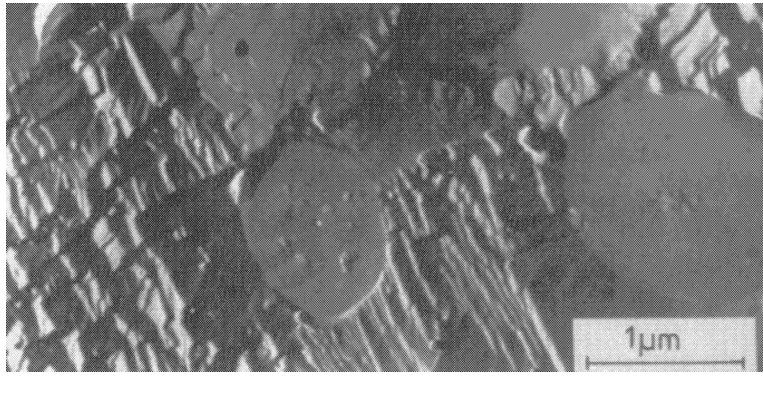

Figure 16.3. BIOVERIT III contains apatite, $AlPO_4$-crystals, and other "complex" phosphates (TEM replica, hydrogen chloride (HCl)-etched).

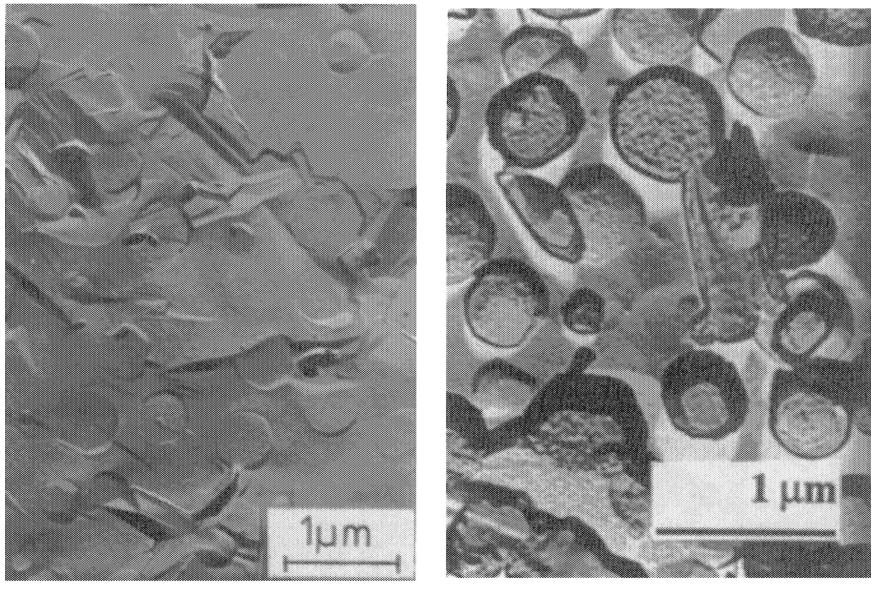

(a) (b)

Figure 16.4. TEM/replica micrograph of BIOVERIT I: a) untreated specimen; b) specimen after one week in Ringer's solution.

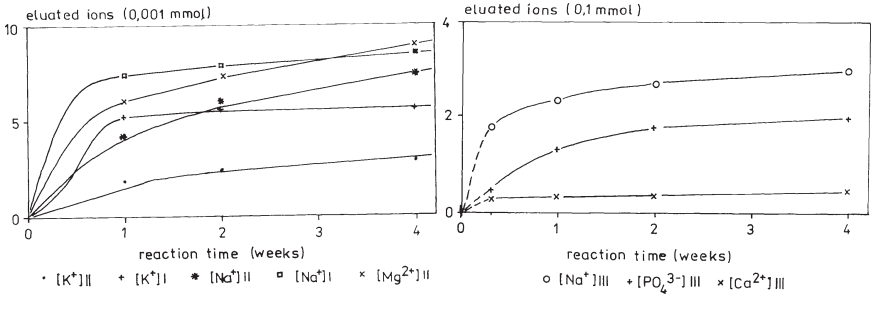

Figure 16.5. Eluation of ions from BIOVERIT I, II, and III (T = 37°C, pH = 7.4, sample 3 g, grain size: 160–315 µm 100 ml tris-buffer solution).

compared with Fig. 16.4a shows more prominent crystals due to solubility of the glassy phase. Solubility of alkali ions and magnesium ions from BIOVERIT I and II was found in tris-buffer-solution (Fig. 16.5). This indicates an ion exchange between the glass-ceramics and simulated body fluid. High resolution

measurements by SIMS show a tendency for phosphate group enrichment at the surface of BIOVERIT I glass-ceramics, in addition to the phosphate contained in the original apatite crystals.

16.5. TISSUE RESPONSE

Results of *in vivo* tests of BIOVERIT I show that one year after operation, the reaction interface between bone (tibia of guinea pig) and glass-ceramic implants is less than 15 μm. Figure 16.6a and 16.6b show a very good bonding of glass-ceramic and bone. Apatite is the main crystal phase of the glass-ceramic; in addition, the Ca^{2+} and phosphate ion content is higher in the reaction zone than in the glass-ceramic. Leaching of alkali ions occurs to a depth of about 5 μm. Optical microscopic investigations (histology) and the calculated bone connection (Fig. 16.6) show a bioactive behavior of BIOVERIT I glass-ceramic in comparison to alumina implants. These results of bone connection of BIOVERIT I and Al_2O_3 can be compared directly because of the experimental model. The shearing strength of the implant–bone boundary has been determined by measuring the mechanical force necessary to push out the implant of BIOVERIT I. The value of about 2.3 MPa found for glass-ceramic implants was on average eight times greater than for alumina implants, measured for comparison in the same model. The surface of the implants after push-out tests was determined by SEM. A typical surface is demonstrated in Fig. 16.7, in

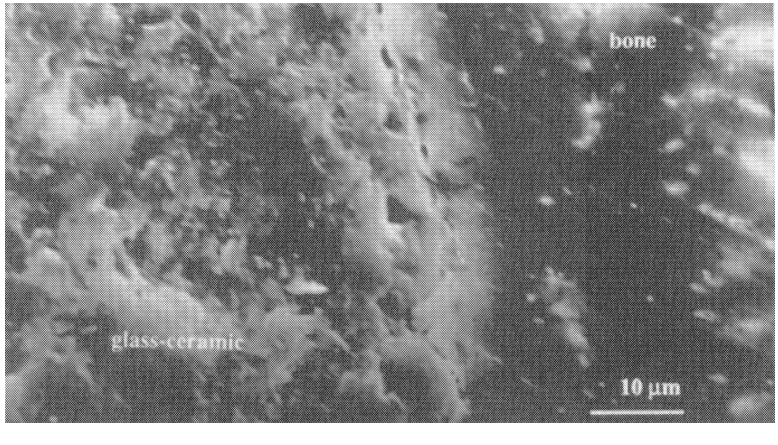

Figure 16.6a. The interface between BIOVERIT I and bone one year after operation (SEM).

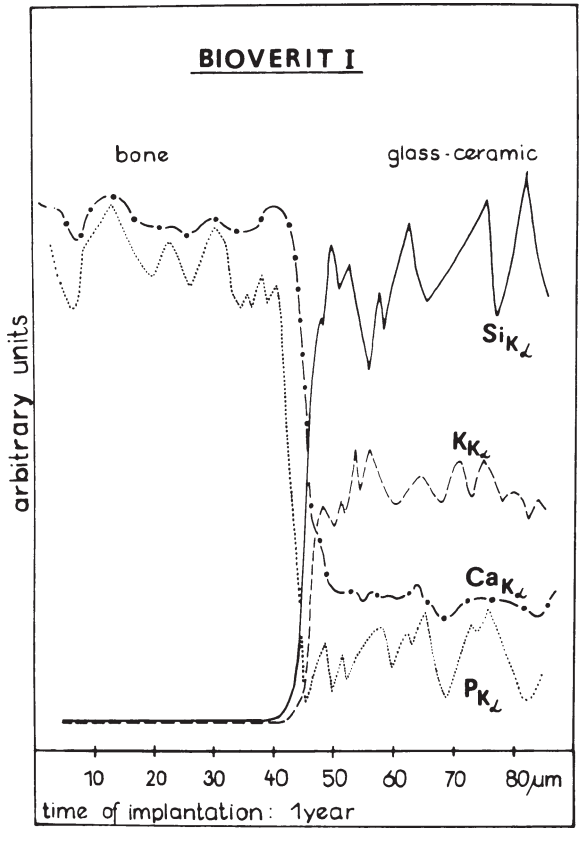

Figure 16.6b. The interface between BIOVERIT I and bone one year after operation (electron microprobe).

comparison to Fig. 16.4a, which shows the surface of an untreated BIOVERIT I glass-ceramic. These studies show the very small solubility of the glassy phase of the glass-ceramic, of less than 0.5 µm. The apatite and mica crystals are directly deposited at the surface of the biomaterial. The black parts of the photograph, where the crystals are not clearly visible, are bone which has remained adherent to the surface of the glass-ceramic. The process of bioactivity is complex. It includes the reaction of the apatite, shown by dense hydroxyapatite implants, new apatite formation, ion transport and surface activity, the role of SiO_2, as described by Hench,[1,2] and biomechanical factors. Animal experiments with BIOVERIT III implants showed good bioactive behavior of the implants. Biocompatibility has been tested and good bonding without intervening tissue

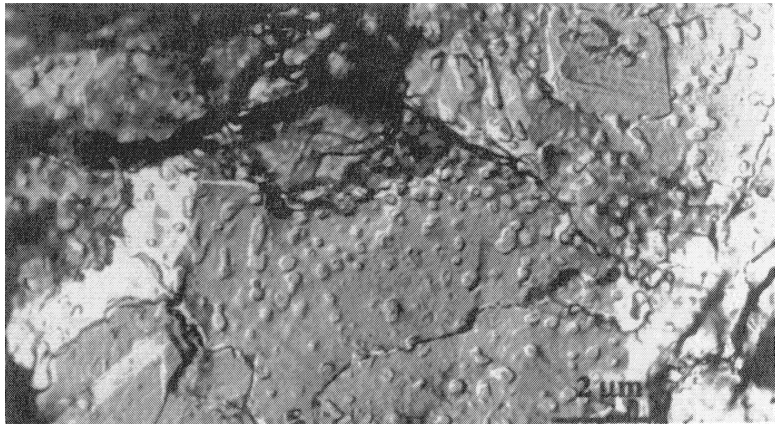

Figure 16.7. BIOVERIT I after pull out test, eight weeks after implantation in tibia of guinea pig (TEM/replica).

was obtained. BIOVERIT II is a biocompatible glass-ceramic with lower bioactivity. Animal experiments demonstrated that bonding occurs without causing any adverse reactions and that the biocompatible implant can be covered with epithelium.

16.6. CLINICAL APPLICATIONS

BIOVERIT I and II can be used as biomaterials for bone substitution. More than 850 implants have been successfully used in clinical cases in the following fields:[14–16]

- Orthopedic surgery (especially different types of spacers).
- Head and neck surgery (especially middle ear implants).
- Stomatology (especially tooth root and veneer laminates).

Orthopedic surgery:

- Reconstruction of the root of the acetabulum in a dislocated hip at the dysplasic stage (pericapsular iliumosteotomy according to Pemperton).
- Ligament fixation in capsule-ligament plastic surgery of the knee joint.
- Osteotomy of the tibial head and augmentation of the tibial plateau.
- Partial replacement of vertebrae in the dorsal part of the spine.

- Ventral spondylodesis in the cervical vertebrae, according to Robinson.
- Distraction osteotomy for maintaining of space.
- Plastic surgery of the shoulder joint, according to Eden and Hybinette.
- Substitution of vertebrae.

Head and neck surgery:

- Collumellization in tympanoplasty.
- Augmentation of the stapes.
- Reconstruction of the posterior wall of the auditory canal.
- Reconstruction of the skull base.
- Maintenance of the base of the orbit.
- Construction of the anterior wall of the frontal sinus.
- Rhinoplasty.

Figure 16.8 shows spacers of BIOVERIT I for treating recurrent dislocations of the shoulder by the Eden–Hybinette operation and Fig. 16.9 shows middle ear implants of BIOVERIT II.

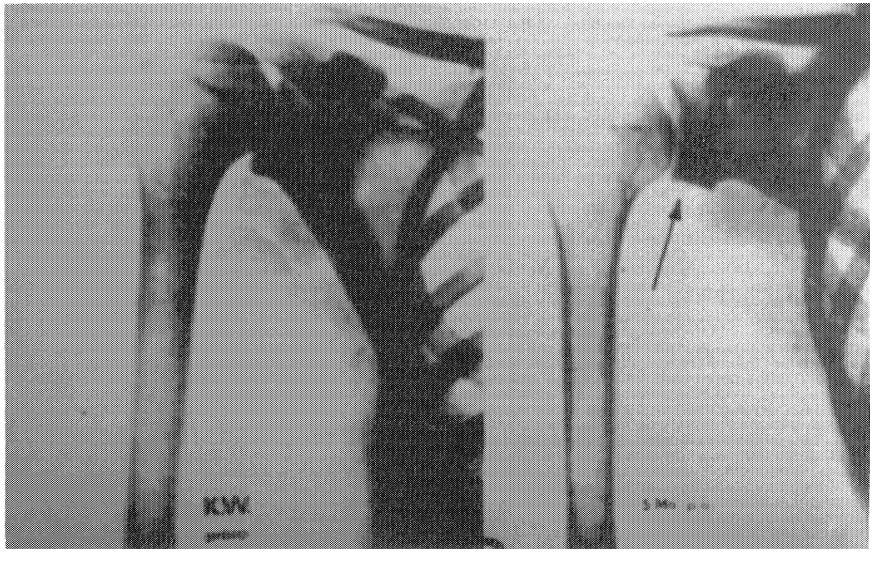

Figure 16.8. BIOVERIT I spacers for treating recurrent dislocation of the shoulder by an Eden–Hybinette operation.

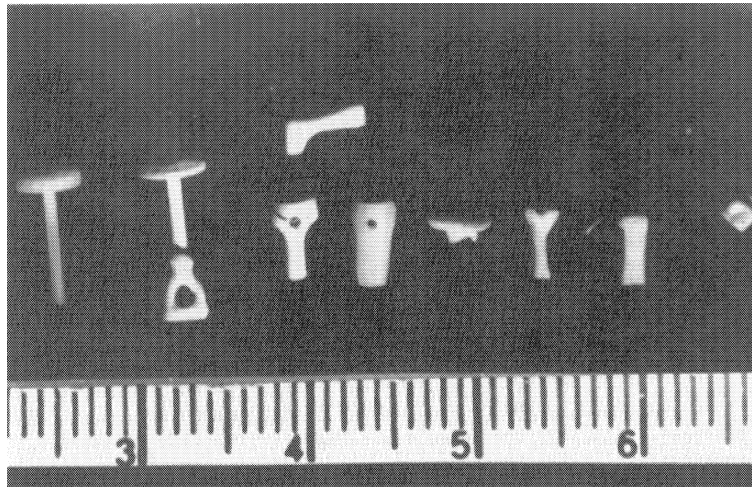

Figure 16.9. Middle-ear implants of BIOVERIT II that have been shaped by the surgeon.

REFERENCES

1. Hench, L.L., Splinter, R.J., W.C. Allen, W.C. *et al.* (1971). Bonding Mechanisms at the Interface of Ceramic Prosthetic Materials, *J. Biomed. Mater. Res. Symp.*, **2**, 117–141.
2. Pantano Jr., C.G., Clark Jr., A.E. and Hench, L.L. (1974). Multilayer Corrosion Films on Bioglass® Surface, *J. Am. Ceram. Soc.*, **57**, 412–413.
3. Strunz, V., Bunte, M., Gross, U.M. *et al.* (1978). Beschichtung von Metallimplantanten mit Bioaktiver Glaskeramik Ceravital, *Dtsch. Zahntirztl.*, **33**, 862–865.
4. Kukubo, T., Shigematsu, M., Nagashima, Y. *et al.* (1982). Apatite and Wollastonite-Containing Glass-Ceramics for Prosthetic Application, *Bull. Inst. Chern. Res.*, **60**, 260–268.
5. Ducheyne, P. and de Groot, K. (1981). *In Vivo* Surface Activity of a Hydroxylapatite Alveolar Bone Substitute, *J. Biomed. Mater. Res.*, **15**, 441–445.
6. Vogel, W. (1979). *Glaschemie*, Verlag Grundstoffindustrie, Leipzig.
7. Höland, W., Vogel, W., Naumann, K. *et al.* (1985). Interface Reactions Between Machineable Bioactive Glass-Ceramics and Bone, *J. Biomed. Mater. Res.*, **19**, 303–312.

8. Vogel, W. and Höland, W. (1987). Development of Glass-Ceramics for Medical Application, *Angew. Chern. Int., Ed. Engl.*, **26**, 527–544.
9. Höland, W., Wange, P., Naumann, K. *et al.* (1991). Control of Phase Formation Process in Glass-Ceramics for Medicine and Technology, *J. Non-Crystalline Solids*, **129**, 152–162.
10. Vogel, W., Vogel, J., Roland, W. *et al.* (1987). Zur Entwicklung Bioaktiver Kieselsaurefreier Phosphatglas Keraminken für die Medizin Wissenschaftliche Zeitschrift FSK Jena, *Natur wiss. R.*, **36**, 841–854.
11. Wange, P., Vogel, J., Horn, L. *et al.* (1990). The Morphology of Phase Formations in Phosphate Glass Ceramics, *Silic. Incl.*, **7–8**, 231–236.
12. Beall, G.H., Montierth, M.R. and Smith, P. (1991). Workable Glass-Ceramics, *Glas Email-Keramo-Technik*, **22**, 409–415.
13. Grossman, D.G. (1983). Stain-Resistant Mica Compositions and Articles Thereof in Particular Dental Constructions, Patent EP 0 083 828.
14. Schubert, T., Purath, W., Liebscher, P. *et al.* (1988). Klinische Indikationen für die Anwendung der Janaer Bioaktiven Maschinell Bearbeitbaren Glaskeramik in der Orthopadie und Traumatologie, *Beitrage Orth. Traumata!*, **35**, 7–16.
15. Beleites, E., Gudziol, H. and Roland, W. (1988). Maschinell Bearbeitbare Glaskeramik für die Kopf-Hals-Chirurgie, *HNO-Praxis*, **13**, 121–125.
16. Pinkert, R., Naumann, K. and Vogel, W. (1987). Individuelle Herstellung Enossaler Zahnimplantate aus der Maschinellen Barbeitbaren Bioaktiven Glaskeramik Jena, *Philip Journal*, **6**, 339–342.

Chapter 17

HYDROXYAPATITES

Racquel Z. LeGeros and John P. LeGeros

17.1. INTRODUCTION

The first successful repair of a bony defect using a calcium phosphate reagent, described as "triple calcium phosphate compound" was reported by Albee in 1920.[1] A half a century later, Levitt *et al*. in 1969[2] and Monroe *et al*. in 1971[3] described a method of preparing a ceramic apatite from mineral fluorapatite, $Ca_{10}(PO_4)_6F_2$, and suggested the possible use of this apatite ceramic in dental and medical applications. Clark *et al*.[4] and Hubbard[5] described methods of preparing calcium phosphate ceramics by sintering commercially-available calcium phosphate reagents, described as "tri-calcium phosphate tribasic". Nery *et al*.[6] in 1975 reported the first clinical application of Hubbard's preparation (they described it as "tri-calcium phosphate" or TCP ceramic). However, X-ray diffraction (XRD) analysis of this "TCP ceramic" showed it to consist of a mixture of beta-tri-calcium phosphate (β-TCP, $Ca_3(PO_4)_6$) and hydroxyapatite (HA, $Ca_{10}(PO_4)_6(OH)_2$).[7] Consequently, Nery proposed that such mixtures be described as biphasic calcium phosphates (BCP).[8,9]

In the mid-1970s, three groups, Jarcho *et al*. in the US,[10–12] de Groot *et al*.[13,14] and Denissen[15] in Europe and Aoki *et al*. in Japan,[16,17] simultaneously but independently worked towards the development and commercialization of hydroxyapatite (HA) — more accurately, calcium hydroxyapatite – as a biomaterial for bone repair, augmentation and substitution. This was probably based on the rationale that the bone mineral has been described as "hydroxyapatite"[18,19] and the observation reported in the early 1970s by Hench of a "chemical bonding" of bone with a bioactive glass ceramic through a calcium phosphate-rich layer.[20]

Currently, apatite-based commercial bioceramics for bone repair include sintered (HA) and unsintered (HAp) apatite preparations, apatites derived from marine algae, coral or from bovine bone and composites of polymer and apatite (Table 17.1.).[7,21–24]

This chapter provides a brief review of the preparation and general properties of pure hydroxyapatite (HA), synthetic unsubstituted and substituted apatites (HAp) and biological apatites, as well as cell and tissue responses to and clinical applications of apatite bioceramics. The reader is also referred to other reviews on the subject.[23–26]

Table 17.1. Commercial HA and HAp Bioceramics.

Derived from marine algae
Algipore® (Friadent, Germany)
Coral derived apatite
Interpore®200, ProOsteon®200, ProOsteon®500 (Interpore Int, CA)
Bovine bone apatite (unsintered)
BioOss® (EdGeitslich, Switzerland)
Bovine bone apatite (sintered)
Endobon® (Merck, Germany)
Ostograf®-N (Ceramed, CO)
Trubone® (Japan)
Synthetic HA (sintered)
Calcitite® (Calcitek, CA)
Osteograf® (Ceramed, CO)
Bioroc® (DePuy-Bioland, France)
Apaceram™ (Pentax Corp., Tokyo)
Synthetic HAP (unsintered)
Osteogen® (Impladent, NY)
Ostim® (Germany)
HA composites
HA/polyethylene, *HAPEX*® (Gyrus, TN)
CHA/collagen, *Healos*™ (Orquest Inc., CA)
HA/$CaSO_4$, *Hapset*® (Lifecore, MN)

17.2. GENERAL STRUCTURE AND PROPERTIES OF CALCIUM HYDROXYAPATITE

The term "apatite" describes a family of compounds having similar structures but not necessarily having identical compositions. Hence, apatite is a description of a structure and not of a composition. Hydroxyapatite (HA), specifically calcium hydroxyapatite, is a compound of a definite composition, $Ca_{10}(PO_4)_6(OH)_2$, and a definite crystallographic structure. The structure of HA, showing the exact atomic positions in the crystal, was determined by Beevers and Mcintyre from a mineral apatite[27] and later refined by Kay *et al*.[19] and Young and Elliott[28] from a synthetic HA.

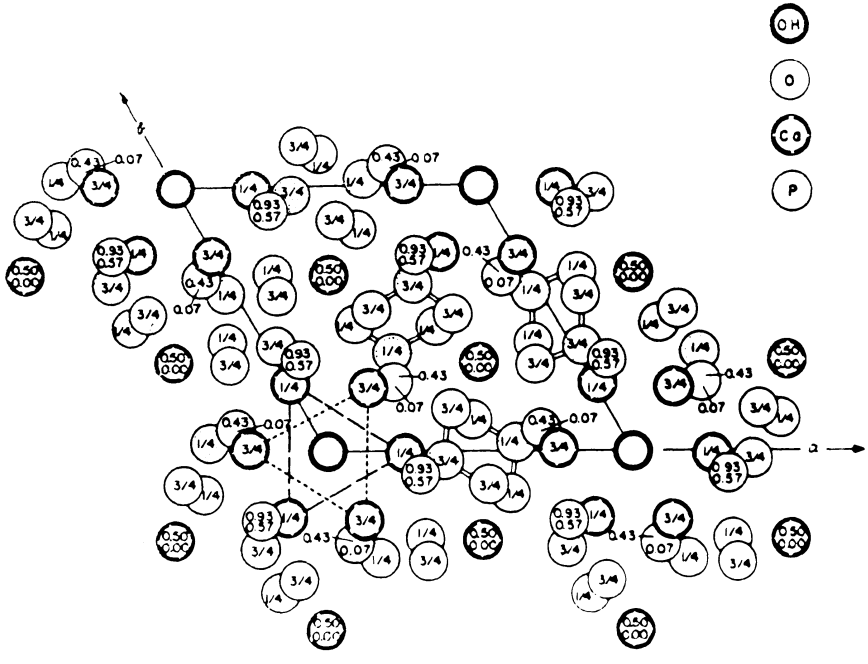

Figure 17.1. The atomic arrangement of calcium hydroxyapatite, $Ca_{10}(PO_4)_6(OH)_2$, in a hexagonal unit cell. The OH ions located in the comers of the unit-cell are surrounded by two groups of Ca(II) atoms arranged in triangle positions at z = 0.25 and at 0.75, two groups of PO_4 tetrahedra also arranged in triangle positions and by a hexagonal array of Ca(I) atoms at the outermost distance (courtesy of Prof. R. Young[28]).

Calcium hydroxyapatite belongs to the hexagonal system with a space group, P63/m. This space group is characterized by a six-fold *c*-axis perpendicular to three equivalent a-axes (a_1, a_2, a_3) at angles 120° to each other. The smallest building unit, known as the unit cell, contains a complete representation of the apatite crystal, consisting of Ca, PO_4, and OH groups closely packed together in an arrangement, shown in Fig. 17.1.[28]

The ten calcium atoms belong to either Ca (I) or Ca(II) subsets depending on their environment. Four calcium atoms occupy the Ca (I) positions: two at levels z = 0 and two at z = 0.5. Six calcium atoms occupy the Ca (II) positions: one group of three calcium atoms describing a triangle located at z = 0.25, the other group of three at z = 0.75, surrounding the OH groups located at the comers of the unit cell at z = 0.25 and z = 0.75, respectively (Fig. 17.2). The six phosphate (PO_4) tetrahedral ions are in a helical arrangement from levels z = 0.25 to z = 0.75. The network of PO_4 groups provides the skeletal framework which

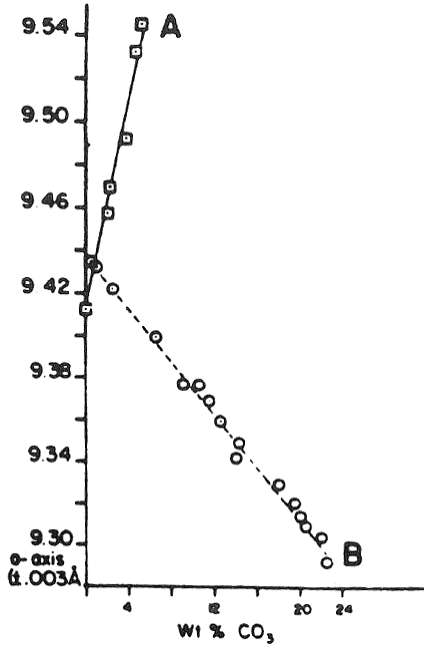

Figure 17.2. The effect of two types of carbonate substitution on the *a*-axis dimensions of synthetic apatites. Type A, CO_3-for-OH substitution, $Ca_{10}(PO_4)_6CO_3$, causes an expansion in the *a*- and contraction in the *c*-axis dimensions.[29,30] Type B, CO_3-for-PO_4, coupled with Na-for-Ca substitution, $(Ca,Na)_{10}(PO_4,CO_3)_6(OH)_2$, causes an expansion in the *a*- and contraction in the *c*-axis dimensions compared to the *a*- and *c*-axis dimensions of unsubstituted HA.[29,36,37]

gives the apatite structure its stability. The oxygen of the phosphate groups are described as one O_I, one O_{II}, and two O_{III}. The atomic arrangements of F-apatite, $Ca_{10}(PO_4)_6F_2$, and of Cl-apatite, $Ca_{10}(PO_4)_6Cl_2$, in which fluoride (F) and chloride (Cl), respectively, substituted for the OH groups in the apatite structure, are similar. The F or Cl atoms substituted for OH differ in the respective position of the OH for which they substitute. The O-H, F and Cl atoms lie along the *c*-axis at the center of the Ca (II) triangles, as described by Young and Elliott.[28]

The apatite structure, idealized as $Ca_{10}(PO_4)_6(OH)_2$, is a very hospitable one, allowing the substitutions of many other ions without significantly changing the hexagonal symmetry. For example, in apatites prepared from solutions, some cations, e.g., Sr^{2+}, Ba^{2+}, Pb^{2+} ions, can fully substitute for calcium (Ca^{2+}), while other ions, e.g., Mg^{2+}, Zn^{2+}, Mn^{2+}, or K^+, are incorporated only to a very limited extent; sulfates, vanadates, borates and acid phosphate (HPO_{4-}) can substitute for

$(PO_4)^{3-}$; and F^-, Cl^- or Br^- ions can substitute for (OH^-).[29–32] Complete F-for-OH substitution is easily achieved, while Cl-for-OH substitution is restricted in apatites prepared from solutions, but full substitution is obtained when prepared by solid-state reaction.[28,29] However, Elliott and Young[28] showed that complete Cl-for-OH substitution causes the loss of hexagonal symmetry and leads to monoclinic symmetry because of the alternating positions of the Cl atoms and an enlargement of the cell in the *b* direction.

Substitutions in the apatite structure result in changes in properties: e.g., lattice parameters, morphology, crystallinity (reflecting crystal size and/or strain) and solubility (Tables 17.2 and 17.3). For example, F-for-OH substitution causes a contraction in the *a*-axis dimensions without changing the *c*-axis, is usually associated with an increase in the crystallinity (reflecting increase in crystal size and/or decrease in crystal strain) and imparts greater stability to the structure.[23,25,28,29] Increased stability is reflected in the observation that F-substituted apatites are less soluble than F-free synthetic and biological apatites.[29,32,33]

Carbonate, CO_3, can substitute either for the hydroxyl (OH) or the phosphate (PO_4) groups, designated as Type A for CO_3-for-OH[34,35] or Type B for CO_3-for-PO_4[29,36,37] substitutions. These two types of substitution have opposite effects on the lattice parameters, *a*-axis and *c*-axis dimensions (Fig. 17.2 and Table 17.2). In the case of Type A, the substitution of larger planar CO_3 groups for smaller linear OH groups causes an expansion in the *a*-axis and contraction in the *c*-axis dimensions.[29,34,35] While for Type B, the substitution of smaller planar CO_3 groups for a larger tetrahedral PO_4 groups cause a contraction in the *a*-axis and expansion in the *c*-axis dimensions compared to the CO_3-free apatites.[29,36,37] Differences in infrared spectral properties were also observed.[29,35,38] LeGeros and coworkers demonstrated that the coupled CO_3-for-PO_4 and Na-for-Ca substitution cause changes in the size and shape of the apatite crystal, from acicular crystals to rods to equi-axed crystals with increasing carbonate content (Fig. 17.3),[29,37,39,40] and in dissolution properties the CO_3-substituted apatite is more soluble than CO_3-free synthetic apatites.[41]

Differences in lattice parameters between substituted and unsubstituted HA reflect the size and the amount of the substituting ions (Tables 17.2 and 17.3).[29] Various substitutions in the apatite, besides those of F- or Cl-for-OH, or CO_3-for-OH, or CO_3-for-PO_4 mentioned above, also affect properties, e.g., crystallinity (Table 17.3), thermal stability and dissolution properties or solubility of the apatite crystals. Sr-for-Ca or Mg-for-Ca substitution cause an increase in the extent of dissolution of the apatite.[29,42,43] When simultaneously present, the substituents in the apatite structure can have synergistic or antagonistic effects on the properties of the apatite. For example, magnesium and carbonate have synergistic

Table 17.2. Lattice Parameters of Mineral, Synthetic and Biological Apatites.

Apatite	Major Substituent*	Lattice Parameters	(+0.003A)
Mineral			
OH Apatite (Holly Springs)	—	9.422	6.880
F-apatite (Durango, Mex)	F	9.375	6.880
Dahllite (Wyoming)	CO_3	9.380	6.885
Staffelite (Staffel, Germany)	CO_3, F	9.345	6.880
Marine phosphorite (w.USA)	CO_3, F	9.322	6.882
Synthetic (non-aqueous)[a]			
OH-apatite	—	9.441	6.882
F-apatite	F	9.375	6.880
Cl-apatite	Cl	9.646	6.771
CO_3 apatite	CO_3	9.544	6.859
Synthetic (aqueous)[b]			
OH-apatite (Ca-deficient)	HPO_4**	9.438	6.882
F-apatite	F	9.382	6.880
(Cl,OH)-apatite	Cl**	9.515	6.858
CO_3-OH-apatite	CO_3**	9.298	6.924
CO_3-F-apatite	CO_3**, F	9.268	6.924
Sr-apatite	Sr	9.739	6.913
Pb-apatite	Pb	9.894	7.422
Ba-apatite	Ba	10.162	7.722
Biological			
CO_3-OH-apatite (human enamel)	HPO_4, Cl, CO_3, Mg	9.441	6.882
F-apatite (shark enameloid)	F, CO_3, HPO_4	9.382	6.880

Table based upon LeGeros.[29]

[a]Prepared at high temperature (1,000°C) by solid-state diffusion.[34,35]

[b]Prepared at 100°C either by precipitation or by hydrolysis methods.[29,36,37] Biological apatites.[29,40]

*Information not reprinted from LeGeros.[29]

**Maximum incorporation in case of Cl^- is less than one mole; in the case of CO_3 it is three moles; in cases of HPO_4 it is unknown. In these cases the substitutions are: F- or Cl-for-OH; CO_3-for OH (Type 1); CO_3-for PO_4 coupled with Na-for-Ca (Type B); HPO_4- for PO_4; Sr, Pb or Ba-for-Ca.

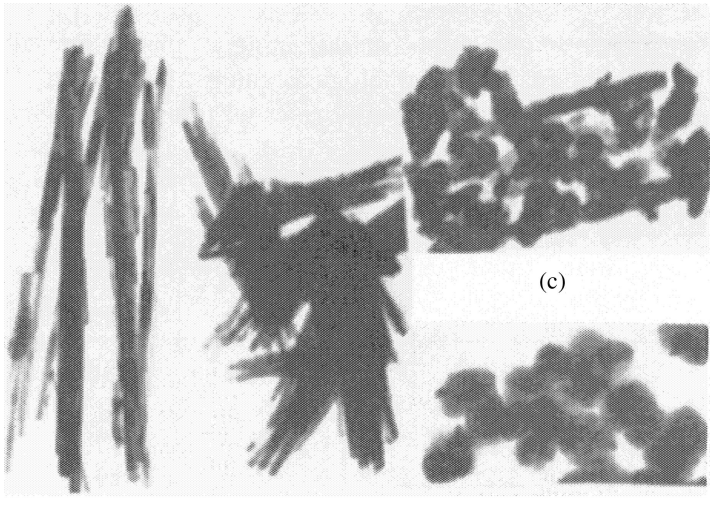

Figure 17.3. Electron micrographs of CO_3-apatite crystals obtained by the conversion of $CaHPO_4$ in solution containing increasing concentration of carbonate ions. Carbonate incorporation causes changes in crystal sizes and shape. Carbonate content: (a) 2.5 wt%; (b) 4.5 wt%; (c) 15.2 wt%; (d) 17.25 wt%. Magnification 40,000X. Apatite crystals change in morphology from acicular to rods to equi-axed crystals with increasing carbonate incorporation.[29,36,37,39]

effects on the crystallinity (Table 17.2) and dissolution properties of synthetic apatites; magnesium and fluoride or carbonate and fluoride have antagonistic effects, the fluoride effect being the more dominant one.[29,41,43,44]

A comprehensive understanding of both the individual and combined effects of substituents in the structure on the properties of apatite is important to the development of substituted HA, as new biomaterials lead to an improved understanding of the interaction between bone mineral and the HA materials presently used for bone repair, augmentation, substitution and coatings of metal dental and orthopedic implants.

17.3. BIOLOGICAL APATITES

Biological apatites, which comprise the mineral phases of calcified tissues (enamel, dentin, bone) and of some pathological calcifications (e.g., human dental calculi, salivary and urinary stones), are usually referred to as calcium hydroxyapatite, HA,[18,19] meaning $Ca_{10}(PO_4)_6(OH)_2$. Actually, the biological

Table 17.3. Qualitative Effects of Some Substituents for Ca^{2+}, PO_4^{3+} or OH in $Ca_{10}(PO_4)_6(OH)_2$ on Lattice Parameters and Crystallinity of Apatites.

Substituent	Ionic Rad(A)*	Lattice Parametersa-axis	(+003A) *c*-axis	Crystallinity
for Calcium, Ca2+	0.99	9.438	6.882	
Strontium, Sr^{2+}	1.12	(+)	(+)	(nc)
Barium, Ba^{2+}	1.34	(+)	(+)	(–)
Lead, Pb2+	1.20	(+)	(+)	(–)
Potassium, K^+	1.33	(nc)	(nc)	(nc)
Sodium, Na^+	0.97	(nc)	(nc)	(nc)
Lithium, Li^+	0.68	(nc)	(nc)	(nc)
Magnesium, Mg2+	0.66	(–)**	(–)**	(–)**
Cadmium, Cd2+	0.97	(–)	(–)	(–)
Manganese, Mn2+	0.80	(–)	(–)	(–)
Zinc, Zn2+	0.74	(+)**	(+)**	(–)**
Aluminum, Al3+	0.51	(+)	(+)	(–)
for OH				
Fluoride, F^-	1.36	(–)	(nc)	(+)
Chloride, Cl^-	1.81	(+)	(–)	(nc)
for PO_4^{3-}				
Carbonate, CO32–		(–)	(+)	(–)
HPO_4^{2-}		(+)	(nc)	(nc)

Table based upon LeGeros.[29]

* R.C. Weast, R.C. (ed.) (1988). *Handbook of Chemistry of Physics, 68th Ed*, CRC Press, Boca Raton, FL. (+) increase, (–) decrease, (nc) no change,

**TCP formed in addition to AP. If prepared at temperatures below 60°C, CO_3, P_2O_7, Mg, Al and Zn when present at a critical concentration in solution cause the formation of amorphous calcium phosphate (ACP).[29,45]

apatites differ from pure HA in stoichiometry, composition, crystallinity (crystal size), dissolution and in other physical and mechanical properties (Fig. 17.4 and Table 17.4).[29,40,46] Biological apatites are usually calcium-deficient (i.e., Ca/P ratio less than the stoichiometric ratio of 1.67 for pure HA) and are always carbonate substituted. It is therefore more appropriate that biological apatites be referred to

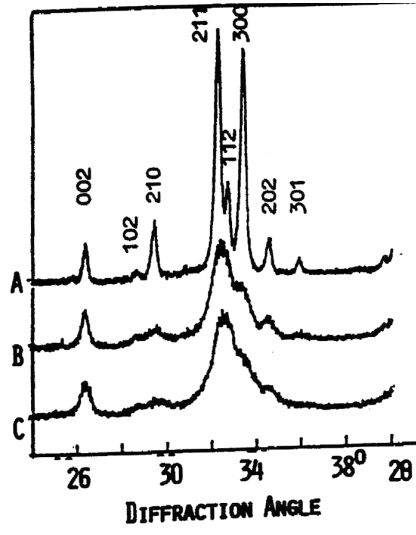

Figure 17.4(a). XRD patterns of human enamel, dentin and bone apatite, showing significantly larger crystals of enamel apatite compared to those of bone or dentin.

as carbonate apatite or carbonate-substituted apatite and not as hydroxyapatite or HA.[29,40,47]

The carbonate in biological apatites substitutes primarily for the phosphate groups in a coupled manner, i.e., CO_3-for-PO_4 (referred to as a Type B substitution) coupled with Na-for-Ca substitution.[29,40] The coupled substitution is necessary to balance charges for the substitution of CO_3 (divalent) for PO_4 (trivalent) ions. Biological apatites of enameloids of some species of fish or of shark enameloid are substituted with F and CO_3.[29] Other minor elements, e.g., sodium (Na^+), magnesium (Mg^{2+}), potassium (K^+), acid phosphate $(HPO_4)^{2-}$, chloride (Cl^-) and fluoride (F^-) and some trace elements (e.g., Sr^{2+}, Zn^{2+} etc.) are associated with biological apatites and may be substituents in the apatite structure, as described below:

$$(Ca,M)_{10}(PO_4,CO_3,Y)_6(OH,F,Cl)_2, \tag{17.1}$$

where M represents other minor (e.g., Mg^+, Na^+, K^+ etc.) and trace elements (e.g., Sr^{2+}, Zn^{2+}, Mn^{2+}) substituting for Ca^{2+} and Y represents acid phosphate, HPO_4^{2-}, sulfates, manganates, vanadates etc substituting for $(PO_4)^{3-}$. Some of these minor and trace elements may be surface- rather than lattice-bound.[48] Lattice-bound

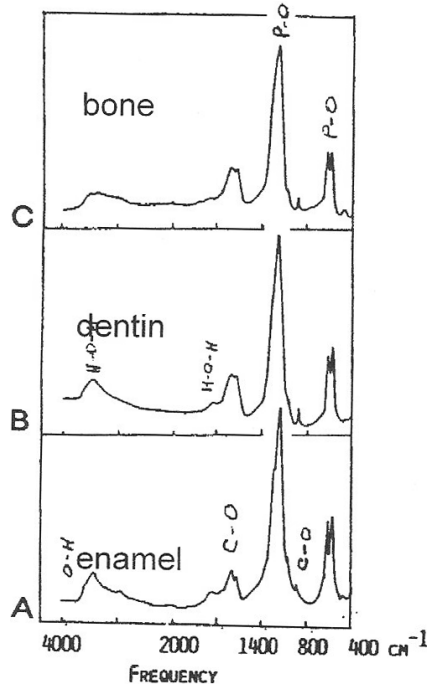

Figure 17.4(b). Fourier transform infrared (FTIR) spectra of human enamel, dentin and bone apatite, showing the presence of carbonate, CO_3(C-O), phosphate, PO_4(P-O) and hydroxyl, OH (O-H), groups.

elements will contribute to changes in lattice parameters; surface elements will not, but contribute to changes in crystal properties.

The biological apatites of enamel differ from those of dentin or bone in crystallinity (mostly reflecting crystal size) and in the concentration of the minor elements, principally carbonate and magnesium ions (Fig. 17.4 and Table 17.4). Enamel apatites contain the least amount of carbonate and magnesium and have the largest crystal size compared to either dentin or bone apatites (Table 17.4). In terms of dissolution properties, enamel apatite is less soluble than dentin or bone (Fig 17.4c) but much more soluble than dense HA, which is prepared at high temperatures (Fig. 17.5). The difference in crystal size and in dissolution properties among enamel, dentin and bone may be attributed in part to the differences in the carbonate and magnesium concentrations.[29,40] Incorporation of either magnesium or carbonate ions has been shown to cause a decrease in crystallinity (Table 17.3) and an increase in the extent of dissolution of synthetic apatites.[29]

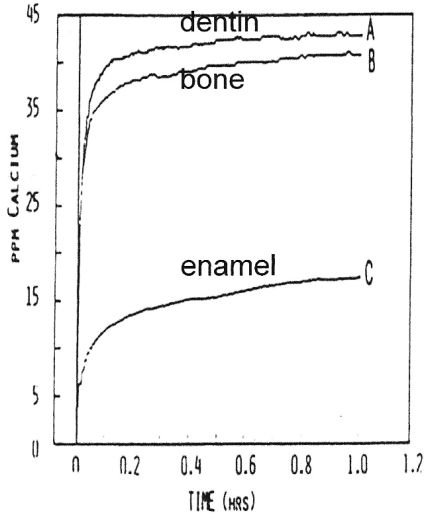

Figure 17.4(c). Comparative dissolution (0.1M KAc, pH 6, 37°C) of human enamel, dentin and bone apatite, showing much lower solubility of enamel apatite compared to bone or dentin apatite.

Sintering enamel, bone or dentine apatite results in changes in crystal morphology, crystal size, lattice parameters and composition (Table 17.4).[29,40] Sintering enamel and dentin apatites above 800°C results in the formation of HA and small amounts of β-TCP (about 5 wt% and about 12 wt% in sintered enamel and dentin, respectively). The β-TCP phase is magnesium-substituted as determined from lattice parameters and chemical analyses and is therefore sometimes referred to as β-TCMP.[29,40] Sintering human bone apatite above 800°C gives mainly HA and minor amounts of CaO (Table 17.4). Compositional changes in biological apatites include the loss of CO_3 as CO_2 and the formation of Mg-substituted β-TCP phase. The formation of the β-TCP after heat treatment of enamel and dentin and calcium-deficient synthetic apatites is attributed to the HPO_4^{2-} content of the apatite before sintering.[33,35]

Sintered animal bones result in the formation of β-TCP (Mg-substituted) or CaO, depending on the age and species of the animals.[29]

17.4. PREPARATION OF HYDROXYAPATITE

HA can be prepared as dense or as macroporous forms, with pores as large as 500 μm. Dense HA is described as having a maximum microporosity of 5%

Table 17.4. Comparative Composition, Crystallographic and Mechanical Properties of Human Enamel, Bone and Hydroxyapatite (HA) Ceramic.

	Enamel	**Bone**	**HA**
Constituents (wt %):			
Calcium, Ca2+	36.0	24.5	39.6
Phosphorus, P	17.7	11.5	18.5
(Ca/P) molar	1.62	1.65	1.67
Sodium, Na^+	0.5	0.7	tr
Potassium, K^+	0.08	0.03	tr
Magnesium, Mg2+	0.44	0.55	tr
Carbonate, $CO_3 2^+$	3.2	5.8	
Fluoride, F^-	0.01	0.02	
Chloride, Cl^-	0.30	0.10	
Ash (total inorganic)	97.0	65.0	100
Total organic	1.0	25.0	
Absorbed H20*	1.5	9.7	
Trace elements: Sr^{2+}, Pb^{2+},Ba2+, Fe3+, Zn2+,Cu2+, etc.			
Crystallographic properties			
Lattice parameters (+/– 0.003A)			
a-axis	9.441	9.419	9.422
c-axis	6.882	6.880	6.880
Crystallinity index(**)	70–75	33–37	100
Crystallite size, A	1300 × 300A	250 × 25–50	
Products after sintering (950°C)	HA + TCP	HA + CaO	HA
Mechanical properties			
Elastic modulus (106 MPa)	0.014	0.020*	0.01
Tensile strength (MPa)	70	150*	100

Table based upon LeGeros.[29]

*Values for cortical bone.[13]

**Information reprinted from LeGeros.[29]

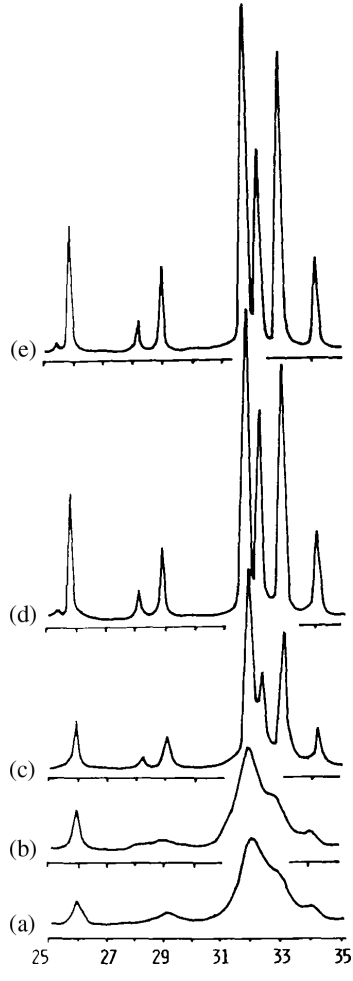

Figure 17.5. XRD patterns of human bone before (a) and after heat treatment at 400°C (b), 700°C (c) and 950°C (d), showing increase in crystal size as a result of heat treatment. Heat treatment at 400°C resulted in the removal of the organic phase which constitutes about 35 wt% of the bone.

by volume, with the micropores measuring about 1 μm in diameter and consisting of crystals with size exceeding 2000 Å.[13,15]

Preparation of dense HA consists of the following steps: preparing the apatite (HAP) powder or using commercially available apatite reagents; compacting or compressing into a desired size and shape under high pressure; and sintering. The different steps are described below.

17.4.1. Preparation of HAP

Pure HA can be obtained from reactions in hydrothermal systems or from solid-state reactions. However, when prepared from aqueous systems, either by precipitation or hydrolysis methods, the apatite obtained is usually calcium-deficient (i.e., the Ca/P molar ratio is lower than the stoichiometric value of 1.67 for pure HA). When the precipitation reaction is carried out under very basic conditions, the precipitate will contain carbonate, which will make the Ca/P molar ratio higher than the stoichiometric value. Unsintered hydroxyapatite preparations will be referred to as HAP.

17.4.1.1. *Precipitation methods*

The apatite preparation methods commonly used in commercial preparations were based on the method of Rathje and of Hayek and Newesely.[49,50] Rathje's method consisted of drop-wise addition of phosphoric acid, H_3PO_4, to a stirring suspension of calcium hydroxide, $Ca(OH)_2$, in water (Reaction 17.2):

$$10Ca(OH)_2 + 3H_3(PO_4)_2 \rightarrow \underset{\text{Apatite(HAP)}}{Ca_{10}(PO_4)_6(OH)_2}. \qquad (17.2)$$

This method is modified by the addition of ammonium hydroxide, NH_4OH, to keep the pH of the reaction very alkaline, to insure the formation of HA after sintering the apatite (HAP) precipitate.[16] Hayek and Newesely's method[50] consisted of the reaction between calcium nitrate, $Ca(NO_3)_2$, and ammonium phosphate, $(NH_4)_2HPO_4$, with added NH_4OH (Reaction 17.3):

$$10Ca(NO_3)_2 + 6(NH_4)_2HPO_4 + 2NH_4OH \rightarrow \text{Apatite (HAP)}. \qquad (17.3)$$

This method is sensitive to the concentrations of each of the reactants and the pH of the reaction for the formation of HA upon sintering of the apatite precipitate.[51] Calcium acetate, $Ca(CH_3COO)_2$, instead of calcium chloride or nitrate is recommended as the calcium source in precipitation reactions because the acetate ions will not be incorporated into the apatite,[36] unlike nitrate or chloride ions which may. The temperature of precipitation ranges from room temperature (about 24°C) to boiling (95–100°C). The concentration of calcium can be adjusted if substitution for calcium (e.g., strontium, magnesium, manganese etc.) in the apatite is desired. Similarly, the phosphate concentration can be adjusted

and replaced with carbonate if carbonate apatite is desired. Other ions, e.g., vanadate, borate, manganate etc., can be similarly added, replacing part of the phosphate component.[29] Fluoride- or chloride-substituted apatite can be prepared by the addition of F^- or Cl^- ions in the reaction.[29,37]

The precipitation method, like the hydrolysis method, usually results in calcium-deficient apatite, which causes the formation of β-TCP with HA upon sintering above 800°C.[29,51–53] If the reaction, either precipitation or hydrolysis, is carried out under very basic pH, the Ca/P approaches the stoichiometric value or exceeds it, depending on the formation of carbonate-apatite before sintering. In this paper, the designation "apatite" (HAP) indicates that the product is not a stoichiometric HA with a Ca/P molar ratio of 1.67.

17.4.1.2. *Hydrolysis method*

Apatite (AP) can also be prepared by the hydrolysis of acid calcium phosphates, e.g., dicalcium phosphate dihydrate, DCPD, $CaHPO_4 \cdot 2H_2O$, octacalcium phosphate, OCP, $Ca_8H_2(PO_4)_6 \cdot 5H_2O$ or monetite, dicalcium phosphate anhydrous, DCP, $CaHPO_4$, in ammonium, sodium or potassium hydroxide carbonate, fluoride or chloride solutions, depending on the desired composition of the apatite.[29,37] Calcium carbonate, $CaCO_3$, can also be hydrolyzed to apatite in ammonium or sodium phosphate solutions or to F-apatite in fluoride-containing solutions. α- or β-TCP, tetra-calcium phosphate (TTCP) and amorphous calcium phosphate (ACP) of special composition can also easily hydrolyzed to calcium-deficient apatite.

Commercially-available calcium phosphate reagents (labeled or mislabeled as "calcium phosphate, tribasic" or "calcium hydroxyapatite") are used as the apatite powder, with or without the addition of appropriate amounts of $CaCO_3$, $Ca(OH)_2$ or CaO[13–15] to make the apatite or apatitic reagent less calcium-deficient and thus minimize the formation of β-TCP phases upon sintering.

Apatites prepared from aqueous systems by precipitation or hydrolysis are usually calcium-deficient and HPO_4-enriched, as shown by the expanded *a*-axis dimensions compared to mineral or ceramic HA (Table 17.2) and the formation of a β-TCP phase upon heat treatment above 800°C.[29,32,52,53] Commercially-available calcium phosphate reagents labeled as "calcium phosphate tribasic" are sometimes mixed phases of apatitic calcium phosphate and monetite (Fig. 17.6a); reagents labeled as "spheroidal hydroxyapatite" were shown by XRD analysis to consist mostly of β-TCP mixed with small amounts of HA and not HA (Fig. 17.6b).[52]

All preparations, commercial or non-commercial, must be characterized using XRD, infrared spectroscopy and chemical analyses (for calcium and

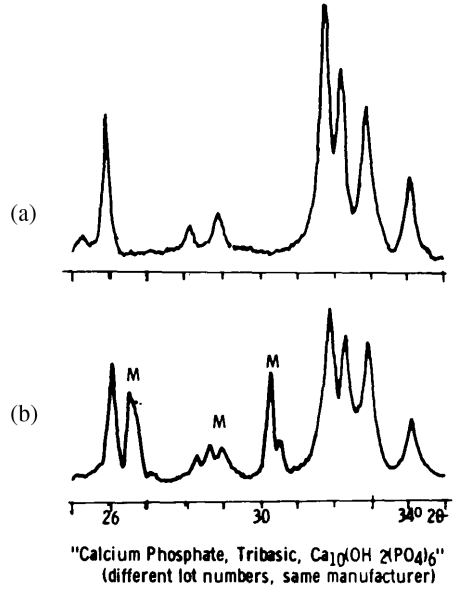

Figure 17.6(a). XRD patterns of commercially available apatitereagents from different manufacturers, labeled "calcium phosphate phosphate tribasic" or "calcium hydroxyapatite", showing apatitic calcium phosphate with poor crystallinity, some mixed with another calcium phosphate phase, $CaHPO_4$, dicalcium phosphate anhydrous or monetite (M).

phosphate concentrations) before use in the preparation of dense HA. This is important since apatite preparations after sintering above 800°C can produce materials consisting of intimate mixtures of β-TCP and HA of varying β-TCP/HA ratios.[7] Some dense or macroporous biphasic calcium phosphates (BCP) are intentionally prepared with the desired β-TCP/HA ratio.[9]

17.4.1.3. *Solid-state reactions*

HA can also be prepared by solid-state reactions as follows:

$$\underset{\text{Monetite}}{6CaHPO_4} + 4\,Ca(OH)_2 \rightarrow \underset{\text{HA}}{Ca_{10}(PO_4)_6(OH)_2} + 6\,H_2O\,, \tag{17.4}$$

$$\underset{\beta\text{-TCP}}{3Ca_3(PO_4)_2} + Ca(OH)_2 \rightarrow \underset{\text{HA}}{Ca_{10}(PO_4)_6(OH)_2} + H_2O\,. \tag{17.5}$$

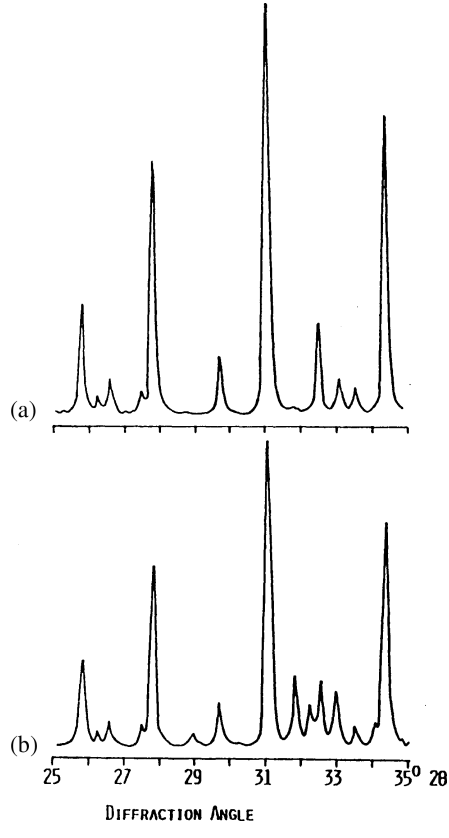

Figure 17.6(b). XRD patterns of commercial reagents labeled as "spheroidal hydroxyapatite" from the same manufacturer but different lot numbers, showing that the reagents are not hydroxyapatite but beta-tricalcium phosphate, β-TCP, in one lot (a) and β-TCP mixed with small amounts of HA in the other (b).

The mixed calcium compounds are compressed and sintered above 950°C. Substituted apatites (e.g., Sr for Ca, F or Cl for OH) can also be prepared by adding appropriate compounds.

17.4.1.4. *Hydrothermal reactions*

The above reactions can also be carried out hydrothermally at 275°C, under steam pressure of 12,000 psi.[29] In addition, β-TCP, $Ca_3(PO_4)_2$ and tetracalcium phosphate (TTCP), $Ca_4P_2O_9$ or $Ca_4(PO_4)_2O$, can be easily converted to HA hydrothermally under these conditions.

Calcium carbonate, $CaCO_3$, (as calcite or aragonite) in the presence of the appropriate amounts of $CaHPO_4$ (monetite) can be transformed to HA as follows:

$$4CaCO_3 + 6CaHPO_4 \rightarrow \underset{HA}{Ca_{10}(PO_4)_6(OH)_2} + 6H_2O + 4CO_2. \quad (17.6)$$

Coralline HA (HA from coral) is prepared by the hydrothermal conversion of coral ($CaCO_3$) in the presence of ammonium phosphate.[21] Carbonate-substituted apatite can be prepared by the hydrothermal conversion of α-TCP in the presence $(NH_4)_2CO_3$.[54]

$$10CaCO_3 + 6(NH_4)_2 \rightarrow Ca_{10}(PO_4)_6(OH)_2 + H_2O + CO_2. \quad (17.7)$$

17.4.2. Preparation of Dense or Macroporous HA

The apatite powder prepared according to any of the methods described in the previous section can be made into either of two forms: dense or macroporous. As mentioned earlier, dense HA is described as having porosity of less than 5% by volume. Dense HA may also be described as microporous. The microporosity is unintentionally introduced and is dependent on the temperature and duration of sintering. For dense HA, the maximum pore size is less than 1 μm in diameter.[13,15]

Macroporosity, on the other hand, can be deliberately introduced by mixing the powder with a volatile component, e.g., hydrogen peroxide or naphthalene, then evaporating the volatile component at low temperature, about 80°C, before sintering.[5,13] Macroporosity can also be a property of the original material, such as bone or coral, which is maintained during the conversion to apatite. Microporosity is affected by sintering temperature; the higher the temperature the lower the percentage of microporosity.

Apatite powder is compressed or compacted into a mold at a pressure of 60–80 MPa. The powder may be mixed with a binder, e.g., 1 wt% cornstarch and water,[16] stearic acid in alcohol[15] or low molecular weight hydrocarbons[55] applied to the die as a lubricant. The compressed body can be sintered in air (conventional method) at the desired temperature, usually 950–1,300°C, heating at the rate of about 100°C per hour and holding at the maximum temperature for several hours before cooling at the same rate as the heating rate.

Hot-pressing techniques are also used, in which heat and pressure are simultaneously and continuously applied. This procedure allows densification

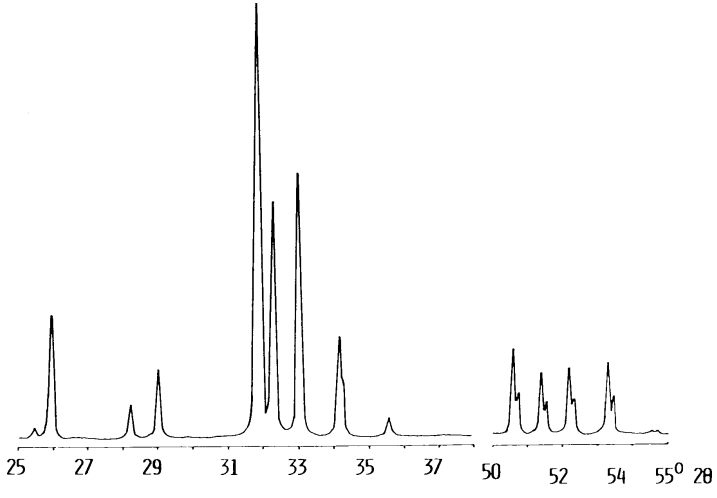

Figure 17.7(a). XRD pattern of powdered dense HA prepared by precipitation and subsequent sintering, showing the presence of only the HA phase. The crystallinity, reflecting crystal size, is comparable to that of mineral HA (Holly Springs, GA).

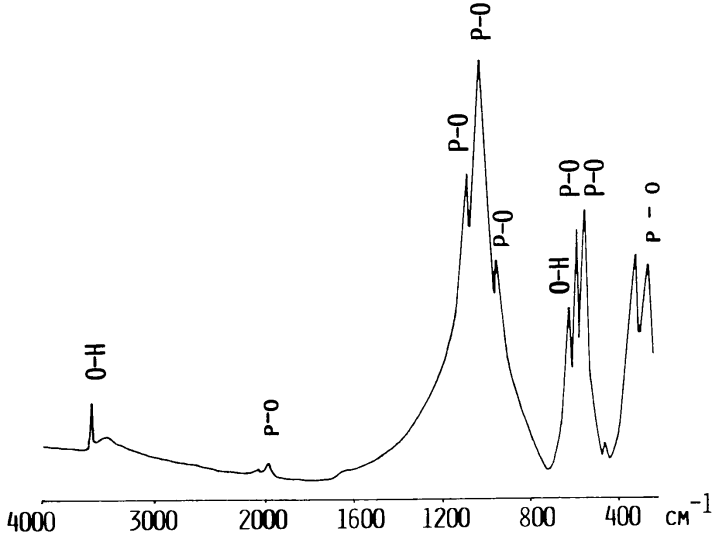

Figure 17.7(b). Infrared spectroscopy (IR) absorption spectrum of the same material as in (A), showing the characteristic absorption bands of O-H and P-O and reflecting the vibrations of the OH and PO_4 groups in the calcium hydroxyapatite, $CA_{10}(PO_4)_6(OH)_2$.

to take place at a much lower temperature than in the conventional sintering process (e.g., 900°C vs 1,300°C). The lower temperature of densification prevents the formation of other calcium phosphate phases, e.g., α- and β-TCP, TTCP, which usually form when HA is sintered at temperatures above 900°C.[13] The disadvantage of this technique is the expensive equipment required and the limited geometry of the end product. Another method of compressing is by hot-isostatic pressing (HIP), where materials are compressed by gaseous pressures at high temperatures. This process results in greater density and higher compressive strength than the conventional method (uniaxial pressing) of compacting.

Using the above methods, dense HA is prepared in tooth forms or in blocks. Particulates in irregular or spherical shapes are obtained by milling and rolling the compacted and sintered blocks. The block form is carved to prepare middle ear implants.[56]

17.5. COMPOSITION OF DENSE HA

Pure HA, $Ca_{10}(PO_4)_6(OH)_2$, has the theoretical composition of 39.68 wt% Ca, 18.45 wt% P, Ca/P wt ratio of 2.151 and Ca/P molar ratio of 1.667. Dense HA materials, commercial or non-commercial, vary in Ca/P ratios, reflecting the β-TCP/HA ratios in the sintered material which in turn reflect the purity (whether consisting of only the apatite phase or mixed with other CaP phases) and/or composition or calcium deficiency of the apatite preparation before sintering. If the Ca/P is 1.67, only HA will be observed in the XRD (Fig. 17.8a) and infrared spectrum (Fig. 17.8b); if the Ca/P is lower than 1.67, β-TCP and other phases such as tetracalcium phosphate (TTCP), $Ca_4P_2O_9$ or $Ca_4(PO_4)_2O$ will be present with the HA phase in the sintered material, depending on the temperature and condition of sintering. If Ca/P is higher than 1.67, CaO will be present with the HA phase. In addition, there will be minor and trace elements from the original reagents used to prepare the apatite powder. Some of the commercial and non-commercial dense HA materials contain up to 10 wt% β-TCP mixed with HA.[15] In addition, impurities in the reagents (e.g., in H_3PO_4) can cause the sintered HA to change color (e.g., from white to blue). According to ASTM designation: F 1185–88, 1990 Annual Book of ASTM Standards, Section 13, the acceptable composition for commercial HA is a minimum of 95% HA, as established by XRD analyses, and the acceptable concentration of trace elements is limited (maximum ppm) as follows: As = 3; Cd = 5; Hg = 5; Pb = 30; total heavy metals (as lead) = 50. The HA is to be associated with less than 5 wt% β-TCP.[57]

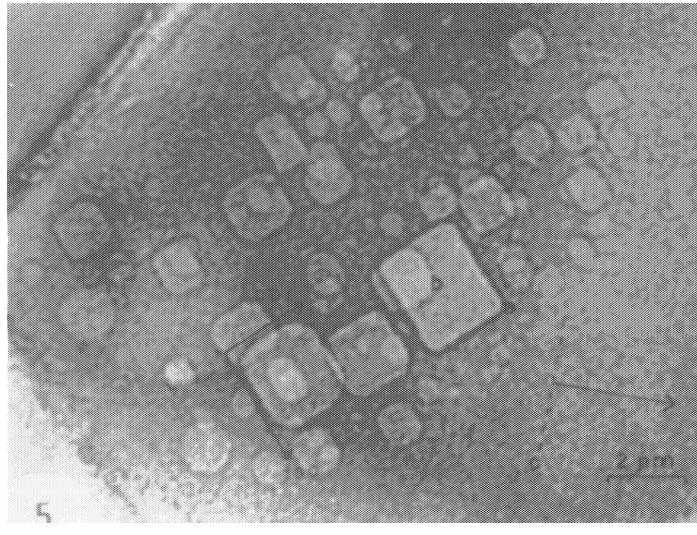

Figure 17.8. Transmission electron microscopy (TEM) of HA crystals sintered at 950°C, showing the presence of characteristic lattice defects (courtesy of Dr. G. Daculsi).[59]

The purity, composition and particle size of the apatite preparation before sintering, the sintering temperature and conditions (e.g., with or without water pressure present) also affect the type and amount of other calcium phosphate phases and/or other calcium compounds which will be present with the HA phase. Many of the interrelationships of these factors are described by the phase diagrams of de Groot *et al.*[13] Reported sintering temperatures for commercial and non-commercial HA range from 950 to 1,500°C. In this temperature range, the following calcium phosphates can form with or without the additional calcium oxide phase: β-TCP, α-TCP (resulting from the transformation of β-TCP at temperatures above 1,300°C), TTCP and oxyapatite according to the reaction outlined below:

$$\underset{\text{Ca-deficient apatite}}{\text{“Apatite” preparation (HAP)}} \xrightarrow[\text{HA}]{>900^\circ\text{C}} \underset{\text{HA}}{Ca_3(PO_4)_6(OH)_2} + \underset{\beta\text{-TCP}}{Ca_3(PO_4)_2}, \tag{17.8}$$

$$\underset{\beta\text{-TCP}}{\beta\text{-TCP}} \xrightarrow[>1{,}100^\circ\text{C}]{} \underset{\alpha\text{-TCP}}{\alpha\text{-TCP}}, \tag{17.9}$$

$$\underset{\text{HA}}{Ca_{10}(PO_4)_6(OH)_2} \xrightarrow[>1{,}300^\circ\text{C}]{} \underset{\alpha\text{-TCP}}{2Ca_3(PO_4)_2} + \underset{\text{TTCP}}{Ca_4(PO_4)_2O}, \tag{17.10}$$

$$\underset{\beta\text{-TCP}}{Ca_3(PO_4)_2} + CaO \xrightarrow[>1{,}400°C]{} \underset{TTCP}{Ca_4(PO_4)_2O}. \qquad (17.11)$$

Apatite prepared from highly alkaline solution in the presence of air may often contain CO_3 and can form CaO and HA upon sintering above 900°C. TTCP can also result from the reaction between β-TCP and CaO. Sintering with water vapor pressure of about 500 mm Hg minimizes the formation of the other CaP phases (β- and α-TCP, TTCP) and HA will be the more stable phase.[58] Thus the Ca/P molar ratio of the apatite preparation, the sintering temperature and conditions determine the final composition of the dense HA. Comparisons of Ca/P molar ratios of several commercial HA ceramics reported values ranging from 1.57 to 1.70.

The composition of dense HA is appropriately determined by using XRD, infrared spectroscopy (IR) and chemical analyses. XRD determines the purity (whether single or multiphasic); the crystallinity of the HA phase; the approximate ratios of the other phases (e.g., α- and β-TCP or TTCP or CaO with the HA phase); and the lattice parameters of the HA and other phases. Infrared spectroscopy gives information to support XRD data to detect additional phases, indicate relative crystallinities and provide evidence of substituents (e.g., CO_3, F).

The combined XRD, IR and chemical analyses will provide information on the presence of substituents in the HA and β-TCP structures.

17.6. PROPERTIES

17.6.1. Crystallographic Properties

Powdered HA (from dense or macroporous forms) gives an XRD pattern characterized by diffraction peaks with small line broadening, $\beta_{1/2}$, and high intensities (Fig. 17.7a), indicating a high degree of crystallinity (large crystals), similar to mineral OH apatite (Holly Springs, GA). The lattice parameters (*a*- and *c*-axis dimensions) are 9.422 and 6.881 + 0.003A, similar to mineral HA (Table 17.4 compared to Table 17.2). Other crystalline phases, e.g., α-TCP, β-TCP, TTCP and CaO, can be detected with XRD when present above 1 wt%. IR absorption spectrum (Fig. 17.7b) shows the characteristic O-H and P-O absorption bands representing the vibrations of the OH and PO_4 groups, respectively, in the HA, $Ca_{10}(PO_4)_6(OH)_2$. Ceramic HA crystals are large and assume rhombic shapes compared to the much smaller acicular apatite crystals before sintering.[32]

Daculsi *et al*. reported for the first time the presence of hexagonal parallelepiped (void type) lattice defects in addition to other defect structure in crystals of ceramic HA sintered at 950°C (Fig. 17.8) but not in those prepared at 1,250°C.[59] It may be logical to assume that the differences in the amount and types of lattice defects could cause differences in reactivity *in vivo*; the material with more lattice defects would be expected to be more reactive than the material with fewer lattice defects. This could explain the observations reported by Niwa *et al.*[60] that, *in vivo*, HA sintered at lower temperatures (700°C) were more reactive than those sintered at higher temperatures (950°C). HA crystals with more lattice defects would be expected to be more reactive than the material with fewer lattice defects.

17.6.2. Mechanical Properties

The properties of the apatite powder and the compression and sintering conditions influence the mechanical properties of the dense HA. Several mechanical properties (compressive strength etc.) were shown to decrease with the increasing amount of microporosity.[15] The density, grain size, compressive, flexural, torsional and dynamic torsional strengths and moduli of elasticity in compression and bending increased with sintering temperature from 1,150°C to 1,350°C.[16,55] The fracture toughness for HA ceramic sintered at 1,100–1,150°C increased but no significant change was observed for HA ceramic sintered at 1,050–1,250°C. At sintering temperatures above 1,250°C, the fracture toughness drops down to a value lower than the value obtained for HA sintered at l,100°C. In addition, the presence of β-TCP also causes a decrease in fracture toughness.[16] The difference in values of mechanical properties has also been attributed to differences in the preparation of apatite powder. The difference in preparation methods causes difference in grain size (small grain size tends to give greater fracture toughness) and in composition.

The various mechanical properties of dense HA are several times greater than those of cortical bone, dentin or enamel (Table 17.5).

de Groot *et al*. reported that the flexural strength and fracture toughness of dense HA are much less in a dry than in a wet condition.[58] The Weibull factor, n, which describes the resistance of a material to fatigue failure, is 50 for HA in a dry environment and 12 in a wet physiological implant bed. Implants with values of n = 10–20 are expected to fail in several months of clinical use. This property makes dense HA ceramic an unsuitable material for load-bearing situations, in spite of its good biocompatibility and osteoconductivity.[58]

Table 17.5. Comparative Mechanical Properties of Dense HA and Human Enamel.

Properties	HA (1)	HA (2)	Enamel
Color	blue	white	
Compressive strength MN/m^2	410 + 75	430 + 95	270
Tensile strength MN/m^2	39 + 4	38 + 4	70
Vickers hardness MN/m^2	4500	4500	3400
Density	97%	99.9%	80%
Starting powder	Commercial reagent	Precipitated	
Preparation	Compressing and sintering	Compressing and sintering	
Modulus of elasticity MN/m^2	$1.1 - 1.3 \times 10^4$	$1.1 - 1.3 \times 10^4$	1.4×10^4
Impact strength MN/m^2	0.18	0.16	
Bending momentum	2.8 + 0.2	3.1 + 0.3	

Denissen *et al.*[15]

17.6.3. Dissolution Properties

In vitro dissolution of HA depends on the type and concentration of the buffered or unbuffered solutions, pH of the solution, degree of saturation of the solution, solid/solution ratio, the length of suspension in the solutions and the composition and crystallinity (reflecting crystal size and strain) of the HA.[33,41,61] In the case of ceramic HA, the degree of micro- and macroporosities, defect structure and the amount and type of other phases present also have significant influence. Comparative XRD patterns (Fig. 17.10a) and dissolution (Fig. 17.10b) of different commercial HA bioceramics reflect their preparation method. For example, bovine-derived HA (unsintered) and unsintered HAP is more soluble than sintered ceramic HA (Fig. 17.10b). For an HA ceramic containing other calcium phosphate phases, the extent of dissolution will be affected by the type and amount of the non-HA phases. The extent of dissolution decreases in the following order:

$$ACP >> TTCP >> \alpha\text{-}TCP >> \beta\text{-}TCP >> HA \qquad (17.12)$$

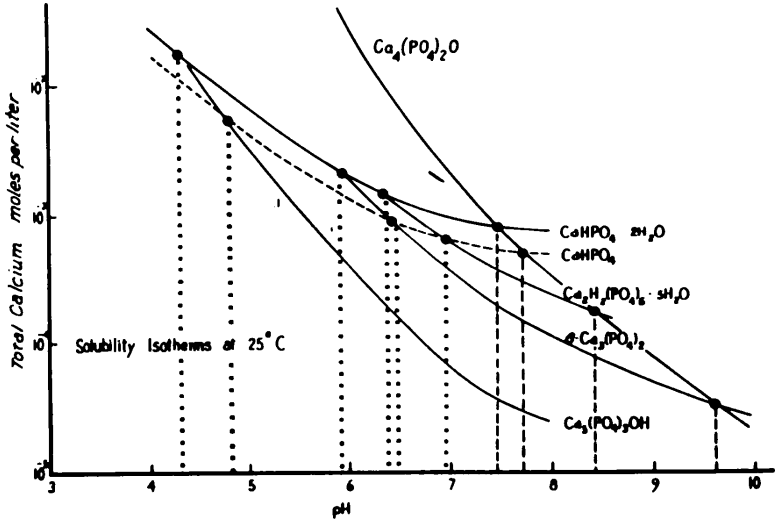

Figure 17.9. Solubility diagrams of different calcium phosphate (CaP) compounds[46] (courtesy of Dr. W. Brown, NIST). Some of these Ca-P compounds are associated with the preparation of HA biomaterial (e.g., β-TCP, TTCP) and others with the possible dissolution, precipitation and transformation of the HA biomaterials *in vivo.*

17.7. SURFACE CHEMISTRY

The surface chemistry of HA ceramic will depend on the composition of the ceramic and on the composition and pH of the solution in the micro-environment. An acid environment will cause partial dissolution of the surface, enriching the population of Ca^{2+}, $H_2PO_4^-$, HPO_4^{2-}, PO_4^{3-}, H^+, OH^- and ion pairs such as $CaH_2PO_4^+$ and $CaOH^{+}$[62] in a hydrated layer. Biological apatites have also been described as having a hydrated layer with ions reflecting the composition of the bone mineral and the biological fluid.[48] *In vivo*, electrolytes from the biological fluids will also be part of the surface chemistry and will contribute to the development of surface charges on the HA implant.[46,62–64] The surface charges will influence cellular interactions at the interface.[62,64] Ducheyne *et al.* reported that the absolute values of zeta potential measured were higher for the unsintered and Ca-deficient apatite compared with those of ceramic and stoichiometric HA and suggested that these values affect the cellular activities involved in bone formation.[62] In addition, proteins will adsorb on modified HA surfaces,[65]a phenomenon well known in the use of apatite for column chromatography.[66] The relationship of specific functional groups of amino acids to the formation of biological

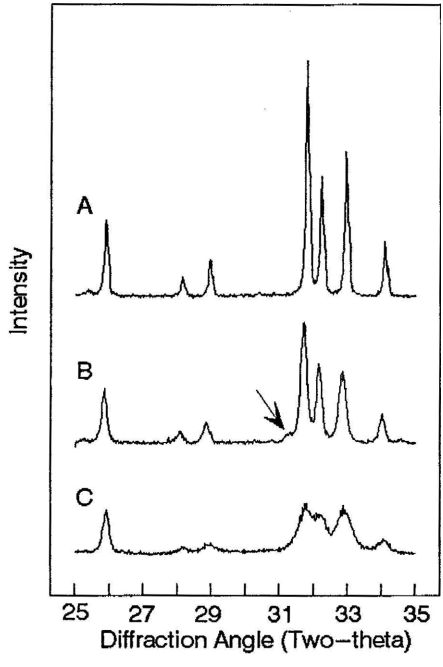

Figure 17.10(a). XRD patterns of commercial HA bioceramics. (a) *Calcitite*® (synthetic HA,sintered); (b) *Interpore*® (coralline HA, coral hydrothermally converted to HA); (c) *BioOss*® (derived from bovine bone, unsintered); and (d) *Osteogen*® (synthetic apatite, unsintered).

apatites and eventual mineralization has been strongly suggested in studies on mineral-organic matrix interactions.[67,68]

17.7.1. Formation of Carbonate-Apatite Crystals on HA Surfaces *In Vitro* and *In Vivo*: Dissolution/Precipitation Processes

Microcrystals observed on the surface of ceramic HA after implantation in bony sites[71–73] were identified also as apatite by selective electron diffraction with transmission electron microscopy (TEM).[69–71] Similar observations were made on the surfaces of crystals of ceramic HA, coralline HA and biphasic calcium phosphate (BCP), after suspension in cell culture or in serum[72–74] and after implantation in non-bony sites[75] and in bony sites.[78] These microcrystals (Fig. 17.11a) sometimes appear to exhibit epitaxial growth on the HA ceramic crystals (Fig. 17.11b). The difference in structures between the HA ceramic and the

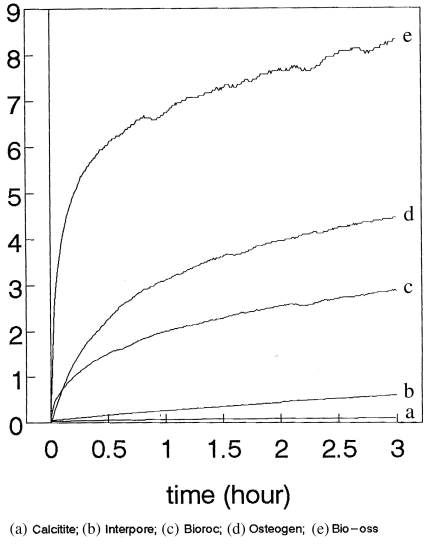

Figure 17.10(b). Comparative dissolution in acidic buffer (0.1M KAc, pH 6, 37°C) of commercial HA bioceramics. (a) *Calcitite*® and (c) *Bioroc*® are both sintered synthetic HA; (b) *Interpore*® is coral-derived ($CaCO_3$ hydrothermally converted to HA); (d) *Osteogen*® is unsintered apatite (HAP); and (e) *BioOss*® is bovine bone apatite (unsintered).

microcrystals were also confirmed by TEM images (Fig. 17.12). In addition, IR spectroscopy has helped to identify these crystals as carbonate-apatite (Fig. 17.13), intimately associated with an organic matrix (Figs. 17.13 and 17.14).[75] Bone apatite crystals, like other biological apatites, are carbonate apatite and are also intimately associated with an organic matrix.[29]

The formation of these microcrystals of CO_3-apatite is believed to be a dissolution-precipitation processes (shown schematically in Fig. 17.15).[76,77] The partial dissolution of the calcium phosphate material, HA, is initiated by the acid condition which results from cellular activity, causing the release of Ca^+, HPO_4^{2-} and PO_4^{3-} and increasing the supersaturation of the microenvironment with respect to calcium phosphate phases which are stable at the pH in this environment. DCPD, $CaHPO_4.2H_2O$, octacalcium phosphate, OCP, $Ca_8H_2(PO_4)_6.5H_2O$, which can form under acid conditions or Mg-substituted β-TCP, $(Ca,Mg)_3(PO_4)_2$, or whitlockite, which can form under either acid or basic conditions, can hydrolyze in the presence of CO_3^{2-} in the biological fluid to CO_3-apatite.[29,76,77] Alternatively, or in addition, CO_3-apatite can form directly at physiological pH, using the calcium and phosphate ions released from partially dissolving ceramic

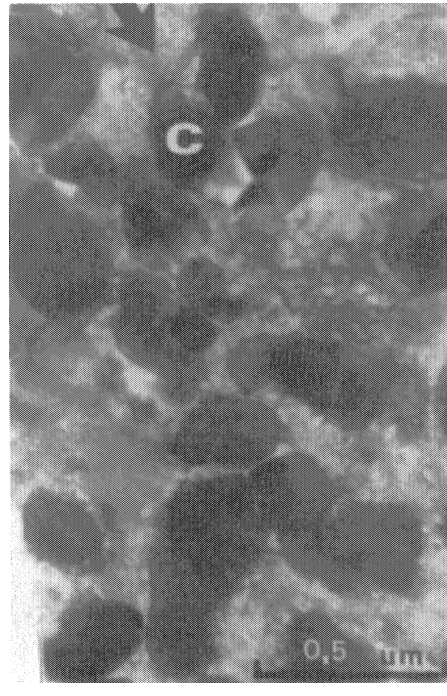

Figure 17.11(a). TEM of dense HA particles after four months implantation in human periodontal pockets. Undecalcified ultrathin section from the implant surface. Magnification, × 100,000 showing the presence of microcrystals (arrow) on the surfaces of the much larger HA crystals (c).

HA and from the biological fluids which contain other electrolytes, notably CO_3^{2-} and Mg^{2+}. These ions become incorporated in the new CO_3-apatite, microcrystals forming on the surfaces of the much larger crystals of the ceramic HA (Fig. 17.11a). The CO_3-apatite can also form by precipitation, deduced from the observed uptake of calcium ions from serum[73] or seeded growth on the ceramic HA crystals. However, cell-induced resorption or dissolution of the HA or BCP (β-TCP and HA) crystals is frequently observed *in vitro* and *in vivo*.[72,74,76,77]

The formation of CO_3-apatite has also been seen *in vitro* and *in vivo* on surfaces of bioactive glasses and glass ceramics.[78] (See Chapters 3 and 13–16). In studies on biphasic calcium phosphate (BCP) materials consisting of different β-TCP/HA ratios, it was observed that the abundance of the CO_3-apatite microcrystals on the surfaces of the large BCP crystals was influenced by the β-TCP/HA ratio: the higher the ratio, the greater the abundance of the CO_3-apatite

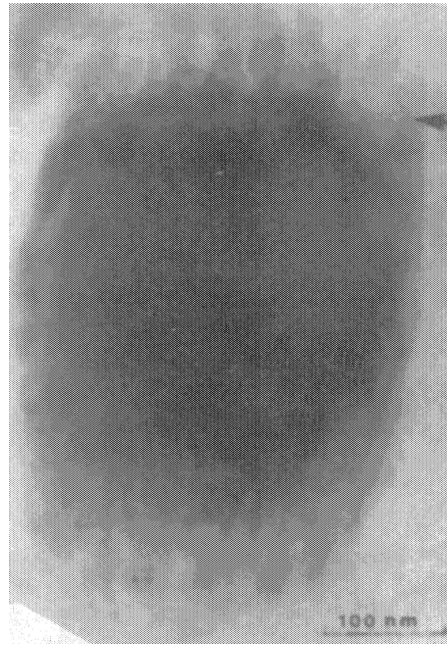

Figure 17.11(b). TEM of dense HA particles after two months implantation in human periodontal pocket, showing epitaxial growth of the new crystals on the HA ceramic crystals. Magnification, × 1,350,000.

microcrystals. This was thought to be due to the higher dissolution properties of the β-TCP component of the BCP causing an increase in the concentration of the calcium and phosphate ions in the microenvironment, leading to the precipitation of the CO_3-apatite.[76] Reactions on material surfaces, including the formation of CO_3-apatite, may be important in establishing the strong "bonding zone" at the bone–material interface unique to bioactive materials.

17.8. TISSUE RESPONSE

17.8.1. Cellular Interaction with HA

HA surfaces appear to be biocompatible with several cell types, such as macrophages, fibroblasts, osteoclasts, osteoblasts, and periodontal ligament cells.[72,74,79,80] The favorable response in terms of cell attachment and cell proliferation (Fig. 17.16a) of different types of cells to dense HA and other bioactive

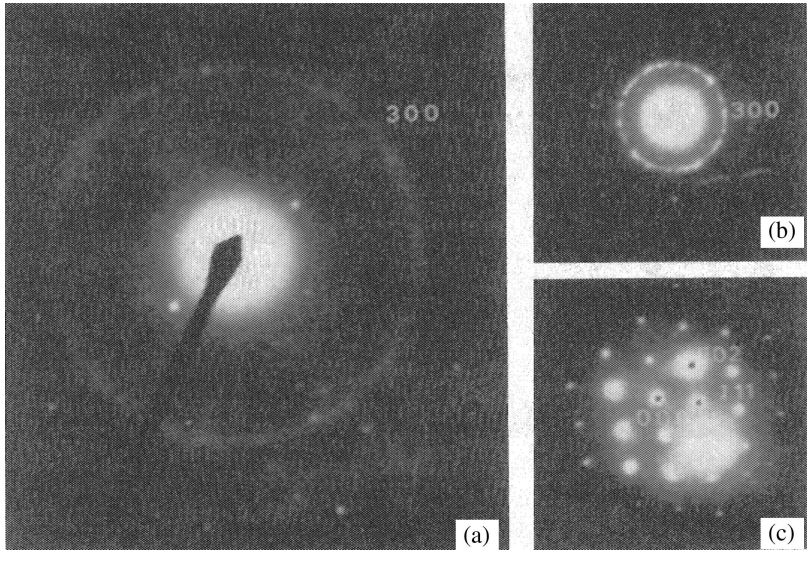

Figure 17.12. Electron diffraction of (c) large crystals of HA ceramic; (b) the microcrystals; and (a) bone apatite crystals. The rings on (c) correspond to the 111 and 002 apatite lattice plane; those in (a) and (b) correspond to the (300) plane of apatite (in collaboration with Dr. G. Daculsi).[76]

materials has been demonstrated in many studies, such as those cited above. The cells cause the dissolution of the HA ceramic crystals intracellularly by phagocytosis (Fig. 17.16b) or extracellularly by producing an acid environment,[81] which causes the partial dissolution of the HA ceramic crystals. The HA material allows the proliferation of fibroblasts, osteoblasts and other bone cells.[72,74,79,80] The cells do not seem to distinguish between HA and bone surfaces, which indicates a significant similarity in the surface chemistry. However, *in vitro* cell response is affected by the composition of the apatites.[82–84] For example, osteoclastic activity (i.e., resorption) was observed to be greater on carbonate-substituted apatite compared to that on fluoride-substituted apatite,[83] and osteoclastic activity (expression of bone markers) was greater on F-substituted compared to F-free apatites.[84]

17.8.2. Osteoconductive Properties

HA, like other calcium phosphate biomaterials, is osteoconductive but not osteoinductive.[10,13] An osteoconductive material allows the formation of bone on

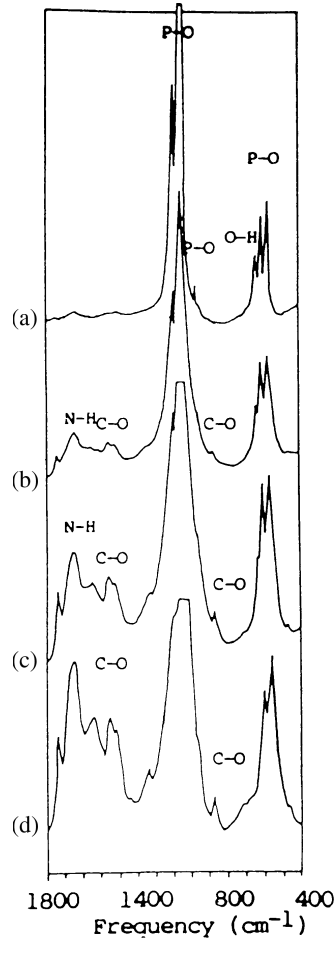

Figure 17.13. Infrared (IR) absorption spectra of BCP (β-TCP/HA, 15/85) material before (a) and after implantation in surgically-created dental defects (in collaboration with Drs. E. Nery and K. Lynch). IR spectra of materials obtained from the core (b), the implant surface (c), and from an area in the bone furthest away from the implant (d), show increasing intensities of the N-H (related to the organic phase) and of the C-O (related to the CO_3 in the CO_3-apatite) absorption bands. In addition, the intensity of the O-H (related to the OH groups in HA material before implantation) shown in (a) become unresolved in materials in (b) and (c) and become more similar to the bone apatite (d).[78]

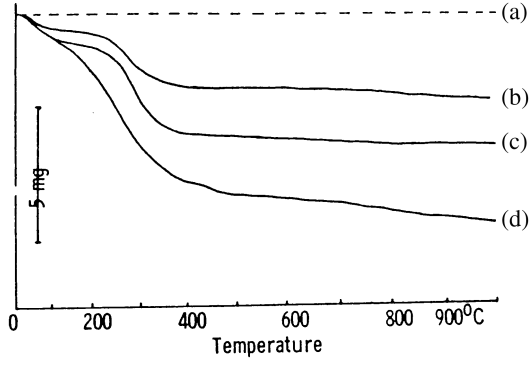

Figure 17.14. Thermogravimetric analyses (TGA) of dense HA (a) before implantation; and of implants recovered after (b) 60, (c) 180, and (d) 365 days from non-osseous sites in hamster. The weight loss below 400°C is due to the loss of adsorbed water and organic phases and above 500°C due to loss of carbonate from the CO_3-apatite (lost as CO_2).[75]

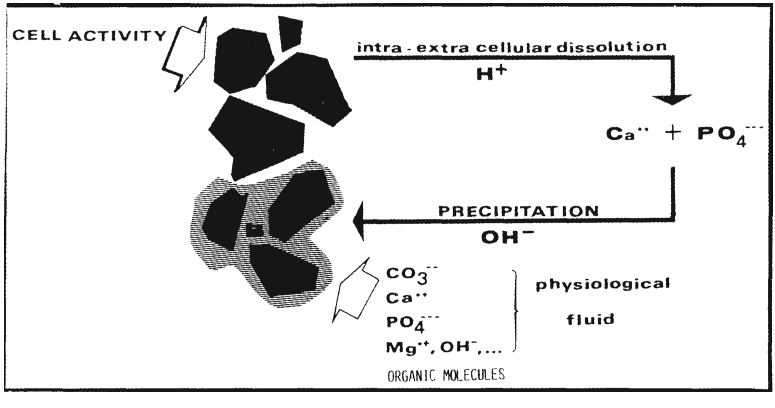

Figure 17.15. Schematic representation of the dissolution/precipitation processes involved in the *in vivo* formation of CO_3-apatite on surfaces of CaP (e.g., HA) implant materials.

its surface by serving as a scaffold or a template (Fig. 17.17). In the case of bioactive glasses and glass ceramics, and calcium phosphate materials such as dense HA, their role is not a passive one but participatory, contributing to the formation of the CO_3-apatite on surfaces and promoting the adhesion of matrix-producing cells and organic molecules as a result of surface chemistry and surface charges.

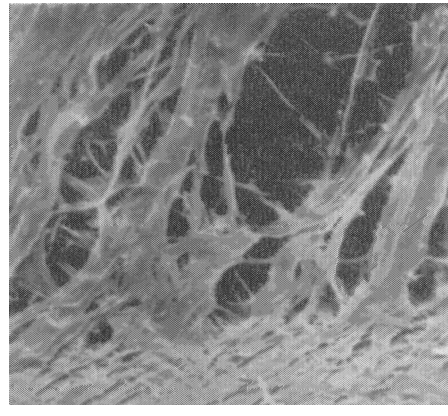

Figure 17.16(a). SEM of dense HA particles colonized by cells.

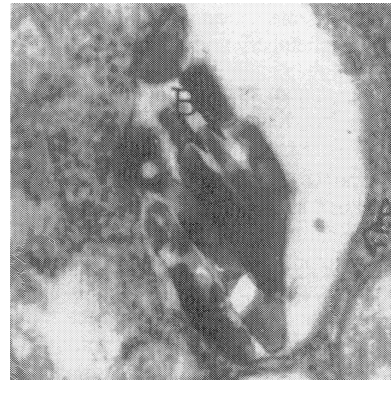

Figure 17.16(b). TEM showing (a) phagocytosed HA crystals and (b) the dissolution of HA crystals.[77]

17.8.3. Osteoinductive Properties

The ability of bone to repair or regenerate itself is due to the bone morphogenetic proteins (BMPs) and osteogenic proteins (e.g., collagen, osteonectin, osteopontin and bone sialoprotein) present in the extracellular matrix.[85,86] Calcium phosphate bioceramics (HA, β-TCP) are bioactive (directly bonds with bone) and osteoconductive, but inherently not osteoinductive.[87] However, osteoinductive properties (ability to form bone in non-bony sites) have been reported for HA and BCP.[88–90] This phenomenon has been attributed to specific combinations of

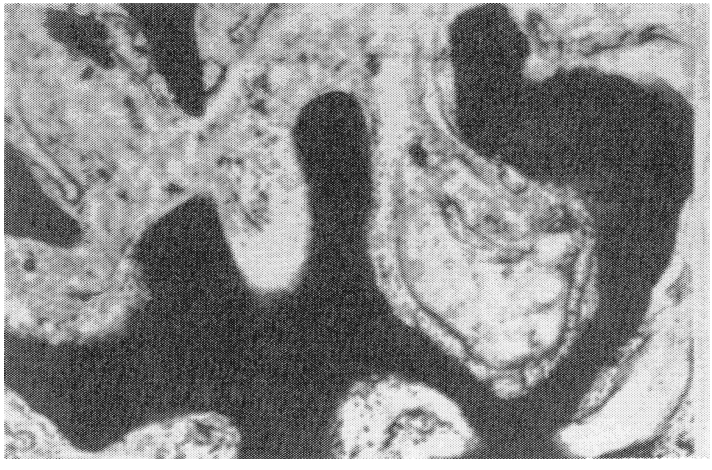

Figure 17.17. Microradiography showing the osteoconductive properties of HA materials; the new bone is shown on the surface of the HA acting as a template.

macro- and microporosities that allow the entrapment of circulating BMPs. The calcium phosphate bioceramics can also be made osteoinductive by incorporating BMPs or other osteogenic proteins.[88,89,91]

17.8.4. Bone–HA Interface

The type of bonding at the material–bone interface depends on the nature of the material.[75,94,95] The interfacial strength between bone and implant biomaterial, as determined from push-out tests, is much greater for the bioactive implant materials (e.g., Bioglass® and HA) compared to other materials, such as titanium, zirconia or alumina (Table 17.6).[95] In the case of bioactive materials, the fracture occurs either in the material or the bone but not at the interface; in the case of inert materials, the separation occurs at the interface.[95] This phenomenon is attributed to the "bonding osteogenesis" occurring at the interface between bone and the bioactive materials, which does not occur with non-bioactive materials.[94] This interface has been referred to as the "bonding zone", described as being electron-dense, consisting of mineralized organic meshwork. Greater interfacial strength was also observed with metal implants coated with plasma-sprayed HA than those without.[96,97] The description of the bone–HA interface depends on the analytical methods used in studying the interface. Light microscope studies and low

Table 17.6. Comparative Properties of Biomaterials.

Materials	Fracture Strength	Bone Contact	Fracture
Bioglass®*	28.9 MPa	92.9%	Cohesive
Hdroxyapatite*	19.6 MPa	95.4%	Cohesive
Titanium**	1.9 MPa	59.5%	Interfacial
Zirconia**	1.3 MPa	33.3%	Interfacial

Fracture strengths per unit area after 24 weeks.

* Bioactive materials

** Non-bioactive materials (Niki *et al*.[85])

resolution scanning electron microscopy (SEM) showed intimate contact between the bone and the HA implant surface (Fig. 17.18a). High resolution TEM of the HA–bone interface showed the presence of highly mineralized collagen in the vicinity of the large HA ceramic crystals, which are associated with much smaller crystals of CO_3-apatites. Electron microprobe analyses showed that the relationship between the calcium and phosphorus concentrations was not significantly different when scanning from the implant (HA) to the interface to the bone regions (Fig. 17.18b).

Histological examination showed that dense HA particles used during the initial periodontal period of wound healing were followed by resorption in some areas and also by osteoid bone formation without intervening fibrous tissue.[9,10,13,60]

17.8.5. Events in the Formation of "Bone-Bonded" Interface

The following events are proposed as responsible for the formation of the strong interface between bone and a bioactive material:[78,79]

- acidification of the microenvironment due to the cellular action on the bioactive material;
- dissolution/precipitation processes resulting in the formation of CO_3-apatite intimately associated with an organic matrix similar to bone apatite;
- production of adhesive proteins and collagen fibrils containing extracellular matrix;

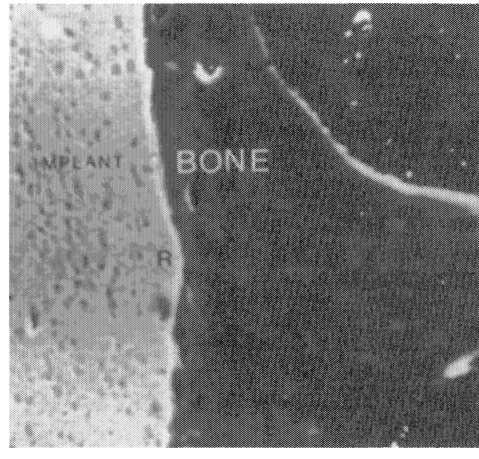

Figure 17.18(a). SEM of the interface between dense HA ceramic implant and bone (magnification X 300).

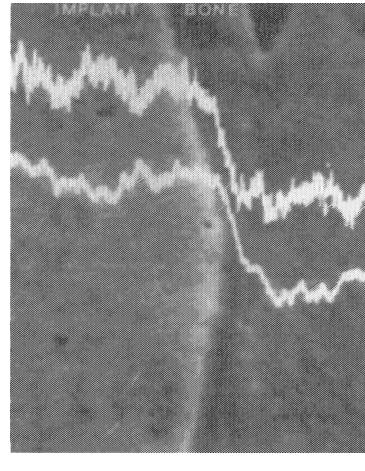

Figure 17.18(b). Electron microprobe analyses showing calcium (Ca) and phosphate (p) concentrations on the regions of the implant, interface and bone (magnification X 2100) (courtesy of Dr. H. Dennissen).

- simultaneous mineralization of the collagen fibrils and incorporation of the CO_3-apatite crystals (originating from the material) in the remodeling new bone; and

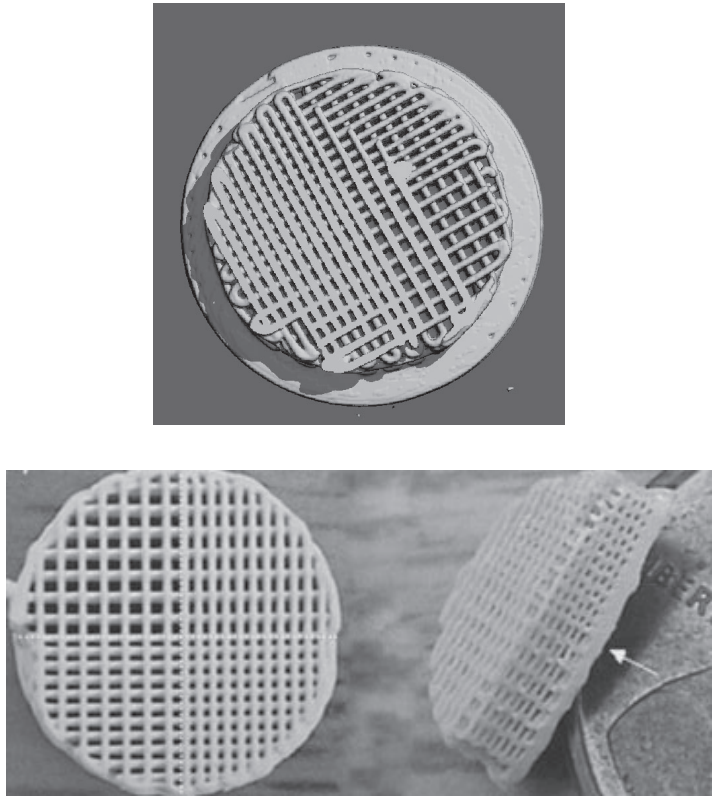

Figure 17.19. HA scaffold with varying macroporosity, prepared using "Direct Write" 3D technology. Printing green state ceramics using colloidal inks (Robocasting) (courtesy of Dr. J. Ricci (NYU)).[99]

- interdigitation of the mineralized collagen between the host bone and the bioactive ceramic surfaces and within the pores provides the interfacial strength.

17.9. CLINICAL APPLICATIONS

Dense HA as tooth forms has been used as immediate tooth root replacements to minimize the alveolar ridge resorption which follows tooth loss and to maintain ridge width and height.[13,16,65] Dense or macroporous HA and unsintered HA (Table 17.1) in block and particulate forms are used in the

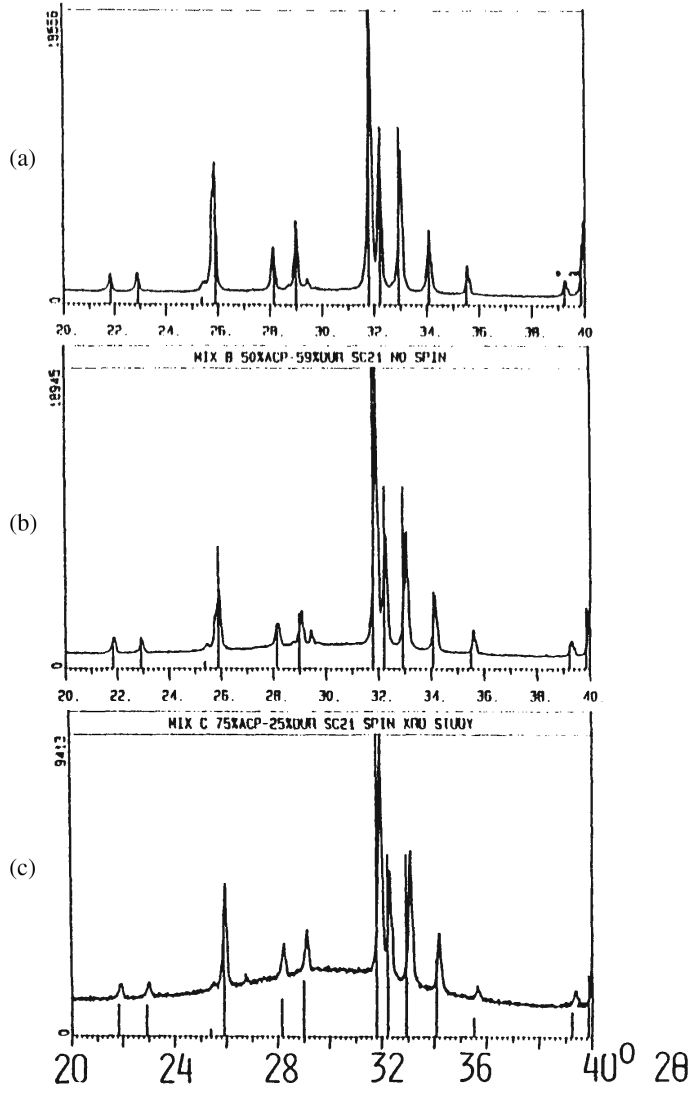

Figure 17.20(a). XRD of coatings on dental implant prepared by plasma-spraying dense HA particles on titanium substrate. The coating composition in the order of increasing relative concentration is: (1) HA with crystallinity lower than starting material (A); (2) amorphous calcium phosphate; and (3) α- and β-TCP of poor crystallinity. Other coatings also contain small amounts of TTCP.[22,130]

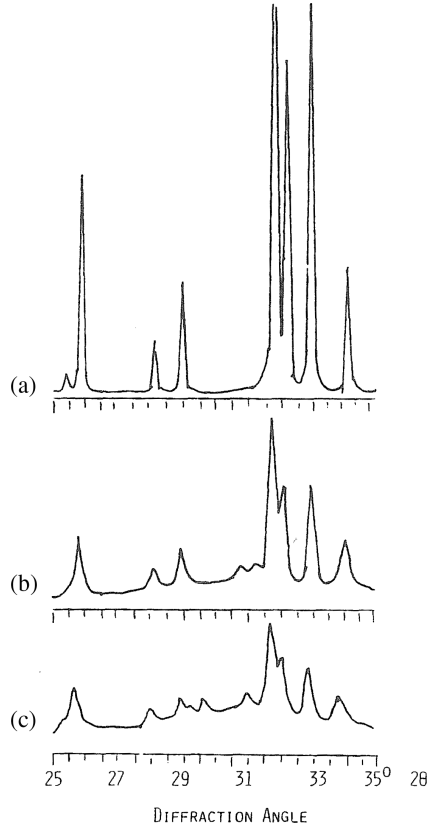

Figure 17.20(b). XRD of coating prepared as in Fig. 17.20a, showing composition gradient from the layer closer to the metal substrate (b) to the coating surface (c). The dense HA material used for plasma spraying is shown in (a).

augmentation of alveolar ridge for better denture fit[11,66,67] or in the repair of bone defects in dental and orthopedic applications,[10,59,68,72] maxillofacial reconstruction,[98] as a filler in association with placing of metal implants or for repair of failing metal dental implants (Fig. 17.19 is an example of a new generation of engineered porous HA scaffolds),[11,99] as a filler in composites or cements,[26] middle-ear implants[11,57] and percutaneous devices.[100] Dense HA has also been used as target materials for plasma-sprayed or ion-sputtered coatings for commercial dental (Fig. 17.20) and orthopedic implants. HA and HAP have also

been used as scaffolds in tissue regeneration,[101] in drug delivery,[102] gene therapy[103], and as bioreactors.[104]

17.9.1. Coatings on Dental and Orthopedic Implants

Dense HA particles are plasma-sprayed on commercial dental and orthopedic metal implants to combine the strength of the metal and the bioactivity and osteoconductivity of the HA. These coated implants are described as "HA-coated". However, X-ray diffraction analysis of plasma-sprayed coupons or implants shows that the coating may differ significantly in crystallinity (i.e., per cent of crystalline phases vs. non-crystalline phases and crystallinity of the HA phase) and in composition from that of the dense HA ceramic used as the source material for plasma-spraying (Fig. 17.21a). The plasma-sprayed HA coating is not homogeneous, consisting principally of HA and amorphous calcium phosphate (ACP) in varying HA/ACP ratios and small amounts of α-TCP,

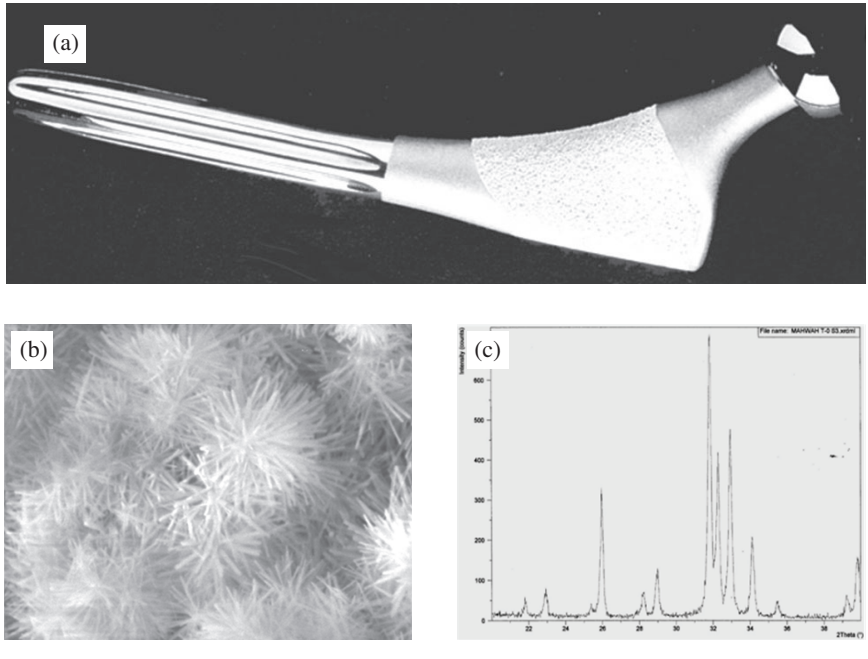

Figure 17.21. (a) Hip-implant partially coated with precipitated apatite; (b) SEM image of the coating; (c) XRD pattern of the coating showing apatite diffraction peaks (courtesy of Mr. F. Dimaano, Stryker-Orthopedics).

β-TCP, TTCP and CaO.[33,105,106] It was also observed that the coating composition of the layer closer to the metal substrate tends to contain more ACP than the outermost layer of the coating (Fig. 17.21b). Since different calcium phosphate phases have different solubilities (Fig. 17.9), it is possible that the stability of the coating, and therefore of the implant, will depend on the composition of the coating.

Alternatives to the plasma-spray method are electrochemical[107] or chemical[108] deposition (or biomimetic) methods of depositing apatite coating on dental or orthopedic implants. These methods use much lower temperatures (37 to 80°C) and provide a homogeneous composition of the coating. See Chapters 20 and 21 for additional details on the science and technology of HA coatings.

ACKNOWLEDGEMENTS

The work involving the authors cited in this paper was supported in part by research grants from NIH nos DE 07223, DE 04123 and SO7RRO76226. The authors gratefully acknowledge the collaboration of Drs. Guy Daculsi (University of Nantes, France), Monique Heughebaert (University of Toulouse, France) and Regina Kijkowska (Technical University, Krakow, Poland) in some of the work cited.

REFERENCES

1. Albee, F.H. (1920). Studies in Bone Growth. Triple Calcium Phosphate as a Stimulus to Osteogenesis, *Ann. Surg.*, **71**, 32–36.
2. Levitt, G.E., Crayton, P.H., Monroe, E.A. *et al.* (1969). Forming Methods for Apatite Prosthesis, *J. Biomed. Mater. Res.*, **3**, 683–685.
3. Monroe, Z.A., Votawa, W., Bass, D.B. *et al.* (1971). New Calcium Phosphate Ceramic Material for Bone and Tooth Implants, *J. Dent. Res.*, **50**, 860–862.
4. Clark, W.J., Driskell, T.D., Hassler, C.R., *et al.* (1973). Calcium Phosphate Resorbable Ceramics, a Potential Alternative to Bone Grafting, *IADR Prog. & Abst.*, **52**, Abstr. #259.
5. Hubbard, W. (1974). *Physiological Calcium Phosphate as Orthopedic Implant Material* (PhD Thesis, Marquette University).

6. Nery, E.B., Lynch, K.L, Hirthe, W.M. *et al.* (1975). Bioceramic Implants in Surgically Produced Infrabony Defects, *J. Periodont.*, **46**, 328–339.
7. LeGeros, R.Z. (1988). Calcium Phosphate Materials in Restorative Dentistry: A Review, *Adv. Dent. Res.*, **2**, 164–183.
8. Ellinger, R.F., Nery, E.B. and Lynch, K.L. (1986). Histological Assessment of Periodontal Osseous Defects Following Implantation of Hydroxyapatite and Biphasic Calcium Phosphate Ceramics. A Case Report, *Int. J. Perio. Restor. Dent.*, **3**, 223–233.
9. Nery, E., LeGeros, R.Z. and Lynch, K.L. (1992). Tissue Response to Biphasic Calcium Phosphate Ceramic with Different Ratios of Biphasic Calcium Phosphate Ceramic with Different Ratios of HA/TCP in Periodontal Osseous Defects, *J. Periodontal.*, **63**, 729–735.
10. Jarcho, M. (1976). Hydroxylapatite Synthesis and Characterization Forms, *J. Mater. Sci.*, **11**, 2027–2035.
11. Jarcho, M. (1981). Calcium Phosphate Ceramics as Hard Tissue Prosthetics, *Clin. Orthopaed.*, **157**, 259–278.
12. Jarcho, M., Bolen, C.H., Thomas, M.B. *et al.* (1976). Synthesis and Characterization in Dense Polycrystalline Form, *J. Mat. Sci.*, **11**, 2027–2035.
13. de Groot, K. (1983). "Ceramic of Calcium Phosphates: Preparation and Properties", in de Groot, K. (ed.), *Bioceramics of Calcium Phosphate*, CRC Press, Boca Raton, FL, pp. 100–114.
14. Peelen, J.G.C., Rejda, B.V. and de Groot, K. (1980). Preparation and Properties of Sintered Hydroxyapatite, *Ceramurgia Int.*, **4**, 71–73.
15. Denissen, H., Mangano, C. and Cenini, G. (1985). *Hydroxylapatite Implants*, Piccini Nuova Libraria, S.P.A., India.
16. Aoki, H., Kato, K., Ogiso, M. *et al.* (1977). Sintered Hydroxyapatite as a New Dental Implant Material, *J. Dent. Outlook*, **49**, 567–575.
17. Aoki, H. (1991). *Science and Medical Applications of Hydroxyapatite*, Takayama Press System Center Co., Tokyo.
18. DeJong, W.F. (1926). La Substance Minerals dans les Os., *Tec. Trav. Chim.*, **45**, 445–458.
19. Kay, M.I., Young, R.A. and Posner, A.S. (1964). Crystal Structure of Hydroxyapatite, *Nature*, **204**, 1050–1053.
20. Hench, L.L., Splinter, R.J., Allen, W.C. *et al.* (1971). Bonding Mechanisms at the Interface of Ceramic Prosthetic Materials, *J. Biomed. Mater. Res.*, **2**, 117–141.
21. Roy, D.M., Linnehan, S.A. (1973). Hydroxyapatite Formed from Coral Skeleton Carbonate by Hydrothermic Exchange, *Nature*, **247**, 220–227.

22. Dard, M., Bauer, A., Liebendorgen, A. *et al.* (1994). Preparation Physcico-Chemical and Biological Evaluation of a Hydroxyapatite Ceramic from Bovine Spongiosa, *Acta Odonto. Stom.*, **185**, 61–69.
23. LeGeros, R.Z., Ito, A., Ishikawa, K. *et al.* (2009). "Fundamentals of Hydroxyapatite and Related Calcium Phosphates", in Basu, B. (ed.), *Advanced Biomaterials: Fundamentals, Processing and Applications*, John Wiley and Sons, Inc., New York, pp. 19–52.
24. LeGeros, R.Z., Daculsi, G. and LeGeros, J.P. (2002). "Bioactive Bioceramics", in Pietrzak, W.S. (ed.), *Musculoskeletal Tissue Regeneration: Biological Materials and Methods*, Humana Press, New Jersey, pp. 153–181.
25. Dorozkin, S. (2009). Calcium Orthophosphates in Nature, Biology and Medicine, *Materials*, **2**, 399–498.
26. Bohner, M. (2000). Calcium Orthophosphates in Medicine: From Ceramics to Calcium Phosphate Cements, *Injury, Int. J. Care Injured*, **31**, S-D17–47.
27. Beevers, C.A. and Mcintyre, D.B. (1956). The Atomic Structure of Fluorapatite and its Relation to that of Tooth and Bone Mineral, *Miner. Mag.*, **27**, 254–259.
28. Young, R.A. and Elliott, J.C. (1966). Scale Bases for Several Properties of Apatites, *Arch. Oral Biol.*, **11**, 699–707.
29. LeGeros, R.Z. (1991). "Calcium Phosphates in Oral Biology and Medicine", in Myers, H. (ed.), *Monographs in Oral Sciences, Vol. 15*, S. Karger, Basel.
30. Mayer, I., Cuisinier, F.J.K.G, Gedalya, S. *et al.* (2008). TEM Study of the Morphology of Mn2+-Doped Calcium Hydroxyapatite and Beta-Tricalcium Phosphate, *J. Inorg.. Biochem.*, **102**, 311–317.
31. Matsunaga, K. (2008). First-Principles Study of Substitutional Magnesium and Zinc in Hydroxyapatite and Octacalcium Phosphate, *J. Chem Physics*, **128**, 245101–245110.
32. LeGeros, R.Z. and LeGeros, J.P. (2008). "Hydroxyapatite" in Kokubo, T. (ed.), *Handbook of Bioceramics and their Applications*, Woodhead Publishing Ltd, London, pp. 367–394.
33. Moreno, E.C., Kresak, M. and Zahradnik, R.T. (1977). Physicochemical Aspects of Fluoride-Apatite Systems Relevant to the Study of Dental Caries, *Caries. Res.*, **11**, 142–177.
34. Bonel, G. (1972). Contribution à l'Etude de la Carbonation des Apatites, *Ann. Chim.*, **7**, 65–88.
35. Elliot, J.C. (1964). *The Crystallographic Structure of Dental Enamel and Related Apatites* (PhD Thesis, University of London).

36. Zapanta-LeGeros, R. (1965). Effect of Carbonate on the Lattice Parameters of Apatite, *Nature*, **206**, 403–405.
37. LeGeros, R.Z., LeGeros, J.P., Trautz, O.R. *et al.* (1971). Conversion of Monetite, $CaHPO_4$, to Apatites: Effect of Carbonate on the Crystallinity and the Morphology of the Apatite Crystallites, *Adv. in X-Ray Anal.*, **14**, 57–66.
38. LeGeros, R.Z., LeGeros, J.P., Trautz, O.R. *et al.* (1970). Spectral Properties of Carbonate in Carbonate-Containing Apatites, *Dev. Applied Spectroscopy*, **7B**, 3–12.
39. LeGeros, R.Z., Trautz, O.R., LeGeros, J.P. *et al.* (1967). Apatite Crystallites: Effect of Carbonate on Morphology, *Science*, **155**, 1409–1411.
40. LeGeros, R.Z. (1981). Apatites in Biological Systems, *Prog. Crystal. Growth. Charact.*, **4**, 1–45.
41. LeGeros, R.Z. and Tung, M.S. (1983). Chemical Stability of Carbonate and Fluoride Containing Apatites, *Caries. Res.*, **17**, 419–429.
42. Sillen, A. and LeGeros, R.Z. (1991). Solubility Profiles of Synthetic Apatites and of Modern and Fossil Bones, *J. Arch. Sci.*, **18**, 385–397.
43. Okazaki, M. and LeGeros, R.Z. (1992). Crystallographic and Chemical Properties of Mg-Containing Apatites Before and After Suspension in Solutions, *Magnesium Res.*, **5**, 103–108.
44. Yao, F. and LeGeros, R.Z. (2010). Carbonate and Fluoride Incorporation in Synthetic Apatites: Comparative Effect on Physico-Chemical Properties and *In Vitro* Bioactivity in Fetal Bovine Serum, *Mater. Sci. Engineer.*, **30**, 423–430.
45. LeGeros, R.Z., Bleiwas, C.B., Retino, M. *et al.* (1999). Zinc Effect on the *In Vitro* Formation of Calcium Phosphates: Relevance to Clinical Inhibition of Calculus Formation, *Am. J. Dent.*, **12**, 65–70.
46. Brown, W.E. and Chow, L. (1976). Chemical Properties of Bone Mineral, *Ann. Res. Mater. Sci.*, **6**, 213–226.
47. Rey, C., Renugoplakrishan, V. and Collins, B. (1991). Fourier Transform Infrared Spectroscopic Study of the Carbonate Ions in Bone Mineral during Aging, *Calcif. Tissue Int.*, **49**, 251–258.
48. Neuman, W.F. and Neuman, M.W. (1958). *The Chemical Dynamics of Bone Mineral*, University of Chicago Press, Chicago, IL.
49. Rathje, W. (1939). Zur Kentnis de Phosphate I. Uber Hydroxyapatite, *Bodenk Pjlernah*, **12**, 121–128.
50. Hayek, E. and Newesely, H. (1963). Pentacalcium Monohydroxyorthophosphate, *Inorg. Syn.*, **7**, 63–65.

51. Bonel, G., Heughebaert, J.-C., M. Heughebaert, M. *et al.* (1988). "Apatitic Calcium Orthophosphates and Related Compounds for Biomaterials Preparation", in Ducheyne, P. and Lemons, J.E. (eds), *Bioceramics: Materials Characteristics Versus* In Vivo *Behavior, Vol. 523*, Ann. NY Acad. Sci., New York, pp. 115–130.
52. LeGeros, R.Z. (1986). Variability of β-TCP/HAP Ratios in Sintered Apatites, *J. Dent. Res.*, **65**, Abstr. #110.
53. LeGeros, R.Z., Lin, S., Rohanizadeh, R. *et al.* (2003). Biphasic Calcium Phosphates: Preparation and Properties, *J. Mater. Sci. Mat. Med.*, **14**, 201–209.
54. Wakae, H., Takeuchji, A., Udoh, K. *et al.* (2008). Fabrication of Cancellous Bone Type Carbonate Apatite Foam by Hydrothermal Conversion of A-Tricalcium Phosphate in Carbonate Solutions, *J. Biomed. Mater. Res.*, **87A**, 957–963.
55. Best, S., Bonfield, W. and Doyle, C. (1990). "Optimization of Toughness in Dense Ceramics", in Heimke, G. (ed.), *Bioceramics, Vol. 2*, German Ceramic Society, Cologne, pp. 57–64.
56. van Blitterswijk, C.A., Hesseling, S.C., Grote, J.J. *et al.* (1990). The Biocompatibility of Hydroxyapatite Ceramic: A Study of Retrieved Human Middle Ear Implants, *J. Biomed. Mater. Res.*, **24**, 433–453.
57. ASTM (2002). *Annual Book of ASTM Standards*. *Section 13. F1185–88*, Standard Specification for Composition of Ceramic Hydroxylapatite for Surgical Implants, Philadelphia, pp. 471–473.
58. de Groot, K., Klein, C.P.A.T., Wolke, J.G.C. *et al.* (1990). "Chemistry of Calcium Phosphate Bioceramics", in Yamamuro, T., Hench, L.L. and Wilson, J. (eds), *Handbook of Bioactive Ceramics, Vol. II*, CRC Press, Boca Raton, FL, pp. 3–16.
59. Daculsi, G., LeGeros, R.Z., LeGeros, J.P. *et al.* (1991). Lattice Defects in Calcium Phosphate Ceramics; High Resolution TEM Ultrastructural Study, *J. Appl. Biomat.*, **2**, 147–152.
60. Niwa, S., Sawai, K., Takahashi, S. *et al.* (1980). Experimental Studies on the Implantation of Hydroxylapatite in the Medullary Canal of Rabbits, *Biomat.*, 1, 65–71.
61. Margolis, H. and Moreno, E.C. (1992). Kinetics of Hydroxyapatite Dissolution in Acetic, Lactic and Phosphoric Acid Solutions, *Calcif. Tissue. Int.*, **50**, 137–143.
62. Ducheyne, P., Kim, C.S. and Pollack, S.R. (1992). The Effect of Phase Differences on the Time-Dependent Variation of the Zeta Potential of Hydroxyapatite, *J. Biomed. Mater. Res.*, **26**, 147–168.

63. Pollack, S.R. (1984). Bioelectrical Properties of Bone: Endogenous Electrical Signals, *Orthop. Clin. N Amer.*, **15**, 3–13.
64. Doss, S.K. (1976). Surface Property of Hydroxyapatite: The Effect on Various Inorganic Ions on the Electrophoretic Behavior, *J. Dent. Res.*, **55**, 1067–1075.
65. Somasundran, P. (1968). Zeta Potential of Apatite in Aqueous Solution and its Change During Equilibrium, *J. Colloid. Interface Sci.*, **27**, 659–666.
66. Gorbunoff, M.J. (1984). The Interaction of Proteins with Hydroxylapatite, *J. Anal. Biochem.*, **136**, 425–432.
67. Spencer, M. and Grynpas, M. (1978). Hydroxyapatite for Chromatography. 1. Physical and Chemical Properties of Different Preparations, *J. Chromat.*, **166**, 423–434.
68. Boskey, A.L. (1984). "Overview of Cellular Elements and Macromolecules Implicated in the Initiation of Mineralization", in Butler, W. (ed.), *The Chemistry and Biology of Mineralized Tissues*, Ebsco Media Birmingham, AL, pp. 335–343.
69. Reddi, H. (1985). Implant-Stimulated Interface Reactions During Collagenous Bone Matrix-Induced Bone Formation, *J. Biomed. Mater. Res.*, **19**, 233–239.
70. Beckham, A., Greenlee, T.K. and Crebo, Jr., A.R. (1971). Bone Formation at a Ceramic Implant Interface, *Calcif. Tiss. Res.*, **8**, 165–171.
71. Ganeles, J., Listgarten, M.A. and Evian, C.I. (1986). Ultrastructure of Durapatite Periodontal Tissue Interface in Human Intrabony Defects, *J. Periodntol.*, **57**, 133–140.
72. Tracy, B.M. and Doremus, R.H. (1984). Direct Electron Microscopy Studies of the Bone–Hydroxylapatite Interface, *J. Biomed. Mater. Res.*, **18**, 719–726.
73. Gregoire, M., Orly, I. and Menanteau, J. (1990). The Influence of Calcium Phosphate Biomaterials on Human Bone Cell Activities: An *In Vitro* Approach, *J. Biomed. Mater. Res.*, **24**, 163–177.
74. LeGeros, R.Z., Orly, I., Gregoire, M. *et al.* (1988). Comparative Properties and *In Vitro* Transformation of HA Ceramics in Serum, *J. Dent. Res.*, **67**, Abstr. # 512.
75. Orly, I., Gregoire, M., Menanteau, J. *et al.* (1989). Effects of Synthetic Calcium Phosphates on the H-Thymidine Incorporation and Alkaline Phosphatase Activity of Human Fibroblasts in Culture, *J. Biomed. Mat. Res.*, **23**, 1433–1440.
76. Heughebaert, M., LeGeros, R.Z., Gineste, M. *et al.* (1988). Physico-Chemical Characterization of Deposits Associated with HA Ceramics Implanted in Non-Osseous Sites, *J. Biomed. Mater. Res.*, **22**, 254–268.

77. LeGeros, R.Z. and Daculsi, G. (1990). "*In Vivo* Transformation of Biphasic Calcium Phosphate Ceramics: Ultrastructural and Physico-Chemical Characterizations", in Yamamuro, T., Hench, L.L. and Wilson, J. (eds), *Handbook of Bioactive Ceramics Vol. II*, CRC Press, Boca Raton, FL, pp. 17–28.
78. LeGeros, R.Z., Daculsi, G., Orly, I. *et al.* (1991). "Substrate Surface Dissolution and Interfacial Biological Mineralization", in J. Davies, E. (ed.), *The Bone–Biomaterial Interface*, University of Toronto Press, Toronto, pp. 76–88.
79. Hench, L.L. (1991). Bioceramics: From Concept to Clinic, *J. Am. Ceram. Soc.*, **74**, 1487–1510.
80. Davies, J.E. (1990). "The Use of Cell and Tissue Culture to Investigate Bone Cell Reactions to Bioactive Materials", in Yamamuro, T., Hench, L.L. and Wilson, J. (eds), *Handbook of Bioactive Ceramics, Vol. I*, CRC Press, Boca Raton, FL, 195–225.
81. Bagambisa, F.B., Joos, U. and Schilli, W. (1990). The Interaction of Osteogenic Cells with Hydroxylapatite Implant Materials *In Vitro* and *In Vivo*, *Int. Oral. Maxillofac. Implants*, **5**, 217–226.
82. Baron, R., Neff, L., Louvard, D. *et al.* (1985). Cell-Mediated Extracellular Acidification and Bone Resorption: Evidence for a Low pH in Resorbing Lacunae and Localization of 100-kD Lysosomal Membrane Protein at the Osteoclast Ruffled Border, *J. Cell. Biol.*, **101**, 2210–2222.
83. Webster, T.J., Ergun, C., Deoremus, R. *et al.* (2002). Hydroxylapatite with Substituted Magnesium, Zinc, Cadmium and Yttrium. II. Mechanisms of Osteoblast Adhesion, *J. Biomed. Mater. Res.*, **59**, 312–317.
84. Fujimori, Y., Mishima, H., Sugaya, K. *et al.* (1988). *In Vitro* Interactions of Osteoclast-Like Cells and Hydroxyapatite Ceramics, *Bioceramics*, **11**, 335–338.
85. Inoue, M., LeGeros, R.Z., Inoue, M. *et al.* (2004). *In Vitro* Response of Osteoblast-Like and Odontoblast-Like Cells to Unsubstituted and Substituted apatites, *J. Biomed. Mater. Res.*, **70A**, 585–593.
86. Urist, M.R. (1965). Bone Formation by Autoinduction, *Science*, **150**, 893–898.
87. Reddi, A.H. (2000). Morphogenesis and Tissue Engineering of Bone and Cartilage: Inductive Signals, Stem Cells and Biomimetic Biomaterials, *Tissue Eng.*, **6**, 351–359.
88. LeGeros, R.Z. (2002). Properties of Osteoconductive Biomaterials: Calcium Phosphates, *Clin. Orthopaed. Rel. Res.*, **395**, 81–98.
89. Kuboki, Y., Takita, H., Kobayash, D. (1998). BMP-Induced Osteogenesis on the Surface of Hydroxyapatite with Geometrically Feasible and Non-feasible Structures. Topology of Osteogenesis, *J. Biomed. Mater. Res.*, **39**, 190–199.

90. Ripamonti, U., Ma, S. and Reddi, A.H. (1992). The Critical Role of Geometry of Porous Hydroxyapatite Delivery System: Induction of Bone by Osteogenin, a Bone Morphogenetic Protein, *Matrix*, **12**, 201–212.
91. LeNihouhanne, D., Daculsi, G., Gauthier, O. *et al.* (2005). Ectopic Bone Formation by Microporous Calcium Phosphate Ceramic Particles in Sheep Muscles, *Bone*, **36**,1086–1093.
92. LeGeros, R.Z. (2008). Calcium Phosphate-Based Osteoinductive Materials, *Chem. Revs*, **108**, 4742–4753.
93. Osborn, J.F. and Neweseley, H. (1980). The Material Science of Calcium Phosphate Ceramic, *Biomaterials*, **1**, 108–111.
94. Niki, M., Ito, G., Matsuda, T. *et al.* (1991). "Comparative Push-Out Data of Bioactive and Non-Bioactive Materials of Similar Rugosity", in Davies, J.E. (ed.), *Bone–Material Interface,* University of Toronto Press, Toronto, pp. 350–356.
95. de Groot, K. (1987). "Hydroxylapatite Coatings for Implants in Surgery", in Vincenzini, P. (ed.), *High Tech Ceramics*, Elsever, Amsterdam, pp. 381–386.
96. Cook, S.D., Thomas, K.A, Dalton, J.E. *et al.* (1992). Hydroxylapatite Coating of Porous Implants Improves Bone Ingrowth and Interface Attachment Strength, *J. Biomed. Mater. Res.*, **26**, 989–1001.
97. Jarcho, M. (1992). Retrospective Analysis of Hydroxyapatite Development for Oral Implant Applications, *Dent. Clin. North. Amer.*, **36**, 19–26.
98. Linkow, L. (1984). Bone Transplants Using the Symphysis, the Iliac Crest and Synthetic Bone Materials, *J. Oral. Implantol.*, **11**, 211–217.
99. Jansen, J.A., van der Waerden, J.P.C.M., van der Lubbe, H.B.M *et al.* (1990). Tissue Response to Percutaneous Implants in Rabbits, *J. Biomed. Mater. Res.*, **24**, 295–307.
100. Simon, J.L., Michna, S., Lewis, J.A. *et al.* (2007). *In Vivo* Bone Response to 3D Periodic Hydroxyapatite Scaffolds Assembled by Direct Ink Writing, *J. Biomed. Mater. Res.*, **83A**, 747–758.
101. Uchida, A., Shinto, Y., Araki, N. *et al.* (1992). Slow Release of Anticancer Drugs from Porous Calcium Hydroxyapatite Ceramic, *J. Orthop. Res.*, **10**, 440–445.
102. Frayssinet, P., Rojuguet, N., Mathon, D. (2006). Bone Cell Transfection in Tissue Culture Using Hydroxyapatite Microparticles, *J. Biomed. Mater. Res.*, **79A**, 225–228.
103. Frayssinet, P., Primout, I., Rouquet, N. *et al.* (1991). Bone Cell Grafts in Bioreactor: A Study of Feasibility of Bone Cell Autograft in Large Defects, *J. Mater. Sci. Mater. Med.*, **2**, 217–221.

104. LeGeros, R.Z., LeGeros, J.P., Kim, Y. *et al.* (1995). Calcium Phosphates in Plasma-Sprayed HA Coatings, *Ceram. Trans.*, **48**, 173–189.
105. LeGeros, R.Z., Coelho, P.G., Holmes, D. *et al.* (2011). "Orthopedic and Dental Implant Surfaces and Coatings", in Zhang, S. (ed.), *Biological and Biomedical Coatings Handbook*, CRC Press, Boca Raton, FL, pp. 301–334.
106. Lin, S., LeGeros, R.Z. and LeGeros, J.P. (2003). Adherent Octacalcium Phosphate Coating on Titanium Alloy Using Modulated Electrochemical Deposition Method, *J. Biomed. Mater. Res.*, **68A**, 810–828.
107. Rohanizadeh, R., LeGeros, R.Z., Marsono, H. *et al.* (2005). Adherent Apatite Coating on Titanium Substrate Using Chemical Deposition, *J. Biomed. Mater. Res.*, **72A**, 428–438.

Chapter 18

SILICON SUBSTITUTED HYDROXYAPATITE

Robert J. Friederichs, William Bonfield and Serena M. Best

18.1. INTRODUCTION

Synthetic hydroxyapatite (HA) is similar in chemical composition to bone mineral and has been utilised in a number of different applications as an orthopaedic implant material. HA is considered to be osseoconductive, meaning that it encourages bone growth on its surface when in the presence of bone-forming cells. To this end, HA has been used in various bone contacting or grafting applications in the form of dense or porous blocks, granules, powders, coatings or as a mineral component in a polymer composite.[1] However, HA has a relatively limited bioactivity compared to some other synthetic bioceramics and glasses. One method that can improve the bioactivity of HA is to modify the chemical composition by substituting ions found in human bone mineral into the HA lattice. LeGeros initially investigated carbonate substitution in hydroxyapatite (CHA) due to its presence in human bone, and other investigators expanded this seminal work.[2,3] See Chapter 17 for details. Carbonate substitution increased solubility, proliferation of osteoblasts and osteoclastogenesis.[4,5] Increased solubility of CHA may be desirable in some applications where resorbtion is desired, but problematic in situations where stability is required (Chapter 20). Dhert *et al*. investigated fluoride substitutions for its stabilising effect on the HA lattice and found that it increased mechanical stability of the tissue/implant interface.[6] Another ion critical to bone formation and repair is silicon (Si).

Silicon was shown to be a critical trace element in connective tissue health (particularly bone and cartilage) by Carlisle.[7] She showed a pronounced change in skeletal structure between chicks that were fed an enhanced-silicon diet opposed to those fed a silicon-deficient diet. A similar experiment using rats found that increased Si intake translated to increased longitudinal growth of bones.[8] The mechanism by which silicon influences bone development is still uncertain, but it appears that Si complexes help enhance production of collagen and other extracellular matrix (ECM) proteins and increases osteoblast (OB) activity (Chapter 4). Silicon has been added to OB cultures *in vitro* and stimulatory effects have been observed. Orthosilicic acid, present in human blood plasma, was added to human OBs *in vitro* and subsequently increased markers of OB activity.[9] Another study supplemented human OBs with sodium silicate and

observed increased OB metabolic activity and proliferation.[10] Silicon plays an important role in bone health, and has been utilised in synthetic calcium phosphates (CaP) such as HA with the aim of improving bioactivity.

18.2. SYNTHESIS OF SILICON SUBSTITUTED HYDROXYAPATITE

Many researchers have studied the synthesis of phase-pure silicon substituted HA (SiHA), with varying degrees of success. Sol-gel, hydrothermal, wet precipitation, solid state and mechanochemical methods have all been used to synthesise SiHA. Ruys and Tanizawa developed early sol-gel and hydrothermal methods that produced SiHA with extraneous phases such as amorphous calcium phosphate and brushite, which confounded the effects of silicon substitution.[11,12] Several wet chemical precipitation methods have produced phase-pure SiHA. Bonfield and co-workers were the first to successfully produce a phase-pure SiHA.[1] In 1999 Bonfield, Best and Gibson developed a wet precipitation method based on work by Akao[13] that used an aqueous reaction between silicon tetraacetate ($Si(OCOCH_3)_4$), calcium hydroxide and orthophosphoric acid to produce a phase-pure SiHA. The HA was substituted with 0.4 weight percentage (wt%) silicon and remained thermally stable up to 1,200°C.[14] The proposed mechanism that Si was incorporated into the HA lattice is listed in Eq. 18.1.

$$Ca(PO_4)_{6-x}\,(SiO_4)_x\,(OH)_{2-x} \tag{18.1}$$

Kim *et al*. produced SiHA using wet chemical methods similar to Gibson, but used tetraethylorthosilicate (TEOS) as the Si source.[15] Kim's use of TEOS claims to have increased thermal stability up to 1,300°C. However, phase purity problems associated with how the TEOS was incorporated in the wet chemical reaction arose and were addressed by Hadden *et al*.[16] Palard used a nitrate-based method similar to Jarcho, but this SiHA was only thermally stable to 1,000°C.[17,18]

18.3. PHYSICO-CHEMICAL IMPLICATIONS OF SILICON SUBSTITUTION

18.3.1. Heat Treatment and Microstructural Changes in Siha

SiHA produced by Bonfield and co-workers' method was shown to be phase pure when heat-treated between 1,000–1,300°C.[19] The onset of

densification occurred at a higher temperature for SiHA compared to HA. The grain size of SiHA also reduced with increasing Si content up to 1.6 wt% with respect to HA heat-treated at 1,200°C. The effect of the smaller grain size was reflected in higher hardness values from SiHA compared to HA heat-treated to 1,200°C or above. The authors suggest that larger amounts of carbonaceous material, perhaps remnants of the silicon tetraacetate and adsorbed carbonate, present in SiHA before sintering may have contributed to the inhibitory effects observed.

18.3.2. Crystal Structure and Chemical Analysis

Gibson *et al*. performed X-ray diffraction (XRD), Fourier transform infrared reflection spectroscopy (FTIR) and X-ray fluorescence (XRF) to determine whether silicon was incorporating into HA. XRD showed that the only phase present was hydroxyapatite (ICCD 09-0432), but upon Rietveld refinement of the data the insertion of silicon for phosphorous produced a contraction along the crystallographic *a*-axis and an expansion along the *c*-axis compared to stoichiometric HA. Silicon substation altered P-O vibration bands in FTIR, and contained three additional peaks. XRF revealed that the amounts of silicon calculated using Eq. 18.1 were approximate to those incorporated into HA.[14] Other studies investigated how silicon substitutes into the phosphate tetrahedral lattice position in HA using ^{29}Si nuclear magnetic resonance (NMR) and neutron diffraction.[20,21] Gomes *et al*. found that charge compensation mechanisms in SiHA can depend on the synthesis route, which can account for the variability in phase purity observed in the literature. The mechanism in Eq. 18.1 was found to occur alongside a second mechanism where B-CO_3 substitution, which inevitably occurs during exposure to the atmosphere in synthesis, decomposes upon heat-treating over ~800°C and creates phosphate/silicate vacancies (Eq. 18.2).[20]

$$Ca_{10}(PO_4)_{6-x-y}(SiO_4)_{x+y}(V_{p-Si})_y(OH)_{2-x}O_y(V_{OH-O})_{x-y}, \quad (18.2)$$

where $V_{P/Si}$ and $V_{OH/O}$ are phosphate/silicate and hydroxyl/oxide pair vacancies respectively.

18.3.3. Surface Charge and Protein Adsorption

The surface charge of SiHA has been characterised using high-resolution force spectroscopy with a functionalised COO^- terminated alkanethiol

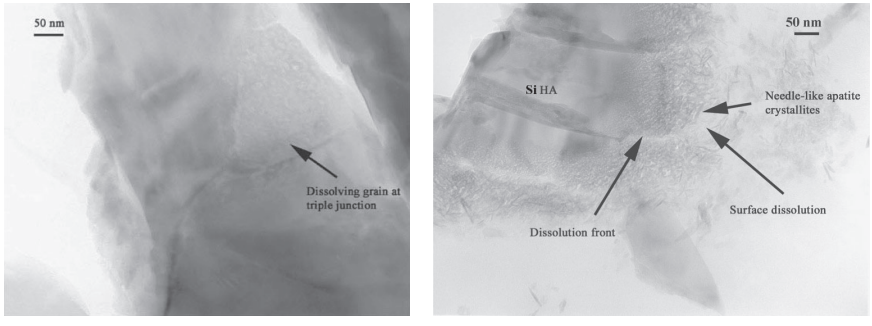

Figure 18.1. TEM micrographs of SiHA granules implanted *in vivo* for 12 weeks. (a) 1.5 wt% SiHA grain dissolving at a triple junction. (b) TEM micrograph of dissolution from 0.8 wt% SiHA granules. Reprinted from Porter *et al.*, with permission from Elsevier.[25]

self-assembling monolayer. This technique revealed larger Van der Waals and adhesive interactions present in SiHA. The surface charge of SiHA was twice more negatively charged compared to HA.[22] This may help explain the accelerated adsorption of adhesive proteins fibronectin and vitronectin onto SiHA compared to HA.[23]

18.3.4. Dissolution of SiHA

Porter *et al*. have studied the ultra-structure of SiHA using transmission electron microscopy (TEM) and found higher concentrations of triple-point defects compared to HA. These defects may increase the solubility of SiHA (Fig. 18.1).[24,25] The dissolution kinetics of SiHA suggest that Si is leaching out of the HA lattice, but it may reprecipitate at the implant interface.[26,27]

18.4. BIOLOGICAL RESPONSE TO SILICON-SUBSTITUTED HYDROXYAPATITE

Several *in vitro* and *in vivo* studies have demonstrated that silicon substitution in HA has desirable implications for bone regeneration. SiHA formed an enhanced apatite layer compared to HA during *in vitro* bioactivity tests using simulated body fluid, and SiHA was found to stimulate OB activity *in vitro*.[28,29] *In vivo* work has shown significantly increased bone apposition and organisation around SiHA implants compared to HA.[30] Organised collagen fibrils also formed

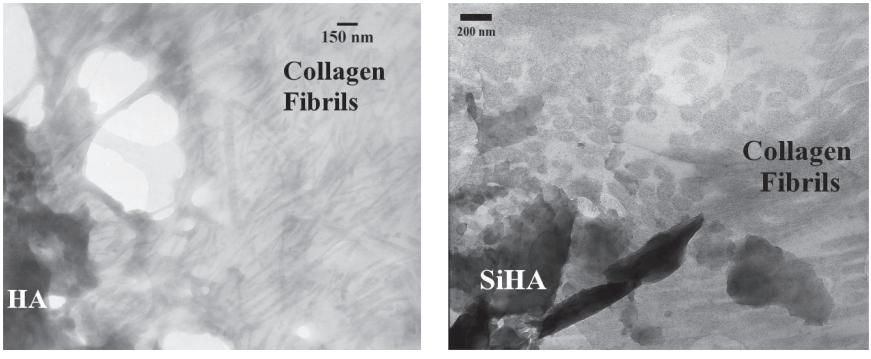

(a) (b)

Figure 18.2. TEM micrographs of granules implanted *in vivo* for six weeks. (a) Disorganised collagen fibrils apposing HA granules. (b) Aligned collagen fibrils (both parallel and transverse) apposing 1.5 wt% SiHA granules. Reprinted from Porter *et al.*, with permission from Elsevier.[31]

faster on SiHA compared to HA (Fig. 18.2).[31] These results have stimulated the major clinical application of SiHA, marketed under the trade name ActiFuse™, as a synthetic bone graft for skeletal reconstruction, particularly for spinal fusion.[32]

18.5. CONCLUSIONS

The importance of silicon in bone health has promoted its use in HA bone-grafting materials. Many synthetic routes have been used to obtain a phase-pure SiHA, with Bonfield and co-workers developing the first working procedure based on common wet chemical precipitation of HA. Greater understanding of how silicon incorporates into the HA lattice can explain some of the variability in phase purity observed in the literature. The mechanisms by which SiHA speeds bone growth are still under investigation. Some possibilities for the success of SiHA are that surface charge becomes more negative, silicon destabilises the HA lattice, increasing solubility, silicon is released from the lattice in a therapeutic manner, topographical effects (reduced grain size and increased concentration of triple points) and bone cells actively detect silicon in the HA lattice. The success of SiHA bone grafts may rely on several of these mechanisms. Once these mechanisms are better understood, SiHA can be further tailored to enhance bone formation around an implant.

ACKNOWLEDGEMENTS

This work is supported by a National Science Foundation Graduate Research Fellowship (R.J.F Grant Number DGE-1042796) and the Cambridge Overseas Trusts (R.J.F).

REFERENCES

1. Bonfield, W., Grynpas, M.D., Tully, A.E. *et al.* (1981). Hydroxyapatite Reinforced Polyethylene — A Mechanically Compatible Implant Material for Bone-Replacement, *Biomaterials*, **2**, 185–186.
2. Doi, Y., Shibutani, T., Moriwaki, Y. *et al.* (1998). Sintered Carbonate Apatites as Bioresorbable Bone Substitutes, *J. Biomed. Mater. Res.*, **39**, 603–610.
3. Legeros, R.Z., Trautz, O.R., Legeros, J.P. *et al.* (1968). Carbonate Substitution in Apatite Structure (1), *Bulletin de la Societe Chimique de France*, **25**, 5–7.
4. Hing, K.A., Merry, J.C., Gibson, I.R. *et al.* (1999). "Effect of Carbonate Content on the Response of Human Osteoblast-Like Cells to Carbonate Substituted Hydroxyapatite", in Ohgushi, H., Hastings, G.W. and Yoshikawa, T. (eds), *Bioceramics*, World Scientific, Nara, pp. 195–198.
5. Spence, G., Patel, N., Brooks, R. *et al.* (2008). Osteoclastogenesis on Hydroxyapatite Ceramics: The Effect of Carbonate Substitution, *J. Biomed. Mater. Res. A*, **92**, 1292–1300.
6. Dhert, W.J.A., Klein, C., Wolke, J.G.C. *et al.* (1991). A Mechanical Investigation of Fluorapatite, Magnesiumwhitlockite, and Hydroxylapatite Plasma-Sprayed Coatings in Goats, *J. Biomed. Mater. Res.*, **25**, 1183–1200.
7. Carlisle, E.M. (1988). Silicon as a Trace Nutrient, *Sci. Total Environ.*, **73**, 95–106.
8. Jugdaohsingh, R., Calomme, M.R., Robinson, K. *et al.* (2008). Increased Longitudinal Growth in Rats on a Silicon-Depleted Diet, *Bone*, **43**, 596–606.
9. Reffitt, D.M., Ogston, N., Jugdaohsingh, R. *et al.* (2003). Orthosilicic Acid Stimulates Collagen Type 1 Synthesis and Osteoblastic Differentiation in Human Osteoblast-Like Cells *In Vitro*, *Bone*, **32**, 127–135.
10. Zou, S., Ireland, D., Brooks, R.A. *et al.* (2009). The Effects of Silicate Ions on Human Osteoblast Adhesion, Proliferation, and Differentiation, *J. Biomed. Mater. Res. B*, **90**, 123–130.

11. Ruys, A.J. (1993). Silicon-Doped Hydroxyapatite, *J. Aust. Ceram. Soc.*, **29**, 83–88.
12. Tanizawa, Y. and Suzuki, T. (1995). Effects of Silicate Ions on the Formation and Transformation of Calcium Phosphates in Neutral Aqueous-Solutions, *J. Chem. Soc.-Faraday Trans.*, **91**, 3499–3503.
13. Akao, M., Aoki, H. and Kato, K. (1981). Mechanical-Properties of Sintered Hydroxyapatite for Prosthetic Applications, *J. Mater. Sci.*, **16**, 809–812.
14. Gibson, I.R., Best, S.M. and Bonfield, W. (1999). Chemical Characterization of Silicon-Substituted Hydroxyapatite, *J. Biomed. Mater. Res.*, **44**, 422–428.
15. Kim, S.R., Lee, J.H., Kim, Y.T. *et al.* (2003). Synthesis of Si, Mg Substituted Hydroxyapatites and their Sintering Behaviors, *Biomaterials*, **24**, 1389–1398.
16. Hadden, D.J., Skakle, J.M.S. and Gibson, I.R. (2008). Optimisation of the Aqueous Precipitation Synthesis of Silicate-Substituted Hydroxyapatite, *Key Eng. Mater.*, **361–363**, 55–58.
17. Jarcho, M., Bolen, C.H., Thomas, M.B. *et al.* (1976). Hydroxylapatite Synthesis and Characterization in Dense Polycrystalline Form, *J. Mater. Sci.*, **11**, 2027–2035.
18. Palard, M., Champion, E. and Foucaud, S. (2008). Synthesis of Silicated Hydroxyapatite Ca-10(Po4)(6-X)(Sio4)(X)(Oh)(2-X), *J. Solid State Chem.*, **181**, 1950–1960.
19. Gibson, I.R., Best, S.M. and Bonfield, W. (2002). Effect of Silicon Substitution on the Sintering and Microstructure of Hydroxyapatite, *J. Am. Ceram. Soc.*, **85**, 2771–2777.
20. Gomes, S., Nedelec, J.M., Jallot, E. *et al.* (2011). Silicon Location in Silicate-Substituted Calcium Phosphate Ceramics Determined by Neutron Diffraction, *Cryst. Growth Des.*, **11**, 4017–4026.
21. Gomes, S., Renaudin, G., Mesbah, A. *et al.* (2010). Thorough Analysis of Silicon Substitution in Biphasic Calcium Phosphate Bioceramics: A Multi-Technique Study, *Acta Biomaterialia*, **6**, 3264–3274.
22. Vandiver, J., Dean, D., Patel, N. *et al.* (2006). Silicon Addition to Hydroxyapatite Increases Nanoscale Electrostatic, Van Der Waals, and Adhesive Interactions, *J. Biomed. Mater. Res. A*, **78**, 352–363.
23. Guth, K., Campion, C., Buckand, T. *et al.* (2010). Surface Physiochemistry Affects Protein Adsorption to Stoichiometric and Silicate-Substituted Microporous Hydroxyapatites, *Adv. Eng. Mater.*, **12**, B113–B121.

24. Porter, A.E., Botelho, C.M., Lopes, M.A. *et al.* (2004). Ultrastructural Comparison of Dissolution and Apatite Precipitation on Hydroxyapatite and Silicon-Substituted Hydroxyapatite *In Vitro* and *In Vivo*, *J. Biomed. Mater. Res. A*, **69**, 670–679.
25. Porter, A.E., Patel, N., Skepper, J.N. *et al.* (2003). Comparison of *In Vivo* Dissolution Processes in Hydroxyapatite and Silicon-Substituted Hydroxyapatite Bioceramics, *Biomaterials*, **24**, 4609–4620.
26. Guth, K., Campion, C., Buckland, T. *et al.* (2010). Effect of Silicate-Substitution on Attachment and Early Development of Human Osteoblast-Like Cells Seeded on Microporous Hydroxyapatite Discs, *Adv. Eng. Mater.*, **12**, B26–B36.
27. Botelho, C.M., Lopes, M.A., Gibson, I.R. *et al.* (2002). Structural Analysis of Si-Substituted Hydroxyapatite: Zeta Potential and X-Ray Photoelectron Spectroscopy, *J. Mater. Sci. Mater. Med.*, **13**, 1123–1127.
28. Balas, F., Perez-Pariente, J. and Vallet-Regi, M. (2003). *In Vitro* Bioactivity of Silicon-Substituted Hydroxyapatites, *J. Biomed. Mater. Res. A*, **66**, 364–375.
29. Botelho, C.M., Brooks, R.A., Best, S.M. *et al.* (2006). Human Osteoblast Response to Silicon-Substituted Hydroxyapatite, *J. Biomed. Mater. Res. A*, **79**, 723–730.
30. Patel, N., Best, S.M., Bonfield, W. *et al.* (2002). A Comparative Study on the *In Vivo* Behavior of Hydroxyapatite and Silicon Substituted Hydroxyapatite Granules, *J. Mater. Sci. Mater. Med.*, **13**, 1199–1206.
31. Porter, A.E., Patel, N., Skepper, J.N. *et al.* (2004). Effect of Sintered Silicate-Substituted Hydroxyapatite on Remodelling Processes at the Bone-Implant Interface, *Biomaterials*, **25**, 3303–3314.
32. Bonfield, W. (2011). Engineering Business Success, *Ingenia*, **46**, 19–24.

Chapter 19

POROUS HYDROXYAPATITE

Edwin C. Shors and Ralph E. Holmes

19.1. INTRODUCTION

The rationale for using hydroxyapatite (HA) as a bone substitute material should be self-evident: natural bone is approximately 70% HA by weight and 50% HA by volume. The rationale for making the material macroporous is not so obvious, and necessitates an appreciation for the architecture of tissues and its effect on regeneration and repair. All of our organs, such as liver, kidney and bone, have a parenchymal and a stromal component. The parenchyma is the physiologically-active part of the organ; the stroma is the framework that supports the organization of the parenchyma. In soft tissues, loss of parenchyma with maintenance of stroma allows a remarkable degree of regeneration and repair. A bone defect might regenerate more predictably if a stromal substitute is implanted to provide a framework for organization of the osteons. By providing the bone defect with a stromal substitute, containing spaces morphologically compatible with the osteons and their vascular interconnections, a partnership between biomaterials and biologic regenerative and repair responses can be encouraged.[1]

Cortical bone consists of osteons or Haversian systems, which are held together by a hard tissue stroma or interstitium (see Section 19.8, Appendix A, for illustrations of bone architecture). The interstium does not have the Haversian canals and blood circulation of the osteons. Interosteonic communications, known as Volkmann canals, traverse the interstitial bone and permit blood to access the deepest osteons and maintain their osteocytes. Interstitial bone accounts for one-third of the volume of long bones, like the femur and tibia, with the remaining two-thirds consisting of the parenchymal osteons.[2,3] When designing an implant for osteoconduction, it would seem logical to mimic the architecture of this interstitial or stromal bone. Osteons average 190–230 μm in diameter, and intercommunicate through Volkmann canals. An idealized bone graft substitute would mimic osteon-evacuated cortical bone and have an interconnected porous system of channels of similar dimensions. These pore dimensions are in accord with the studies of Klawitter and Hulbert,[4] which established a minimum pore size of 100 μm for bone in-growth into ceramic structures.

Cancellous bone differs from cortical bone in being open-spaced and trabecular. The trabeculae represent "unrolled" osteons on both surfaces,

which are in apposition to a central framework of interstitial bone. An ideal cancellous bone graft substitute would mimic osteon-evacuated cancellous bone and have a thin lattice interconnected by pores of 500–600 μm. This chapter emphasizes the effects of porosity, since that is where bone regeneration takes place.

19.2. PROCESSING

19.2.1. Sintered HA

The most widely-used process to fabricate porous HA implants utilizes isostatic compaction and sintering (Chapter 1) of calcium phosphate powders that contain naphthalene particles.[5] Volatilization of the naphthalene particles leaves a porosity which consists of spherical voids communicating by a narrow-necked aperture wherever the particles were in contact. To permit bone in-growth of any depth, these apertures must exceed 100 μm or they will represent blind ends and discontinuities in bone. Another sintering process for creating a macroporous structure utilizes pretreatment with hydrogen peroxide.[6]

19.2.2. HA Cement

More recently, water-setting HA cements have been employed to create HA materials with various porosities.[7–9] The most completely-characterized HA cement in this group[10] is made by reacting tetra-calcium phosphate and calcium hydrogen phosphate in an aqueous environment.

$$Ca_4(PO_4)_2 + CaHPO_4 \rightarrow Ca_5(PO_4)_3OH \qquad (19.1)$$

Under *in vitro* conditions at 37°C, the HA cement sets in approximately 15 minutes and the isothermal chemical reaction is completed in 4 hours. Porosity is obtained by mixing the cement prior to set with sucrose granules and then dissolving the granules in water.

19.2.3. HA Conversion by Hydrothermal Exchange

During the early 1970s in the Material Research Laboratory at Pennsylvania State University, a process was developed that utilized the skeletal structure of marine invertebrates, especially reef building corals, as a template to make porous structures of other materials.[11] The calcium

carbonate skeleton is reacted with dominium hydrogen phosphate and, by means of a hydrothermal exchange of carbonate and phosphate, is converted to HA.

Under suitable temperature and pressure conditions the exchange results in a nearly pure HA. The HA structure is an exact replica of the porous marine skeleton, including its interconnected porosity. Prior to the exchange reaction, the organic component of these corals is removed with sodium hypochlorite. The extreme chemical and thermal conditions of the exchange reaction destroy any residual organic material. Of interest to present day environmental concerns is the lack of any impact due to harvesting these corals. Known as "nuisance coral" in the South Pacific, they are over-abundant and must be routinely removed from harbors and shipping lanes.

19.3. COMPOSITION

The chemical compositions of the different HA preparations are traditionally evaluated with X-ray diffraction. Preparations typically demonstrate a crystalline structure which is essentially pure HA with trace levels of beta tri-calcium phosphate, also known as beta-whitlockite (Fig. 19.1). This beta form of tri-calcium phosphate is also present within human bone at similar low concentrations.

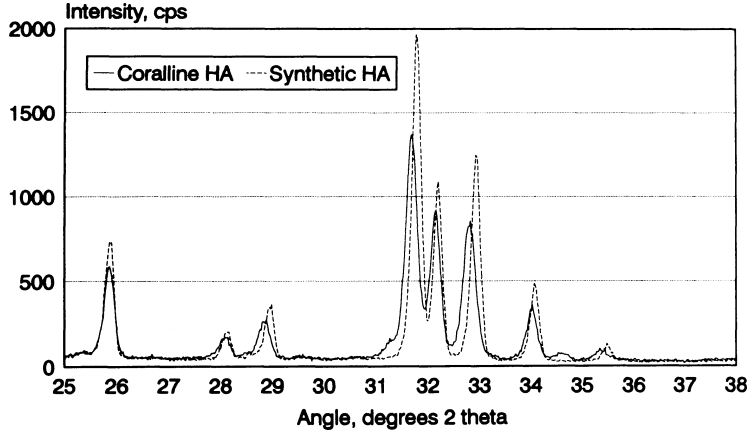

Figure 19.1. X-ray diffraction scan of synthetic HA standard compared with HA from hydrothermal exchange of coral skeleton carbonate with phosphate.

19.4. PROPERTIES

The porosity of sintered and cement forms of HA is dependent on the numbers and dimensions of the volatilized or dissolved particles. The degree of particle compaction and contact helps to determine the interconnectivity of the porosity. For example, the sintered HA material studied by Klein[6] contained pores of 150–250 μm. The volume fraction porosity and the pore interconnectivity were not reported. The HA cement material studied by Costantino[10] had a volume fraction porosity of 10% and 20%. The pore dimensions and connectivity were not reported.

Early research identified two species of coral as having suitable pore sizes for conversion into HA and subsequent use as a bone substitute.[12] The characteristics of the porosity in marine invertebrates were found to be genus and species dependent. Within a species and between members of that species, the average pore diameters were quite uniform, with a low range of variation throughout the structure. Accurate taxonomic identification thus assured a consistency of pore size and for the first time offered a legitimate educational reason for biomaterials students to visit and study in the West Indian and South Pacific littorals.

To mimic the osteon-evacuated stroma of cortical bone, the coral skeleton from the genus *Porites* was selected (Fig. 19.2). The solid framework and pore network are continuous with interconnected domains. The solid components of the implant framework average 75 μm and the interconnections average 95 μm.

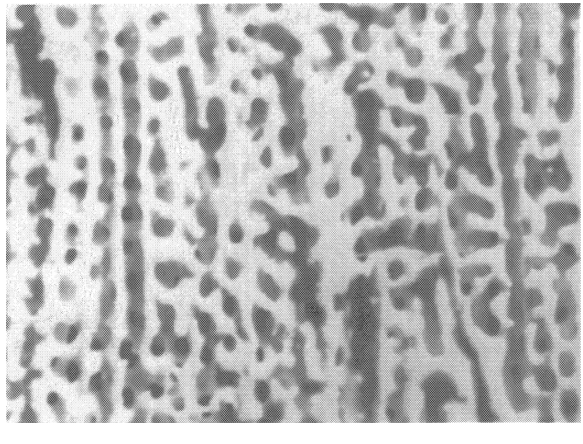

Figure 19.2. Microstructure of *Porites* coral skeleton after conversion to hydroxyapatite (HA200). Fenestrations of pore channel walls resulting in high degree of interconnectivity are easily seen.

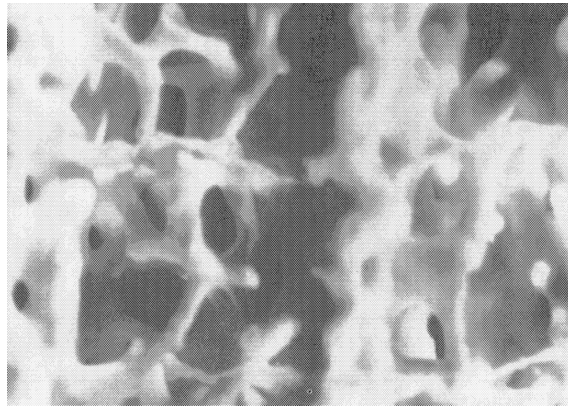

Figure. 19.3. Microstructure of *Goinopora* coral skeleton after conversion to hydroxyapatite (HA5OO). Trabecular framework with large interconnected pores is apparent.

The pores average 230 μm diameter and their interconnections average 190 μm diameter. The void volume fraction is 65%.[13]

To mimic the osteon-evacuated stroma of cancellous bone, the genus *Goniopora* was selected (Fig. 19.3). The solid components of its framework average 130 μm with interconnections that average 220 μm diameter. The pores average 600 μm diameter and their interconnections average 260 μm diameter. The void volume fraction is 63%.[13]

For brevity and ease of association with pore size, the HA form of *Porites* is called HA200 while that for *Goniopora* is called HA500. Both structures are comparable with human bone, Table 19.1.

Table 19.1. Comparison of the Microstructure of HA500 and Human Cancellous Bone (±SE).[17]

	HA500	**Iliac Bone**[14]	**Iliac Bone**[15]
Volume fraction (%)	35.1 ± 1.5	20.5 ± 0.4	20.3 ± 0.4
Surface area (mm^2/mm^3	5.3 ± 0.2	3.0 ± 0.1	3.4 ± 0.1
Ratio of surface area to volume fraction	15.3 ± 0.6	14.6 ± 0.6	17.3 ± 0.2
Mean trabecular width (μm)	131.9 ± 4.4	136.6 ± 4.5	120.3 ± 1.6
Mean pore width (μm)	245.0 ± 9.0	529.6 ± 22.9	468.2 ± 27.2

From White *et al.*[17]

Table 19.2. Biomechanical Properties of HA200.[17]

Property	Test	Orientation	Mean	Range
Crush Strength (psi)	Compression	Parallel	1343	997–1675
		Perpendicular	626	257–963
Ultimate strength ($N\text{-}cm^{-1}$)	Compression	Perpendicular	373	251–544
Stiffness ($N\text{-}cm^{-1}$)	Compression	Perpendicular	8300	3310–11470
Energy absorption (N-cm)	Compression	Perpendicular	9.9	4.5–13
Tensile strength ($gm\text{-}cm^{-2}\times10^{4}$)	4-point bending	Not reported	Not reported	2.4–3.3
Young's modulus ($gm\text{-}cm^{-2}\times10^{4}$)	4-point bending	Not reported	Not reported	5.2–6.0
Elastic modulus ($dynes\text{-}cm^{-2}\times10^{10}$)	Resonance frequency	Parallel	4.8	3.6–5.8
		Perpendicular	2.6	1.9–3.2

Table 19.3A. Failure Stress Values for HA500 (+SD).[36]

Direction	Tensile	Compressive	Transverse	Torsional	Bending
Parallel	188.7 ±---	851.7 ± 319.7	143.0 ± 41.3	41.3 ± 11.2	403.3 ± 97.5
Perpendicular	95.4 ± 49.4	489.0 ± 160.3	268.0 ± 98.5	40.2 ± 15.1	529.5 ± 224.7
Diagonal	122.0 ± 67.2	661.3 ± 267.0	495.7 ± 51.9	46.3 ± 18.0	332.8 ± 137.2

Table 19.3B. Moduli of HA500 (±SD).

Direction	Tensile	Compressive	Flexure	Rigidity
Parallel	56.0 ± ---	80.2 ± 54.4	110.0 ± 29.3	0.9 ± 0.4
Perpendicular	32.7 ± 11.7	36.5 ± 14.5	159.8 ± 69.4	0.9 ± 0.4
Diagonal	23.6 ± 14.1	56.2 ± 31.1	111.7 ± 35.2	1.1 ± 0.8

From Tencer *et al.*[36]

19.4.1. Biomechanical Propetties

Biomechanical properties of sintered and cement forms of porous HA depend on the degree of porosity. The biomechanical properties of HA200 and HA500 are presented in Tables 19.2 and 19.3.

The biomechanical properties of HA200 and HA500 are distinctly anisotropic, i.e., different in one direction than in the others, as a result of the growth characteristics of most scleractinian corals. The relationship between compressive strength and channel axis of the pores in HA200 has been well defined.[16] In the absence of any bone in-growth the ultimate compressive strength of HA200 is significantly less than cortical bone, while that of HA500 is similar to cancellous bone. The stiffness of HA200 as defined by conventional destructive testing is comparable with bone graft, but the implant material still fails like a ceramic with a brittle fracture. Like its dense form, porous HA materials have a low fatigue strength relative to most metals and polymers. Although not well studied, crack propagation has been considered to be partially ameliorated by the presence of pores.[17]

19.4.2. Surface Chemistry

The surface chemistry of the porous sintered and cemented HA are presumably not different from their dense forms. In the converted HA it has been noted that the crystallite size of the HA is significantly smaller than the crystallite size within the original coral. Although this reaction has been studied in detail, the explanation for this polycrystalline morphology is not well defined.[18,19] A high power scanning electron photomicrograph (Fig. 19.4) demonstrates this high surface area, which may be a factor in the osteoconductive behavior of this porous HA material.

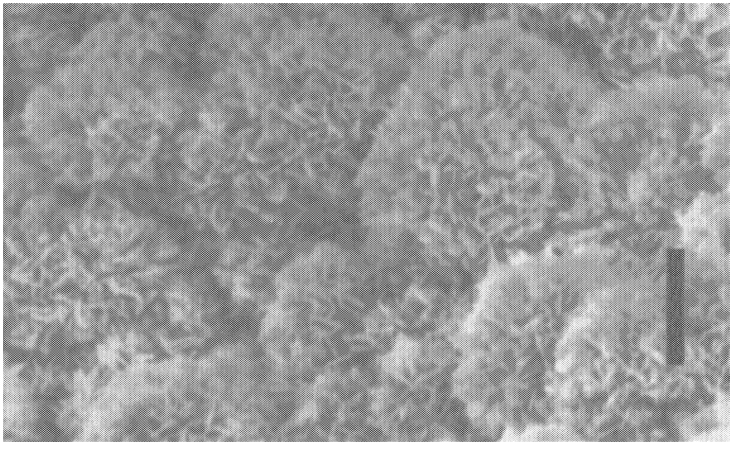

Figure 19.4. High power scanning electron micrograph of HA200 showing polycrystalline surface. Reference line indicates 15 μm.

19.5. TISSUE RESPONSE

19.5.1. In-growth

The tissue response to porous HA implants is inherently different from dense HA because of the opportunity for in-growth. Porosity and interconnectivity are key determinants of amount and type of in-growth. In highly porous and interconnected implants like HA200 and HA500, fibrovascular tissue in-growth starts by day three or four. By 28 days this in-growth is completed throughout the implant and apposition of bone against the pore walls has begun.[20–22] The spatial apposition of bone then progresses temporally from the implant surface towards the center.[23] A transient appearance of multinucleated giant cells has been reported.[24] The eventual bone–HA bonding within pores is considered to be like that documented for dense HA. Studies in several dog models have found bone in-growth to be nearly complete by three months (equivalent to six months in man). Data from HA200 in Table 19.4 and HA500 in Table 19.5 summarizes these studies.

Table 19.4. Tissue Volume Fractions (%) of HA200 Implants Retrieved from the Dog Radius After 3, 6, 12, 24, and 48 Months (± SE).[26]

Months	n	Soft Tissue	Bone	HA Matrix
3	3	12.1 ± 2.4	49.4 ± 2.4	38.6 + 1.5
6	3	13.7 ± 1.8	46.1 ± 2.1	40.2 ± 3.6
12	3	11.6 ± 2.3	52.7 ± 3.1	35.7 ± 1.2
24	3	7.7 ± 0.5	54.8 ± 1.0	37.6 ± 1.5
48	2	6.2 ± 1.1	54.3 ± 4.2	39.6 ± 3.2

Table 19.5 Tissue Volume Fractions (%) of HA500 Implants Retrieved from the Dog Proximal Tibial Metaphysis After 2, 4, 6, and 12 Months (± SE).[27]

Months	n	Soft Tissue	Bone	HA Matrix
2	2	57.3 ± 1.4	10.3 ± 0.6	32.6 ± 1.3
4	2	50.1 ± 1.6	11.6 ± 0.7	38.3 ± 1.5
6	2	51.2 ± 1.6	13.0 ± 0.7	35.9 ± 1.4
12	2	49.0 ± 1.7	17.3 ± 0.9	33.8 ± 1.6

The histologic appearance of the initial bone in-growth demonstrates an irregular and unorganized orientation of the collagen fibers and distribution of osteocytes that is characteristic of immature woven bone.[23] This initial bone is subsequently replaced with mature parallel fiber lamellar bone. This sequence is similar to normal bone formation. The woven bone of the embryo and newborn skeleton is gradually replaced with a parallel fiber lamellar bone which will remodel throughout life.[25] In dog studies, normal physiologic remodeling of the mature bone, reflecting the influence of Wolff's law, can be observed by 12 months. In diaphyseal radius implants of HA200 the intramedullary portion showed a substantial remodeling with removal of the bone in-growth (and preservation of bone in-growth within the intracortical portion).[26] In metaphyseal tibial implants of HA500 the HA pores within the cancellous region contained trabecular bone in-growth while the pores within the cortical shell regions contained osteonal bone in-growth.[27] The findings of these normal physiologic behaviors of bone (maturation sequence and response to Wolff's law) within the pores of HA characterizes the implant composition and microstructure (pore shape, size, and interconnectivity) as highly biocompatible.

19.5.2. Union and Incorporation

In orthopedic terminology, the tissue response of bone in-growth into graft or implant surface pores is called union. An implant or graft is said to be united when sufficient bone in-growth (approx. 200–500 μm depth) has occurred to unite host bed and implant as measured by histometry and shear testing. When bone in-growth throughout the pores is present, it is conceptually conceivable that the bone could occupy the pore center without contacting the pore walls, or it could contact the pore walls and thicken into the pore center. Apposition of bone in-growth against the walls of the implant or graft matrix is called incorporation. An implant or graft is said to be incorporated when the matrix is substantially coated with bone in-growth. In addition to traditional measures of osteocompatibility,[28] studies of animal specimens and human biopsies should ideally utilize an easy, accurate, and unbiased system of image acquisition and analysis which includes the measurement of specific implant matrix surface area and fraction of this area covered by bone in-growth.[29] As exemplified by the data in Table 19.6, the tissue response to porous HA implants can result in a high degree of incorporation.

Table 19.6. Porous HA Matrix Surface Areas (mm^2/mm^3) and Surface Fractions (%) Covered by Bone In-Growth in Implant Specimens Retrieved after 11–17 Months (±SD).[37]

Months	Surface Area	Surface Fraction
11	9.6 ± 0.8	88.8 ± 8.8
12	9.3 ± 0.9	90.2 ± 6.9
14	9.2 ± 0.4	89.3 ± 8.4
15	9.3 ± 0.4	96.6 ± 1.8
16	9.0 ± 0.6	92.2 ± 5.6
17	9.2 ± 0.7	90 ± 5.6

Table 19.7. Crush Strength (psi) in Compression of HA200 Before and after Bone In-Growth.[38]

	Before		After	
Orientation	Mean	Range	Mean	Range
Parallel	1343	997–1675	4776	2750–8479
Perpendicular	626	257–963	4529	2475–7562

19.5.3. Effect on Strength

In porous HA the tissue responses result in an implant–bone composite that significantly changes the original biomechanical properties. A high correlation (r = 0.92) was reported between the bending strength of porous HA and the amount of pore space occupied by bone in-growth.[30] In HA200 compressive strength was found to increase 3.5–7.2-fold and anisotropy of the original matrix was neutralized after bone in-growth (Table 19.7). In HA500 compressive strength was found to increase 2.7–6.8-fold after bone in-growth.[12]

19.5.4. Biodegradation

Two mechanisms — cell mediated and dissolution — participate in the biodegradation and resorption of HA in the body. The activity of both of these mechanisms is directly related to implant surface area. Because of its lower surface area, dense HA has demonstrated very low rates of biodegradation. Porous HA, on the other hand, can undergo a significant degree of resorption. Scanning electron microscopy of HA cement after setting revealed that it

is composed of small petal-like crystals with an interconnected microporosity averaging 2–5 nm in diameter. Experimental study of a macroporous form of this microporous HA cement has not been reported. However, when a microporous-only form of HA cement was used to obliterate the frontal sinus of cats, only 27% of the HA cement remained after 18 months.[31] HA converted by hydrothermal exchange has much larger micropores, 1–5 μm in diameter, resulting in a much smaller total surface area. Perhaps not surprisingly, converted HA only resorbs 1–2% per year.

The different sequences of biodegradation are probably important from a functional point of view. When placed in the cat sinus, a retreating front of HA cement resorption was replaced by an advancing front of new bone repair. The lack of mechanical strength at this front, of no consequence in the frontal sinus, might have serious consequences in a weight-bearing long bone. In contrast, HA200 and HA500 demonstrate no bulk front of resorption and replacement. The individual HA matrix members of converted HA become thinner by 1–2% per year, apparently replaced by bone, resulting in maintenance of the bulk dimensions of the implant and its mechanical strength, until it is finally "thinned" out of existence. The mechanisms of biodegradation of these different forms of HA, along with the biomechanical consequences, need further study.

19.6. CLINICAL APPLICATIONS

Of the different forms of porous HA materials, only the converted HA forms, HA200 and HA500, have undergone major clinical trials. Clinical applications in maxillofacial and orthopedic surgery continue to be evaluated. A representative study will be reviewed from each field of application. These studies are small and a larger database is required before all indications and contraindications can be determined.

19.6.1. Maxillofacial Surgery

In 92 consecutive patients undergoing orthognathic surgery, a total of 355 HA200 implants were placed in the maxilla (294), mandible (4), and midface (20).[32] In the 47 patients who had maxillary surgery, 202 implants were positioned directly adjacent to the maxillary sinus. Of these 202, 58 were placed in a maxillary step osteotomy, 99 in the lateral maxillary wall osteotomy, and 45 between the pterygoid plate and maxillary tuberosity. The remaining maxillary implants were placed interdentally (53) and midpalatally (36) after

segmentalization and expansion. Of the 41 mandible implants, 28 were positioned in the buccal cortical defect left by a sagittal split osteotomy, 10 were used for chin onlay, and 3 were used for chin interpositional inlay. Of the 20 midface implants, 12 were used for the lateral orbital rim, 7 for infraorbital only, and 1 for nasofrontal interposition.

These procedures, representing a broad spectrum of maxillofacial surgery, were associated with long-term complications in 4 of the 92 patients (4.3%). One patient developed bilateral maxillary sinusitis two months post-surgery, responded well to antibiotics and had no further problems. Two patients developed intranasal exposure of midpalatal implants which were removed at 6 and 14 months with no further problems. The fourth patient had persistent drainage from an interdental implant which was removed 21 months after surgery with no further problems. Cephalometric measurement and analysis of post-surgery facial bone position revealed stability equivalent to that seen after the use of autogenous bone grafts. Biopsies taken from 9 patients at 4–16 months post-surgery revealed structurally-intact implants that were both united and incorporated.[33] The biopsy specimens were composed of 48.5% HA200 matrix (range: 36.5–56.7%), 18% bone (range: 6.7–31%), and the remainder was soft tissue and vascular space. Up to nine months woven bone was still apparent, with longer-term biopsies showing only parallel-fiber lamellar bone.

Another maxillofacial application of interest is the use of HA200 in the form of 2–3 mm diameter granules placed in the floor of the maxillary sinus. The in-growth of bone into these granules provides more bone stock into which titanium cylinders and screws may be placed for use in dental restoration. In a series of four patients receiving implants in five maxillary sinuses, five biopsies were retrieved.[34] Histometric analysis demonstrated a mean bone in-growth of 23.1%, soft tissue in-growth of 44.9% and HA matrix of 31.9%. After biopsy confirmation of bone in-growth, a total of 12 dental implants were placed and subsequently used for dental restoration. Clinical studies of HA200 alone, mixed with cancellous autografts and infiltrated with bone marrow aspirate continue.

19.6.2. Orthopedic Surgery

A series of 46 patients with traumatic defects of their long bones underwent reconstruction with HA500 and stabilization with plate and screw fixation.[35] The mechanism of injury was motor vehicle accident in 32 cases, falls in 10, and gunshot injuries in 4. There were 25 men and 212 women, with an average age of 34.5 years (range: 17–67 years). All operations were performed between six hours

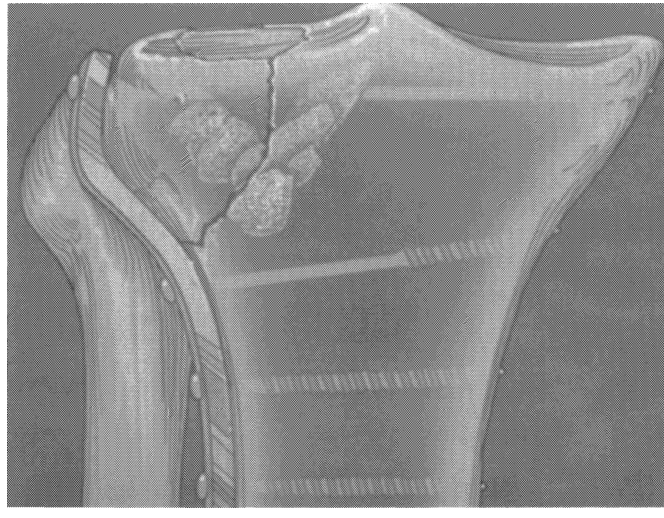

Figure 19.5. Illustration of tibial plateau fracture treated with porous HA implant. After returning the fragment to its anatomic position, a defect remained in the cancellous interior of the metaphysic, which was grafted with blocks of porous HA.

and five days from the time of injury. No supplemental autogenous bone graft was used in any of these 46 cases.

Metaphyseal (end-shaft) defects arising from axial compression injuries to adjacent joint surfaces constituted 34 of the cases. The location of the defect was tibial plateau in 23, distal tibia in 4, distal radius in 3, and distal femur in 4. All but three cases had displaced osteochondral fragments impacted into the crushed cancellous bone of the metaphysis. Following reduction and rigid internal fixation of all major components of the fracture, the resultant metaphyseal defects varied in volume from 1 to 120 cm^3 (mean: 9.5 cm^3; median: 2.5 cm^3). A satisfactory press fit of the HA500 block was achieved in all cases. An illustrative case is drawn in Fig. 19.5.

Diaphyseal (mid-shaft) defects, secondary to high energy bending forces, constituted the remaining 12 cases. The location of the defect was tibia in three cases, femur in two cases, humerus in three cases, radius in three cases, and ulna in two cases. The volume of cortical defects implanted with HA500 ranged from 1 to 4 cm^3. An illustrative case is drawn in Fig. 19.6.

Fracture union was achieved in all cases. As judged by disappearance of all cortical and cancellous fracture lines, fracture union occurred at an average of 28 weeks, identical with that noted in a comparable group of historical autograft

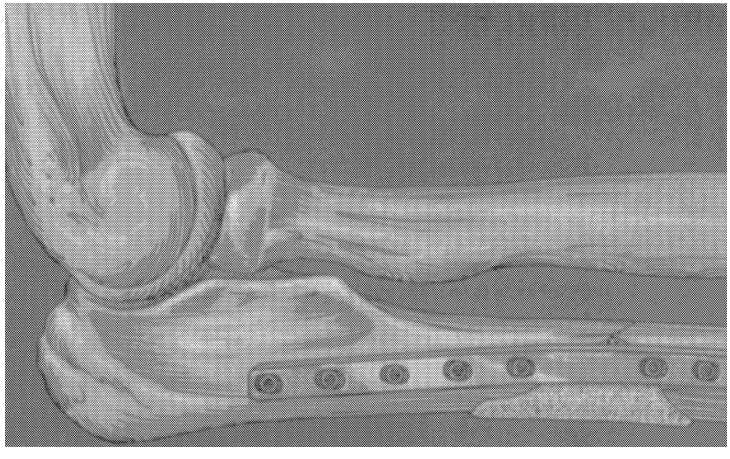

Figure 19.6. Illustration of radius fracture in forearm treated with porous HA implant. After stabilization with plate and screws, a segment of cortical bone was missing, this was then grafted with a block of porous HA.

controls. Four complications occurred in these 46 patients. These consisted of one early loosening of a humeral plate, one soft tissue slough, one contiguous septic arthritis, and one loss of reduction followed by a late onset infection. None of these complications were attributable to the porous HA implant.

Biopsy of the HA500 implant was performed in ten patients at the time of elective hardware removal. Fluoroscopic imaging was used to ensure that the biopsy was taken from the center of the implant. The time from surgery to biopsy averaged 11 months (range: 7–18 months). The biopsies cases included seven proximal tibial metaphyseal fractures, two distal tibial metaphyseal fractures, and one humeral diaphyseal fracture. Histologic evaluation showed compact bone in the superficial (cortical) portions of the biopsy specimens with regenerated osteons filling the HA pores. The deeper (cancellous) sections demonstrated normal appearing trabeculae in apposition to the HA matrix. Histometric analysis was performed on all biopsies and revealed an average bone volume fraction of 40.7%, HA matrix of 31.8%, and soft tissue and vascular space of 27.5%.

19.7. SUMMARY

A variety of possibilities exist for the fabrication of porous HA materials with differing porosities, interconnectivities, mechanical properties, surface chemistry, and tissue responses. The effects of these differing properties on the

success of clinical applications need more study. The diversity of reconstructive requirements for clinical defects of the skeleton is great and there is need for equally-diverse ceramic implant materials. Because HA materials are so brittle, their acceptance by clinicians remains low. New forms of HA materials that incorporate collagen or other similar polymers must be developed so clinicians can easily shape and fix the implants and that patients can walk without fear of failure while bone repair is taking place. (See Chapter 32 for a discussion of ceramic–polymer hybrid materials that offer the potential to satisfy this need.)

The cellular partnership between host repair and an implant providing a stroma or interstitium represents an exciting challenge to biomaterials scientists and clinicians. Future optimizations of these material and microstructural components will be combined with impregnation of bone growth factors and population by cultured osteoblast cells to reward the patients, clinician and biomaterials scientist with even more predictable and successful surgical outcomes.

19.8 APPENDIX A

An Illustration of the Microstructure of Human Cortical Bone.

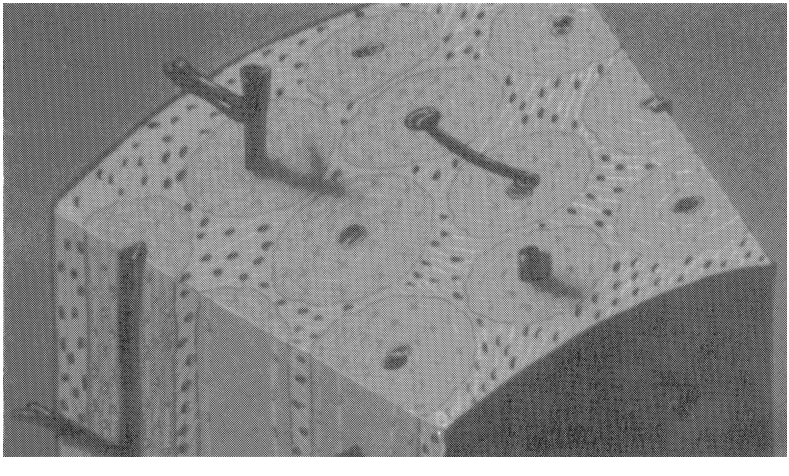

The cylindrical osteons or Haversian systems represent the parenchymal component of bone. Blood flowing through the Haversian canals supply osteocytes contained between the osteonal lamellae. Interstitial or stromal bone occupies the space between osteons. Note fenestrations or Volkmann canals in the interstitial bone which permit interosteonic passage of blood supply.

REFERENCES

1. Holmes, R.E. (1990). "Alloplastic Implants", in McCarthy, J.G. (ed.), *Reconstructive Plastic Surgery, 3rd ed.*, W. B. Saunders Co., Philadelphia, PA, pp. 698–731.
2. Currey, J.D. (1964). Some Effects of Ageing in Human Haversian System, *J. Anat.*, **98**, 69–75.
3. Evans, F.G. and Bang, S. (1966). "Physical and Histological Differences Between Human Fibular and Femoral Compact Bone", in Evans, F.G. (ed.), *Studies on the Anatomy and Function of Bone and Joints*, Springer-Verlag, New York, pp. 142–150.
4. Klawitter J.J. and Hulbert, S.F. (1971). Application of Porous Ceramics for the Attachment of Load Bearing Orthopedic Applications, *J. Biomed. Mater. Res. Symp.*, **2**, 161–229.
5. Hubbard, W. (1974). *Physiological Calcium Phosphates as Orthopedic Biomaterials* (PhD Thesis, Marquette University).
6. Klein, C., Patka, P. and den Hollander, W. (1989). Macroporous Calcium Phosphate Bioceramics in Dog Femora: A Histological Study of Interface and Biodegradation, *Biomaterials*, **10**, 59–62.
7. Brown, W.E. and Chow, L.C. (1986). "A New Calcium Phosphate, Water-Setting Cement", in Brown P.W, (ed.). *Cements Research Progress*, American Ceramic Society, Westerville, OH, pp. 352–379.
8. Capano, P.J. (1987). *The Chemical Synthesis, and Biomedical and Dental Applications of the First Truly Successful* In Vivo *Replacements for Bones, Teeth, and Similar Materials* (PhD Thesis, University of Texas at Austin).
9. Constantz, B., Young, S.W., Kienapfel, H. *et al.* (1991). Pilot Investigations of a Calcium Phosphate Cement in a Rabbit Femoral Canal Model and a Canine Humeral Plug Model, *Transactions of the 17th Annual Meeting, Society for Biomaterials, Scottsdale, AZ, May 1–5*, 92.
10. Costantino, P.D., Friedman, C.D., Jones, K. *et al.* (1991). Hydroxyapatite Cement: I. Basic Chemistry and Histologic Properties, *Arch. Otolaryngol. Head Neck Surg.*, **117**, 379–384.
11. Roy, D.M. and Linnehan, S.K. (1974). Hydroxyapatite Formed from Coral Skeletal Carbonate by Hydrothermal Exchange, *Nature*, **241**, 220–222.
12. Holmes, R., Mooney, V., Bucholz, R. *et al.* (1984). A Coralline Hydroxyapatite Bone Graft Substitute, *Clin. Orthop.*, **188**, 252–262.

13. Hanusiac, W.M. (1977). *Polymeric Replamineform Biomaterials and a New Membrane Structure* (PhD Thesis, Pennsylvania State University).
14. Malluche, H.H., Meyer, W., Sherman, D. *et al.* (1982). Quantitative Bone Histology in 84 Normal American Subjects: Morphometric Analysis and Evaluation of Variance in Iliac Bone, *Calcif. Tissue Internat.*, **34**, 449–455.
15. Merz, W.A. and Schenk, R.K. (1970). Quantitative Structural Analysis of Human Cancellous Bone, *Acta. Anat.*, **15**, 54–66.
16. Tencer, A.F., Mooney, V., Brown, K.L. *et al.* (1985). Compressive Properties of Porous Coated Hydroxyapatite for Bone Grafting, *J. Biomed. Mater. Res.*, **19**, 957–969.
17. White, E. and Shors, E.C. (1973). Biomaterials Aspects of Interpore-200 Porous Hydroxyapatite, *Dent. Clin. North Am.*, **30**, 49–67.
18. Eysel, W. and Roy, D.M. (1973). Hydrothermal Flux Growth of Hydroxyapatite by Temperature Oscillation, *J. Crystal Growth*, **20**, 245–250.
19. Eysel, W. and Roy, D.M. (1975). Topotactic Reaction of Aragonite to Hydroxyapatite. *Zeitschrift für Kristallographic*, **141**, 11–24.
20. Finn, R.A., Bell, W.H. and Brammer, J.A. (1980). Interpositional Grafting with Autogenous Bone and Coralline Hydroxyapatite, *J. Maxillofac. Surg.*, **8**, 217–227.
21. Piecuch, J.F., Topazian, R.G., Skoly, S. *et al.* (1983). Experimental Ridge Augmentation with Porous Hydroxyapatite Implants, *J. Dent. Res.*, **62**, 148–151.
22. Butts, T.E., Peterson, L.J. and Allen, C.M. (1989). Early Soft Tissue Ingrowth into Porous Block Hydroxyapatite, *J. Oral Maxillofac. Surg.*, **41**, 475–479.
23. Holmes, R.E. (1979). Bone Regeneration within a Coralline Hydroxyapatite Implant, *Plast. Reconstr. Surg.*, **63**, 626–633.
24. Itatani, C. and Marshall, G.J. (1984). Cellular Responses to Implanted Replamineform Hydroxyapatite, *Trans. Orthop. Res. Soc.*, **9**, 123.
25. Ogdon, J.A. (1980). "Chondro-Osseous Development and Growth", in Urist, M.R. (ed.), *Fundamental and Clinical Bone Physiology*, J.B. Lippincott, Philadelphia, PA, pp. 108–171.
26. Holmes, R.E., Bucholz, R.W. and Mooney, V. (1987). Porous Hydroxyapatite as a Bone Graft Substitute in Diaphyseal Defects: A Histometric Study, *J. Orthop. Res.*, **5**, 114–121.
27. Holmes, R.E., Bucholz, R.W. and Mooney, V. (1986). Porous Hydroxyapatite as a Bone Graft Substitute in Metaphyseal Defects, *J. Bone Joint Surg.*, **68A**, 904–911.

28. Tencer, A.F., Holmes, R.E. and Johnson, K.D. (1986). "Osteocompatibility Assessment", in von Recum, A.F. (ed.), *Handbook of Biomaterials Evaluation: Scientific, Technical, and Clinical Testing of Implant Materials*, Macmillan Publishing Company, New York, pp. 321–338.
29. Holmes, R.E., Hagler, H.K. and Coletta, C.A. (1987). Thick-Section Histometry of Porous Hydroxyapatite Implants Using Backscattered Electron Imaging, *J. Biomed. Mater. Res.*, **21**, 731–739.
30. Martin, R.B., Chapman, M.W., Holmes, R.E. *et al.* (1989). Effects of Bone Ingrowth on the Strength and Non-Invasive Assessment of a Coralline Hydroxyapatite Material, *Biomaterials*, **10**, 481–488.
31. Friedman, C.D., Costantino, P.D., Jones, K. *et al.* (1991). Hydroxyapatite Cement:II. Obliteration and Reconstruction of the Cat Frontal Sinus, *Arch. Otolaryngol. Head Neck Surg.*, **117**, 385–389.
32. Wolford, L.M., Wardrop, R.W. and Hartog, J.M. (1987). Coralline Porous Hydroxylapatite as a Bone Graft Substitute in Orthognathic Surgery, *J. Oral Maxillofac. Surg.*, **45**, 1034–1042.
33. Holmes, R.E., Wardrop, R.W. and Wolford, L.W. (1988). Hydroxylapatite as a Bone Graft Substitute in Orthognathic Surgery: Histologic and Histometric Findings, *J. Oral Maxillofac. Surg.*, **46**, 661–671.
34. Smiler, D.G. and Holmes, R.E. (1987). Sinus Life Procedure using Porous Hydroxyapatite: A Preliminary Clinical Report, *J. Oral Implantology*, **13**, 17–32.
35. Bucholz, R.W., Carlton, A. and Holmes, R.E. (1987). Hydroxyapatite and Tricalcium Phosphate Bone Graft Substitute, *Orthop. Clin. North Am.*, **18**, 323–334.
36. Tencer, A.F., Shors, E.C., Woodard, P.L. *et al.* (1991). "Mechanical and Biological Properties of a Porous Polymer-Coated Coralline Ceramic", in Yamamuro, T., Hench, L.L., Wilson J. (eds), *Handbook of Bioactive Ceramics, Vol. II, Calcium Phosphate and Hydroxylapatite Ceramics*, CRC Press, Boca Raton, FL, pp. 209–221.
37. Holmes, R.E. and Roser, S.M. (1987). Porous Hydroxyapatite as a Bone Graft Substitute in Alveolar Ridge Augmentation: A Histometric Study, *Int. J. Oral Maxillofac. Surg.*, **16**, 718–728.
38. Piecuch, J.F., Goldberg, A.J., Shastry, C.V. *et al*. (1984). Compressive Strength of Implanted Porous Replamineform Hydroxyapatite, *J. Biomed. Mater. Res.*, **18**, 39–45.

Chapter 20

STABILITY OF CALCIUM PHOSPHATE CERAMICS AND PLASMA SPRAYED COATINGS

C.P.A.T. Klein, J.G.C. Wolke and K. de Groot

20.1. INTRODUCTION

In hard tissue replacement, permanent attachment of limb prostheses or total tooth implants, a biomaterial must interface with bone. The biocompatibility of implant materials is optimal when the material elicits the formation of normal tissues at its surface and establishes a contiguous interface capable of transferring the loads which normally occur at the implantation site. To what extent bone-plus-implant will be able to function as an integrated mechanical unit depends on: the mechanical and physiological characteristics of the living bone; the chemical, mechanical and physical properties of the implant; and the interaction between bone and implant.[1–3]

The main inorganic phases of bones and teeth of vertebrates, as well as hard tissues of humans, although chemically quite complex, appear to be predominantly in a single structural state closely resembling that of hydroxyapatite, $Ca_{10}(PO_4)_6(OH)_2$, (HA). Biological apatites are known for their occurrence in non-stoichiometric form, usually with low Ca/P ratios, and contain, besides structural imperfections and defects, substantial amounts of foreign ions such as CO_3^{2-}, citrate, Mg^{2+} and Na^+, and trace amounts of Cl^-, F, K^+, Sr^{2+} and other metal ions (see also Chapter 17).[4–6]

The synthetic form has been shown to be chemically and crystallographically similar, although not identical, to naturally occurring HA and has thus received a great deal of attention for use as bone graft substitute.[7,8]

Calcium phosphate implant materials are composed of the same ions which make up the bulk of the natural bone mineral. Because of this, these materials, when implanted in bone, are capable of participating in calcium phosphate solid-solution equilibria at their surfaces. The required calcium and phosphate ions needed to establish their equilibria may be derived from the implant, the surrounding bone, or both.[9–11]

The biocompatibility of synthetic HA is not only suggested by its composition but also by results of *in vivo* implantation, which has produced no local or systemic toxicity, no inflammation and no foreign body response. Many

investigators have demonstrated direct bone apposition of new bone to HA. This bone contact appears to be direct, without an intervening fibrous layer. During mechanical testing, fracture often occurs through the bone and/or HA, rather than at the bone–HA interface. The intimate bonding of new bone to HA is the main advantage of using HA as a bone graft substitute.[12–16]

Calcium phosphate ceramics can be made with properties resembling those of hard tissues. Dense ceramics with a compressive strength >500 Mpa, as well as porous ceramics allowing bony in-growth, can be prepared. Another approach to influence the processes at the biomaterial–bone interface is the use of biomaterials with controlled chemical breakdown characteristics, i.e., bioactive/biodegradable materials. With time, such biomaterials should be totally resorbed by the body and replaced by tissues. Consequently, the function of totally biodegradable biomaterials is merely to serve as a scaffolding or filler of space, thereby permitting tissue infiltration and replacement. Essentially, this is the same function as that of bone grafts. A major advantage of the use of resorbable bioceramics over autologous bone grafts is a ready supply, controlled variations in size and elimination of a second surgical procedure. However, a disadvantage of this type of bioceramic is the serious strength reduction that occurs during the resorption process. Consequently, mechanical design factors must be seriously taken into account to prevent fracturing of the resorbable ceramic during the intermediate stages of healing. Biodegradable implants are preferable when they are used ultimately to restore the normal function of bone. These implants should encourage bone growth and facilitate integration of the implant with bone, the rate of its resorption should match the rate of the bone formation, and the reduction in implant strength should closely match the increase in strength of the healing tissues.

So-called tri-calcium phosphates (TCP) appear to be the most suitable bioceramics of this type.[17] With a nominal composition of $Ca_3(PO_4)_2$, this material has a Ca/P ratio of 1.50. TCP is found in two different whitlockite crystallographic configurations, α-TCP and the more stable β-TCP.[8,13] Due in part to its crystalline structure, the biodegradation rate of TCP has been shown to be much greater than that of HA.[8,18] While the exact mechanism of biodegradation remains unclear, some researchers suggest that when placed in an acidic environment, TCP dissolves *in situ.*[13] Other investigators noted osteoclast-like cells attached to the surface of the implanted TCP and suggest a cellular breakdown by macrophages.[19,20]

As the material resorbs, new bone fills the area once occupied by the TCP implant. While much of the TCP implant is resorbed within the first months, some material remains in the defect site for extended periods, perhaps years in

humans.[20–22] The material that is not resorbed appears to be incorporated within the new bone structure. Resorbable TCP or β-whitlockite ceramics give rise to more bone remodeling activity than HA ceramics. Depending on the Ca/P ratio, an irregular or more planar bone formation is present at the ceramic surface.[13,24–26]

Data on biodegradability of the different calcium phosphate ceramics (HA or TCP, dense or porous) are conflicting. The reported experimental conditions show a variety of surgical procedures and animal models. Also, manufacturing conditions, crystal structure, Ca/P ratio, impurities, degree and type of porosity were not clearly defined.[27]

Because the mechanical properties of calcium phosphate bioceramics are limited, they should either be unloaded or loaded only in compression. To achieve the high strength necessary for implants, metal alloys can be coated with calcium phosphate particles. The bone-bonding capacity of these coatings may help cementless fixation of orthopedic prostheses. It has been shown that skeletal bonding is enhanced immediately after implantation.[13,28,29] Coatings on metals and other substrates (ceramics, polymers and composites) have been applied by a variety of methods including, dip, plasma spraying, electrophoretic deposition, sputter coating, hot isostatic pressing and ion assisted sputtering (see also Chapter 21).[30,31]

Variations of the material properties of calcium-phosphate coatings affect the bone-bonding mechanism and the rate of bone formation. Local supersaturation in the constituent ions of the bone mineral phase, arising from enhanced solid-solution exchange at the coating surface, could be a cause of bone tissue growth enhancement.[32] Variation in Ca/P ratios (2.0–1.5), i.e., tetra-calcium phosphate, HA and α/β-TCP, lead to differences in degradability and to differences in bone contact.[20,33–35] Composition changes by addition of fluorine to apatite or magnesium to β-whitlockite will also influence the stability of the coating.[36,39] Understanding the cause of biodegradation of calcium phosphates and enhancement of bone tissue in-growth or bonding requires knowledge of the characteristics of the calcium-phosphate coating itself and the coating process.

20.2. CALCIUM PHOSPHATE BIOCERAMICS

20.2.1. Density

Dense ceramics are usually made by compressing a powder into a pellet, which is then subjected to a heat treatment that causes the powder particles to fuse by means of solid-state diffusion. Such process is called sintering and is described in Chapter 1. Depending on variables such as sintering temperature, time and

particle size distribution, a dense shape can be produced. “Dense” is defined as less than 5% (in volume) porous. Several methods are used to introduce macropores into a bioceramic as described in Chapter 19.[41,42]

Both the material tensile and compressive strength depend on the material volume portion occupied by interstices. These interstices or porosities are usually classified as comprising either micropores (having a diameter of several microns due to the incomplete sintering of the particles) or macropores (having a diameter of several hundred microns allowing bone in-growth).

20.2.2. Stability

Although calcium phosphate bioceramics are usually obtained by sintering at high temperatures, sometimes with the exclusion of water vapor, it is the stability at ambient and body temperatures that determines their fate after implantation. Since solid-state reactions hardly ever occur at room temperatures, solid, unstable phases will only react at their surfaces. If the surface continually dissolves, the whole implant may dissolve. If surface reactions lead to the formation of a thin layer of a second stable phase, the virtual absence of solid-state reactions causes the unstable solid to be stabilized. As Driessens showed,[43] there are only two calcium phosphate materials that are stable at room temperature when in contact with aqueous solutions, and it is the pH of the solution that determines which one is stable. At a pH lower than 4.2, the component $CaHPO_4\ 2H_2O$ (dicalcium phosphate) is the most stable, while at higher pH (>4.2), HA is the stable phase (Fig. 20.1). High-temperature stability of calcium phosphates is best illustrated by the phase diagrams shown in Figs. 20.2–20.4. These focus on temperatures at which sintering processes usually take place, 1,000–1,500°C.

Figure 20.2 shows that when the ambient atmosphere contains no water, various calcium phosphates can be found at high temperatures, such as tetracalcium phosphate (=C4P), α-tricalcium-phosphate (α-C3P), monetite (=C2P) and mixtures of calcium oxide (CaO) and C4P. HA is not stable under these conditions.

If the partial water pressure is increased from 0 to 50 mmHg (Fig. 20.3) then the situation is quite different: HA can be found (=Ap). If the ratio Ca/P is not exactly equal to 10/6, a wide range of apatite-containing mixtures is thermodynamically stable, e.g., tetra-calcium phosphate, triphosphate and calcium oxide (CaO).

The two phase diagrams, Figs. 20.3 and 20.4, stress the importance of temperature, exact Ca/P ratio and partial pressure of water vapor in the ambient atmosphere in the determination of stable phases. β-Triphosphate turns into

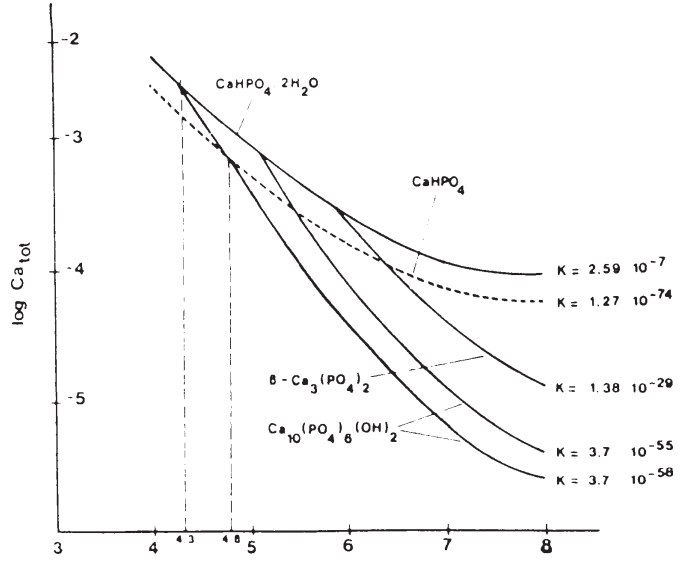

Figure 20.1. Solubility of various phases in the system CaO P_2O_5 H_2O as function of pH (horizontal axis).

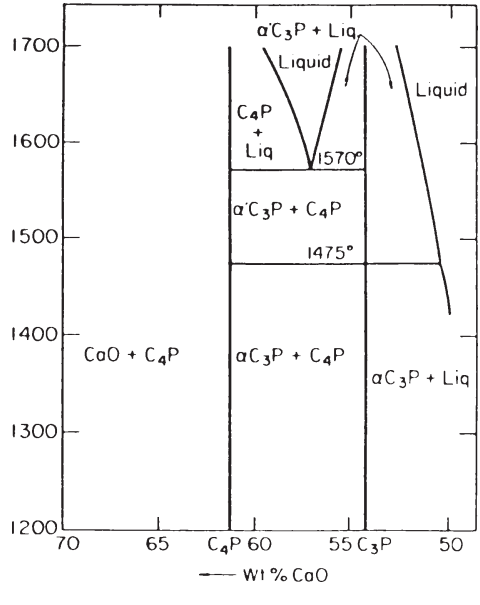

Figure 20.2. Phase diagram of the system CaO P_2O_5 at high temperature (vertical axis °C). No water present.

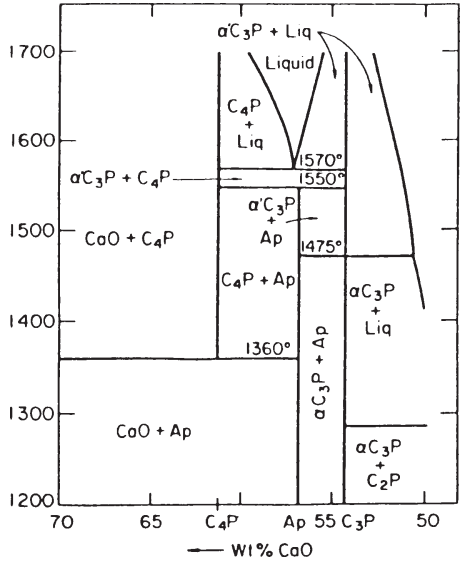

Figure 20.3. Phase diagram of the system CaO P_2O_5 at high temperature (vertical axis °C). Water vapor P_{H_2O} = 500 mmHg.

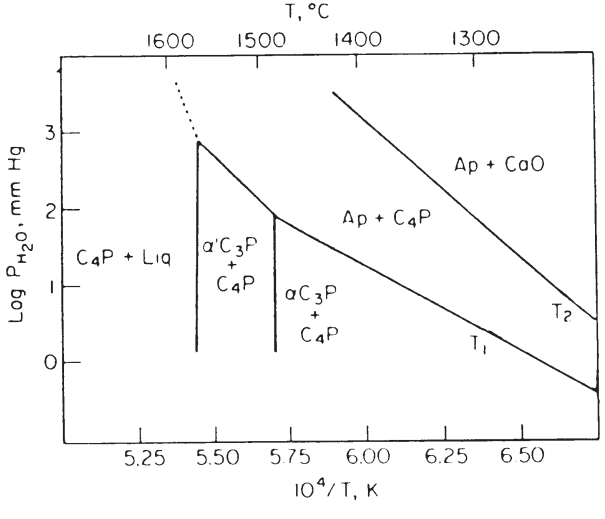

Figure 20.4. Influence of ambient water vapor pressure (vertical axis P_{H_2O} in mmHG) on phase composition.

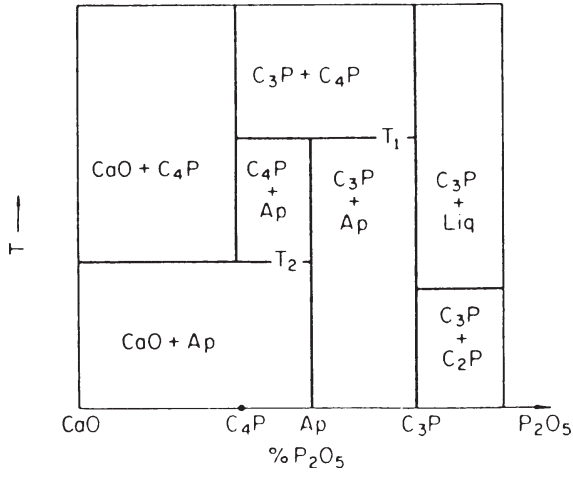

Figure 20.5. Enlarged part of Fig. 20.3. Instead of 1,360°C, we use T_2, and instead of 1,475°C we use T_1 to indicate that these values hold only for P_{H_2O} = 500 mmHG.

α-triphosphate around 1,200°C; the latter phase is considered to be stable in the range 700–1,200°C.

The importance of partial water pressure is shown more clearly in Fig. 20.5, an enlarged part of Fig. 20.3. This diagram shows that for a Ca/P ratio higher than 10/6, at temperature of 1,300°C ($10^4/T = 6.4$, if T is expressed in °K), the stable phase is C3P + C4P, if the vapor pressure is 1 mmHg ($\log P_{H_2O} = 0$). The stable phases are Ap + C4P at 10 mmHg. Mixtures of Ap + CaO are stable at pressures of around 100 mm Hg. Thus, with a Ca/P ratio exceeding that of apatite by only a few percent, stable phases can vary from C3P + C4P($\log P_{H_2O} = 0$), Ap + C4($\log P_{H_2O} = 1$) and Ap + CaO ($\log P_{H_2O} = 2$). Control over temperature, Ca/P ratio and vapor pressure during sintering provides the stability to produce a wide range of well-defined calcium phosphate products.

If these conditions are not controlled, a less well-defined end product may result.[44] Both Ca^{2+} and PO_4^{3-} ions, as well as the OH^- group in HA, can be replaced by other ions, several of them present in physiological surroundings, for example fluorine, magnesium or carbonate. In synthetic apatite, carbonate can partially substitute for OH^- and PO_4^{3-} ions in the crystal lattice, while magnesium is incorporated only to a very limited extent. Further, these ions decrease the crystallinity of synthetic apatite and promote the formation of amorphous calcium phosphate. Magnesium ions stabilize triphosphates (see Chapter 17 for details).

20.2.3. Biodegradation of Calcium Phosphate Bioceramics

Biodegradation data on different calcium phosphate ceramics are contradicting. Many authors[18,28,45–50] report rather fast degradation of β-whitlockite, while others[51,53] report a minimal or very slow resorption. Many investigators[18,54–56] found no degradation of HA, whereas another described resorption.[57] It is thought that the chemical composition of the ceramic determines whether or not calcium phosphate materials with 1< Ca/P ratio >2 are degradable.[17,50] This question has been investigated by Klein *et al*.[35,43,58,59] A well-defined series of HA and β-whitlockite crystal structures were investigated, with microporosity ranging from 2 to 55% and with macroporosity of either 0 or 30%. These experiments show that the composition, Ca/P ratio, impurities like F^- or Mg^{++} and structural relationships (micro-/macrostructure) are important factors associated with biodegradation. Ceramics with a Ca/P ratio 1.67 are more stable. Microporosity plays a more dominant role than the macroporosity. Microporosity determines the geometry of "necks" between sintered particles, while macroporosity determines the amount of necks in contact with the environment. The "neck" formation depends on preparation technique, sintering temperature and the pressure applied to compress the powder into a tablet before sintering. Varying the surface chemistry by addition of F^- or Mg^{++} ions decreased the biodegradation rate.

LeGeros *et al*.[8] studied the influence of the β-TCP/HA ratios on biodegradation and *in vivo* transformation. The higher the ratio, the greater the extent of dissolution; β-TCP will dissolve earlier than HA. The processes of dissolution and precipitation appeared to occur simultaneously and are correlated with the ratio. The resorption of β-TCP/HA appears to occur simultaneously with bone formation. For the same material (HA) and the same pH, dissolution rates vary considerably in different buffers.

Table 20.1 shows that the dissolution rate of HA at pH 7.2 varies from 97.4 when buffered in citrate to 44.3 in Gomori's buffer. Without buffers, dissolution studies yield quite different results. In addition to Klein *et al*.,[35] Bauer *et al*.[60] showed that in deionized water the pH may change from 8.6, when tri-phosphate is incubated, to 12.3 for tetra-calcium phosphate. Solubilities decrease rapidly with increasing pH; one expects to find a very low apparent dissolution rate for tetra-calcium phosphate under such conditions. This explains the finding by Adam *et al*.[61] that dissolution of tetra-calcium phosphate is lower than that of HA. When the same buffer is used, HA has a lower solubility rate than both tri-phosphate and tetra-calcium phosphate; however, it is uncertain that this is relevant *in vivo*, where the fluids are probably saturated with respect to calcium and phosphate.

Table 20.1. Concentration of Ca and P (ppm) after One Week Incubation in Various Buffers.

	Citrate		Gomori's		Deionized H_2O	
Material	**Ca**	**P**	**Ca**	**P**	**Ca**	**P**
TCP[a]	85.0	45.9	48.9	19.6	4.6	1.7
HA[a]	97.4	43.8	44.3	17.6	5.1	2.2
Tetra[a]	70.3	47.9	77.6	18.6	9.7	2.2
TCP[b]	153	82.5	17.1	8.0	3.3	1.5
HA[b]	44.0	19.8	10.8	4.3	44.4	2.3
Tetra[b]	351	127	94.4	9.0	8.8	0.2

[a]30 mg sintered powder particles/30 ml buffer: [b]coated plug (= 15 mg coating)/30 ml buffer.

20.3. PLASMA–SPRAYED COATINGS OF CALCIUM PHOSPHATE

20.3.1. Plasma Spray Technique

The plasma spray technique is described in Chapter 21. The very high temperature of plasma spraying can lead to dehydroxylation or phase transformations in the coating. The transition temperature of tri-calcium phosphate is around 1,200°C, HA decomposes at 1,300°C, tetra-calcium phosphate and fluorapatite are stable above 1,300°C. Hence the capacity of the plasma flame to induce phase transitions decreases in this order. However, HA shows dehydroxylation, β-whitlockite changes to α-whitlockite and tetra-calcium phosphate will turn into an HA crystalline structure. Plasma spraying decreases crystallinity.

Ideally, only a thin outer layer of each powder particle should become molten in the plastic state in which phase transition is unavoidable. This plastic state is necessary to ensure dense and adhesive coatings, but should comprise a negligible volume fraction of the calcium phosphate particles. By choosing an optimum relation between particle size and type of gas (heat content of a plasma, and thus ability to increase the temperature of a particle, depends strongly on the gas used), speed of the plasma (the longer a particle resides in a plasma, the higher its temperature) and cooling process of the coated surface, one obtains coatings with the desired calcium phosphate(s) and crystallinity.

Figure 20.6 shows the influence of different plasma gases on the coating crystallinity. Plasma gas argon mixed with hydrogen gives a higher degree of crystallinity, but without hydrogen the powder particles cannot enter the gas. This is because the high velocity and viscosity of the argon gas causes the particles to

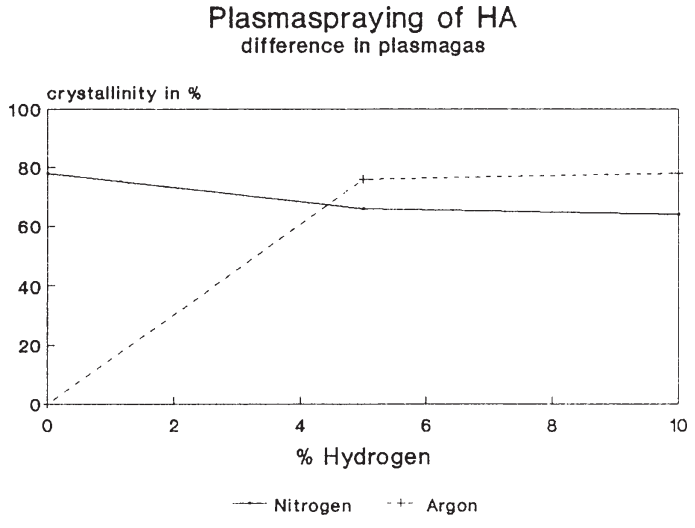

Figure 20.6. The influence of different plasma gases on the crystallinity of the coating.

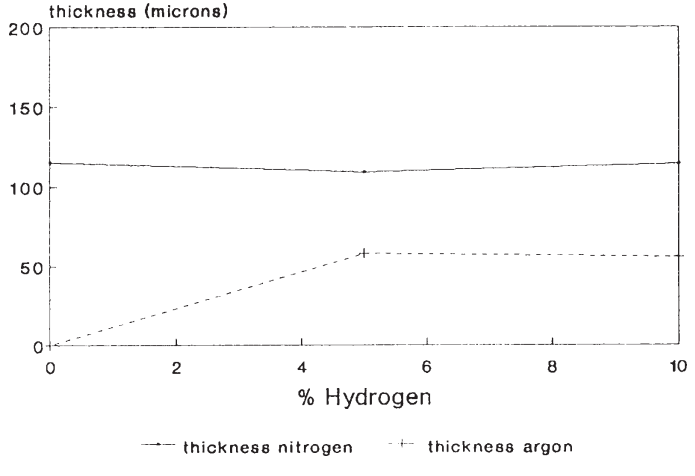

Figure 20.7. The influence of different plasma gases on the thickness of the coating.

bounce back from the flame, instead of entering. Figure 20.7 shows that the plasma gas nitrogen gives a thicker coating layer compared to argon. An important criterion is the calcium oxide formation which can react with water and destroy the coating layer. Figure 20.8 shows that using higher hydrogen content

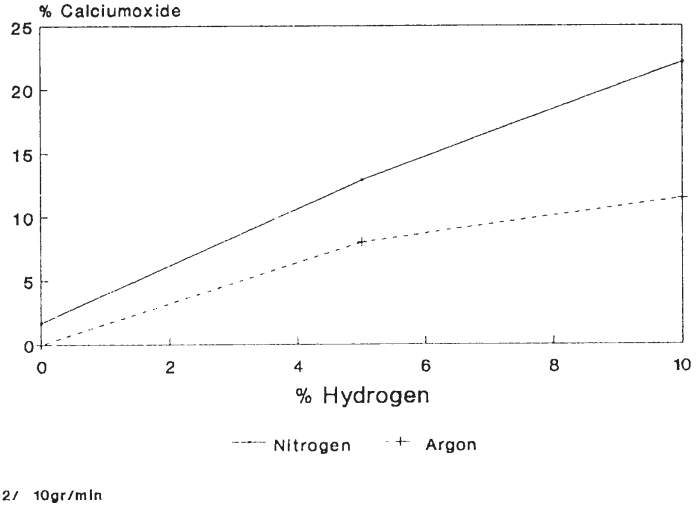

Figure 20.8. The influence of different plasma gases on the % calcium oxide in the coating.

results in more calcium oxide than the use of nitrogen only. Hydrogen leads to more enthalphy in the flame and a lower flame velocity, thus the particles undergo more melting and decomposition.

20.3.2. Physico-Chemical Properties

An important aspect of plasma-sprayed ceramic coatings is their thickness. A mismatch in thermal properties coupled with the fast coating rate of the coating material during the plasma spray process gives rise to stresses in the coating and substrates; these stresses increase with the thickness of the coating. The compressive stress at the coating–substrate interface weakens the bond strength, therefore, the thinner the coating, the higher its bond strength.

It has been shown (through finite element analysis) that bond strength usually suffers from significant stress concentration effects. Since these effects are a function of variation in elastic modulus, the testing method, shape of testing sample and thickness of the brittle layer, bond strength measurements have only a relative value.

For plasma-sprayed coatings, two methods are used to determine bond strength.

Table 20.2. Tensile Strength of Different Glues.

	Strength	Failure Mode	n
Araldite® AV 118	60.8 MPa	100% Glue/HA	5
3M	38.3 MPa	100% Glue/HA	5
Lee Insta-Bond	5.4 MPa	100% HA/Ti	3
Concise	11.7 MPa	100% HA/Ti	3

Table 20.3. Tensile Strength of Different Coating Thickness Glued with Araldite® AV 118.

	Strength	Failure Mode	n
40 μm	66.8 MPa	100% Glue/HA	5
80 μm	60.7 MPa	100% Glue/HA	5
120 μm	45.3 MPa	100% HA/Ti	2

1. Scratch testing, in which a sharp needle under a given weight necessary to reach the underlying metallic surface is an indication of the comparative "bond strength".
2. Tensile and shear testing, in which, by means of a glue, loads normal and parallel, respectively, are applied to the ceramic coating. The loads expressed in force per area are the tensile and shear strength, respectively.

HA coatings have only been subjected to the second test: tensile and shear strength determination. We have coated rods with a layer of 50 μm. For tensile strength measurement we coated the cross section (having an area of 0.95 cm^2), and for shear strength, the cylindrical surface. Araldite® AV 118 glue was used to apply a force. For tensile strength the glue was put on the coated cross section and then subjected to a normal force (in tension). The values were in the order of 70 MPa, and the failure mode occurred at the glue–HA interface. The measured values therefore represent more the adhesive strength in shear; the coated rod was potted into the glue and then pulled out of it. We found values of around 30 MPa and, due to the fact that shearing results in wear attrition, it was not possible to determine the mode of failure, although usually more than half of the coating still seemed to be present.

Our values are about twice as high as those reported by Kay *et al*.[50] Since we found that our strength actually represented the adhesive strength of the glue, it might well be that Kay *et al*. used another type of glue, and hence also measured an "apparent" bond strength instead of the true one, where the failure mode

should have been at the right interface. The roughness of the coating is important if the main failure mode is at the glue–ceramic interface; increasing the roughness increases the contact area, and hence, the "apparent" bond strength.

20.3.3. Bone Attachment of Plasma Sprayed Calcium Phosphate Coatings (Push-Out Test)

The thickness of the coating is a primary influence on the strength of the coated device. A thick coating will have mechanical properties that are somewhat similar to that of the bulk material. If the coating is too thick, it spalls from the metal.

Mechanical and histological evaluations of uncoated and plasma-sprayed HA were performed. The attachment characteristics of interface shear strength were determined by mechanical push-out testing. The results showed variability, probably due to different implantation procedures (cortical or cancellous bone, loaded or unloaded), different coating techniques (grit-blasted titanium surface, particle size) and/or treatment of the tissue-implant sample before the push-out test (formaldehyde fixation or fresh wet bone). However, with identical specimen preparation, there still exists a large scatter in data (Table 20.4).

Dhert *et al*.[36] has studied, with finite element analysis, the push-out test and the effect of varying conditions of the push-out model on the interfacial shear strength. Distance between implant and support jig is very critical for the occurrence of peak stresses in the interface. The clearance of the hole in the support jig should be at least 0.7 mm, to give the most uniform distribution of stresses along the interface. Many researchers have reported that clearance should be minimal,

Table 20.4. Mean Push-Out Strength (MPa) +SD of Various Studies on HA Coatings.

Week	Boone	Cook	Dhert	Geesink	Geesink	Klein	Poser	Verheyen
3								2.9 ÷ 0.3
4	5.8 ÷ 0.8							
5		7.0 ÷ 3.2						
6				49.1 ÷ 2.3				5.8 ÷ 0.4
10		7.3 ÷ 2.2						
12	8.2 ÷ 2.8		13.2 ÷ 2.1	54.8 ÷ 2.6	34.5 ÷ 6.5	8.2 ÷ 1.1	9.8 ÷ 3.8	
25			17.3 ÷ 6.1					3.3 ÷ 0.4
104					29.7			
108						44.0		

however, this will lead to unrealistically low apparent push-out strength values. Variations of the Young's modulus of the implants resulted in a wide range of interface shear stresses. A low Young's modulus results in considerably higher stresses at the medial site of the cortex, from which the load is applied on the implant. A high modulus results in slightly higher stresses at the lateral site of the cortex, where the jig edge supports the bone. In this situation the interface stress distribution is much more uniform compared to the situation with a low Young's modulus implant. Only materials with similar Young's modulus can be compared. Variation of the cortical thickness showed a reciprocal relationship between cortical thickness and interface shear strength. The diameter of the implant hardly affected the interface stress distribution.

20.3.4. Biodegradation of Calcium Phosphate Coatings

Variations of the material properties of calcium phosphate coatings affect the bone-bonding mechanism and the rate of bone formation. Local supersaturation in the constituent ions of the bone mineral phase, arising from enhanced solid–solution exchange at the coating surface, may be a cause for the bone growth enhancement.

Variation in Ca/P ratios (2.0–1.5), i.e., tetra-calcium phosphate, HA and *a/B-TCP*, lead to differences in degradability and differences in bone bonding. HA (Ca/P ratio 1.67) and tetra-calcium phosphate (Ca/P ratio 2.0) give a strong, intimate bone contact. α-TCP and uncoated titanium evoked remodeling of bone and less bone contact.

Composition changes by addition of fluorine to apatite or magnesium to β-whitlockite also influence the stability of the coating. HA showed lower push-out data (not significant) and higher degradation of the coating than fluorapatite. Magnesium whitlockite showed significant lower bone contact and push-out data and higher degradation. Parallel *in vitro* solubility studies showed that the solubility of tetra-calcium phosphate and α-TCP is much higher than that of HA. Fluorapatite showed lower solubility than HA, while magnesium whitlockite shows a very high solubility. Understanding the causes of enhancement of bone tissue in-growth bonding requires knowledge of the characteristics of the calcium phosphate coating and the coating process.[20,36,37]

The particle size distribution should be not too broad, otherwise the particles do not melt uniformly; some will be overheated or vaporized. Differences in particle size of the sintered powder used for plasma spraying gives differences in crystalline/amorphous structure of the coating. A particle size distribution of 1–45 μm gives a coating with an almost totally amorphous structure, due to the

complete melting of the very small particles. However, fluorapatite coating with this particle size distribution (1–45 µm) gives a crystalline coating comparable with a distribution of 1–125 µm. The powder port used may influence the crystallinity and stability of the coating. A heat treatment after the plasma spraying can have an effect on the coating properties, because recrystallization occurs.

In vitro and *in vivo* experiments established the factors which may influence coating stability, solubility, crystallinity and bone tissue response. Factors involved with the plasma spray-coating procedure, such as starting powder compound (FA, HA, Mg-TCP or Tetra-calcium phosphate), powder particle distribution (1–45 µm, 1–125 µm) of HA versus fluorapatite coatings (HA-45, HA-125, FA-45 and FA-125), the plasma spray powder port factor (2 or 6) of HA coatings ($HA_{45/2}$, $HA_{45/6}$, $HA_{125/2}$, $HA_{125/6}$) and the effect of post heat treatment of 1 hour at 600°C were examined. In the *in vitro* study the materials were compared using solubility tests, X-ray diffractometry and scanning microscopy. The different coatings were incubated in buffer solutions for three months and at different time intervals the Ca and P concentrations were measured. Before and after incubation the non-heat-treated and heat-treated coatings were examined by X-ray and SEM. Solubility (Table 20.5) and crystallinity (Fig. 20.9) depended on Ca/P ratio, particle distribution and post-heat treatment.

Table 20.5. Solubility of Different Calcium Phosphate Coatings.

	Ca^{++} citrate	Ca^{++} gomori	P^{-} Citrate	P^{-} Gomori	
FA-45	325	150	153	56	No
	150	80	83	35	H.T.
FA-125	325	120	150	47	No
	170	70	82	31	H.T.
HA-45/2	400	330	184	127	No
	360	200	184	80	H.T.
HA-45/6	400	240	175	99	No
	400	225	195	93	H.T.
Mg-TCP	500	800	152	275	No
	500	800	210	300	H.T.
TETRA	400	450	118	75	No
	220	150	76	27	H.T.

No = no heat treatment, H.T. = heat treatment.

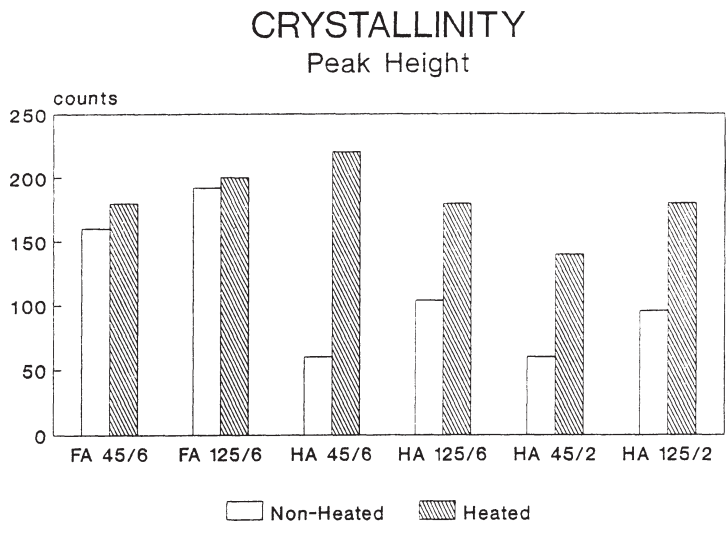

Figure 20.9. The peak height at 25.7° and 29° of the XRD patterns of HA coatings before and after a heat treatment. HA-125 coatings are more crystalline than HA-45. Heat treatment increased the crystallinity for all HA coatings.

X-ray diffraction (XRD) patterns of FA-45 and FA-125 plasma-sprayed coatings showed a well crystallized material. XRD patterns of HA-45 coatings compared with HA-125 coatings showed almost entirely amorphous phases of HA-45 and a more crystalline HA-125 coating.

After heat treatment of the different plasma sprayed coatings, FA coatings showed no significant change in crystallinity and HA-45 and HA-125 coatings showed a higher crystallinity. A difference in powder port factor did not affect the degree of crystallinity. XRD patterns of fluorapatite coatings (FA-45, FA-125) demonstrated both in non-heat-treated and heat-treated coatings a crystalline structure. The crystallinity of fluorapatite was hardly altered by factors such as temperature (1 hr, 600°C) or particle size distribution (1–45 μm, 1–125 μm). However, during plasma spraying HA decomposes. XRD patterns of HA coatings showed less crystallinity. HA-45 especially showed an amorphous structure, probably because of the complete melting of the very small particles. HA coatings became more crystalline after a heat treatment, probably because of recrystallization (Fig. 20.10). The post-heat treatment influenced both crystallinity and degree of solubility. The plasma spray powder port factor examined for HA coatings was not very significant. Incubation of different calcium phosphate coatings showed precipitation of Ca^{2+} and P^{-} ions at the surfaces of nearly all non-heat-treated

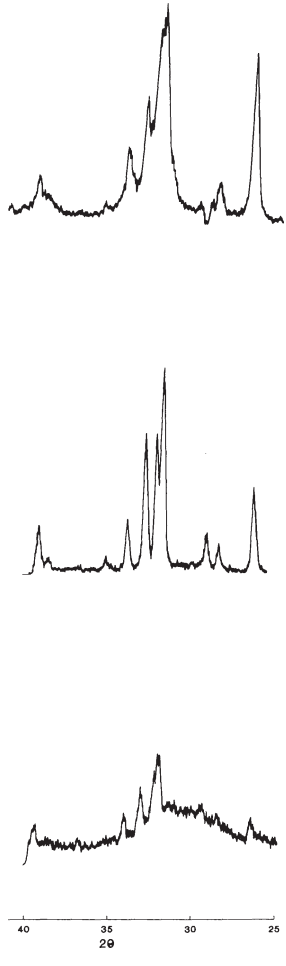

Figure 20.10. XRD patterns of: (above) non-heat-treated HA-45 coating after incubation in Gomori's buffer; (middle) heat-treated HA-45 coating; (below) non-heat-treated HA-45.

coatings (HA, Mg-TCP, Tetra) except FA coatings. In all heat-treated coatings no precipitation was observed (Figs. 20.11a and 20.11b).

In *in vivo* experiments the same factors were studied in relation to coating stability and bone tissue response. Different calcium phosphate plasma-sprayed coatings were implanted in goat femora for three months. After the implantation period the samples were prepared for histology and histometry.

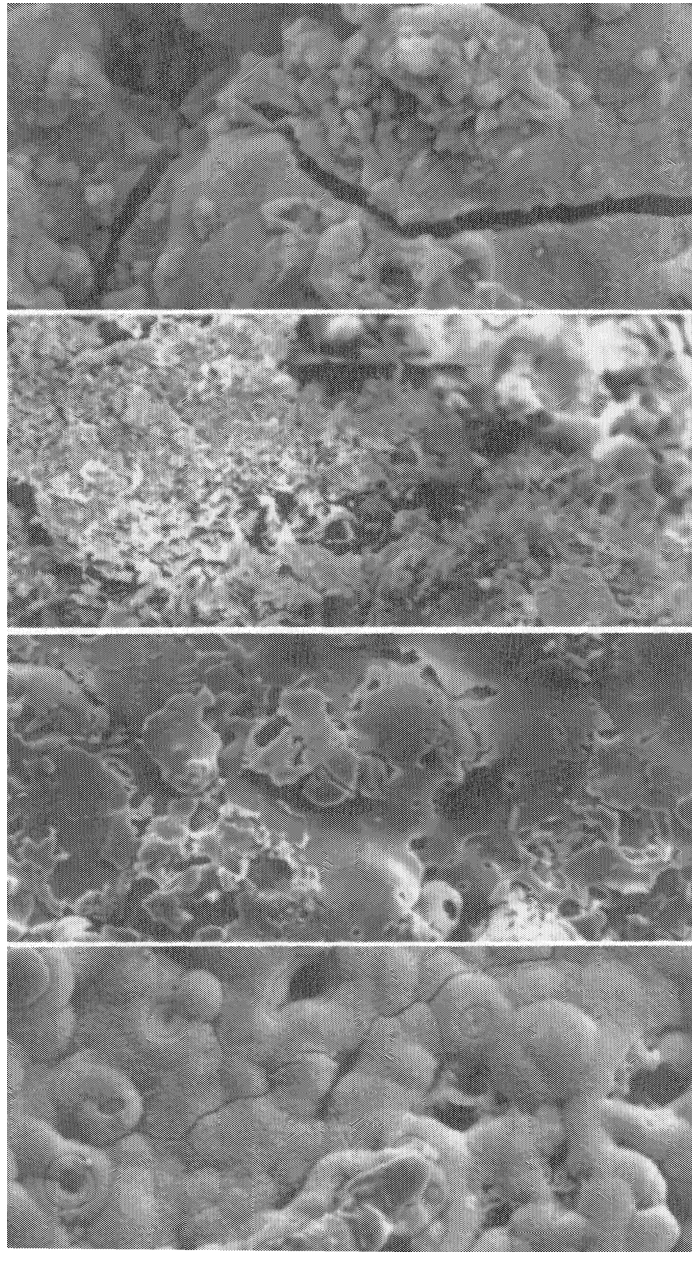

Figure 20.11a. SEM photographs of different calcium phosphate coatings without a heat treatment and after three months incubation in Gomori's buffer. From top to bottom: TETRA, Mg-TCP, FA-45 and HA-45. All coatings except FA showed precipitation of calcium and phosphate.

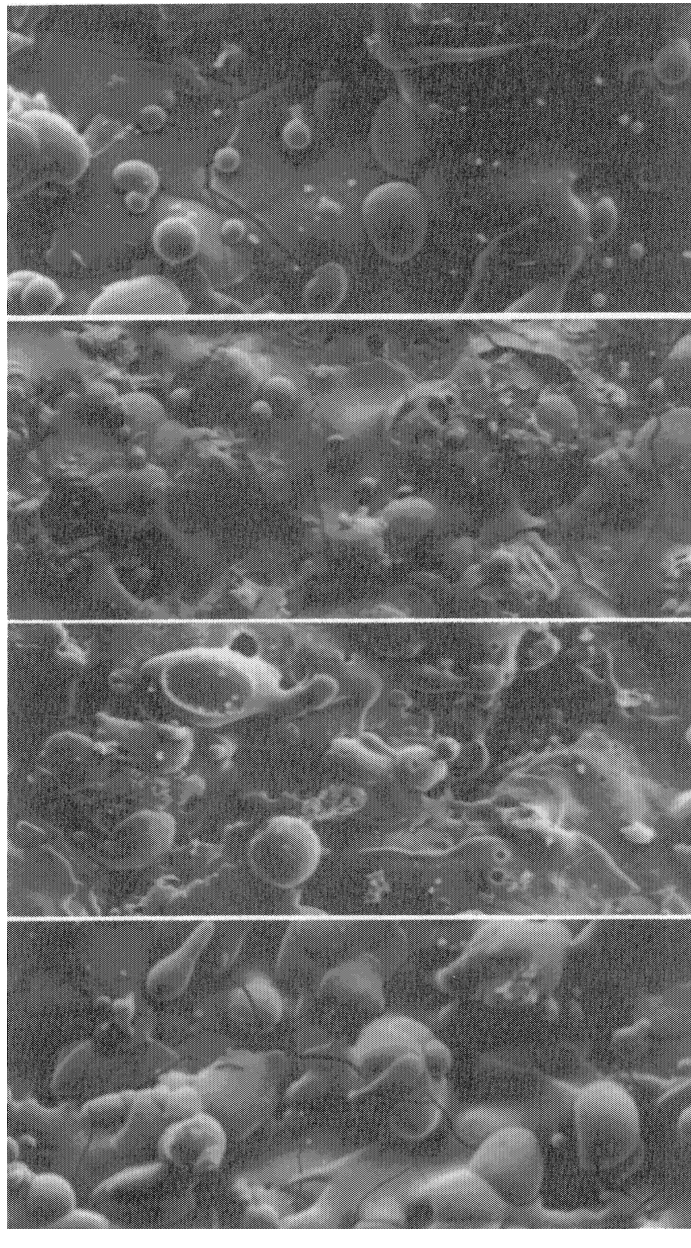

Figure 20.11b. SEM photographs of different calcium phosphate coatings with a heat treatment and after three months incubation in Gomori's buffer. From top to bottom: TETRA, Mg-TCP, FA-45 and HA-45. No coating showed precipitation of calcium and phosphate.

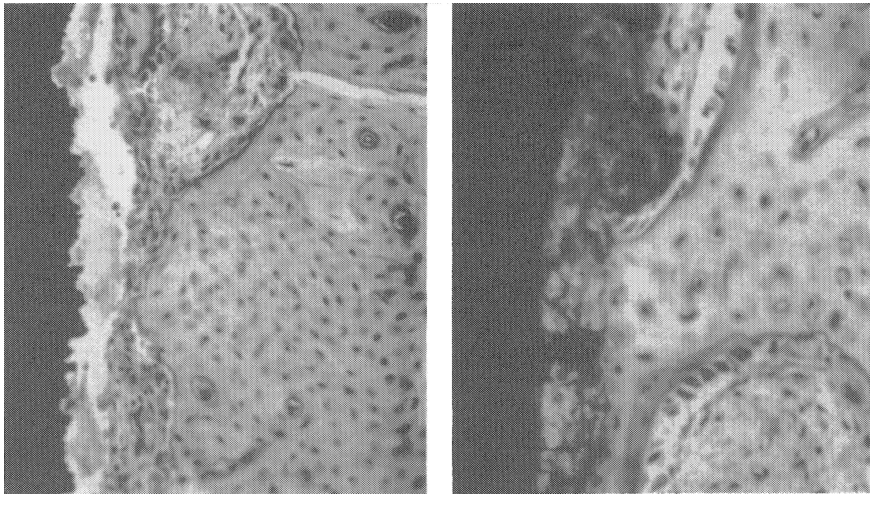

Figure 20.12. HA-45 coating implanted in goat femur for three months. Signs of degradation give rise to high cellular response (left). Heat-treated HA-45 coatings were more stable (right).

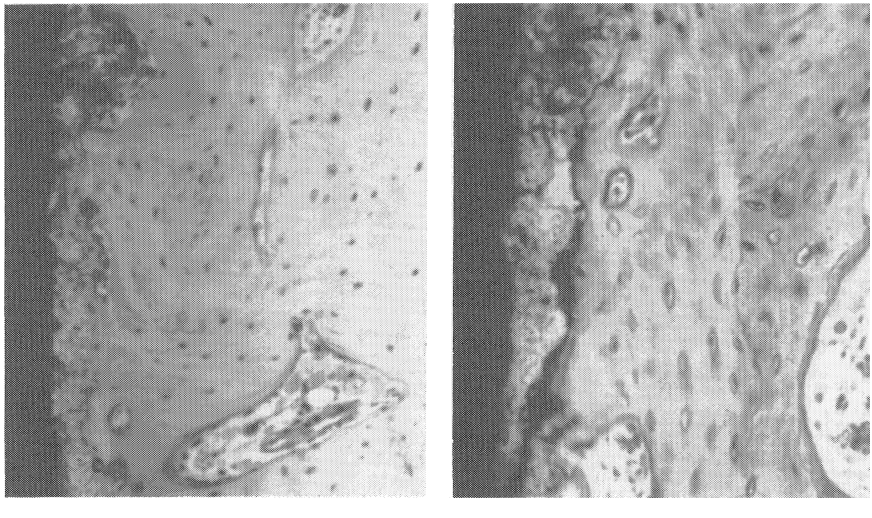

Figure 20.13. Both FA-45 coating (left) and FA-45 heat-treated (right) showed a highly stable, less cellular response and more direct bone contact.

An enhancement of the coating stability of HA-45 and HA-125 because of a heat treatment after the plasma spray procedure was demonstrated. Increased crystallinity, caused by recrystallization during heat treatment, is probably the reason for the promoted stability. The enhanced stability of HA coatings leads to increased direct bone contact. It was found that α-TCP coatings evoked more remodeling activity than the more stable HA coatings during the first weeks of implantation; after a longer period the difference in bone response is less. Also, this study demonstrated that the stable FA and heat-treated HA coatings were incorporated into the bone, with the formation of lamellar bone next to the implants and with little remodeling, while the more unstable non-heat-treated HA coatings showed remarkable remodeling and cellular response. In the first months of implantation, less stable coatings can induce high bone remodeling activity with fewer bone contacts (Figs. 20.12 and 20.13).

20.4. CONCLUSIONS

There were few effects of powder port (2 or 6) on HA coatings *in vivo*. However, a heat treatment enhanced the coating stability of both HA coatings prepared with powder port 2 and 6. Comparing the XRD pattern data of HA coatings with coating stability data, it seemed that *in vitro* tests showed that heat treatment and particle size were factors that influenced the degree of crystallinity, while *in vivo* only the heat treatment factor is clearly detectable. Comparing data of an *in vitro* solubility study of HA coatings, it also seemed that the heat treatment is the most significant factor influencing stability/solubility of the coating. FA-45 and FA-125 non-heat-treated coatings showed a significantly higher stability than the HA coatings, which were not further improved by a heat treatment. The degree of crystallinity of FA coatings was also not altered by a heat treatment. FA coatings are very stable and not subjected to factors such as particle size distribution or temperature. Comparing the FA data of the *in vitro* study with the *in vivo* study, it appeared that after a heat treatment the solubility was decreased significantly, while crystallinity, coating stability and bone tissue response for non-heat-treated and heat-treated FA coatings remained similar.

REFERENCES

1. Andrade, J.D. (1973). Interfacial Phenomena and Biomaterials, *Med. Instrum.*, **7**, 110–119.

2. Clark, A.E., Hench, L.L. and Paschall, H.A. (1976). The Influence of Surface Chemistry on Implant Interface Histology. A Theoretical Basis for Implant Materials Selection, *J. Biomed. Mater. Res.*, **10**, 161–177.
3. Hench, L.L. (1988). "Bioactive Ceramics", in Ducheyne, P. and Lemons, J. (eds), *Bioceramics: Materials Characteristics Versus* In Vivo *Behavior*, *Ann. N.Y. Acad. Sci.*, **523**, 54–71.
4. Engstrom, A. (1972). "The Ultrastructure of Bone", in Bourne, G.H. (ed.), *The Biochemistry and Physiology of Bone*, Academic Press, New York, pp. 237–257.
5. Meyer, L.L. and Fowler, B.O. (1982). Lattice Defects in Non Stoichiometric Calcium Hydroxylapatites, *Inorg. Chern.*, **21**, 3029–3035.
6. McConnell, D. (1973). Applied Mineralogy. Vol. 5 Apatite, Springer-Verlag, New York.
7. Alexander, H., Parsons, J.R., Ricci, J.L. *et al*. (1987). "Calcium Based Ceramics and Composites in Bone Reconstruction", in Williams, D.F. (ed.), *CRC Critical Reviews in Biocompatibility*, CRC Press, Boca Raton, FL, pp. 43–77.
8. LeGeros, R.Z., Parsons, J.R., Daculsi, G. *et al*. (1988). Significance of the Porosity and Physical Chemistry of Calcium Phosphate Ceramics: Biodegradation Bioresorption, *Ann. N.Y. Acad. Sci.*, **523**, 286–271.
9. Osborn, J.F. and Newesely, H. (1980). "Dynamic Aspects of the Implant Bone-Interface", in Heimke, G. and Hanser, C. (eds), *Dental Implant*, Verlag, Munich, pp. 111–123.
10. Cameron, H.U., MacNab, I. and Pilliar, R.M. (1977). Evaluation of Biodegradable Ceramic, *J. Biomed. Mater. Res.*, **11**, 179–186.
11. Kato, K., Aoki, H., Tabota, I. *et al*. (1979). Biocompatibility of Apatite Ceramic in Mandibles, *Biomater. Med. Devices Artif. Organs*, **7**, 291–304.
12. Jarcho, M., Kay, J.F., Gumaer, K.I. *et al*. (1979). Tissue Cellular and Subcellular Events at a Bone Ceramic Hydroxylapatite Interface, *J. Bioeng.*, **1**, 79–92.
13. Jarcho, M. (1981). Calcium Phosphate Ceramics as Hard Tissue Prosthetics, *Clin. Orthop.*, **157**, 259–278.
14. Tracy, B.M., Doremus, B.M. (1984). Direct Electron Microscopy Studies of the Bone Hydroxylapatite Interface, *J. Biomed. Mater. Res.*, **18**, 719–726.
15. Ricci, J., Alexander, H., Parsons, R.H. *et al*. (1986). "Partially Resorbable Hydroxylapatite-Based Cement for Repair of Bone Defects", in Saha, S.

(ed.), *Biomedical Engineering: Recent Developments*, Pergamon Press, New York, pp. 469–474.

16. Parsons, J.R., Ricci, J.L., Alexander, H. *et al*. (1988). Osteoconductive Composite Grouts for Orthopaedic Use, *N.Y. Acad. Sci.*, **523**, 190–207.
17. Koster, K., Heide, H. and Konig, R. (1977). Resorbable Calcium Phosphate Ceramics Under Load, *Langenbecks Arch. Chir.*, **343**, 174–181.
18. Klein, C.P.A.T., Driessen, A.A., de Groot, K. *et al*. (1983). Biodegradation Behavior of Various Calcium Phosphate Materials in Bone Tissue, *J. Biomed. Mater. Res.*, **17**, 769–784.
19. Eggli, P.S., Muller, V. and Schenk, R.K. (1988). Porous Hydroxyapatite and Knead Phosphate Cylinders with Two Different Pore Size Ranges Implanted in the Cancellous Bone In Rabbits, *Clin. Orthop.*, **232**, 127–137.
20. Klein, C.P.A.T., Patka, P., van der Lubbe, H.B.M. *et al*. (1991). Plasma-Sprayed Coatings of Tetracalcium Phosphate, Hydroxylapatite, and α-Knight on Titanium Alloy: An Interface Study, *J. Biomed. Mater. Res.*, **25**, 53–65.
21. Hulbert, S.F., Hench, L.L., Forbers, D. *et al*. (1982). History of Bioceramics, *Ceramics Internat.*, **8**, 131–140.
22. Boretos, J.W. (1987). Advances in Bioceramics, *Advanced Ceramic Materials*, **2**, 15–30.
23. Bowers, G.M., Vargo, J.W., Levy, B. *et al*. (1986). Histologic Observations Following the Placement of Knead Phosphate Implants in Human Intrabony Defects, *J. Periodontal.*, **51**, 286–287.
24. Van Blitterswijk, C.A., Grote, J.J., Kuypers, W. *et al*. (1986). Macropore Tissue Ingrowth: A Quantitative Study on Hydroxylapatite Ceramic, *Biomaterials*, **7**, 137–143.
25. Klein, C.P.A.T., Patka, P. and den Hollander, W. (1989). Macroporous Calcium Phosphate Bioceramics in Dogs Femora; A Histological Study of Interface and Biodegradation, *Biomaterials*, **10**, 59–62.
26. Fellows, B.J., Bauer, G., Gottschalk, G. *et al*. (1987). "Investigation into the Nature of Bioactivity in the Calcium Phosphate System", in Vincenzini, P. (ed.), *Ceramics in Clinical Applications*, Elsevier, New York, pp. 283–288.
27. Klein, C.P.A.T. and de Groot, K. (1990). "Implant Systems Based on Bioactive Ceramics", in Heimke, G. (ed.), *Osseo-Integrated Implants Vol. II, Implants in Oral and ENT Surgery*, CRC Press, Boca Raton, FL, pp. 193–208.
28. Geesink, R.G.T., de Groot, K. and Klein, C.P.A.T. (1987). Chemical Implant Fixation Using Hydroxyapatite Coatings, *Clin. Orthop.*, **225**, 147–170.

29. Cook, S.D., Thomas, K., Kay, J.F. *et al*. (1988). Hydroxylapatite Coated Titanium for Orthopaedic Implant Applications, *Clin. Orthop. Rel. Res.*, **232**, 225–243.
30. Lacefield, W.R. (1988). "Hydroxyapatite Coatings", in Ducheyne, P. and Lemons, J.E. (eds.), *Bioceramics; Material Characteristics Versus* In Vivo *Behavior, Vol. 523*, *Ann. NY. Acad. Sci*., New York, pp. 72–80.
31. Ducheyne, P., McGuckin, J.F. (1990). "Composite Bioactive Ceramic-Metal Materials", in Yamamuro, T., Hench, L.L. and Wilson, J. (eds.), *Handbook of Bioactive Ceramics*, CRC Press, Boca Raton, FL, pp. 175–186.
32. de Groot, K., Klein, C.P.A.T., Wolke, J.G.C. *et al*. (1990). "Plasma-Sprayed Coatings of Calcium Phosphate", in Yamamuro, T., Hench, L.L. and Wilson, J (eds.), *Handbook of Bioactive Ceramics, Vol. II*, CRC Press, Boca Raton, FL, pp. 133–142.
33. Klein, C.P.A.T., de Blieck-Hogervorst, J.M.A., Wolke, J.G.C. *et al*. (1991). "A Study of Solubility and Surface Features of Different Calcium Phosphate Coatings *In Vitro* and *In Vivo:* A Pilot Study", in Vincenzini, P. (ed.), *Ceramics in Substitutive and Reconstructive Surgery*, Elsevier, Amsterdam, pp. 363–374.
34. Klein, C.P.A.T., de Blieck-Hogervorst, J.M.A., Wolke, J.G.C. *et al*. (1990). "Solubility of Hydroxyapatite, Tricalcium Phosphate and Tetracalcium Phosphate Coatings on Titanium *In Vitro*", in Lee, A.J.C. (ed.), *Advances in Biomaterials, Clinical Implant Materials*, Elsevier, Amsterdam, pp. 277–282.
35. Klein, C.P.A.T., de Blieck-Hogervorst, J.M.A., Wolke, J.G.C. *et al*. (1990). Studies of the Solubility of Different Calcium Phosphate Ceramic Particles *In Vitro*, *Biomaterials*, **11**, 509–512.
36. Dhert, W.J.A., Klein, C.P.A.T., Wolke, J.G.C. *et al*. (1991). A Mechanical Investigation of Fluorapatite, Magnesium Whitlockite and Hydroxyapatite Plasma Sprayed Coatings in Goats, *J. Biomed. Mater. Res*., **25**, 1183–1200.
37. Dhert, W.J.A., Klein, C.P.A.T., Wolke, J.G.C. *et al*. (1991). "Fluorapatite, Magnesium-Whitlockite, and Hydroxyapatite Coated Titanium Plugs: Mechanical Bonding and the Effect of Different Implantation Sites", in Vincenzini, P. (ed.), *Ceramics in Substitutive and Reconstructive Surgery*, Elsevier, Amsterdam, pp. 385–394.
38. Davis, S.D., Gibbons, D.F., Martin, R.L. *et al*. (1972). Biocompatibility of Ceramic Implants in Soft Tissue, *J. Biomed. Mater. Res.*, **6**, 425–449.

39. Heling, L., Heindel, R. and Merin, B. (1981). Calcium Fluorapatite: A New Material for Bone Implants, *J. Oral Implantol.*, **9**, 548–555.
40. Klein, C.P.A.T., Wolke, J.G.C., de Blieck Hogervorst, J.M.A. *et al*. (1992). Heat-Treatment Influences Plasma Sprayed Calcium Phosphate Coatings, *Proc. Fourth World Congress 1992*, Berlin.
41. Driessen, A.A., Klein, C.P.A.T. and de Groot, K. (1982). Preparation and some Properties of Sintered Kneed-Whitlockite, *Biomaterials*, **3**, 113–116.
42. van Raemsdonk, W., Ducheyne, P. and de Meester, P. (1984). "Calcium Phosphate Ceramics", in Ducheyne, P. and Hastings, G.W. (eds), *Metal and Ceramic Biomaterials, Vol.2*, CRC Press, Boca Raton, FL, pp. 143–166.
43. Driessens, F.C.M. (1983). "Formation and Stability of Calcium Phosphates in Relation to the Phase Composition of the Mineral in Calcified Tissues", in de Groot, K. (ed.), *Bioceramics of Calcium Phosphate*, CRC Press, Boca Raton, FL, pp. 1–31.
44. de Groot, K., Klein, C.P.A.T., Wolke, J.G.C. *et al*. (1990). "Chemistry of Calcium Phosphate Bioceramics", in Yamamuro, T., Hench, L.L. and Wilson, J. (eds), *Handbook of Bioactive Ceramics, Vol. II*, CRC Press Boca Raton, FL, pp. 3–16.
45. Bhaskar, S.N., Brady, J.M., Getter, L. *et al*. (1971). Biodegradable Ceramic Implants in Bone, *Oral Surg.*, **32**, 336–346.
46. Levin, M.P., Getter, L. and Cutright, D.E. (1975). A Comparison of Iliac Marrow and Biodegradable Ceramic in Periodontal Defects, *J. Biomed. Mater. Res.*, **9**, 183–195.
47. Boyne, P.J., Strunz, T.J. and Shaghat, J.P. (1982). Three Year Long Term Study of Implants of Hydroxylapatite in Dog Alveolar Bone, *8th ANN. Meet. Soc. Biomaterials*.
48. de Groot, K. (1987). "Dental and Other Head and Neck Uses of Calcium Phosphate Bioceramics", in Ducheyne, P. and Lemons, J. (eds), *Bioceramics: Materials Characterization Versus* In Vivo *Behavior*, *N.Y. Acad. Sci*., New York, p. 272.
49. Janke, K. (1987). "Ceramic Implants in Ear, Nose and Throat Surgery", in Vincenzini, P. (ed.), *Ceramics in Clinical Applications (Materials Science Monogr. 39)*, Elsevier, New York, pp. 207–217.
50. Thomas, K.A., Kay, J.F., Cook, C.D. *et al*. (1987). The Effect of Surface Macrostructure and Hydroxylapatite Coating on the Mechanical Strength

and Histologic Profiles of Titanium Implant Materials, *J. Biomed. Mater. Res.*, **21**, 1395–1414.

51. Nery, E.B., Pflughoeft, L.K.L. and Rooney, G.E. (1989). Functional Loading of Bioceramic Augmented Alveolar Ridge: A Pilot Study, *J. Prosthet. Dent.*, **43**, 338–343.
52. Duquette, P. (1973). *An Evaluation of the Osteogenic Potential of a Porous, Single Phase, Knead Phosphate Ceramic* (PhD Thesis, Indiana).
53. Wagner, W., Tetsch, P., Ackermann K.L. *et al*. (1981). Tierexperimentelle Untersuchungen zur Knochenregeneration Genormter Defekte nach der Implantation einer Trikalziumphosphat Keramik, *Dtsch. Zahnarztl. Z*, **36**, 82–85.
54. Patka, P., den Otter, G., de Groot, K. *et al*. (1985). Reconstruction of large Bone Defects with Calcium Phosphate Ceramics: An Experimental Study, *Neth. J. Surg.*, **37**, 38–44.
55. van Blitterswijk, C.A., Koerten, H.K. and Grote, J.J. (1986). "Biological Performance of Whitlockite", in Christel, P., Meunier, A. and Lee, A.J.C. (eds), *Advances in Biomaterials, Vol. 6*, Elsevier, Amsterdam, pp. 1197–1217.
56. Aoki, H., Kato, K. and Tabata, T. (1979). Osteocompatibility of Apatite Ceramics in Mandibles, *Rep. Inst. Med. Det. Eng.*, **11**, 33–35.
57. Strub, J.R. and Gaberthuel, T.W. (1978). Trikalziumphosphat und desen Biologisch Abbaubare Keramik in der Parodontale Knochen Chirurgie, Eine Literaturubersicht, *Schweiz. Monatsschr. Zahnheilkd.*, **88**, 798–803.
58. Klein, C.P.A.T., de Groot, K., Driessen, A.A. *et al*. (1985). Interaction of Biodegradable Kneed-Whitlockite Ceramics with Bone Tissue: *In Vivo* Study, *Biomaterials*, **6**, 189–192.
59. Klein, C.P.A.T., de Groot, K., Driessen, A.A. *et al*. (1986). A Comparative Study of Different Kneed-Whitlockite Ceramics in Rabbit Cortical Bone with Regard to their Biodegradation Behavior, *Biomaterials*, **7**, 144–146.
60. Bauer, G., Fellows, B.J., Gottschalk, H. *et al*. (1985). Auswirkung des pH-werts Verschiedener Calciumphosphat Keramiken auf die Biologische Umgebung DVM-AK "Implantate", *Bioactive Werkstoffe*, **6**, 103.
61. Adam, P., Nebelung, A.O. and Vogt, M. (1988) Loslichkeit und Umwandlungen Biokeramischer Schichten, Z. *Zahnarztl. Implantol,* **4**, 15–21.

Chapter 21

HYDROXYAPATITE COATINGS

William R. Lacefield

21.1. INTRODUCTION

Ceramic coatings are used on metallic substrates in a variety of applications, including enhancement of corrosion resistance of a metal or the creation of a more refractory surface for high temperature service. In the biomedical field, coatings have been used to modify the surface of implants, and in some cases to create an entirely new surface, which gives the implant properties which are quite different from the uncoated device.[1] Because of its similarity to the inorganic component of bone and tooth structure, synthetic hydroxyapatite [$Ca_{10}(PO_4)_6(OH)_2$] (HA) was one of the first materials considered for coating metallic implants. As bulk HA is brittle and relatively weak when compared to common implant metals and alloys and high strength ceramics like aluminum and zirconium oxides (Chapter 2), the best use of HA in load-bearing implant applications is as a coating on one of these stronger implant materials. In spite of the relatively good tissue response to metallic implant surfaces, such as the passive titanium oxide layer present on titanium, with the use of calcium phosphate materials as coatings it is possible to present a surface which is conducive to bone formation.[2]

One reason for the use of HA or a similar calcium phosphate surface is to cause earlier stabilization of the implant in surrounding bone. This is the case, for example, in a dental implant, where the healing time is reduced and the prosthetic attachment can be placed earlier. Another reason to use an HA coating is to extend the functional life of the prosthesis, as in the case of a cementless hip prosthesis, stabilized by the HA coating in the surrounding femur without the use of polymethylmethacrylate bone cement. Under the proper conditions a cementless prosthesis should remain functional longer than a cemented device in which stability is threatened by fracture of the bone cement after a limited number of years in service.

The specific function of an implant should be considered when determining what properties are desired in a coating. For example, a carbon coating on a heart valve prosthesis increases wear resistance and provides a non-thrombogenic surface to the device (Chapter 24). Where HA coatings are used currently, these

two factors are not of primary importance. Of major importance is that the HA coating enables the implant to present a surface to the surrounding bone or soft tissue which will elicit the optimum tissue response. Not only does the surface need to be of a composition that is conducive to the proper tissue response, but the breakdown of the coating or the release of ions from the coating should not cause an adverse reaction. Dense HA has a very low dissolution rate in neutral and alkaline aqueous solutions (Chapters 17 and 20). If there is a decrease in density or crystallinity or if non-HA material is created during the coating process, the dissolution rate can be much greater. This does not rule out the possibility that some coating dissolution can take place without compromising biocompatibility; in fact, the presence of Ca and PO_4 ions in the area around the implant may be more conducive to bone formation than a surface which does not release ions.

A coating should be strongly bonded to the metal substrate to maintain implant integrity as well as to facilitate proper transmission of load from the implant to the surrounding bone. An HA coating which separates from the implant *in vivo* would provide no advantage over an uncoated implant and may be less desirable than no coating at all. In a worse case condition, a weakly-bonded HA coating may separate from the implant and fragments of the coating would be in close proximity to the bare metal surface. Any movement of the loose ceramic coating fragments on the substrate surface could result in disruption of the passive oxide layer on metal surfaces, such as TiO_2 on titanium and Cr_2O_3 on cobalt-chromium alloys. Although reformation of the oxide layer occurs quite rapidly, a momentary increase in metallic ion release will take place. Also, the oxide that forms under *in vivo* conditions existing at the time of reformation may not be as passive or protective as was the previous oxide layer.

21.2. PROCESSING

Industrial and laboratory techniques used for coating HA and other ceramic materials onto metallic substrates include plasma spraying, electrophoretic deposition, sputtering and hot isostatic pressing. The plasma spray method will be discussed in detail, as it is currently the most widely-used method for coating commercially-available implant devices with HA.[1–4] A number of alternative ways of coating implants with HA are briefly reviewed, as the use of some of these provide coatings which are essentially 100% crystalline HA or are potentially advantageous in particular applications, such as for coating porous-surfaced implants.

The first consideration in evaluating methods for producing HA coatings is whether the composition and properties of the starting material are altered so that the *in vivo* performance of the coating is compromised.[5] This alteration can be either contamination of the coating by foreign materials or changes in the basic structure and chemistry of the starting material due to exposure to high temperatures during processing. One source of contamination of HA coatings can occur due to the breakdown of the equipment used, such as the copper anode nozzle in the plasma-spraying process. Other deposition techniques have different sources of contamination, such as the electrolyte solution used in the electrophoretic deposition method.

Another potential problem area, in addition to the alteration of the HA or other coating material during deposition, is that changes in the substrate itself may occur if it is subjected to high temperatures for an extended period. This may occur either during deposition of the coating or during a subsequent heat treatment, which may be used to increase density or crystallinity of the coating. It is possible that during high temperature heat treatment or sintering any of the available metallic substrate materials can be adversely affected by excessive time and temperature combinations. A decrease in mechanical properties of metallic substrates may result from a number of microstructural changes, including grain growth in wrought alloys of titanium and stainless steel, changes in the α-β structure of titanium alloy and embrittlement of cast cobalt-chromium alloys by carbide precipitation at the grain boundaries. These changes are not likely to occur with ceramic substrate materials, such as aluminum oxide.

21.2.1. Plasma Spraying

Plasma spraying, the most common means of applying HA coatings to implant devices, employs a plasma, or ionized gas, partially to melt and carry the ceramic particulate onto the surface of the substrate.[1,3] In flame spraying, another thermal spraying technique, the carrier gasses are not ionized and the temperatures generated are considerably lower than in plasma spraying.

A schematic of a typical plasma-spraying process is shown in Fig. 21.1. The carrier gas is usually argon, which is ionized as it passes within the high temperature discharge zone as the current arcs across the gap between the anode and the cathode. The nozzle of the plasma gun is kept from melting by water cooling, as temperatures developed in the plasma may exceed 10,000°C. As the ceramic particulate remains in the heated plasma zone for only a fraction of a second, usually only partial melting of the powder takes place. Distance of the substrate from

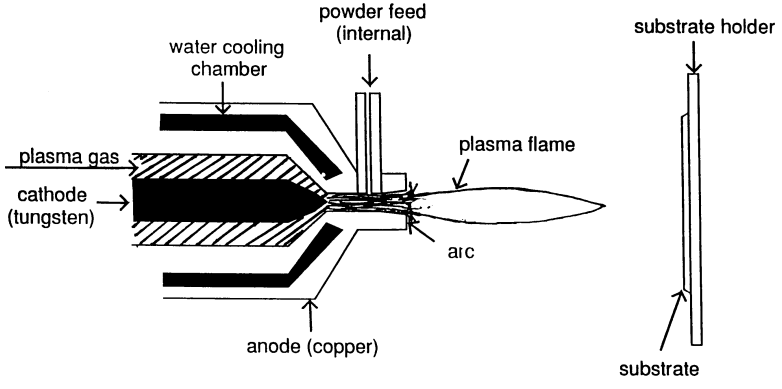

Figure 21.1. Typical plasma-spraying operation with powder fed into the plasma stream internally.

the plasma is one of the critical factors controlling the degree of melting of the particle and the ability of the particulate to flow into a dense coating. One advantage of the plasma-spraying process is that during the coating process the substrate remains at a relatively low temperature (generally less than 300°C), so the mechanical properties of the metallic implant materials are not compromised.

Other factors which influence the degree of melting of the particulate during plasma spraying include the variables controlling the temperature of the plasma, such as current, anode–cathode gap distance, and gas mixture. The carrier gas may be pure argon, but hotter plasma is produced by small additions of hydrogen or other gases. A gas composition of 90% Ar, 10% H gives significantly hotter plasma than 100% Ar, with other conditions remaining constant.

Another factor influencing the degree of melting of the particulate is the position at which the material enters the plasma stream. If the material enters within the nozzle near the start of the plasma zone, it is known as an internal feed system. If the powder is fed into the plasma outside the nozzle, it is an external feed system. As the material stays longer in the plasma for the internal feed system, lowering plasma temperatures can usually be used to achieve the same degree of melting as the external feed system.

Plasma spraying of HA usually takes place under normal atmospheric conditions, as opposed to the plasma spraying of some metallic powders during which a vacuum or an inert atmosphere is used to minimize oxidation. The higher heat-transfer conditions present during atmospheric plasma spraying results in greater deposition efficiency for HA and other ceramic materials when compared with plasma spraying in a vacuum.

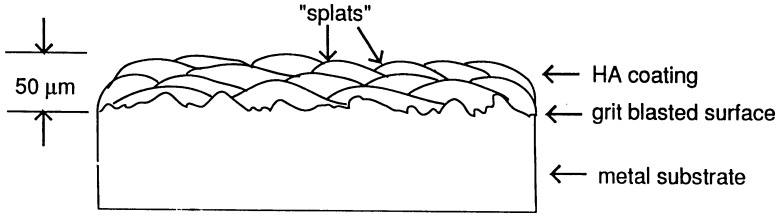

Figure 21.2. Formation of plasma-sprayed HA coating on surface of grit-blasted metal substrate.

Pure, 100% crystalline HA particles in the 20–40 μm range are typically used as the starting material for plasma spraying. When the softened particulate impinges on the substrate surface, individual particles deform into characteristic shapes called "splats". Figure 21.2 shows a schematic of the formation of a plasma-sprayed HA coating on a metal substrate surface. Three passes of the HA spray are typically made for any given area of the implant surface. Deformation and spreading of individual particles takes place on impact with the substrate, and the final coating thickness typically averages 40–60 μm. The flow of the softened HA is usually sufficient to form a dense coating with less than 2% residual porosity.

HA coatings produced by the plasma-spraying process typically contain considerable amorphous calcium phosphate material and small amounts of crystalline phases other than HA (see Chapter 17). It is possible to increase the crystallinity and in some cases the bond strength of plasma-sprayed HA coatings by a post-deposition heat treatment. However, this extra step is usually not feasible commercially because of factors such as the adverse effects of the annealing temperature on the mechanical properties of the substrate metal or alloy, the time and expense of the additional operation and the contamination of the HA surface.

21.2.2. Other Coating Techniques

Because of the difficulty in producing highly-crystalline coatings and reproducibly high bond strength using the plasma-spraying technique, other coating methods have been investigated for commercial applications.[1]

1. An electrophoretic deposition process, in which HA particulate is suspended in an alcohol or other suitable solution and then subjected to an electric field, is a method which deposits the HA on an implant surface with minimal

alteration of the starting material. This is a useful technique for placing HA on porous surfaces which cannot be completely coated with line-of-sight techniques such as plasma spraying.[6] However, as the HA is only weakly deposited and the individual particles are not bonded together, high temperature sintering is necessary after deposition. Because of low bond strength, electrophoretically-deposited coatings are perhaps best used for porous implant designs where the presence of an HA coating is only necessary for a limited time period.

2. Hot isostatic pressing (HIP) can be used to densify HA powder placed on the surface of a metallic implant. In order to achieve a uniform application of pressure on the particulate mass, an encapsulation material (e.g., a noble metal foil) is necessary. The advantage of the method is that lower sintering temperatures (less than 900°C) are required to attain densification and bonding of the HA coating, thus the chances of altering the microstructure or mechanical properties of the metal substrate are reduced.
3. Ion beam sputtering and radio frequency (RF) sputtering are thin film deposition techniques in which a target material is bombarded with an ion beam in a vacuum chamber, and atomic-sized fragments of sputtered material form coatings on suitably placed substrates. The typical coatings sputtered from an HA target are amorphous on deposition, as the sputtered components from the HA target (Ca, P, O and H) do not possess enough energy to recombine into HA. A heat treatment in the order of 500°C is usually sufficient to provide enough thermal energy to form a crystalline coating that is predominantly HA. Although sputter-deposited coatings generally have better bond strength and mechanical properties than thick coatings, the durability of thin 1 μm coatings in the body has not yet been demonstrated.
4. Thermal spray techniques other than plasma spraying are also potential candidates for the production of commercial HA coatings on implants. One approach involves the use of the high velocity oxy-fuel (HVOF) technique. In this method the much higher velocity of the particles causes them to fuse and flow into irregularities on the metal surface more easily, in spite of being subjected to much lower temperatures than plasma spraying, thus the initially high crystallinity of the HA can be maintained.

21.3. COMPOSITION

The composition of plasma-sprayed HA coatings is somewhat different to that of the starting material, as might be expected because of the high degree of

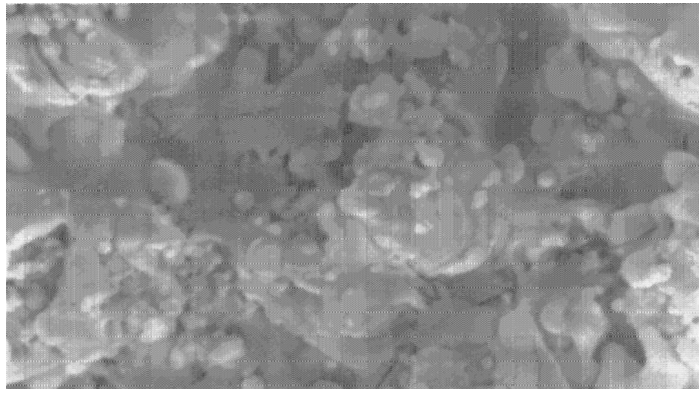

Figure 21.3. SEM micrograph of plasma-sprayed HA coating surface showing partially melted structure with some porosity and microcracks (500X).

melting experienced by the ceramic particulate.[7–10] There are several analytical techniques which are useful for evaluation and analysis of HA coatings. Observation of the coating surface by scanning electron microscopy (SEM) or light microscopy (LM) can be useful prior to the use of other techniques which determine the composition and physical properties.

Figure 21.3 is an SEM showing a typical plasma-sprayed surface of HA on a Ti substrate. The structure appears to be highly melted, with little evidence of the crystalline nature of the coating at this magnification, although comparison of X-ray diffraction (XRD) patterns showed the crystallinity on this particular specimen to be on the order of 50%. Other features of the surface include very low porosity levels, another indication of the high degree of melting experienced by the HA particulate. Also, microcracks can be observed scattered throughout the structure of plasma-sprayed HA coatings, perhaps as a result of a very rapid cooling rate.

XRD has been widely used as a means of determining the composition and structure of plasma-sprayed HA coatings as well as for estimating the percentage of crystallinity and identifying secondary crystalline phases generated as a result of the high temperature spraying process.[7–8] Figure 21.4 shows a diffraction pattern of HA powder prior to plasma spraying. In the plot of the intensity vs 2Θ, there are numerous sharp peaks and a low background, indicative of highly-crystalline HA material. Figure 21.5 is an XRD pattern of the resulting plasma-sprayed coating, made using the powder with the diffraction pattern given in Fig. 21.4. Several changes in the diffraction pattern can be noted, including an increase in the background area under the peaks. Truly amorphous materials

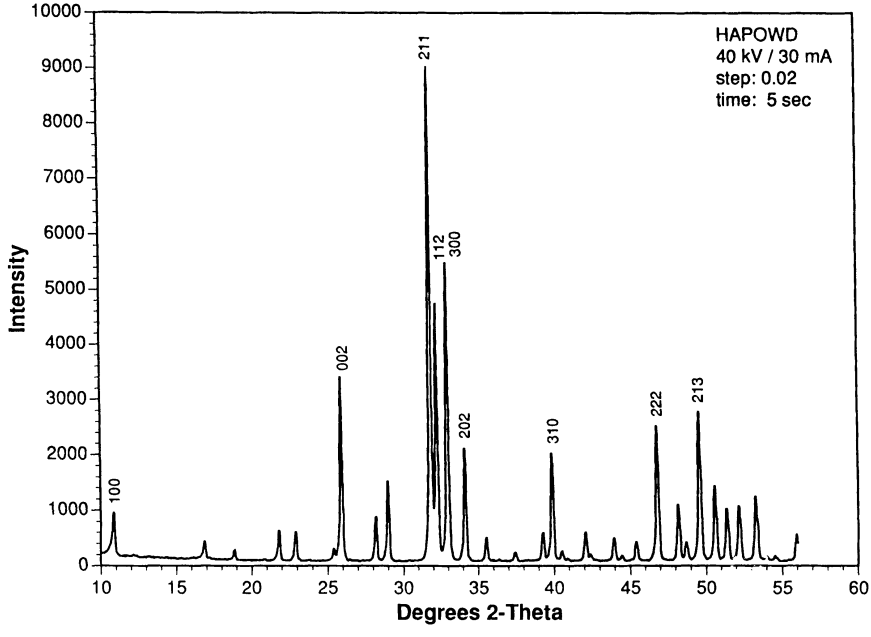

Figure 21.4. XRD pattern of HA powder.

exhibit only a "glass bulge", with no sharp peaks discernible. A slight bulge in combination with peaks indicates a material which is partly crystalline and partly amorphous. A second change in the pattern would be the appearance of new peaks, as indicated by arrows to the left. These new peaks are indicative of one or more crystalline phases which have been generated by the plasma-spraying process, such as α and β-tri-calcium phosphate, calcium oxyphosphate, calcium pyrophosphate, or calcium oxide. Matching of diffraction patterns to determine other crystalline phases has to be made with care because of possible overlapping of some of the major peaks.

Lattice parameter determination by XRD is another way to find out whether changes have taken place in the HA as a result of the coating process or subsequent exposure to a physiologic solution. HA normally possesses a hexagonal structure with a P63/m space group with lattice parameters of a = b = 9.42 A and c = 6.88 A. If the HA is pure and free of vacancies a monoclinic form with the space group P21/b can exist. Any changes in the lattice composition due to the substitution of fluorine, carbonates etc. alters the a and c lattice parameters (see Chapter 17 for details).[11]

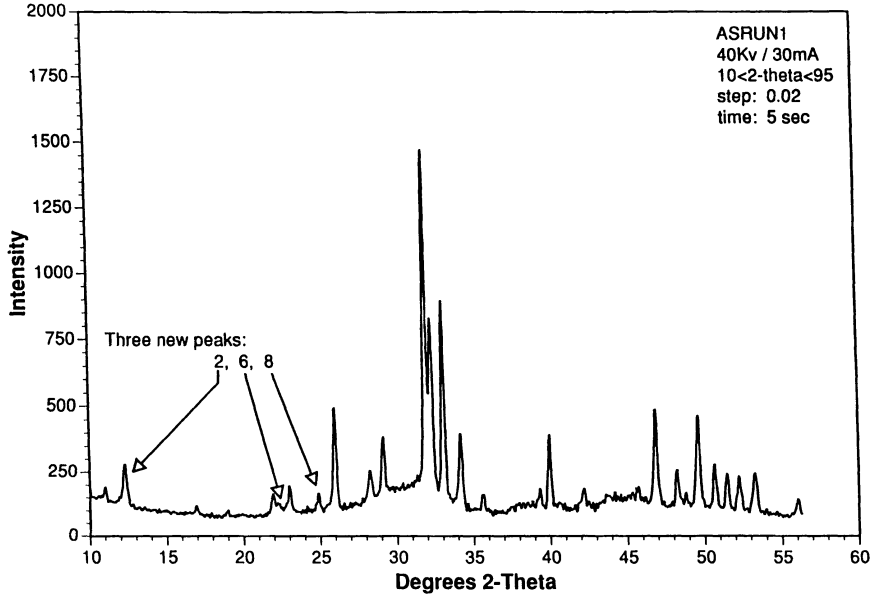

Figure 21.5. XRD pattern of plasma-sprayed HA coating.

Other analytical techniques, such as Fourier transform infrared analysis (FTIR) and Raman spectroscopy, can provide structural information in addition to that obtained by XRD analysis.[1] FTIR is a technique which is sensitive to the asymmetrical vibrational modes of groups such as PO_4 and OH and is therefore useful in determining changes which take place in the relative concentrations of those groups. Figure 21.6(A) is the FTIR spectrum of pure HA powder prior to plasma spraying, and Fig. 21.6(B) is the plasma-sprayed coating using the same powder. One of the absorption bands for phosphate groups occurs at 1,090 cm^{-1}. The larger bulge in the left side of the spectrum is indicative of amorphous material or the presence of moisture. The decrease in the absorption bands at 3,572 cm^{-1} for the coating indicates that some of the OH groups were driven off during the high temperature process. The FTIR spectrum can be also be used to determine the presence of carbonate in the coatings and other crystalline phases such as calcium pyrophosphate ($Ca_2P_2O_7$). Raman spectroscopy, a technique which is sensitive to symmetrical vibrational modes, has also been valuable for evaluating certain changes that occur in plasma-sprayed HA coatings, such as the loss of OH, which are not readily determined by XRD. Additional information on the characterization of calcium phosphate phases is given in Chapter 17.

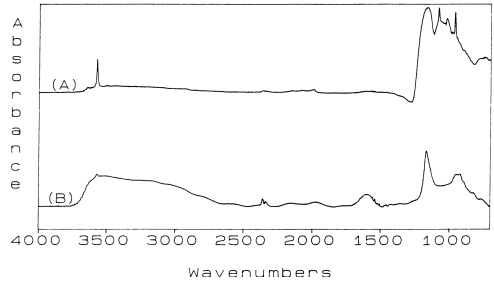

Figure 21.6. (A) FTIR spectrum of HA powder. (B) FTIR spectrum of plasma-sprayed HA coating.

21.4. PROPERTIES

Two important properties of plasma-sprayed HA coatings are bond strength to the implant and dissolution rate in solution.[12] Bond strength measurements are often used by manufacturers for purposes of quality control, as small changes in the conditions of the plasma-spraying process can cause major alteration of the adherence of coating to substrate.

The most commonly-used method of determining tensile bond strength involves the coating of a metallic disc followed by testing utilizing a variation of ASTM C633. To test the adherence of HA coatings to an implant material such as titanium, the surface of the substrate disc is first prepared in the same way as the actual surface on an implant, using all cleaning and grit blasting steps. The coated disc is then fixed to a stainless steel rod and bonded to another rod using a heat cured epoxy, as shown schematically in Fig. 21.7. The two rods are pulled in tension until failure occurs, with exact alignment retained during the test. The tensile strength is then calculated by dividing the load at failure by the cross-sectional area of the disc.

The tensile bond strengths of plasma-sprayed HA coatings on various substrate metals reported in the literature range from less than 7 MPa to more than 80 MPa, depending in large part on the measurement technique used, although other factors such as coating conditions and surface roughness of the substrate certainly affect the values obtained. The use of heat-cured epoxy is somewhat controversial because of the possibility of the epoxy penetrating through the coating to the metal interface and artificially-strengthening the bond. Plasma-sprayed HA is melted more completely (and is therefore denser) than the typical thermal-sprayed ceramics such as Al_2O_3, so penetration of epoxy is not as much of a problem. Factors such as compressive stresses generated during cooling of the

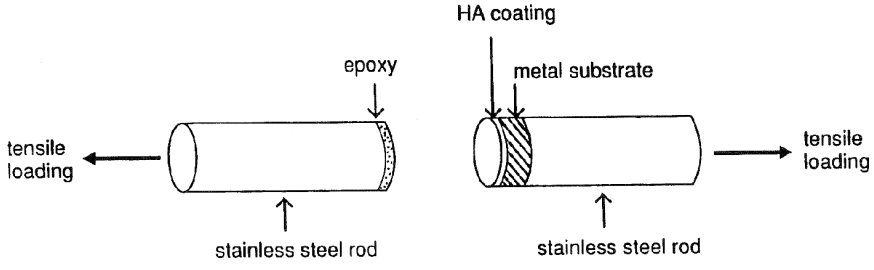

Figure 21.7. Tensile bond testing of HA-coated specimens using a modified ASTM C633 procedure.

heat-cured epoxy are additional sources of error in bond test measurements of plasma-sprayed HA coatings.

The roughness of the substrate is of primary importance in achieving high bond strength of a plasma-sprayed HA coating, and coarse aluminum oxide grit is generally used to roughen the implant surface prior to deposition. The bonding of the plasma-sprayed HA coatings to metal appears to be entirely mechanical in nature, as there is no evidence of any degree of chemical bonding in as-deposited coatings.[12]

The dissolution rate of HA coatings is of interest because a rapidly-dissolving coating may not remain on the implant for a sufficient time to allow full stabilization in bone or the desired tissue response *in vivo*, as discussed in Chapter 20. A coating which is breaking down quickly *in vivo* will release a higher quantity of Ca and PO_4 ions to the surrounding tissues than a more stable coating with a lower dissolution rate will. The quantity of ions released (typically in the ppm range) can be determined by placing the coated specimen in a simulated physiologic solution and monitoring the Ca ion content for given time periods. One means of measuring ion release is by atomic absorption, in which the quantity of ions in a solution is determined by lamps which measure the absorbance of a particular species, such as Ca.

Plasma spraying of HA powder produces calcium phosphate coatings with a crystalline structure which is primarily HA, usually with small amounts of other crystalline phases. However, there is also a considerable amount of amorphous material generated during the plasma-spraying operation, as the crystallinity typically ranges between 40 and 80%. The dissolution rate of plasma-sprayed HA coatings is quite variable and typically is considerably higher than fully dense, 100% crystalline HA, either in the human body or in simulated physiologic solutions. This is mainly due to the presence of amorphous material and other, more

soluble, crystalline calcium phosphate and calcium oxide phases present in plasma-sprayed HA coatings. High dissolution rates are generally seen as undesirable for HA coatings, although another calcium phosphate material — tri-calcium phosphate — is used with the objective of complete dissolution within a predictable time period. Although ongoing development and optimization of the plasma spraying of HA is aimed at higher crystallinity coatings without sacrificing bond strength, there is no evidence that very high crystallinity (approaching 100%) is better *in vivo*. Further *in vitro* and *in vivo* research which correlates the crystallinity, secondary phase composition, and ion release rate with tissue response to an HA-coated implant is necessary before optimum coating conditions can be established.

21.5. SURFACE CHEMISTRY

The surface chemistry of HA coatings is mainly dependent on the coating technique used as well as the composition of the starting material.[5] For plasma-sprayed HA coatings, the amorphous content of the coating as well as the presence of more soluble crystalline phases, such as tri-calcium phosphate, result in a surface which is actively releasing Ca and PO_4 ions. Techniques such as electrophoretic deposition produce HA coatings that are essentially 100% crystalline and therefore may be less active as far as ion release, depending in part on the final density of the material after sintering.[6] Sputter-deposited coatings have different surface chemistries and ion release rates depending on the degree of crystallization and the presence of other elements, such as fluorine. More radical surface modifications under investigation include the incorporation of agents which induce the formation of bone, such as bone morphogenic proteins, into HA coatings.

One concern with any coating method is whether the starting material is contaminated during the coating process. Surface analytical techniques such as Auger electron spectroscopy (AES) and X-ray photoelectron spectroscopy (XPS) are useful for determining trace amounts of contaminants introduced during the coating, handling or sterilization operations (see Chapter 37). For plasma-sprayed HA, the main contaminant introduced during the process is copper from the anode nozzle or tungsten from the internal cathode. Higher plasma temperatures, used in conjunction with an external feed system, cause a more rapid deterioration of the plasma spray gun nozzle, and may result in more Cu contamination of the coating. However, with the internal feed system there is the increased risk of abrasion of the inside of the nozzle by the ceramic particulate carried by the plasma stream. In actual practice, minute quantities of Cu as well as Cu

particulate have been identified on the surface of plasma-sprayed HA coatings by AES and energy dispersive spectroscopy (EDS) from both internal and external feed systems.

The surface chemistry of the portion of the metal implant covered by HA should not be a factor except in cases where the coating dissolves or separates from the substrate. In cases of delamination or dissolution of the coating, the substrate must have an acceptable surface which was not contaminated or adversely altered during the coating operation. Surface chemistry of the metal substrate may also be altered by the operations used to texture the surface. In the grit blasting of metallic substrates for plasma-sprayed HA coatings, the embedding of aluminum oxide particles is unavoidable. These particles are difficult to remove, but may pose no problem because of the relative inertness of aluminum oxide.

Alteration of the implant surface may occur during sterilization with gamma irradiation, indicated by a light tan color observed in some HA coatings after treatment. This color change may be a result of displacement of electrons from their proper locations in the electron shells, and the white color characteristic of the coating prior to sterilization can be restored by annealing if esthetics are a concern. Other surface changes which may occur as a result of sterilization procedures include contamination of the coating in a steam autoclave and formation of cytotoxic products on rough HA surfaces sterilized by ethylene oxide. Potential problems of surface contamination with wet heat (autoclave) and chemical sterilization (ethylene oxide) is the reason that HA-coated implants are now sterilized by gamma irradiation or dry heat.

21.6. TISSUE RESPONSE

The area of primary concern with the use of any implant system is the body's response to the device. Animal studies have been done on HA-coated implants to predict the response in humans.[1,12] Most investigations matched HA-coated implants against identical uncoated implants to determine if the coating enhances stabilization of the implant in the newly developing bone. Some studies found no significant difference between HA-coated and uncoated implants; in a majority it appears that bone forms sooner around the implant when an HA coating is present. Some long-term animal studies found that there was little difference between HA-coated and uncoated implants after six months or more *in vivo.* Thus, the main advantage of HA coatings may be in short-term stabilization of the implant.

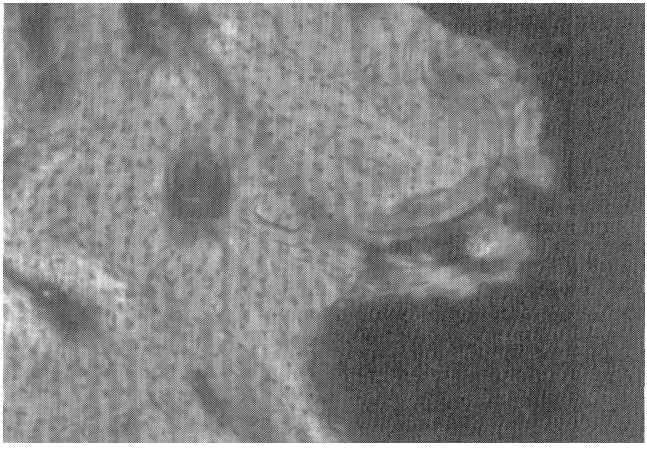

Figure 21.8. Bone formed around an HA-coated screw type implant on a dog (original magnification × 190).

Animal studies often involve histological examination of the tissues surrounding an implant after killing the animals at preset time periods. The presence of bone directly against the implant surface is seen as evidence of proper tissue response, as opposed to the presence of fibrous tissue. Several techniques, including high voltage SEM, have been used to determine if cell attachment is present or if a very thin layer of fibrous tissue exists between the bone and implant surface. An example of bone formed against an HA coated screw implant in a canine study is given in Fig. 21.8 (implant removed). Whether a chemical bond between an HA surface (or any other implant surface such as TiO_2) and bone is formed is still controversial and will require high resolution TEM to resolve.

Push-out tests have been used to measure the ability of the implant to resist forces tending to shear the bond between the implant surface and bone. Some tests have indicated that HA coatings enhance fixation of the implant in the surrounding bone. However, these tests have been performed on smooth-sided implants without grooves or other features designed for retention, and the bond strength of the implant to bone is typically quite low (e.g., 7 MPa). It is not practical to rely on the bond of an HA coating to bone to provide long-term stability of an implant in the absence of any other retentive features.

There are reports from practitioners of HA-coated implants being removed where the coating has fractured and fragments remain bonded to the surrounding bone. This indicates that the bond strength of the HA coating may be stronger to bone, in some cases, than to the metal substrate after a time *in vivo.* Figure 21.9

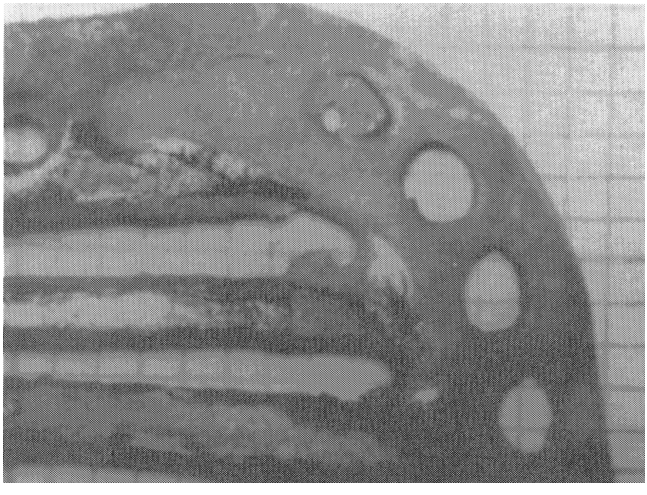

Figure 21.9. Removed HA-coated subperiosteal implant, showing remaining bone and sections of bare metal where coating has separated.

shows an HA-coated cobalt-chromium subperiosteal dental implant, in which part of the coating was stripped off when the device was removed from the surrounding bone. Most of the HA-coated implants removed clinically were plasma-spray coated many years ago, and progress has been made in the quality and bond strength of the coatings since then.

21.7. CLINICAL APPLICATIONS

The use of HA coatings is an attempt to enhance the response of the surrounding bone or soft tissue to a metallic or ceramic implant.[12] The widest use of HA coatings is on metallic dental endosseous and subperiosteal implants, and to a lesser extent on metallic orthopedic devices, such as total hips and knees.

On dental and orthopedic implants with plasma-sprayed HA coatings, the coating itself covers only a portion of the device. In a one or two stage root form dental implant, only the portion to be placed within the bone is HA coated, with the exception of some devices in which the coating extends onto the neck, i.e., transgingival area, of the implant. Subperiosteal dental implants are usually entirely coated except for the posts to which the superstructure (e.g., full denture) will be attached. For orthopedic implants, generally only a portion of the contact surface between the implant and bone is HA coated. In some total hip designs,

only the proximal end of the shaft portion is HA coated, based on the premise that some mobility of the distal end is desirable.

There are few long-term controlled clinical studies which use plasma-sprayed HA-coated implants. There are, however, observations made by clinicians who evaluate the results of HA-coated implants and feel they are superior to uncoated devices. In the case of dental implants, it is commonly felt that the use of HA coatings is more advantageous in the maxilla than in the mandible, so some practitioners will use HA-coated Ti root form implants in the maxilla and uncoated Ti in the mandible. Similarly, for cast cobalt-chromium subperiosteal implants, plasma-sprayed HA-coated devices are more likely to be used in the maxilla than the mandible.

Some of the coating techniques, other than plasma spraying, under consideration for the deposition of HA on medical and dental implants produce coatings which are 100% crystalline HA. Chapter 23 describes an alkaline solution-based technique that produces a calcium-phosphate coating on Ti implants that is used clinically.

Reports from the early use of HA dental implants by practitioners and the results of some animal studies indicate that plasma sprayed HA coatings cause faster adaptation of bone to an implant device than uncoated titanium or other implant alloys do, although the long-term advantages of the use of these coatings in either dental or orthopedic devices is debated. The popularity of HA coatings, especially for endosseous dental implants, is due to the perception that an implant coated with a substance which is similar to bone *should* result in a more optimum response from either the surrounding bone or soft tissue. HA coatings continue to interest both the clinician and the researcher as studies improve the design of implants which utilize HA coatings and optimize factors such as crystallinity and ion release rates to attain the proper tissue response in each particular orthopedic and dental application.

REFERENCES

1. Lacefield, W.R. (1988). “Hydroxylapatite Coatings”, in Ducheyene, P. and Lemons, J. (eds), *Bioceramics: Materials Characteristics Versus* In Vivo *Behavior*, Annals of the New York Academy of Sciences, New York, pp. 72–80.
2. Geesink, R.G.T., de Groot, K. and Klein, C.P.A.T. (1987). Chemical Implant Fixation Using Hydroxyl-Apatite Coatings, *Clin. Orthop.*, **2**, 147–170.
3. de Groot, K., Geesink, R.G.T., Klein, C.P.A.T. *et al.* (1987). Plasma Sprayed Coatings of Hydroxyapatite, *J. Biomed. Mater. Res.*, **21**, 1375–1387.

4. Kay, J.F., Jarcho, M., Logan, G. *et al.* (1986). The Structure and Properties of Hydroxylapatite Coatings on Metal, *Transactions 12th Annual Meeting of the Society for Biomaterials IX*, 13.
5. Radin, S. and Ducheyne, P. (1990). The Effect of Plasma Sprayed Induced Changes in the Characteristics on the *In Vitro* Stability of Calcium Phosphate Ceramics, *Transactions 16th Annual Meeting of the Society for Biomaterials XIII*, 128.
6. Ducheyne, P., Radin, S., Heughbaert, M. *et al.* (1990). Calcium Phosphate Ceramic Coatings on Porous Titanium: Effect of Structure and Composition on Electrophoretic Deposition, Vacuum Sintering and *In Vitro* Dissolution, *Biomaterials*, **11**, 244–254.
7. Koch, B., Wolke, J.G.C. and de Groot, K. (1990). X-ray Diffraction Studies on Plasma Sprayed Calcium Phosphate-Coated Implants, *J. Biomed. Mater. Res.*, **24**, 655–667.
8. Ducheyne, P., van Raemdonck, W., Heughebaert, J.C. *et al.* (1986). Structural Analysis of Hydroxyapatite Coatings on Titanium, *Biomaterials*, **7**, 97–103.
9. Koeneman, J., Lemons, J., Ducheyne, P. *et al.* (1990). Workshop on Characterization of Calcium Phosphate Materials, *J. Applied Biomaterials*, **1**, 79–90.
10. Filiaggi, M.J. and Pilliar, R.M. (1989). Interfacial Characterization of a Plasma-Sprayed Hydroxylapatite/Ti-6Al-4V Implant System, *1Oth Annual Conference Canadian Biomaterials Society*, pp. 23–25.
11. Kay, M.I., Young, R.A. and Posner, A.S. (1964). Crystal Structure of Hydroxyapatite, *Nature*, **204**, 1050–1052.
12. Thomas, K.A., Kay, J.F., Cook, S.D. *et al.* (1987). The Effect of Surface Macrotexture and Hydroxyapatite Coating on the Mechanical Strengths and Histological Profiles of Titanium Implant Materials, *J. Biomed. Mater. Res.*, **21**, 1395–1406.
13. Cook, S.D., Thomas, K.A., Kay, J.F. *et al.* (1988). Hydroxyapatite-Coated Porous Titanium for Use as an Orthopedic Biologic Attachment System, *Clin. Orthop.*, **230**, 303–312.

Chapter 22

BIOACTIVE GLASS COATINGS

Larry L. Hench and Orjan Andersson

Editor's Note: *This chapter is an abbreviated version of Chapter 13 of the first edition of An Introduction to Bioceramics. Numerous studies were conducted to develop reliable coatings of bioactive glasses on a metallic load bearing prosthesis. Structural failures occurred due to attack of the metal–glass phase boundary between the glass coating and the metal substrate material and such devices never became clinically important and therefore the topic is mostly deleted from this second edition. A short summary of the studies conducted by Hench and Anderson and colleagues at the University of Florida and Abo Akademi in Turku, Finland follow with a few key citations.*

22.1. INTRODUCTION

Bioactive glasses are not strong enough to be used for load-bearing applications. One approach to solving this problem is to combine the glass with a fracture tough phase, such as a metal or a polymer, to produce a composite (Chapters 25 and 26). The other alternative is to apply the glass as a coating on a mechanically tough substrate, the subject of this chapter. Coating a substrate with a bioactive glass serves three purposes.

(1) The substrate is protected from corrosion and degradation of properties.
(2) Tissues are protected from corrosion products which may induce systemic effects. Figure 22.1a shows tissues adjacent to a bone plate and metallic screw after only 18 months following implantation in a 58 year old woman. An extensive concentration of corrosion products is present in the tissue. Figure 22.1b shows tissues adjacent to a bioactive glass coated stainless steel implant, after 18 months in a monkey. No corrosion products are present.
(3) The bioactive glass coating provides interfacial attachment to bone, e.g., bioactive fixation, thereby eliminating the need for polymeric bone cements. Studies reviewed in Reference 1 provide evidence from animal studies of strong interfacial bonding between 45S5 Bioglass®-coated femoral head prostheses and bone in a monkey model.

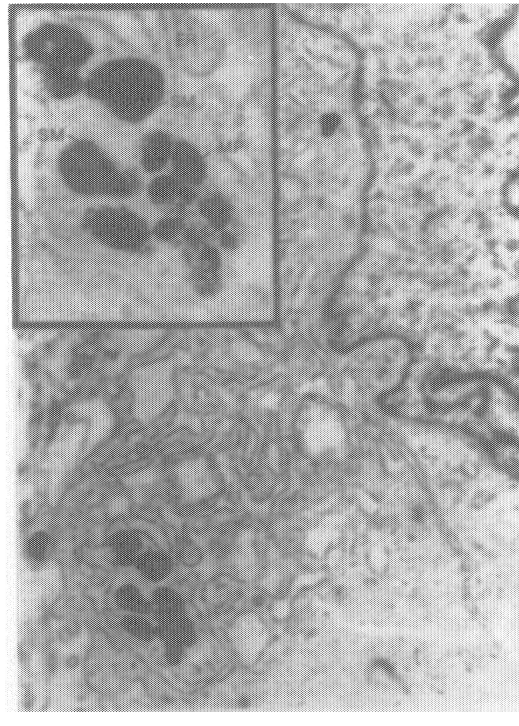

Figure 20.1a. Fibroblast-like cell containing aggregates of metallic particles in cytoplasmic vacuoles (23,000X). Inset: high magnification electron micrograph to demonstrate metallic particles within membrane-bound vacuoles (55,000X).

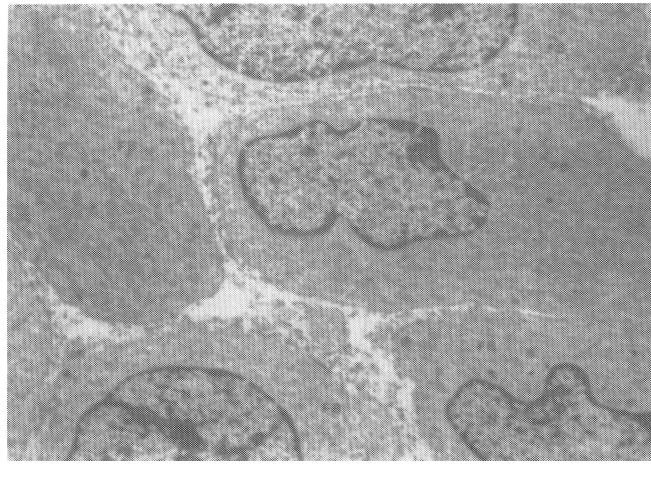

Figure 22.1b. Representitive field from tissue surrounding Bioglass®-coated implants.

The metals commonly used as load-bearing prostheses in orthopedics and dentistry have been used as substrates for bioactive glasses including: 316L stainless steel, Ti-6–4 alloy, and Co-Cr-Mo alloys. Medical grade alumina has also been used as a substrate. Chapter 2, Table 2.4 summarizes the properties of alumina.

Three methods are used to apply bioactive glasses as coatings.

(1) Enameling or glazing, using glass frits to provide a protective first layer or ground coat, applied between the substrate and the bioactive glass.
(2) Flame-spray coating, where the glass is applied to the substrate as a stream of molten particles. The particles fuse to the substrate upon impact.
(3) Rapid-immersion coating, where the metallic substrate is heated to form an oxide layer of critical thickness and is then rapidly inserted into a container of molten glass. The oxide layer dissolves in the glass forming an adherent bond between the substrate and the glass coating.

Chapter 13 in the first edition of this book reviews the principles, results, and problems of these coating methods.

22.2. THE PROBLEM

The problem of obtaining a bioactive glass coating with high mechanical integrity is the chemical reactivity of this type of glass. Compositions of silicate-based glasses that form a bond with tissues have <60 mole% SiO_2 (Chapter 3). Such glasses have a random, two-dimensional, sheet-like, network structure, with many open pathways for ion transport. It is this structure that results in the rapid formation of a calcium phosphate (CaP) and hydroxycarbonate apatite (HCA) layer on the glass, which provides binding sites to collagen (Chapter 3). The open network also makes it easy for other cations, such as Fe, Cr, Ni, Co, Mo, Ti, or Ta, to pass through the glass or react with the surface. If these cations are present they rapidly react with the surface and prevent formation of the CaP layer and its crystallization to HCA, and thereby inhibit or eliminate the bioactivity of the glass. Only a few percent of multivalent cations are needed to make a glass non-bioactive. See Hench[1] and Gross *et al*.[2] for a review of these compositional factors.

22.3. ENAMELING

Glass coatings have been applied to metallic substrates for millennia in a process called enameling. The glass is melted and homogenized and quenched into either water or air, forming a frit, and then ground into a powder (Chapter 37).

The metal is coated with the powder by painting, spraying, or dipping. An aqueous slurry of the glass powder is often used. After drying, the coated part is then heated to above the softening temperature of the glass (400–600°C), where the glass fuses to an oxide layer on the metal, forming a mechanical–chemical bond at the interface. The outer layer of the powder sinters together (Chapter 1) and forms a coherent layer of glass fused to the metal.

In order to facilitate adherence of the glass to the metal, two layers of glass are applied on the substrate. The first layer of glass provides interfacial bonding of glass to the metal, achieves an appropriate match of coefficients of thermal expansion (CTE) of the metal and the glass, has a high durability and a suitably low glass transition temperature, Tg, and low viscosity, and still retains bioactivity of a top layer of glass fused to it. The Tg of the inner layer of glass must not be lower than that of the outer layer, since it would soften too much during firing of the top layer. Optimization of glass compositions to produce and control the range of thermal and chemical properties listed above has been achieved by Karlsson[3,4] and Andersson[5,6] and coworkers at Abo Akademie University, Turku, Finland. A phenomenological model for glass optimization was developed using the following steps:

(1) Define the compositional ranges of interest.
(2) Design an experimental plan (select compositions) that allows regression analysis of the results and avoids cross-correlation.
(3) Measure the properties of interest for the selected compositions.
(4) Conduct a computer-based regression analysis to describe the relationship between composition and property.[5,6]

22.4. RESULTS AND APPLICATIONS

Details of development of bioactive glass coatings on various metals are given in the first edition of *An Introduction to Bioceramics* and References 1, 3–7. Clinical applications have not been obtained due to difficulty in achieving long-term stability of the glass–metal interface, even though a glass–bone bond is achieved.

22.5. REFERENCES

1. Hench, L.L. (1990). “Bioactive Glasses and Glass-Ceramics: A Perspective”, in Yamamuro, T., Hench, L.L. and Wilson, J. (eds), *Handbook of Bioactive Ceramics, Vol. I*, CRC Press, Boca Raton, FL, pp. 7–23.

2. Gross, U., Kinne, R., Schmitz, H.J. *et al.* (1988). The Response of Bone to Surface Active Glass/Glass-Ceramics, *CRC Critical Reviews in Biocompatibility* **4**, 25–30.
3. Westerland, T., Hatakka, L. and Karlsson, K.H. (1983). A Model for Optimizing Glass Batch Compositions, *J. Am. Ceram. Soc.*, **66**, 574–579.
4. Hatakka, L. and Karlsson, K.H. (1986). Optimization of Batch Costs for an Industrial Furnace, *Glass Technology*, **27**, 17–20.
5. Andersson, H., Karlsson, K.H., Kangasniemi, K. *et al.* (1988). Models for Physical Properties and Bioactivity of Phosphate Opal Glasses, *Glastech. Ber.*, **61**, 300–305.
6. Andersson, H. and Karlsson, K.H. (1991). On the Bioactivity of Silicate Glass, *J. Non-Cryst. Solids*, **129**, 145–151.
7. Hench, L.L., Hench, J.W. and Greenspan, D.C. (2004). Bioglass: A Short History and Bibliography, *J. Aust. Ceram. Soc.*, **40**, 1–42.

Chapter 23

BIOACTIVE HA COATINGS BY TI SURFACE ACTIVATION

Tadashi Kokubo and Seiji Yamaguchi

23.1. INTRODUCTION

Various types of bioactive ceramics have been developed, and many are now being used clinically as important bone substitutes. However, these materials have low fracture toughness, and thus cannot be used under high-loading conditions. Under these conditions, metals such as stainless steel, Co–Cr–Mo alloys and Ti and its alloys are used because of their high fracture toughness. Among these, Ti and its alloys exhibit better biocompatibility. However, even Ti and its alloys do not bond to the living bone, and therefore their attachment to the surrounding bone is not stable over a long period of time. In order to impart bone-bonding properties to these metals, hydroxyapatite (HA) coating has been attempted, and resulting composites are already used clinically. However, the coated HA is not stable in the living body over a long period of time. Moreover, incorporation of Ca and/or P onto the surfaces of these metals has been attempted by using ion implantation, electrochemical treatments and hydrothermal treatments.[1] These methods require special apparatus and cannot be easily applied to large devices with complex shapes.

Bioactive titanate layers were recently reported to form on the surfaces of Ti and its alloys by simple chemical and heat treatments.[1] The titanate layers are tightly bonded to the metal substrates through a graded interface. This treatment is easily applied to implants of any shape. Some of the bioactive metals prepared by this method are already used clinically.

23.2. CONCEPT FOR FORMING BIOACTIVE TITANATE SURFACE LAYER

Bioactive ceramics such as Bioglass®, glass-ceramic AW and sintered HA bond to the living bone through an apatite layer that is formed on the ceramic surfaces in the living body. This apatite layer was found to be formed even in an acellular simulated body fluid (SBF) with ion concentrations nearly equal to that of human blood plasma.[2] It was also found that an apatite layer is formed even on

pure titania gel in SBF.[3] This indicates that if Ti and its alloys were modified by chemical and heat treatments to form a titanate surface layer, the resulting material could form an apatite layer on its surface in the living body through which it could bond to the living bone.[1] Examples of Ti and its alloys formed with bioactive titanate layers on their surfaces by simple chemical and heat treatments are described below.

23.3. FORMATION OF BIOACTIVE SODIUM TITANATE LAYER

Ti metal was soaked in 5 M NaOH solution at 60°C for 24 h and then heat-treated at 600°C for 1 h. A layer of sodium hydrogen titanate ($Na_xH_{2-x}Ti_yO_2y_{+1}$) elongating perpendicular to the surface about 1 μm in thickness was formed on the surface of Ti metal by the NaOH treatment. This was transformed to a layer of sodium titanate ($Na_2Ti_6O_{13}$) accompanied with rutile (TiO_2) through the subsequent heat treatment, as shown in Fig. 23.1.[4] Auger electron spectroscopy (AES) confirmed that this surface layer gradually changed to the Ti metal substrate.[5]

Apatite was formed on the surface of the sodium titanate layer in SBF within one day and integrated with the layer, as shown on scanning electron

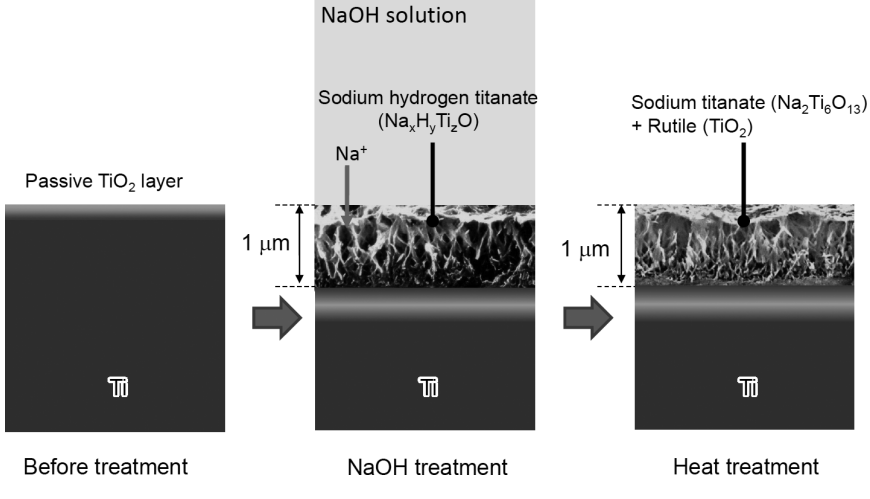

Figure 23.1. Structural change of the surface of Ti metal subjected to NaOH and heat treatments.

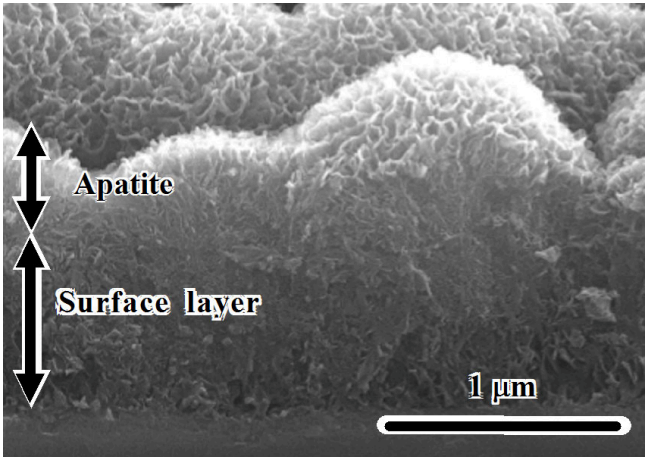

Figure 23.2. Cross-sectional SEM image of NaOH- and heat-treated Ti metal after soaking in SBF for one day.

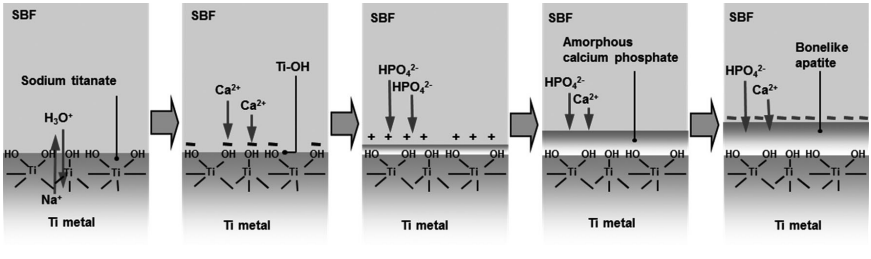

Figure 23.3. Process of apatite formation on NaOH- and heat-treated Ti metal in SBF.

micrograph (SEM) in Fig. 23.2.[4] According to X-ray photoemission spectroscopy, transmission electron microscopic observation and zeta-potential measurement, apatite was formed in SBF by the following process, shown in Fig. 23.3.[6] Sodium titanate releases Na^+ ions via exchange with H_3O^+ ions in SBF to form Ti–OH groups on its surface. The Ti–OH groups are negatively charged because the pH of the surrounding SBF increases,[7] and therefore preferentially combine with Ca^{2+} ions to form calcium titanate. As Ca^{2+} ions accumulate, the calcium titanate surface becomes positively charged to combine with phosphate anions, forming amorphous calcium phosphate, which is eventually transformed to crystalline bone-like apatite. Ti metal formed with the sodium titanate surface layer

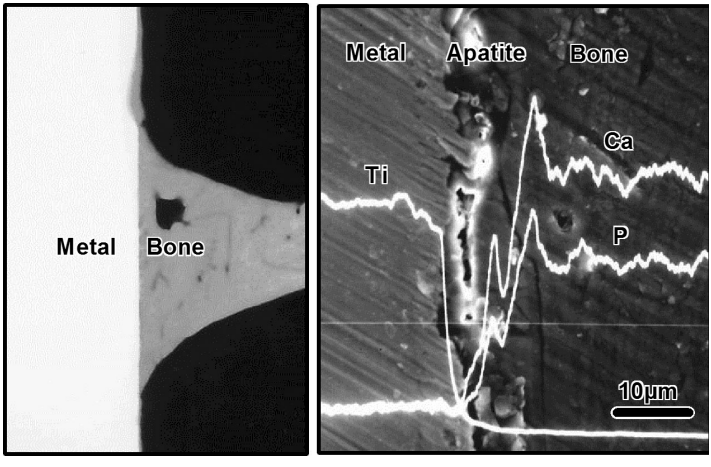

Figure 23.4. Contact microradiograph (left-hand side) and scanning electron micrograph-energy dispersive X-ray analysis picture (right-hand side) showing spontaneous bonding and integration of titanium metal, which was subjected to NaOH and heat treatments, to rabbit tibial bone after eight weeks' implantation.

precipitated apatite on its surface, which was implanted in the tibia of a rabbit, and tightly bonded to the living bone through the apatite layer, as shown in Fig. 23.4.[8] A total hip joint equipped with the porous Ti metal layer on which the sodium titanate layer was formed has been used clinically in Japan since 2007, as shown in Fig. 23.5.[9,10]

Moreover, the NaOH and heat treatments are effective for forming the bioactive sodium titanate layer on conventional Ti-based alloys such as Ti–6Al–4V, Ti–15Mo–5Zr–3Al and Ti–6Al–2Nb–Ta, but not for new Ti–Zr–Nb–Ta alloys because Na^+ ion release from the sodium titanate layer in the body are suppressed by the alloying elements.

23.4. FORMATION OF BIOACTIVE CALCIUM TITANATE LAYER

Ti–Zr–Nb–Ta alloys are important as implants, because they are free from suspected cytotoxic elements and can exhibit low elastic modulus and high mechanical strength.[11] Alloys of this type were soaked in 0.1 M $CaCl_2$ solution at 40°C for 24 h after the NaOH treatment and subjected to the heat treatment at

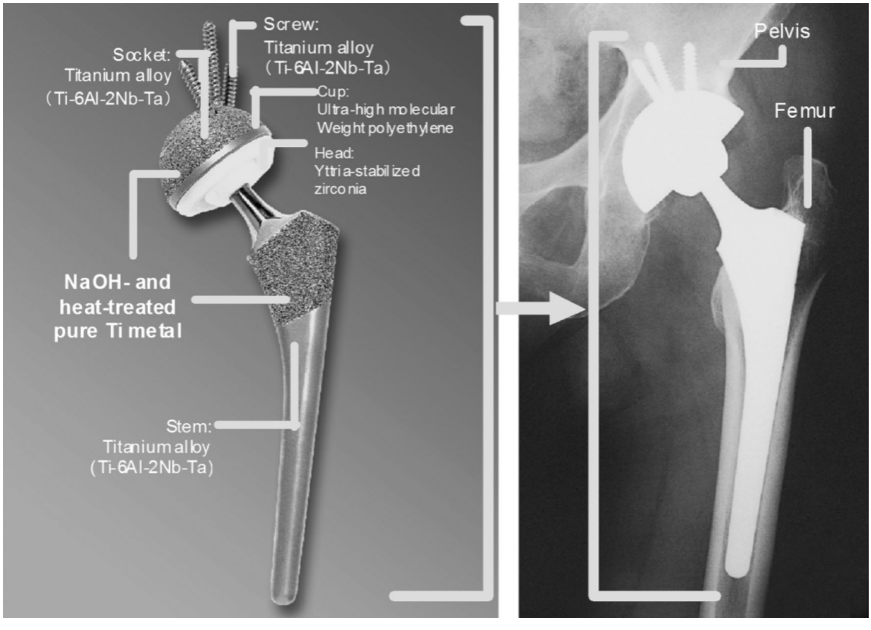

Figure 23.5. Clinical application of artificial hip joint formed with bioactive porous Ti metal on its surface in Japan since 2007.

600°C for 1 h. Na^+ ions in the sodium hydrogen titanate formed by the NaOH treatment were completely replaced with Ca^{2+} ions during the $CaCl_2$ treatment. Calcium titanate accompanied with rutile was formed after the subsequent heat treatment, as shown in Fig. 23. 6.[12] However, this calcium titanate layer did not form the apatite layer in SBF because Ca^{2+} ions were sparingly released from the calcium titanate layer. The alloys were then soaked in water at 80°C for 24 h to form Ca-deficient calcium titanate by partial exchange of Ca^{2+} ions in the calcium titanate layer on the top surface with H_3O^+ ions in water, as shown in Fig. 23.7.[12] As a result, the alloys formed the apatite layer in SBF because Ca^{2+} ions were readily released from the calcium titanate layer. Owing to this, not only the negatively charged Ti–OH groups were formed but also the ionic activity product of apatite in SBF was increased. These treatments imparted a higher apatite-forming ability even to Ti. When implanted in the tibia of a rabbit, Ti and its alloys subjected to these treatments bonded tightly to the surrounding bone, Fig. 23.8.[13] The so-formed bioactive Ti and its alloys are useful in various types of implants.

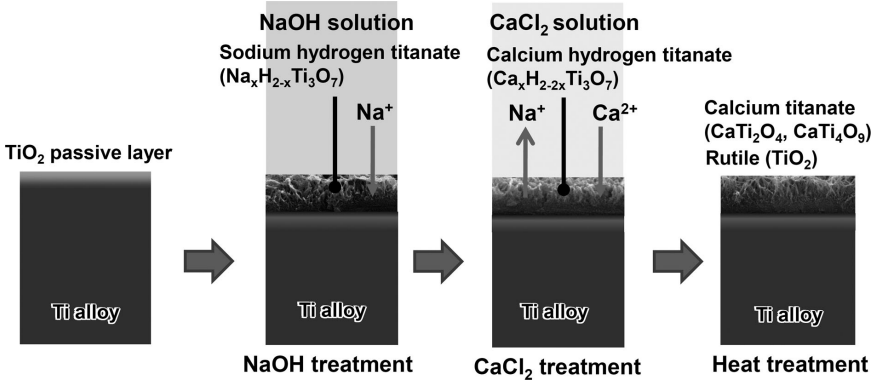

Figure 23.6. Surface structural changes of Ti-15Zr-4Nb-4Ta alloy with NaOH, $CaCl_2$ and heat treatments.

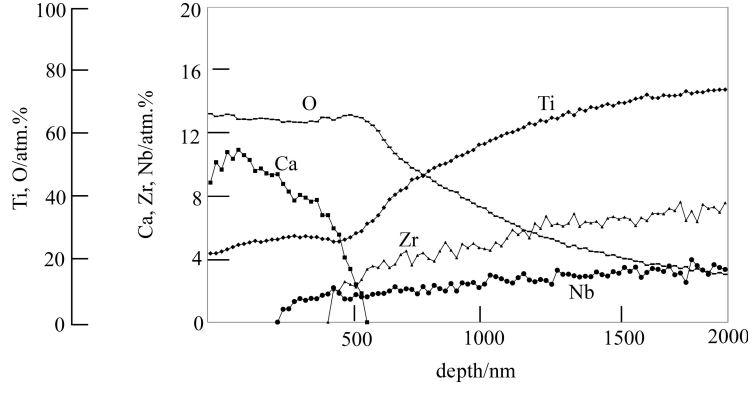

Figure 23.7. AES depth profiles of the surface of Ti-15Zr-4Nb-4Ta alloy subjected to NaOH, $CaCl_2$, heat and water treatments.

23.5. FORMATION OF BIOACTIVE TITANIUM OXIDE LAYER

Both the sodium and calcium titanate layers described above adopt a feather-like structure composed of thin needle-like phases, as shown in Figs 23.1 and 23.6. However, this type of surface layer is not resistant to shearing stress caused by treatments such as screwing in dental implants. A bioactive titanium oxide layer with a dense rough surface prepared by the following process may be suitable. Ti and its alloys were soaked in an aqueous solution with a pH less than 1.1 (e.g., H_2SO_4/HCl mixed acid solution) at 70°C for 1 h and then heat-treated at 500–650°C for 1 h. A layer of titanium hydride with a dense rough surface was

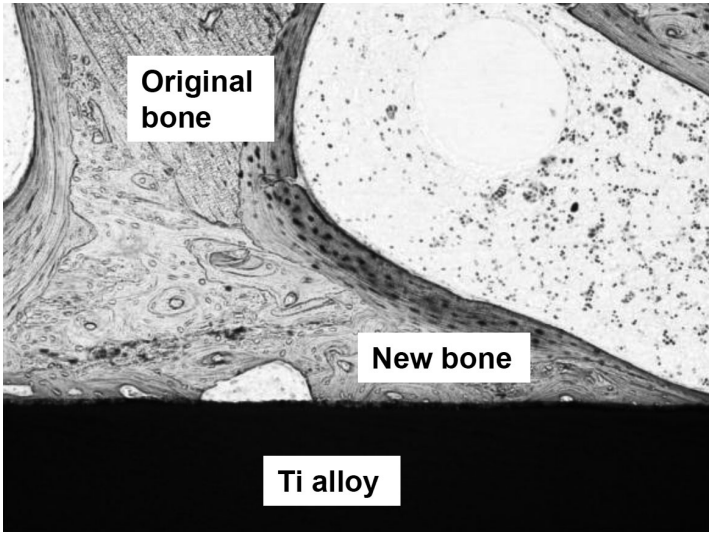

Figure 23.8. Optical micrograph of stained section of bone–implant interface at 16 weeks after implantation into tibia of rabbit for Ti-15Z-4Nb-4Ta alloy subjected to NaOH, $CaCl_2$, heat and water treatments.

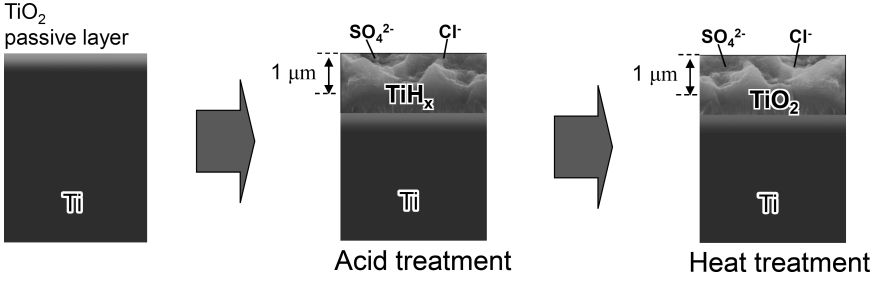

Figure 23.9. Structural changes of surfaces of Ti metal by acid and heat treatments.

formed on the Ti metal by the acid treatment that transformed to the rutile layer by the subsequent heat treatment without appreciable change in surface roughness, as shown in Fig. 23.9.[14]

Ti and its alloys formed with this rutile layer precipitated apatite on their surfaces in SBF, as shown in Fig. 23.10.[14] This was in contrast to Ti and its alloys formed with the rutile layer only by the heat treatment, which did not form the apatite layer.[14] According to the depth profile of the radio-frequency glow discharge optical emission spectra and zeta-potential measurement, the apatite layer

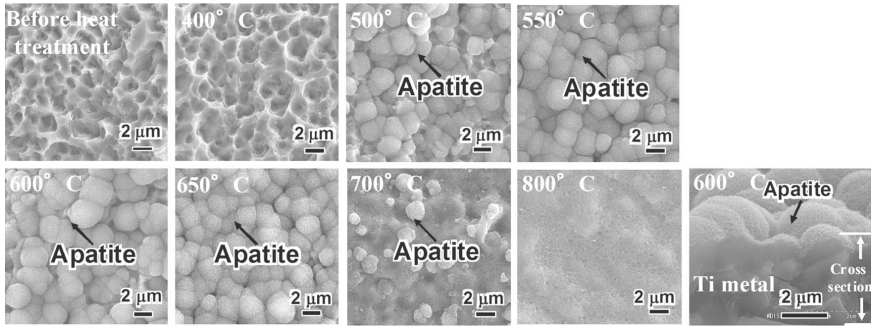

Figure 23.10. SEM photographs of surface of Ti metal soaked in SBF for one day, after heat treatment at various temperatures following acid treatment.

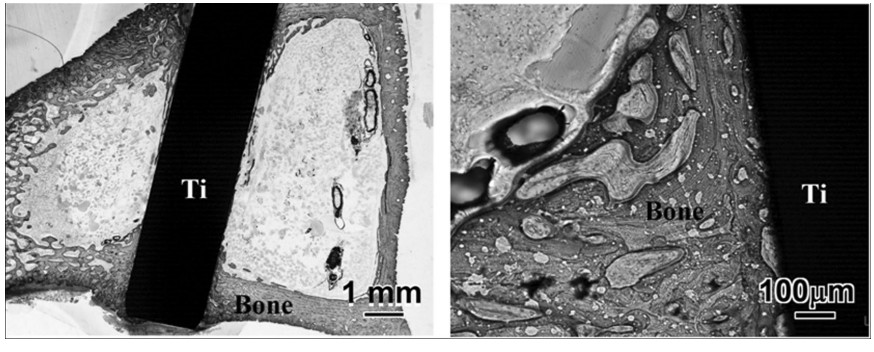

Figure 23.11. Optical microphotograph of strained section of acid- and heat-treated Ti metal implanted into rabbit tibia for four weeks.

is formed on the titanium oxide layer in SBF by the following process. Acidic groups such as SO_4^{2-} and Cl^- ions that are adsorbed on titanium hydride during the acid treatment remain on rutile even after the subsequent heat treatment and then dissociate in SBF to provide the acidic environment on rutile. Titanium oxide is positively charged in an acid environment, preferentially combining with phosphate anions, in contrast to the sodium and calcium titanate layers, which are negatively charged. As phosphate ions accumulate, its surface becomes negatively charged to combine with Ca^{2+} ions, forming calcium phosphate, which is eventually transformed to apatite.[14]

When implanted in the tibia of rabbit, the Ti metal formed with the titanium oxide layer by this process tightly bonded to the living bone, as shown in Fig. 23.11.[14] Porous Ti metal that was subjected to HCl and subsequent heat

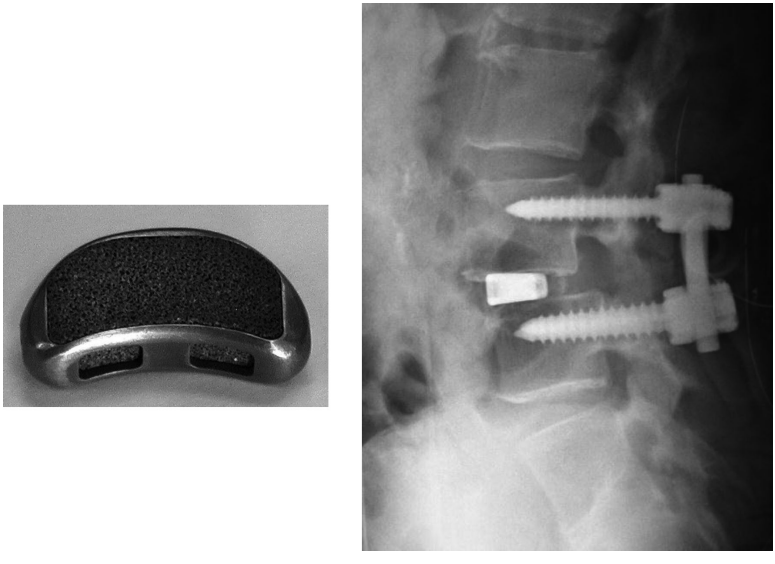

Figure 23.12. Clinical trial of spinal fusion by porous bioactive Ti metal for five patients (November 2008–June 2009).

treatments after the NaOH treatment to form a bioactive titanium oxide layer exhibited osteoinductivity and osteoconductivity.[15] This bioactive porous Ti was successfully subjected to clinical trials for use in a spinal fusion device in five patients, as shown in Fig. 23.12.[16] This type of device can be fixed to the surrounding bone without using an autograft.

23.6. SUMMARY

Novel bioactive titanate layers can be formed on the surface of Ti and its alloys by simple chemical and heat treatments. Bioactive metals prepared by this method are predicted to be useful in various types of implants in orthopaedic and dental fields.

REFERENCES

1. Kokubo, T. and Yamaguchi, S. (2010). Bioactive Ti Metal and its Alloys Prepared by Chemical Treatments: State-of-the-Art and Future Trends, *Adv. Eng. Mater.*, **12**, B579–B591.

2. Kokubo, T. and Takadama, H. (2006). How Useful is SBF in Predicting *In Vivo* Bone Bioactivity?, *Biomaterials*, **15**, 2907–2915.
3. Li, P., Ohtsuki, C., Kokubo, T. *et al.* (1994). The Role of Hydrated Silica, Titania, and Alumina in Inducing Apatite on Implants, *J. Biomed. Mater. Res.*, **28**, 7–15.
4. Yamaguchi, S., Takadama, H., Matsushita, T. *et al.* (2009). Cross-Sectional Analysis of the Surface Ceramic Layer Developed on Ti Metal by NaOH-Heat Treatment and Soaking in SBF, *J. Ceram. Soc. Jpn.*, **117**, 1126–1130.
5. Kim, H.-M., Miyaji, F., Kokubo, T. *et al.* (1999). Graded Surface Structure of Bioactive Titanium Prepared by Chemical Treatment, *J. Biomed. Mater. Res.*, **45**, 100–107.
6. Kim, H.-M., Himeno, T., Kawashita, M. *et al.* (2003). Surface Potential Change in Bioactive Titanium Metal During the Process of Apatite Formation in Simulated Body Fluid, *J. Biomed. Mater. Res.*, **67A**, 1305–1309.
7. Textor, M., Sitting, C., Franchiger, V. *et al.* (2001). "Properties and Biological Significance of Natural Oxide Films on Titanium and its Alloys", in Brunette, D.M., Tengrall, P., Textor, M. *et al.* (eds), *Titanium in Medicine*, Springer Verlag, New York, 172–230.
8. Yan, W.-Q., Nakamura, T., Kobayashi, M. *et al.* (1997). Bonding of Chemically Treated Titanium Implants to Bone, *J. Biomed. Mater. Res.*, **37**, 267–275.
9. Kawanabe, K., Ise, K., Goto, K. *et al.* (2009). Osteoinductive Porous Titanium Implants: Effect of Sodium Removal by Dilute HCl Treatment, *J. Biomed. Mater. Res.*, **90B**, 476–481.
10. Kokubo, T. (2005). Design of Bioactive Bone Substitutes Based on Biomineralization Process, *Mater. Sci. Eng. C.*, **25**, 97–104.
11. Geetha, M., Singh, A.K., Asokamani, R. *et al.* (2009). Ti Based Biomaterials, the Ultimate Choice for Orthopedic Implants — A Review, *Prog. Mater. Sci.*, **54**, 397–425.
12. Yamaguchi, S., Takadama, H., Matsushita, T. *et al.* (2010). Apatite-Forming Ability of Ti–15Zr–4Nb–4Ta Alloy Induced by Calcium Solution Treatment, *J. Mater. Sci. Mater. Med.*, **21**, 439–444.
13. Fukuda, A., Takemoto, M., Saito, T. *et al.* (2011). Bone Bonding Bioactivity of Ti Metal and Ti–Zr–Nb–Ta Alloys with Ca Ions Incorporated on their Surfaces by Simple Chemical and Heat Treatments, *Acta Biomater.*, **7**, 1379–1386.

14. Kokubo, T., Pattanayak, D.K., Yamaguchi, S. *et al.* (2010). Positively Charged Bioactive Ti Metal Prepared by Simple Chemical and Heat Treatments, *J. R. Soc. Interface*, **7**, S503–S513.
15. Takemoto, M., Fujibayashi, S., Neo, M. *et al.* (2006). Osteoinductive Porous Titanium Implants: Effect of Sodium Removal by Dilute HCl Treatment, *Biomaterials*, **27**, 2682–2691.
16. Fujibayashi, S., Takemoto, M., Neo, M. *et al.* (2011). A Novel Synthetic Material for Spinal Fusion: A Prospective Clinical Trial of Porous Bioactive Titanium Metal for Lumbar Interbody Fusion, *Eur Spine J.*, **20**, 1486–1495.

Chapter 24

PYROLYTIC CARBON COATINGS

Reinhold H. Dauskardt and Robert O. Ritchie

24.1. INTRODUCTION

Carbon is the most frequently found element in all organic molecules and compounds and as such performs a vital role in biological processes. As a crystalline material it can exist in a bewildering number of forms, some of which offer the most outstanding biocompatibility, chemical inertness and thromboresistance of any of the ceramics (or "bioceramics") used in biomedical applications. These properties have, for example, made various forms of carbon the preferred material where interface to blood flow is required. Alternatively, they can be attached to both soft and hard tissue, which is a prerequisite for a wide range of biomedical devices. Where device design and mechanical strength of the carbon form permit, components may be fabricated entirely of carbon. However, in the majority of biomedical applications carbon is used as a versatile coating, the principal mechanical properties often being derived from the underlying substrate material.

Three types of carbon are commonly used for biomedical devices: the low temperature isotropic (LTI) form of pyrolytic carbon, glassy (vitreous) carbon and the ultralow-temperature isotropic (ULTI) form of vapor-deposited carbon.[1–3] These three forms of carbon have a disordered lattice structure and are collectively referred to as turbostratic carbons. Although pyrolytic carbons were developed originally for elevated temperature applications (e.g., as coatings for nuclear fuel particles), LTI pyrolytic carbon has found wide appeal in the biomedical materials industry, in particular for mechanical cardiac valve prosthetic devices, as it has been shown to be highly thromboresistant and to have inherent cellular biocompatibility with blood and soft tissue. Moreover, it displays excellent durability, strength and resistance to wear, and had been thought to be immune to cyclic fatigue failure.

Indeed, the majority of modern mechanical heart valve prostheses utilize components manufactured from silicon-alloyed, LTI-pyrolytic carbon, either as a coating on a polycrystalline graphite substrate or as a monolithic material (where the substrate has been machined away). Alternatively, more complex shapes and even flexible materials may be obtained from coating fabricated metal

components or polymeric sheets or fabrics with a thin, impermeable layer of ULTI carbon by vapor deposition. Larger components can be fabricated by the controlled heating of a preformed polymeric body to form glassy carbon. Due to its inherently low density and weakness, however, glassy carbons are typically used as a thick coating which is reinforced by the underlying substrate.

With the exception of the LTI carbons which are co-deposited with silicon, all the carbons in clinical use are pure elemental carbon. Up to 20 weight percentage (wt%) silicon is most often added to LTI carbon to improve mechanical properties without significant changes in biocompatibility. Structurally, the clinically important turbostratic carbons are from the disordered end of the wide range of crystalline states of carbon to the perfect, three-dimensional graphite forms through the partially ordered graphite-like structures to the nearly amorphous state. Note, however, that by far the most important structural carbons for use in biomedical applications are the LTI pyrolytic carbons. For this reason more attention will be directed to these materials in our subsequent discussions.

In the following sections, we first discuss the composition, structure and processing procedures of the three clinically significant turbostratic carbons. These are unique compared to those of the more perfectly crystalline states of diamond or graphite. Then the important resulting biomedical and mechanical properties are considered. Finally, we will examine a number of biomedical applications and devices and conclude by discussing some important issues in device reliability and life prediction procedures.

24.2. CARBON STRUCTURES

While the microstructure of turbostratic carbon might seem very complicated due to its disordered nature, it is in fact quite closely related to the structure of graphite. In a graphite crystal, the carbon atoms are arranged in flat sheets or layer planes and the sheets stacked in a regular sequence to produce the three-dimensional graphite lattice as shown in Fig. 24.1a. Each carbon atom is strongly covalently bonded to the six nearest neighbor atoms, forming a hexagonal array within each layer, while the layers are relatively weakly bonded by van der Waals attractions. The weak bonding between planes results in the highly anisotropic properties of single crystals of graphite. However, when a solid is composed of many small crystals having random orientations, the bulk material behaves in an isotropic fashion.[4,5]

In graphite, the layer planes are stacked in a regular ABAB sequence. It is possible to disorder the sequence by disrupting the stacking through random

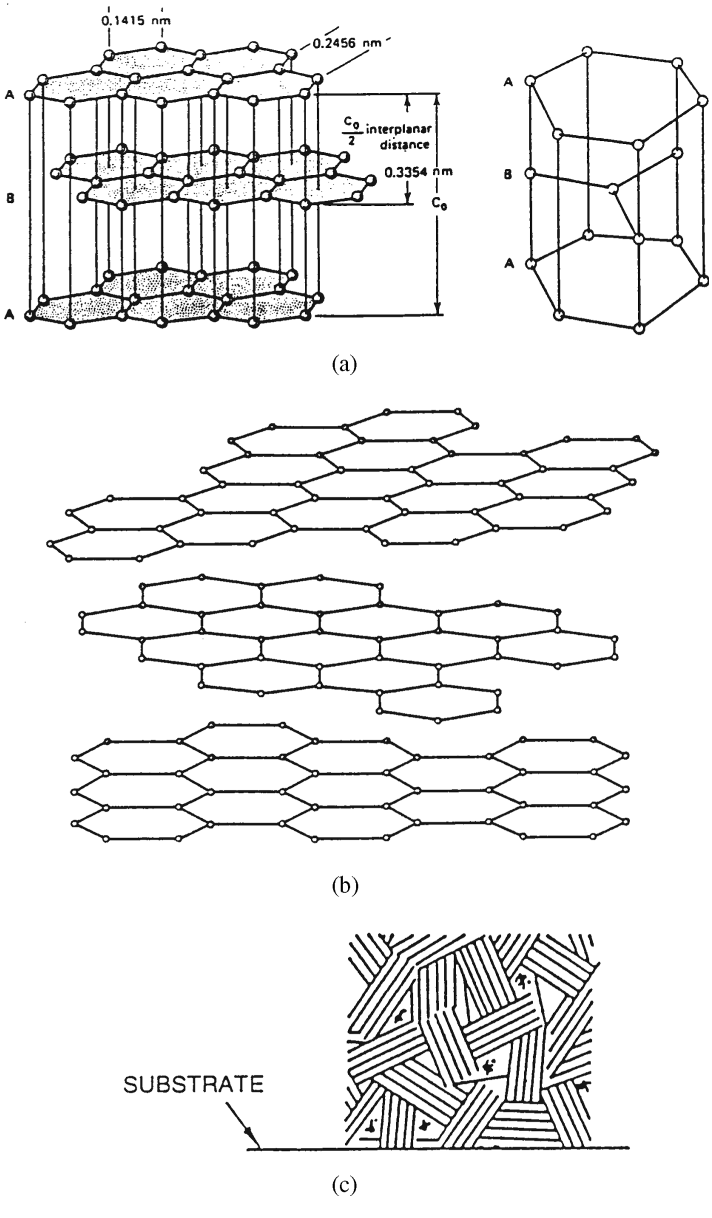

Figure 24.1. The crystallographic arrangement of carbon atoms in (a) hexagonal graphite where parallel layer planes are in a regular sequence and (b) a turbostratic carbon where the layers are arranged without order. Randomly oriented turbostratic crystallites are assembled to produce a bulk material in (c).

rotations or displacements of the layers relative to each other. Carbon materials having such disordered lattice plane stacking are known as *turbostratic* structures (Fig. 24.1b). In graphite the crystal size might be as large as 100 nm in diameter, the disordered regions of turbostratic carbon or "crystallites" are only around 10 nm in size. Randomly oriented turbostratic carbon crystallites are assembled to produce the bulk material as shown in Fig. 24.1c. This random packing results in isotropic mechanical and physical properties at the macroscale.

Missing carbon atoms leads to many vacant lattice sites in each of the turbostratic layer planes. Imperfect matching of small segments of these planes also leads to wrinkles or distortions within each plane. Furthermore, there may also be a substantial fraction of disorganized carbon between crystallites in the bulk material. As might be expected, such distortion and voiding in the structure may result in a marked effect on both the density and strength of turbostratic carbons. Densities, therefore, range from 1,400 kg/m^{-3} to a theoretical limiting value of 2,200 kg/m^{-3}. High density LTI carbons are the strongest bulk form of turbostratic carbon and their strength can be increased by adding silicon, as discussed in the following section. ULTI carbon can also be produced with high densities and strengths, but is available only as a thin coating (0.1–1.0 μm) of pure carbon. Glassy carbon is inherently a low density material and as such is weak.

24.3. PROCESSING

Dense and high strength LTI pyrolytic carbon components are typically made by co-depositing carbon and silicon carbide on a polycrystalline graphite substrate via a chemical vapor-deposition, fluidized-bed process using a gas mixture of a silicon containing carrier gas with a hydrocarbon (e.g., propane, methyltrichlorosilane and helium gas mixtures) at elevated temperatures.[1–3] The resulting material contains typically 10 wt% silicon, often in the form of discrete submicron β-SiC particles randomly dispersed in a matrix of roughly spherical micron-size subgrains of pyrolytic carbon; the carbon itself has a subcrystalline turbostratic structure, with a crystallite size of typically less than 10 nm.

The system used for production of pyrolytic carbon coatings is shown schematically in Fig. 24.2. The fluidized bed coater is in principle a simple apparatus which consists of a vertical tube furnace (or reactor) containing a bed of granular particles, usually zirconium oxide. The reactant gas stream enters the reactor and fluidizes (i.e., supports and agitates) the bed of particles in which the components to be coated are suspended. Due to the high temperatures (typically

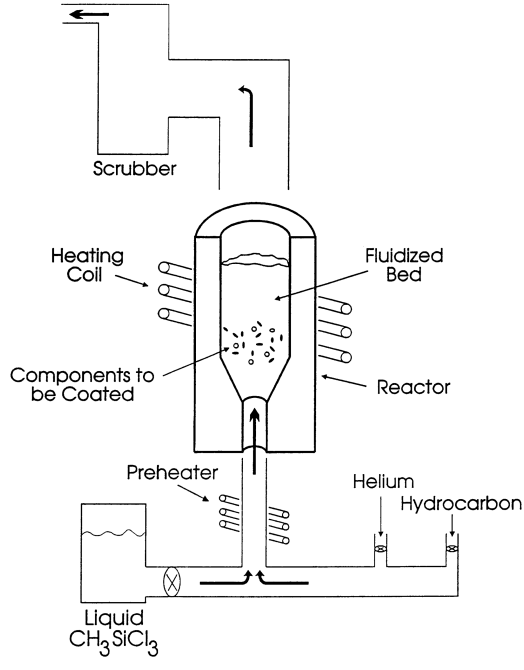

Figure 24.2. Fluidized bed process for coating components with LTI pyrotytic carbon.

in the range 1,000–1,500°C), the hydrocarbon gas "cracks" or pyrolyzes according to the reactions:

$$C_3H_8 \rightarrow 3C + 4H_2, \text{ and} \tag{24.1}$$

$$CH_3Cl_3Si \rightarrow SiC + 3HCl. \tag{24.2}$$

The solid products of these pyrolysis reactions are carbon and silicon carbide, which deposit as a coating on everything in the bed, including the fluidizing particles and the graphite components to be coated. The fluidizing bed system is equipped with metering devices so that the quantity of carrier gas, hydrocarbon and silicon-containing hydrocarbon can be controlled to give the proper concentrations for deposition.

The silicon carbide present in silicon alloyed pyrolytic carbon does not dissolve in the carbon matrix but instead forms discrete second-phase particles of silicon carbide with cubic crystal symmetry, as shown schematically in Fig. 24.3. The quantity of silicon present has a marked influence on the

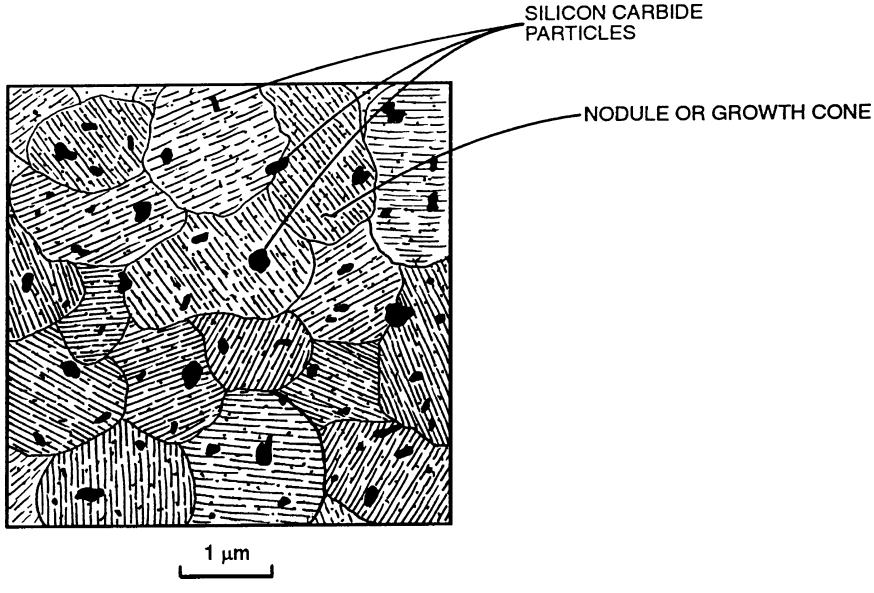

Figure 24.3. Schematic illustration of the microstructure of silicon alloyed LTI pyrolytic carbon. Nodules or growth cones, with sizes dependent on the processing parameters, are comprised of millions of crystallites of turbostratic carbon. Randomly dispersed throughout the matrix are particles of silicon carbide which vary in size from 1 to 1,000 nm.

mechanical properties of pyrolytic carbon. As the silicon content increases, fracture strength, wear resistance, hardness and the elastic modulus increase significantly. Both the content and distribution of silicon carbide particles is quantitatively measured using X-ray diffraction (XRD) and scanning electron microscopy (SEM) techniques and must be carefully controlled to achieve optimum properties.

Glassy or vitreous carbons are formed by slowly heating a solid polymeric perform, such as cellulosics or phenol-formaldehyde resin, to drive off volatile constituents. The heating rate during formation must be carefully controlled to allow diffusion of the volatiles through the polymeric mass and prevent bubble formation within the part. This requirement typically limits the thickness of glassy carbon components to less than 7 mm. These carbons are composed of random crystallites of the order of 5 nm in size. While the glassy carbons only achieve a maximum density of ~1,500 kg/m^{-3}, they have, in fact, quite a low porosity. This leads to the low permeability of glassy carbons to liquids and gasses since the porosity is not interconnected.

The ULTI vapor-deposited carbons can be produced with much higher densities and strengths but only as a thin coating, typically in the range of 0.1–1.0 mm in thickness. The coating is formed by a hybrid vacuum process by using a catalyst to deposit carbon from a carbon-bearing precursor. With variations in processing parameters, the density, crystallite size and isotropy of the coating can be varied within quite wide ranges. In addition, cooling of the substrate during coating allows the coating of low melting point materials such as Dacron®, Teflon® and polyurethane parts and sheets (Trademark, E. I. DuPont de Nemours, Inc., Wilmington, Delaware).

The adhesion of the ULTI coating to the substrate is naturally an important design consideration, particularly when used on flexible substrates. When used as a coating on certain clinical stainless steels and titanium (Ti-6Al-4V) alloys, a bond strength exceeding 70 MPa is achieved. This excellent bond strength is, in part, due to the formation of carbides at the carbon/metal interface. The bond strength with other materials that do not form carbides is typically lower.

24.4. MECHANICAL AND BIOMEDICAL PROPERTIES

The mechanical properties of the various turbostratic carbons are closely related to their microstructures, with a strong correlation of most of these properties with coating density. Other microstructural features such as crystallite size, structure and orientation, grain size and composition are also important in determining the resulting properties. Some of the more important mechanical properties of the clinically useful turbostratic carbons, together with a typical polycrystalline graphite substrate onto which coatings might be deposited, are presented in Table 24.1.

24.4.1. Strength and Modulus

Due to the highly anisotropic properties of graphitic crystals, the macroscopic mechanical properties of polycrystalline carbons depend strongly on degree of crystal orientation. Also, the porosity of the material affects the strength by reducing the internal area over which the stress is distributed and by creating local regions of high stress. Accordingly, carbons with a high degree of preferred orientation and high density are extremely strong and stiff in directions parallel to the preferred layer planes. On the other hand, in turbostratic carbons where the crystallites are randomly arranged and the material is not fully dense, lower strengths and dramatically reduced moduli are measured. Therefore, while typical

Table 24.1. Structural and Mechanical Properties of Graphite and Biomedical Turbostratic Carbons.

	Polycrystalline Graphite Substrate	Silicon Alloyed LTI Pyrolytic Carbon	Glassy (Vitreous) Carbon	ULTI Vapor Deposited Carbon
Density (kg/m^{-3})	1,500–1,800	1,700–2,200	1,400–1,600	1,500–2,200
Crystallite Size (nm)	15–250	3–5	1–4	8–15
Expansion Coefficient ($10^{-6}\,K^{-1}$)	0.5–5	5–6	2–6	—
Hardness (DPH)	50–120	230–370	150–200	150–250
Young's Modulus (GPa)	4–12	27–31	24–31	14–21
Flexural Strength (MPa)	65–300	350–530	69–206	345–690
Fracture Strain (%)	0.1–0.7	1.5–2.0	0.8–1.3	2.0–5.0
Fracture Toughness (MPam-1/2)	–1.5	0.9–1.1	—	—

LTI pyrolytic and ULTI vapor-deposited materials still retain a comparatively high strength, their moduli are uncharacteristically low. The greater porosity of the glassy carbons generally results in even lower strengths, contributing to a weak structure, which is albeit still stronger than polycrystalline graphite.

The moduli of the turbostratic carbons are close to 21 GPa and hence are close in magnitude to the modulus of bone (see Chapter 1). A carbon implant device under physiological loading and in contact with bone can therefore deform elastically with the bone and minimize stress concentrations which might otherwise develop. As a comparison, the modulus of surgical stainless steel or titanium alloys is almost an order of magnitude higher than that of bone (Chapter 1).

24.4.2. Hardness and Wear

The hardness or resistance of a material to indentation is an important property of turbostratic carbons since, as with most materials, it closely correlates with resistance to wear. Hardness is also important for LTI pyrolytic carbons since it correlates with the silicon carbide content, carbon crystal size and the deposition temperature and is therefore an indirect indicator of these parameters. In addition, wear rates typically decrease noticeably with increasing hardness. Silicon-alloyed LTI pyrolytic carbon has superior wear resistance compared to other forms of graphite or even unalloyed pyrolytic carbon. Excellent wear

resistance is particularly important for components of artificial heart valves which articulate against each other and are exposed to significant wear and possible cavitation erosion during a patient's lifetime.

24.4.3. Fracture Resistance

The high strength and low moduli of turbostratic carbons results in large strains to failure when compared to other brittle ceramics. For example, while the total strain to rupture of an alumina ceramic specimen is 0.1% and those for polycrystalline graphites are in the range 0.1–0.7%, the fracture strain for LTI pyrolytic carbons is 1.5–2.0% and can be as high as 5% for ULTI vapor-deposited carbons. The high fracture strains are thought to result in part from the network of strong C–C covalent bonds in the graphitic layer planes, which must be broken before failure by shear or cleavage can be accommodated.[6] These large fracture strains are important properties for coatings of flexible polymeric substrates, which must be able to sustain significant bending and flexing without cracking of the coating.

While the high fracture strains measured using smooth, uncracked specimens are high, they are sometimes incorrectly taken as an indication of material toughness. The catastrophic failure of many engineering structures occurs well below their strength or fracture strain. The toughness or "resistance to fracture" of turbostratic carbons must, therefore, be measured in the presence of cracks or flaws which may be present in the final device.

Using a fracture mechanics approach, the *fracture toughness* or critical stress intensity factor, K_c, can be measured by inserting an "atomically-sharp" crack of known length into a specimen and loading until fast fracture occurs. (In simple terms, the stress intensity, K, is given as $Q\sigma\sqrt{\pi a}$, where σ is the applied stress, a is the crack size and Q is a geometry-dependent factor of order unity.) Using this approach, the toughness of silicon alloyed pyrolytic carbon has been measured in the range 0.9–1.1 $MPa\sqrt{m}$, only slightly higher than that of soda lime glass and less than half the fracture toughness of alumina or silicon nitride ceramics. Similar to other ceramics, these low values of fracture toughness remain a significant limitation for the reliable design of many pyrolytic carbon devices, particularly in the presence of tensile residual stresses in the coatings of composite components. Therefore, while the fracture strain does affect the fracture toughness depending on the specific fracture mechanism, the *magnitude* of the uniaxial fracture strain measured in a tensile specimen will be quite different to the highly constrained fracture strain in the triaxial stress field ahead of a sharp crack. For this reason, fracture strain and fracture toughness often show poor correlation.

In linear-elastic materials, it is also possible to express the toughness as a critical strain energy release rate, G_c, which is related to the fracture toughness by $G_c = K_c^2/E$ (where E is Young's modulus). It is interesting to note that because of the low moduli of the turbostratic carbons, in this formulation the converted toughness appears to be quite high, typically 0.04–0.3 kJ/m^{-2}, compared to other ceramics which have much higher moduli and hence lower G_c values in the range 0.02–0.1 kJ/m^{-2}. This apparent contradiction in toughness rankings is best rationalized by recognizing that the actual energy required to cause fracture in a device might be largely due to the large deflections which result from the low moduli of turbostratic carbons. However, such fractures can occur at very low stresses depending on the device configuration. The onset of fracture is therefore nearly always calculated from a design stress approach using the fracture toughness, K_c; energy calculations based on G_c are rarely used in mechanical design against fracture.

24.4.4. **Cyclic Fatigue**

An important finding concerns the assumed insensitivity of turbostratic carbons and other brittle ceramic materials to cyclic fatigue degradation.[7–9] Early studies claimed that the fatigue endurance strength of these materials was virtually identical to the single cycle fracture stress, i.e., that cyclic stresses less than this stress do no microscopic damage. However, studies employing fracture-mechanics type testing procedures with precracked samples demonstrate that fatigue cracks can grow under alternating loads in monolithic pyrolytic carbon and pyrolytic carbon-coated graphite composites in both ambient temperature air and blood-analog environments. The typical crack growth rate per loading cycle, da/dN, for a pyrolytic carbon composite, together with similar data for other brittle ceramic materials, are shown in Fig. 24.4 as a function of the stress intensity range, $\Delta K = K_{max} - K_{min}$, where K_{max} and K_{min} are the maximum and minimum values of the applied cyclic stress intensity. Also included in the figure for comparison is the crack growth behavior of two structural metallic alloys.

While the data in Fig 24.4 show a clear (cyclic) fatigue effect, in view of past skepticism over fatigue in brittle materials, it is necessary to demonstrate unequivocally that the crack growth is cyclically induced and not simply a consequence of stress corrosion (static fatigue) cracking at maximum load. To achieve this, crack extension was monitored with the stress intensity cyclically varied between K_{max} and K_{min} and the stress intensity held constant at the same value of K_{max}. This procedure was periodically repeated throughout the range of growth rates; a typical result, for K_{max} is shown in Fig. 24.5, where 1.36 MPa$\sqrt{m}$

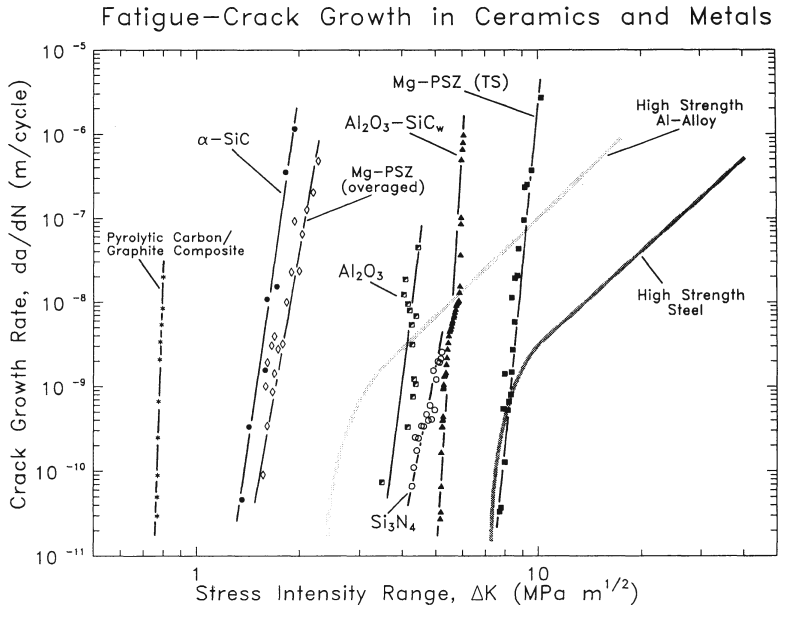

Figure 24.4. Cyclic fatigue crack growth behavior of a LTI carbon/graphite composite shown in comparison with a range of ceramics including alumina, silicon nitride, silicon carbide and zirconia, and two structural metallic alloys.

and K_{min} = 0.14 MPa√m. Whereas crack extension proceeds readily under cyclic loading conditions (Region a), upon removal of the cyclic component by holding at the same K_{max} (Region b), crack-growth rates are markedly reduced. Clearly, similar to behavior reported for other ceramics, a true cyclic fatigue effect is apparent. Furthermore, subcritical fatigue crack growth rates under cyclic loading appear to be far in excess of those under equivalent sustained loading.

These observations of cyclic fatigue crack growth in ceramics and pyrolytic carbons have important consequences for the many prosthetic devices which are exposed to repeated physiological loading. This phenomenon is particularly important in heart valve applications, as the human heart typically beats 38 million times each year, necessitating the structural design of prostheses for fatigue lifetimes in excess of patient lifetime, i.e., between 10^9 and 10^{10} cycles. Indeed, some structural failures of mechanical heart valves manufactured from pyrolytic carbon have been attributed to progressive fracture by fatigue. We discuss the importance of cyclic fatigue effects in life prediction and device reliability in a later section.

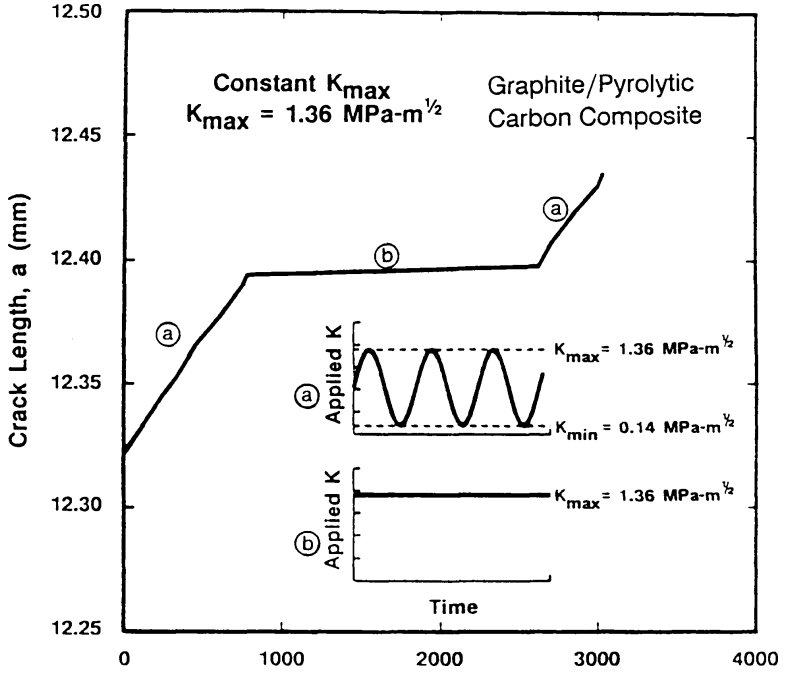

Figure 24.5. The effect of sustained load vs. cyclic loading conditions, at a constant K_{max}, on the subcritical crack growth in pyrolytic carbon coated graphite tested in Ringer's solution at 37°C. Note how crack growth rates under cyclic loading (Region a) are far in excess of those measured under sustained loading (Region b).

24.4.5. Stress Corrosion Cracking

Similar to other ceramics, turobstratic carbons are prone to subcritical crack growth under the synergistic action of an applied load and a moist (or corrosive) environment. Such stress corrosion (static fatigue) crack growth behavior is plotted in terms of the crack velocity with respect to time (da/dt) as a function of the applied monotonic stress intensity in Fig. 24.6. The data include an LTI pyrolytic carbon/graphite composite in an environment of Ringer's lactate (blood analog) solution at a temperature of 37°C, glassy carbon in water and in air, and data for a pyrolytic graphite in air. Crack velocities span many orders of magnitude from 10^{-9} to 10^{-1} m/sec and, similar to cyclic fatigue crack growth, show a marked sensitivity to the applied stress intensity. Like cyclic fatigue, it is important to characterize the stress corrosion cracking behavior of turbostratic carbons in order to permit reliable design.

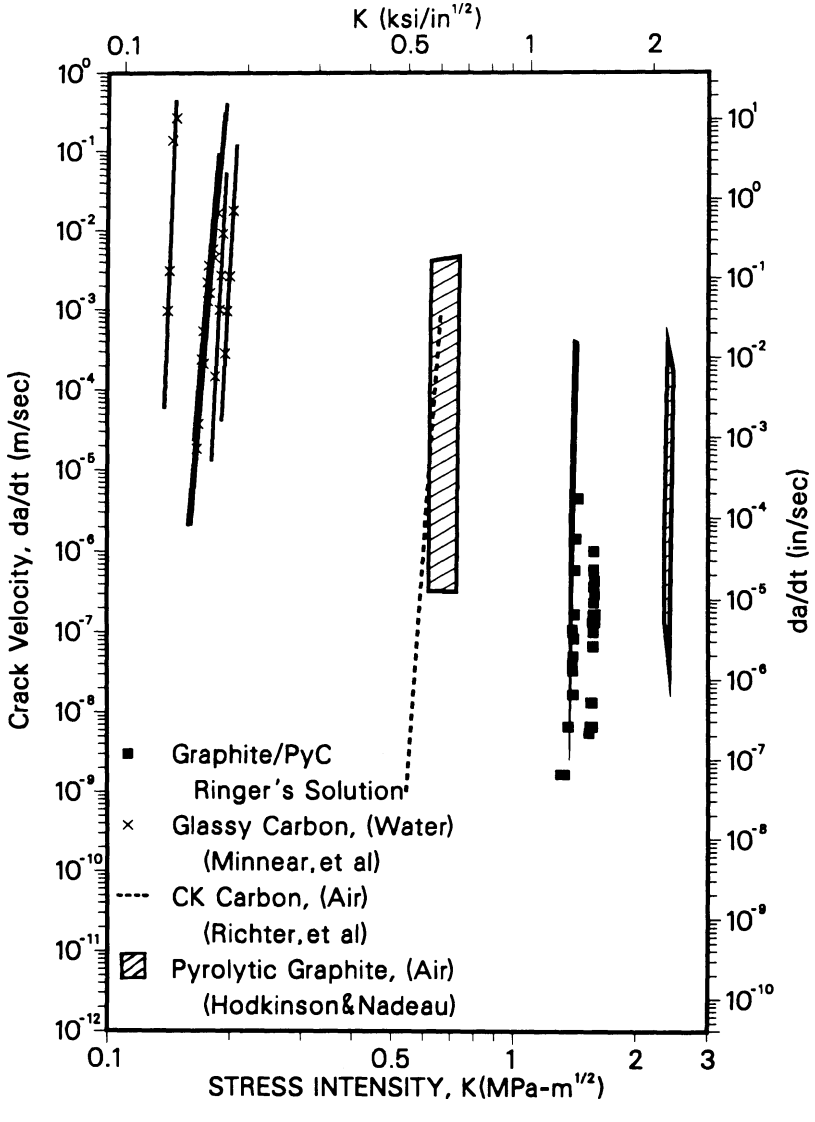

Figure 24.6. Stress corrosion crack growth behavior of a graphite/LTI carbon coated composite tested in 37°C Ringer's solution, shown in comparison with data for glassy carbon tested in water and air and for pyrolytic graphite in ambient temperature air.

24.4.6. Residual Stress

Biomedical turbostratic carbon coatings often exist in a state of residual stress. Like most coatings cooled from a higher processing temperature, the residual thermal stress state depends on the difference in thermal expansion mismatch between the coating and the underlying substrate material. Variation in the structure and grain size of the coating from the interface with the substrate to the coating surface may also affect the residual stress state. Both effects depend on the coating thickness. For LTI pyrolytic carbon-coated graphite components, the greater thermal expansion coefficient of pyrolytic carbon compared to graphite results in a tensile residual stress in the coating. Depending on processing temperature and microstructural variation, measurements indicate a tensile stress of up to 60 MPa in the coating. Such residual stresses may be detrimental to the integrity of the coating. The residual stress must be added to the nominal applied stress when evaluating the likelihood for fracture in the coating.

24.4.7. Biocompatibility

From a biomaterials viewpoint, the greatest attribute of the three forms of turbostratic carbon is their excellent cellular biocompatibility and thromboresistance.[1–3] This is particularly true of the high purity LTI pyrolytic and ULTI vapor deposited carbons. Depending on the polymeric precursor and the processing temperature, the purity of the glassy carbon forms may result in variability in biocompatibility. While the biocompatibility of the turbostratic carbons has been studied extensively, no theory explaining their excellent properties exists.

In cardiovascular applications, the compatibility of LTI pyrolytic carbons with blood has received the most attention. Unlike soft and hard tissue reactions to implanted materials, which tend to be slow to develop, the rejective reactions in blood are dramatic and swift. Most materials in contact with blood quickly activate the tissue's clotting mechanism. LTI carbon has been shown to be equivalent to siliconized glass, which causes little damage to blood. Theories to explain the excellent cellular biocompatibitily of LTI carbon with blood range from conditioning of the carbon surface with a passivating protein layer, through selective adsorption to the complete inertness of the LTI carbon surface to proteins in general. A general observation, however, is that smooth or polished surfaces are better than rough surfaces, possibly because roughness may provide locations where cells can adhere and serve as thrombotic nuclei.

While ULTI vapor-deposited coatings have also been shown to have excellent biocompatibility and thromboresistance with blood, glassy carbons

have been studied primarily for attachment to both soft and hard tissue. When implanted, glassy carbons in general do not provoke an inflammatory response in adjacent tissue. Similar behavior has been reported for the LTI and ULTI carbons. Note, however, that although smooth surfaces promote better thromboresistance, rougher surfaces which allow tissue in-growth and attachment provide stronger interfaces to soft or hard bone tissue.

24.5. APPLICATIONS

The excellent cellular biocompatibility of the three biomedical turbostratic carbons together with selected mechanical properties have resulted in a wide range of successful applications. Bokros has compiled a list of applications and these are reproduced in Table 24.2. We restrict our discussion to cardiovascular and dental applications in the following sections.

24.5.1. Cardiovascular

Mechanical cardiac valve prostheses are designed to regulate blood flow continuously in hostile physiological environments for periods in excess of patient lifetimes. Valve components are exposed to cyclic loading, flexing and bending, wear at surfaces exposed to articulation and cavitation erosion on surfaces exposed to blood flow. These requirements represent one of the most demanding biomaterial applications. They also represent, however, one of the greatest successes of bioceramics in the form of silicon alloyed LTI pyrolytic carbon, which is currently used in the majority of artificial heart valves.

Many modern heart valves are based on the tilting disk design, which open and close as the heart beats, allowing blood flow under near-normal rheological conditions. Some designs involve two semicircular leaflets (bileaflet valves) instead of a single disk or occluder. The disk or leaflets are contained in a circular housing which has a cloth sewing ring on the outer diameter to facilitate attachment to the heart (Fig. 24.7). The disk or leaflets and housing are manufactured from LTI carbon-coated graphite, although some devices use a cobalt-chromium or titanium alloy housing. Unfortunately, the complex shapes of some of the metal housings require the use of casting and welding technologies in their manufacture. As a result, serious problems have arisen with some of these devices, leading to catastrophic failures by fatigue of the valve housing.

One of the primary restrictions on artificial heart valves is the uncertain lifetime under complex physiological loading due to degradation by cyclic fatigue

Table 24.2. Successful Applications of Glassy, LTI and Vapor-Deposited ULTI Carbons (After J.C. Bokros).

		Material Characteristics Contributing to Success			
Application	**Material**	**Cellular Compatibility**	**Strength**	**Wear Resistance**	**Stiffness**
Mitral and aortic heart valves	LTI	X	X	X	
Dacron® and Teflon® heart valves sewing rings	ULTI	X			
Blood access device	LTI/titanium	X			
Dacron® and Teflon® vacular grafts	ULTI	X			
Dacron®, Teflon® and polypropylene septum and aneurysm patches	ULTI	X			
Pacemaker electrodes	Porous glassy carbon-ULTI-coated porous titanium	X			
Blood oxygenator microporous membranes	ULTI	X			
Otologic vent tubes	LTI	X	X		
Subperiosteal dental implant frames	ULTI	X			
Dental endosseous root form and blade implants	LTI	X	X		X
Dacron-reinforced polyurethane aoplastic trays for alveolar ridge augmentation	ULTI	X			
Percutaneous electrical connectors	LTI	X	X		
Hand joints	LTI	X	X	X	X

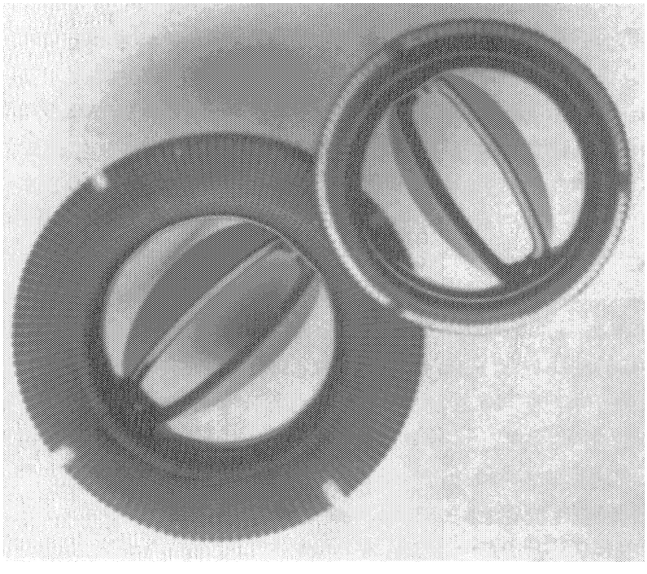

Figure 24.7. A typical bileaflet artificial heart valve with components made from silicon alloyed LTI pyrolytic carbon (courtesy Baxter Medical Inc.).

or stress corrosion. While heart valves manufactured from pyrolytic carbon-coated graphite are currently used extensively, with more than 200,000 in use (in 1993), several structural failures of LTI carbon-coated components have been attributed to cyclic fatigue. These conclusions are questionable due to difficulty in distinguishing fractographic features produced under cyclic and monotonically loaded conditions.

The identical morphology of cyclic fatigue and overload (fast) fracture surfaces is not unique to pyrolytic carbon (Fig. 24.8a and b); similar behavior is shown by the graphite core of the composite material (Fig. 24.8c and d), and by most ceramic materials where cyclic fatigue fractures are documented. This is in marked contrast to metallic materials where the characteristic cyclic fatigue fracture mode, i.e., striations (Fig. 24.8e), is quite distinct to the transgranular cleavage (Fig. 24.8f), microvoid coalescence or intergranular fracture seen for failure under monotonic loads. The reason for this is not clear, due to current uncertainties in the micromechanisms of ceramic fatigue. The implication is that post failure analysis of fracture surfaces in pyrolytic carbon can be very deceptive.

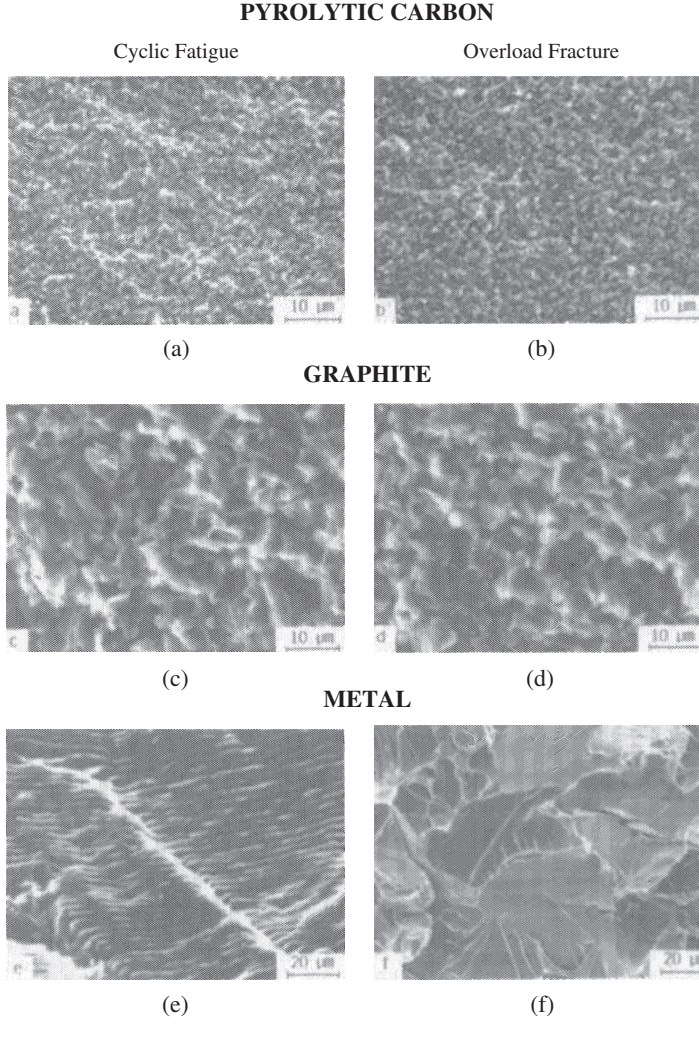

Figure 24.8. Low and high magnification SEMs of cyclic fatigue and overload (fast) fracture in (a and b) the LTI pyrolytic carbon cladding, (c and d) the polycrystalline graphite substrate and (e and f) a metallic material (low-strength ferritic steel), showing (e) fatigue striations and (e) transgranular cleavage fracture.

24.5.2. Dental

The close elastic modulus match between glassy and LTI carbons and bone make the carbons candidate materials for a number of load-bearing dental implant applications. Artificial tooth roots with sizes up to 11 mm in length and 5 mm in diameter have been manufactured from glassy carbon. LTI carbon with its superior strength has been used in more complex implant designs. Where the size and complexity of the implant does not allow construction from carbon, components can be fabricated from metal alloys and coated with a thin impermeable layer of ULTI vapor-deposited carbon. Subperiosteal dental implants and endosseous tooth root replicas have been fabricated using these techniques. Such designs combine the superior mechanical properties of the metal with the chemical properties of carbon.

24.6. DEVICE RELIABILITY

Careful mechanical design and accurate life prediction, which must accurately simulate realistic failure modes, are essential elements for the reliable use of ceramic implants exposed to complex physiological loading and environmentally-induced degradation in many clinical applications. The structural design of cardiovascular-assist devices places particularly demanding requirements on the pyrolytic carbon-coated components. To maintain structural integrity, prosthetic heart valves must therefore be designed to endure fatigue lifetimes greater than ~10^9 cycles in blood analog environments; current FDA requirements demand that this is achieved using so-called damage-tolerant design procedures. These procedures rely upon the fracture-mechanics based concept that a conservative (worst-case) estimate of the structural life can be defined in terms of the time, or number of loading cycles, for the largest undetected crack to grow to critical size, generally defined in terms of the material's fracture toughness, K_c. A similar analysis might be required for other forms of crack growth, for example, stress corrosion cracking in components subject to sustained (noncyclic) loads.

There are three principal material property inputs to such calculations: the initial flaw population or size of the largest (worst-case) crack pre-existing in the device (which must be defined by quality control); the critical crack size for catastrophic failure of the device (which in most cases is defined by the material's fracture toughness, K_c); and the rate at which the incipient cracks will grow subcritically between these two limits. Of these, the crucial input for fatigue life

prediction is the rate of subcritical crack growth; specifically, relationships are required which define the crack growth increment per cycle, da/dN, as a function of a crack-driving force such as the stress intensity, K. In prostheses fabricated from metallic materials such as cobalt and titanium alloys, such cyclic fatigue crack growth data are widely available in handbooks or can be measured using ASTM standard techniques. In prostheses manufactured from pyrolytic carbons, fatigue data have only recently become available, in part because it had been incorrectly assumed that pyrolytic carbon was immune to cyclic fatigue failure. Damage-tolerant design and life-prediction procedures for both metallic and pyrolytic carbon implants are based on fatigue crack propagation data derived from conventional ASTM-style (e.g., compact-tension) test pieces containing long (typically ~2–20 mm in length), pre-existing through-thickness cracks.

Whereas all current analyses for pyrolytic-carbon/graphite implants utilize crack-propagation data conventionally measured on specimens with long, through-thickness cracks, the reality of actual flaw growth for valves in service is more likely primarily associated with small, part-through (half-penny shaped) cracks, which initiate predominantly on the surface of the pyrolytic carbon coating and propagate both along the surface of the pyrolytic carbon and depth-wise toward the graphite core.[10] Such small crack behavior is undoubtedly of special importance to most ceramics simply because ceramic components will, in general, not be able to tolerate the presence of physically long cracks. Although the collection of small-crack data is both complex and labor-intensive, life-prediction procedures should be based on such data.

Studies of small crack growth behavior in other ceramic and ceramic-composite materials suggest that a reasonable correspondence can be obtained between the growth rate behavior of long, through-thickness cracks and small, part-through surface cracks, *provided cyclic crack growth rates are characterized in terms of the appropriate stress intensity factor, incorporating both external (applied) and internal (residual) stresses.* Such internal stresses may result during fabrication of the pyrolytic-carbon/graphite composite and/or from surface damage such as scratches or gouges incurred during handling of the device. With the appropriate characterization, in principle either form of growth-rate data could be utilized for life prediction.

Despite the highly successful and expanding use of pyrocarbons in the biomedical industry, since their initial development during the mid-1970s, little fundamental materials research has been published on these materials. Little is known about the mechanistic role of the microstructure in influencing their fracture and fatigue properties, so critical for the structural integrity of heart valve prostheses. For the continued use of turbostratic carbons as a

structural material for such safety-critical applications as medical implant devices, the mechanistic and microstructural basis underlying critical mechanical properties, such as strength, ductility, toughness and resistance to fatigue, wear and erosion, must be further investigated. See Chapter 25 for further discussion.

ACKNOWLEDGEMENT

This work was supported by the Director, Office of Energy Research, Office of Basic Energy Sciences, Materials Sciences Division of the U.S. Department of Energy under Contract No. DE-AC03–76SF00098.

REFERENCES

1. Bokros, J.C., LaGrange, L.D. and Schoen, F.J. (1972). "Control of Structure of Carbon for use in Bioengineering", in Walker, P.L. (ed.), *Chemistry and Physics of Carbon*, Dekker, New York, pp. 103–171.
2. Bokros, J.C., Akins, R.J., Shim, H.S. *et al.* (1976). "Carbon in Prosthetic Devices", in Deviney, M.D. and O'Grady, T.M. (eds), *Petroleum Derived Carbons*, American Chemical Society, Washington, DC, pp. 237–265.
3. Haubold, A.D., Yapp, R.A. and Bokros, J.C. (1986). "Carbons for Biomedical Applications", in Bever, M.B. (ed.), *Encyclopedia of Materials Science and Engineering, Vol. 1*, Pergamon Press, Oxford, pp. 514–520.
4. Kotlensky, W.V. (1965). Deformation in Pyrolytic Graphite, *Trans. Met. Soc. AIME*, **223**, 830–832.
5. Kotlensky, W.V. and Martens, H.E. (1965). Structural Changes Accompanying Deformation in Pyrolytic Graphite, *J. Am. Ceram. Soc.*, **48**, 135–138.
6. More, R.B., Haubold, A.D. and Beavan, L.A. (1989). Fracture Toughness of Pyrolite, Carbon, *Trans. Society for Biomaterials*, **15**, 180.
7. Dauskardt, R.H. and Ritchie, R.O. (1989). Cyclic Fatigue-Crack Growth Behavior in Ceramics, *Closed Loop*, **17**, 7–17.
8. Ritchie, R.O., Dauskardt, R.H., Yu, W. (1990). Cyclic Fatigue-Crack Propagation, Stress-Corrosion and Fracture-Toughness Behavior in Pyrolytic Carbon-Coated Graphite for Prosthetic Heart Valve Applications, *J. of Biomed. Maters. Res.*, **24**, 189–206.

9. Ritchie, R.O. and Dauskardt, R.H. (1991). Cyclic Fatigue in Ceramics: A Fracture Mechanics Approach to Subcritical Crack Growth and Life Prediction, *J. Ceramic Soc. Japan*, **99**, 1047–1062.
10. Ritchie, R.O., Dauskardt, R.H. and Pennisi, F.J. (1992). On the Fractography of Overload, Stress Corrosion and Cyclic Fatigue Failures in Pyrolytic-Carbon Materials Used in Prosthetic Heart-Valve Devices, *J. Biomed. Mater. Res.*, **26**, 69–76.

Chapter 25

PYROLYTIC CARBON PROSTHESES: CLINICAL RESULTS

Jonathan Shute

25.1. INTRODUCTION

Pyrolytic carbon is a unique biomaterial with many valuable characteristics, as described in Chapter 24. During the last few decades, pyrolytic carbon has been the subject of many clinical and scientific studies. Implants such as artificial heart valves and small joint replacements containing pyrolytic carbon are being widely used with much clinical success.

25.2. PYROLYTIC CARBON IN ARTIFICIAL HEART VALVES

Heart valve replacements are implants that replace calcified or damaged heart valves. These heart valves can either be mechanical or bioprosthetic. For background information regarding alternative types of heart valves, see the suggested reading list. The design of prosthetic heart valves has evolved significantly over the last 50 years. Artificial heart valves started as a ball and cage design and over time have shifted towards the use of leaflets. Improved heart valve development has been accompanied by a reduction in blood flow issues and undesirable coagulative responses.[1]

The use of bileaflet mechanical pyrolytic carbon heart valves has increased since 1990.[2] These valves are constructed entirely of, or coated with, pyrolytic carbon and have been used for aortic, mitral, and tricuspid valve replacements.[2–4] While some of the factors involved in failure of heart valve replacements are still unclear, a significant amount of clinical data has been collected on the survivability of implant recipients.

In 2006, Chang *et al*. reported results from 138 tricuspid valve replacement (TVR) surgeries performed on 125 patients with mean ages of 43.7 ± 16.6 years. One hundred and three of the TVR implants were assorted mechanical valves with components or parts made from pyrolytic carbon, and 35 of the TVR implants were bioprosthetic valves. Of the original 125 patients, 116 were available for follow-up with a mean follow-up of 7.1 ± 5.1 years. In the bioprosthesis group, 22.9% of individuals had died within 30 days of implantation; in the

mechanical pyrolytic carbon group, 13.6% had died within 30 days of implantation. The survival rate, or freedom from mortality, related to valve replacement for the remaining 116 patients was 96.2 ± .6%, 89.5 ± 0.7%, and 89.5 ± 0.9% at 5, 10, and 16 years respectively. They found no statistical difference between the survival rates of the pyrolytic carbon and biprosthetic implants.[2]

A study of 485 patients who received pyrolytic carbon heart valve replacements was published in 2006 by Bryan *et al*.[3] In their randomized study, 234 CarboMedic heart valves and 251 St. Jude Medical heart valves were implanted. The distribution of valve replacements varied with 160 mitral, 288 aortic, and 137 mitral and aortic replacements. Patients had a median follow-up of 10 years and the mean freedom from valve related mortality at 10 years was 93.0% and 95.0% for St. Jude Medical heart valve and CarboMedic recipients, respectively. There were 25 mortalities related to valve related issues and 14 patients required reoperation. Freedom from all valve related issues including bleeding, thromboembolism, and reoperation at 10 years was 46.2% and 51.6% for St. Jude Medical and CarboMedic recipients, respectively.[3]

Similar results have been seen for the survivability of pyrolytic carbon replacement valves in other studies. A 25-year clinical study regarding the survivability rate of the St. Jude Medical mechanical valve was recorded in 2010 by Toole *et al*., consisting of 945 patients. From this patient population, 537 received aortic valve replacements (AVR) and 408 received mitral valve replacements (MVR) with mean ages of 56 ± 14 years and 56 ± 13 years, respectively. Freedom from mortality in the patients receiving AVR was approximately 94%, 89%, 84%, and 60–75% for 5, 10, 16, and 25 years respectively. Patients receiving MVR had greater longevity than those receiving AVR. Freedom from mortality in patients receiving MVR was approximately 96%, 93%, 90%, and 85–89% for 5, 10, 16, and 25 years respectively.[4]

The survivability of patients receiving mechanical heart valves has been clinically assessed over the last two decades and much has been found regarding the reasons for mortality, morbidity, and failure of devices. Figure 25.1 shows the freedom from mortality for various pyrolytic carbon mechanical heart valves from multiple studies. For most studies, roughly 90% of patients survive to the 10-year check-up after mechanical heart valve implantation.[4–6] If no valve replacement surgery were to occur, the survival rate could be dramatically lower for many patients. As a greater understanding of heart valve related morbidity and mortality is established, survival may increase even further and could potentially be as safe as any other type of implantation.

Currently, the main concerns associated with mechanical heart valve implantation are thromboembolism and other bleeding effects. When the

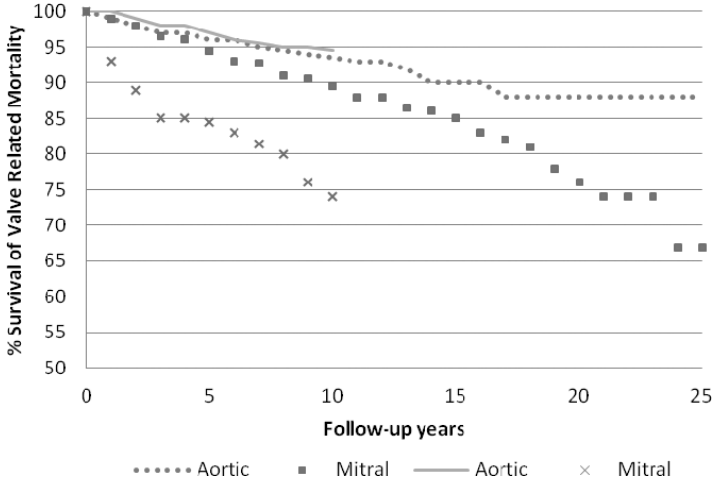

Figure 25.1. Freedom from heart valve related mortality for recipients of various types of pyrolytic carbon heart valves.[2,4]

coagulation cascade is improperly activated, the formation of a thrombosis, or clot, may occur. In regions of the body with high amounts of blood flow, such as the heart, the thrombosis is at high risk of detaching from its growth site and entering the bloodstream. When the thrombosis breaks free of its growth site it is referred to as a thromboembolism. Thromboembolism is a common complication for mechanical valve recipients and methods to minimize this effect are being investigated by bioengineers and researchers around the world. This issue is complex and is tied to multiple factors, including the material properties and geometric construction of the implant.[5,6]

One way to measure the risk of thromboembolism is to determine the hemocompatability of a material. Understanding how the material responds to platlets, which are tied to the formation of thrombosis, can enhance the understanding of why implantation of the material increases the risk for thromboembolism. The hemocompatability of pyrolytic carbon was tested in comparison to other materials by Forti *et al*. in 2010. They tested pyrolytic carbon samples against titanium alloy, tissue culture polystyrene, and γ-irradiation sterilized polystyrene in whole plasma and evaluated protein adsorption, platelet activation, and the composition of materials on the surface layer. The results of the tests indicated that the surfaces of pyrolytic carbon samples had high levels of fibrinogen adsorption, relatively low levels of fibronectin and proteins adsorption, and low platelet adherance. They also found that protein adsorption to the

surfaces of materials increased with increasing contact angle and that the roughness of the samples did not seem to affect protein adsorption and platelet adhesion.[5]

Considering results from the tests performed by Forti *et al*., the hemocompatability of pyrolytic carbon is expected to be relatively good. However, other mechanisms *in vivo* may also enhance the chance for platelet adhesion and activation and therefore may only be valuable in living studies. As the mechanisms for protein adsorption and coagulation are better understood from the material–protein interface in the body, the ability to delay or inhibit coagulation may be improved. Correcting for the inherent issues caused by the material's interaction with the body may require additional surface layers, specialized therapy, or re-evaluation of the material.

Geometric structure also plays a significant role in the hemocompatability of implanted devices. A bileaflet mechanical valve has two "leaf"-like faces that rotate on hinges.[1] When pressure is applied to the interior side of the valve, the leaves rotate up to 90 degrees. When the valve opens, a large area for blood flow becomes available. A larger area for blood flow can improve the hemocompatability of the valve substantially. The way the blood flows through the valve can influence the shearing of platelets and blood cells. Optimizing blood flow is critical in preventing coagulation and other complications. *In vitro* studies have been performed to evaluate the stresses at which coagulation occurs. Hellums criteria, an experimentally-determined threshold, states that if the product of the shear stress and the duration of time exceed 3.5 Pa, platelets will activate. Other studies have indicated that turbulent stresses ranging from 10 to 100 Pa can trigger activation. The degree of shear stress is related to a geometric constraint known as the effective orifice area (EOA). The EOA is the area in which blood flows through the valve in the forward pumping motion and is defined in Equation 25.1 as:

$$\mathrm{EOA}(\mathrm{cm}^2) = \frac{Q_{\mathrm{rms}}}{51.6\sqrt{\Delta \mathrm{p}}}, \tag{25.1}$$

where Q_{rms} is the root mean square systolic/diastolic flow rate (cm^3/s) and Δp is the mean systolic/diastolic pressure drop (mmHg).[6] As the EOA increases, the pressure drop and the shearing stresses on the walls of the valve are reduced. This reduces the chances for shearing-based coagulation. Improving the geometric designs of heart valves and identifying other coagulation-based issues with mechanical implants are necessary to properly design the appropriate structure for an artificial heart valve.

Bioprosthetic heart valves are often used because of their superior anticoagulative response throughout the lifetime of the patient. Most implants require administration of anticoagulants immediately after implantation, but not all implants require lasting therapy. Mechanical valve recipients must be treated with anticoagulants, such as warfarin, throughout the course of their life. Bioprosthetic valve recipients usually only require daily administration of aspirin.[2] Anticoagulant therapy is a complex issue and research on how to improve the quality of treatment or reduce treatment duration is still under investigation. An in-depth analysis on anticoagulants is beyond the scope of this chapter.

Alternatives to anticoagulation therapy have been under investigation for nearly as long as the development of implants. Some investigators are looking into surface modifications and have found a particular method that shows significant decreases in platelet adhesion. In 2011, Slaughter *et al*. reported on a new type of surface modification known as Forcefield Technology.[7] The forcefield surface modification technique involves the application of a small voltage across the surface of a pyrolytic carbon disk. The voltage difference across the surface attracts proteins to the surface of the disk that are resistant to platelet adherence. In an experiment comparing platelet adherence, forcefield modified surfaces demonstrated excellent results against non-forcefield controls. Confluence of cells and platelets onto the surfaces of materials were compared with scanning electron microscopy and confluence was found to be 3.3% ± 2.2% and 81.7% ± 24% for the forcefield-modified disks and controls, respectively. This new method is still in the early stages of development but may provide an alternative to anticoagulants in the future.[7]

25.3. PYROLYTIC CARBON IN ARTHROPLASTY

As a surfacing material, pyrolytic carbon has become well established and been used in multiple devices. Pyrolytic carbon has also been established as a good choice for use as a bulk material in some implants. While materials such as stainless steel and alumina possess the strength that is necessary for high load bearing implants, pyrolytic carbon is suitable for use in smaller implants with lower load bearing requirements. For this and other reasons, pyrolytic carbon was selected as a material choice for finger joint arthroplasty.[8–10]

Diseases such as arthritis present significant lifestyle challenges that sometimes include painful or even debilitating degradation of the bones in the hand. Some individuals experience severe joint issues associated with their proximal interphalangeal (PIP) joints and may require surgery or implantation for correction. The goal of these implantations is to improve grip strength, widen the

range of joint motion, reduce pain, and enhance the satisfaction of the patient overall. PIP joint prostheses are structurally similar to a total knee replacement. The rolling motion of the two faces in the PIP joint ease movement and increase the biomechanical accuracy of the replacement to that of the native joint. The use of pyrolytic carbon in implants in the past has shown low wear and good biocompatibility and thus was considered a good choice for a highly motile prosthetic joint. Many studies have been performed on the use of pyrolytic carbon in PIP joint arthroplasty and the efficacies of the prosthetics have been evaluated.[8]

In 2007, Bravo *et al*. published data from their study regarding 35 patients who in total received 50 PIP joint replacements.[9] The reasons for implantation were various forms of arthritis: 10 patients had posttraumatic arthritis, 11 had rheumatoid arthritis, and 14 had osteoarthritis. There was a distribution of 15 index finger, 18 middle finger, 10 ring finger, and 7 small finger joint replacements. Before surgery the average range of motion was 40°, pain score on a scale of 0–10 (0 being painless) was 6, grip strength was 19 kg and pinch strength was 3 kg. After implantation, the average range of motion was 47°, pain score was 1, grip strength was 25 kg, and pinch strength was 4 kg. The average follow-up was 2.25 years. Two patients requested unnecessary amputation of the joint and there was a revision rate of 8%. There were 14 revisions in total (5 for minor reasons) and patient satisfaction was recorded at approximately 80%.[9]

A study comparing the effectiveness of silicone PIP joint arthroplasty versus pyrolytic carbon arthroplasty was performed by Branam *et al*. in 2007.[10] In the pyrolytic carbon group there were 19 joint replacements in 9 patients and in the silicone group there were 22 joint replacements in 13 patients. The average follow-ups for the pyrolytic carbon and silicone groups were 19 and 45 months, respectively. There was an increase in the flexion range of motion for the pyrolytic carbon group (increase of 3°) and a decrease in the silicone group (decrease of 2°). Additional surgery was required on three joints in the silicone group due to complications and one case of sepsis. No complications demanding surgery occurred in the pyrolytic carbon group. The range of deformity was larger and statistically significant in silicone joints. Patients reported greater satisfaction with the postimplantation appearance of the pyrolytic carbon joints and both groups reported a significant decrease in pain.[10]

Pyrolytic carbon PIP joint arthroplasty offers a relatively simple surgical correction for an issue that is currently difficult to treat otherwise. For use as an implant material in PIP joint arthroplasty, pyrolytic carbon has shown much success regarding improvements in strength, range of motion, and quality of life. Most of the reported complications are from the loosening or dislocation of the implants.[10] Few issues with biocompatibility have been recorded.

25.4. SUMMARY

Clinical uses of pyrolytic carbon have shown exceptional results in comparison with other materials. Development of heart valve replacements with pyrolytic carbon appears to be promising for the future. Survival for pyrolytic carbon heart valves is on par with other materials but still presents some issues. Thromboembolism and bleeding must be addressed through material modifications and the improvement of implant geometry. Future advances in anticoagulation drugs or a better understanding of the coagulation response with pyrolytic carbon will also greatly improve the quality of pyrolytic carbon heart valves. For clinical applications like proximal interphalangeal joint replacement, pyrolytic carbon is currently one of the best material choices. Studies have shown excellent joint recovery, reductions in pain, and improved patient satisfaction. Future studies on pyrolytic carbon may broaden the spectrum of implants and improve on the results for those implants being used today.

Author's Note: *This review of pyrolytic carbon, pyrolytic carbon implants, and its associated data is done without the influence of any organization, manufacturer or external parties. All information contained within is presented based upon a critical review of the published literature and is presented to enhance the public's knowledge base on the topic of pyrolytic carbon.*

REFERENCES

1. Mohammadi, H., Mequanint, K. (2011). Prosthetic Aortic Heart Valves: Modeling and Design, *Med. Eng. Phys.*, **33**, 131–147.
2. Chang, B., Lim, S., Yi, G. *et al.* (2006). Long-Term Clinical Results of Tricuspid Valve Replacement, *Ann. Thorac. Surg.*, **81**, 1317–1324.
3. Bryan, A.J., Rogers, C.A., Bayliss, K. *et al.* (2007). Prospective Randomized Comparison of CarboMedics and St. Jude Medical Bileaflet Mechanical Heart Valve Prostheses: Ten-Year Follow-Up, *J. Thorac. Cardiov. Sur.*, **133**, 614–622.
4. Toole, J.M., Stroud, M.R., Kratz, J.M. *et al.* (2010). Twenty-Five Year Experience with the St. Jude Medical Mechanical Valve Prosthesis, *Ann. Thorac. Surg.*, **89**, 1402–1409.
5. Forti, S., Lunelli, L., Volpe, C.D. *et al.* (2011). Hemocompatibility of Pyrolytic Carbon in Comparison with Other Biomaterials, *Diam. Relat. Mater.*, **20**, 762–769.

6. Dasi, L.P., Simon, H.A., Sucosky, P. *et al.* (2009). Fluid Mechanics of Artificial Heart Valves, *Clin. Exp. Pharmacol. P.,* **36**, 225–237.
7. Slaughter, M.S., Pederson, B., Graham, J.D. *et al.* (2011). Evaluation of New Forcefield Technology: Reducing Platelet Adhesion and Cell Coverage of Pyrolytic Carbon Surfaces, *J. Thorac. Cardiov. Sur.*, **142**, 921–925.
8. Nunley, R.M., Boyer, M.I., Goldfarb, C.A. (2006). Pyrolytic Carbon Arthroplasty for Posttraumatic Arthritis of the Proximal Interphalangeal Joint, *J. Hand Surg.*, **31A**, 1468–1474.
9. Bravo, C.J., Rizzo, M., Hormel, K.B. *et al.* (2007). Pyrolytic Carbon Proximal Interphalangeal Joint Arthroplasty: Results With Minimum Two-Year Follow-Up Evaluation, *J. Hand Surg.*, **32A**, 1–11.
10. Branam, B.R., Tuttle, H.G., Stern, P.J. *et al.* (2007). Resurfacing Arthroplasty Versus Silicone Arthroplasty for Proximal Interphalangeal Joint Osteoarthritis, *J. Hand Surg.*, **32A**, 775–788.

SUGGESTED READING

Connolly, J.M., Bakay, M.A., Alferiev, I.S. *et al.* (2011). Triglycidyl Amine Crosslinking Combined With Ethanol Inhibits Bioprosthetic Heart Valve Calcification, *Ann. Thorac. Surg.*, **92**, 858–865.

Halkos, M.E. and Puskas, J.D. (2009). Are All Bileaflet Mechanical Valves Equal?, *Curr. Opin. Cardiol.*, **24**, 136–141.

Sacks, M.S., Schoen, F.J. and Mayer, Jr., F.J. (2009). Bioengineering Challenges for Heart Valve Tissue Engineering, *Annu. Rev. Biomed. Eng.,* **11**, 289–313.

Mohammadi, H. and Mequanint, K. (2011). Prosthetic Aortic Heart Valves: Modeling and Design, *Med. Eng. Phys.*, **33**, 131–147.

Chapter 26

BIOCERAMIC COMPOSITES

Paul Ducheyne, Michele Marcolongo and Evert Schepers

Editor's Note: *This chapter is an abbreviated version of Chapter 15 of the first edition of An Introduction to Bioceramics. Numerous studies were conducted to develop reliable composites of bioactive glasses and ceramics reinforced with a metallic phase. Structural failures occurred due to attack of the metal–glass phase boundaries in the composite material and the materials never became clinically important and therefore the topic is mostly deleted from this second edition. A short summary of the pioneering studies by Professor Ducheyne and colleagues follow with two key citations.*

26.1. SUMMARY

Early development of bioceramics was prompted by considerations of biocompatibility, but implant devices must posses an appropriate range of mechanical properties. For many biomedical applications, ceramics alone, either bioactive or inert, cannot meet diverse requirements of safe and effective *in vivo* functioning under load-bearing conditions. This turned attention toward composite materials which could take advantage of the desirable properties of each of the constituent materials, while mitigating the more limited characteristics of each component. Bioceramic composites can be divided in to three categories: bioinert, bioactive, and biodegradable composites. The ceramic phase can be the reinforcing material, the matrix material, or both. Synthesizing a successful composite follows identification of desirable properties as well as inferior characteristics of each material. Several bioceramic composites fabricated and analyzed are shown in Table 26.1. These include stainless steel fiber/bioactive glass (the first bioceramic composite) and titanium fiber/bioactive glass composites. These discontinuous metal fiber/ceramic composites maintain bioactivity while increasing the fracture toughness and strength of the material in comparison with that of the ceramic alone. There are also ceramic reinforced/bioactive ceramic composites (e.g., zirconia reinforced/AW glass and apatite/wollastonite (AW) two-phase bioactive glass ceramic), and bioceramic augmented polymeric matrices (e.g., calcium phosphate reinforced polyethylene, discussed in Chapter 27).

Table 26.1. Bioceramic Composites.

Inert	Carbon fiber reinforced carbon
	Carbon fiber polymetric matrix materials (polysulfone, poly aryl ether ketone, poly ether ketone ketone, poly ether ether ketone)
	Carbon fiber reinforced bone cement
Bioactive	AW Glass-Ceramic
	Stainless steel fiber reinforced Bioglass®
	Titanium fiber reinforced bioactive glass
	Zirconia reinforced AW glass-ceramic
	Calcium phosphate particle reinforced polyethylene
	Calcium phosphate fiber and particle reinforced bone cement
Resorbable	Calcium phosphate fiber reinforced polylactic acid

Many of these composites are bioactive and have higher mechanical strength than the bioceramics themselves (see Reference 3 for details).

26.2. FABRICATION METHODS

Stainless steel fiber/bioactive glass composites are made of 45S5 bioactive glass and AISI 316L stainless steel fibers.[1,2] The nominal composition for the bioactive glass is: 45wt% SiO_2, 24.5% CaO, 24.5% NO, and P_2O_5. AISI 316L stainless steel has the following compositional range for the more important alloying elements: 16–20wt% Cr, 10–14% Ni, 2–4% Mo, less than 0.03% C. The preparation of the stainless steel fiber/bioactive glass composite involves a number of steps, which include preparing the fiber preform, impregnating the preform with the glass matrix, and heat treating the composite. Initially, the required amount of fiber for a given geometry is weighed and compacted under pressure, the fibers are sintered at 1,250°C, and then the uniformity of the preform's density is inspected using radiography. The surface of the sintered metal fiber preform is oxidized for 10 min in air at 800°C. The total metal shrinkage is controlled by holding the porous preform at 400°C for 20 min, then it is immersed into molten glass maintained at 1,350–1,380°C, and finally the glass-impregnated preform is annealed at 400–500°C for 4 hours and furnace cooled. The processing parameters have been optimized experimentally to achieve this successful procedure. Variables which affect glass impregnation are: viscosity of the molten glass, thermal expansion coefficients of the metal substrate and glass, oxidation and

roughness of the metal surface, metal temperature at time of immersion, duration of immersion, time and temperature of annealing, volume fraction of the metal fibers, and size of porosity.

26.3. ANIMAL TESTS

26.3.1. Stainless Steel Fiber Reinforced Bioactive Glass as Tooth Root Implant

Beagle dogs were used as experimental animals in a dental root implant study. The premolars were extracted at least one year prior to implantation. With appropriate anesthesia, cavities were prepared in the edentulous areas. Low-speed drills (approximately 300 RPM) with abundant cooling by physiological saline were used for all the preparations. Three dogs received subgingivally six fiber-reinforced bioactive glass implants with a pin of bioactive glass on the surface and one bulk bioactive glass, as a control. They were killed four months after implantation. In one animal, five bulk bioactive glass implants were installed in the lower jaw and two in the upper jaw. This animal was killed after 16 months.

Following the usual preparation for light and SEM, no difference in the reaction pattern between bulk bioactive glass and fiber-reinforced composite glass was observed at four months (Fig. 26.1). The various reaction layers

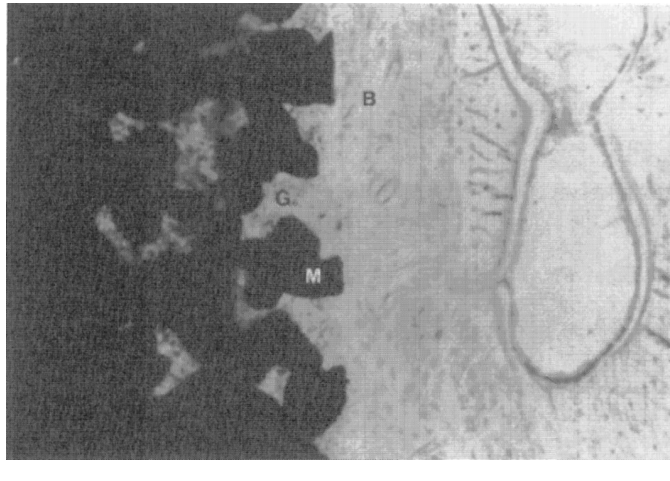

Figure 26.1. Micrograph of the interfacial zone between stainless steel-bioactive glass composite and bone tissue.

present on the composite glass were similar to those reported previously. Energy dispersive X-ray (EDX) analysis clearly demonstrated the formation of a Si-rich layer covered by a CaP-rich layer at the outer surface. Histologically, connection between the implant surface and bone is readily apparent: it is preferentially present at the cortical bone border. No interposed fibrous tissue can be seen between the implant and the bone. The osteocytes at the interface are regularly distributed and some cell processes in the canaliculi of these cells appear to be in a very close relationship with the reacted implant surface. EDX analysis of the CaP-rich layer in such an interface shows an increasing Ca and P concentration at the outer glass surface and a smooth transition of the Ca and P peak intensities towards the bone tissue. This results in a compositional gradient between bioactive glass and bone tissue. In contrast, when the implant is surrounded by fibrous tissue, the Ca and P profiles increase toward the outer surface but drop immediately to zero when the neighboring tissue is scanned. This fibrous encapsulation of the implant is preferentially seen at the apical part of the implant, near the infra-alveolar nerve where no bone tissue is present at the time of installation. The fibrous tissue capsule consists of densely-packed collagen fibers and contains few cells. These observations confirm that bioactive glass is not osteoinductive, since bone connection is only formed when bone tissue is present in the immediate vicinity of the glass surface at the time of installation. This lack of osteoinductivity is also substantiated by the absence of bone tissue at the glass surface around a perforation to the maxillary sinus. Close adaptation of the epithelial tissue to the glass surface is observed here. Whereas no osteoinduction can be ascribed to the glass, it is osteoconductive. An out-growth of bone can be observed in the apical and the cervical directions, where it starts from the initial contact area with cortical bone.

When the implant is intact, EDX analysis does not reveal any ion diffusion from the metal fibers into the outer glass rim of the implant or in the surrounding tissues. Thus, the outer glass rim is effective in preserving the biocompatibility of the bioactive glass itself, and prevents any influence of the stainless steel fiber. However, if metal fibers are directly exposed to the surrounding tissue fluids, Fe ions from the stainless steel fibers are detected by EDX point analysis in tissues of these areas. Other metal ions are not detected, but this can be due to the detection limit of this technique (approximately 0.01–0.1%). These metal ions inhibit the interfacial osteogenesis in these areas and can even elicit an inflammatory cell reaction. Since these reactions are not consistently observed, it is suggested that the tissue response in areas with a cracked glass rim is due to the synergistic action of dissolved glass ions and metal fiber ions.

REFERENCES

1. Ducheyne, P. and Hench, L.L. (1982). The Processing and Static Mechanical Properties and Metal Fibre Reinforced Bioglass®, *J. Mater. Sci.*, **17**, 595–606.
2. Schepers, E., De Clercq, M. and Ducheyne, P. (1988). "Tissue Response to a Bioactive Glass-Metal Interface", in de Putter, C., de Lange, D., de Groot, K. *et al.* (eds), *Implant Materials in Biojunction, Advances in Biomaterials, Vol. 8*, Elsevier, Amsterdam, pp. 79–85.
3. Hench, L.L., Hench, J.W. and Greenspan, D.C. (2004). Bioglass: A Short History and Bibliography, *J. Aust. Ceram. Soc.*, **40**, 1–42.

Chapter 27

DESIGN OF BIOACTIVE CERAMIC-POLYMER COMPOSITES

William Bonfield

27.1. INTRODUCTION

The basis for tailor-making bioactive hydroxyapatite (HA)-polymer composites as skeletal implants to mimic hard tissue is reviewed. HA-reinforced polyethylene composite was originally conceived as a biomaterial for bone replacement on the basis of producing appropriate mechanical compatibility, as well as the necessary biocompatibility.[1] It was demonstrated that an increase in the volume fraction of particulate HA from 0 to 0.5 (50 volume percentage) produced an increase in the Young's modulus of this composite, so as to approach the lower band of the range of values associated with bone itself. Cortical bone at the ultrastructural level is a HA-reinforced collagen composite.[2] Thus, the equivalence of microstructure and deformation behavior give HA-polyethylene composites a special property as a bone analogue material. HA-reinforced polyethylene composites offer the potential of a stable implant–tissue interface during physiological loading. The fracture characteristics of the composite depend on the HA volume fraction. There is a transition from ductile to brittle fracture as the volume fraction increases above approximately 0.45.[3] Hence, it is possible to tailor-make the composition of the composite, so as to achieve any particular combination of Young's modulus combined with the appropriate fracture characteristics. With respect to bone substitution, an optimum combination appears to be approximately 0.4 volume fraction of HA, when the fracture toughness of the composite is still significantly greater than that of cortical bone. *In vivo* studies in a loaded animal model demonstrated that, with a volume fraction of HA greater than approximately 0.2, the composite demonstrated bone apposition around the implant.[4,5] High resolution electron microscopy[6] demonstrated continuous HA lattice images across the composite–bone interface, indicating continuity at the ultrastructural level. This result was in contrast to the control polyethylene implants, which demonstrated fibrous encapsulation. HA-reinforced polyethylene composite, with a volume fraction of 0.4 of HA, has now been used clinically as an implant for reconstruction of the orbital floor.[7] The particular properties of the composite allowed the implant to be shaped by the clinician during the

operation and to be implanted without any fixation. Results have demonstrated successful osteointegration of the implants and good clinical results in this lightly-loaded application.

Following from the work on HA-reinforced polyethylene composite have been studies on other particulate-filled composites with potential as biomaterials. This includes work on HA-reinforced polyhydroxybuterate[8] and HA-reinforced polylactide.[9] In both cases the use of degradable polymer matrices offers interesting potential for skeletal scaffolding materials. However, it is still essential in the formulation of these composites to obtain the required mechanical properties necessary for a loaded application. With respect to thermosetting materials, HA additions have been made to polymethylmethacrylate (PMMA) bone cement in an attempt to introduce some bioactivity to this material.[10] This route presents some difficulty, due to the brittle nature of the matrix material, and a more promising alternative appears to be PEMA bone cement,[11] which, with considerable ductility, approaches more closely the behavior observed for polyethylene. It should be emphasized that a ductile polymer matrix is an essential precursor for effective stiffening and strengthening with HA additions.

To achieve the desired mechanical properties, it is necessary experimentally to have precise control of the processing conditions, so as to ensure a homogeneous distribution of HA.[12] In addition, the mean particle size and the particle size distribution, as well as the surface area, of the HA can be varied, so as to produce different mechanical properties. The technology to tailor-make bioactive composites of any particular combination to deliver a range of prescribed mechanical and biological behaviors is now well established for the HA-polyethylene system,[13,14] as well as having considerable potential for other bioceramic-polymer combinations.

27.2. ANALOGUE COMPOSITE DESIGN

The key data[15] for the HA-polyethylene system are shown graphically in Fig. 27.1, which plots volume fraction of HA against Young's modulus and strain to fracture.[16] From a starting value of 1.3 GPa for zero volume fraction (i.e., 100% polyethylene), the Young's modulus increases with volume fraction to exceed the lower bound of values associated with cortical bone at the 0.5 volume fraction (50 volume percentage) HA composition. A 0.5 volume fraction of HA corresponds to –0.75 weight fraction (75 weight percentage), i.e., HA is the major constituent of the composite. The stiffening produced is accompanied by a decrease in strain to failure, but the composite retains appreciable ductility until a HA volume

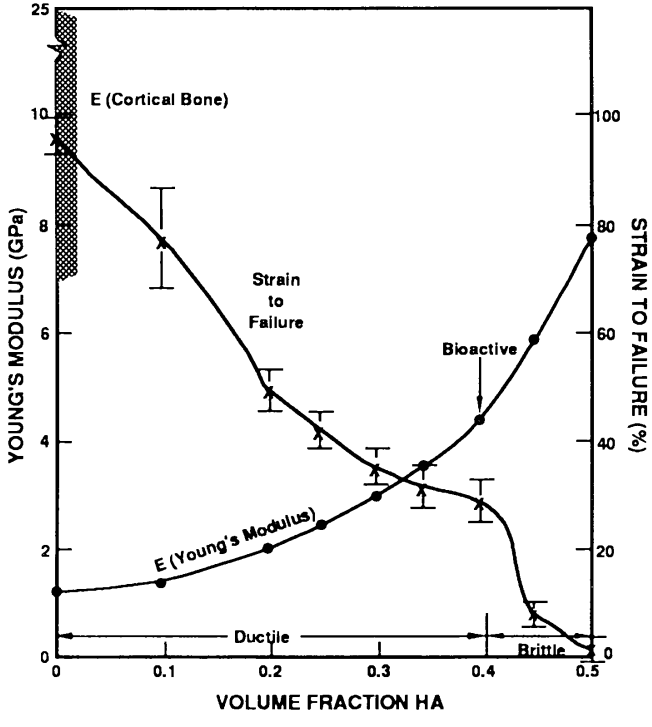

Figure 27.1. Effect of volume fraction of HA on Young's modulus (E) and strain to failure of HA-reinforced polyethylene composite, in comparison to cortical bone, as represented by Hench,[16] based on data by Bonfield.[15] (Reproduced by courtesy of the *Journal of the American Ceramic Society.*)

fraction of –0.4. Composites with volume fractions <0.4 deliver the ceramic in a fracture tough condition.

Biological activity is also indicated in Fig. 27.1. The result established *in vivo* is that fibrous encapsulation is noted for polyethylene controls and for composites with less than 0.2 volume fraction of HA, but bone apposition is achieved for composites with HA volume fraction greater than 0.2. In terms of the interfacial shear strength of the implant–tissue interface, the transition from fibrous encapsulation to bone apposition for the HA-polyethylene system produces approximately a ten-fold increase in value (from –1 to –10 MPa). Hence, formulation of an HA-polyethylene composite, with HA volume fraction between 0.2 and 0.4, gives a bioactive, fracture-tough, modulus-matching bone implant.

The medical application of such analogue composites is in prostheses requiring fixation to bone and a stable implant–tissue interface. The matching of deformation behavior across the implant–tissue interface means that polyethylene wear debris is not a problem. However, the composite is not intended for an articulating application, such as for a joint surface. With that restriction, there remain a myriad of potential skeletal implant applications for appropriately-designed HA-reinforced polyethylene composites.

The experimental data shown in Fig. 27.1 can not be modelled on the basis of simple rule-of-mixture calculations combining polyethylene (E = 1.3 GPa) with HA (E = 80 GPa), an approach which gives theoretical values much higher than the measured results. A statistical finite element approach, based on the concept of Voronoi cells,[17–19] has been applied to the results of Fig. 27.1 and gives satisfactory agreement between experiment and theory. The details of this approach are beyond the scope of this short chapter, but give confidence that the curves shown in Fig. 27.1 may be used as first-order predictors for the experimental behavior of other HA polymer composites, as well as a guide to the formulation of alternative bioceramic-polyethylene combinations. An extensive review with 111 references by S.M. Rea and the author summarizes this topic.[20]

ACKNOWLEDGEMENTS

The author acknowledges the considerable input of colleagues over the past decades to the program of research on bone analogue materials and the continuing support of the UK Science and Engineering Research Council.

REFERENCES

1. Bonfield, W., Grynpas, M.D., Tully, A.E. *et al.* (1981). Hydroxyapatite Reinforced Polyethylene – A Mechanically Compatible Implant, *Biomaterials*, **2**, 185–186.
2. Bonfield, W. and Li, C.H. (1967). Anisotropy of Non-Elastic Flow in Bone, *J. Appl. Phys.*, **38**, 2450–2455.
3. Bonfield, W., Behiri, J.C., Doyle, C. *et al.* (1984). "Hydroxyapatite Reinforced Polyethylene Composites for Bone Replacement", in Ducheyne, P., Van der Perre, G. and Aubert, A.E. (eds), *Biomaterials and Biomechanics*, Elsevier, Amsterdam, pp. 421–426.
4. Bonfield, W., Doyle, C. and Tanner, K.E. (1986). "*In Vivo* Evaluation of Hydroxyapatite Reinforced Polyethylene Composites", in Christel, P.,

Meunier, A. and Lee, A.J.C. (eds), *Biological and Biomechanical Performance of Biomaterials*, Elsevier, Amsterdam, pp. 153–158.

5. Doyle, C., Luklinska, Z.B., Tanner, K.E. *et al.* (1990). "An Ultrastructural Study of the Interface Between Hydroxyapatite Polymer Composites and Bone", in Heimke, G., Soltsz, U. and Lee, A.J.C. (eds), *Clinical Implant Materials*, Elsevier, Amsterdam, pp. 339–344.
6. Bonfield, W. and Luklinska, Z.B. (1991). "High Resolution Electron Microscopy of a Bone–Implant Interface", in Davies, J.E. (ed.), *The Bone–Biomaterials Interface*, University of Toronto Press, Toronto, pp. 89–94.
7. Downes, R.N., Vardy, S., Tanner, T.E. *et al.* (1991). "Hydroxyapatite Polyethylene Composite in Orbital Surgery", in Bonfield, W., Hastings, G.W. and Tanner, K.E. (eds), *Bioceramics Vol. 4*, Butterworth Heinmann, Oxford, pp. 239–246.
8. Doyle, C., Tanner, K.E. and Bonfield, W. (1991). *In Vitro* and *In Vivo* Evaluation of Polyhydroxybutyrate and of Polyhydroxybutyrate Reinforced with Hydroxyapatite, *Biomaterials*, **12**, 841–847.
9. Van Sliedregt, A. (1993). *Hydroxyapatite-Polylactide Composites for Reconstructive Surgery* (Doctoral Thesis, University of Leiden).
10. Sogal, A. and Hulbert, S.F. (1992). "Mechanical Properties of a Composite Bone Cement-Polymethylmethacrylate and Hydroxyapatite", in Yamamuro, T., Kokubo, T. and Nakamura, T. (eds), *Bioceramics, Vol. 5*, Kobunshi Kankokai, Kyoto, pp. 213–224.
11. Khorasani, S.N., Deb, S., Behiri, J.C. *et al.* (1992). "Modified Hydroxyapatite Reinforced PEMA Bone Cement", in Yamamuro, T., Kokubo, T. and Nakamura, T. (eds), *Bioceramics, Vol. 5*, Kobunshi Kankokai, Kyoto, pp. 225–232.
12. Abram, J., Bowman, J., Behiri, J.C. *et al.* (1984). The Influence of Compounding Route on the Mechanical Properties of Highly Loaded Particulate Filled Polyethylene Composites, *Plast. Rub. Proc. Appl.*, **4**, 261–269.
13. Bonfield, W., Bowman, J. and Grynpas, M.D. (1980). Prosthesis Comprising Composite Materials, UK Patent Application 8032647 (1980), UK Patent GB2085461B, The Patent Office, London (1984).
14. Bonfield, W., Bowman, J.A. and Grynpas, M.D. (1991). Composite Material or Use in Orthopaedics, US Patent 5, 1991, 017, 627.
15. Bonfield, W. (1988). "Hydroxyapatite Reinforced Polyethylene as an Analogous Material for Bone Replacement", in Ducheyne, P. and Lemons,

J.E. (eds), *Bioceramics: Materials Characteristics Versus* In Vivo *Behavior*, Annals of the New York Academy of Sciences, New York, pp. 173–177.

16. Hench, L.L. (1991). Bioceramics: From Concept to Clinic, *J. Am. Ceram. Society*, **74**, 1487–1510.
17. Guild, F.J. and Young, R.J. (1989). A Predictive Model for Particulate-Filled Composite Materials, Part 1 Hard Particles, *J. Mater. Sci.*, **24**, 298–306.
18. Guild, F.J. and Bonfield, W. (1993). Predictive Modelling of Bioactive Hydroxyapatite-Polyethylene Composites, *Biomaterials*, **14**, 985–993.
19. Guild, F.J. and Bonfield, W. (1998). Predictive Modelling of the Mechanical Properties and Failure Processes in Hydroxyapatite-Polyethylene (HADEX™) Composite, *J. Mater. Med.*, **9**, 497–502.
20. Rea, S.M. and Bonfield, W. (2004). Biocomposites for Medical Applications, *J. Aust. Ceram. Soc.*, **40**, 43–57.

Chapter 28

CALCIUM PHOSPHATE CEMENTS

Sanjukta Deb

28.1. INTRODUCTION

Bone grafts are frequently required for surgical procedures in orthopaedics, craniomaxillofacial, dental and spinal surgery. A large proportion of the bone grafts are derived from autologous bone, which remains the gold standard despite the numerous synthetic bone substitutes that are commercially available. Autologous bone has all the prerequisites for new bone formation because it is osteoconductive, osteogenic and osteoinductive. However, it has its own limitations, such as the amount of autogenous bone available, increased morbidity, increased anaesthesia time, blood loss and postoperative donor site complications. Allografting is another option which does not involve second site morbidity and the substitute generally is able to maintain osteoinductive effects. However, to eliminate risks arising due to disease transmission and immunogenic response, aggressive processing leads to the loss of the inductive effects and results are often inconsistent. The third group of materials are synthetic, which can be classified into different groups, either based on their chemistry or the nature of the additives, to provide function such as inclusion of growth factors, platelet rich plasma etc. The majority of bone substitutes are based on calcium phosphates ceramics, calcium sulphates and bioactive glasses, presented in the form of granules, blocks, pastes and putties. Calcium phosphate cements comprise a promising group that are mouldable and undergo *in situ* setting, which may or may not produce a resorbable material depending on the composition. Current synthetic bone grafts are primarily made either from calcium phosphate ceramics or self-setting calcium phosphate cements and composite materials. Calcium phosphates are ranked as the materials with the greatest promise both as candidates for bone tissue engineering or bone substitute materials. Cato *et al*. recently summarised the different types of bone graft materials available and analysed the results of recent prospective, controlled, randomised studies using bone grafts with different biological entities in the systems, which highlights the importance of calcium phosphates in bone regeneration.[1]

28.2. CALCIUM PHOSPHATE CEMENTS

Current strategies in developing calcium phosphate bone substitutes are focused towards *in situ* setting of the cements under physiological conditions with adequate mechanical properties, which can be tailored to resorb by controlling structure and composition. Calcium phosphates show excellent biocompatibility and are able to integrate biologically with bone in the living body due to their similarity to poorly crystalline carbonated hydroxyapatite (HA), which forms the mineral component of bone and teeth, see Chapter 17. This is one of the main reasons for their widespread use as a bone substitute or bone repair material and thus has been widely researched and used in orthopaedics, dental applications and increasingly they are being applied in spinal surgery.[2–4]

Calcium phosphate biomaterials can be divided in two major categories: the ceramic calcium phosphates and the calcium phosphate cements. The ceramic calcium phosphates are clinically applied in the form of blocks or granules, which exhibit excellent biocompatibility that is able to support bone growth and osseointegrate mainly at the surface. Ceramic calcium phosphates are thus limited by poor resorbability, lack of adhesiveness, require pre-shaping and are brittle in nature. These limitations led to the development of self-setting calcium phosphate cements (CPCs), which was a significant step towards the clinical application of calcium phosphates. The self-setting cements confer the ability to mould the material into any desired shape, such that it can be easily introduced in irregularly-shaped bone cavities. Excellent cytocompatibility, bioactivity, mouldability and resorbability make calcium phosphate cements a unique group of materials which have made a significant impact in the field of bone regeneration. This chapter will provide a brief overview of calcium phosphate cements and their applications.

28.3. CALCIUM PHOSPHATE CEMENTS CHEMISTRY

Calcium phosphate cement is a generic term that describes hydraulic cements formed from a mixture of precursors that constitute one or several calcium phosphate powders and a liquid or aqueous component that sets to a hardened mass, with the end product being a calcium phosphate material. The concept of CPCs was first introduced by LeGeros *et al*. and Chow *et al*., and since has received much attention due to the *in situ* handling properties and the ability to shape and mould in comparison to calcium phosphate bioceramics.[5–7]

Calcium orthophosphates are salts of calcium derived from orthophosphoric acid, which may be obtained by precipitation at room temperature or at high temperatures. These compounds (see Table 28.1) can be used as reactants for

Table 28.1. Calcium Orthophosphate Compounds.

Compound	Chemical Formula	Ca/P Ratio	pH Stability Range in Aqueous Solutions at 25°C	Abbreviation
Compounds obtained at room temperature under aqueous conditions				
Monocalcium phosphate monohydrate	$Ca(H_2PO_4)_2\ H_2O$	0.50	0.0–2.0	MCPM
Dicalcium phosphate dihydrate	$CaHPO_4\ 2H_2O$	1.00	2.0–6.0	DCPD
Octacalcium phosphate	$Ca_8(HPO_4)2(PO4)_4\ 5H_2O$	1.33	5.5–7.0	OCP
Precipitated hydroxyapatite	$Ca_{10}(PO_4)_6\ (OH)_2$	1.67		PHA
Amorphous calcium phosphate	$Ca_xH_y(PO_4)_z \cdot nH_2O,$	1.35–1.5	Metastable	ACP
Calcium deficient hydroxyapatite	$Ca_{10-x}(HPO4)_x\ (PO_4)_{6-x}(OH)_{2-x}$	1.50–1.67	6.5–9.5	CDHA
Compounds obtained at high temperature				
Monocalcium phosphate anhydrous	$Ca(H_2PO_4)_2$	0.50	Stable only above 100°C	MCPA
Dicalcium phosphate anhydrous	$CaHPO_4$	1.00	Stable only above 100°C	DCP
α-Tricalcium phosphate	$\alpha Ca_3(PO_4)_2$	1.50		αTCP
β-Tricalcium phosphate	$\beta Ca_3(PO_4)_2$	1.50		βTCP
Tetracalcium phosphate	$Ca_4(PO_4)_2\ O$	2.00		TTCP
Sintered hydroxyapatite	$Ca_{10}(PO_4)_6(OH)_2$	1.67		s-HA

CPCs, wherein the setting and hardening of these materials are controlled by dissolution-precipitation reactions at room or body temperature and involve crystalline phase transformations. CPCs generally consist of a concentrated mixture of one or several calcium phosphate powders and an aqueous solution and only those transformations that can occur at physiological temperature under aqueous conditions can be considered for *in vivo* applications.

28.3.1. Apatite and Brushite Based Calcium Phosphate Cements

Calcium phosphate cements typically consist of a solid and liquid component, which, when mixed at specific molar ratio and pH, can yield cements that can be divided into two major types: apatite and brushite. The precursors and their solubility isotherms determine the rate of setting and products formed, where water serves as a medium to dissolve the precursors. When the pH of the cement paste is below 4.2 the product formed is dicalcium phosphate dihydrate (DCPD), known as brushite, where a pH higher than 4.2 yields the apatite cements or the calcium deficient hydroxyapatite (CDHA), as shown in Fig. 28.1.

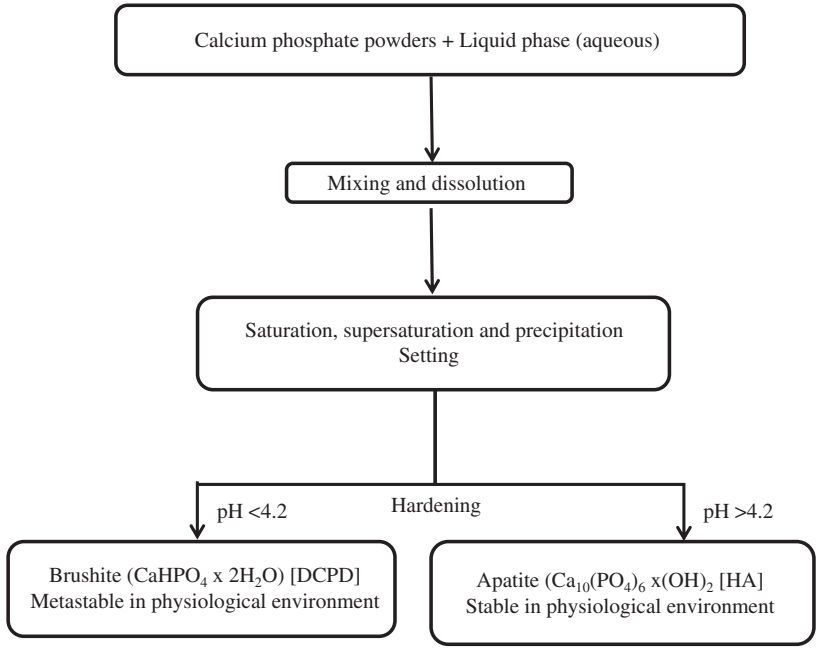

Figure 28.1. Schematic of the formation of calcium phosphate cements.

The final product, as a result of the reaction, is important, as it governs the *in vivo* bioresorbability. There seems to be a greater emphasis, so far in literature, on the apatite-forming cements and their *in vivo* application due to its similarity to the mineral component of bone.[2,3,8] However, in the last decade or so a number of investigators have focussed on the brushite cements due to their metastable nature and rapid resorbability.[9–12]

28.3.1.1. *Apatite cements*

Calcium phosphate cements form via the dissolution of the precursors in an aqueous medium, leading to the precipitation of the final product after supersaturation occurs. The solution thermodynamics largely govern the setting reaction of calcium phosphates. The rate of the reaction is also dependent on the chemical composition, pH and the granulometry of the precursors used to form the cement. The precipitation occurs and the newly formed crystals and subsequent crystal growth leads to the hardening of the cement. One of the first CPCs was the classic Brown and Chow formulation, wherein a mixture of equimolar amounts of tetracalcium phosphate (TTCP) and DCPD were reacted in a 4:1 powder to liquid ratio, with water as the liquid phase, the acid–base interaction leading to a poorly formed CDHA. This highly viscous paste could be moulded but not injected and is therefore used mainly as a contouring material in craniofacial surgery. In the 1990s, it was established that there were about 15 different binary combinations of calcium orthophosphates, which gave pastes upon mixing with water or aqueous solutions, so that the pastes set at room or body temperature into a solid cement.[2]

The mixture of TTCP and DCPD has a singular point around a pH of 8.5 and the most stable form being HA at this pH is thus precipitated. The driving force towards crystallisation is the relative stability of the salts and phases such as OCP that may form during the process, but because it is metastable and more soluble than HA, it is eventually transformed into HA. The reaction is shown in Equation 28.1.

$$2Ca_4(PO_4)_2O + 2CaHPO_4 \rightarrow Ca_{10}(PO_4)_6(OH)_2 \qquad (28.1)$$

The apatite forming CPCs can form either precipitated hydroxyapatite (PHA) or CDHA. During the actual formation of cements the pH border shifts and brushite may be formed up to a pH of 6, whereas the apatitic cements form at pH greater than 6.5. There are three main groups of CPCs that form the apatite

cements. The first type involves the reaction of two calcium phosphates, as exemplified by the classic Brown and Chow cement with one acidic component and one basic in nature.[13] Most formulations use TTCP, as it is the only basic component with a Ca/P ratio higher than PHA and hence can be reacted with other calcium phosphates with a lower Ca/P ratio to yield PHA or CDA. The reaction in Equation 28.1 clearly shows that it does not produce any acidic or basic byproducts and thus can be used for clinical applications. Norian SRS® and Biocement D® are examples of commercial apatite type CPCs that form a nonstoichiometric carbonate apatite or dahllite $[Ca_8 \cdot (HPO_4)_{0.7}(PO_4)_{4.5}(CO_3)_{0.7}(OH)_{1.3}]$ as the end-product, which are formed in an aqueous environment with low crystallinity, and thus are very similar to the mineral content of the hard tissues in the body.[2]

The second type of setting associated with CPCs involve only one phase, wherein a metastable calcium phosphate undergoes hydrolysis in aqueous media, thus the Ca/P ratio remains the same for both the starting component and the hydrolysed product. Examples include the interaction of α-TCP or β-TCP with aqueous solutions, nanocrystalline TTCP and an aqueous solution etc., yielding CDHA as a result of the recrystallisation process.[14–16]

$$Ca_xH_y(PO_4)_z \cdot nH_2O + H_2O \rightarrow Ca_{10-x}(HPO_4)_x(PO_4)_{6-x}(OH)_{2-x} + nH_2O$$

$$3(\alpha\text{- or } \beta\text{-})Ca_3(PO_4)_2 + H_2O \rightarrow Ca_9(HPO_4)(PO_4)5(OH)$$

$$3Ca_4(PO_4)_2O + 3H_2O \rightarrow Ca_9(HPO_4)(PO_4)5(OH) + 3Ca(OH)_2$$

The third type of CPC can be obtained by the interaction of two or more calcium phosphates with other salts such as calcium carbonates, strontium carbonate, magnesium phosphate etc. Strontium substitutes are being increasingly researched with a view to enhance radio-opacity and also improve osteoblastic activity. The commercial cement Norian SRS®, a skeletal repair system marketed by Norian, is an example of this type, wherein mixtures of calcium phosphates with Ca/P ratios lower than PHA are used and calcium carbonate is added to provide the extra calcium ions. The final setting product is a carbonated HA with a Ca/P ratio between 1.67 and 1.69.

28.3.1.2. *Brushite cements*

Brushite based cements were first reported by Mirtchi and Lemaitre via reacting an acidic calcium phosphate and basic β-tricalcium phosphate in the

presence of water, as shown in Equation 28.2.[17] The formation of brushite requires large amounts of water in contrast to apatite cements, and thus are truly hydraulic cements. An example of the acid–base type interaction was the formulation reported by Lemaitre *et al*., where β-TCP was reacted with the acidic monocalcium phosphate monohydrate (MCPM) to form brushite, as shown in Equation 28.2.[17]

$$\beta\text{-}Ca_3(PO_4)_2 + Ca(H_2PO_4)_2 \cdot H_2O + 7H_2O \rightarrow 4CaHPO_4 \cdot 2H_2O \qquad (28.2)$$

It can be observed from Equation 28.2 that the acidic MCPM can be substituted with orthophosphoric acid, whilst β-TCP may be replaced with α-TCP and different CPCs can be obtained, such as the reaction shown in Equation 28.3. Thus, an array of cement formulations can be prepared and are available as constituents of different bone substitutes.

$$Ca_9(HPO_4)(PO_4)_5(OH) + 3H_3PO_4 + 17H_2O \rightarrow 9CaHPO_4 \cdot 2H_2O \qquad (28.3)$$

The reaction in the formation of brushite is very rapid and the hardening occurs in ~30 seconds, making it difficult to handle in a clinical situation. During setting of a β-TCP and MCPM cement, the cement pH varies from being very acidic with pH values of ~2.5 in the early stages of setting to almost neutral pH values of ~6.0. Brushite cements are formed via consuming water in their setting reaction and they have fairly weak mechanical properties. The inhibition of crystal growth during setting results in the formation of smaller-sized crystals which may improve mechanical properties via close packing of the crystals. Brushite-based cements can be stable, dissolve or reprecipitate to a more thermodynamic stable calcium phosphate phase, such as OCP and HA, or disintegrate.[18,19] Brushite is thermodynamically metastable and as a consequence it is difficult to predict the behaviour of brushite in a physiological environment, and for this reason discordant data is reported in literature.[20] Studies have indicated that acidic calcium phosphates, namely brushite and monetite, are osteoconductive, osteoinductive and resorb at a faster rate than HA.[21,22] However, research over the last two decades has made it possible to create brushite cements in clinically acceptable times and these cements are of interest in bone regeneration due to their biocompatibility and rapid resorption.[10] *In vivo* studies have shown that HA allows the formation of a bond between bone and the external surface, whereas the use of brushite led to the observation of a gap of around 400 μm existing between the new bone and the cement, indicating the resorption of brushite.[23]

In vitro aging in liquid medium is dependent on factors that can be divided for simplicity into two categories. The first correlates to the composition of the liquid medium as: concentration of free calcium and phosphorous ions, pH value, refreshing frequency of the media and weight/volume ratio between medium and sample. The second category relates to the cement formulation and working temperature. Bohner *et al*. reported the aging of brushite cement in distilled water at different temperatures and observed that high temperature and low pH (due to the presence of large amounts of phosphoric acid in the base formulation) trigger the conversion of brushite into monetite.[24] Monetite can also be formed by dehydration of brushite to form the anhydrous dicalcium phosphate (DCP) or by modifying the precipitation conditions to favour the crystallisation of monetite. Preformed monetite can be obtained by the modification of α- or β-TCP block immersed in phosphoric acid solution or by hydrothermal modification of brushite matrix that is obtained from calcium phosphate cement formulations.[25] Monetite can be formed under very low pH conditions and precipitation of it can occur in calcium hydroxide-based DCP cements in the presence of excess phosphoric acid. Monetite can also be prepared using β-TCP-based cements in the presence of excess MCPM or via thermal dehydration of brushite.[10] Monetite DCP, unlike brushite, is slightly less soluble and appears not to transform to HA, which has the tendency to precipitate as insoluble HA, slowing its replacement by bone.[26] Thus, the finding that monetite is osteoconductive and resorbable *in vivo* makes it a very suitable material as a scaffold for bone tissue engineering. However, it may not be applied as an *in situ* setting material due to the extremely low pH requirements.[27,28]

28.4. PROPERTIES

The setting reaction of calcium phosphates occur in three main stages: the dissolution of the precursors, which is dependent on the solubility parameters and the mean particle size of the powders; the formation of new crystals; and finally, the entanglement of the crystals lead to the hardening. The hardening process can take several days; however, an early setting occurs, at which stage 5–15% of the reaction has taken place. In general, most CPC formulations either set too fast, as in the brushites, or too slow, such as in the apatitic cements. Ideally, calcium phosphate cements should set in a time that provides the clinician adequate time to perform the implantation and prevent delays due to slow setting. Generally, calcium orthophosphate cements must set slowly enough to provide sufficient time for a surgeon to perform implantation but fast enough to prevent delaying the operation. The setting should also ensure that adequate

mechanical properties are attained at this stage. The most common method employed to study the hardening of the cements is the application of Gillmore and Vicat needle test methods, which are standard recommended methods (ASTM C266-89; ASTM C191-92) that examine the indentation on the surface of the cements at different periods of time, with setting being indicated by no visual indent on the surface of the cements. Other techniques for determining setting time that have been applied are isothermal differential scanning calorimetry, Fourier transform infrared spectroscopy, impedance spectroscopy etc. The setting time can be regulated in either case with the introduction of additives. The trend is to introduce either seed crystals in the powder or phosphate ions in the liquid phase for the quicker precipitation of the apatites, whereas in citrates, pyrophosphates are added in the liquid phase to enhance the setting time of brushite forming cements. The setting of calcium phosphates is exothermic, however, as the process is slow, the temperature rise is not high enough to cause tissue damage during the hardening of the cement. The mixing of the powder and liquid is a critical step that allows the particulates to be wetted by the liquid phase for the onset of the dissolution step in the formation of a CPC. It is imperative that the powder particles are homogenously mixed with the liquid phase and the inclusion of air bubbles should be avoided, as both can compromise the mechanical properties of the cement. It has been often noted that different operators mixing the cements can result in varying mechanical properties. It is customary to mix the powder and liquid phase using a pestle and mortar under sterile conditions in the operating theatre prior to it being either moulded or placed in a syringe for dispensing it into the bone defects. However, this has been shown to generate a large degree of variation in the resulting properties, which has led to the advent of proprietary mechanical mixing devices such as the electrically powered mixing machine for Norian SRS/CRS® or Mini-malax® mixing system for Cementek® cement, Teknimed S.A. The flow characteristics of calcium phosphate cement are important, as these cements either need to be injected or moulded and placed in the bone defect site by the clinician. Placing putty-like pastes requires high viscosity cements that can be moulded by the clinician, whereas it is desirable to have a low viscosity for an injectable CPC. Injection of high viscosity cements is not only difficult to handle but the high injection forces may lead to phase separation, thus affecting cement setting.[29,30] Habib *et al.* recently reported the potential of an electromechanical approach to improve the injectability of CaP pastes and demonstrated that injectability dramatically improved through ultrasonication-assisted delivery devices.[31] Low viscosity cements are favoured for injectability, but it increases the risk of extravasation and limits clinical application, especially in spinal procedures.

28.4.1. Porosity

There are two main types of porosity in CPCs: micro- and macroporosity. Pore sizes below 5 μm are considered micropores and sizes greater than 100 μm are macropores. Porosity in bone substitutes is an important requirement for bone formation because it allows the migration and proliferation of the cells and is responsible for vascularisation. The porosity also has a role to play in the resorption and biointegration of the material with the host tissue. Typically, CPCs are microporous and the pore size range from 0.1 to 10 μm. The minimum recommended pore size for bone substitutes is approximately 100 μm, but some researchers suggest bone formation is better with pore sizes around 300 μm. However, this is not definitive and reports in the literature vary. Microporosity in the calcium phosphate cement causes an increase in surface area, which is beneficial due to the higher adsorption of bone-inducing proteins. Micropores can also enhance the formation of apatite via dissolution and reprecipitation but can profoundly influence the mechanical properties.[32] Porosity has a marked influence on the mechanical properties of CPCs, however few systematic investigations are reported. In a related study Zhang *et al*. used an α-TCP cement, formed via hydrolysis, and demonstrated that the coarser the microstructure the larger the critical flaw size, causing fracture, and in macroporous systems the critical flaw size increased with macroporosity.[33] Thus, by controlling the microstructure, the relationship between strength and porosity can be moderated.

28.4.2. Mechanical Properties

CPCs are brittle in nature and exhibit superior behaviour in compression in comparison to tensile and shear properties. The compressive strength of different CPCs may vary from 10–00 MPa, with tensile strengths being much lower, between 1 and 10 MPa. The mechanical properties of CPCs show a wide range of variation from the mean values and are not narrowly distributed. Although important mechanical properties required to characterise CPCs include compressive, tensile and fracture toughness, most data available in literature are limited to compression tests. The compressive strength of different CPCs have been reported by numerous workers, however, there is a wide variation due to the inherent porosity, particle size, powder to liquid ratio, use of accelerators and seed content, combined with the variation in testing methodology, especially due to different pre-sampling treatments. A number of commercial bone substitutes are shown in Table 28.2, with available composition and their compressive strengths.

Table 28.2. The Compressive Strength of Some Commercial Calcium Phosphate Bone Cements.

Cement	Powder Composition	Compressive Strength in MPa	Manufacturer
BoneSource®	TTCP & DCPD	36	Stryker, Synthes
Norian SRS®	α-TCP + $CaCO_3$ + MCPM	50	Norian
Calcibon®	α-TCP + DCP + PHA + $CaCO_3$	60	Biomet
Injectable JectOS®	DCP + TCP + Zirconia	35	Rotamed
Cementek®	α-TCP + TTCP+ sodium glycerophosphate	15–25	Teknimed

28.5. *IN VIVO* BEHAVIOUR OF CPCS

CPCs are a promising group of materials in bone repair and regeneration. They can be made into any shape and applied as an *in situ* setting cement as pastes or in preformed shapes, as shown in Fig. 28.2. Cells have the ability to attach to CPCs and allow osteoblasts to attach, proliferate and differentiate. When osteoblasts differentiate they produce collagen type I, alkaline phosphatase, proteoglycans and the matrix proteins osteocalcin, osteopontin and bone sialoprotein, which indicate bone formation. CPCs are very biocompatible, osteoconductive, can stimulate tissue regeneration and undergo gradual remodelling. Apatite CPCs are capable of setting at both physiological temperature and pH, are similar to the mineral content of bone, mechanically adequate and set at neutral pH.[34] They have been shown to stimulate bone in-growth to a greater extent than unfilled defects.[3,35,36] Apatitic calcium phosphate cements possess excellent biological properties but there is controversy regarding their resorbability. Some studies suggest that the resorption of these cements is extremely slow and others differ in their observations. The resorption is thought to occur via cell mediated processes and osteoclastic activity, which can degrade the material from the surface and continue to the core. The biodegradation of apatite cements is faster than ceramic apatites, nevertheless they are slow.[3,37–41] Brushite and monetite cements have been shown to be cytocompatible and research in this field has expanded rapidly in the recent years.[10] Brushite, in contrast to apatite cement, is metastable and has a much faster resorption *in vivo*. Studies have shown brushite cement to be completely converted to octacalcium phosphate after immersion in Dulbecco's

Figure 28.2. Porous blocks, granules and different shaped macroporous and microporous CPCs.

modified Eagle medium (DMEM) cell culture medium; in contrast, Grover *et al*. observed that aging of brushite in fetal bovine serum inhibited both dissolution of brushite and the formation of HA.[18,42] Bohner *et al*. reported the ageing of brushite cement in distilled water at different temperatures and observed that high temperature and low pH (due to the presence of large amounts of phosphoric acid in the base formulation) triggers the conversion of brushite into monetite.[24] Brushite cements have a fairly rapid rate of resorption and form a gap between the cement and newly formed bone because the rate of resorption exceeds the rate of bone formation. Brushite cements eventually convert to HA, which slows down the resorption rate, and bone is able to form in direct contact. In contrast, monetite does not transform to HA and may resorb completely.

28.6. MODIFICATION OF CPCS

One of the main drawbacks of CPCs is their brittle nature and poor mechanical properties that limit clinical applications to non-load bearing areas.

The other important consideration is the poor cohesion of the cement in the early stages after setting, which has led to several efforts in improving the early washout of the cement. Polymeric materials such as alginate, chitosan and gelatin have been incorporated in CPCs to enhance the anti-washout and mechanical properties. Shie *et al*. reported on the addition of a 2% solution of gelatin to a calcium carbonate and MCPM mixture to form a CPC, which increased the setting time and hardened in a clinically acceptable time with improved strength.[43] Miyazaki *et al*. used a number of water soluble polymers, such as poly(acrylic acid) and poly(vinyl alcohol), and added them to TTCP-DCPD cements, with the result of an increase in the compressive strengths but with shorter working and setting time.[44] The molecular weight and concentration of poly(acrylic acid) added to the TTCP-DCPD cements yielded optimised properties with increased compressive strength and acceptable setting time.[45–46] Matsuya *et al*. reported that the use of a less reactive poly acid, namely poly(methyl vinyl ether-maleic acid), with TTCP yielded cements with significantly higher compressive strength.[47] Both poly(acrylic acid) and poly(methyl vinyl ether-maleic acid) were subsequently used to form apatite cements using commercial HA cements, BoneSource® (Stryker) and two other experimental CPC cements, which formed cements in clinically acceptable times, with the experimental CPCs showing significantly higher compressive and diametral tensile strengths. *In vivo* studies showed that these cements elicited an acute inflammatory response which subsided within a week.[48]

Regenerative medicine aims to minimise reliance on autografting procedures in bone repair, and thus synthetic scaffolds are being intensively researched to apply tissue engineering approaches for functional replacement of bone tissue. Thus, the established cytocompatibility and the biomimetic nature of the calcium phosphate phase, which allows for cell attachment, proliferation and expression of osteoblast phenotypes, render them as a preferred group of materials to function as scaffolds for bone tissue engineering. CPCs in general are dense materials containing micropores, however it is well established that an interpenetrating macro- and microporous structure is desirable for bone tissue engineering. This has led to efforts in creating macroporous scaffolds or injectable CPCs with porosity, although increasing porosity is expected to decrease the mechanical properties, even further limiting the clinical applications. Processing strategies for introducing porosity in CPC cements include soluble porogens, degradable fibres, gas foaming and rapid protyping.[49] A study by Lopez-Herida *et al*. on the effect of mesoporosity in CPCs recommended that porogens should have a minimum size of 40 μm and be incorporated at approximately by 30 wt% in CPC.[50,51]

Fibre reinforcement has been used to enhance mechanical properties of composites and naturally has been explored for improving the properties of

CPCs.[52] It is desirable to have CPCs with adequate strength during the early stages of implantation, to be able to provide mechanical stability. Randomly dispersed short fibres made of polymers improve the fracture toughness of CPCs and the incorporation of resorbable fibres in addition allows the formation of pores as they are lost via degradation. An interconnecting porous structure is known to favour bone regeneration and benefits from the potential to allow vascularisation, thus degradable fibres prepared from polyglycolide, polylactide and polycaprolactone have been included in CPCs. The addition of electrospun ultrafine fibres made from poly(ε-caprolactone) (PCL) (PCL12: 1.1 μm, PCL15: 1.4 μm, PCL18: 1.9 μm) and poly(l-lactic acid) (PLLA4: 1.4 μm) to Calcibon® at different weight fractions of 1%, 3%, 5% and 7% improved fracture resistance, with the toughness dependent on the amount of fibres incorporated but independent of the diameter. The fibres created channel-like porous structures in the cement and the degradation caused a dramatic increase in the interconnected porosity.[53] Fibres prepared from bioactive glass with the ternary SiO_2–CaO–P_2O_5 system have also been reported to enhance the elastic modulus and work of fracture of CPCs with a slight decrease in setting times, indicating that the properties of the CPCs can be tailored according to surgical requirements.[54] Silk fibroin fibres used in α-TCP cements provide a substantial reinforcement of the cement, and mesenchymal stem cells were able to successfully differentiate into osteogenic lineage and thus could have potential for *in vivo* bone regeneration.[55] These systems are able to sustain cell growth; however more extensive studies are required to determine the rate of degradation of the fibres within a CPC matrix. The dispersion of the fibres and interfacial adhesion between the matrixes needs to be investigated further to correlate their mechanical properties to composite formation.

28.7. CPCS AND DRUG DELIVERY

The fact that CPCs have a low setting temperature and are microporous in nature make them suitable as candidates for drug delivery. The important prerequisite for a drug delivery carrier is the ability to retain the drug in a specific target site and to deliver it progressively with time in the surrounding tissues. Drugs can be incorporated within the precursors of the calcium phosphates to form the cement, which is a distinct advantage over just adsorption on the surface, but the activity of the drug must not be affected. CPCs have been used to incorporate bisphosphonates, a class of drugs used for the prevention or treatment of osteoporosis. The advantage of such systems is that it not only functions as a bone

substitute but also provides therapeutic action via the local regulation of osteoclastic activity, characteristic of osteoporosis.[56]

Growth factors are often added to scaffolds or bone substitutes to enhance tissue regeneration. Growth factors are expensive, sensitive to heat, solvents and different pH environments, and one alternative approach to enhance bone formation is the incorporation or substitution with trace elements. Strontium is present in small amounts in the mineral phase of bone and recently the beneficial effect of strontium has been recognised in the treatment of osteoporosis.[57] Research findings have also shown that partial substitution of Ca^{2+} with Sr^{2+} ions in HA improve mechanical properties and the rate of dissolution caused by the distortion of the HA lattice.[58] Strontium is also known to modulate bone cell recruitment and thereby stimulates bone formation and inhibits osteoclast activity to a certain extent. Furthermore, strontium increases radio-opacity, which is one of the requirements for cements used in spinal surgery. Based on these properties, the inclusion or substitution of Sr in CPCs has the potential to enhance the bioactivity of CPCs. New routes of introducing Sr in CPCs were proposed by Wang *et al*, which revealed that by mixing 50 wt% Sr- amorphous calcium phosphate (Sr-ACP) and 50 wt% dicalcium phosphate dehydrate (DCPD), strontium could be doped into HA lattice, increasing the lattice dimensions and lattice volume, whereas mixing 50 wt% ACP with amorphous strontium phosphate and 50 wt% DCPD yielded HA and Sr-HA separately in the hydrated cement.[59] Recently, Romieu *et al*. reported on a calcium-strontium mixed injectable and radio-opaque hydraulic cement setting to form a strontium-calcium deficient carbonate apatite with a radio-opacity three times greater than cortical bone.[60] The compressive strength reported was approximately 20 MPa, which still limits the use for non-load-bearing applications; however, the enhanced radio-opacity confers the potential application in spinal applications. Sr-substituted calcium phosphate cements prepared with Sr-substituted β-TCP and MCPM were loaded with an antibiotic doxycycline hyclate via adsorption in the set cement, and by adding in the liquid phase it was reported that efficient drug binding occurred and cements that were formed with the antibiotic in the liquid phase released higher fractions of the drug, indicating that the Sr substitute CPCs could also be considered as a vehicle for drug delivery.[61]

28.8. APPLICATIONS

Different physical forms, such as injectable/mouldable pastes, preset material, granules and printed blocks of brushite and monetite, have been used as

bone substitute materials. A number of CPCs are currently available commercially as bone substitutes. CPCs are capable of setting at both physiological temperature and pH and have been shown to stimulate bone in-growth to a greater extent than unfilled defects.[34,36] Despite excellent biological properties, the mechanical properties of CPCs are weak, they are predominantly dense and the merits of one CPC above another are often difficult to distinguish. Norian SRS® (Synthes), BoneSource® (Stryker), Hydroset® (Stryker) and Calcibon® (Biomet) are some examples of apatite cements. Examples of commercial brushite cements include chronOS Inject® (Synthes), PD VitalOs®, Calcibon® (Biomet), Norian SRS (Synthes, Inc, West Chester, Pennsylvania), JectOS® (Kasios) and ProOsteon (Biomet, Parsippany, New Jersey). CPCs have been more recently modified to function as injectable bone substitutes; some commercial examples currently available to the surgeon are BoneSource®, BoneSave®, HydroSet® (Stryker, Kalamazoo, Missouri), Actifuse® (ApaTech® Limited, Elstree, Hertfordshire, UK) and Vitoss® Synthetic Cancellous Bone Filler (Orthovita, Inc., Malvern, PA). The mechanism of action of these substitutes provides a foundation for cells to migrate to from the wound edges, eventually leading to the repair of the bony defect.

Current strategies in the development of CPCs include tailoring of cement properties to enhance resorbability, enhancing clinical handling, substituting calcium phosphates and combining fast and slow resorbing cements and polymeric composite CPC cements.[48,52,53,62–64] Indeed, be they dense porous materials or injectable cements, the sheer number of synthetic bone substitutes now available to the surgeon makes selection of any one particular synthetic substitute over another a difficult task, a choice typically dictated by a surgeon's personal preference.

28.9. SUMMARY

A large proportion of orthopaedic, craniomaxillofacial and dental surgical procedures require bone grafts, and with the growing demands there still remains a need to design synthetic bone grafts that mimic the structure and composition of bone and good surgical handling properties. Bone grafts currently fall into three main categories: autografts, allografts and synthetic grafts. Autografting is the gold standard; however, it is associated with a second site morbidity, inadequate volume of graft material and sometimes the need for further surgical intervention. Current synthetic bone grafts are primarily made either from CPCs or self-setting CPCs and composite materials; however, structurally and mechanically these are yet to match the autografting procedure. In addition, most bone substitutes are only able to integrate with the edges of the wound bed, with the

core remaining isolated compounded with lack of vascularisation or replacement of the material with new bone, leading to failures, especially in larger sized defects.

Augment™ Bone Graft (rhPDGF/β-TCP), a biosynthetic bone graft substitute marketed by BioMimetic Therapeutics (NASDAQ: BMTI) for autograft in foot and ankle fusions, was the subject of a recent clinical trial, which established that it had a comparable performance to that of autografts. Another clinical trial using β-tricalcium phosphate (β-TCP)/HA with bone marrow aspirates by Bansal *et al*. also showed that the combination of the two provided similar outcomes as autografting in posterior stabilisation using pedicle screw and rod assembly, and fusion in unstable lumbar and dorsal spinal injuries.[65] Though the merits of one synthetic bone substitute above another are often difficult to distinguish, the fact that synthetic bone substitutes account for less than 10% of all bone substitutes used in grafting procedures simply highlights the fact that synthetic substitutes so far fall below the standards set by autologous bone.

REFERENCES

1. Cato, T., Laurencin, M.A., Khan, Y. *et al.* (2011). Medscape Reference, Drugs, Diseases and Procedures. Available at: http://emedicine.medscape.com/article/1230616-overview. [Accessed 21 March 2012].
2. Dorozhkin, S.V. (2009). Calcium Orthophosphates in Nature, Biology and Medicine, *Materials*, **2**, 399–498.
3. Ginebra, M.P. (2008). "Calcium Phosphate Bone Cements", in Deb, S. (ed.), *Orthopaedic Bone Cements*, Woodhead Publishing Limited, Cambridge, pp. 206–230.
4. Verlaan, J.J., Lopez-Heredia, M.A., Alblas, J. *et al.* (2011). "Injectable Bone Cements for Spinal Column Augmentation: Materials for Kyphoplasty/Vertebroplasty", in Ducheyne, P. (ed.), *Comprehensive Biomaterials, Vol. 6*, Elsevier, New York, pp. 147–160.
5. Brown, W.E. and Chow, L.C. (1985). Dental Restoration Cement Pastes, US Patent 4518430.
6. LeGeros, R., Chohayeb, A. and Shulman, A. (1982). Apatitic Calcium Phosphates: Possible Dental Restorative Materials, *J. Dent. Res.*, **61**, 343.
7. LeGeros, R.Z. (2008). Calcium-Phosphate Based Osteoinductive Materials, *Chem. Revs*, **108**, 4742–4753.

8. Ginebra, M.P., Espanol, M., Montufar, E.B. *et al.* (2010). New Processing Approaches in Calcium Phosphate Cements and their Applications in Regenerative Medicine, *Acta Biomater.*, **6**, 2863–2873.
9. Bohner, M. (2010). Resorbable Biomaterials as Bone Graft Substitutes, *Mater. Today*, **13**, 24–30.
10. Tamimi, F., Sheikh, Z. and Barralet, J. (2012). Dicalcium Phosphate Cements: Brushite and Monetite, *Acta Biomater.*, **8**, 474–487.
11. Cama, G., Barberis, F., Capurro, M. *et al.* (2011). Tailoring Brushite for *In Situ* Setting Bone Cements, *Mater. Chem. Phys.*, **130**, 1139–1145.
12. Cama, G., Barberis, F., Botter, R. *et al.* (2009). Preparation and Properties of Macroporous Brushite Bone Cements, *Acta Biomaterialia*, **5**, 2161–2168.
13. Brown, W.E. and Chow, L.C. (1983). A New Calcium Phosphate Setting Cement, *J. Dent. Res*., **62**, 672–679.
14. Brunner, T.J., Grass, R.N., Bohner, M. *et al.* (2007). Effect of Particle Size, Crystal Phase and Crystallinity on the Reactivity of Tricalcium Phosphate Cements for Bone Reconstruction, *J. Mater. Chem*., **38**, 4072–4078.
15. Gbureck, U., Grolms, O., Barralet, J.E. *et al.* (2003). Mechanical Activation and Cement Formation of Beta-Tricalcium Phosphate, *Biomaterials*, **24**, 4123–4131.
16. Bohner, M., Gbureck, U. and Barralet, J.E. (2005). Technological Issues for the Development of More Efficient Calcium Phosphate Cement, Bone Cements: A Critical Assessment, *Biomaterials*, **26**, 6423–6429.
17. Mirtchi, A.A. and Lemaitre, J. (1989). Calcium Phosphate Cements: Study of the β-Tricalcium Phosphate–Monocalcium Phosphate System, *Biomaterials*, **10**, 475–480.
18. Constantz, B.R., Barr, B,M,, Ison, I.C. *et al.* (1998). Histological, Chemical, and Crystallographic Analysis of Four Calcium Phosphate Cements in Different Rabbit Osseous Sites, *J. Biomed. Mater. Res*., **43**, 451–461.
19. Selen, M. and Cuneyt, T.A. (2010). Brushite ($CaHPO_4{\cdot}2H_2O$) to Octacalcium Phosphate ($Ca_8(HPO_4)_2(PO_4)_4{\cdot}5H_2O$) Transformation in DMEM Solutions at 36.5 °C, *Mater. Sci. Eng.*, **30**, 245–254.
20. Grover, L.M., Gbureck, U., Wright, A.J. *et al.* (2006). Biologically Mediated Resorption of Brushite Cement *In Vitro*, *Biomaterials*, **27**, 2178–2185.
21. Ohura, K., Bohner, M., Hardouin, P. *et al.* (1996). Resorption of, and Bone Formation From, New Betatricalcium Phosphate — Monocalcium Phosphate Cements: An *In Vivo* Study, *J. Biomed. Mater. Res.*, **30**, 193–200.

22. Munting, E., Mirtchi, A.A. and Lemaitre, J. (1993). Bone Repair of Defects Filled with Phospocalcic Hydraulic Cement: An *In Vivo* Study, *J. Mater. Sci. Mater. Med.*, **4**, 337–344.
23. Apelt, D., Theiss, F., El-Warrak, A.O. *et al.* (2004). *In Vivo* Behaviour of Three Injectable Hydraulic Calcium Phosphate Cements, *Biomaterials*, **25**, 1439–1451.
24. Bohner, M., Merkle, H.P. and Lemaitre, J. (2000). *In Vitro* Aging of a Calcium Phosphate Cement, *J. Mater. Sci. Mater. Med.*, **11**, 155–162.
25. Galea, L.G., Bohner, M., Lemaitre, J. *et al.* (2002). Use of Injectable Calcium Phosphate Cement for Fracture Fixation: A Review, *Clin. Orthop. Relat. Res*., **395**, 23–32.
26. Tamimi, F., Torres, J., Gbureck, U. *et al.* (2009). Craniofacial Vertical Bone Augmentation: A Comparison Between 3D Printed Monolithic Monetite Blocks and Autologous Onlay Grafts in the Rabbit, *Biomaterials*, **30**, 6318–6326.
27. Gbureck, U., Holzel, T., Klammert, U. *et al.* (2007). Resorbable Dicalcium Phosphate Bone Substitutes Prepared by 3D Powder Printing, *Adv. Funct. Mater.*, **17**, 3940–3945.
28. Tamimi, F., Torres, J., Kathan, C. *et al.* (2008). Bone Regeneration in Rabbit Calvaria with Novel Monetite Granules, *J. Biomed. Mater. Res. A*, **87**, 980–985.
29. Habib, M., Baroud, G., Gitzhofer, F. *et al.* (2008). Mechanisms Underlying the Limited Injectability of Hydraulic Calcium Phosphate Paste, *Acta Biomater.*, **4**, 1465–1471.
30. Habib, M., Baroud, G., Gitzhofer, F. *et al.* (2010). Mechanisms Underlying the Limited Injectability of Hydraulic Calcium Phosphate Paste. Part II: Particle Separation Study, *Acta Biomater.*, **1**, 250–256.
31. Habib, M., Baroud, G., Galea, L. *et al.* (2012). Evaluation of the Ultrasonication Process for Injectability of Hydraulic Calcium Phosphate Pastes, *Acta Biomater.*, **8**, 1164–1168.
32. Hannink, G. and Arts, J.J. (2011). Bioresorbability, Porosity and Mechanical Strength of Bone Substitutes: What is Optimal for Bone Regeneration? *Injury Int. J. Care Injured*, **42,** S22–S25.
33. Zhang, J.T., Trancret, F. and Bouler, J.M. (2011). Fabrication and Mechanical Properties of Calcium Phosphate Cements (CPC) for Bone Substitution, *Mater. Sci. Eng.*, **31**, 740–747.

34. Driessens, F.C.M., Boltong, M.G., Bermudez, O. *et al.* (1994). Effective Formulations for the Preparation of Calcium Phosphate Bone Cements, *J. Mater. Sci. Mater. Med.*, **5**, 164–170.
35. Caulier, H., van Der Waerden, J.P.C.M., Paquay, Y.C.G.J. *et al.* (1995). Effect of Calcium Phosphate (Ca-P) Coatings on Trabecular Bone Response: A Histological Study, *J. Biomed. Mater. Res.*, **29**, 1061–1069.
36. Kurashina, K., Ogiso, A., Kotani, A. *et al.* (1998). Histological and Microradiographic Evaluation of Hydrated and Hardened Alpha-Tricalcium Phosphate/Calcium Phosphate Dibasic Mixtures, *Biomaterials*, **19**, 701–706.
37. Friedman, C.D., Costantino, P.D., Takagi, S. *et al.* (1998). BoneSource™ Hydroxyapatite Cement: A Novel Biomaterial for Craniofacial Skeletal Tissue Engineering and Reconstruction, *J. Biomed. Mater. Res.*, **43B**, 428–432.
38. Larsson, S. and Thomas, B. (2002). Use of Injectable Calcium Phosphate Cement for Fracture Fixation: A Review, *Clin. Orthop. Relat. R.*, **395**, 23–32.
39. Ooms, E.M., Wolke, J.G.C., van de Heuvel, M.T. *et al.* (2003). Histological Evaluation of the Bone Response to Calcium Phosphate Cement Implanted in Cortical Bone, *Biomaterials*, **24**, 989–1000.
40. Gómez, E., Martín, M., Arias, J. *et al.* (2005). Clinical Applications of Norian SRS (Calcium Phosphate Cement) in Craniofacial Reconstruction in Children: Our Experience at Hospital La Paz Since 2001, *J. Oral Maxil. Surg.*, **63**, 8–14.
41. Hidaka, N., Yamano, Y., Kadoya, Y. *et al.* (2002). Calcium Phosphate Bone Cement for Treatment of Distal Radius Fractures: A Preliminary Report, *J. Orthop. Sci.*, **7**, 182–191.
42. Grover, L.M., Knowles, J.C., Fleming, G.J.P. *et al.* (2003). *In Vitro* Ageing of Brushite Calcium Phosphate Cement, *Biomaterials*, **24**, 4133–4141.
43. Shie, M.Y., Hen, D.C.C., Wang, Y. *et al.* (2008). Immersion Behaviour of Gelatin Containing Calcium Phosphate Cement, *Acta Biomater.*, **4**, 646–655.
44. Miyazaki, K., Horibe, T., Antonucci, J.M. *et al.* (1993). Polymeric Calcium Phosphate Cements: Analysis of Reaction Products and Properties, *Dent. Mater.*, **9**, 41–45.
45. Majekodunmi, A.O. and Deb, S. (2007). Poly (Acrylic Acid) Modified Calcium Phosphate Cements: The Effect of the Composition of the Cement Powder and of the Molecular Weight and Concentration of the Polymeric Acid, *J. Mater. Sc. Mater. Med.*, **18**, 1883–1888.

46. Majekodunmi, A.O., Nicholson, J.W. and Deb, S. (2003). Effect of Molecular Weight and Concentration of Poly(Acrylic Acid) on the Formation of a Polymeric Calcium Phosphate Cement, *J. Mat. Sci. Mater. Med.*, **14**, 747–752.
47. Matsuya, Y., Antonucci, J.M., Matsuya, S. *et al.* (1996). Polymeric Calcium Phosphate Cements Derived from Poly(Methyl Vinyl Ether-Maleic) Acid, *Dent. Mater.*, **12**, 2–7.
48. Khashaba, R.M., Moussa, M.M., Mettenburg, D.J. *et al.* (2010). Polymeric-Calcium Phosphate Cement Composites-Material Properties: *In Vivo* and *In Vitro* Investigations, *Int. J. Biomater.*, doi: 1155/2010/691452.
49. Ginebra, M.P., Espanol, M., Montufar, E.B. *et al.* (2010). New Processing Approaches in Calcium Phosphate Cements and their Applications in Regenerative Medicine, *Acta Biomater.*, **6**, 2863–2873.
50. Lopez-Heredia, M.A., Sariibrahimoglu, W.Y., Bohner, M. *et al.* (2012). Influence of the Pore Generator on the Evolution of the Mechanical Properties and the Porosity and Interconnectivity of a Calcium Phosphate Cement, *Acta Biomater.*, **8**, 404–414.
51. Lee, G.-S., Park, J.-H., Shin, U.S. *et al.* (2011). Direct Deposited Porous Scaffolds of Calcium Phosphate Cement with Alginate for Drug Delivery and Bone Tissue Engineering, *Acta Biomater.*, **7**, 3178–3186.
52. Canal, C. and Ginebra, M.P. (2011). Fibre-Reinforced Calcium Phosphate Cements: A Review, *J. Mech. Behav. Biomed.,* **4**, 1658–1671.
53. Zuo, Y., Yang, F., Wolke, J.G.C. *et al.* (2010). Incorporation of Biodegradable Electrospun Fibers into Calcium Phosphate Cement for Bone Regeneration, *Acta Biomater.*, **6**, 1238–1247.
54. Nezafati, N., Moztarzadeh, F., Hesaraki, S. *et al.* (2011). Synergistically Reinforcement of a Self-Setting Calcium Phosphate Cements with Bioactive Glass Fibres, *Ceram. Int.*, **37**, 927–934.
55. Yili, Q., Yang, Y., Juan, L. *et al.* (2011). Preliminary Evaluation of a Novel Strong/Osteoinductive Calcium Phosphate Cement, *J. Biomater. Appl.*, **26**, 311–327.
56. Roussiere, H., Fayon, F., Alonso, B. *et al*. (2008). Reaction of Zoledronate with β-Tricalcium Phosphate for the Design of Potential Drug Device Combined Systems, *Chem. Mater*., **20**, 182–191.
57. Bonnelye, E., Chabadel, A., Saltel, F. *et al.* (2008). Dual Effect of Strontium Ranelate: Stimulation of Osteoblast Differentiation and Inhibition of Osteoclast Formation and Resorption *In Vitro*, *Bone*, **42**, 129–138.

58. Chen, D.M., Fu, Y.F. and Gu, G.Z. (2003). Preparation and Solubility of Solid Solution of Strontium Substituted Hydroxyapatie, *Chin. J. Biomed. Eng.*, **20**, 278–282.
59. Wang, X. and Ye, J. (2008). Variation of Crystal Structure of Hydroxyapatite in Calcium Phosphate Cement by the Substitution of Strontium Ions, *J. Mater. Sci. Mater. Med.*, **19**, 1183–1186.
60. Romieu, G., Garric, X., Munier, S. *et al.* (2010). Calcium-Strontium Mixed Phosphate as Novel Injectable and Radio-Opaque Hydraulic Cement, *Acta Biomater.*, **6**, 3208–3215.
61. Alkhraisat, M.H., Rueda, C., Cabrejos-Azama, J. *et al.* (2010). Loading and Release of Doxycycline Hyclate from Strontium-Substituted Calcium Phosphate Cement, *Acta Biomater.*, **6**, 1522–1528.
62. Nilsson, M., Wielanek, L., Wang, J.S. *et al.* (2003). Factors Influencing the Compressive Strength of an Injectable Calcium Sulphate-Hydroxyapatite Cement, *J. Mater. Sci. Mater. Med.*, **14**, 399–404.
63. Chew, K.K., Low, K.L., Hussein, S. *et al.* (2011). Reinforcement of Calcium Phosphate Cement with Multi-Walled Carbon Nanotubes and Bovine Serum Albumin for Injectable Bone Substitute Applications, *J. Mech. Behav. Biomed.*, **4**, 331–339.
64. Liao, H., Walboomers, X.F., Wouter Habraken, J.E.M. *et al.* (2011), Injectable Calcium Phosphate Cement with PLGA, Gelatin and PTMC Microspheres in a Rabbit Femoral Defect, *Acta Biomater.*, **4**, 1752–1759.
65. Bansal, S., Chauhan, V., Sharma, S. *et al.* (2009). Evaluation of Hydroxyapatite and Beta-Tricalcium Phosphate Mixed with Bone Marrow Aspirate as a Bone Graft Substitute for Posterolateral Spinal Fusion, *Indian J. Orthop.*, **43**, 234–239.

Chapter 29

RADIOTHERAPY GLASSES

Delbert E. Day and Thomas E. Day

29.1. INTRODUCTION

Radiotherapy glasses are defined as radioactive glasses used for *in situ* irradiation, beta or gamma radiation, of targeted organs inside the body.[1,2] Glasses used for this purpose must not only be biocompatible, but also chemically insoluble in the body during the time that the glass is radioactive, to prevent the unwanted release of the radioisotopes from the targeted site. The development of radiotherapy glasses was motivated by the need to deliver large (>10,000 rads), localized doses of beta radiation to diseased organs in the body in such a way as to minimize, and ideally avoid, damage to adjacent healthy tissue. Irradiating malignant tumors inside the body by external beam radiation is limited in several important ways. A major limitation is that the maximum dose which can be safely delivered is constrained by the need to protect surrounding healthy tissue and is usually too small (≤3,000 rads) to be therapeutic. Furthermore, external irradiation with energy radiation such as gamma often causes damage to healthy tissue. The lower energy beta radiation is not well suited for delivery by external means because its smaller range in tissue may be too small for it to reach the target site. Since beta radiation is preferred in many cases, a means of *in situ* radiation is advantageous.

For use as *in vivo* radiation delivery vehicles, radiotherapy glasses should be: biocompatible and nontoxic to the body; chemically insoluble during the time the glass is radioactive; and have high chemical purity. Aluminosilicate glasses containing yttrium and rare earth (RE) cations such as Sm, Ho, Re, and Dy satisfy these criteria.[3–5] Furthermore, they have the advantage that radioisotopes such as Y-90, Sm-153, and Ho-166 can be made by neutron activation as the last step in the manufacturing process, so that the glass can be manufactured in the normal way, avoiding the handling of radioactive materials.

Yttrium aluminosilicate (YAS) glasses have been successfully used clinically for 25 years.[6–18] This application uses YAS glass microspheres, containing Y-90, to irradiate malignant tumors in the liver. Depending upon the size of the liver, desired dose, and diameter of the microspheres, the surgeon injects 1–15 million microspheres of radioactive YAS glass, 15–35 μm in diameter, into the hepatic artery, the primary blood supply for the target tumors. Microspheres are sized so that the blood carries them into the capillary bed of the liver, but they

are too large to pass completely through the liver and enter the circulatory system. Since the distribution of the radioactive microspheres follows the blood flow, the microspheres will concentrate in the tumor, which has a greater than normal blood supply, and irradiate the tumor with beta rays. Typically, 80% of the dose reaches the tumor. Since Y-90 has a half-life of 64.1 hrs, the radioactivity decays to a negligible level in about 21 days.

Radiotherapy glasses can be made in a variety of shapes, such as irregular particles, fibers, or spheres. Microspheres are the shape of choice since the diameter can be carefully controlled and the smooth spherical surface helps with easy injectable delivery of the particles to the target.

29.2. PROCESSING

A typical manufacturing sequence for preparing radiotherapy glass microspheres is given in Fig. 29.1.[5] The first step is the melting of a homogeneous mixture of high purity powders, such as Y_2O_3, Al_2O_3, and SiO_2, in a platinum crucible. Melting typically occurs at 1550–1650°C for the RE aluminosilicate

1. **GLASS MELTING**
   - a. Select chemically pure raw materials (oxides) which do not contain any impurities that would form undesirable radioisotopes during neutron irradiation.
   - b. Mix raw materials to form a homogeneous mixture of powders.
   - c. Melt raw materials to form homogeneous glass.
2. **SPHERIODIZATION (MICROSPHERE FORMATION)**
   - a. Crush glass to particles of desired size.
   - b. Inject particles into gas-oxygen flame to melt each particle and form solid glass sphere (flame spray powder).
   - c. Collect microspheres in suitable container.
3. **SIZING** -- screen or separate microspheres into desired size range.
4. **NEUTRON ACTIVATION** -- irradiate microspheres in nuclear reactor (several days) until desired level of radioactivity is achieved. Package microspheres for delivery to physician.

Figure 29.1. Steps in manufacturing radiotherapy glass microspheres.

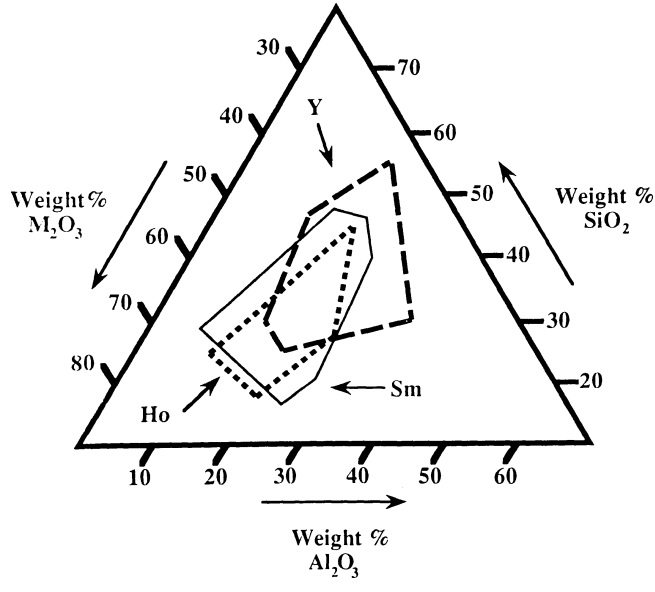

Figure 29.2. Glass formation region (<1,600°C) for Y_2O_3, $Ho2O_3$, or Sm_2O_3 aluminosilicate glasses.

compositions inside the glass forming areas depicted in Fig. 29.2. After melting, the chemically-homogeneous melt is quenched to room temperature and crushed to a powder of the desired size. This powder is spheriodized by passing the particles through a gas/oxygen flame, where each particle is melted, forms a sphere by surface tension forces, and becomes solid during cooling. The microspheres are then screened to obtain microspheres of the desired size. An example of the uniform and highly spherical microspheres made in this way is shown in Fig. 29.3. The final step is the irradiation of the glass microspheres with neutrons to form the desired quantity of radioisotope. YAS glasses are easily irradiated, forming Y-90, to a specific activity up to 5 mCi/mg of glass. After irradiation the microspheres are ready for packaging and shipment. It is important that high purity raw materials, free of neutron-activatable impurities, be used and that care is taken during the various manufacturing steps to avoid chemical contamination of the glass.

29.3. COMPOSITIONS

As evident from Fig. 29.2, glasses can be obtained from a wide range of Y, Sm, and Ho aluminosilicate compositions which melt below 1,600°C. Since a

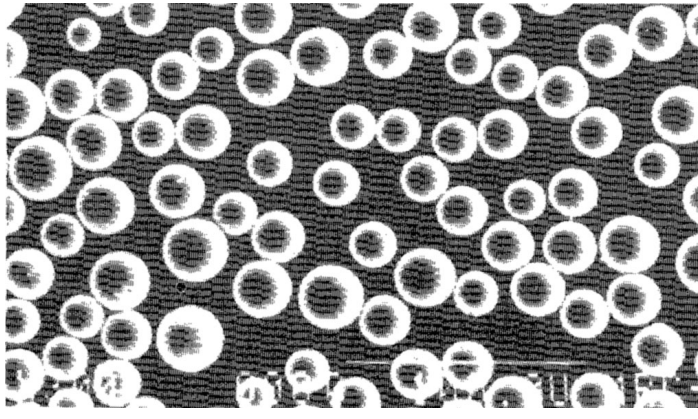

Figure. 29.3. Appearance of "typical" glass microspheres, made according to the procedure described in Fig. 29.1. The white bar in the lower right hand corner is 100 μm.

large range of beta-emitting RE radioisotopes can be incorporated into aluminosilicate glasses, it is possible to select one which is best suited to the particular type and size of the target organ. This compositional flexibility is an inherent advantage of radiotherapy glasses.[3–5] In cases where some amount of gamma radiation is desired, neutron-activatable gamma emitting radioisotopes, such as Na-24, K-42, or P-32, can also be incorporated into the aluminosilicate glass matrix.

An aluminosilicate glass is well suited for radiotherapy use since: no unwanted radioisotopes are formed by the neutron activation of Al, Si, or O; these glasses have a high chemical durability, being essentially insoluble in the body; microspheres with a high specific activity can be easily obtained because of the large amount (40–70 wt%) of RE oxide which can be present in the glass; homogeneous melts can be prepared at reasonable temperatures (<1,600°C); and particles of the glass are easily spheriodized in a flame because of the viscosity characteristics of the glass.

29.4. PROPERTIES

29.4.1. Chemical Durability

Glasses used for radiotherapy purposes need to be highly durable during the time they are radioactive, since the means of confining the radioisotope to the target organ is to keep it inside a chemically-insoluble microsphere. *In vitro* and clinical

tests on radioactive YAS glasses have demonstrated their superior chemical durability. Patients injected with radioactive YAS glass microspheres since 1991 show no reports of any premature or unwanted release of radioactive Y-90 in the body.

In vitro tests on a wide range of YAS glasses, containing 9–30 Y_2O_3, 11–35 Al_2O_3, and 48–72 SiO_2, mol%, have shown that these glasses have an excellent chemical durability in deionized water and in saline at 37°C; this durability varies only slightly with chemical composition.[3–5] An example of the small amount of yttrium released from a typical YAS glass is shown in Fig. 29.4. The only data of practical interest is that for the first three weeks, since the glass is no longer radioactive after that time. Slightly more yttrium is leached from YAS glasses at higher temperatures, 50°C, or in the HCl solution (both of which are used for accelerated testing), but the amount present in deionized water at three weeks (<5 ppm/cm^2 of glass) is too small to be of concern clinically.

A comparison of the small amount of yttrium released from a glass in either bulk form, as glass microspheres, or powder is shown in Table 29.1. The results for microspheres, which are relevant to the use of such glasses in the body, show that little yttrium is released from the microspheres or powder, even though the surface area of these samples is 300 times larger than that of the bulk sample. There is no significant difference in the amount of yttrium released from microspheres tested in either deionized water or saline at 37°C.

The *in vitro* test data in Table 29.1 for the YAS microspheres have been used to calculate the amount of radioactive Y-90 that would be released in a patient injected with 300 mCi of Y-90. The solid data points in Fig. 29.5 show the

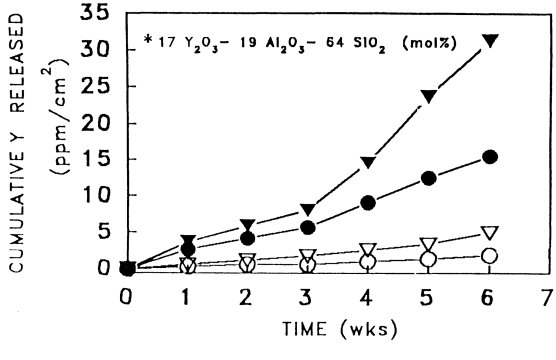

Figure 29.4. Cumulative concentration of Y dissolved from YAS-4 glass and present in 100 ml of solution. Open circles and triangles are for DI water at 37 and 50°C, respectively, while closed circles and triangles are for 12M HCl (pH = 2) at 37 and 50°C, respectively.[5]

Table 29.1. Weight Percent Yttrium Released Per gm of $17Y_2O_3$-$19Al_2O_3$-$64SiO_2$, Mol% Glass[5].

Conditions	% Y Related/gm of Glass	
	3 weeks	4 weeks
DI Water at 37°C		
CM* bulk glass	0.02	0.04
CM microspheres (25 to 35 mm)	0.06	0.09
CM powder (20 to 38 mm)	0.20	0.27
SG* powder (20 to 38 mm)	0.11	0.20
Saline at 37°C		
CM bulk glass	0.03	0.07**
CM microspheres	0.04	0.11**
SG powder	0.81	1.19

*CM means conventionally melting glass while SG means a glass prepared by sol-gel techniques.
**Measured at six weeks.

calculated amount of radiation released to the body due to the very slight dissolution of the YAS glass beads. The calculation takes into account the decay of the Y-90 (half-life of 64.1 hrs). The solid line labeled C in Fig. 29.5 was calculated assuming that all of the radioactive Y-90 dissolved from the microspheres was absorbed in the most susceptible tissue, bone marrow. Even in this worst-case scenario, the total dose to the bone marrow is estimated at less than 5 mrads, which is roughly equivalent to a chest X-ray or about the same dose a person living in Leadville, Colorado, receives in one year from cosmic radiation. The *in vitro* tests in deionized water and saline up to 50°C indicate that the YAS glass microspheres should have an extremely good chemical durability in the body. The lack of any detectable release of radioactive Y-90 from YAS glass microspheres that have been injected into humans, that is, no depression of bone marrow activity, substantiates the *in vitro* test results and demonstrates the suitability of these glasses for use in humans.

Overall, the RE aluminosilicate glasses have excellent durability in deionized water and saline but their durability should be expected to vary somewhat with temperature, with the RE concentration, and the specific RE cation in the glass.[3–5] In general, the durability in deionized water or saline tends to decrease slightly with increasing concentration of the RE cation in the glass, as shown in Fig. 29.6, where slightly more yttrium is dissolved from YAS glasses of higher

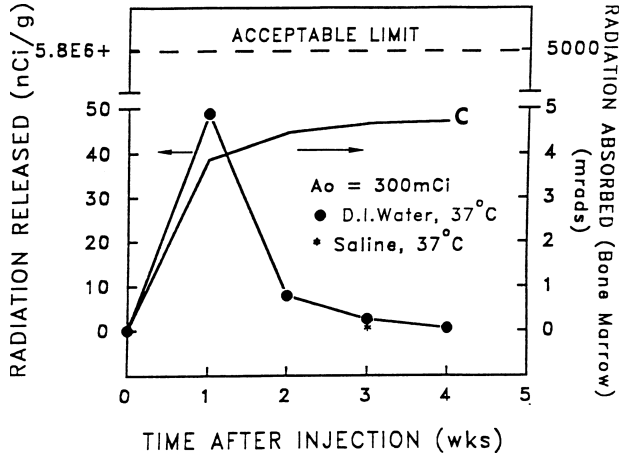

Figure 29.5. Calculated amount of Y-90 radiation released (nCi/g) from YAS-4 microspheres (25–35 μm immersed in (•) DI water (pH 6.9) at 37°C for up to four weeks or in (*) isotonic saline (pH 6.2) at 37°C for three weeks. Calculated from data (Table 28.1), assuming an initial injected dose of 300 mCi and taking into account the decay of the radioactive Y-90. Curve C represents cumulative absorbed dose (rnrads) assuming that all radiation from released Y-90 is absorbed by bone marrow.[5]

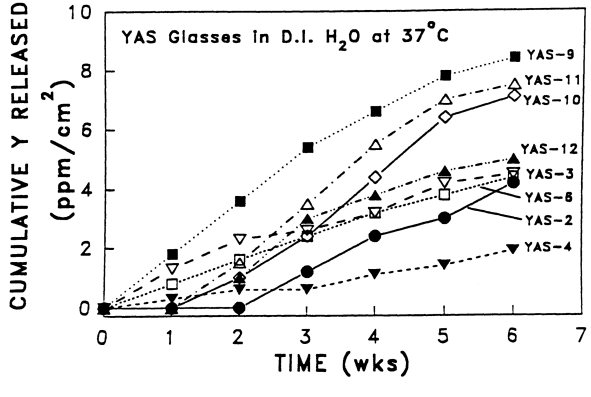

Figure 29.6. Cumulative concentration (ppm) of Y released into 100 ml of DI water at 37°C per surface area (cm^2) of bulk glass. The YAS-4, YAS-12, and YAS-9 glasses contain 17.0, 30.0, and 27.4 mol% Y_2O_3, respectively. Experimental error ± 2.0 ppm.[5]

yttrium content, YAS-9 and -11 contain 27.4 and 30 mol% Y_2O_3, respectively, while the YAS-4 glass contains 17 mol% Y_2O_3. Samarium aluminosilicate (SmAS) glasses are also highly durable in deionized water at 37°C, with a dissolution rate

that ranges from about 30 x 10^{-9} gm/cm^2/min to 2 x 10^{-9} gm/cm^2/min, which is quite similar to the dissolution rate for YAS glasses. Chemical durability of these glasses is considered acceptable for human use and there has been no reported release of Sm-153 from SmAS glass microspheres injected into the kidneys of rabbits.

The excellent chemical durability of RE aluminosilicate glasses is attributed to the absence of alkali and alkaline earth oxides in these glasses, which typically lower the chemical durability of silicate glasses, and to the presence of small highly-charged cations, which can form strong chemical bonds with oxygen. The RE aluminosilicate glasses have a strongly-bonded, three-dimensional network structure that is not easily attacked by aqueous solutions having a pH between 6 and 8. *In vitro* measurements of the chemical durability of Y, Sm, Ho, and a few Re aluminosilicate glasses indicate that most RE aluminosilicate glasses should have a chemical durability satisfactory for *in vivo* use.

29.4.2. Density and Refractive Index

Since the molecular weight of the rare earth oxides is much higher than that of Al_2O_3 and SiO_2, the density of the RE aluminosilicate glasses depends primarily on the concentration of the RE oxide.[5] As shown in Fig. 29.7, the density of YAS glasses ranges from about 2.8 gm/cm^3 at 10 mol% Y_2O_3 to about

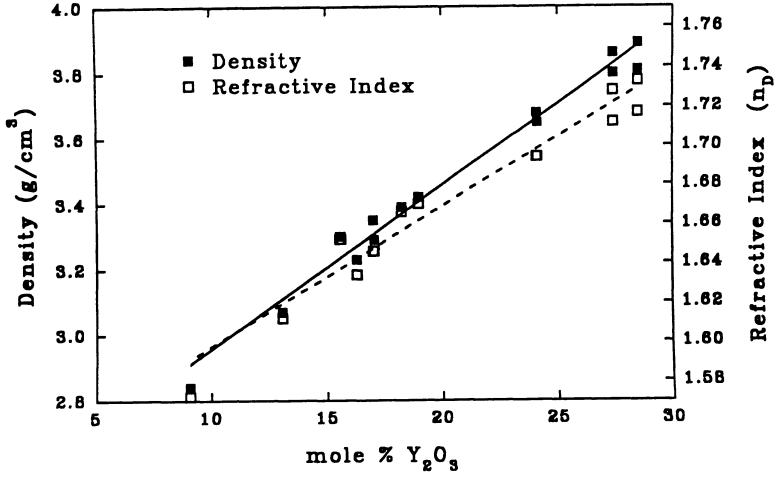

Figure 29.7. Density (solid line) and refractive index (dashed line) of YAS glasses. Lines are least squares fit to data points.

4.0 gm/cm^3 for glasses containing 30 mol% Y_2O_3. Comparable SmAS glasses have a higher density, ranging from about 3.4 to 4.6 gm/cm^3, which is consistent with the higher molecular weight of Sm_2O_3.

The density of the RE aluminosilicate glasses is obviously considerably higher than that of blood, but this has not caused any problems in the injection of these glasses into humans or test animals. During injection, precautions are necessary to insure that the microspheres do not settle out of solution, but simple agitation is adequate to keep the microspheres suspended.

The refractive index of the glasses is not important to their use for radiotherapy purposes, but this is another property which depends primarily upon the concentration of the RE oxide, Fig. 29.7. The relative amounts of alumina and silica in these glasses is of lesser importance to properties such as refractive index, density, and thermal expansion coefficient.

29.5. CLINICAL RESULTS: UP TO 1993

Clinical results in this section are as reported in the first edition of this book.

The tissue response to radiotherapy glasses varies according to the tissue being irradiated, and clinical data relating tissue response to radiotherapy glasses exists only for the liver and kidney. This chapter discusses effects only in the liver.

The liver is referred to as a reverting postmitotic cell type. This means that the liver does not normally divide or renew itself, as does the skin or lining of the digestive tract, but has the capability to do so. If the capacity of the liver to function is decreased by some type of injury (chemical, trauma, etc.), it will be stimulated to renew itself in order to maintain normal body function.

Liver tumors, like other tumor types, undergo rapid mitotic division and are highly sensitive to ionizing radiation. All tissues that are rapidly dividing cell types are extremely sensitive to the effects of ionizing radiation. This is due to the large percentage of time that the cells' genetic material is condensed in the nucleus. Ionizing events reaching the condensed genetic material in the nucleus of the cell will lead to cell death. Since the normal liver is not usually in a dividing state it is resistant to the effects of low to moderate levels of ionizing radiation.

The "average" doses that have been delivered with radiotherapy glasses to liver tumors have ranged from 5,000 to 15,000 rads.[6–10] This would normally be considered a large human dose and it is difficult to predict the exact dose delivered to just the tumor. As previously mentioned, the distribution of the glass microspheres in the liver is believed to depend on the blood flow. Many hepatic tumors are classified as hypervascularized, which means that the blood flow to

the tumors exceeds that to the normal surrounding tissue, and, consequently, a larger than normal fraction of microspheres will be transported and deposited in the tumor. This increases the radiation dose to the tumor while minimizing the exposure of the surrounding normal tissue. This localization of the radiation explains why patients treated with radioactive Y-90 glass microspheres can tolerate much higher doses than those treated by whole liver radiation methods.

One study used dogs as a model for hepatic arterial injection of both non- and radioactive YAS glass microspheres. Doses exceeding 30,000 rads were delivered to the livers of these dogs. Delivered doses of non- and radioactive microspheres (143–562 mg) were measured in units of mCi per gm of liver tissue and ranged from 1 to 12 times the anticipated human dose. The dogs were grouped by varying dose levels and a control group that received nonradioactive microspheres was used to determine the physical impact of the microspheres alone on liver function.

Doses of nonradioactive microspheres delivered were up to six times that of the anticipated human dose. Minimal changes were detected, such as changes within the walls of the central veins, in the appearance of the hepatocytes, and in the tissue architecture. Hepatocellular function and damage were within normal limits. There were no signs of portal fibrosis or cirrhosis.

Changes seen in the liver injected with radioactive YAS microspheres were similar to the findings of other irradiation studies in dog liver. These changes included histologic changes in the portal areas of the liver. Doses as high as 35,000 rads were delivered, but did not cause total necrosis and were judged by clinical standards as compatible with survival. Doses up to 15,000 rads were well tolerated and showed little change in liver function. No microspheres were found in the bone marrow. Even in dogs receiving more than 15,000 rads, no bone marrow suppression occurred. At doses above 25,000 rads, the consequences of hepatic cirrhosis would probably pose significant problems.

In a preliminary study, a transient increase in body temperature has been noted, but this lasted only a few days. In some patients with a history of previous liver disease (chronic alcoholism), ulcerations of the lower stomach and upper small intestine have occurred. When treated, these conditions were self-limiting. In almost all patients receiving YAS radiotherapy glasses, liver enzymes were mildly elevated. This effect was not dose-related and lasted from a few days to weeks.

Clinical applications of radiotherapy glasses have been on liver and kidney tumors. Most of this work has been with liver tumors, since patients with liver cancer can enter the terminal phase within four to six months of diagnosis. This has sparked a major effort in investigating ways of delivering ionizing radiation *in vivo* to treat these malignant tumors.

Work is currently underway to discover whether very large doses delivered to the kidneys will reduce the shedding of malignant cells, which can spread the tumor, during surgical removal of a diseased kidney.

In summary, any tissue that is relatively insensitive to low or moderate amounts of ionizing radiation in which these unique microspheres can be deposited, by either the blood flow or surgical implantation, is a potential candidate for this new form of radiotherapy.

29.6. SUMMARY

RE aluminosilicate glass microspheres have proved to be well suited for radiotherapeutic use in humans. These microspheres provide a new and unique method of irradiating diseased internal organs with beta radiation, in amounts which exceed those that can be delivered by other means. YAS glass microspheres have been safely used to irradiate, up to 15,000 rads, malignant tumors in the liver. Since the glass microspheres tend to distribute themselves in the liver in proportion to the blood flow, the actual dose to the tumors is believed to be much larger than the average dose to the entire liver, since the microspheres tend to concentrate in the tumors because of their vascularity. In one case, 80% of the YAS microspheres were estimated to lodge in the tumor vascular bed, giving an estimated dose of 32,000 rads. Samarium aluminosilicate glass microspheres have been used to irradiate, up to 15,000 rads, the kidneys in rabbits without any harmful side effects or detectable damage to adjacent tissue.

A major advantage of the RE aluminosilicate glass microspheres is excellent chemical durability in the body. Since the glasses are insoluble in body fluids, the radioactive RE isotope is confined to the target organ and prevented from entering the circulation. The maximum time which these glass microspheres will remain in the body is currently unknown, but YAS microspheres have been in one patient for more than four years with no reported problems.

29.6.1. Clinical Results: Up To 1993[10]

In one group of 39 adenocarcinoma patients treated with 5,000 to 11,000 rads in a phase I–II study, the average survival time was 9.7 months from the date of treatment with the microspheres. This compares with a median survival time of 12 months from the time of diagnosis for patients treated with conventional chemotherapy. All of the patients treated with the YAS glass microspheres had undergone one chemotherapy treatment and diagnosis may have occurred several months prior to injection with the YAS microspheres.

Treatment with glass microspheres takes about one hour, followed by a few hours in the hospital for observation; treatment is as a "day-patient". Chemotherapy requires several repeated treatments over several weeks. Increased liver enzymes are a common side effect following treatment with the glass microspheres, and transient fever, increased pain, and nausea and vomiting are less common side effects.

Radiotherapy glass microspheres are being considered for treating other diseases and other types of cancer. Using radiotherapy glasses to kill cancer cells in diseased kidneys prior to surgical removal has already been mentioned. Ideally, it should be possible to use radiotherapy glass microspheres to irradiate any diseased organ with a capillary bed. The *in situ* irradiation of arthritic joints with beta emitting RE aluminosilicate glass microspheres is also under study. The stifle joints in rabbits have been injected with usable quantities of glass microspheres without any noticeable physical damage to the joint for periods up to one year. In rabbits the glass microspheres were found imbedded in a layer of the synovial tissue. In this application, the radioactive glass microspheres were used to perform a radiation synovectomy of the diseased joint.

29.7 NEW DEVELOPMENTS: 1993–2012

29.7.1 Clinical Results: Destroying Malignant Tumors

The technological innovation described in this chapter is the development and application of radioactive YAS glass microspheres that are being used to treat patients with a generally inoperable and deadly form of primary liver cancer; what is called hepatocellular carcinoma (HCC).[11] The incidence of this deadly disease (HCC) is increasing worldwide and is considered the sixth most common cancer in the world (one million new cases annually) and ranks third as the cause of cancer-related deaths (500,000 deaths per year). In the US, the National Cancer Institute estimates that there were 19,160 new cases of HCC and 16,780 deaths in 2007. Life expectancy for patients diagnosed with HCC is measured in months. The five year survival rate for patients with HCC is less than 7%.[12]

Liver cancer, especially HCC, has been and still is a difficult disease to treat, but the availability of Y-90 glass microspheres has opened a new avenue for treating liver cancer, what is called radioembolization. This refers to the combined effect of the radiation and the embolization of the capillaries in a malignant tumor(s). The Y-90 microspheres not only safely deliver a much larger dose of radiation to the tumor(s), but the roughly 2–8 million glass microspheres in a typical injection become lodged (embolize) in the capillaries, thereby reducing

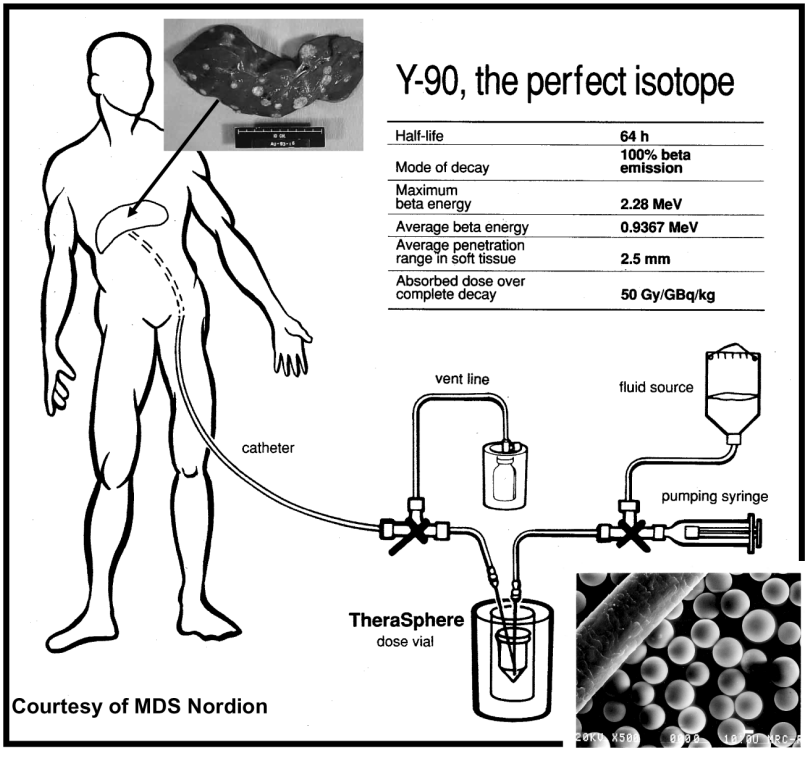

Figure 29.8. Schematic view of the infusion of Y-90 glass microspheres into tumors in the liver. Bottom inset shows YAS microspheres along with a human hair and inset at top shows a liver with multiple tumors (light spots).

the blood (nourishment) flow to the malignant tumor(s). These two synergistic effects help shrink and destroy the tumor(s).[11]

Typically, the procedure is done on an out-patient basis, with the patient receiving what amounts to an injection of several million radioactive Y-90 glass microspheres through a catheter inserted in the femoral/hepatic artery (Fig. 29.8). The microspheres are released into the blood stream as close as possible to the tumor(s) in order to maximize the number of microspheres deposited in the malignant tumor(s). The microspheres are sized so that they are small enough to enter the capillaries of the tumor(s), but are too large to pass through the capillaries. Typically, only a small fraction, 2–10%, of the radioactive microspheres reaches healthy tissue. The chemical stability of the glass ensures safety.[13]

After a brief period of observation, the patient is discharged if there are no complications. The inoperable HCC tumor(s) in the patient's liver continue to be irradiated *in situ* by the localized Y-90 beta radiation as the patient returns to a normal routine. In about four weeks the microspheres are no longer radioactive.

Initially, patients received only one injection of Y-90 glass microspheres, since the radiation dose was much larger than doses used previously. As confidence in the safety of *in situ* irradiation increased and the benefits became better known, patients received multiple injections when necessary. The *in situ* irradiation of HCC tumors with radioactive YAS glass microspheres is increasingly recognized as having many advantages.[11] With Y-90 radioembolization, it is possible to irradiate multiple, small tumors at much higher doses, 5–50 times, compared to use of external beam. The localized beta radiation destroys tumors regardless of the tumor origin and the relatively low toxicity of the beta radiation toward healthy tissue permits repeated injections. Compared with chemotherapy and other radiation procedures, the side effects are small; a small fraction of patients report flu-like symptoms such as fatigue, a slight fever, or abdominal pain for a few days.

29.7.2. Survival Data

Of greatest interest is the survival data for patients treated with the Y-90 glass microspheres. For patients with inoperable HCC, the stage of the disease at the time of treatment is especially important to survival. The survival data for a group of 229 patients with HCC who received no specific treatment provides a reference point.[14] The median survival time for this group was 51 days; 21 days for patients at an advanced stage and 249 days for patients with an early stage disease. For a group of 42 patients treated with Y-90 glass microspheres, the median survival was 236 days (advanced stage) and 660 days (early stage).[15] In another group of 150 patients with inoperable HCC, the median survival time for the entire group was 800 days (2.2 yrs) after treatment with the Y-90 glass microspheres.[16] Finally, the 1, 2, and 5 year survival rates for a group of 20 patients, aged 42 to 82, with inoperable HCC and treated with Y-90 glass microspheres were reported to be 100%, 75%, and 46%, respectively.[17] These survival rates are encouraging.

29.8 CONCLUSIONS

The radioembolization of HCC tumors with radioactive YAS glass microspheres is recognized as a safe and effective way of treating this deadly form of cancer. Glass technology and science have made an important contribution to the

success of this new procedure for treating patients with inoperable liver cancer. There are other opportunities where microspheres of YAS and other RE aluminosilicate glasses can be used as *in situ* radiation devices to destroy malignant tumors in other organs in the body.[18]

REFERENCES

1. Ehrhardt, G.J. and Day, D.E. (1987). Therapeutic Use of Yttrium-90 Microspheres, *Nucl. Med. Bioi. Inti. J. Radiat. Appl. Instr., Pan B*, **14**, 233–242.
2. Brown, R.F., Lindesmith, L. and Day, D.E. (1991). Ho-166 Containing Glass for Internal Radiotherapy, *Nucl. Med. Bioi. Inti. J. Radiat. Appl. Instr., Pan B*, **18**, 783–790.
3. Hyatt, M.J. and Day, D.E. (1987). Glass Formation and Properties in the Yttria-Alumina Silica System, *J. Am. Ceram. Soc. Comm.*, **70**, 283–287.
4. Erbe, E.M. and Day, D.E. (1990). Properties of Sm_2O_3–Al_2O_3–SiO_2 Glasses for *In Vivo* Applications, *J. Am. Ceram. Soc.*, **73**, 2708–2713.
5. Erbe, E.M. (1991). *Structure and Properties of Y_2O_3–Al_2O_3–SiO_2 Glasses* (PhD Thesis, University of Missouri-Rolla).
6. Herba, M.J., Illescas, F.F., Thirlwell, M.P. *et al*. (1988). Hepatic Malignancies: Improved Treatment with Intraarterial Y-90, *Radiology*, **169**, 311–314.
7. Houle, S., Yip, T.K., Shepherd, F. *et al*. (1989). Hepatocellular Carcinoma: Pilot Trial of Treatment with Y-90 Microspheres, *Radiology*, **172**, 857–860.
8. Wollner, L., Knutsen, C., Smith, P. *et al*. (1988). Effects of Hepatic Arterial Yttrium 90 Glass Microspheres in Dogs, *Cancer*, **61**, 1336–1344.
9. Day, D.E. and Ehrhardt, G.J. (1991). U.S. Patents 4,789,501; 5,011,677 and 5,011,797. Biomedical Materials, *MRS Bulletin*, **XVI**, 26–81.
10. Harbert, J.C. and Ziessman, H.A. (1987). "Therapy with Intraarterial Microspheres", in Freeman, L.M. and Weissmann, H.S. (eds), *Nuclear Medicine Annual*, Raven Press, New York, pp. 295–319.
11. Salem, R. and Thurston, K.G. (2006). Radioembolization with Yttrium-90 Microspheres: A State-of-the-Art Brachytherapy Treatment for Primary and Secondary Liver Malignancies, Part 3: Comprehensive Literature Review and Future Direction, *J. Vasc. Interv. Radiolology*, **17**, 1571–1594.
12. El-Serag, H.B., Mason, A.C. and Key, C. (2001). Trends in Survival of Patients with Hepatocellular Carcinoma between 1977 and 1996 in the United States, *Hepatology*, **33**, 62–65.

13. Erbe, E.M. and Day, D.E. (1993). Chemical Durability of Y_2O_3–Al_2O_3–SiO_2 Glasses for the *In Vivo* Delivery of Beta Radiation, *J. Biomed. Mater. Res.*, **27**, 1301–1308.
14. Okuda, K., Ohtsuki, T., Obata, H. *et al*. (1985). Natural History of Hepatocellular Carcinoma and Prognosis in Relation to Treatment: Study of 850 Patients, *Cancer*, **56**, 918–928.
15. Keppke, A.L., Salem, R., Reddy, D. *et al*. (2007). Imaging of Hepatocellular Carcinoma after Treatment with Yttrium-90 Microspheres, *Am. J. Roentgenology*, **188**, 768–775.
16. Kulik, L.M., Atassi, B., Holsbeeck, L.V. *et al*. (2006). Yttrium-90 Microspheres (TheraSphere™) Treatment of Unresectable Hepatocellular Carcinoma: Downstaging to Resection, RFA and Bridge to Transplantation, *J. Surgical Oncology*, **94**, 572–586.
17. Gaba, R.C., Lewandowski, R.J., Kulik, L. *et al*. (2009). Radiation Lobectomy: Preliminary Findings of Hepatic Volumetric Response to Lobar Yttrium-90 Radioembolization, *Ann. Surg. Oncol*., **16**, 1587–1596.
18. White, J.E. and Day, D.E. (1994). Rare Earth Aluminosilicate Glasses for *In Vivo* Radiation Delivery, *Key Eng. Mat.*, **94–95**, 181–208.

Chapter 30

DENTAL GLASS-CERAMICS AND ZrO_2-CERAMICS

Wolfram Höland, Marcel Schweiger and Volker M. Rheinberger

30.1. INTRODUCTION

Biomaterials used in restorative dentistry are important products for humans who want to regain the full range of their chewing functions or improve the aesthetic appearance (malposition) of their teeth. Therefore, dental biomaterials are products which considerably enhance the quality of human life. Typical products are dental inlays, onlays, crowns, veneers bridges, posts or abutments for implant therapy. This category of materials must fulfill a combination of properties. They must be able to match or even surpass the optical (translucency, opalescence, fluorescence), chemical and mechanical properties of natural teeth. For example, chemical durability is essential to prevent the occurrence of caries. With regard to mechanical properties, abrasive wear behavior must be similar to that of natural teeth, whereas flexural strength and toughness have to be considerably higher than natural teeth to allow construction of functionally-adequate dental bridges, posts or abutments in high load-bearing regions. A historical review of the development of biomaterials for restorative dentistry shows that ceramics were used to produce dental restorations as early as the beginning of the 19th century. But aesthetic veneering of metal frameworks (crowns, bridges) only became possible after leucite-based ($KAlSi_2O_6$) porcelain-fused-to-metal (PFM) materials had been developed.[1] Significant advances in the development of materials that match, or even outperform, the optical, mechanical and chemical properties of natural teeth were accomplished with the introduction of glass-ceramics. For the first time, materials capable of meeting the challenges of metal-free tooth replacements became available.

30.2. MICA-TYPE GLASS-CERAMICS

DICOR® (Corning Inc./Dentsply Int., USA) was the first glass-ceramic developed for restorative tooth replacements (Table. 30.1).[2] Mica crystals of the type of tetrasilicic mica, $KMg_{2.5}Si_4O_{10}F_2$, were precipitated by means of controlled crystallization in the SiO_2–MgO–K_2O–F system. See Chapter 16 for

details of these glass-ceramics. The first clinical tests with inlays and crowns were performed as early as 1979. This glass-ceramic featured translucent properties and was capable of reproducing the optical characteristics of natural teeth. Flexural strength was approximately 150 MPa. The base glass was processed by means of molding technology. Additional heat treatment was required to convert the base glass into the glass-ceramic. In addition to applications that involved the use of molding technology, machinable types of mica glass-ceramics, such as DICOR® MGC, became available to manufacture dental devices. This was an important development, pointing towards promising new technologies.

30.3. LEUCITE-TYPE GLASS-CERAMICS

At the end of the 1980s, special molding technology which eliminated the need for additional heat treatments became available, allowing the fabrication of inlays and crowns from leucite, $KAlSi_2O_6$, glass-ceramics.[3] The principles of controlled surface nucleation and surface crystallization in base glasses of the SiO_2–Al_2O_3–K_2O–Na_2O system were applied in these glass-ceramics.[4] The resulting product is IPS Empress® (Ivoclar Vivadent AG, Liechtenstein; Tables 30.1 and 30.2). With this material, the lost-wax technique and subsequent viscous flow molding processes enable the fabrication of highly individualized inlays and crowns, offering a high degree of accuracy of fit. The molding processes are performed in specially-designed ceramic press furnaces of Ivoclar Vivadent AG, using a temperature range of 1,000–1,200°C. The IPS Empress® glass-ceramic exhibits a coefficient of thermal expansion, CTE, of $15 \cdot 10^{-6}$ K^{-1} m/m to $18.25 \cdot 10^{-6}$ K^{-1}m/m. It offers a flexural strength of approximately 160 MPa, which can be increased by glazing and additional heat treatment. Wear behavior in relation to natural dentition deserves particular mention. Since this glass-ceramic is characterized by similar abrasive properties as natural teeth, the opposing tooth structure of the human dentition is not damaged during mastication.

In 2005, IPS Empress® Esthetics, an even more translucent version of the above leucite glass-ceramic, was developed. The improved optical qualities allow fabrication of dental replacements that are even more similar to natural teeth. Typical applications are dental inlays, veneers and crowns (Fig. 30.1). Inlays and crowns can be accomplished in a single appointment by machining the material with diamond tools in a CEREC unit (Sirona, Germany). Patients do not need to see their dentist twice to have their restoration completed.

30.4. LITHIUM DISILICATE GLASS-CERAMICS

Lithium disilicate ($Li_2Si_2O_5$) glass-ceramics expand the range of indications of glass-ceramic biomaterials to include dental bridges. Wide-ranging developments have been undertaken in conjunction with this material system.[5–7] To develop the new material, the main crystal phase was produced in the special base glass of the SiO_2–Li_2O–K_2O–ZnO–P_2O_5–Al_2O_3–La_2O_3 system by means of heterogeneous nucleation and crystallization. In the process, an interlocking microstructure with a crystal content of more than 60% vol. was achieved.[4] The resulting product was called IPS Empress®2 (Ivoclar Vivadent AG; Table 30.1).

Table 30.1. Timeline for Development of Glass-Ceramics for Dental Restoration.

1979	DICOR® glass-ceramic: first clinical tests as moldable glass-ceramic for dental restoration
1991	IPS Empress®: moldable leucite based glass-ceramic for inlays, crowns, veneers
1997	IPS Empress® Cosmo Post: ZrO_2-containing glass-ceramic for fixation of ZrO_2 posts
1998	IPS ProCAD®: machinable leucite-based glass-ceramic for inlays, crowns, veneers
1999	IPS d.SIGN®: leucite-apatite glass-ceramic to veneer metal frameworks, especially dental crowns and long-span bridges
2000	IPS Empress®2/IPS Eris for E2: lithium disilicate glass-ceramic veneered with fluoroapatite glass-ceramic to fabricate dental crowns and small three-unit dental anterior bridges
2004	IPS Empress® Esthetic: leucite based glass-ceramic with high optical properties close to the natural tooth
2005	IPS e.max® Press MO: lithium disilicate as moldable glass-ceramic for veneered crowns and three-unit dental bridges
2005	IPS e.max® Ceram and Zir Press: Fluoroapatite glass-ceramic to veneer high toughness sintered ZrO_2 frameworks (especially crowns and posterior bridges)
2005	IPS e.max® CAD MO: machinable lithium disilicate glass-ceramic, especially for veneered dental crowns
2005	IPS e.max® ZirCAD: machinable yttria-stabilized zirconia
2007	IPS e.max® Press LT and CAD LT: medium translucent lithium disilicate glass-ceramic
2009	IPS e.max® Press HT and IPS e.max CAD HT: high translucent (HT) lithium disilicate glass-ceramic as moldable (Press) and machinable (CAD) glass-ceramic for dental application
2011	IPS e.max® CAD-On: lithium disilicate glass-ceramic fused to a ZrO_2-framework, especially for posterior dental bridges

Table 30.2. Clinical Application of Special Types of Glass-Ceramics as Biomaterials for Dental Restoration.

Glass-Ceramic Product	Number of Units (One unit represents one crown or inlay etc.)
IPS Empress® System (1991–2010)	43 million
IPS Empress®CAD (and ProCAD®) (1998–2010)	7 million
IPS e.max® System (2005–2010)	36 million
IPS d.SIGN® (1999–2010)	89.5 million

Figure 30.1. Bioceramics for dental restoration (Ivoclar Vivadent AG). (a) Left: dental bridge (framework of lithium disilicate glass-ceramic veneered with fluoroapatite glass-ceramic) on a mirror. (b) Right: dental bridge (framework of ZrO_2 ceramic fused to a lithium disilicate glass-ceramic) on a mirror. (c) Middle: dental inlay, crown and veneer of leucite glass-ceramic.

A significant improvement over IPS Empress®2 was achieved in the SiO_2–Li_2O–K_2O–Al_2O_3–ZrO_2 system and resulted in the development of the product IPS e.max® (Ivoclar Vivadent AG; Tables 30.1 and 30.2).[8] This glass-ceramic showed a high fracture toughness, K_{IC} value of 2.3 $MPa \cdot m^{0.5}$, and high flexural strength (440 MPa) and translucency. The product group of IPS e.max® encompasses several types of material. The biomaterial IPS e.max® Press presents a moldable glass-ceramic and the biomaterial IPS e.max® CAD a machinable glass-ceramic. The IPS e.max® Press ceramics are distinguished by the fact that these materials are processed into inlays, crowns and bridges by the application of molding technology at a temperature of 920°C. The glass-ceramic can be veneered with fluoroapatite glass-ceramic (Fig. 30.1).

An intermediate product, which is easy to machine, has been developed. This lithium metasilicate glass-ceramic demonstrates a singular blue color. After the blue glass-ceramic has been machined and tried in the mouth of the patient, it undergoes heat treatment at 840°C. During thermal treatment, it is transformed into a lithium disilicate glass-ceramic with aesthetics of natural teeth.

30.5. FLUOROAPATITE GLASS-CERAMICS

The needle-like fluoroapatite crystals, $Ca_5(PO_4)_3F$, contained in glass-ceramics (IPS e.max® Ceram, IPS e.max® ZirPress, Ivoclar Vivadent AG) may produce a favorable light-scattering effect, such that the resulting translucency corresponds to that of natural teeth.[8,9] The objective was to develop a veneering ceramic that offered tooth-like optical properties. This, however, does not mean that the material should be bioactive. The tooth-like translucency and the CTE of 9.5 10^{-6} K^{-1}m/m enabled the resulting glass-ceramic to be used on lithium disilicate glass-ceramics as well as on high-toughness $3Y_2O_3$–ZrO_2 sintering ceramics. Sintered ceramic devices are achieved by machining open-pore materials and subsequently sintering them to a high density. The high toughness of approximately 4.5 $MPa \cdot m^{0.5}$ allows the fabrication of metal-free long-span bridges.

30.6. ZrO_2-CONTAINING GLASS-CERAMICS

With the objective to achieve high levels of toughness and a CTE that is adjusted to that of ZrO_2 sintered ceramics, a ZrO_2-containing glass-ceramic (IPS Empress® Cosmo Post, Ivoclar Vivadent AG) was developed (Table 30.1). Controlled crystallization was used to produce $Li_2ZrSi_6O_{15}$ as the main crystal phase.[10]

This glass-ceramic offers the advantage over other products that it can be pressed onto ZrO_2 posts by means of a molding process. The resulting dental posts are suitable for the build-up of devitalized teeth and offer metal-free, highly aesthetic solutions for patients.

30.7. LEUCITE-APATITE GLASS-CERAMICS

Glass-ceramics were also developed to veneer dental metals frameworks, e.g. long-span bridges. A preferred material is a leucite-apatite glass-ceramic (IPS d.SIGN®, Ivoclar Vivadent AG) from the SiO_2–Al_2O_3–K_2O–Na_2O–CaO–P_2O_5–F system (Tables 30.1 and 30.2). The leucite content enables this glass-ceramic to attain the required coefficient of thermal expansion of approximately $12 \cdot 10^{-6}$ K^{-1}m/m. The fluoroapatite needles provide the product with the required translucent qualities. The nucleation and crystallization mechanisms in the base glasses of this material are conducted by means of a two-fold reaction. Leucite is formed by surface crystallization, while apatite is precipitated according to the mechanisms of internal processes.[9] This glass-ceramic can be applied in two different techniques: sintering or molding on dental frameworks.[8,11]

30.8. ZrO_2 CERAMICS

Sintered ceramics of Al_2O_3 and ZrO_2-type are widely used in dentistry.[8] The preferred processing technology is machining by milling. The ZrO_2 ceramic of the type IPS e.max® Zir CAD (Ivoclar Vivadent AG) is characterized by a K_{IC} value of 4.5 $MPa \cdot m^{0.5}$. Based on this very high toughness, the biomaterial is used to produce dental copings, frameworks of dental bridges and dental abutments. The product of a dental framework can be veneered with the fluoroapatite glass-ceramic IPS e.max® Ceram or ZirPress.

A technology was developed to fuse two machined products, a lithium disilicate (IPS e.max® CAD HT) and a zirconia framework to produce a dental bridge. The final product is IPS e.max® CAD-On (Table 30.1, Fig. 30.1). This is the strongest veneering material with excellent aesthetics for posterior bridges.

30.9. CONCLUSION

Considering all the products presented together, glass-ceramic and sintered bioceramics cover the entire range of indications for anterior and posterior

restorative tooth repair and, therefore, fully fulfill the dental restoration requirements of patients.

REFERENCES

1. McLean, J.W. (1972). "Dental Porcelains", in Dickens, D. and Cassels, J.M. (eds), *Dental Materials Research, NBS Publications 354*, National Bureau of Standards, Washington, DC, pp. 77–83.
2. Grossman, D.G. (1972). Machinable Glass-Ceramic Based on Tetrasilicic Mica, *J. Am. Ceram., Soc.*, **55**, 446–449.
3. Wohlwend, A. and Schärer, P. (1990). Die Empress-Technik-Ein Neues Verfahren zur Herstellung von vollkeramischen Kronen, Inlays und Facetten, *Quint. Zahntech*., **16**, 966–978.
4. Höland, W. and Beall, G.H. (2012). *Glass-Ceramic Technology, 2nd Edition* John Wiley and Sons, Inc., Hoboken, NJ.
5. Freiman, S.W. and Hench, L.L. (1972). Effect of Crystallization on the Mechanical Properties of Li_2O-SiO_2 Glass-Ceramics, *J. Am. Ceram. Soc.*, **55**, 86–90.
6. Haedley, T.J. and Loehman, R.E. (1984). Crystallization of a Glass-Ceramic by Epitaxial Growth, *J. Am. Ceram. Soc.*, **67**, 620–625.
7. Beall, G.H. (1989). Design of Glass-Ceramics, *Solid State Sci*., **3**, 333–354.
8. Höland, W., Schweiger, M., Watzke, R. *et al.* (2008). Ceramics as Biomaterials for Dental Restoration, *Expert Rev. Med. Devices*, **5**, 729–745.
9. Höland, W., Ritzberger, C., Apel, E. *et al.* (2008). Formation and Crystal Growth of Needle-Like Fluoroapatite in Functional Glass-Ceramics, *J. Mater. Chem*., **18**, 1318–1332.
10. Schweiger, M., Frank, M., von Clausbruch, S.C. *et al.* (1998). Microstructure and Properties of Pressed Glass-Ceramic Core to Zirconia Post, *Quint. Dent. Technol*., **21**, 73–79.
11. Höland, W., Rheinberger, V., Apel, E. *et al.* (2007). Principles and Phenomena of Bioengineering with Glass-Ceramics for Dental Restoration, *J. Europ. Ceram. Soc*., **27**, 1521–1526.

Chapter 31

BIOACTIVE GLASS FOR TOOTH REMINERALIZATION AND PAIN DESENTIZATION

David C. Greenspan and Larry L. Hench

31.1. INTRODUCTION

Tooth pain is often due to a clinical condition called dentin hypersensitivity and is a common occurrence in the general adult population. The incidence has been reported to be anywhere from 4% to as high as 57% of adults.[1,2] In periodontal patients, the rate of dentin hypersensitivity can be as high as 98%.[3] The condition has been characterized by a short sharp pain arising from exposed dentin in response to stimuli; typically thermal, evaporative, chemical or tactile.[4–6] This chapter reviews the development of a novel class of biomaterials that are highly effective in the treatment and prevention of dentin hypersensitivity. The material is 45S5 Bioglass®, see Chapter 3, processed to be a powder that is composed of small particles that are several micrometers in diameter. The commercial product is trademarked NovaMin®. The technical description of this material in the dental literature for use in treatment of dentin hypersensitivity is an inorganic, amorphous, calcium, sodium phosphosilicate (CSPS) material. This chapter also describes the mode of action of CSPS particles that results in the superior performance in the reduction of tooth sensitivity by physically occluding dentin tubules.

31.2. NOVAMIN® AND SENSITIVITY: MODE OF ACTION

The currently accepted theory for tooth hypersensitivity is the hydrodynamic theory proposed by Brännström,[7] based upon the concept that open dentinal tubules allow fluid flow through the tubules, which results in pressure changes that excite the nerve endings in the dental pulp. Clinical replicas of sensitive teeth viewed under a scanning electron microscope (SEM) reveal varying numbers of open or partially occluded dentinal tubules.[8] In patients with dentin hypersensitivity, there are a greater number of tubules per area and the diameter of the tubules is greater than in patients with no sensitivity.[9] In general, tubules are not exposed at the tooth root surface because of the cementum covering the tooth root, or because of a natural smear layer of dentinal debris and organic matter that covers

the tooth surface and masks the tubules. When the smear layer is present, the fluid flow that can occur through the dentin is only a few percent of that possible following acid removal of the smear layer, which "opens" the tubules.

The first approach to the treatment of dentinal hypersensitivity is to treat the tooth with a chemical agent, such as potassium nitrate or potassium chloride, which penetrates into the dentinal tubules and depolarizes the nerve synapses, reducing sensitivity by preventing the conduction of pain impulses.[10] While these materials have consistently shown clinical efficacy in the treatment of sensitivity, it may take weeks for the patient to perceive a reduction in pain and sensitivity. The second approach is to treat the tooth with a chemical or physical agent to physically occlude dentinal tubules, which reduces sensitivity by prevention of pulpal fluid flow (e.g., potassium oxalate, ferric oxalate, strontium chloride).[11] Although both approaches are effective at reducing or eliminating hypersensitivity, the duration of relief is highly variable. Hypersensitivity usually reappears due to toothbrush abrasion, the presence of acid challenges in the mouth, and/or degradation of the coating material.[12]

The use of CSPS in periodontal surgery (45S5 Bioglass® used commercially as PerioGlas®, see Chapter 9),[13] where tooth sensitivity is routinely found, coupled with the need for improved materials to treat tooth sensitivity, led to the initial investigations of this material for treating tooth sensitivity. CSPS surfaces form a strong attraction with collagen.[14–16] Because dentin consists of more than 50% collagen, it was believed that the CSPS particles would bind to the exposed dentin surface as well as physically fill the open tubules. It was further hypothesized that the subsequent ionic release and surface reaction would help to form a protective hydroxycarbonate apatite (HCA) layer that would impart rapid and continual relief from tooth sensitivity. The earliest studies conducted demonstrated that the material would in fact rapidly occlude dentin tubules and form a protective layer on the dentin surface.[17] To understand the details of the mechanisms of this action, it is necessary to review the combination of ionic reactions that occur in an aqueous environment as well as other factors such as pH changes and the surface changes in the particles themselves. All have a critical role in producing the protective effect of this material.

31.3. ROLE OF pH AND IONIC RELEASE

When particles of the CSPS material are exposed to an aqueous environment, such as water or saliva, there is an immediate release of sodium ions, as described in Chapter 3. The release of Na from the particle surfaces locally increases the pH which can cause a more rapid precipitation of the ions to form

the HCA layer. The immediate release of Na from the CSPS particles is necessary but not sufficient for the formation of the calcium phosphate layer. However, the rapid release of sodium allows for the release of calcium and phosphate ions from the particles within minutes of exposure to the aqueous environment by producing a porous surface layer. An amorphous calcium phosphate layer was found to form on the particle surfaces within an hour of exposure to a simple organic buffer, as discussed in Chapter 3. It is important to realize that this unique attribute of the composition of calcium sodium phosphosilicate sets it apart from all other materials that have been shown to act as physical occluding materials. The slow network dissolution of the particles is critical because the particles act as reservoirs to continuously release calcium ions and phosphate ions into the local environment, over many days in some cases.

In addition to the release of these ions, the role of soluble silica in the formation of calcium phosphate mineral is important. It is an attribute of the NovaMin® particles that they release silica into the localized oral environment at a concentration of 15–40 ppm. This is one of the critical factors in the early stages of the precipitation of an amorphous calcium phosphate phase. In order to be effective at occluding tubules, the particles must not only release the proper level of ions over time, but they must be able to remain on the dentin surface over a long period of time. There is a strong adherent interaction between the reacted surface of the particles and collagen, and this interaction is strongest for the 45S5 composition used in NovaMin®. Development of the negative surface charge at the particle surface due to the initial reactivity allows for binding to the side groups on Type I collagen fibers. Because exposed dentin has a high content of exposed collagen, this is likely to be the mechanism that allows the CSPS particles to attach to and remain on the dentin surface. Once deposited onto the dentin, the particles will continue to provide long-term release of calcium and phosphate into the local environment, leading to long-term protection of the dentinal tubules.

31.4. EVIDENCE OF EFFICACY FOR CSPS

Standard *in vitro* models are used to demonstrate the mode of action of various desensitizing agents.[18] The dentin block model has a number of variations to test the ability of materials to occlude tubules and to remain on the dentin surface through various challenges that would normally be found in the oral environment. There has been extensive testing of CSPS using a number of these models and they have repeatedly demonstrated the rapid occlusion of tubules and the persistence of the particles on the dentin surface.[18] A single application of the proper concentration (above 3%) of CSPS either in a

daily-use dentifrice or a professionally-applied prophylaxis paste is effective at blocking at least 75% of open tubules. In many cases, the single application is sufficient to block over 95% of tubules. Furthermore, a single application of CSPS in these models will resist repeated acid challenges. When tested in a model where the material is repeatedly applied and alternately subjected to twice daily acid challenges, the results demonstrate continual blockage of the dentin tubules. Additional testing has shown that the CSPS continues to release calcium ions over a long period of time, compared with other calcium-containing products that release a burst of calcium but then provide little in the way of calcium ions to protect the exposed dentin.

SEM is one of the analytical methods used to evaluate the ingredients used for tubule occlusion in treating tooth sensitivity. Figure 31.1a is an SEM image that shows a typical prepared dentin block used in the types of *in vitro* studies described above. The piece of dentin has been ground and polished, and then acid etched to remove the smear layer and to open the dentin tubules. Figure 31.1b shows a dentin block that has been treated one time with the CSPS material and subjected to a subsequent acid challenge. After the acid challenge the sample was gently rinsed and dried for SEM analysis. Note that the majority of tubules are completely closed and the remainder are at least partially closed. Particles are retained on the surface of the dentin block even after rinsing. This evidence substantiates and helps to explain the long-lasting effect of even a single use of the CSPS particles.

While *in vitro* studies are extremely useful in helping to differentiate, rank, and evaluate various materials for their effectiveness in treating tooth sensitivity,

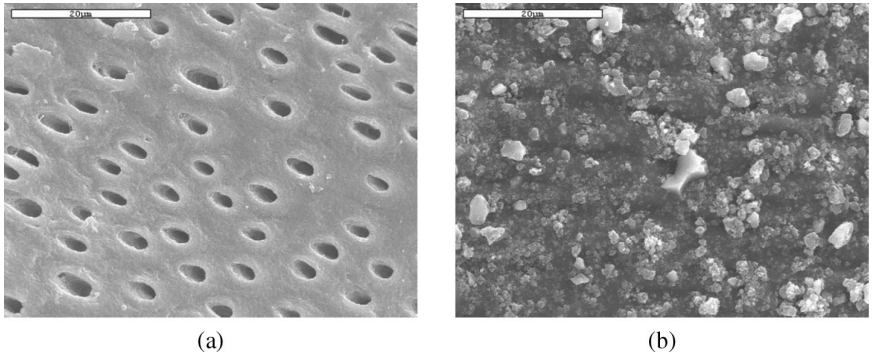

(a) (b)

Figure 31.1. SEM images from *in vitro* dentinal occlusion study showing prepared and treated dentin. (a) prepared dentin slab showing open tubules. (b) dentin after a single application of 45S% Bioglass® CSPS for two minutes and 30 second water rinse.

the clinical trial is the ultimate test for these materials. There have been a number of clinical studies performed with this material. One study compared the efficacy of a strontium chloride ingredient and a placebo to a daily-use CSPS dentifrice in reducing tooth sensitivity in a six week prospective study. The results showed that, compared to placebo, both ingredients reduced sensitivity, but the CSPS material showed statistically greater reductions in sensitivity at the six week end point compared with the other materials.[19] More recently, a review of a number of clinical studies has substantiated these early findings.[20]

31.5. COMMERCIALIZATION OF CSPS FOR TREATING TOOTH SENSITIVITY

During the past 10 years, a number of consumer and professional products containing CSPS have been introduced into the market. The first product developed by NovaMin® Technologies was Oravive®, a daily-use, fluoride-free dentifrice that contains 5% of the CSPS ingredient NovaMin®. This product was cleared for use by FDA through a 510(k) product as a medical device for the rapid and continual reduction of tooth sensitivity through physical tubule occlusion. Other products that have been introduced are listed in Table 31.1, along with a description of the product. Today, CSPS has been formulated into over 15 products and is sold in over 20 countries, including the U.S., Canada, India, China, and a number of countries in Europe. These products have proven to be highly effective and the CSPS material has an unparalleled safety profile. Sensodyne

Table 31.1. A List of Some of the Current CSPS Products Available.

Product	Description
SootheRx (U.S.)	7.5% CSPS, Daily use, professionally supplied
X-Pur (Canada)	5.0% CSPS, Daily use, professionally supplied
Nanosensitive (Germany)	7.5% CSPS
Sensishield (U.K.)	5.0% CSPS
Nutri-émail (France)	7.5% CSPS
Vantaj	5.0% CSPS
SHY-NM	5.0% CSPS
Odontis Sensiblock (Brazil)	7.5% CSPS

Repair and Protect, manufactured by GlaxoSmith Kline (GSK), is an over the counter dentifrice that provides NovaMin® technology to the consumer in many parts of the world.

31.6. CONCLUSION

Development of new applications and refinements in the manufacture and use of CSPS continues in the area of oral health care. Over the past 10 years, studies have shown that the surface activity and ionic release from specific compositions of CSPS materials have produced the most effective treatment for tooth sensitivity to date. The interactions of the material with native collagen along with the reactivity of the particles insures that the material will immediately occlude patients' dentin tubules and will remain at the dentin surface, allowing this ionic release to build a thin mineral layer that will continue to occlude the tubules and will resist challenges of acidic environments.

The science behind the development of this class of materials has led to investigations of CSPS for oral health care applications beyond the treatment of tooth sensitivity. The potential of these materials for remineralization of both enamel and dentin has been studied *in vitro* and *in situ* and holds promise.[21,22] The unique ionic reactions and potential antimicrobial[23,24] and anti-inflammatory[25] properties might prove useful in treating or even preventing gingivitis.[26]

REFERENCES

1. Rees, J.S. and Addy, M. (2002). A Cross-Sectional Study of Dentine Hypersensitivity, *J. Clin. Perodontol.*, **29**, 997–1003.
2. Irwin, C.R. and McClusker, P. (1997). Prevalence of Dentine Hypersensitivity in a General Dental Population, *K. Ir. Dent. Assoc.*, **43**, 7–9.
3. Chabanski, M.B., Gillam, D.G., Bulman, J.S. *et al.* (1996). Prevalence of Cervical Dentine Sensitivity in a Population of Patients Referred to a Specialist Periodontology Department, *J. Clin. Periodontol.*, **23**, 989–992.
4. Canadian Advisory Board on Dentin Hypersensitivity. (2003). Consensus-Based Recommendations for the Diagnosis and Management of Dentin Hypersensitivity, *J. Can. Dent. Assoc.*, **69**, 221–226.
5. Orchardson, R. and Collins, W.J. (1987). Clinical Features of Hypersensitive Teeth, *Br. Dent. J.*, **162**, 253–256.

6. Dowell, P. and Addy, M. (1983). Dentine Hypersensitivity — A Review. Aetiology, Symptoms and Theories of Pain Production, *J. Clin. Periodontol*., **10**, 341–350.
7. Brännström, M. and Astrom, A. (1972). The Hydrodynamics of the Dentine; Its Possible Relationship to Dentinal Pain, *Int. Dent. J*., **22**, 219–227.
8. Absi, E.G., Addy, M. and Adams, D. (1989). Dentine Hypersensitivity: The Development and Evaluation of a Replica Technique to Study Sensitive and Nonsensitive Cervical Dentine, *J. Clin. Periodontol*., **16**, 190–195.
9. Ishikawa, S. (1969). A Clinic-Histological Study on the Hypersensitivity of Dentine, *J. Jpn. Stomatol. Soc*., **36**, 68–88.
10. Schiff, T., Bonta, Y., Proskin, H.M. *et al.* (2000). Desensitizing Efficacy of a New Dentifrice Containing 5.0% Potassium Nitrate and 0.454% Stannous Fluoride, *Am. J. Dent*., **13**, 111–115.
11. Orchardson, R. (2006). Managing Dentin Hypersensitivity, *J. Am. Dent. Assoc.*, **137**, 990–998.
12. West, N.X., Hughes, J.A. and Addy, M. (2002). Dentine Hypersensitivity: The Effects of Brushing Toothpaste on Etched and Unetched Dentine *In Vitro*, *J. Oral. Rehabil*., **29**, 167–174.
13. Froum, S.J., Cho, S.C., Rosenberg, E. *et al.* (1998). Comparison of Bioglass® Synthetic Bone Graft Particles and Open Debridement in the Treatment of Human Periodontal Defects, *J. Perio*., **69**, 698–709.
14. Zhong, J.P., LaTorre, G.P. and Hench, L.L. (1994). "The Kinetics of Bioactive Ceramics Part Vii: Binding of Collagen to Hydroxyapatite and Bioactive Glass", in Andersson, O.H. and Yli-Urpo, A. (eds), *Bioceramics 7. Proceedings of the 7th International Symposium on Ceramics in Medicine*, Butterworth-Heinemann Ltd, Oxford, pp. 61–66.
15. Orefice, R., Hench, L.L. and Brennan, A. (2009). Evaluation of the Interaction of Collagen with the Surface of a Bioactive Glass, *J. Biomed. Mater. Res*., **90**, 114–120.
16. Efflandt, E.S., Magne, P., Douglas, W.H. *et al.* (2002). Interaction between Bioactive Glass and Human Dentin, *J Mater. Sci. Mater. Med.*, **13**, 557–565.
17. Litkowski, L.J., Hack, G.D., Sheaffer, H.B. *et al.* (1997). "Occlusion of Dentin Tubules By 45S5 Bioglass®", in Sedel, L. and Rey, C. (eds), *Bioceramics 10. Proceedings of the 10th International Symposium on Ceramics in Medicine*, Elsevier, New York, pp. 411–414.

18. Burwell, A., Jennings, D., Muscle D. *et al.* (2010). NovaMin and Dentin Hypersensitivity — *In Vitro* Evidence of Efficacy, *J. Clin. Dent.*, **21**, 66–71.
19. Du, M.Q., Bian, Z., Jiang, H. *et al.* (2008). Clinical Evaluation of a Dentifrice Containing Calcium Sodium Phosphosilicate (NovaMin) for the Treatment of Dentin Hypersensitivity, *Am. J. Dent.*, **21**, 210–214.
20. Alauddin, S.S., Greenspan, D. and Anusavice, K.J. (2005). *In Vitro* Human Enamel Remineralization Using Bioactive Glass Containing Dentifrice, *J. Dent. Res.*, **84**, 2546.
21. Litkowski, L.J., Quinlan, K.B. and Pandya, A.J. (2007). *In Situ* Comparison of Surfaces by Optical Profilometry, *J. Dent. Res.*, **86**, 1412.
22. Gendreau, L., Barlow, A.P.S. and Mason, S.C. (2011). Overview of the Clinical Evidence for the Use of NovaMin in Providing Relief from the Pain of Dentin Hypersensitivity, *J. Clin. Dent.*, **22**, 90–95.
23. Stoor, P., Soderling, E. and Salonen, J.L. (1998). Antimicrobial Effects of a Bioactive Glass Paste on Oral Microorganisms, *Acta. Odontol. Scand.*, **56**, 161–165.
24. Allan, I., Newman, H. and Wilson, M. (2001). Antibacterial Activity of Particulate Bioglass Against Supra and Subgingival Bacteria, *Biomaterials*, **22**, 1683–1687.
25. Rechtenwald, J.E., Minter, R.M., Rosenberg, J.J. *et al.* (2002). Bioglass Attenuates a Proinflammatory Response in Mouse Peritoneal Endotoxicosis, *Shock*, **17**, 135–138.
26. Tai, B.J., Jun, B., Bian, Z. *et al.* (2006). Anti-Gingivitis Effect of a Dentifrice Containing Bioactive Glass (NovaMin®) Particulate, *J. Clin. Periodontol.*, **33**, 86–91.

Chapter 32

POROUS BIOACTIVE CERAMIC AND GLASS SCAFFOLDS FOR BONE REGENERATION

Julian R. Jones

32.1. INTRODUCTION

Regenerative medicine is the future for bone repair, but in some ways it is already the present. Bone can heal itself if the defect is small, but otherwise it needs assistance. Today, annually, orthopaedic and neurological surgeons perform half a million bone graft operations in the USA and 300,000 operations in Europe. In the majority of those procedures they are treating bone defects caused by trauma, tumour removal or non-union of fractures using temporary templates that stimulate the body's own natural regenerative processes. However, the scaffold is the patient's own bone, taken from the pelvis; i.e., an autograft. Actually, it is a ready-made tissue-engineered living construct of a porous scaffold (the composite of hydroxycarbonate apatite (HCA) and collagen) containing osteoprogenitor cells and other adult stem cells.

Unfortunately, there are many drawbacks to using the patient's bone, some of which are obvious, some a little less so. The most important is that there is only so much bone you can take from places that do not really need it. The body is not wasteful in bone production. In most places in the body it is needed for bearing loads such as body weight. If bones are not loaded, the body tends to take the bone away through remodelling by osteoclast action. The pelvis is the most common site that can be a bone donor. This requires surgeons to carry out two operations to heal one defect; in fact surgeons usually work in pairs, with one operating on the pelvis and one working on the original defect. This doubles the resources needed for the operation and of course the cost. More importantly, removing bone from the pelvis creates another defect that needs to be healed (without the help of more bone). The healing of this defect is extremely painful and lengthy. Patients generally feel more pain at the donor site than at the original defect and one in four patients will experience complications at the defect site, even 12 months after the operation. Some will require further surgical intervention, which is not ideal for the patient, the healthcare service or the economy.

Artificial bone graft materials are needed to regenerate bone defects without the need for graft operations so that patients can heal in a pain-free manner and return to their normal lives more quickly, including that those still of a working age can return to work more rapidly. Bone can also be sourced from bone banks, but the bone in these banks is from cadavers and has to be irradiated to remove biologicals that would otherwise transmit disease or trigger immunorejection by the patient, and unfortunately the irradiation reduces the mechanical properties of the bone. An artificial bone graft that can replace the need for grafts would have a massive impact on the global economy. The device market itself is thought to be worth $2 billion, without taking into account the economic impact of reduced operating costs and faster recovery times. However, there are differences in the engineering design criteria for an artificial bone graft and a scaffold for bone regeneration. This is because many artificial bone grafts are designed to augment the bone and stay there for a long time rather than regenerate the bone to its original state and function. Depending on the design and the claims a company can make when marketing the materials, there are also differences in the regulatory procedures that have to be undertaken.

32.2. AN IDEAL SCAFFOLD

An ideal scaffold to regenerate a bone defect and leave no trace of an implant must possess the following characteristics:[1]

1. Be biocompatible and bioactive, promoting osteogenic cell attachment, bone formation and bond to the bone without scar tissue sealing it off from the body.
2. Act as a template for bone growth and therefore have an interconnected porous structure that can allow bone in-growth and vascularisation.
3. Resorb safely in the body and have a controllable degradation rate.
4. Exhibit mechanical properties similar to that of the host bone.
5. Have a fabrication process which allows the scaffold to be shaped to fit a range of defect geometries and be up-scalable for mass-production.
6. Be sterilisable and meet the regulatory requirements for clinical use.

Current products are far from this ideality. Bone defect fillers need not be scaffolds; particles and granules are often preferred by orthopaedic surgeons for their ease of handling. If the material is designed to augment bone for long periods it should not degrade but can be remodelled by osteoclasts, which will take many

months or perhaps even years. Currently there are no tissue engineering constructs available as commercial products, largely due to the amount of time and investment needed to take the products to market. Surgeons are very aware of the potential benefits of tissue engineering strategies, such as the fact that osteoprogenitor cells cultured on a template would enhance bone production rate, so they do what they can by aspirating blood and bone marrow from within the bone defect and its surroundings. They then mix the blood and marrow with synthetic bone graft particles or granules to form a putty-like mixture that can be press-fitted into bone defects. The aim is that the putty can be easily handled and the blood and bone marrow may contain osteoprogenitor cells that will activate when reimplanted.

32.3. COMMERCIALLY AVAILABLE SYNTHETIC BONE GRAFTS

There are numerous synthetic bone graft materials available as commercial products, but none that fulfil all the criteria listed above. Bioceramics are usually chosen because they can be bioactive but they are brittle materials. Some porous metallic constructs are available (e.g., titanium alloys), but they are not bioactive or degradable. Polymers can be tough but they have poor compressive strength and polymers are not bioactive unless expensive biological growth factors are incorporated; thus, there are no polymeric synthetic bone grafts. Composites would provide a combination of bioactivity and compressive strength from bioceramics and toughness from biodegradable polymers; however, it is difficult to synthesise composites in such a way that the bioceramics are not masked by the polymer. Consequently, most commercial bone graft substitutes are bioactive ceramics.

32.3.1. Commercial Bioactive Glasses

Chapter 3 shows that 45S5 Bioglass® has considerable use in bone regeneration because it is arguably the most bioactive material,[2] bonding to bone rapidly and stimulating bone growth by its dissolution products. However, there are relatively few clinical products based on this material. What are the reasons? Some are related to business and marketing, others due to scientific reasons. Considering the scientific reasons, all the processing techniques for making porous scaffolds from particles involve sintering. Sintering is the fusion of particles at high temperature. (See Chapter 1 for more details.) Raising the temperature above the glass transition temperature (T_g) causes local flow of the glass and

allows particles to fuse. However, to maintain the amorphous glass structure and properties, the temperature must not be heated above the crystallisation temperature ($T_{c\ onset}$). Unfortunately for the original Bioglass® composition (46.1% SiO_2, 24.4% Na_2O, 26.9% CaO and 2.6% P_2O_5, in mol %), the low silica content causes T_g and $T_{c\ onset}$ to be too close together, so it is not possible to sinter the glass without crystallising, which leads to formation of a glass-ceramic and reduction in bioactivity.

Therefore, Bioglass® particles are only available commercially as PerioGlas® and NovaBone®, from NovaBone Products LLC (Alachua, FL). PerioGlas® are particles used for filling bone defects in the jaw following periodontal disease, and NovaBone® is an orthopaedic bone defect filler. The particle size range is 90–710 μm. Biogran®, also made of Bioglass® granules, was marketed by Orthovita Corp. Finer (<15 μm) particles are marketed under the name NovaMin® (GlaxoSmithKline, UK) for use in toothpaste to promote mineralisation of microtubules in enamel, with the aim of reducing tooth sensitivity.

Other slight variations on the Bioglass® composition have been released as commercial products, such as BonAlive® (SiO_2 53 wt%, Na_2O 23%, CaO 20%, P_2O_5 4%) by Vivoxid® (Finland) and StronBone® (44.47 mol% SiO_2, 27.26% Na_2O, 21.47% CaO, 2.39% SrO, 4.42% P_2O_5) by RepRegen (UK), which has recently received its CE mark, allowing it to be sold as a bone defect filler in Europe. The potential advantage of StronBone® is the inclusion of small amounts of strontium, which is thought to help fight osteoporosis.

32.3.2. Porous Commercial Synthetic Hydroxyapatites

As bone mineral is a hydroxyapatite (HA), an obvious choice of material for a synthetic bone graft is a synthetically produced apatite. Many synthetic bone grafts are made from synthetic hydroxyapatite (sHA), chemical formula $Ca_{10}(PO_4)_6OH_2$. However, bone mineral is a carbonated hydroxyapatite (CHA), approximated by $(Ca,X)_{10}(PO_4,HPO_4,CO_3)_6(OH,Y)_2$, where X is a cation, either a magnesium, sodium or strontium ion that can substitute for the calcium ions, and Y is an anion (a chloride or fluoride ion) that can substitute for the hydroxyl group.[3]

Conventional sHA is produced by creating an HA powder by solution chemistry, which is sintered. It is a crystalline ceramic and stoichiometric HA (Ca/P ratio of 1.67) is commonly produced by precipitation by reacting calcium hydroxide with orthophosphoric acid solution (at pH >9) at temperatures of between 25 and 90°C.[4] sHA was first used clinically in 1978, when dense sintered HA cylinders were used as immediate dental root implants after tooth extraction.[5]

Several methods have been used to produce porous sHA. The simplest way to generate porous scaffolds from ceramics such as HA is to sinter spherical particles. Porosity is often increased by adding sacrificial porogens, which are often particles that will be removed after compaction or during sintering. The sacrificial particles can either be soluble, e.g., salt or sucrose,[6] or combustible, e.g., PMMA microbeads. However, these methods give rise to a heterogeneous pore distribution and the interconnectivity of the pores is low. To improve interconnectivity, open-celled polyurethane foams can be immersed in slurries of sHA. The foams are then heated at 250°C to burn out the organic components (pyrolysis) and sintered at 1,350°C for 3 hours, producing a scaffold with 300 µm interconnected pore diameters.[7] This method is successful, but leaves the foam struts hollow and is difficult to upscale for mass production.

A successful porous sHA product, ApaPore® (Apatech Ltd., Elstree, UK), is a porous HA that has an interconnected macroporosity and some microporosity. It has been successfully used in impaction grafting for the cemented revision of failed total joint arthroplasties, spinal fusions and bone defect treatment. Although Apatech have not disclosed how they produce their product, its morphology indicates that it is made by a process similar to the gel-cast foaming process, which has been the most successful published method for producing an interconnected porous ceramic.[8] In the gel-cast foaming process, suspensions of sHA particles and organic monomers are foamed with the aid of a surfactant (Fig. 32.1).

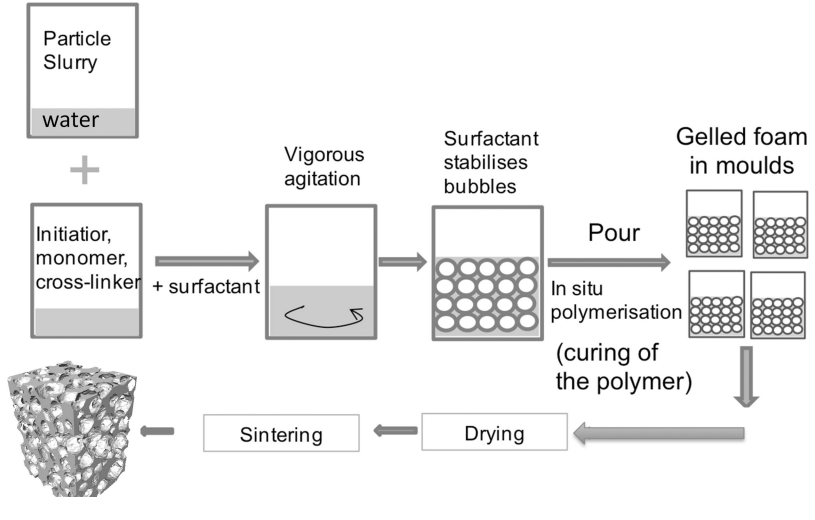

Figure 32.1. Schematic of the gel-cast foaming process.

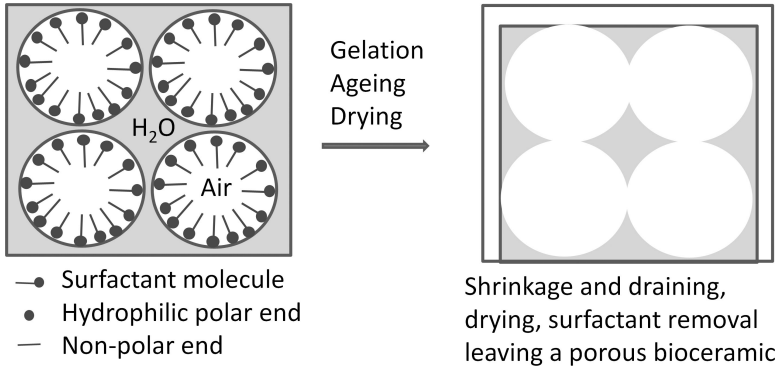

Figure 32.2. Schematic showing how surfactants stabilise air bubbles in agitated water.

The surfactant is critical to obtaining an interconnected pore network. It works by reducing surface tension, which stabilises bubbles that form by air entrapment. The slurry is typically expanded to three or four times the initial slurry volume. Using *in situ* polymerisation of monomers, the porous network sets. The increase in viscosity during the gelation process also helps to stabilise the bubbles. Figure 32.2 shows how the surfactant works. They are "surface active agents" and are molecules with a hydrophilic end and a hydrophobic end. When surfactants are added to water, they lower the surface tension because the hydrophilic end of the molecule affiliates itself with the water; the hydrophobic end is in the air. The surfactant must be of suitable type and be homogeneously dispersed to obtain spherical pores. To obtain an interconnected pore network, the bubbles must be large and touching each other in the solution until gelation. On gelation, the surfactant films must rupture, opening up interconnecting channels between the bubbles, which now become the pores. The surfactant and polymer are then removed by a sintering process, which also fuses the ceramic particles together and provides strength. As the particles are bound together in a polymer matrix, rather than coating a polymer foam, the struts of the gel-cast foam are not hollow, which improves their strength when compared to polymer foam replicates.

Hi-Por Ceramics Ltd. (Sheffield, UK) market a foamed competitor, and Ossatura™ (Isotis Orthobiologics, USA) is a granular macroporous (75%) material composed of approximately 80% sHA and 20% β-TCP (tricalcium phosphate). TCP undergoes dissolution in aqueous solutions and therefore is incorporated in the product so that it will degrade more rapidly than the HA, leaving pores for bone to grow into.

Very popular HA bone graft materials have also been derived from special species of corals (Porites)[9] and from bovine bone.[10] These can contain some of the minor and trace elements originally present in the coral or in the bone. Bio-Oss® (Osteohealth, Shirley, New York) is a porous bovine bone.[10] Osteograf-N™ (CeraMed Co, Denver, CO) and Endobon™ (Merck Co, Darmstadt, Germany) are sintered materials.

Porous coralline HA is sold as Interpore™ and Pro-Osteon™[9], which are manufactured by Interpore International, Inc., Irvine, CA. HA grafts derived from coral, or coralline HA, are prepared by hydrothermal conversion of coral, which is primarily $CaCO_3$, at 260°C and 15,000 psi in the presence of ammonium phosphate.[9] A secondary phase of β-tricalcium phosphate (β-TCP) also forms during the hydrothermal conversion. The main problem with corralline-derived HA is sourcing the coral template, as only particular types of coral have a suitable structure.

Bovine-derived apatites are produced by the removal of the organic matrix. The resulting material is then either left unsintered or sintered above 1,000°C. The unsintered bone mineral consists of small crystals of HCA, whereas the sintered bone mineral consists of much larger apatite crystals without CO_3.[3] Coralline HA contains traces of Mg, Sr, CO_3 and F. Bovine bone-derived apatite contains Mg, Na and CO_3.[3] The advantage of these materials is that they have an interconnected macroporous network that is conserved from the coral and bone, without the need for porogens or foaming processes. A disadvantage is the lack of supply of the coral and ethical and environmental issues regarding coral harvesting.

Although sHA has excellent biocompatibility and osteoconductivity, it does not resorb in the body and therefore will not fulfil the criteria of an ideal tissue scaffold. Consequently, it is not an ideal material for regenerative medicine applications, but is an excellent material for use as a permanent bone defect filler or permanent grafting material (bone substitute).

The rate of dissolution of HA materials depends on porosity and crystallinity.[11] Although stoichiometric sHA has very low degradation rates, degradation can be increased by substituting in other components that are found in biological apatites. The type and extent of substitution affects the rate of dissolution. Bone has 5–8 wt% CO_3^{2-} and carbonate substitution (nominally for PO_4) that contributes to the most soluble apatite (HCA)[12], however, F substitution (for OH) decreases the solubility to lower than sHA. Higher dissolution also leads to higher bioactivity.

Synthetic carbonated apatite (HCA) is synthesised by adding calcium nitrate into the solution reaction and sintering in a CO_2 atmosphere to prevent carbonate loss.[13,14] However, Apatech decided to opt for silicon-substituted

(nominally for PO_4) apatite.[15] The concept of using Si is based upon the composition of bioactive glasses that are more osteogenic than apatites and the main difference is that bioactive glasses release soluble silica, as discussed in Chapter 3. Very small amounts of Si were introduced into the HA composition. Cell culture tests, using human bone cells, and *in vivo* tests in rabbits indicated that 0.8 wt% Si produced the best quality bone (see Chapter 18).[16,17]

The improved bioactivity of the Si-HA compared to sHA is likely to be due to a combination of the Si-producing defects (more grain boundaries and smaller grains) in the crystal structure, increasing the dissolution rate of the HA and the release of soluble silica. Small structural differences were observed between sHA and Si-HA, with Si-HA having a unit cell with a shorter a axis and larger c axis and a lower number of OH groups. The incorporation of silicon in the HA lattice also caused an increase in the distortion of the PO_4 tetrahedra. Si-HA is marketed as various products under the name Actifuse®, which is now a market leader as a synthetic graft for spinal fusion operations. It is a granular material that the surgeons tend to mix with blood and insert into titanium alloy or polyether-ether-ketone (PEEK) cages, which are used to replace herniated intervertebral discs. The Actifuse® actively fuses the vertebrae together in an operation that would commonly use bone from the pelvis or bone spurs harvested from other regions of the spine. It is 80% porous Si-HA (0.8 wt%), produced by a similar method as their ApaPore® product, where a cage or screw fixation device is used to relieve the graft site from physiological loads. It is applied as a granular structure that is combined with localised blood or with blood marrow aspirate, in a ratio of 1–1.5:1 (blood/BMA to Actifuse®) to allow for optimal handling and placement.

The limitation with all these materials is that they cannot be used in load-bearing applications because of their low fracture strength.[12]

32.4. POROUS BIOACTIVE GLASSES

In terms of commercial products, bioactive glass is lagging behind apatites somewhat. However, they still have the potential to outperform all the commercial products currently available. The delay in the development of bioactive glass scaffolds has been due to the fact that the commercially available (and FDA approved) composition (Bioglass®) cannot be made into porous scaffolds without it crystallising. However, NovaBone Products now has a porous 45S5 Bioglass® product in the market that has a minimal amount of crystallisation. There are two options for creating amorphous porous glasses: change the composition so as to

create a melt-derived bioactive glass that can be sintered and ensure the new composition is still bioactive; or make the glass by an alternative route.

There are two processing routes to produce bioactive glasses: the traditional melt-derived approach and the sol-gel process, each yielding very different glasses.

32.4.1. New Melt-Derived Glasses

Bioglass® cannot be made into scaffolds or even easily drawn into fibres without it crystallising, because of its random 2D amorphous structure. It has less than 50% silica content so that the silica network is disrupted enough to be degradable in aqueous solutions (i.e., body fluid). This means it must have greater than 50% of its other components, the majority of which are calcia (CaO) and soda (Na_2O), which act as network modifiers. This composition means that Bioglass® has a network connectivity (the number of bridging oxygen bonds, -Si-O-Si-, bonds per silicon atom) of two. If the network connectivity increases above 2.4, bioactivity is significantly reduced, which is why bioactivity is lost in melt-derived glasses that have silica content greater than 60 mol% (see Chapter 3).

Recently, new compositions have been devised that do not crystallise on drawing and sintering. One is 13–93 (54.6 mol% SiO_2, 6% Na_2O, 22.1% CaO, 1.7% P_2O_5, 7.9% K_2O, 7.7% MgO), which was developed in Finland. Porous scaffolds have been produced, using the polymer foam replication technique,[18] but this composition takes seven days to form an HCA layer in simulated body fluid tests. In contrast, 45S5 Bioglass® particles formed the same layer within eight hours in the same test. This is because the network connectivity is higher in glass composition 13–93 compared to 45S5 Bioglass®, due to the increased silica content.

In order to obtain a similar result without compromising bioactivity, ICIE16 (49.46% SiO_2, 36.27% CaO, 6.6% Na_2O, 1.07% P_2O_5 and 6.6% K_2O, in mol%) was developed by Elgayar *et al.*[19] Also, to improve on the pore morphology, the gel-cast foaming process that was used so successfully on HA ceramics was adapted to produce porous bioactive glass scaffolds (Fig. 32.1).

Fine particles (<38 μm) in an aqueous slurry were foamed under vigorous agitation. During the *in situ* polymerisation, the viscosity increased until a gel (a solid covalent network containing water) forms. Just prior to gelation, the foam is poured into a mould. The pouring window is short: too early and the foam cannot hold its weight and will collapse, too late and it will gel in the foaming vessel. After gelation, the foam is a composite of glass particles within the newly formed polymer matrix (Fig. 32.3).

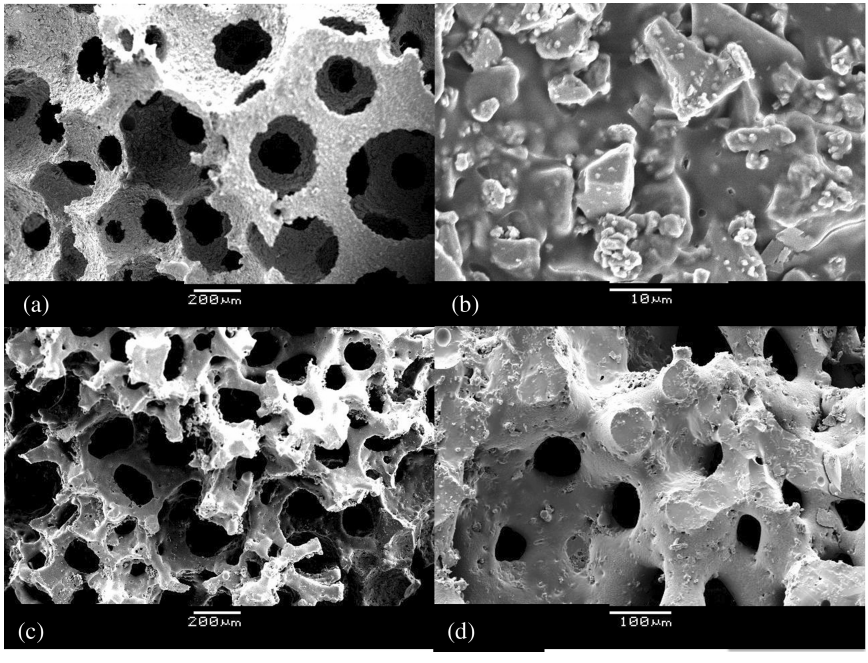

Figure 32.3. Scanning electron microscope images from the gel-cast foaming process of a bioactive glass: (a, b) immediately after foaming (a) low and (b) high magnification showing gelation glass particles dispersed in a polymer foam; (c, d) after drying, polymer removal and sintering at (c) low magnification, showing the pore network, and (d) higher magnification, showing that the particles have fused together well during sintering. More detail can be found in Wu *et al.* (2011). *Acta Biomater*., 7, 1807–1816.

To make the porous glass, the surfactant and polymer are removed. The composite is usually held at around 300°C to remove the polymer. At this point, the particles are effectively balancing on each other in the shape of a foam. As the temperature increases above T_g the particles sinter together. The sintering temperature depends on the sintering window of the glass composition being used, but is usually around 700°C. The scaffolds have large interconnecting pores (Fig. 32.3). The smooth surface of the struts indicate that sintering was completed efficiently. One disadvantage of this process is that there are many variables, which makes upscaling a challenge. The amount of glass loading particle size is also important; small particles sinter more easily as they have a higher surface area, surfactant concentration and thermal processing parameters. All are critical for a strong foam.

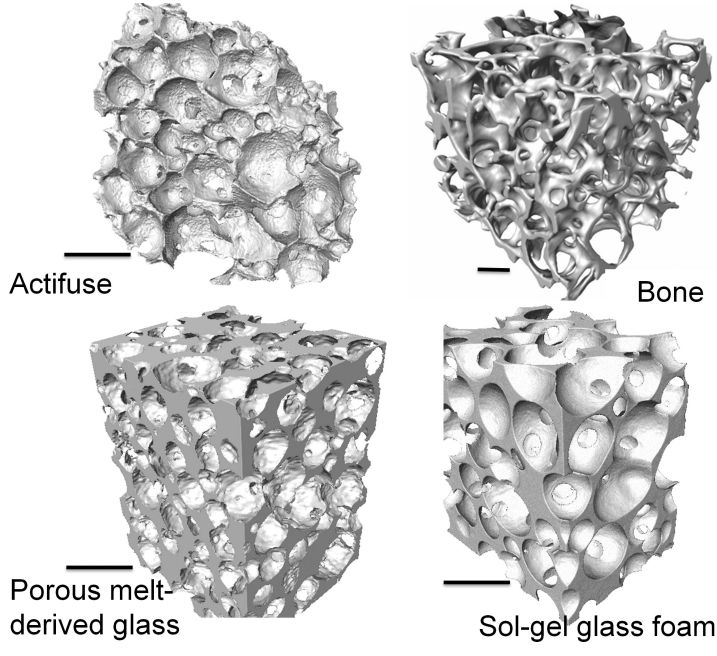

Figure 32.4. X-ray microtomography images of: Actifuse®, cancellous bone and bioactive glass foams (melt-derived and sol-gel derived). Scale bars are 500 μm.

Another challenge is that for a surfactant to operate, water must be present, hence the need for the slurry to be water-based. This means that the glass will start to react with the water. Although the amount of time the glass is exposed to the water is short, it can trigger crystallisation of the glass to occur at a lower temperature. Gel-cast foam glass scaffolds have been made with 60% porosity, interconnect sizes in excess of 100 μm and compressive strengths greater than 15 MPa, which is at the upper end of that of cancellous bone.

Before sinterable melt-derived glass compositions were developed, the sol-gel process was used to produce porous glass scaffolds. Figure 32.4 shows 3D images comparing the pore networks of Actifuse®, cancellous human bone, gel-cast foam and sol-gel foam bioactive glass scaffolds. All have similar interconnected pore networks. Other techniques struggle to create porous scaffolds that mimic the structure of cancellous bone so closely while obtaining compressive strengths that also match the bone.

Recent developments in rapid prototyping have allowed the development of higher strength (>150 MPa) porous melt-derived glasses. The strength is a result of

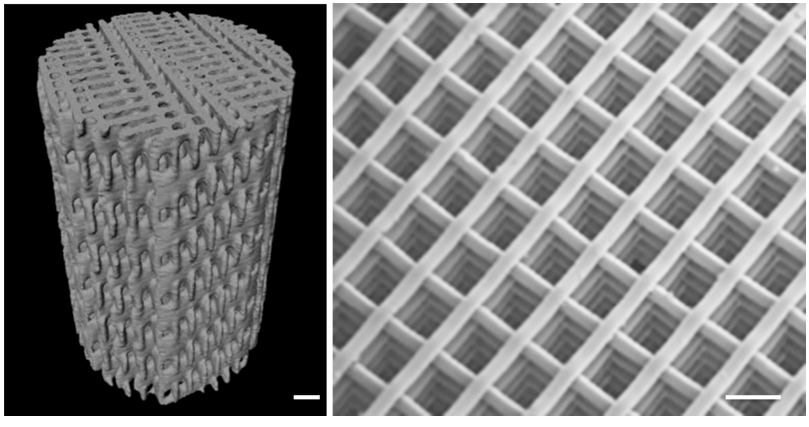

Figure 32.5. Bioactive glass scaffolds produced by the robocasting rapid prototype method. X-ray microtomography image (left) and SEM image (right) (courtesy of E. Saiz and Q. Fu. Further information in *Adv. Funct. Mater*., 2011, **21**, 10581063).

alignment of thick glass struts (>50 μm) in the scaffold. This is similar to the strength of cortical bone. Rapid prototyping techniques can build objects in almost any net shape, by depositing material layer by layer. The method is often also known as solid freeform fabrication. The advantage over foaming is that the scaffold structure is dictated by computer aided design files (CAD). The CAD file could even be generated from a CAT scan of a tissue, allowing complete replication of the structure of a tissue. Bioactive glass scaffolds are produced by a printing process called robocasting. Pores were in excess of 500 μm (Fig. 32.5) and porosity was 60%. The glass composition used was 6P53B (51.9 SiO_2, 9.8 Na_2O, 1.8 K_2O, 15.0 MgO, 19.0 CaO, 2.5 P_2O_5, in mol%). Inks were made by mixing 30 vol% glass particles in 20 wt% Pluronic® F-127 solution. Glass scaffolds were fabricated by extruding the inks through a 100 μm syringe nozzle using a robotic deposition device. The inks were printed on an alumina substrate in a reservoir of non-wetting oil. The scaffolds were air-dried for 24 hours and subjected to a controlled-heat treatment to decompose the organics and sinter the glass particles (700°C).

32.4.2. Sol-Gel Derived Bioactive Glasses

For a melt-derived glass to bond to bone, the silica content has to be 60 mol% or lower. However, HCA layer formation and bone bonding can be achieved for glasses with up to 90 mol% silica if the glass is sol-gel derived.[20] This is because

sol-gel glasses have a lower network connectivity than their nominal composition suggests. This is due to OH being incorporated into the silica network during the process and because sol-gel glasses have an inherent nanoscale porosity, which increases their specific surface area (>100 m^2g^{-1} compared to 2 m^2g^{-1}) for melt-derived glasses, and thereby increases their bioactivity and degradation rate.[21]

The first sol-gel derived bioactive glasses were developed in the early 1990s.[20,21] The 58S (60 mol% SiO_2, 36 mol% CaO and 4 mol% P_2O_5) composition was found to form the HCA surface layer more rapidly than similar compositions of melt-derived glass.[23]

The sol-gel process involves the hydrolysis of alkoxide precursors to create a sol, see Chapter 1. In the case of silicate-based bioactive glasses, the silicate precursor would be an alkoxide such as tetra-ethyl orthosilicate (TEOS) or similar. If other components apart from silica are required in the glass composition they are added to the sol either as other alkoxides or as salts. In the case of 58S, phosphate is incorporated by adding tri-ethyl phosphate (TEP) and calcium by adding nitrate tetra-hydrate. The sol can be considered as a solution of silica species that can undergo polycondensation to form silica nanoparticles which then coalesce during gelation. Water and ethanol are byproducts of the condensation reaction, which must be evaporated by using carefully controlled low heating rates. The final step is to heat the dried gel to at least 600°C in order to remove the nitrates from the calcium nitrate. During the thermal processing, the coalesced nanoparticles sinter together, leaving interstitial nanoporosity. The nanopores are usually in the range of 1–30 nm diameter and can be tailored during processing by controlling the pH of the catalyst,[24] the nominal composition[25] and the final temperature. It is, however, difficult to produce large crack-free monoliths (greater than 10 mm thickness), because the driving off of water, organics and nitrates cause capillary stresses that cause cracking.

Although sol-gel glasses can degrade more rapidly and be more bioactive than the melt-derived glasses, perhaps the biggest benefit of using the sol-gel route over melt-derived is that porous scaffolds with interconnected macropores suitable for tissue engineering applications can be easily produced by introducing a foaming step.[26] The sol-gel foaming process has some similarities to the gel cast foaming process, in that a surfactant is added and the sol is foamed by vigorous agitation as the viscosity rapidly increases (Fig. 32.6). However, in the sol-gel process, no polymer is added to gel the system as the sol gels spontaneously. On gelation, the spherical bubbles become permanent in the gel and as drainage occurs in the foam struts, the gel shrinks and the bubbles merge and interconnects open up at the point of contact between neighbouring bubbles.

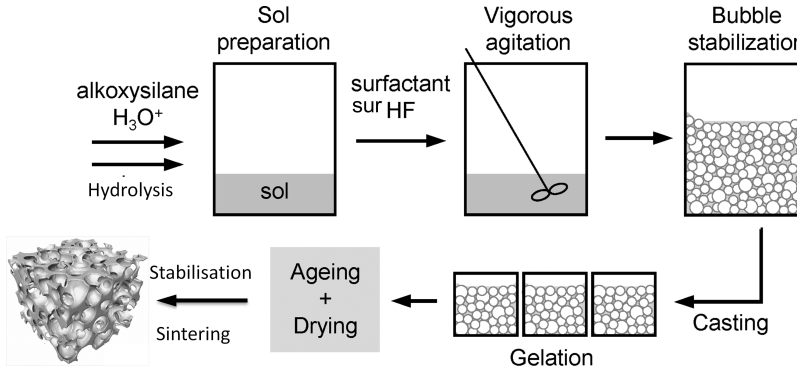

Figure 32.6. Schematic of the sol-gel foaming process.

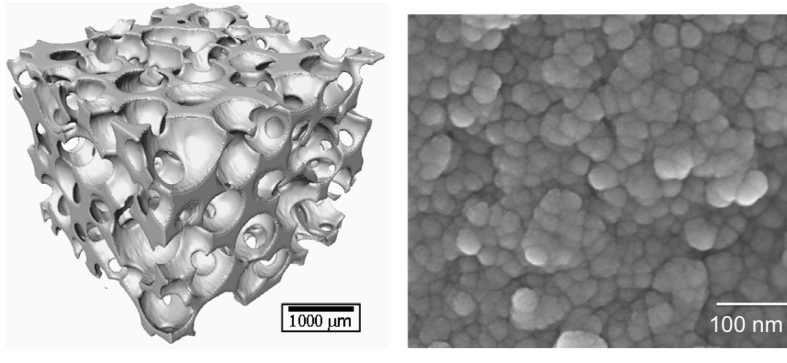

(a) (b)

Figure 32.7. Sol-gel foam bioactive glass scaffolds. (a) X-ray microtomography image of the macroporosity (reprinted with permission from Jones *et al.* (2007). *Biomaterials,* 28, 1404–1413); (b) electron microscopy image of the nanoporosity.

The sol-gel foam scaffolds have a hierarchical structure of interconnected macropores (Fig. 32.7a and Fig. 32.4), which mimic the porous structure of cancellous bone and allow the scaffold to act as a 3D template for tissue growth, and a nanoporous porosity that allows control of degradation (Fig. 32.7b). Cell response studies on the bioactive glass foam scaffolds have found that primary human osteoblasts lay down mineralised immature bone tissue, without additional signalling species. This occurred in scaffolds of both the 58S composition[27] and the 70S30C composition,[28] which showed that phosphate is not required in

the glass composition for bone matrix production and mineralisation to occur. Compressive strengths of 2.4 MPa have been obtained while maintaining modal interconnect diameters above 100 μm.[1] Strength values are similar to those of clinically used porous HA.[10] Although their compressive strength may be suitable, bioactive scaffolds suffer similar problems to sHA for brittleness.

32.5. GLASS-CERAMICS

The first attempt to improve toughness of glasses and ceramics was with a third class of materials that is in widespread use in Japan: glass-ceramics, particularly the apatite-wollastonite glass-ceramics that originated from Bioglass®. Glass-ceramics are polycrystalline materials produced by heating a parent glass above its crystallisation temperature. The most successful glass-ceramic has been A/W (apatite/wollastonite) bioactive glass-ceramic. It has a very fine-grained apatite (A) and wollastonite (W=$CaSiO_3$) crystals bonded by a bioactive glass interface produced by hot-pressing powders together.[29] Mechanical strength, toughness and stability of A/W glass-ceramics (AW-GC) in physiological environments are excellent and bone bonds to A/W-GC implants with high interfacial bond strengths. The bioactivity of this glass-ceramic was attributed to apatite formation on its surface in the body, brought about by the dissolution of calcium and silicate ions from the glass ceramic.[30] The AW-GC material was approved for orthopaedic applications in Japan with particular success in vertebral replacement and spinal repair.[31] It showed bioactivity and a high compressive strength (80 MPa). It is used clinically as artificial vertebrae and in iliac crest reconstruction. Bioactive glass-ceramics are reviewed in detail in Kokubo.[30] No A/W scaffolds have been developed.

32.6. THE FUTURE: BIOACTIVE NANOCOMPOSITES AND HYBRIDS

As no bioceramic or biopolymer fulfils all of the criteria for an ideal scaffold listed above, new materials must be developed. There have been several attempts to combine bioactive glasses with biodegradable polymers to create a scaffold material with degradability, bioactivity and toughness. These attempts commonly used biodegradable polymers that are already approved for clinical use for some applications, such as the polyesters poly(lactides) or poly(glycolides) (and their co-polymers). Composite scaffolds with interconnected pore networks have been produced by incorporating bioactive glass particles into polylactide

foams. However, their application in bone regeneration is flawed, as the bioactive particles are generally covered by the polymer matrix. The host bone will therefore not come into contact with the glass. This may be rectified as the polymer phase begins to degrade and the glass is exposed. However, it is not as simple as that due to how the polymer degrades. Polyesters degrade by hydrolysis (chain scission by reaction with water). Initially, degradation is slow and depends on rate of water uptake (diffusion) into the polymer. Once the chain scission begins, molecular weight will decrease. The pH will then drop locally due to the acidic degradation products (e.g., lactic or glycolic acid), which will catalyse the degradation process (self catalysis). This will make the degradation rate extremely rapid, causing the scaffold to breakdown and rapidly lose mechanical strength, possibly leaving the defect unhealed. The autocatalysis can even cause thicker sections of polymer to degrade faster than thin sections. Co-polymerisation of poly(lactides) with poly(glycolides) can help tailor the degradation rate of the polymers, but the degradation rate will not be linear. Nanoscale composites may allow a closer relationship between the glass and the polymer and overcome this problem.

The aim of creating nanocomposites is to have a nanoscale interaction between the bioactive inorganic phase and the organic phase, creating a tough material. This intimate interaction should allow bone cells to come into contact with both phases at one time, and the material should degrade congruently, in a more linear fashion than conventional polyesters or their composites. Nanocomposites are a nanoscale version of a conventional composite, where nanoparticles are dispersed in a polymer matrix. Alternatives are hybrids, where the inorganic and organic phases are indistinguishable above the submicron scale.[32] As the sol-gel process is initially a room temperature process, soluble polymers can be incorporated into the sol so that the polymer network is incorporated as the silica network forms. This nanoscale interaction can produce unique properties.

When covalent bonds are formed between the components, it is possible to achieve fine control of degradation rate and mechanical properties (a class II hybrid; Fig. 32.8). These materials are termed *hybrids* herein but certain types have also been called ceramers and ormosils, and have the greatest potential to combine the desired properties of the constituent materials for bone regeneration.

The sol-gel foaming process, yielding ideal pore networks for bioactive glass scaffolds, can also be applied to a hybrid sol to produce a hybrid foam (Fig. 32.9).

However, there are complex chemical challenges associated with this procedure, including which polymer to use and how to incorporate calcium. Traditionally, calcium nitrate has been used as a precursor and donator of calcium

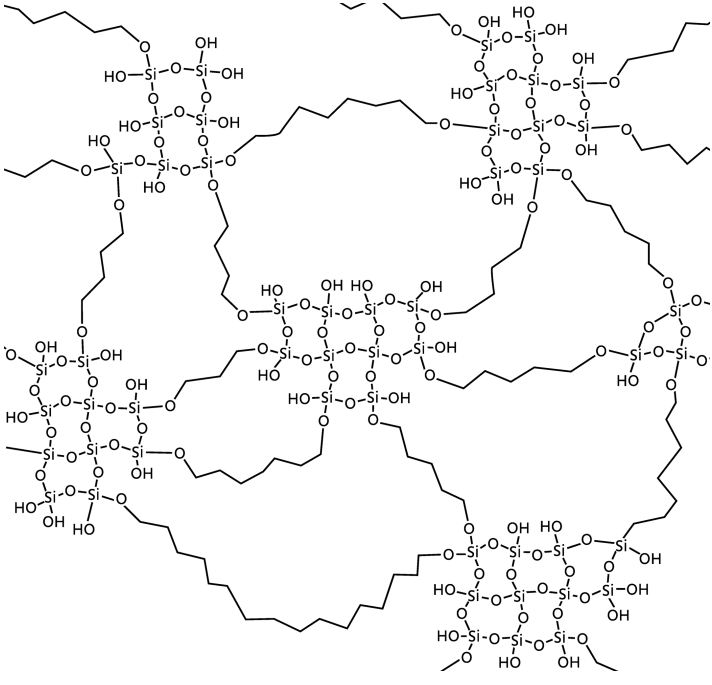

Figure 32.8. Schematic of a hybrid material (2D representation; courtesy of Esther Valliant, Imperial College London).

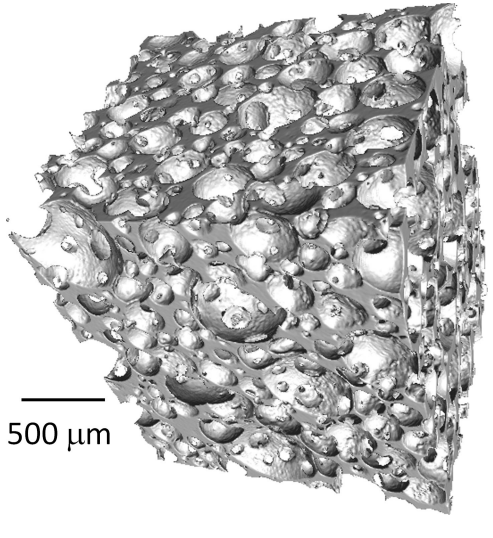

Figure 32.9. 3D X-ray microtomography image of a sol-gel foam hybrid.

into the inorganic network. However, temperatures of at least 600°C are needed to drive off the nitrate byproducts that are toxic to cells. The temperature must also reach 450°C before calcium nitrate dissociates and calcium is incorporated into the network.[21] Hybrids cannot be heated to high temperatures, as the polymer will be damaged. Therefore another calcium precursor is needed. The best method for introducing calcium is yet to be found.

Many bioresorbable polymers, e.g., poly(lactides), cannot be simply introduced into the sol, as they are not soluble in the sol. Bioactive glass/poly (vinyl alcohol) (PVA) hybrid scaffolds were produced using the sol-gel foaming technique. PVA was chosen because it is soluble in water and could be added to a typical sol used to synthesise bioactive glass. The scaffolds produced had pore networks very similar to the bioactive glass foams with macropore diameters of up to 500 μm. Compression testing on these foams demonstrated that polymer addition increased with strain to failure of up to 8% strain, compared to ~1% without the polymer added. A problem with the silica/PVA nanocomposites is that the PVA was not covalently bonded to the inorganic phase; therefore the scaffold is likely to breakup quite rapidly in body fluid.

Although conventional polyesters are insoluble in water, they can be functionalised so that not only are they incorporated in the sol-gel process, they can also form covalent bonds with the silica network, creating a true hybrid material. The functionalisation of the polymer involves the introduction of coupling agents.

One example is silica/poly (ε-caprolactone) (PCL) hybrids.[34] Hydroxyl groups at either end of poly (ε-caprolactone diol) polymer chains can be reacted with 3-isocyanatopropyl tri-ethoxysilane (IPTS). This process results in a polymer end capped with a tri-ethoxysilyl group. When the end capped with PCL is introduced into a sol the siloxane groups hydrolyse and then Si-OH groups from the end-capped polymer condense with the Si-OH groups from the hydrolysed TEOS in the sol to yield an interconnected PCL-silica network. The Young's modulus and tensile strength of the bioactive glass/PCL hybrid with 60 wt% polymer were 600 and 200 MPa, respectively, which is in the range of cancellous bone. However, the mechanical properties were measured on dense materials and would be dramatically lower if the materials were processed into porous scaffolds. The molecular weight of the PCL was low, at 6,693, indicating that long-term mechanical properties and stability in body fluid may also be low. Polymer chains must entangle with each other if the material is to have toughness, and the molecular weight should be two orders of magnitude higher for entanglement to happen. Polymers that can be functionalised using side groups of the chain rather than end-capping would therefore be preferable.

Alternatives to conventional polyesters are natural polymers. A popular strategy is to try to mimic the structure of bone as closely as possible, as its mechanical properties are superior to any biomedical composite produced to date. Reasons for bone's superior properties are that it has a hierarchical structure and is a nanocomposite containing collagen, which itself is a triple helix of polypeptides (amino acid chains). Collagen is a structural protein with a triple helix structure of collagen analogous to that of a rope and gives it excellent mechanical strength.

Collagen would therefore be an ideal choice to use as a natural polymer in hybrid synthesis. Unfortunately the triple helix structure that gives collagen its properties makes it very insoluble. It will dissolve in acetic acid, but only in very low concentrations. Therefore it is not possible to produce a hybrid with significant amounts of polymer using collagen, so it would remain brittle. There is also the dilemma of where to source the collagen. Currently, it cannot be synthesised in any significant quantity so it must be sourced from animals. Although collagen is unlikely to be rejected by a patient's body, because the amino acid structure of collagen is similar for most species and therefore cannot be detected as foreign, patients may refuse an implant on religious or moral grounds, due to the animal species it originates from, e.g., bovine or porcine.

Natural polymers can also be functionalised. Gelatin has great potential as it is hydrolysed collagen and when collagen is dissolved in acetic acid, it denatures. The benefit of gelatin is that it is water-soluble. It also contains COOH (carboxylic acid), NH and NH_2 groups along its backbone that are available for functionalisation. A similar process to that used for the PCL-diol is used, except that glycidoxypropyl tri-methoxysilane (GPTMS) is used as the coupling agent.[35] The glycidol group (epoxy ring) can open and react with the functional groups on the polymer chain, depending on the pH conditions. The functionalised polymer has short molecules bonded to it with Si-OH groups on the end of them, ready to undergo condensation with other Si-OH groups from the silica in the sol to form Si-O-Si bonds. Hybrids have also been produced with poly-γ-glutamic acid (γ-PGA), which is a much simpler polypeptide than gelatin.[36] γ-PGA is synthesised by a biotechnology route, i.e., produced by bacteria.

Another popular natural polymer is chitosan (2-amino-2-deoxy-2-Ducan), which is a polysaccharide derived from crustacean shells.[37] The chitosan is reacted with methanesulphonic acid to form butyrylchitosan, which is then reacted with acryloxypropyl tri-methoxysilane (APTMS) to form a silanated butyrylchitosan, which was then introduced into a sol of hydrolysed TEOS.

The covalent coupling of polymers to the bioactive silica is necessary to be able to control the degradation or dissolution of the hybrids, especially if the

polymers are water soluble. However, careful control of the chemistry should allow complete control of degradation rate and the mechanical properties. The future may well be the use of human recombinant proteins, but much development is needed to increase their yields.

32.7. REGULATORY ISSUES

Once a promising new scaffold material has been developed and tested in the laboratory with cell culture tests and long-term mechanical tests as a function of degradation, it is time to translate the work from the bench to the bedside. This is not a trivial (or inexpensive) process. It takes considerable time and investment. Difficult decisions also have to be made. An important early decision is for which class of material regulatory approval should be sought. At the time of writing, regulatory bodies, such as the FDA and the EU, are (quite rightly) making regulatory approval more difficult to achieve. Although it may disadvantage new companies with potentially important new products, safety must be paramount. The regulatory class depends on the claims made by a company. For example, in the EU, if a company claims that a scaffold will bond to bone, degrade over time and stimulate bone regeneration, it will be a Class III medical device. If the company claims a new material will simply do the same as other bone grafts and fill space it will be a Class II device, but then the marketing or sales people in the company cannot claim performance superior to current products. Of course, to obtain regulatory approval of a Class III device takes more investment and may involve lengthy clinical trials. Claiming pharmaceutical properties of an implant may also mean that approval is needed from pharmaceutical (rather than device) regulatory bodies such as the UK Healthcare Products Regulatory Agency (MHRA). See Chapters 38 and 39 for details of regulatory guideline and procedures.

32.8. SUMMARY

Granules of silicon-doped HA, with interconnected pores in excess of 100 μm, are the current market leader for bioactive ceramic synthetic bone grafts. Bioactive glass foams have the potential to improve performance but no bioceramics will ever fulfil all the criteria for an ideal scaffold. Inorganic/organic hybrids have the potential to be tough bioactive and biodegradable scaffolds. A massive challenge is expanding this technology to regenerate real load-bearing defects such as the hip. Replacing metals as load bearing devices is the ultimate,

but perhaps unachievable, goal. Tissue engineering approaches are not yet widely used in the clinic, except that surgeons often mix blood and bone marrow with implants, hoping to activate some stem cells already belonging to the patient. Incorporating osteoprogenitor cells within scaffolds may be the best solution if healthy bone is to be achieved in large defects.

REFERENCES

1. Jones, J.R., Ehrenfried, L.M. and Hench, L.L. (2006). Optimising Bioactive Glass Scaffolds for Bone Tissue Engineering, *Biomaterials*, **27**, 964–973.
2. Oonishi, H., Hench, L.L., Wilson, J. *et al.* (2000). Quantitative Comparison of Bone Growth Behavior in Granules of Bioglass®, A-W Glass-Ceramic, and Hydroxyapatite, *J. Biomed. Mater. Res.*, **51**, 37–46.
3. LeGeros, R.Z. (2002). Properties of Osteoconductive Biomaterials: Calcium Phosphates, *Clin. Orthopaed. Rel. Res.*, **395**, 81–98.
4. Kato, K., Aoki, H., Tabata, T. *et al.* (1979). Biocompatibility of Apatite Ceramics in Mandibles, *Biomater. Med. Dev.*, **7**, 291–297.
5. Denissen, H.W., Kalk, W., Veldhuis, A.A.H. *et al.* (1989). 11-Year Study of Hydroxyapatite Implants, *J. Prosth. Dent.*, **61**, 706–712.
6. Andrade, J.C.T., Camilli, J.A., Kawachi, E.Y. *et al.* (2002). Behavior of Dense and Porous Hydroxyapatite Implants and Tissue Response in Rat Femoral Defects, *J. Biomed. Mater. Res.*, **62**, 30–36.
7. Zhang, C., Wang, J.X., Feng, H.H. *et al.* (2001). Replacement of Segmental Bone Defects Using Porous Bioceramic Cylinders: A Biomechanical and X-Ray Diffraction Study, *J. Biomed. Mater. Res.*, **54**, 407–411.
8. Sepulveda, P., Binner, J.G.P., Rogero, S.O., *et al.* (2000). Production of Porous Hydroxyapatite by the Gel-Casting of Foams and Cytotoxic Evaluation, *J. Biomed. Mater. Res.*, **50**, 27–34.
9. Roy, D.M. and Linnehan, S.K. (1974). Hydroxyapatite Formed from Coral Skeletal Carbonate by Hydrothermal Exchange, *Nature*, **247**, 220–222.
10. Valentini, P., Abensur, D., Wenz, B. *et al.* (2000). Sinus Grafting with Porous Bone Mineral (Bio-Oss) for Implant Placement: A 5-year Study on 15 Patients, *Int. J. Periodon. Rest. Dent.*, **20**, 245–254.
11. Koerten, H.K. and van der Meulen, J. (1999). Degradation of Calcium Phosphate Ceramics, *J. Biomed. Mater. Res.*, **44**, 78–86.
12. de Groot, K. (1983). *Bioceramics of CaP*, CRC Press, Boca Raton, FL.

13. Merry, J.C., Gibson, I.R., Best, S.M. *et al.* (1998). Synthesis and Characterization of Carbonate Hydroxyapatite, *J. Mater. Sci. Mater. Med.*, **9**, 779–783.
14. Gibson, I.R. and Bonfield, W. (2002). Novel Synthesis and Characterization of an AB-Type Carbonate-Substituted Hydroxyapatite, *J. Biomed. Mater. Res.*, **59**, 697–708.
15. Gibson, I.R., Best, S.M. and Bonfield, W. (1999). Chemical Characterization of Silicon-Substituted Hydroxyapatite, *J. Biomed. Mater. Res.*, **44**, 422–428.
16. Botelho, C.M., Brooks, R.A., Best, S.M. *et al.* (2006). Human Osteoblast Response to Silicon-Substituted Hydroxyapatite, *J. Biomed. Mater. Res. A*, **79**, 723–730.
17. Hing, K.A., Revell, P.A., Smith, N., *et al.* (2006). Effect of Silicon Level on Rate, Quality and Progression of Bone Healing within Silicate-Substituted Porous Hydroxyapatite Scaffolds, *Biomaterials*, **27**, 5014–5026.
18. Fu, Q., Rahaman, M.N., Bal, B.S. *et al.* (2008). Mechanical and *In Vitro* Performance of 13–93 Bioactive Glass Scaffolds Prepared by a Polymer Foam Replication Technique, *Acta Biomater*., **4**, 1854–1864.
19. Elgayar, I., Aliev, A.E., Boccaccini, A.R. *et al.* (2005). Structural Analysis of Bioactive Glasses, *J. Non-Cryst. Solids*, **351**, 173–183.
20. Li, R., Clark, A.E. and Hench, L.L. (1991). An Investigation of Bioactive Glass Powders by Sol-Gel Processing, *J. Appl. Biomater.*, **2**, 231–239.
21. Lin, S., Ionescu, C., Pike, K.J. *et al.* (2009). Nanostructure Evolution and Calcium Distribution in Sol-Gel Derived Bioactive Glass, *J. Mater. Chem.*, **19**, 1276–1282.
22. Pereira, M.M., Clark, A.E. and Hench, L.L. (1994). Calcium-Phosphate Formation on Sol-Gel-Derived Bioactive Glasses *in vitro*, *J. Biomed. Mater. Res.*, **28**, 693–698.
23. Sepulveda, P., Jones, J.R. and Hench, L.L. (2002). *In Vitro* Dissolution of Melt-Derived 45S5 and Sol-Gel Derived 58S Bioactive Glasses, *J. Biomed. Mater. Res.*, **61**, 301–311.
24. Brinker, J. and Scherer, G.W. (1990). *Sol-Gel Science: The Physics and Chemistry of Sol-Gel Processing*, Academic Press, Boston, MA.
25. Arcos, D., Greenspan, D.C. and Vallet-Regi, M. (2002). Influence of the Stabilization Temperature on Textural and Structural Features and Ion Release in SiO_2-CaO-P_2O_5 Sol-Gel Glasses, *Chem. Mater.*, **14**, 1515–1522.
26. Sepulveda, P., Jones, J.R. and Hench, L.L. (2002). Bioactive Sol-Gel Foams for Tissue Repair, *J. Biomed. Mater. Res.*, **59**, 340–348.

27. Gough, J.E., Jones, J.R. and Hench, L.L. (2004). Nodule Formation and Mineralisation of Human Primary Osteoblasts Cultured on a Porous Bioactive Glass Scaffold, *Biomaterials*, **25**, 2039–2046.
28. Jones, J.R. Tsigkou, O., Coates, E.E. *et al.* (2007). Extracellular Matrix Formation and Mineralization of on a Phosphate-Free Porous Bioactive Glass Scaffold Using Primary Human Osteoblast (HOB) Cells, *Biomaterials*, **28**, 1653–1663.
29. Nakamura, T., Yamamuro, T., Higashi, S. *et al.* (1985). A New Glass-Ceramic for Bone-Replacement-Evaluation of its Bonding to Bone Tissue, *J. Biomed. Mater. Res.*, **19**, 685–698.
30. Kokubo, T. (1991). Bioactive Glass-Ceramics — Properties and Applications, *Biomaterials*, **12**, 155–163.
31. Neo, M., Kotani, S., Nakamura, T. *et al.* (1992). A Comparative Study of Ultrastructures of the Interfaces between Four Kinds of Surface-Active Ceramic and Bone, *J. Biomed. Mater. Res.*, **26**, 1419–1432.
32. Valliant, E.M. and Jones, J.R. (2011). Towards Softer Materials for Synthetic Bone Graft Applications: Hybrid Materials, *Soft Matter.*, **7**, 5083–5095.
33. Pereira, M.M., Jones, J.R., Orefice, R.L. *et al.* (2005). Preparation of Bioactive Glass-Polyvinyl Alcohol Hybrid Foams by the Sol-Gel Method, *J. Mater. Sci. Mater. Med.*, **16**, 1045–1050.
34. Rhee, S.H. and Lee, S.J. (2007). Effect of Acidic Degradation Products Of Poly(Lactic-Co-Glycolic)Acid on the Apatite-Forming Ability of Poly(Lactic-Co-Glycolic)Acid-Siloxane Nanohybrid Material, *J. Biomed. Mater. Res. A*, **83**, 799–805.
35. Mahony, O., Tsigkou, O., Ionescu, C. *et al.* (2010). Silica-Gelatin Hybrids with Tailorable Degradation and Mechanical Properties for Tissue Regeneration, *Adv. Funct. Mater.*, **20**, 3835–3845.
36. Poologasundarampillai, G., Ionescu, C., Tsigkou, O. *et al.* (2010). Synthesis of Bioactive Class II Poly(γ-Glutamic Acid)/Silica Hybrids for Bone Tissue Regeneration, *J. Mater. Chem.*, **40**, 8952–8961.
37. Zhu, A., Zhang, M. and Shen, R. (2003). Covalent Immobilization of O-Butyrylchitosan with a Photosensitive Hetero-Bifunctional Crosslinking Reagent on Biopolymer Substrate Surface and Blood Compatibility Characterization, *J. Biomater. Sci. Polym. Ed.*, **14**, 411–421.

Chapter 33

TREATMENT OF CHRONIC WOUNDS WITH BIOACTIVE BORATE GLASS FIBERS

Steven Jung

33.1. INTRODUCTION

Since the first *in vivo* experiments conducted by Larry Hench in the late 1960s, it has been known that bioactive glasses were biocompatible materials that formed strong bonds with living tissue.[1] Since those first experiments, most research with regards to bioactive glass has been targeted towards understanding and improving bone regeneration and bone bonding. Many papers discuss the formation of hydroxyapatite on the surface of bioactive glass using *in vitro* methods, and numerous case studies in humans and animals prove the efficacy of bioactive glass in stimulating bone regeneration.[1,2]

Soft tissues such as skin and muscle have been reported to have bonded to bioactive glass, but typically this was just a side comment with no significant emphasis in the study's conclusions. Millions of people with conditions like diabetes and venous stasis (vascular insufficiency in the lower legs) have few effective treatment options for healing chronic wounds often associated with these diseases. The worldwide market for soft tissue regenerative materials and dressings reached nearly $7 billion dollars (US) in 2010 and is expected to grow at ~10% a year.[3] In comparison to the worldwide bone regeneration market of $5.8 billion (US) in 2010,[4] wound healing is a larger market with great personal and socio-economic impact. Wound healing and soft tissue regeneration has an unmet need with regards to effective treatment options and a new and highly effective material/dressing is needed to fulfill it.[3]

In this chapter, results from a human clinical trial that used a new type of bioactive borate glass fiber to treat chronic wounds are described.[5] Patients in the study were selected because they had failed to heal with conventional wound dressings and treatment and were considered chronic and non-healing.

33.2. RATIONALE BEHIND BIOACTIVE BORATE GLASS AND FIBERS

It is known that silicate-based bioactive glasses such as 45S5 bond to soft tissue, but these glasses as a whole have some properties that are difficult

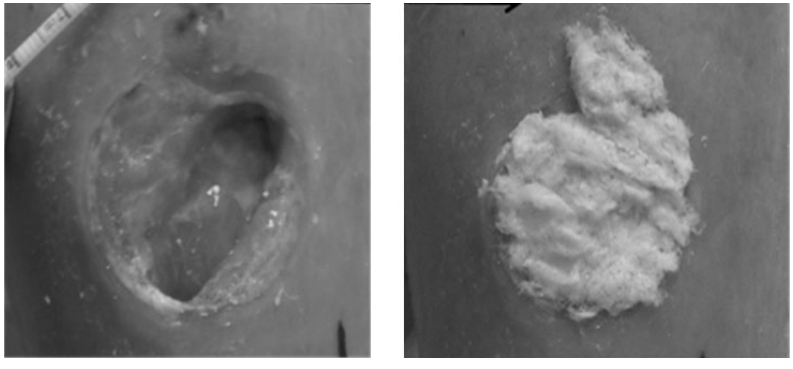

Figure 33.1. Photograph of wound before (left) and after (right) treatment with bioactive borate glass nano-fibers.

to overcome when processing a final form other than milled particles, such as small diameter nano-sized fibers. A material made from nano-sized fibers was selected to mimic the natural fibrous microstructure of a blood clot since that is what the body generates during the initial stage of connective tissue healing.[6] Overall handling of the material is another important consideration of the material with respect to the clinicians that will ultimately use the material in practice. In general, the easier the material is to work with, the better the outcome of the respective treatment. Figure 33.1 shows a wound prior to treatment (left) and the same wound covered with the bioactive borate glass fibers (right). The fibers are flexible and easily manipulated to fit the contours of a complex shaped wound.

The borate glass compositions studied for wound healing have *in vivo* reaction rates that are approximately ten times faster than the well known silicate based 45S5 glass. This enhanced reaction rate allows for the fibers to fully react at the wound site in a matter of a few days, which is convenient since the typical wound patient is seen two to three times a week in clinic. The bioactive borate glasses also contain trace elements, such as copper and zinc, that stimulate important biological functions such as angiogenesis (blood vessel formation)[7] and epithelialization,[8] respectively.

33.3. PATIENT CRITERIA AND TREATMENT

Each patient was treated by conventional methods, which included typical debridement of non-viable tissue and/or wound exudates followed by wound

coverage, for a minimum of four weeks without forward progress prior to qualifying for enrollment. Each patient was seen two to three times weekly until the wound resolved or up to eight weeks. Due to the size of some of the wounds, the eight-week limit was extended in several cases since significant healing had occurred. During each visit at the hospital out-patient wound clinic, the wound was rinsed with a sterile saline solution to remove any wound exudates. Once the wound was clean, it was documented by photograph and dimensions of maximum length, width, and depth were recorded to monitor wound healing progress. The patient was asked about any pain and sensation at the wound site, or if they had any additional comments about the treatment. Finally, the wound surface was covered with the borate glass fiber dressing and the entire wound was covered with a conventional bandage. This process was followed two to three times weekly until the wound was resolved.

33.4. SUMMARY OF THE HUMAN CLINICAL TRIAL

At the time this chapter was written, 47 patients had continuously enrolled in the clinical study over the course of 15 months. Twenty six patients had healed and were released from the outpatient care, seven patients dropped out of the study for various reasons, including changing doctors, moving out of the area, and a few stated no reason at all, but stopped attending appointments, and 14 continued treatment with forward progress. The types of wounds included lower leg venous stasis ulcers, pressure ulcers on the lower back (sacrum) and on the feet, and an amputee stump revision. A few examples illustrating the different types of wounds treated and the clinical outcomes are described.

One instance involved treatment of a chronic, non-healing venous stasis ulcer on the lower leg of a 70-year old female. The patient had the following chronic health problems: diabetes, PVD, PAD, neuropathy, Charcot foot, previous chronic wounds, previous recurring leg infections, and venous insufficiency. The wound was four months old and began from a small bruise. What was initially just a bruise from falling had grown to a deep wound about the size of a golf ball, as shown in Fig. 33.2a. This wound was complicated by undermining (areas of skin that have pockets of underlying tissue voids), hydrostatic pressure in the lower leg, and by the fact that vascular deficiency from the patient's other health conditions inhibited healing. As the treatment progressed, several indications that the wound was progressing became evident (Figs 33.2b–33.2d). Within three weeks, the wound had fully granulated (filled from the bottom), as shown by the

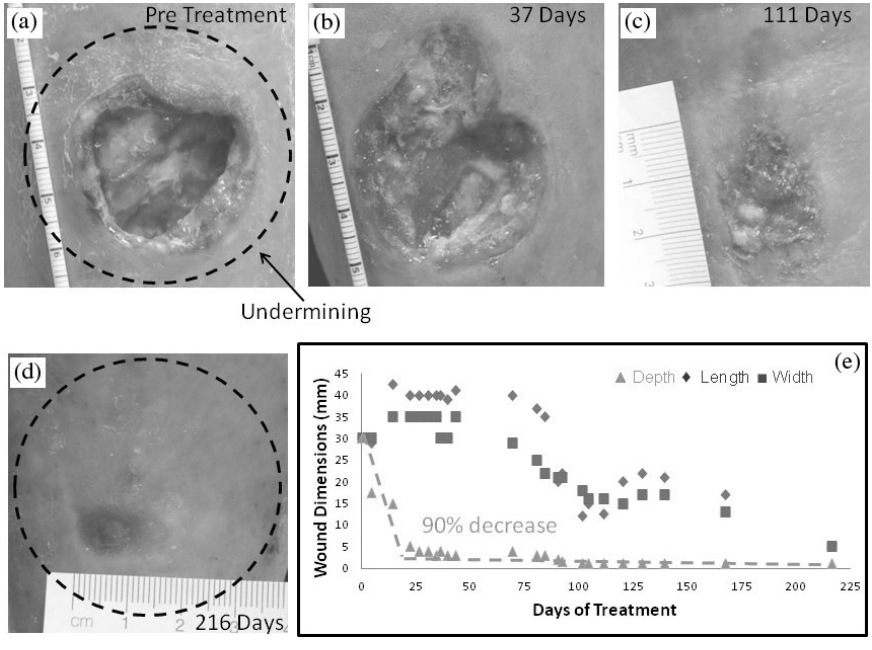

Figure 33.2. Images and wound measurements from a venous stasis ulcer treated with borate-based bioactive nano-fibers. The dashed circles at days pretreatment and 216 were added to guide the eye to the area of regenerated tissue.

data in Fig. 33.2e. At five weeks, the distinct change from an irregularly-shaped wound in Fig. 33.2a to a rounded wound in Fig. 33.2b (five weeks) indicated that the wound had "moved" and was healing. After 111 days (33.2c), the wound was filling in from the top which is normal, and the bottom of the wound was continually shrinking. The image in Fig. 33.2d shows the wound the day the patient was released. The wound had fully epithelialized with only a small circle of fragile tissue remaining. There was no noticeable scar and there was feeling reported by the patient in the regenerated tissue.

A second instance involved a deep sacral ulcer over the lower back/tail bone area on a 39-year old paraplegic male patient (Fig 33.3a). The dressing application and procedure was the same as discussed above. This treatment yielded not only fast healing of the wound, but also little scar tissue was formed, as shown in the following photographs. This wound was termed a "killer wound", since it was located adjacent to exposed portions of the patient's spinal cord, and if the spinal cord were to become infected, the patient could expire.

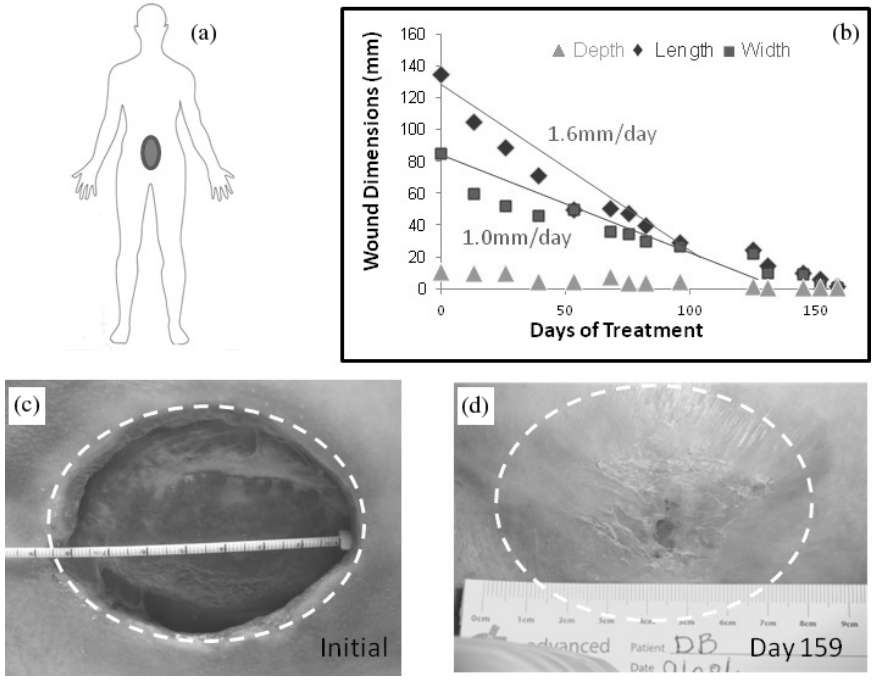

Figure 33.3. Images and wound measurements from a sacral ulcer treated with borate-based bioactive nano-fibers. The dashed circles at days initial and 159 were added to guide the eye to the area of regenerated tissue.

The wound closure data for the sacral ulcer is shown in Fig. 33.3b. It is apparent that the wound reacted positively to the fibers, as the length and width dimensions decreased at ≥ 1 mm/day. The image of the wound prior to treatment is shown in Fig. 33.3c. The wound had areas of significant undermining and was considered a wet wound. After 159 days (Fig. 33.3d) the wound had fully healed with minimal scarring and was no longer releasing any exudates. The dashed oval represents the area of the original wound to guide the eye.

A third instance involved a pressure wound on the heel of a 55-year old adult male patient. The wound had existed for about two years without healing under conventional treatment. The healing process was complicated by the patient's chronic health issues, including diabetes with peripheral neuropathy, hypertension, renal failure with dialysis three times weekly, degenerative disk disease of the lumbar spine, and chronic foot wounds. The dressing applied and procedure was the same as discussed above.

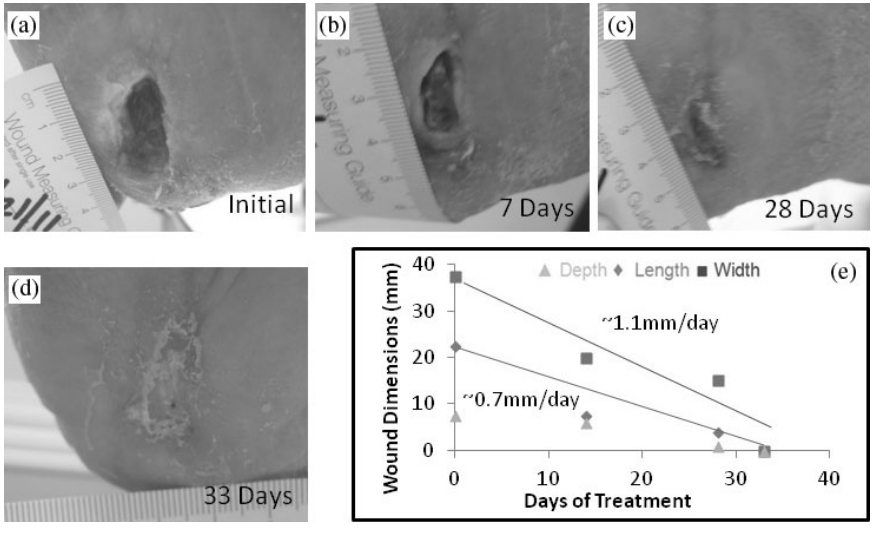

Figure 33.4. Images and wound measurements from a heel wound treated with borate-based bioactive nano-fibers.

The images of the healing progression are shown in Figs 33.4a–33.4d and the data in Fig. 33.4e. Within the first week of treatment, the wound had fully granulated (Fig. 33.4b) and within two weeks the wound had decreased in size by over 50%. After 28 days, the wound was nearing full epithelialization (Fig. 33.4c) and was completely healed in just over a month (Fig. 33.4d).

33.5. SUMMARY

The most important observations from this work include: the ability to use bioactive borate glasses to convert a chronic non-healing wound to an acute wound that healed; the lack of scarring present in the regenerated tissue; and the successful stimulation of granulation tissue in deep tissue wounds. The composition and microstructure of the bioactive borate glass materials appear to work together to promote healing and provide successful clinical outcomes. Finally, the data and images shown in this chapter illustrate the possibilities for enhancing treatment options for servicing the wound-healing market worldwide.

REFERENCES

1. Hench, L.L., Hench, J.W. and Greenspan, D.C. (2004). Bioglass: A Short History and Bibliography, *J. Aust. Ceram. Soc.*, **40**, 1–42.
2. Rahaman, M.N., Day, D.E., Bal, B.S., *et al*. (2011). Bioactive Glass in Tissue Engineering, *Acta Biomater*, **7**, 2355–2373.
3. Espicom Healthcare Intelligence (2010). World Medical Market Forecasts to 2015. Available at: http://marketresearch.com/Espicom-Healthcare-Intelligence-v1129/Medical-Forecasts-2738245. [Accessed 21 March 2011].
4. Kalorama Information Market Intelligence Report. (2011). Biomaterials. Available at: MarketResearch.com.
5. Jung, S.B. (2011). Wound Healing Power of Glass, *Nanotech Insights*, **2**, 2–4.
6. Cormack, D.H. (1987). *Ham's Histology, 8th Edition*, J.B. Lippincott Company, Philadelphia, PA.
7. Harris, E.D. (2004). A Requirement for Copper in Angiogenesis, *Nutrition Reviews*, **62**, 60–64.
8. Lansdown, A.B.G., Mirastschijski, U., Stubbs, R.N., *et al*. (2006). Zinc in Wound Healing: Theoretical, Experimental, and Clinical Aspects, *Wound Repair Regen.*, **15**, 2–15.

Chapter 34

BIOACTIVE GLASS-CERAMICS FOR LOAD-BEARING APPLICATIONS

Oscar Peitl, Edgar D. Zanotto, Francisco C. Serbena and Larry L. Hench

34.1. INTRODUCTION

One of the great challenges in biomaterials is developing a material that matches the biomechanical properties of bone and also has sufficient bioactivity to bond to living bone and soft tissues.[1,2] Biocomposites come close to achieving this goal but have been limited in clinical applications due to unstable interfaces between the phases, as discussed in Chapter 26. Another approach has been to improve the mechanical properties of bioactive ceramics by making a glass-ceramic, such as the A/W glass-ceramic (for example Cerabone®), discussed in Chapters 13 and 14. The high strength and high toughness of the A/W glass-ceramic makes it a load-bearing replacement for cortical bone loaded under compression. A/W glass-ceramic has been used successfully in more than 60,000 clinical cases, including vertebral replacement and iliac crest repair (Chapter 14). However, its elastic modulus is about one order of magnitude higher than that of cortical bone, giving rise to the possibility of long-term stress shielding when the material is used as a bone replacement (Chapter 1).[3] Also, the level of bioactivity of A/W glass-ceramic is insufficient for bonding to soft connective tissues,[4] as needed for some clinical applications. This chapter describes a new approach to achieving high strength, high toughness glass-ceramics with bioactivity equivalent to the grandfather 45S5 bioactive glass.[1,2,5]

34.2. BIOACTIVE GLASS-CERAMIC COMPOSITIONS

The effects of crystallization on the *in vitro* activity of osteoblast cultures in simulated body fluid (SBF), in animals and humans, of monolithic and powdered glass-ceramics of the system P_2O_5–Na_2O–CaO–SiO_2 have been developed to exhibit similar levels of bioactivity as the "gold standard" 45S5 Bioglass®.[1,2,4,6] Glasses within the composition range $1Na_2O$–2CaO–$3SiO_2$ and $1.5Na_2O$–1.5CaO–$3SiO_2$ with 0-6% P_2O_5 showed that crystallization slows down, but does *not* inhibit, the development of a crystalline hydroxycarbonate apatite (HCA) layer, even on

Table 34.1. Glass Compositions Studied (wt%).

Component	SiO_2	Na_2O	CaO	P_2O_5
1.07N2C3S	50.3	18.5	31.3	
1.5N1.5C3S	50.5	24.8	24.8	
1.5N1.5C3S + 4P	48.5	23.8	23.8	4.0
1.5N1.5C3S + 6P	47.5	23.2	23.2	6.0

fully crystallized glass-ceramics of these compositions.[1,2] Table 34.1 summarizes some of the glass compositions studied.[5]

34.3. *IN VITRO* TESTS OF BIOACTIVITY

The range of onset time for crystallization of HCA in *in vitro* tests using SBF-K9 varied from 8 h for a $1.5Na_2O–1.5CaO–3SiO_2$ glass containing 6% P_2O_5 to 32 h for a fully crystallized $1.07Na_2O–2CaO–3SiO_2$ glass-ceramic without phosphorous.[1,5] Nonetheless, *in vitro* HCA layer formation on these glass-ceramics, even for the least bioactive, is much faster than on partially- or fully-crystallized commercial bioceramics, such as sintered hydroxyapatite (HA) and A/W (Cerabone®), which usually takes at least seven days.[2] Peitl *et al*. concluded that two simultaneously-acting factors are responsible for the high bioactivity level of these glass-ceramics: a highly-soluble crystal phase (1N2C3S) and the existence of phosphorus ions in substitutional solid solution, which are able to be readily released from the crystal structure.[1,2] Both factors contribute to a faster HCA layer formation on glass-ceramics of this system by the same five stages of surface reaction mechanisms observed for the 45S5 Bioglass®, described in Chapter 3.

All five surface reaction stages go to completion within two–five hours for glasses and glass-ceramics of highest bioactivity in this system.[1–6]

34.4. MECHANICAL PROPERTIES OF GLASS-CERAMICS: GENERAL

There is a large body of literature describing the mechanical properties of different types of glass-ceramics.[7–14] However, effects of the crystallized volume fraction at *constant* grain size and of varying grain size with *constant* crystallized volume fraction on mechanical properties of glass-ceramics have seldom been investigated. There are only a few studies of mechanical properties of bioactive glass-ceramics. Several papers compare the mechanical behavior of the parent

glasses with (almost) fully crystallized glass-ceramics but do not consider partially-crystallized glass-ceramics of varied microstructure.[7–9] Some studies compared the mechanical behavior of glass-ceramics, varying the crystal size for a fixed volume percentage of crystal phase, whereas others describe the effect of volume fraction of crystal phase, but neglect the crystal size effect.

In this work, we studied *independently* two important microstructural factors that affect the material's mechanical behavior: crystalline volume fraction (at constant crystal size) and crystal size (at constant crystallized volume fraction). Production of tailored microstructures by controlling internal nucleation and growth (and the resulting level of internal residual stress) was the biggest challenge. This study is the first to focus on these two interdependent microstructural effects, plus the possible effect of residual stress on the mechanical behavior of glass-ceramics in general and bioactive glass-ceramics in particular.[5] Our goal is to obtain an optimized bioactive glass-ceramic that combines improved mechanical properties, such as relatively low elastic modulus, high fracture strength and relatively high toughness, with a bioactivity level comparable to that of 45S5 Bioglass®. Successful development of these mechanical and bioactivity properties in a fine-grained bioactive glass-ceramic resulted in a patent filed in the USA and in the European Community.[15] Recent efforts describe the optimized mechanical properties and interpretation of the mechanical behavior of this glass-ceramic system.[5]

34.5. EXPERIMENTAL PROCEDURES

High purity silica and reagent-grade calcium carbonate, sodium carbonate and sodium phosphate were used to obtain glasses of approximate compositions 1.07N2C3S and $1.5Na_2O–1.5CaO–3SiO_2$, with 0, 1, 2, 4 and 6 wt% P_2O_5. The exact nominal compositions are given in Table 34.1. Details are given in References 1, 2, 5 and 15. The strategy used to study and control crystallization follows that proposed by Kalinina and Filipovich,[16] who employed a two-step heat treatment to measure nucleation rates. The procedure consists of growing the nuclei formed in the first step by a second heat treatment at a higher temperature.[1,2,5]

Crystal growth rates were determined by optical microscopy, considering the size of the biggest crystal (the *primogenitus*) as function of time and temperature of the second treatment. Measurements were taken on polished and hydrofluoric acid (HF) etched surfaces. Table 34.2 shows the range of temperatures and times used to develop the desired microstructures. The glass-transition temperatures (*Tg*) were determined using differential scanning calorimetry (DSC) to study the effect of P_2O_5 content on the nucleation rates. From the DSC curves, the Hruby parameter *KGL* was calculated to estimate the glass stability against crystallization during heating.[5]

Table 34.2. Thermal Treatment Ranges Used to Produce Different Microstructures for the Compositions Studied.

Composition	Nucleation		Growth		Volume (%)
	T (°C)	t (min)	T (°C)	t (min)	Crystallized
1.07N2C3S	600	960	690	60	100
1.5N1.5C3S	520–560	3–180	620–640	6–22	10–100
1.5N1.5C3S +4P	540–590	30–6000	650–700	5–80	5–100
1.5N1.5C3S +6P	540–590	60–9000	650–700	10–70	10–100

Some mechanical properties — flexural strength, elastic modulus, microhardness and indentation fracture toughness — were measured using rectangular bars with dimensions of $5 \times 3.5 \times 35$ mm^3. The effect of the crystalline volume fraction with a constant grain size was evaluated for five different percentages of crystals, 0, 15, 34, 60 and 100%, with an average grain diameter of 13 μm (with a very narrow grain size distribution). For the crystalline volume fractions that presented the best flexural strength and indentation fracture toughness, we developed thermal treatments to produce microstructures having the widest possible range of crystal sizes without adding any nucleating agent. In this way, microstructures with crystal sizes in the range 5–21 μm and with constant crystalline volume fraction had their mechanical properties investigated.[5]

34.6. MECHANICAL PROPERITES OF OPTIMIZED BIOACTIVE GLASS-CERAMICS

Bioactive glasses having chemical composition between $1Na_2O$–$2CaO$–$3SiO_2$ (1N2C3S) and $1.5Na_2O$–$1.5CaO$–$3SiO_2$ (1N1C2S), containing 0, 4 and 6 wt% P_2O_5, were crystallized through double-stage thermal treatments. By carefully controlling these treatments it was possible to separate and optimize the effects of two important microstructural features, crystallized volume fraction and crystal size, on the mechanical properties. Fracture strength, elastic modulus and indentation fracture toughness were measured as a function of crystallized volume fraction for a *constant* crystal size. Glass-ceramics with crystalline volume fraction between 34 and 60% exhibited improvement of three times in fracture strength, as illustrated in Fig. 34.1, and an increase of 40% in indentation fracture toughness compared with the parent glass.[5]

For the optimal crystalline concentration (34 and 60%), these mechanical properties were then measured for *different* grain sizes, from 5 to 21 μm. The

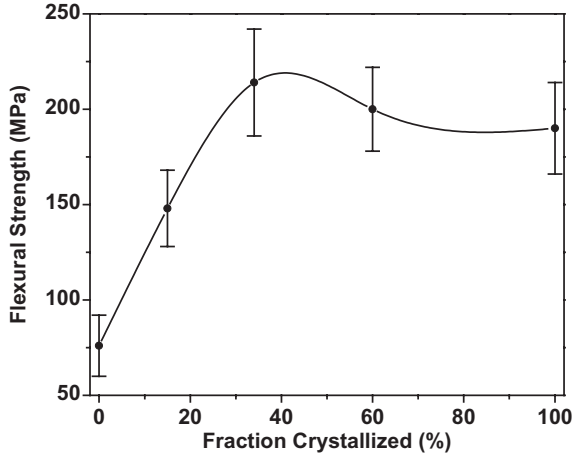

Figure 34.1. Dependence of flexural strength on percent crystallinity for 1.5N1.5C3S+4P glass-ceramics with 13 μm crystal size.

glass-ceramic with the highest fracture strength and indentation fracture toughness had 34% crystallized volume fracture and 13 μm crystals, as shown in Fig. 34.2.[5] Compared to the parent glass, the average fracture strength of this glass-ceramic was increased from 80 MPa to 220 MPa, which is substantially greater than the flexural strength of cortical bone. The indentation fracture toughness increased from 0.60 to 0.95 MPa.m$^{1/2}$, as discussed in Peitl *et al*.[5]

The increase in indentation fracture toughness was analyzed with different theoretical models, which demonstrated that it is due mainly to crack deflection. Residual stresses do not significantly contribute to toughening; in fact they cause a decrease in toughness at low volume fraction of crystals due to the increased average tensile stresses in the glass matrix.[5] The estimated fracture toughness of our 34% crystallized glass-ceramic is about half that of commercial glass-ceramics A/W and BIOVERIT, but it is twice as large as that of 45S5 Bioglass®. The partially-crystallized bioactive glass-ceramics with high strength and high toughness are reasonably machinable; i.e. they can be easily cut or drilled by a surgeon using a hand tool with no cracking or spalling. Importantly, the bioactivity level is equivalent to that of the gold standard 45S5 Bioglass® and by far the highest of all glass-ceramics.[2]

Fortunately, the elastic modulus, E, of the optimized bioactive glass-ceramic increased only slightly, from 60 to 70 GPa, for the strongest glass-ceramic with 34% crystal phase, as shown in Fig. 34.3. This is an important finding since the E of biomaterials should be as close as possible to that of

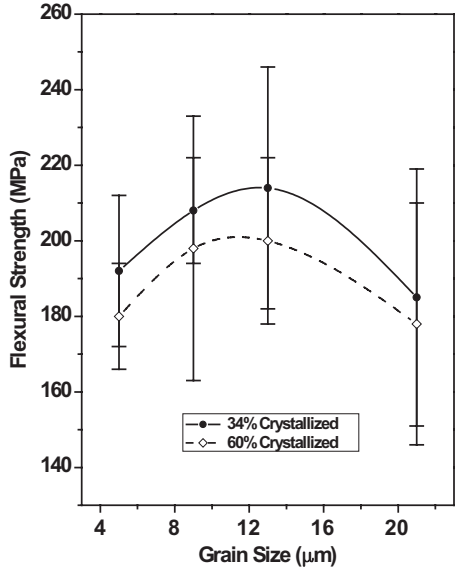

Figure 34.2. Flexural strength (S_F) for 1.5N1.5C3S+4P partially-crystallized glass-ceramic, as function of the crystal size. Solid line = 34% crystallinity, dotted line = 60% crystallinity.

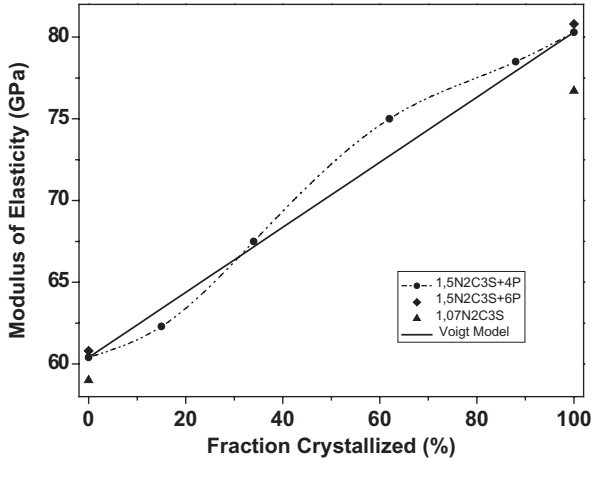

Figure 34.3. Young's modulus as function of volume percentage of crystallinity for three compositions.

cortical bone to avoid stress shielding in load-bearing applications. Thus, the best glass-ceramic is a unique bioactive ceramic that combines excellent mechanical properties with a high level of bioactivity. Clinical trials of this biomaterial are now underway.[17,18]

34.7. CONCLUSION

The flexural strength of the optimized bioactive glass-ceramic is significantly greater than that of cortical bone and comparable to that of apatite-wollastonite (A/W) bioactive glass-ceramic, which has been used successfully in orthopedic compressive load-bearing applications for decades. The optimized bioactive glass-ceramic described in this chapter has the advantage that it exhibits a much lower elastic modulus than A/W glass-ceramic and has an elastic modulus similar to that of cortical bone. The level of bioactivity of the partially-crystallized glass-ceramics that exhibit high strength and toughness is equivalent to that of 45S5 Bioglass®. These results thus demonstrate that it is possible to design bioactive glass-ceramics with improved microstructures that should be possible to use clinically in flexural as well as compressive load-bearing applications. However, prior to extensive clinical trials it is necessary to conduct studies of static and dynamic fatigue of these materials in simulated clinical load-bearing environments to ensure that the mechanical properties do not degrade over time.

ACKNOWLEDGEMENTS

The authors are grateful to Brazilian funding agencies CNPq, Capes (NanoBiotech research network) and Fapesp (Thematic grant # 07/08179-9).

REFERENCES

1. Peitl, O., Zanotto, E.D. and Hench, L.L. (2001). Highly Bioactive P_2O_5-Na_2O-CaO-SiO_2 Glass-Ceramics, *J. Non-Cryst. Solids*, **292**, 115–126.
2. Peitl, O., LaTorre, G. and Hench, L.L. (1996). Effect of Crystallization on Apatite Layer Formation of Bioactive Glass 45S5, *J. Bio. Mater. Res.*, **30**, 509–514.
3. Hench, L.L. and West, J.K. (1996). Biological Applications of Bioactive Glasses, *Life Chem. Rep.*, **13**, 187–241.
4. Moura, J., Teixeira, L.N., Ravagnani, C. *et al.* (2007). *In Vitro* Osteogenesis on a Highly Bioactive Glass-Ceramic (Bioglass®), *J. Bio. Mater. Res.*, **82A**, 545–557.

5. Peitl, O., Zanotto, E.D., Serbena, F.C. *et al.* (2012). Compositional and Microstructural Design of Highly Bioactive P_2O_5-Na_2O-CaO-SiO_2 Glass-Ceramics, *Acta Biomater.*, **8**, 321–332.
6. Jabur, O.R. and Barros, V.M.R. (2008). Bone Formation on Ti Implants in Intra-Bony Defects Sites Filled with Different Bone Substitutes: Histomorphometric Analysis in Dogs, *International Congress of Implantology, September 2008, Ribeirão Preto,* Brazil.
7. Freiman, S.W. and Hench, L.L. (1968). Kinetics of Crystallization in Li_2O-SiO_2 Glasses, *J. Am. Ceram. Soc.*, **51**, 382–387.
8. Sambell, R.A., Bowen, D. and Phillips, D.C. (1992). Carbon Fiber Composites with Ceramic and Glass Matrices, Part 1, Discontinuous Fibers, *J. Mater. Sci.*, **7**, 663–666.
9. Thompson, J.Y. (1995). Characterization of Mechanical Behavior on Microstructural Phenomena in Li_2O-$2SiO_2$ Glass-Ceramics (PhD Thesis, University of Florida).
10. Davidge, R.W. and Green, T.J. (1968). The Strength of Two-Phase Ceramic/Glass, *J. Mater. Sci.*, **3**, 629–634.
11. Borom, M.P., Turkalo, A.M. and Doremus, R.H. (1975). Strength and Microstructure in Lithium Disilicate Glass-Ceramics, *J. Am. Ceram. Soc.*, **58**, 385–391.
12. Miyata, N., Tanigawa, K. and Jinno, H. (1983). "Fracture Behavior of Glass Matrix/Glass Particle Composites", in Bradt, R.C., Hasselman, D.P.H. and Lange, F. (eds), *Fracture Mechanics of Ceramics, Vol. 5*, Plenum, New York, pp. 609–623.
13. Mecholsky, J.J. (1983). "Toughening in Glass-Ceramics through Microstructural Design", in Bradt, R.C., Evans, A.G., Hasselman, D.P.H. *et al.* (eds), *Fracture Mechanics of Ceramics, Vol. 6*, Plenum, New York, pp. 165–180.
14. Levi, E.A., Khodakovskaya, R.Y., Pobedimskaya, E.A. *et al.* (1980). X-ray Measurements of Microstresses in Glass-Crystalline Materials, *Soviet Physics Doklady*, **25**, 882.
15. Hench, L.L., Peitl, O., LaTorre, G. *et al.* (1997). Bioactive Ceramics and Method of Preparing It, US Patent No: US5981412, 1997 and European Patent: 97925614.6-2111, 1997.

16. Kalinina, A.M. and Filipovich, V.N. (1980). Stationary and Non-Stationary Crystal Nucleation Rate in A Glass of $2Na_2O.1CaO.3SiO_2$ Stoichiometric Composition, *J. Non-Cryst. Solids*, **38**, 723–728.
17. Roriz, V.M., Rosa, A.L., Peitl, O. *et al.* (2010). Efficacy of a Bioactive Glass-Ceramic (Biosilicate®) in the Maintenance of Alveolar Ridges and in Osseo Integration of Ti Implants, *Clin. Oral Implan. Res.*, **21**, 148–155.
18. Zanotto, E.D. (2010). A Bright Future for Glass-Ceramics, *Am. Ceram. Soc. Bull.*, **89**, 19–27.

Chapter 35

POROUS WALL, HOLLOW GLASS MICROSPHERES

George G. Wicks, Steven Serkiz, Shuyi Li and William Dynan

35.1. INTRODUCTION

The Savannah River National Laboratory (SRNL) has developed a novel class of materials for a variety of new and exciting applications in energy, environmental remediation, homeland security and medicine.[1–6] This unique material is called porous wall, hollow glass microspheres (PW-HGMs), which consist of tiny glass microballoons, smaller than the diameter of a human hair (Fig. 35.1). The average sizes of the PW-HGMs range from 2 to 100 μm, with an average diameter of about 50 μm. The unique characteristic of these materials that distinguishes them from other glass microspheres is an interconnected porosity in the thin outer walls (which are 1–2 μm thick), which can be controlled on a scale of 100 to 3,000 Å.[7–10] It is the through-wall porosity, extending continuously from the outside to the inside of the microspheres, that creates unique and desirable properties (Fig. 35.2). The open channels can be used to fill the microballoons with materials of interest, providing a contained environment (Fig. 35.3). Other techniques can then be used to open and close the pores, and either chemical or mechanical techniques can be used to release the "payloads" on demand. This wall porosity can also be used to generate new nanostructures of materials of interest both outside the microspheres as well as within their contained cocoons.

SRNL and the Georgia Health Sciences University have joined forces in an interdisciplinary collaboration to study the potential applicability of these unique materials for medical applications, in areas such as drug delivery and MRI contrast agents.[11,12] To investigate the potential for drug delivery, we performed experiments using fluorescently-labeled macromolecules of various known dimensions, including dextrans, proteins, and nucleic acids. A large dextran, with an estimated diameter of about 14.4 nm, failed to enter the microspheres, whereas dextrans with a diameter of 6.0 nm or less were observed to enter the interior volume. Results suggest that the microsphere walls act as molecular sieves, admitting small molecules but excluding larger ones. Protein, RNA, and DNA studies are also consistent with this interpretation.

Based on the ability to control the pores to release payload on demand, we expect to be able to load the microspheres with therapeutic molecules, such as

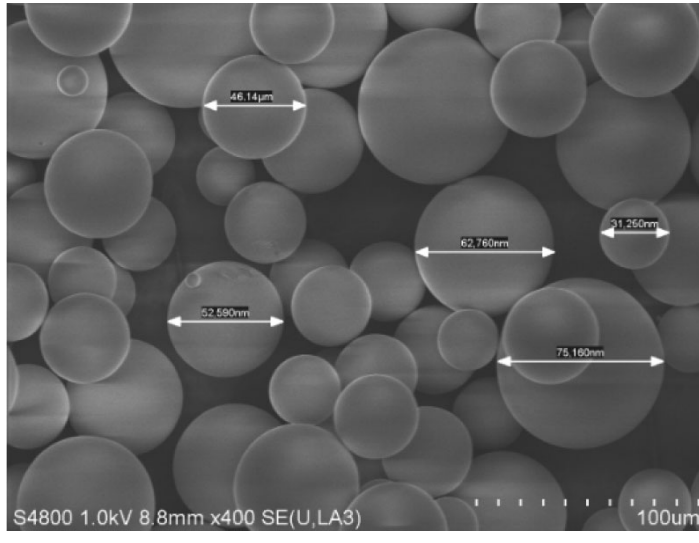

Figure 35.1. PW-HGMs and size distributions.

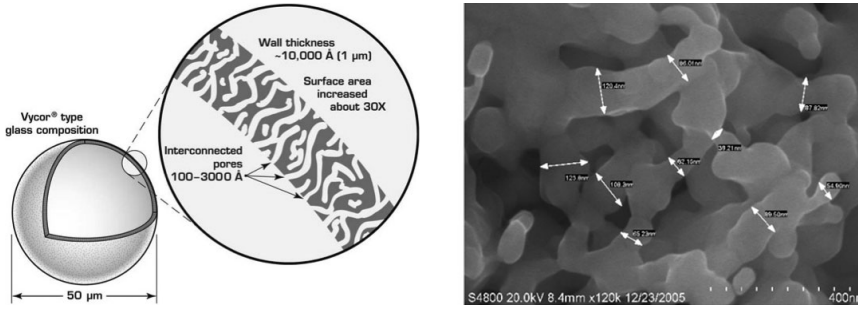

Figure 35.2. (Left) schematic representation of PW-HGMs and through-wall porosity and (right) scanning electron microscopic view, showing surface view of interconnected porosity on PW-HGM walls.

cytokines, antibodies, or small RNAs, and release them at the site where they are needed. We are currently exploring the potential applications of PW-HGMs in the area of regenerative medicine. It should be possible, for example, to load the microspheres with chemoattractant molecules, implant them in a tissue matrix, and use them to recruit mesenchymal stem cells.

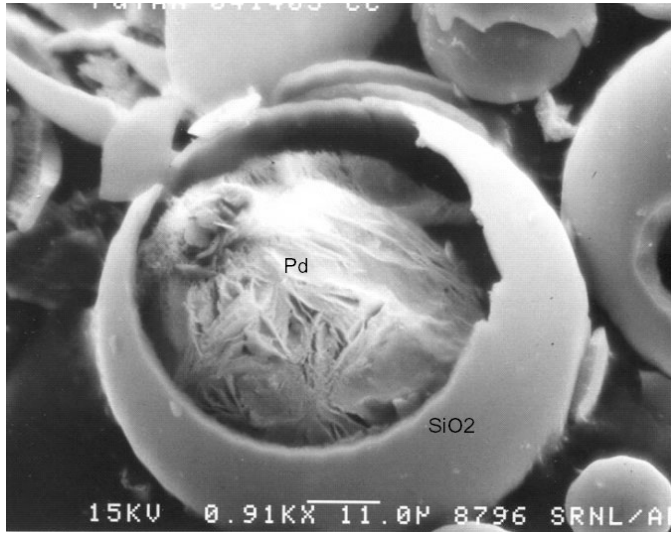

Figure 35.3. SRNL microsphere filled with palladium (top of microballoon removed to view contents).

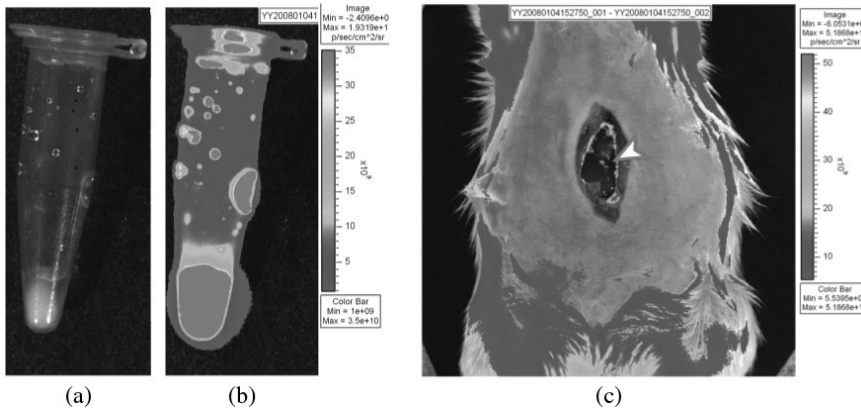

Figure 35.4. PW-HGMs were incubated with 70 kDa fluorescein-dextran and washed. (a) White light image. (b) Fluorescence image of same tube. (c) Visualization in a mouse. Mouse was anesthetized, laparotomized, liver was injected with 10, 30, and 50 µl boluses of beads, and mouse was immediately imaged for green fluorescence. Arrowhead denotes signal at injection site. Note also signal around periphery of liver, possibly following leakage along injection track.

As a first step toward determining whether PW-HGMs could be used *in vivo*, we tested the ability to detect them using a small animal imaging system. We loaded PW-HGMs with fluorescently-labeled dextran, transferred them to a microcentrifuge tube, and performed imaging to measure the fluorescent signal. The method proved to be very sensitive, as evidenced by the ability to detect even very small droplets of PW-HGM slurry on the walls of the tube. We injected the same PW-HGMs into the liver of an anesthetized, laparotomized mouse (Fig. 35.4). The image shows clear localization at the site of injection, with some signal also around the periphery of the liver, possibly following leakage along the injection track. In experiments elsewhere, we have also shown the ability to detect PW-HGMs *in situ* following intratumoral injection.[11]

REFERENCES

1. Wicks, G.G., Heung, L.K. and Schumacher, R.F. (2008). Microspheres and Microworlds-SRNL's Porous, Hollow Glass Balls Open New Opportunities for Hydrogen Storage, Drug Delivery, and National Defense, *Ceramic Bulletin*, **87**, 23–28.
2. Wicks, G.G. and French, A. (2010). A Whole New (Small) World of Opportunity… Porous Wall Hollow Glass Microsystems Offer Exciting Potential for Use in Targeted Drug Delivery, Hydrogen Storage and Other Applications, *Ceramic Industry*, 23–24.
3. Wicks, G.G., Heung, L.K. and Schumacher, R.F. (2008). *Unique Porous Wall Hollow Glass Microspheres for Hydrogen Storage, Separations and Other Related Applications*, Presented at The First Inter-Society ACerS/ ASM Int'l Conference Materials Innovations in an Emerging Hydrogen Economy, Feb. 24–17, 2008, Cocoa Beach, FL.
4. Mohtadi, R., Tange, T., Matsunaga, G. *et al.* (2008). "A New Way for Storing Reactive Complex Hydrides On-Board of Automobiles", in Wicks, G.G. and Simon, J. (eds), *Ceramic Transactions Vol. 202*, John Wiley and Sons, Inc., Hoboken, NJ, pp. 91–96.
5. Heung, L.K., Wicks, G.G. and Schumacher, R.F. (2008). "Encapsulation of Palladium in Porous Wall Hollow Glass Microspheres", in Wicks, G.G. and Simon, J. (eds), *Ceramic Transactions Vol. 202*, John Wiley and Sons, Inc., Hoboken, NJ, pp. 143–148.

6. Mohtadi, R., Matsunaga, T., Wicks, G.G. *et al.* (2011). Hollow Glass Microspheres as Micro Media for Complex Hydrogen Storage Compounds, *J. S. C. Nat. Acad. Sci.*, **9**, 1–4.
7. Heung, L.K. and Wicks, G.G. (2010). Hollow Porous-Wall Glass Microspheres for Hydrogen Storage, U.S. Patent No. 7,666,807, 2010.
8. Schumacher, R.F., Heung, L.K. and Wicks, G.G. (2010). Hollow Porous-Wall Glass Microspheres for Hydrogen Storage, European Patent No. EP 1,809,570, 2010.
9. Mohtadi, R.F., Wicks, G.G. and Heung, L.K. (2008). A Novel Storage Concept for On-Board Storage of Reactive Metal Hydrides, U.S. Patent Application No. 12/035,908, 2008.
10. Li, S., Dynan, W.S., Wicks, G.G. *et al.* (2010). Porous-Wall Hollow Glass Microspheres as Carriers for Biomolecules, Patent Cooperation Treaty Application No. PCT/US2010/042117, 2010.
11. Li, S., Nguyen, L., Xiong, H. *et al.* (2010). Porous-Wall Hollow Glass Microspheres as Novel Potential Nanocarriers for Biomedical Applications, *Nanomed-Nanotechnol*., **6**, 127–136.
12. Li, S., Nguyen, L., Xion, H. *et al.* (2011). Nanocarrier for Biomedical Applications, *J. S. C. Natl. Acad. Sci.*, **9**, 30–32.

Chapter 36

MOLECULAR MODELING OF BIOACTIVE GLASSES AND REACTIONS

Paul Robinson II and Larry L. Hench

36.1. INTRODUCTION

Understanding the interaction of proteins and cells with surfaces is one of the great challenges of biomaterials research. Molecular modeling of the interaction of surface sites with amino acids offers the potential to understand the effectiveness of binding of charged molecules with the material surface. West, Hench and colleagues used various levels of quantum mechanics-based semi-empirical molecular orbital (MO) models to attack this problem. The models are based upon the knowledge gained from surface chemical analyses of the bioactive glass surface, especially the early formation of a biologically active sol-gel derived silica and silanol-rich surface layer.[1]

36.2. MO MODELS OF SILICA

The quantum mechanics-based molecular orbital models involved constructing silica ring and chain structures composed of silica tetrahedra bonded with siloxane (–Si–O–Si–) bonds.[1–5] The terminal oxygen atoms of the poly tetrahedra were charge saturated with silanols (–Si–OH), based on the findings from Fourier transform infrared reflection spectroscopy (FTIR) studies of the bioactive glass surfaces.[1,4–6]

Results from the MO calculations showed energetically favorable reaction pathways for metastable states of penta-coordinated silicon in the reaction tetrahedra that could bind with H_2O and also either carboxyl or amine sites on the amino acids used to model proteins.[1,3,7–11] The findings led to a series of papers that describe an inorganic route to synthesis of polypeptide bonds.[12–14] These inorganic reaction pathways might be relevant in the activation of genes or modification of cell membrane proteins that control cell cycle, as described in Chapter 4.

36.3. PROTEIN-SILICA INTERACTIONS

An MO model was used by Lobel, West and Hench to understand the reaction pathways for diatoms to create hydrated silica frustules using the soluble silica in sea water.[13,14] Similar protein template-based reactions might have

been involved in the key genetic mutations associated with the role of soluble hydrated silica in biosilicification or onset of bone mineralization.[1,11] Latour and Hench continued these studies to understand details of proteins in the surface reactions of biomaterials.[8,10] The importance of fluorine ions in silica chemistry and silica-based glasses was also explored by Drs. Hayakawa and Hench.[15]

Ab initio (AI) calculations of similar silica molecular structures, published by Nedelec and Hench, confirmed the level of accuracy of the earlier semi-empirical MO models and provides some assurance that the conclusions from the MO models are valid.[16]

All of the above studies are described in detail along with new MO calculations in the review by Lobel, West and Hench.[11] The review includes: a comparison of various calculational chemistry methods for use in biomaterials research; examples of molecular modeling of calculated biomaterials reaction pathways; and new modeling results of molecular interactions of biological silicon with protein and saccharides that have largely eluded experimental analysis.

MO modeling of bioactive glass surfaces has been extended to fractal geometry. Fractals are a ubiquitous phenomenon found throughout nature. West, Mecholsky and Hench determined a structure parameter, a_0, correlated with fracture geometry at the atomic level, e.g. the maximum strained diameter of silica rings in bioactive glasses. This structure parameter is directly proportional to the fracture energy and the fractal dimension. It is encouraging that the fractal dimensions determined from MO simulations of atomic silica glass and silicon single crystal surfaces were found to agree with macroscopic measurements from flexure specimens scaling 3–5 orders of madnitude.[17]

36.4. NEW MODELS AND RESULTS

Modern computational modeling of bioactive glasses primarily focuses on the initial *in vivo*, five-step dissolution process of the glass network, described in Chapter 3, and the reactivity of the glass surface. The rapid formation of the subsequent bioactive hydroxyapaptite layer indicates a high level of bioactivity that ultimately depends on the rate of silica network dissolution and release of soluble silica products as either modified siloxane “fragments” or “polysiloxane chains” into the tissue environment.[18,19] Reviews by Tilocca detail modern computer modeling of bioactive glasses that study the bioactivity as a function of surface dissolution rates, composition and aqueous interaction.[18–20]

Classical molecular dynamics (MD) simulations have atomic resolutions of 0.1 nm for durations near 10 μs, but are often constrained in the melt-to-quench processing of bioactive glasses by several limitations: cooling rates are far too high for melt-to-quench simulations;[19] MD has a limited thermodynamic trajectory due to the uncertainty governing initial empirical potentials;[20] MD can introduce fictitious long-range order caused by the replicated boundaries of the analysis window.[19] By contrast, AI simulations based on first principles can simulate quantum interactions related to surface reactions and dynamic behavior in melts. Pure AI obviates the need for starter empirical potentials, yet at the cost of shorter run times (~40 ps) with relatively few atoms (100–300). The lack of long-range order in silicate glass heightens the complexity of the computational simulation approach, demanding the use of combined techniques of MD and AI (AI/MD).[19] Such a combination allows the atomic quantum behavior from AI to propagate from an initial molecular structure over shorter trajectories established by MD.[19] Researchers have investigated the bulk structural effects in various Bioglass® compositions.[21,22] Models based on the AI/MD and Car–Parrinello techniques have been applied to study the hydration of glass surfaces in relation to their bioactivity.[19,23,24] Three principal parameters are analyzed in the simulated bioactive glass structure to assess bioactivity: the number of bonding oxygens (BO); the network connectivity (NC); and the distribution of network-forming atoms (Q^n), which can be indirectly measured by nuclear magnetic resonance (NMR).[20,21] The prevalence of Si–O–Si bonds adds rigidity to the silica network, reduces the critical dissolution processes at the glass surface and correspondingly reduces bioactivity.[22] Consequently, high values of BO, NC or Q^n observed in simulation results imply a low bioactivity.

Figure 36.1 depicts the compositional dependence of bioactivity for the four component bioactive glasses. Region B is glass compositions that do not exhibit bioactivity. Region C are compositions that rapidly dissolve in contact with water or body fluids. Region A is the compositional range of glasses that are osteoconductive and bond to bone; the central portion of Region A is the small compositional range of glasses that are most bioactive (Region S) and bond to both soft connective tissues as well as bone and give rise to rapid osteostimulation and bone regeneration, as discussed in Chapters 3 and 4. The center of Region S is the grandfather composition 45S5 Bioglass®. Even now, after hundreds of compositions have been made and tested, the original 45S5 composition maintains the highest level of bioactivity of all known bioceramics.[1,25] Why? Modeling studies of bioactive glasses give insight to potential atomic interactions, which has led to

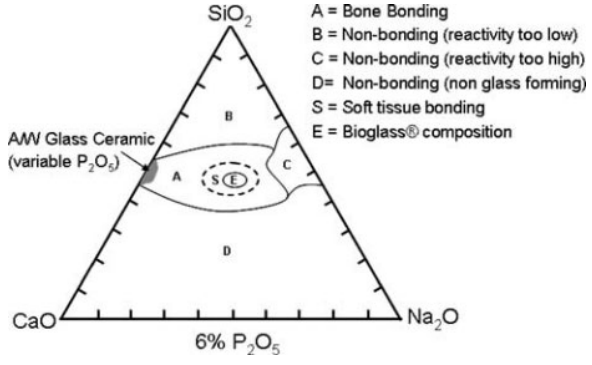

Figure 36.1. Compositional dependence of bioactive glasses.

understanding the role of each chemical constituent in bioactivity. An update on the role of these constituents based on new simulations follows.

36.5. ROLE OF SILICA

Experiments have demonstrated a reduction in bioactivity of Bioglass® compositions containing >60% SiO_2.[25] Surface relaxations of silanols only slightly restore NC at the surface, which results in higher concentrations of orthosilicate tetrahedra on the surface compared to the bulk. These free silicate species are released in solution and interact with cells as part of the ionic dissolution products that have been shown to regulate genes and cell cycles that promote osteoblastic activity (see Chapter 4).[26–28] Tilocca *et al*. used MD to compare the Q^n distributions for compositions of known bioactivity from high (45% SiO_2, S45), intermediate (55% SiO_2, S55) and no bioactivity (65% SiO_2, S65).[19,23,24] This study confirmed an observed trend of decreasing bioactivity with increasing number of bonded network-forming Si atoms (high Q^n). The model also considered the structural prevalence of silica chain fragments versus rings. Results suggest that a glass structure with a high fraction of silica chains is characteristic of highly bioactive surfaces, while a dominance of silica rings is indicative of a bioinactive surface.[18,19] While experiments have confirmed that silica dissolution benefits cell growth (Chapter 4) the proliferation and differentiation of osteoblasts on 70% SiO_2-30% CaO binary foams confirmed experimental findings that phosphorous is not necessary for bioactivity[1] and the silica concentration could be increased above 60% for sol-gel processed foams.[29] Models and computer simulations of these binary foams would enhance our knowledge of the importance of Si/Ca concentration on bioactivity.

36.6. ROLE OF CALCIUM AND PHOSPHOROUS

MD melt-to-quench simulations suggest that a larger Ca content increases rigidity in the phosphate structure.[30] In addition, Ca^{2+} and PO_4^{3-} ions form nano-aggregates of calcium-phosphate rich regions at the surface that reduce bioactivity.[22,31] Although not strictly required, some introduction of P_2O_5 has been experimentally found to enhance bioactivity.[1,32] Tilocca and Cormack showed that increasing the P_2O_5 fraction leads to repolymerization of the silica network. This increase in network connectivity supports why relatively high P_2O_5 content (>10 mol%) reduces bioactivity.[22,33] However, a small amount of P_2O_5 has been observed to enhance bioactivity. This apparent contradiction may be explained by a higher fraction (82%) of orthophosphate groups prevalent in Class A glasses than other phosphate groups having higher BO bonds.[19,30] A higher proportion of free orthophosphates may yield higher release rates at the surface that accelerates bioactivity.[20]

36.7. ROLE OF SODIUM

Since bioactivity depends on surface chemistry, recent MD trends have shifted focus of calculations to the glass surface interface with water.[20] One approach is to probe the water affinity of the silica network. Tilocca concludes that surface hydroxylation, Si network fragmentation, sodium content and free silica fragments have key influences on bioactivity.[19] Small-shell MD simulations of S45 and S65 composition suggest that Na^+ concentrations are high on the surface.[26,34] Understanding the relationship between surface dissolution, ionic release and the triggering of osteogenic cellular processes is the next step in molecular simulations of bioactive surfaces.[35]

36.8. CONCLUSION

Molecular simulations aid in the understanding of effects of constituents on the surface dissolution rates and subsequent bioactivity that assist in answering questions such as:

- What surface reactions dictate high bioactivity in the original 45S5 composition?
- What happens to the structure during a melt-to-quench cycle in wet environments when the bioactive compositions vary?

MO modeling applied to bioactive glasses has given insight to protein interactions on silica surfaces. Computational modeling of fractal geometry has related a materials parameter at the atomic level to the macroscopic geometry of fracture surfaces. AI/MD techniques have been used to model bioactive glasses in dry and wet environments. These modern computational approaches show the effects of Ca, P, Si and Na in bulk glass compositions and the relation to surface reactions at the quantum level. Advances in computational modeling may lead to future studies of more complex multi-component systems such as bioactive borate-based glasses,[36] better evaluate the influence of crystallization on bioactivity of new glass-ceramics[37] and guide research in designing novel bioactive compositions with controlled bioactivity specific to individual patients' needs.

REFERENCES

1. Hench, L.L. and West, J.K. (1996). Biological Applications of Bioactive Glasses, *Life Chem. Rep.*, **13**, 187–241.
2. West, J.K., Zhu, B.F., Cheng, Y. *et al.* (1990). Quantum Chemistry of Sol-Gel Silica Clusters, *J. Non-Crystalline Solids*, **121**, 51–55.
3. West, J.K. and Hench, L.L. (1994). AM-1 Molecular Orbital Calculations of Silica-Alanine-Nitrogen Interaction, *J. Biomed. Maters. Res.*, **29**, 625–633.
4. West, J.K. and Hench, L.L. (1994). A PM3 Molecular Orbital Model of Silica Rings and Their Vibrational Spectra, *J. Non-Crystal. Solids*, **180**, 11–16.
5. Bendale, R.D. and Hench, L.L. (1995). Molecular Orbital Models of Strained Tetrahedral Edge Shared Active Sites on Dehydroxylated Silica: An AM1 and PM3 Study, *Surface Science*, **338**, 322–328.
6. West, J.K., West, D.J. and Hench, L.L. (1998). Molecular Orbital Models of AM1 and PM3 Multi-Ring Silica Clusters and their IR Spectra, *Phys. Chem. Glass.*, **39**, 314–317.
7. Lobel, K.D. and Hench, L.L. (1998). *In Vitro* Adsorption and Activity of Enzymes on Reaction Layers of Bioactive Glass Substrates, *J. Biomed. Mater. Res.*, **39**, 575–578.
8. West, J.K., Latour, R.A. and Hench, L.L. (1997). Molecular Modeling Study of Adsorption of Poly-L-Lysine onto Silica Glass, *J. Biomed. Mater. Res.*, **37**, 585–591.
9. Lobel, K.D. and Hench, L.L. (1996). *In-Vitro* Protein Interactions with a Bioactive Gel-Glass, *J. of Sol-Gel Science and Tech.*, **7**, 69–76.

10. Latour, R.A., West, J.K., Hench, L.L. *et al.* (1997). "Adsorption of L-Lysine onto Silica Glass: A Systematic Approach combining Molecular Modeling with Experimental Analysis", in Sedel, L. and Rey, C. (eds), *Bioceramics 10,* Pergamon, Oxford, pp. 541–544.
11. Lobel, K.D., West, J.K. and Hench, L.L. (2000). "Computer Models of Molecular Structure of Biomaterials", in Vander Sloten, J. (ed.), *Computer Technology in Biomaterials Science and Engineering*, John Wiley and Sons, Inc., Hoboken, NJ, pp. 45–88.
12. Hench, L.L. and West, J.K. (1994). Inorganic Pathways for Biosynthesis: A Molecular Orbital Modeling Approach, *J. Vac. Soc. Technol. A*, **12**, 2962–2965.
13. Lobel, K.D., West, J.K. and Hench, L.L. (1996). A Computational Model for Protein-Mediated Biomineralization of the Diatom Frustule, *Mar. Biol.*, **126**, 353–360.
14. Lobel, K.D., West, J.K. and Hench, L.L. (1996). Molecular Orbital Model of the Diatom Frustule: Potential for Biomimetics, *J. Maters. Sci. Letters*, **15**, 648–650.
15. Hayakawa, S. and Hench, L.L. (2000). AM1 Study on Infra-Red Spectra of Silica Clusters Modified by Fluorine, *J. Non-Crystalline Solids*, **262**, 264–270.
16. Nedelec, J.M. and Hench, L.L. (2000). Effect of Basis Set and Electronic Correlation on *Ab-Initio* Calculations on Silica Rings, *J. Non-Crystalline Solids*, **277**, 106–113.
17. West, J.K., Mecholsky, J.J. and Hench, L.L. (1999). The Application of Fractal and Quantum Geometry to Brittle Fracture, *J. Non-Crystalline Solids*, **260**, 99–108.
18. Tilocca, A. (2009). Structural Models of Bioactive Glasses from Molecular Dynamics Simulations, *P. Roy. Soc: A-Math. Phy. Eng. Sci.*, **465**, 1003–1027.
19. Tilocca, A. (2010). Models of Structure, Dynamics and Reactivity of Bioglasses: A Review, *J. Mater. Chem.*, **20**, 6848–6858.
20. Tilocca, A. (2012). "Molecular Dynamics Methods for Modeling Complex Interactions in Biomaterials", in Navarro, M., and Planell, J.A., (eds), *Nanotechnology in Regenerative Medicine: Methods and Protocols, Methods in Molecular Biology*, Humana Press, New York, pp. 285–301.
21. FitzGerald, V., Pickup, D.M., Greenspan, D. *et al.* (2007). A Neutron and X-Ray Diffraction Study of Bioglass® with Reverse Monte Carlo Modelling, *Adv. Funct. Mater.*, **17**, 3746–3753.

22. Tilocca, A., Cormack, A.N. and de Leeuw, N.H. (2007). The Structure of Bioactive Silicate Glasses: New Insight from Molecular Dynamics Simulations, *Chem. Mater.*, **19**, 95–103.
23. Tilocca, A. and Cormack, A.N. (2009). Modeling the Water-Bioglass Interface by *Ab Initio* Molecular Dynamics Simulations, *ACS Appl. Mater.*, **1**, 1324–1333.
24. Tilocca, A. and Cormack, A.N. (2008). Exploring the Surface of Bioactive Glasses: Water Adsorption and Reactivity, *J. Phys. Chem. C*, **112**, 11936–11945.
25. Ogino, M., Ohuchi, F. and Hench, L.L. (1980). Compositional Dependence of the Formation of Calcium Phosphate Films on Bioglass, *J. Biomed. Mater. Res.*, **14**, 55–64.
26. Tilocca, A. and Cormack, A.N. (2010). Surface Signatures of Bioactivity: MD Simulations of 45S and 65S Silicate Glasses, *Langmuir*, **26**, 545–551.
27. Hench, L., Polak, J., Xynos, I. *et al.* (2000). Bioactive Materials to Control Cell Cycle, *Mater. Res. Innov.*, **3**, 313–323.
28. Xynos, I.D., Edgar, A.J., Buttery, L.D. *et al.* (2001). Gene-Expression Profiling of Human Osteoblasts Following Treatment with the Ionic Products of Bioglass 45S5 Dissolution, *J. Biomed. Mater. Res.*, **55**, 151–157.
29. Saravanapavan, P., Jones, J.R., Verrier, S., *et al*. (2004). Binary CaO-SiO_2 Gel-Glasses for Biomedical Applications, *Bio-Med. Mate. Eng.*, **14**, 467–486.
30. Tang, E., Di Tommaso, D. and de Leeuw, N.H. (2010). An *Ab Initio* Molecular Dynamics Study of Bioactive Phosphate Glasses, *Adv. Eng. Mater.*, **12**, B331–338.
31. Tilocca, A. and Cormack, A. (2008). The Effect of Nanoscale Inhomogeneity and Silicate Network Connectivity on the Activity of Glasses with Biological Applications, *Nuovo Cimento B*., **123**, 1415–1423.
32. Hench, L.L. (2005). Bioceramics, *J. of the Am. Cer. Soc.*, **81**, 1705–1728.
33. Tilocca, A., Cormack, A.N. and de Leeuw, N.H. (2007). The Formation of Nanoscale Structures in Soluble Phosphosilicate Glasses for Biomedical Applications: MD Simulations, *Faraday Discuss.*, **136**, 45–55.
34. Tilocca, A. and de Leeuw, N.H. (2006). Structural and Electronic Properties of Modified Sodium and Soda-Lime Silicate Glasses by Car-Parrinello Molecular Dynamics, *J. Mater. Chem.*, **16**, 1950–1955.

35. Cormack, A.N. and Tilocca, A. (2012). Structure and Biological Activity of Glasses and Ceramics, *Philos. T. Roy. Soc. A*, **370**, 1271–1280.
36. Yao, A.,Wang, D., Huang, W., *et al*. (2007). *In Vitro* Bioactive Characteristics of Borate-Based Glasses with Controllable Degradation Behavior, *J. of the Am. Cer. Soc.*, **90**, 303–306.
37. Peitl, O., Zanotto, E.D., Serbena, F.C. *et al.* (2012). Compositional and Microstructural Design of Highly Bioactive P_2O_5-Na_2O-CaO-SiO_2 Glass-Ceramics, *Acta Biomater.*, **8**, 321–332.

Chapter 37

CHARACTERIZATION OF BIOCERAMICS

Larry L. Hench

37.1. INTRODUCTION

The final form and properties required of a bioceramic depend upon the function served by the material as an implant (Chapter 1). The forms used include: powders, coatings and bulk shapes. The properties of interest for most implant applications are mechanical performance and surface chemical behavior. Control of properties requires control of each of the processing steps illustrated in the top half of Fig. 37.1. (See Chapter 1 for a review of these processing steps.) In order to ensure that the required final properties are achieved prior to

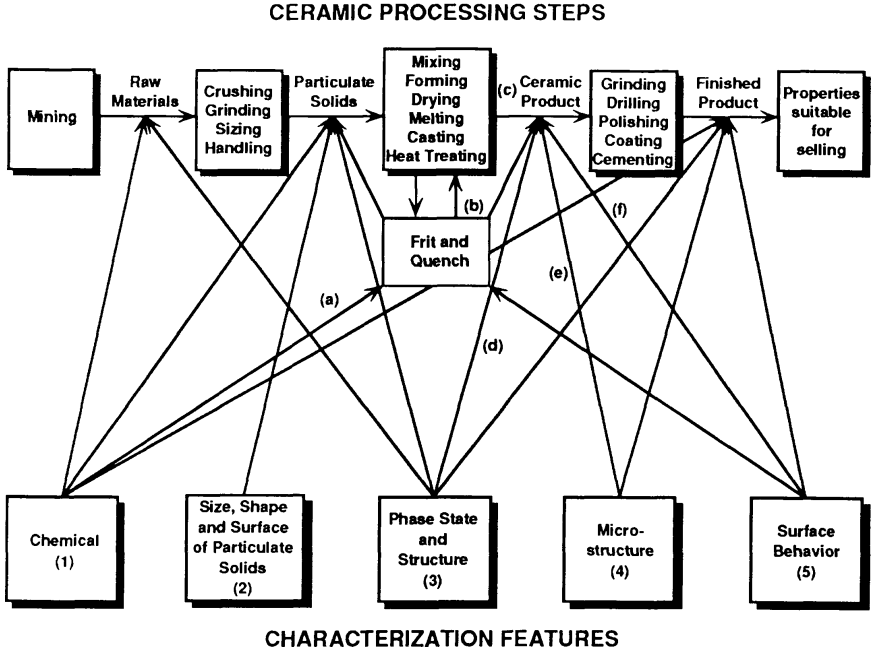

Figure 37.1. The relationship between characterization features and products of ceramic processing steps.

implantation, it is essential to characterize the bioceramic. This chapter summarizes the concepts and instrumental methods involved in the characterization of a bioceramic.

Characterization has been defined by the Materials Advisory Board of the National Research Council in the United States as:

> Characterization describes those features of the composition and structure (including defects) of a material that are significant for a particular preparation, study of properties, or use, and suffice for the reproduction of the material.

Thus, to characterize a bioceramic it is necessary to evaluate its composition, structure and surface sufficiently that the material and its properties can be reproduced.[1]

37.1.1. The Goal of Characterization is the Assurance of Reproducible Properties

The bottom half of Fig. 37.1 illustrates the five major classes or features of characterization. They are:

1) Chemical composition.
2) Size, shape and surface of particulates.
3) Phase state and structure.
4) Microstructure.
5) Surface.

Information is required on all five features to achieve reproducibility of properties for a material and device.

The arrows between the bottom and top half of Fig. 37.1 relate the characterization features, one of the five classes, to the appropriate output in the ceramic processing sequence. Two points are emphasized. First, each characterization feature indicated can be quantitatively evaluated. Second, characterization is directed towards the output of the processing steps and not to the processing method itself. The same analytical techniques may be used to investigate processing variables, but that is not materials characterization. This is an important distinction, since different processing steps can lead to similar properties.

To establish the physical origin of properties and ensure their reproducibility it is necessary to determine the composition and structure of the product and not just the specifics of the manufacturing process used. Practically, it is essential

to control the reproducibility of processing to ensure reproducibility of product properties.

37.1.2. Characterization is the Critical Step in Relating Processing to Properties

The mechanical and surface properties important for biomedical applications of ceramics depend upon all five characterization features shown in Fig. 37.1. Because bioceramics are used within the body, microstructural and surface characteristics are especially critical. The high chemical reactivity of body fluids, enzymes and cells can easily lead to the attack of grain boundaries, surfaces and interfaces between phases. Characterization of a material prior to exposure to *in vitro* and *in vivo* environments is essential if the results of such tests are to be understood and related to the potential long-term performance of the ceramic as an implant.

37.2. STRATEGY OF A CHARACTERIZATION PROGRAM

Many biomaterials have been tested in animals and even in people without adequate characterization. This is often because the developers of new biomaterials are unaware of the importance of characterization. It may also be because of expense. A strategy is necessary to minimize costs but still ensure that sufficient tests are done.

The steps in establishing a characterization strategy follow.

1) Determine the analytical costs of various instrumental methods available for each of the five classes of characterization features shown in Fig. 37.1.
2) Determine the level of accuracy required of the tests for each feature.
3) Decide the statistical confidence level desired for the tests.
4) Establish the number of samples required to achieve the desired confidence in reproducibility.
5) Determine the relative importance of the five characterization features on the final properties desired.
6) Determine relationships between properties and each of the characterization features.
7) Based upon the results of steps 1–6, compute the economics of alternative analytical tests to achieve reproducibility of properties within the desired confidence levels.
8) Select the least expensive test or combination of tests.

37.3. EXAMPLE OF A CHARACTERIZATION PROGRAM

Let us consider as an example the characterization of a bioactive glass dental implant, 45S5 Bioglass® Endosseous Ridge Maintenance Implant (ERMI)®. The ERMI® is an FDA approved Class III device (Chapters 8, 38 and 39). The clinical use of the ERMI® is described in Chapter 8. The characterization program is described in terms of the five characterization features shown in Fig. 37.1. The tolerances given in the example are used only to illustrate the steps involved in establishing a characterization program. The actual tolerances imposed commercially by the manufacturer are company confidential.

The property of most concern for the final product is its bioactivity; i.e., ability to bond to tissues. This is a surface chemical property. The mechanical requirements for the ERMI® are minimal since it is a buried implant (Chapter 8) and is subjected only to small compressive loads. The characterization strategy is therefore designed to ensure reproducible bioactivity of the ERMI®.

37.3.1. Feature 1: Chemical Composition

The nominal composition of the 45S5 glass is 45% SiO_2, 24.5% Na_2O, 24.5% CaO, and 6% P_2O_5, all in weight percent. Extensive studies of composition versus implant behavior, discussed in Chapter 3, show that SiO_2 content is the primary compositional variable that affects the rate of bonding and bioactivity of the implant.

Animal experiments show that with compositions which vary from 42 to 52% SiO_2, the implant will bond to both bone and soft tissue. There is very little effect on bioactivity with variations in Na_2O or CaO content. P_2O_5 content can also vary ±2% with little effect on bioactivity. Consequently, analytical limits on the bulk composition of the implant can be set with tolerances of ±1% for all four major chemical constituents. This level of compositional control is easy to achieve in glass processing. The tolerance of chemical analysis can be set at any value up to ±0.5% and detect variations within the ±1% control range. Automated analytical methods such as X-ray fluorescence, routinely used in the glass industry, are inexpensive and achieve this level of tolerance easily for Si, Na, Ca and P.

In vivo studies, reviewed in Chapters 3 and 15, show that cation impurities with 3+, 4+, 5+ charges, such as Al^{3+} or Ta^{5+}, can inhibit formation of a hydroxycarbonate apatite (HCA) layer on a glass and destroy bioactivity. The compositional limit for the impurities varies for each element but the effect becomes significant at concentrations >1%. Thus, a limit for total impurity content of

multivalent cations is set at 0.5%, which allows for a margin of analytical error. X-ray fluorescence analysis is also suitable for this measurement and it can be obtained at the same time as the bulk compositional analysis of a glass batch, thereby minimizing costs.

37.3.2. Feature 2: Size, Shape and Surface of Particulate Solids

The ERMI® can be made from either a raw glass batch or from glass frit. (A raw glass batch is a mixture of the constituent oxide powders which are melted in a crucible, refined, homogenized and cast into the final implant shape, following a schedule similar to that illustrated in Chapter 1.) A glass frit is an intermediate processing step which produces large glass particles by quenching a molten batch of glass into water or onto a steel plate or rollers. The particles of a glass frit are either remelted and cast into a shape in a forming process or ground into a specific powder size for use in applications such as periodontal repair or bone augmentation, see Chapters 3 and 6–12.

If a glass frit is used in processing it results in an additional, intermediate processing step, as indicated in the top half of Fig. 37.1. The frit can be analyzed for chemical composition (path A), remelted (path B) and cast into an implant (path C). Since no additional finishing is required, the implant can then be characterized for phase state and structure (path D), microstructure (path E) and surface behavior (path F).

This sequence of processing-characterization steps has the advantage that chemical compositional analysis of a large batch of glass frit is less expensive than analysis of many small raw batches of glass. A disadvantage is the potential for pick-up of impurities during fritting-remelting operations. There is also the economic advantage that a composition that does not meet specifications will be detected before the costs of fabricating implants are incurred.

The decision as to which combination of processing and characterization steps to follow is based upon relative economics and depends very much upon the scale of operations and the ability to control the cleanliness of each process step. The goal of characterization is to ensure that, whichever sequence is chosen, the results are the same and within the tolerance levels required for good manufacturing practices by regulatory agencies (Chapters 38 and 39).

An advantage of the intermediate glass fritting step is that mixtures of compositions can be made and then formed into shapes and densified by sintering or hotpressing. This is the sequence of processing followed in the manufacture of A/W glass-ceramic (Cerabone®), as described in Chapters 13 and 14.

The resulting glass-ceramic has a composite structure with superior mechanical properties and still retains bioactivity.

A decision on which processing steps to use in making implants must be accompanied by a decision on characterization steps. The characterization strategy must be compatible with processing and vice versa. The costs of characterization are additional to processing costs and must not be excessive.

37.3.3. Feature 3: Phase State and Structure

The objective of this characterization step is to determine whether the implant is crystalline or amorphous. ERMI® implants are amorphous, glassy materials and crystals are undesirable because they can lead to heterogeneous surface reactions. Improper melting, casting or annealing can lead to crystallization (Chapter 1). Therefore, a characterization step is necessary to ensure that crystallization has not occurred. Several methods are available, including X-ray diffraction (XRD). The XRD spectrum (A) in Fig. 37.2 shows that a 45S5 Bioglass® implant is amorphous; no diffraction peaks are present. There is only a

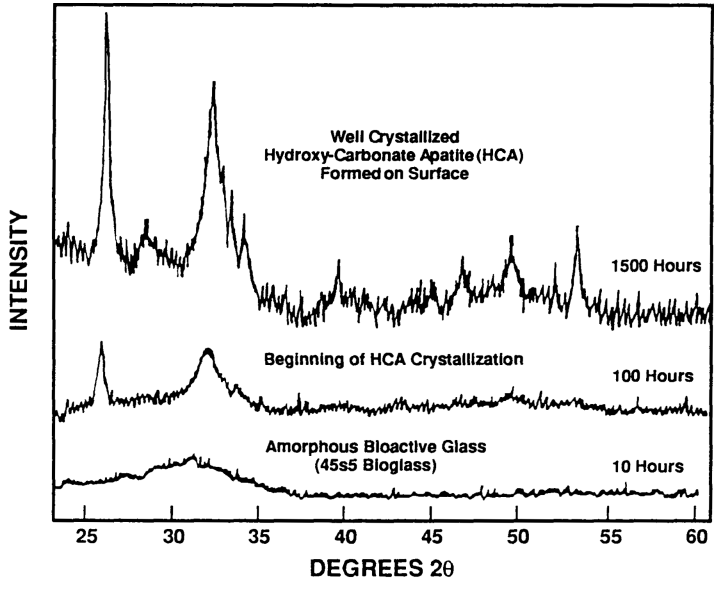

Figure 37.2. XRD pattern of the surface of 45 wt% bioactive silica glass containing 6 wt% P_2O_5 after exposure to a simulated physiological solution for 10, 100 and 1500 hours.

broad diffraction region, characteristic of the short range ordering of the silicate structure in glasses (Chapter 1).

Crystals grown in glass due to processing problems are usually visible to the eye and the least expensive method of characterization is visual inspection by an optical microscope.

Complex multi-phase, polycrystalline materials, such as bioactive glass-ceramics, require characterization of the type of each crystal phase present and the volume fraction of the crystal phases. A mixture of crystal phases and glassy matrix, such as in A/W glass-ceramic, requires an analysis capable of determining the volume fraction of the amorphous matrix. This is difficult, except by subtraction; i.e., one must determine the crystal phase percentages by XRD or optical microscopy, then subtract from 100% to obtain the percent of glass present. Figure 37.3 shows an XRD spectrum of A/W glass ceramic with a mixture of apatite and wollastonite crystal phases.

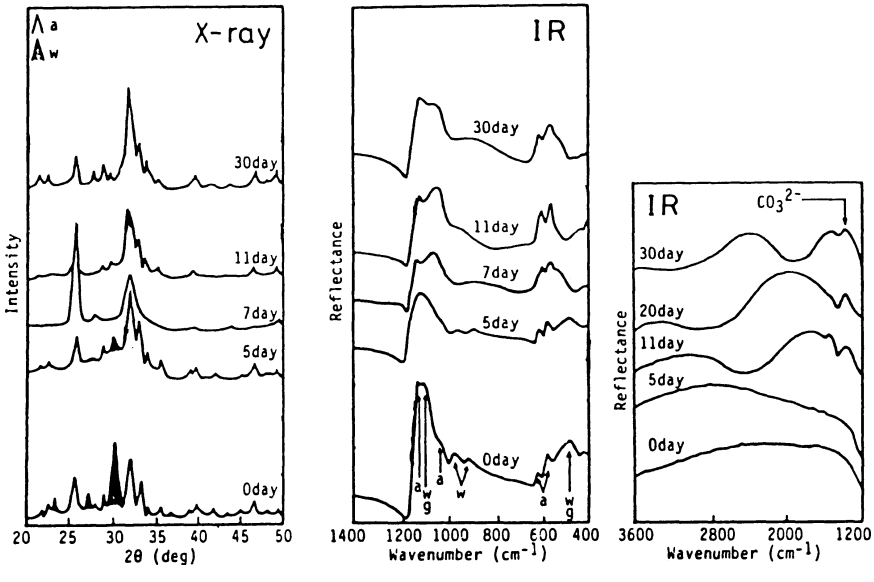

Figure 37.3. Thin film XRD patterns and FT-IR reflection spectra of the surface of A/W glass-ceramic exposed to simulated body fluid (K-9) for various times; a = apatite crystal phase, w = wollastonite crystal phase, g = glassy phase. Note the disappearance of the wollastonite phase as a surface layer of HCA grows. (Modified from Kokubo, T., Hayashi, T., Sakka, S., *et al.* (1987), "Surface Structure of Load-Bearing Bioactive glass-ceramic A-W" in Vincenzini, P. (ed.), *Ceramics in Clinical Applications*, Elsevier, Amsterdam, pp. 175–184.)

37.3.4. Feature 4: Microstructure

This is one of the most important characterization features for bioceramics. Microstructure usually controls mechanical properties and can influence surface behavior due to the presence of phase boundaries, missing grains or inclusions. For example, the ASTM and ISO standards for alumina implants (Chapter 2) establish a limit of <7 μm on mean grain size. Quantitative microscopy, using either optical or scanning electron microscopy (SEM), is the method usually used in analyzing microstructure. Characterization involves the determination of size distribution of grains, size distribution and volume fraction of porosity, phase boundary area and connectivity of phases in a multiphase microstructure. For details of the use of quantitative microscopy (also called stereology) to obtain these features, consult DeHoff.[2]

For a glass implant such as an ERMI, microstructure is not so important. Visual inspection is sufficient to ensure that inclusions or bubbles are absent. However, microstructural characterization of a multiphase glass-ceramic requires analysis of the size, volume fraction and distribution of each of the phases. This can be a big effort and is usually done with an image analyzing computer. In Chapters 13 and 16 micrographs of the complex microstructures present in multiphase bioceramics are shown. A characterization program must establish which of the many microstructural features is most important in controlling the mechanical and surface properties of the material and concentrate the analysis on one or two features, otherwise costs become prohibitive.

Microstructural characterization of a two-phase bioactive composite, such as polyethylene-HA (Chapter 16), is particularly important, since the volume fraction of the phase controls mechanical properties. The second phase must be dispersed homogeneously to be effective. A critical volume fraction of the bioactive phase is necessary for the composite to be bioactive. Thus, analysis of volume fraction and distribution of the two phases are critical in a characterization program for composites.

37.3.5. Feature 5: Surface Behavior

The surface of a biomaterial becomes an interface with tissues upon implantation. Consequently, characterization of the surface features is of vital concern if an implant is to achieve reliable long-term behavior. There are many different surface analytical methods available. The most important problem is often the determination of which surface feature is relevant to the biological and biomechanical performance of an implant. Experiments are required to establish

the relationships between surface analysis and *in vivo* and *in vitro* behavior. Only after these relationships are known is it possible to decide on the characterization method(s) to use and the tolerances required to ensure reproducibility.

The characterization of Bioglass® ERMI® dental implants is used to illustrate surface analytical methods and how to decide on a characterization criterion. There are two approaches for analyzing the mechanisms and reactions at an implant surface. First, the constituents released into a test environment or surrounding tissues can be analyzed. The traditional wet chemical methods, such as atomic emission, absorption spectroscopy or inductively coupled plasma (ICP) chemical analysis, can be used to do this. See Adair and Casey for a summary of analytical methods available and their levels of tolerance.[3]

When bioactive glass implants are exposed *in vivo* or *in vitro* to solutions Na, Ca, Si and P, ions are released from the glass surface. The loss of cations is due to ion exchange with H+ and H_3O+ ions from the solution. These reactions correspond to surface reaction Stages 1 and 2 discussed in Chapter 3. The decrease of P in the solution is due to the formation of an amorphous calcium-phosphate layer on the glass surface (Stage 4). Solution analysis, however, provides no understanding of the changes occurring on the surface of the implant. For example, Stage 3-formation of the silica gel layer or Stage 5-crystallization of the HCA layer cannot be identified from solution analysis alone.

A second approach, surface analysis of the material, is also required to determine compositional gradients or phase changes taking place. Figure 37.4 summarizes the range of instrumental methods available for surface characterization. They can be classified into two groups: those sampling deep (up to 1.5 μm) into the surface and those that examine only the "outer surface" (0.5–5.0 nm) of the material.

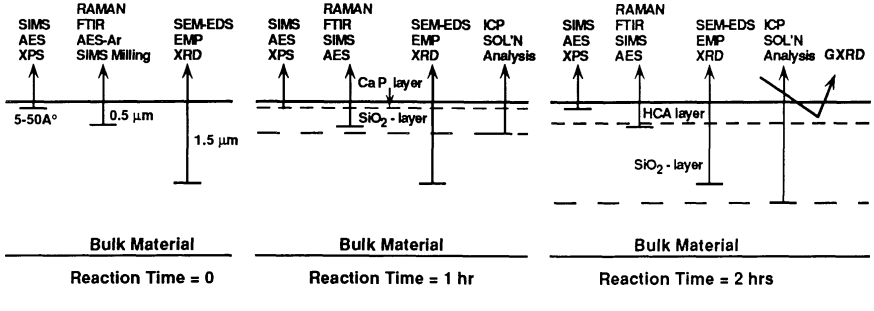

Figure 37.4. Alternative methods for surface characterization of a bioactive implant. (a) Surface before reaction, reaction time = 0. (b) After one hour reaction. (c) After two hours reaction. Note the effect of instrumental sampling depth on the surface analysis.

Results from several of these methods applied to the surface characterization of bioactive glasses, ceramics and glass-ceramics follow.

Figure 37.4 also summarizes the problem faced in characterizing the surface and interface of a bioactive ceramic. The composition and phases of the material change with time. Thus, analysis of the surface prior to implantation, Fig. 37.4a, may or may not be predictive of the interface of the material after implantation, illustrated in Figs 37.4b and 37.4c. The analytical methods chosen must be capable of following these kinetic changes in a reproducible manner. For a bioactive glass-ceramic or bioactive composite with multiple phases, the time-dependent changes of each phase need to be understood before a characterization program can be established.

37.3.6. Infrared Reflection Spectroscopy (IRRS)

This is one of the most versatile, rapid and cost-effective means of surface analysis, especially with the use of a Fourier transform IR (FTIR) spectrometer.[4] As shown in Fig. 37.4, IRRS examines the surface of a glass or ceramic to a depth of approximately 0.5 μm, depending upon the index of refraction and density of the surface layer. It is non-destructive, requires no vacuum or sample preparation and is applicable to samples of any dimension, even those with curvature. An implant can be analyzed before and after *in vitro* or *in vivo* testing.

An FTIR can be used in either specular reflection or diffuse reflection mode, as discussed by LaTorre and Hench.[4] The diffuse mode is particularly useful when there is considerable scattering from surface reaction layers. Analysis of powders requires use of a diffuse scattering stage.

The IRRS method gives quantitative information of the chemical composition of the surface since it is sensitive to the vibrational modes which are characteristic for each molecular constituent of the material. Since Si-O-Si bonds differ in energy from Si-O-Na or Si-O-Ca bonds, their vibrational frequencies are different. Changes in these vibrations can be detected when the surface composition is altered by chemical reaction with a solution, as illustrated in Fig. 37.3 for A/W bioactive glass-ceramic. Thus, the kinetics of surface compositional change can be followed with IRRS. Details are discussed in Chapters 3 and 13.

An FTIR surface analysis can also detect phase changes occurring within a surface layer. The crystallization of an HCA layer on a bioactive glass surface is apparent in Fig. 37.5. The single P-O mode of the amorphous calcium phosphate layer (surface reaction Stage 4, discussed in Chapter 3) is transformed into two separate P-O modes when the apatite crystals are formed. Eventually three P-O modes characteristic of well-developed apatite crystals are observed, as

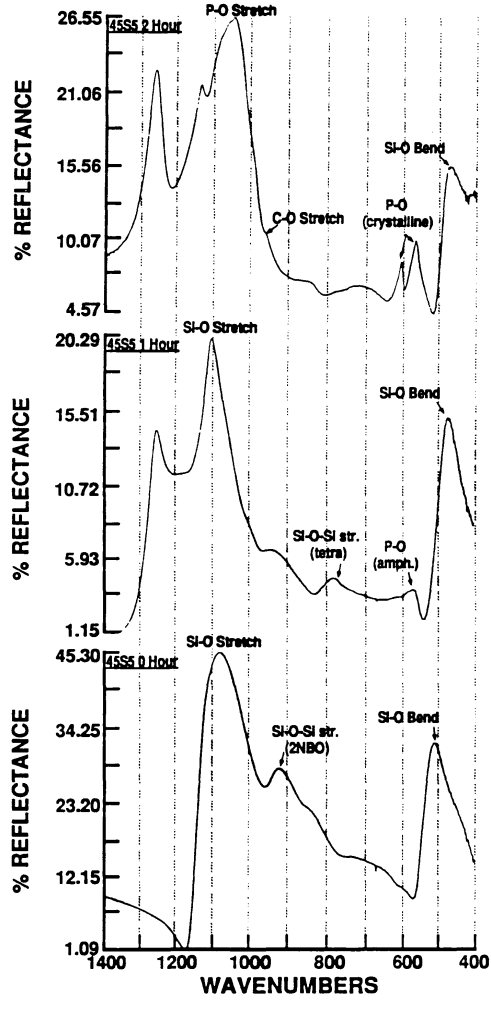

Figure 37.5. FTIR diffusion reflection spectra of a 45S5 bioactive glass before reaction (0 hrs) and after 1 hr and 2 hr reaction in simulated body fluid. Note the formation of amorphous calcium phosphate at one hour and HCA at two hours.

shown in Fig. 37.5, after longer times.[5] The crystalline HCA layer is also detected with XRD, as shown in Fig. 37.2. Because of its versatility and speed, the diffuse reflection FTIR method can be used as a quantitative quality assurance test method with either bulk samples, such as the ERMI dental implant, or powders.

Infrared microscopy combines optical microscopy with IR spectroscopy, which makes it useful for analysis of surface features, surface profiles and microstructural features. This method is described in the LaTorre and Hench article and applied to the analysis of a bioactive glass–bone interface.[4]

Fourier transform Raman spectroscopy (FT-Raman) can also be used for the analysis of surfaces before and after reaction. It is a method with very high resolution and is especially sensitive to the extent of crystallization of the surface. The Raman modes arise from molecular vibrations of the surface but electron transitions involved are different than IR modes, which yield complementary information on the composition and phase state of the surface layers.

37.3.7. Scanning Electron Microscopy (SEM) with Energy Dispersive X-ray Spectroscopy (EDS)

SEM-EDS is a rapid characterization method for surfaces and interfaces and it is probably the most widely-used instrument for this purpose. It must be remembered that there is a deep sampling depth of several μm (Fig. 37.4) for this method. The important advantage of the SEM method is that microstructural and surface features can be observed and their dimensions and area fraction measured. The composition of the surface and microstructural features can then be analyzed chemically with EDS. The size of the electron beam can be modified and the area analyzed varied. A characterization program must experimentally establish a standard sampling area and standards for the analytical results, with appropriate calibrations, in order for the data to be quantitative.

Figure 37.6 shows SEM-EDS results from the interface between a 45S5 Bioglass® implant and a rat tibia, bonded for 30 days. Areas 1 and 2 show a large Si signal from the silica-rich layer formed on the glass. Areas 3 and 4 are from the calcium phosphate-rich layer and bone, respectively.

37.3.8. Electron Microprobe Analysis (EMP)

This electron beam method is excellent for determining the thickness and compositional gradient of reaction layers formed on bioceramic implants. Figure 37.7 illustrates the type of data obtained for a 45S5 Bioglass® bone interface. The intensity of the X-ray signal for each element (which is proportional to composition) is plotted as a function of distance across the interface. Moving from the surface of the implant to the bone, there is a large increase in concentration of Si due to the formation of a repolymerized SiO_2 layer on the glass. The thickness of this layer is about 80 μm.

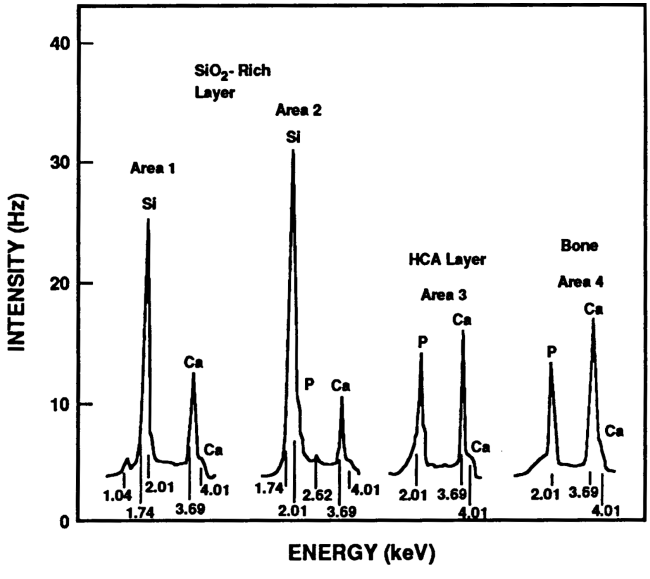

Figure 37.6. SEM-energy-dispersive X-ray analysis of the interface between a 45S5 Bioglass® implant and a rat tibia, bonded one month. Areas 1 and 2 show a large signal from the silica-rich layer formed on the glass. Areas 3 and 4 are from the calcium phosphate-rich film and bone, respectively.

Next, there is a gradual decrease in the Si signal accompanying a progressive increase in Ca and P intensity as the electron beam traverses the HCA layer grown on the glass. The thickness of the HCA layer is about 20 μm. The Ca and P signals then drop to a constant value characteristic of bone mineral. The dashed line in Fig. 37.7 is the Vickers hardness gradient across the interface.

Determining interfacial compositional profiles, such as shown in Fig. 37.7, is essential in understanding the behavior and *in vivo* performance of a bioactive implant, but is not desired for characterization of an implant. The objective of characterization of the surface is to ensure that a profile such as in Fig. 37.7 will be routinely obtained without having to perform 30–180-day tests in animals.

37.3.9. Auger Electron Spectroscopy (AES)

As shown in Fig. 37.4, AES examines the outermost surface of a material with a resolution on the scale of 0.1 nm. AES combined with Ar ion milling, which removes 1 to 50 Å slices of a surface between AES analysis, is one of the

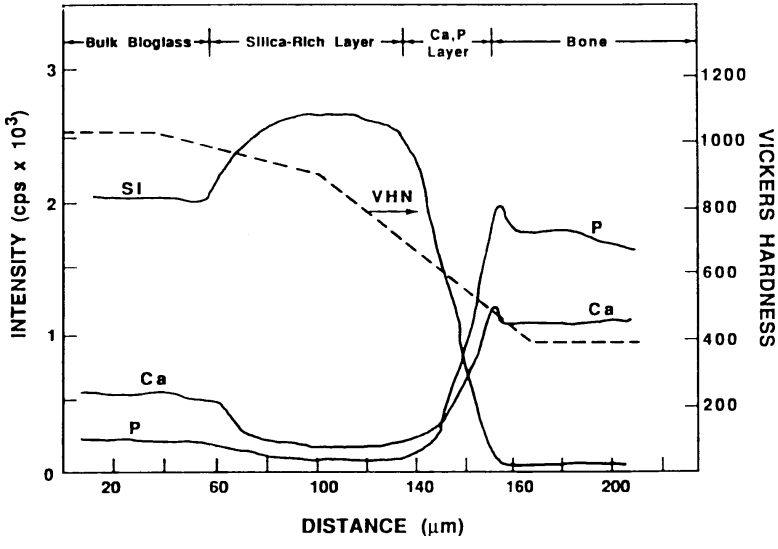

Figure 37.7. Compositional profile across a rat tibia-bioactive glass (45S5) interface after one year. Obtained with electron beam microprobe. Dashed line is Vickers hardness gradient across the interface.

most accurate methods for determining compositional gradients within the outermost layers of a bioceramic.[7] Figure 37.8 illustrates a compositional profile of a 45S5 Bioglass® implant removed from a rat bone after only one hour of implantation. The SiO_2-rich layer and CaP-rich layer have already developed within this short reaction time. C and N signals from adsorbed biological constituents are also detected within the interfacial reaction layers. This result is especially important from the standpoint of surface characterization because it means that the kinetics of formation of the surface reaction layers on the implant is the most important feature of the material.

37.3.10. Secondary Ion Mass Spectroscopy (SIMS)

This method also involves the removal of surface layers of the material, atom by atom, and the measurement of the concentration of the atoms removed with a mass spectrometer. It yields a very accurate compositional profile including many elements. The instrument is expensive and requires considerable expertise in its operation but produces the best overall results for complex interfaces.

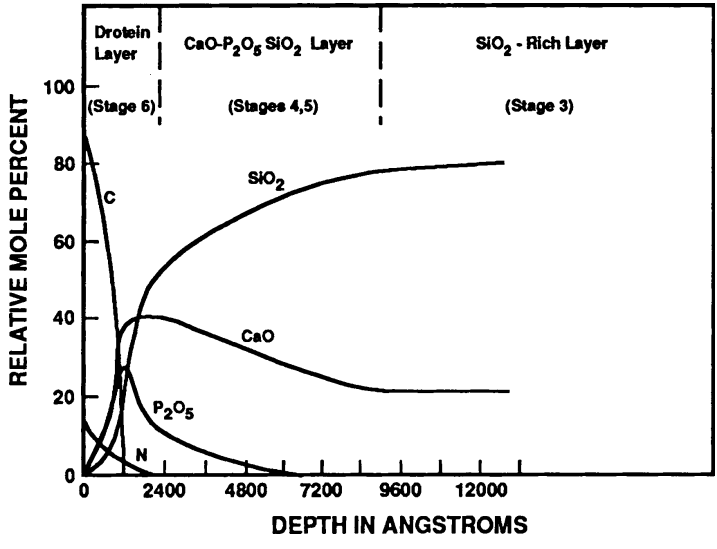

Figure 37.8. Surface compositional profile of bioactive glass (45S5 Bioglass®) obtained with AES and Ar-ion beam milling after one hour exposure to rat bone.

37.3.11. Surface Charge Analysis

The surface charge of a bioceramic influences the adsorption of proteins and other biological constituents and affects the response of tissues in contact with it. The sign and magnitude of surface charge are determined by the composition of the material, the crystal phases in the material, the defects in crystalline phases and the pH of the solution in contact with the material. A material will have a zero point of charge (ZPC) at a particular pH where surface positive charges balance surface negative charges. At pH values above this point, also known as the isoelectric point (IEP), the material will exhibit a positive charge. At pH values below the IEP the material will exhibit a negative charge. The pH of body fluids is acidic, <7, during wound healing, slightly alkaline, 7.4, in normal conditions, and alkaline, >7.4, during bone mineralization. Thus, it is important that bioceramics used in bone repair have surface charges compatible with the range of solution pH occurring during the healing and mineralization of bone.

One of the most useful methods for determining surface charges of bioceramics is a zeta potential measurement. Ducheyne and coworkers discuss this method and its use in characterizing the behavior of various calcium phosphate ceramics.[8] They have shown that the cationic defect structure of stoichiometric

and Ca-deficient hydroxyapatite has a large effect on the surface charge of the materials. They also show that the magnitude and duration of the changes in zeta potential of the apatites are related to an ion exchange between the hydrated layer around the ceramic surface and a net precipitation of new material. The zeta potential method should be considered as a characterization method for calcium phosphate ceramics to determine the relative effect of defect structures on surface properties.

37.3.12. The Decision

Deciding on a specific test or combination of tests is difficult but must be done. As discussed in Chapter 3, experiments established that the critical step in the reaction stages of a bioactive glass implant is formation of the HCA layer. The tissue response correlates directly with the time of HCA formation. Thus, the critical characterization test is the determination of the time of HCA formation. As described above, many different analytical methods can be used to show development of an HCA layer on the glass: XRD, FTIR, FT-Raman, SEM-EDS, EMP, AES and SIMS. Which one should be chosen?

Step 7 in "Development of a Characterization Strategy" states that the decision on test(s) to be used should be based upon relative economics, without sacrifice of accuracy. Economic analysis of the alternative methods listed above requires taking into account a number of factors: time of analysis, time and cost of sample preparation, cost of analysis, cost of instrument, maintenance costs, operator costs, operator skill, reproducibility with different operators, and availability of instrument.

When these factors are taken into consideration, the favored characterization method for bioactive glasses is FTIR analysis, before and after an *in vitro* test simulation of the physiological environment. The characterization requirement is that the glass develops a fully crystallized HCA reaction layer within a specified period of time, for example 20 hours, when exposed to a simulated body fluid (SBF) at 37°C.

The SBF chosen for the characterization program was based upon experiment. Kokubo and coworkers[9] showed that the *in vitro* behavior of A/W glass-ceramic most closely matched *in vivo* behavior when the material was tested in the SBF composition listed in Table 37.1. This composition was based upon analysis of human body fluids, previously reported,[10] and includes important constituents, such as soluble calcium, phosphate ions and carbonate ions. The chemicals used in making up the SBF solution are given in Table 37.2, courtesy of Professor Kokubo.

Comparative studies of various bioactive glass compositions and SBF solutions, summarized in Chapter 3, showed that the rate of HCA formation on

Table 37.1. Ion Concentration (mM) of SBF and Human Blood Plasma.

Ion	Simulated Fluid	Blood Plasma
Na^+	142.0	142.0
K^+	5.0	5.0
Mg^{2+}	1.5	1.5
Ca^{2+}	2.5	2.5
Cl^-	147.8	103.0
HCO_3^-	4.2	27.0
HPO_4^{2-}	1.0	1.0
SO_4^{2-}	0.5	0.5

Table 37.2. Reagents for Preparing SBF#9.

Order	Reagent	Purity	Amount
1	NaCl	For Biological work	7.996g
2	$NaHCO_3$	Certified A.C.S.	0.350g
3	KCl	Certified A.C.S.	0.224g
4	$K_2HPO_4 \cdot 3H20$	99+%	0.228g
5	$MgC1_2 \cdot 6H20$	Assay 99.7%	0.305g
6	1N–HCl		40 ml (about 90% of total amount of HCl to be added)
7	$CaCl_2$	Assay 99.6%	0.278g
8	Na_2SO_4	Certified A.C.S.	0.071g
9		Assay 100.1%	6.057g
3	$NH_2C(CH_2OH)$		

many bioactive glasses exposed to the solutions given in Table 37.1 correlates well with *in vivo* results.

Thus, the critical surface characterization test for a bioactive glass is the time taken for HCA formation when exposed to SBF K-9 at 37°C.

37.4. CONCLUSION

This chapter shows that it is necessary to characterize many different features of an implant in order to determine which is critical to achieve reproducibility. After the critical characterization feature(s) are determined, it is necessary to

establish the tolerances needed for reproducible performance. Then it is possible to compare relative economics of the methods suitable for characterization. A systematic effort is required to develop a cost-effective set of tests that guarantee reproducibility. It is time consuming to follow such a systematic test program but the eventual savings and reliability are worth it in the end. Regulatory requirements are fulfilled by achieving such reliability and reproducibility (Chapters 38 and 39).

REFERENCES

1. Hench, L.L. and Gould, R.W. (eds) (1971). *Characterization of Ceramics*, Marcel Dekker, New York.
2. DeHoff, R.T. (1968). "Curvature and the Topological Properites of Interconnected Phases", in DeHoff, R.T. and Rhines, F.N. (eds), *Quantitative Microscopy*, McGraw-Hill, New York, pp. 291–324.
3. Adair, J.H. and Casey, J.A. (eds) (1993). *Characterization Methods for the Solid-Solution Interface in Ceramic Systems*, American Ceramic Society, Westerville, OH.
4. LaTorre, G. and Hench, L.L. (1993). "Analysis of Bioactive Glass Interfacial Reactions Using Fourier Transform Infrared Reflection Spectroscopy", in Adair, J.H. and Casey, J.A. (eds), *Characterization Methods for the Solid-Solution Interface in Ceramic Systems*, American Ceramic Soc., Westerville, OH, pp. 177–195.
5. Andersson, O.H., LaTorre, G. and Hench, L.L. (1992). "The Kinetics of Bioactive Ceramics, Part II: Surface Reactions of Three Bioactive Glasses", in J. Hulbert, E. and Hulbert, S.F. (eds), *Bioceramics, Vol. 3*, Rose-Hulman Institute of Technology, Terre Haute, IN, pp. 46–53.
6. Hench, L.L., Andersson, O.A. and LaTorre, G.P. (1991). "The Kinetics of Bioactive Ceramics, Part III: Surface Reactions for Bioactive Glasses Compared with an Inactive Glass", in Bonfield, W., Hastings, G.W. and Tanner, K.E. (eds), *Bioceramics, Vol. 4*, Butterworth-Heinemann Ltd., Guildford, pp. 155–162.
7. Hench, L.L. and Clark, D.E. (1982). "Surface Analysis of Glasses", in Casper, L.A. and Powell, D.J. (eds), *Industrial Applications of Surface Analysis*, American Chemical Society, Columbus, OH, pp. 204–228.
8. Ducheyne, P., Kim, C.S. and Pollack, S.R. (1992). The Effect of Phase Differences on the Time Dependent Variation of the Zeta Potential of Hydroxyapatite, *J. Biomed. Mater. Res.*, **26**, 147–168.

9. Kokubo, T., Kushitani, H., Sakka, S. *et al.* (1990). Solutions Able to Reproduce *In Vivo* Surface-Structure Changes in Bioactive Glass-Ceramic A-W, *J. Biomed. l Mater. Res.*, **24**, 721–734.
10. Gamble, J. (1967). *Chemical Anatomy, Physiology and Pathology of Extracellular Fluid, 6th Edition*, Harvard University Press, Cambridge, MA.

Chapter 38

REGULATION OF MEDICAL DEVICES: HISTORICAL

Emanuel Horowitz and Edward Mueller

Editor's Note: *This chapter is an abbreviated version of Chapter 19 of the first edition of An Introduction to Bioceramics emphasizing the historical needs and approaches taken to ensure safety and efficacy of medical devices and the biomaterials used to make them. Numerous changes have taken place during the last 20 years regarding the regulation of medical devices. The following chapter by Dr. David Greenspan summarizes the current status of medical device regulation and provides websites for details regarding obtaining FDA and EU clearance that are beyond the scope of this textbook.*

38.1. INTRODUCTION

The government regulation of medical devices and biomaterials is a complex and difficult task. Regulations should be effective in protecting patients from undue risk without discouraging technical innovations and development. A renowned surgeon, Dr. Dwight Harken, often stated that "A device is safe when it is safer than the disease it corrects and is the best available". Dr. Harken's words illustrate what must be at the heart of a good regulatory system, i.e. a capability of assessing risk-to-benefit ratios. It is important to characterize unambiguously product performance and to be able to assess risks and benefits in a comparable and defensible fashion. To do this requires a strong interplay between all areas of science, engineering, and medicine and most importantly an understanding, by the public, that regulations do not create new knowledge but instead coordinate existing knowledge. Because a product has been assessed in a regulatory sense does not mean it will never fail to perform.

In this chapter, a brief review of the Food and Drug Administration's (FDA) regulation of medical devices is provided. This review will discuss the revision to the Medical Devices Act and will discuss initiatives the Food and Drug Administration Center for Devices and Radiological Health (FDA/CDRH) considered to facilitate and improve the review process. A section is devoted to the role of standards and shows how they play an increasingly important role.

38.2. THE BEGINNING OF REGULATION: PRE-FOOD, DRUG AND COSMETICS ACT (1938)

Prior to 1938 and the passage of the Food, Drug and Cosmetics Act, the federal government had limited power to regulate unsafe practices and protect the health and safety of the public. The FDA, which was established in 1930, had evolved from the Food, Drug and Insecticide Administration, which was formed in 1927. In 1937 an elixir of sulfanilamide containing a poisonous solvent was marketed, resulting in the death of 107 people, mostly children. This incident dramatized the need for new legislation designed to protect the public. The following year, Congress passed the Federal Food, Drug and Cosmetics Act of 1938.

38.2.1. The Food, Drug and Cosmetics Act of 1938

The Act of 1938 authorized the FDA to regulate medical devices by establishing requirements for their safety. In addition, it defined a medical device as *any instrument, apparatus, or contrivance, including any and all components or parts, that were intended for use in the diagnosis, cure, treatment or prevention of disease in man or in other animals.*

Regulations were established to control misbranded or adulterated medical devices which were involved in interstate commerce. Misbranding meant that the labeling was incorrect or misleading or it did not properly identify the manufacturer, packager, or distributor or provide information on the quantity of the contents of the package. Adulteration included devices which were dirty and/or were prepared or packaged under unsanitary conditions.

The 1938 legislation lacked true effectiveness because, unlike drugs, it did not require premarket clearance for medical devices which were involved in interstate commerce. This meant that medical devices could be marketed before being cleared by the federal government in accordance with accepted clearance procedures. During the period that this law was in effect the FDA was limited to enforcing labeling provisions and removing fraudulent medical devices from the marketplace.

The medical advances in science and engineering during the 1940s and 1950s impacted strongly on medical technology. New materials made of polymers, metals, alloys, and ceramics were introduced and found application in newly designed medical devices, while advances in electronics led to the development of entirely new and more complicated medical systems. As the number of medical devices and implants being used on patients increased, particularly in

applications which involved life-saving or life sustaining treatment, the number of adverse reactions and failures grew. It soon became clear that the provisions of the Act of 1938, drafted to protect the public from unsafe or ineffective devices, was inadequate. This led to the confusing situation where some courts of law ruled that certain medical devices could be treated as drugs and regulated accordingly. It was clear that new and more effective legislation was necessary.

38.2.2. The Medical Device Amendments of 1976

In 1969 president Richard Nixon appointed Dr. Theodore Cooper, the Director of the National Institutes of Health's National Heart Institute, to chair a presidential commission, later known as the Cooper Committee, to study the need for increased federal regulation of medical devices.[1] The Cooper Committee found that problems traceable to medical devices had caused about 10,000 injuries and more than 700 deaths over a 10-year period. Their findings and recommendations spurred the passage of the Medical Devices Amendments of 1976,[2] which became law on May 28, 1976. The FDA now had the legal authority to regulate medical devices, especially with regard to their labeling, marketing, manufacture, processing, distribution, and use. A sharp distinction was drawn between medical devices and drugs. Those products that are not metabolized or are not dependent on being metabolized in order to achieve their intended purpose were to be regulated as devices and not drugs. Furthermore, the 1976 definition of a device was somewhat expanded and encompassed instruments, apparatus, implements, machines, contrivances, implants, *in vitro* reagents, or other similar or related articles. It included any component or part which was used in the diagnosis of disease or other conditions, or in the cure, mitigation, treatment, or prevention of disease in man or other animals. Actions which were prohibited under the law included adulteration and misbranding of devices destined for interstate commerce.

The medical device types covered by the legislation of 1976 numbered about 1,700 and were categorized in the following ways:

- over-the-counter devices which did not require a prescription;
- prescription devices;
- investigational devices which were in the development phase and could be used on humans only to obtain safety and effectiveness data; and
- custom devices which met the special needs and requirements of an individual patient.

Also included were critical devices which were defined in the Good Manufacturing Practice Regulation (GMP) as devices which were life supporting or life sustaining.

38.2.3. The Safe Medical Devices Act (SMDA) of 1990

The Act of 1990[3,4] provided new enforcement authority for the FDA, to strengthen the ability of the agency to regulate medical devices and prevent the use of unsafe and ineffective products. The law also modified the classification and reclassification of medical devices and, in turn, affected the premarket notification and premarket approval procedures. It also changed the good manufacturing practices requirements. Most significantly, the new law provided the FDA with a much broader authority to collect data and monitor devices after they have been cleared for marketing. Some of these new authorities, briefly discussed below, include user reporting, tracking, post marketing surveillance, special controls and standards, and revisions to premarket notification 510(k) and premarket approval (PMA) requirements.

38.2.3.1. *User Reporting*

When a medical device fails in service and causes death or serious injury, user facilities, which include hospitals, nursing homes, outpatient treatment and surgical facilities, are required to report such cases to the manufacturer and, in cases of death, to the FDA. User facilities must submit a semiannual report to the FDA which summarizes their reports of such incidents. This user reporting provision is an extension of the existing mandatory device reporting regulation, which required manufacturers to report death and serious injury information to the FDA.

38.2.3.2. *Tracking*

Manufacturers of certain high-risk medical devices are required to establish a method for tracking their products whose failure would jeopardize the heath of the patient. For life-sustaining medical devices, used outside a user facility, and some kinds of permanent implants, the new regulations require that the device manufacturer establishes a system for identifying and locating a device at any given time.

All device manufacturers must report any removals or corrective actions taken to reduce the risk to the patient's health or remedy a violation of a medical

device requirement. This requirement is intended to facilitate recall and notification provisions of the medical device law.

38.2.3.3. *Post-Market Surveillance*

The post-market surveillance study provisions of the Act are probably the most far reaching and immediate for devices manufactured from new materials. Two types of studies are outlined in the new law: mandatory and discretionary. Manufacturers of permanent implant devices and life-sustaining and life-supporting devices which are brought to market after January 1, 1991 are required to conduct post-market studies of the performance of their products. In addition, the FDA may require the manufacturer of any device to initiate such a study of its performance, regardless of when the device was first marketed. The Congress' intention for these studies is expansion of the information available on the performance of the device over a larger population and for a longer period of time, beyond that gathered during the premarket testing. The FDA will probably define the aspects of the device that are to be studied, e.g. specific populations may be targeted for study as "high risk" with the use of a new material, the qualifications of the principal investigator, and the characteristics of an acceptable study. The study protocol and the qualifications of the principal investigator require FDA approval prior to initiation of the study.

38.2.3.4. *Special Controls*

The 1990 Act redefines Class II to include any device which, by application of special controls, can be considered to be safe and effective. The classification and explanation of medical devices in Class I, Class II, and Class III are discussed later in this chapter. Special controls may include performance standards, post-market surveillance and patient registries. Furthermore, the procedures for establishing performance standards are simplified.

38.2.3.5. *510(k)/PMA revisions*

The reclassification of Class III provisions for pre-amendment devices requires that manufacturers submit to the FDA, upon request, a summary of information known to them about their devices, including any adverse safety and effectiveness data. Then the FDA will decide whether such devices will remain in Class III or be down-classified into Class II or Class I.

With regard to 510(k) devices, the manufacturer is obliged to submit to the FDA with the pre-market notification, or make available, a summary statement containing safety and effectiveness information and data upon which an evaluation of the device may be performed. Some new provisions have been introduced on information required with regard to pre-market approval applications which support the safety and effectiveness claim. The requirements and time constraints are quite involved and those interested in these requirements should refer to the PMA paragraphs in the law or consult the FDA.

38.2.4. Future Directions

An important focus of the FDA's future activities in medical devices is risk assessment. There is a great need in the device area to weigh a product's risks against its benefits. In some cases the calculation is reasonably straightforward, e.g. comparing the morbidity and mortality of a damaged heart valve with the use of a prosthetic valve. For many other devices, the relationship is more convoluted. How does one measure the benefits of a breast implant? How does one measure the risks of a material like silicone gel or oil, when its basic toxicology and pharmacokinetics are still uncertain? Straightforward or convoluted, the process is difficult.

To confound the issue, societal messages associated with risk assessment are mixed and inconsistent. Many people have been led to believe that no amount of risk from a medical product is acceptable, and that the government's role is to guarantee that the products it regulates are absolutely safe. That view is considered unrealistic, and greatly hampers the ability to communicate effectively about risk/benefit issues.

With regards to biomaterials and risk/benefit decision making, the FDA needs a systematic means for evaluating/comparing clinical performance against *in vitro* assessments of material and device characteristics and properties. As in medicine, biomaterials biocompatibility assessments are not absolute measurements but are very much comparative evaluations. Imperative in such an approach is the use of consistent (standardized) methods of evaluation and a common knowledge base.

A direction the FDA is currently exploring involves development of a compendium of knowledge about the performance and potential risks of specific biomaterials in specific environments — a biomaterials database. Such a compendium could be a resource for both manufacturers and government, particularly to streamline and improve the quality of the product approval process. Conceptually, this compendium could be compared to the drug master file used by drug manufacturers to develop "me too" pharmaceuticals with reduced testing requirements.

For example, if a new product were manufactured from a certain formulation of a material, using a manufacturing process comparable with that listed in

the compendium, the requirements for pre-clinical testing may be reduced or waived. Such a system could eventually become an integral part of internationally-harmonized procedures for pre-market approval. As currently envisioned, this compendium would be a series of networked databases, as opposed to a single comprehensive database.

A second project proposed by the FDA, as part of the U.S. government's Advanced Materials and Processing Program (AMPP), involves the development of a systematic way to retrieve and study explanted devices on a national level. The proposal, planned to begin in 1994, involves close interactions with university medical centers, professional societies, industry, and standards organizations to establish research protocols and a uniform system for collecting, storing, and analyzing information about the fate of implanted devices in the body. This kind of information, if widely disseminated and shared, would be valuable to new materials and device research, development, and sound regulation. The explant/retrieval database would be one of the networked databases in the above mentioned compendium.

A third area the FDA has been working on is the definition of types of research needed to evaluate effectively product risks and benefits. In 1990, the FDA published a document entitled "Research Agenda for the 1990s",[5] which attempted to address these issues. This document, which is currently being updated, has been circulated widely in an attempt to stimulate needed research. See Reference 6 for additional discussion of this subject.[6]

REFERENCES

1. Study Group on Medical Devices (1970). *Medical Devices: A Legislative Plan,* Department of Health, Education and Welfare, Washington, DC.
2. Medical Device Amendment of 1976 (1990). *Federal Food, Drug and Cosmetic Act as Amended and Related Laws, May 28, 1976,* US Government Printing Office, Washington, DC, 0-248-576QL3.
3. Safe Medical Devices Act (1990). *Highlights of Safe Medical Devices Act of 1990,* US Department of Health and Human Services, Center for Radiological Health, Rockville, MA.
4. House of Representatives Conference Report (1990). *Conference Report No. 101-959,* House of Representatives, Washington, DC.
5. FDA/CDRH Special Publication (1989). *Research Agenda for the 1990s,* US Food and Drug Administration, Silver Spring, MD.
6. Mueller, E., Kammula, R. and Marlowe, D. (1991). Regulation of Biomaterials and Medical Devices, *MRS Bulletin*, **9**, 39–41.

Chapter 39

REGULATION OF MEDICAL DEVICES: CURRENT STATUS

David C. Greenspan

39.1. INTRODUCTION

The regulation of medical devices, like medical devices themselves, has evolved and grown more sophisticated over the past 25 years and will likely continue to evolve. Whereas medical devices of 20 and 30 years ago were either metals, polymers or ceramics, devices now contain combinations of materials, nanoparticles, cells and biological molecules. This makes the regulation of medical devices a complex and often a difficult process. The basic premise of the regulatory function is to ensure that medical devices are safe and efficacious for the patient while, at the same time, allowing for new and improved treatments and therapies to enter the market. The product development processes for medical devices, as for most other technologies, have also grown more sophisticated during the past 25 years. Concepts such as design control and risk management, which were always a part of a product development process, have now become more formally integrated into the early stages of the development of medical devices as well as the later stages of the regulatory process. These changes have brought about the more formal use of voluntary standards in the development and regulation of medical devices. Another major factor in the regulation of medical devices is the globalization of the medical device market and the attempts to harmonize these very complex regulatory processes, including the very important clinical trials process.

This chapter will briefly review the regulatory process, focusing on the Food and Drug Administration (FDA) procedures and the Medical Device Regulations promulgated by the European Union (EU). The role of design control and risk management in the regulatory processes will also be discussed, as will the role of voluntary standards in gaining regulatory approvals. While it is beyond the scope of this chapter to go into any great detail on any of the aspects of regulatory systems, it is hoped that the information presented can be a general guideline for the approach to gaining regulatory clearance of medical devices.

39.2. A BRIEF HISTORICAL PERSPECTIVE OF MEDICAL DEVICE REGULATION

While it is not strictly necessary to delve into the history of how the medical device regulations came about, it is instructive to learn that these government regulations all stem from the need to protect the health and safety of the public. The U.S. and Europe have been the two major medical device markets to date, although in recent years Asian markets have grown substantially. Therefore, this section will deal mostly with U.S. and EU device regulations.

Prior to the enactment of the Food, Drug and Cosmetic Act of 1938, the FDA in the U.S. had limited powers to provide for the safety of the general public (see Chapter 38). It was an event in 1937 (the deaths of over 100 children due to a contaminated elixir) that led to the passage of the legislation strengthening the FDA's ability to ensure the safety of drugs.[1] This legislation, for the first time, set a definition for a medical device. Medical devices were defined as: *any instrument, apparatus, or contrivance, including any and all components or parts that are intended for use in the diagnosis, cure, treatment or prevention of disease in man or in other animals*. It also authorized the FDA to set requirements for insuring the safety of medical devices. It also established requirements for labeling as a way of controlling misbranding or adulterating medical devices and drugs. However, this legislation lacked true effectiveness (in hindsight) since it did not require that medical devices have premarket clearance as drugs did. Thus, the regulations were essentially limited to regulating the labeling of medical devices.

In the late 1960s, with the rapid growth in the medical device industry, a presidential committee[2] was formed to investigate the need for increased federal regulation of medical devices. The committee found safety issues with medical devices that had caused nearly 1,000 deaths and significantly more injuries over a ten-year period. The report by this committee led to the Medical Devices Amendments of 1976, which gave the FDA the authority to regulate medical devices, not only with respect to labeling, but to manufacture, processing, marketing, distribution and use of the devices.[3] The legislation also refined the definition of a medical device to delineate them from drugs. Thus, those products that are not metabolized by the body or are not dependent on being metabolized were to be regulated as devices and not as drugs. Furthermore, the definition was expanded to include instruments, machines, implants, *in vitro* reagents and similar articles used in healthcare. It also included diagnostic materials and components, and these regulations extended not only to man but animals. Another critical part of this legislation was the ability of the Agency to require good manufacturing practices (GMP) standards for medical device manufacturers. The

legislation also created the classification system, whereby medical devices are regulated into one of three categories, based on risk, complexity and the life-sustaining nature of the devices.

In 1990, the Safe Medical Devices Act provided new enforcement authority to the agency and strengthened the FDA's ability to regulate devices and required user facilities to report any serious adverse events to the agency.[4] The amendment also required medical device companies to perform post-market surveillance of devices that were permanently implanted and life sustaining or life supporting. The act also required medical device manufacturers of certain high-risk devices to provide a method for tracking their devices used outside a user facility.

Until 1993, devices marketed in Europe were subject to control by the individual countries and through various regulatory mechanisms. In 1993, the EU passed the Medical Device Directive (EU 93/92) which harmonized the regulation of medical devices throughout the EU.[5] The passage of this directive was based on "The New Approach", which used conformity of products based upon following consensus standards and control of the design, testing and manufacturing of medical devices. The EU directive used a device classification system that was very similar to that adopted by the FDA. Class I devices were of lowest risk, Class II devices were divided into two categories based on more serious risk of harm if they failed, and Class III devices were, as in the U.S., significant risk devices; that is, posing a risk of serious injury or death due to failure of the device. This classification system is defined in the annexes of this EU directive. The directive also specified rules for conducting clinical studies on devices not yet cleared to enter the market. The directive established Notified Bodies; organizations that were certified to review device dossiers to determine if the manufacturer had followed the regulations and could therefore be allowed to market their devices in the EU. This certification process allowed manufactures to affix the "CE Mark" to their devices, which is necessary to be able to sell the device in the EU. The basis for this scheme is the conformity assessment; that is an audit of the documentation and test results, including clinical studies in many cases, which will ensure that a device is manufactured to meet the requirements of the EU regulations and is safe and effective.

In 1997, the U.S. Congress passed the FDA Modernization Act. The main thrust of this act was to move FDA regulations towards harmonized standards with other nations. It also clarified the classification system and the requirements necessary for the clearance of a medical device. The Act also further clarified what had become the major pathway for clearance of medical devices, the 510(k)

premarket notification route. The purpose of this provision was to accelerate the review and decision process for medical devices, which had grown significantly since the original 1976 Device Amendments.

Canadian Medical Device Regulations were instituted by the Canadian Department of Justice in March, 1998 (SOR 98-282). These regulations followed mostly from the European Medical Device Directives, but have some features of the FDA regulatory system. Unlike both FDA and EU regulations, the medical devices in Canada are broken down into four classes, with Class I being that of lowest risk, as in the U.S. and EU systems. Class IV devices are of highest risk. Both Class III and Class IV devices require clinical evidence of efficacy and safety along with full design files, quality systems and other requirements.

In 2002, the FDA created the Office of Combination Products, as the growth of the medical device industry had gone beyond simple devices and now used combinations of materials and drugs or products of biological origin (animal products or human tissue, or proteins and organic molecules), and these were not clearly within the authority of the existing regulatory structure. This Act also revised and strengthened the GMP regulations and placed more reliance on international standards and risk assessment during the design phase of medical device development.

The EU, in 2007 issued sweeping changes in the original Medical Device Directives. This strengthened the clinical investigational requirements for medical devices which included: increased record retention; requirements for more pre-clinical data in the development of medical devices; a number of clarifications on the classifying medical devices based on risk; and a number of changes to labeling requirements, software and other administrative changes related to the Notified Bodies. Taken together, these regulations have clarified a number of the processes used for the regulation of medical devices and strengthened post-market surveillance.

39.3. THE REGULATORY PROCESS AT THE FDA, CANADA AND IN THE EU

From the history of the various regulatory agency legislations and development of laws governing medical devices, the processes of getting a device through the regulatory systems have much more in common than they have differences. Therefore, it is worthwhile to focus on the general processes and those parts of the regulatory process that are most critical to the success or failure of gaining regulatory clearance or approval. In this regard, the role of voluntary standards in the development, testing and analysis of medical devices has become

critical to the entire process. In addition, good manufacturing practices and quality systems are critical to the success of any medical device manufacturer. This section will touch on these very important features of the regulatory process.

39.3.1. How Medical Devices are Classified

As mentioned briefly above, medical devices are classified according to risk to the patient (safety) and the efficacy of the device that relate to the stated claims. The level of regulatory controls and oversight is directly related to the risk of the device to the patient, with Class I being lowest risk and Class III devices being highest risk.

- Class I devices are those considered to be low-risk and subject to "general controls", essentially to prevent mislabeling and adulteration. These devices generally pose no risk of loss of life to the patient.
- Class II devices are those subject to "special controls" as well as general controls, and these are based on a higher risk to the patient and include invasive and non-invasive devices, some implantable devices and diagnostic devices and equipment. These special controls include performance standards and in some cases clinical evidence of safety and efficacy.
- Class III devices, which are highest risk to patients, include devices such as long-term implantable heart valves. They are required to have an approved premarket approval application (PMA) prior to being allowed to begin commercial sales.

As the risk increases, the controls necessary by the manufacturer to ensure safety and efficacy increase. For Class III devices and for many Class II devices, human clinical trials are required. Full quality systems are required by FDA for all Class II and Class III devices. The FDA website (www.fda.gov) is an excellent source for searching "device classification" to determine if a final rule has been issued with respect to a particular device. For example, Title 21 CFR (Code of Federal Regulations), Section 872.3930 (accessible online at: http://www.gpo.gov/fdsys/pkg/CFR-2008-title21-vol8/pdf/CFR-2008-title21-vol8-part803.pdf) is the particular section that contains the final rule for "Bone Grafting Materials, Synthetic". Under that section, one can find the classification of the category (Class II) and that this particular regulation is related to dental bone grafting materials, not all synthetic bone grafting materials. This section will also state any recognized consensus standards that pertain to the particular device.

Depending on the classification of the device, and whether there is a predicate device or not, a device may follow a premarket notification 510(k) path or may require a PMA. The FDA has set out very clear rules that govern what information a manufacturer must supply for a particular device in each of these categories. These regulations can be found in Title 21 CFR regulations as well.

39.3.2. Premarket Notification 510(k)

At least 90 days before it intends to market a device for the first time, a company must submit to the FDA's Document Mail Center a premarket notification. This is also commonly known as a 510(k) submission. This document must contain sufficient information to allow the FDA to ascertain that the device is substantially equivalent to one that is already legally marketed. A 510(k) notification is also required if a manufacturer makes a significant change to an already marketed device, and the manufacturer cannot begin to market that changed device until FDA notifies the company that it may do so, or if the Agency has not responded to the notification within 90 days from receipt of the documentation.

Title 21 CFR 807, "Premarket Notification Procedure", defines those cases where this route to marketing of a device is applicable and also specifies (Section 807.87) what information is necessary, as well as the form in which the information must be submitted. In many cases for Class II devices, human clinical studies may be required to demonstrate equivalence. Rules for conduct of clinical studies may require prior approval from FDA as well as a local Investigational Review Board, depending on whether the device is categorized as "significant risk" or "non-significant risk". If prior approval by FDA is required, the information and procedures for gaining this approval to conduct a human clinical study are detailed in S21 CFR Section 812. This section covers the procedures for the conduct of clinical studies with medical devices, including application, responsibilities of sponsors and investigators, labeling, records and reports.

39.3.3. Premarket Approval

For medical devices that are not found to be substantially equivalent, the PMA process (21 CFR Section 814) is used by FDA to determine the safety and efficacy of the device in question, to either allow the device to be marketed or to request additional information or testing prior to allowance of marketing. Devices

that require PMAs are Class III devices with high risk that pose a significant risk of illness or injury, or devices found not substantially equivalent to Class I and II predicate through the 510(k) process. The PMA process is much more involved than a 510(k) submission, and includes the submission of clinical data to support claims made for the device.

39.3.4. EU Conformity Assessments

Unlike the U.S., where FDA regulates devices through most phases of development, production, distribution and use, in the EU the regulation of medical devices is regulated through the Medical Device Directives (EU 93/42). This EU legislation set out rules that govern how medical devices are to be classified, regulated and approved for marketing within the member states of the EU. This legislation, and numerous amendments to the legislation, established mechanisms for the classification of medical devices similar to the FDA system, mechanisms for controlling clinical studies for unapproved medical devices, for allowing commerce uniformly throughout all the member states and, most importantly, for the creation of Notified Bodies, i.e. organizations that would be responsible for granting the conformity mark, or CE Mark, to medical devices that meet certain requirements. This legislation also established rules requiring manufacturers to comply with ISO 13485 quality system requirements for medical devices.

The classification of medical devices in Europe follows the same general guidelines as does FDA; that is Class I devices are lowest risk, Class II carry more risk and Class III are significant risk devices. In the EU Directive, Class II devices are sub-divided into Class IIa and Class IIb and these sub-divisions are based on the risk to the patient. The specific classification rationale is listed in Annex IX of the legislation and there are numerous rules that govern how one classifies a device. These rules include how invasive the device is, whether it is intended to be a long-term implant, if it is active, whether is uses a source of power to perform its function or contains emitting electromagnetic radiation, along with many other criteria. This system differs from the U.S. system, where devices are classified specifically by type (such as metal hip prosthesis or as mentioned above, synthetic dental bone graft). Overall, the classifications of devices in the EU are going to be very similar to those in the U.S., given that in both systems the basic tenets are safety and efficacy of the devices for their intended uses.

Perhaps the biggest difference in the two regulatory systems is the use of the Conformity Assessment in the EU. Under this system, the manufacturer must operate with a quality management system (default system is ISO 13485 for medical devices) and that each member state authorizes certain Notified Bodies,

the organizations qualified to assess the conformity of the quality management system as it pertains to the specific medical devices being manufactured by a particular company. If, under this system, a company is found to conform to the standards, then it is given the "CE Mark", which must be affixed to the device (or device package), and which is the symbol that the company is legally allowed to place that device into commerce. This conformity assessment depends on the company complying with some 40 elements of the "essential requirements" that are written into the EU 93/42 directive.

The objectives of establishing the essential requirements in these directives was to consider all areas where a company might do something, or fail to perform some tasks, that could result in a risk to the patient. The risk assessment was the driving force that led to the adoption of these essential requirements. These can be categorized into six main areas: internal production control; the type of conformity examination to be carried out to ensure compliance with the directives; how to assess that a device conforms to its intended use and function; guidelines for following a quality assurance system in development and production; how to verify that the product is functioning according to its stated intended use; and rules for how a company is to pursue a company-wide quality assurance system.

In Canada, medical devices are regulated through Health Canada and their system is something of a hybrid between the U.S. system of laws and regulations and the EU system of conformity assessment. In Canada, the main regulation is the Medical Devices Regulation (SOR/98-282). This statute defines medical devices, control of manufacturing and labeling and clinical investigations, and sets out a classification system. Unlike either the EU or U.S. systems, there are four classes of medical devices, with Class I being of lowest risk and Class IV being of highest risk. This legislation defines rules for safety and efficacy of medical devices and rules for applying for a Medical Device License. While the particulars of the Canadian system have some real differences compared with both the EU and U.S. systems, most of the requirements to satisfy the Canadian regulations will also be needed to comply with the U.S. FDA and EU Directives.

39.4. DESIGN AND DEVELOPMENT — AN INTEGRAL PART OF THE REGULATORY PROCESS

The FDA, EU and Canada require that device manufacturers maintain a "quality system" as part of the requirements for approval of medical devices. In the EU, ISO:13485;2003 — "Medical devices — Quality management systems — Requirements for regulatory purposes"[6] is used as the "default" format for a quality system; the use of ISO 13485 is not required, but for all practical purposes is

used by the vast majority of medical device manufacturers. This document is based on the more general standard, ISO 9001 — "Quality Management Systems — Requirements", and sets forth a method for how a company should operate to ensure the highest quality for their products and services. While it is beyond the scope of this chapter to go into any great depth of detail, one section of ISO 13485 in particular, "Product Realization", and a subsection, "Design and development", lay out a specific method of going about developing a medical device.

Basically, the design and development of a medical device should follow a logical sequence, starting with establishing "design inputs", such as patient needs, user needs, sterilization needs, packaging and labeling requirements, biocompatibility requirements, clinical requirements and other market needs and requirements. These inputs are the start of the design process. While these "requirements" cannot be completely known, the process of figuring out the right materials, sterilization methods, physical design etc. lead to "outputs", which are specific specifications and details of all aspects of the device. These outputs can then be tested or verified by methods such as testing the biocompatibility of a new material or new use of an existing material and so on. There are other steps in this process and one can see that the process is an iterative one. Both the FDA (21 CFR 820) and Canada (SOR 98-282) have specific requirements for quality systems. The FDA regulations vary somewhat from the ISO regulations, while the Canadian requirements specify ISO 13485 (CAN/CSA-ISO 13485:03) for Class II, III and IV devices.

As part of the design process, the use of a risk management system has become more and more important in gaining approval of a medical device. Risk management is specifically required in ISO 13485, and there is an ISO Standard (ISO 14971-2008) that describes the various components of performing a risk assessment on a medical device, both in the design phase and in the manufacturing or process stages. In recent years, the FDA has been requiring submission of full risk management documentation along with 510(k)s for Class II and Class III devices. While this may seem onerous to the manufacturer, the conduct of a detailed risk management process can be quite beneficial in the design and development of a medical device. The process uses established methodologies to identify, evaluate and minimize any risk factors in medical devices. Risks are defined as situations that can occur from misuse, design or handling of a device that can lead to the device malfunctioning or causing injury or death. The process should take into account all types of risks, from design to manufacturing to end user and patient factors. Once risks are identified, these are evaluated as to the probability of occurrence and the likelihood that these risks can be identified prior to occurrence. These factors lead to a "level of risk", which if too great must

be mitigated by the manufacturer of the device. By focusing on the entire process of development and use of a device, this risk assessment can be used to produce safer and more effective devices.

Another major component in the regulatory process for medical devices is the evaluation of the safety of the device. There is an ISO Standard (ISO 10993)[7] that describes and defines the types of compatibility and toxicology testing necessary for devices, based upon their length of contact with the body, the type of tissue that they contact and the classification of the device. The standard calls for numerous separate tests, from cytotoxicity to mutagenicity, genotoxicity, reproductive toxicity, sensitization and tests for interaction with blood and effects of materials after implantation. While not all of these tests must be performed by the manufacturer, depending on the classification of the device, it is necessary to justify the tests that are performed and the test conditions used in the performance of the various tests. There are currently 17 sections to this standard, including sections on how to prepare extracts of samples and how to choose reference materials and sample preparation. The testing is expensive, and to complete an entire suite of required tests may take as long as a year for long-term implantable devices. Therefore it is wise for the manufacturer to familiarize themselves with the details of these tests and the procedures early in the process. It is generally not sufficient to perform these types of tests if they do not comply with the standards, unless a rigorous justification has been given and accepted by the appropriate regulatory authorities.

Clinical studies may also be necessary to gain clearance for a medical device, as explained in the first section of this chapter. The conduct of clinical studies is regulated in all of the medical device regulations. In many cases, a clinical study on a device which is in development requires pre-approval from the regulatory body where the investigation will be conducted. In the U.S., the FDA has a mechanism known as an investigational device exemption (IDE) that requires a clinical plan along with supporting safety data be submitted prior to being allowed to begin the study. The FDA will review the submission and within 90 days either allow the study to begin or they may find deficiencies in the proposed study that must be corrected prior to beginning the study. In the EU, the Medical Device Directives require that the Competent Authorities (nation-specific government agencies that oversee medical devices) be notified prior to starting a clinical trial. In the case of Class IIa and IIb, as well as Class III devices, a company may start the trial 60 days after notification, unless the Competent Authority makes a decision to the contrary. There is an ISO Standard (ISO 15155, Parts 1 and 3) that describes the general requirements for and plans to conduct human clinical trials. There are also a number of guidance documents that are available

from the FDA that cover various aspects of designing and conducting clinical studies, and many of these deal with specific device types or categories of devices.

39.4.1. Regulatory Guidance and Standardization

All of the main regulatory bodies (FDA, European Commission and Health Canada) have extensive websites that publish various guidance documents, from how to construct and conduct clinical studies, to when it is necessary to notify the agency of a change in devices, to guidance on specific testing of certain devices. While the amount of information can be voluminous, and somewhat daunting for first-time users and developers of medical devices, it is well worth the effort to become comfortable using the sites and accessing the information within these various sites. It is ultimately up to the device manufacturer to be compliant and up to date with all of the regulations and guidance for navigating the complex world of medical devices.

The use of standards in the development and approval of medical devices is now heavily relied upon by every regulatory authority. Anyone that intends to bring a new device to the market, or is looking to modify an existing device, should be reviewing the various standards that exist to help perform the various tasks necessary to ensure compliance with the government regulations and, more importantly, to be performing the work on the product necessary to ensure that the device is safe and effective for the intended use. Most medical device manufacturers are familiar with the ISO standards for Biocompatibility and Toxicity testing for Medical Devices and with ISO 13485, Quality Management Systems. There are dozens, if not a few hundred, different ISO standards that relate to all aspects of medical devices, from labeling and graphic symbols, to how to conduct a human clinical study, to how to conduct a literature search for use in classifying a medical device. In addition to ISO, a number of other organizations that are involved in creating various standards for medical devices and the testing and compliance of such devices are listed in the reference section.

39.5. CONCLUSION

The process of regulation of medical devices has grown more complex as the devices themselves have grown more complex in their chemistry, structure and application to the treatment of diseases and defects in the body. That increase in complexity makes the process something of a “black box” to many and something that is often uncomfortable. However, as the complexity of this field has increased, so have the resources available to manufacturers to enable them to

navigate through the processes. The basic tenants of medicine, and of medical devices, first, do no harm, and second, ensure safety and efficacy of the device for the intended use by the patient, are still the cornerstone of all medical device regulations. If approached properly and wisely, the process can be a very successful one and the introduction of new and advanced technologies will be a benefit to society.

REFERENCES

1. Hutt, P.B. (1989). A History of Government Regulation of Adulteration and Misbranding of Medical Devices, *Food Dr. Cosmet. Law J.*, **44**, 100–105.
2. Study Group on Medical Devices. (1970). *Medical Devices: A Legislative Plan*, Department of Health, Education and Welfare, Washington, DC.
3. Medical Device Amendment of 1976. (1990). *Federal Food, Drug and Cosmetic Act as Amended and Related Laws, May 28, 1976*, U.S. Government Printing Office, Washington, DC, 0-248-576QL3.
4. Safe Medical Devices Act of 1990. (1990). *House Report 101–808, 101st Congress, 1st Session*, US Department of Health and Human Services, Center for Radiological Health, Rockville, MA.
5. Council Directive 93/42/EEC of 14 June, 1993 Concerning Medical Devices. *Official J. Eur. Commiss*., No. L 169/1, July 12, 1993.
6. ISO 13485:2007, Medical devices — Quality management systems — Requirements for Regulatory Purposes. International Organization for Standardization, Geneva, Switzerland. (2007 ed.).
7. ISO 10993 Parts 1–17. Biological Evaluation of Medical Devices. International Organization for Standardization, Geneva Switzerland (2003 ed.).

RESOURCES FOR ADDITIONAL INFORMATION

http://ec.europa.eu/index_en.htm
http://www.fda.gov/MedicalDevices/default.htm
http://www.iso.org/iso/home.htm
http://www.ansi.org/ American National Standards Institute
http://www.aami.org/Association for the Advancement of Medical Instrumentation
http://www.astm.org/index.shtml

Chapter 40

Technology Transfer of Bioceramics: From Concept to Commerce

Larry L. Hench and Giuseppe Cama

40.1. INTRODUCTION

Chapter 1 discusses the increasing need for affordable healthcare for a progressively aging population. Developing new biomaterials and devices that are more cost effective and have longer survivability is one of the ways to meet this need. However, making the transition from a laboratory concept into a clinical application and eventually into the healthcare market is difficult. This transition has been given several names: from "bench to bedside", "translational research and development", and from "concept to commerce". Developing a characterization program that assures quality assurance, as required for meeting good manufacturing practice (GMP) standards, is one of the challenges that must be met in order to achieve this transition. How to satisfy this need at minimal cost is summarized in Chapter 37. Establishing evidence for safety and efficacy of the biomaterials and devices sufficient for obtaining regulatory approval is another critical need. This can be difficult, as described in detail in Chapters 38 and 39. The goal of this chapter is to summarize the various steps that must be undertaken in order to make a smooth transition from laboratory-scale discoveries through testing and scale-up towards eventual production of a new bioceramic medical device. This summary is based upon the author's 40-year experience of observing what is needed for a successful transition of the seminal discovery[1] of bioactive glasses to become successful clinical products.[2,3] This chapter also describes what is often overlooked or is missing in the effort to make the transfer of technology from the laboratory into a profitable business. Details are presented in Hench.[4]

40.2. TECHNOLOGY TRANSFER PATHS

It is possible to accelerate technology transfer from the laboratory to production by separating the tech transfer process into five discrete paths (Fig. 40.1).[4–6] Each tech transfer path has a distinctly different output (Table 40.1). All five paths must be followed to completion in order for a concept to become a

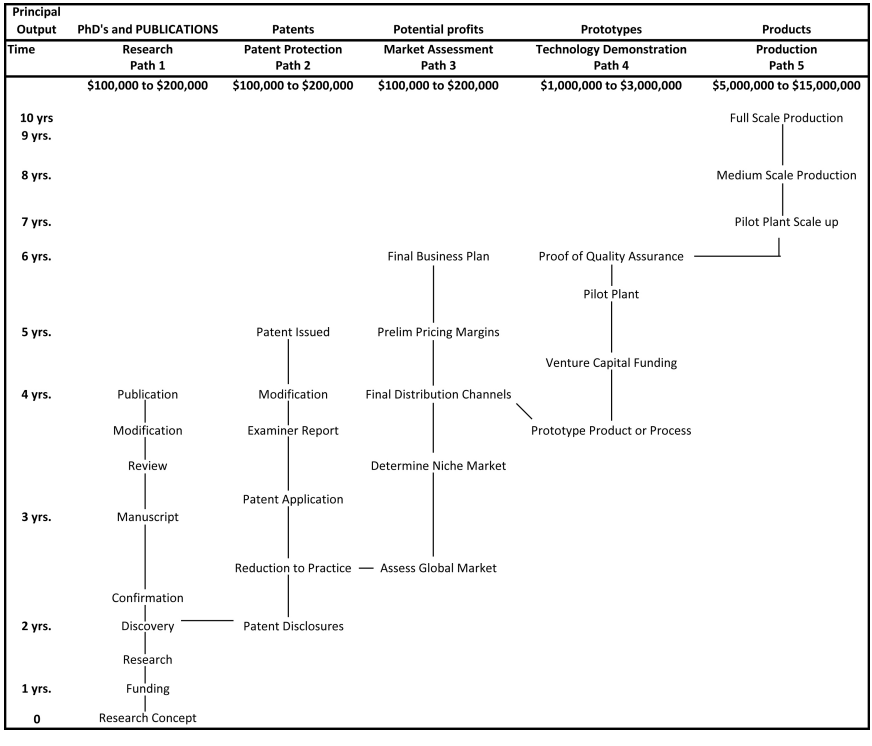

Figure 40.1. Five pathways for technology transfer.

Table 40.1. Technology Transfer Paths and Outcomes.

Path	Outcomes
1. Research	PhDs and Publications
2. Patent Protection	Patents Issued and IP Protected
3. Market Assessment	Profit and Risk Potential Projected
4. Technology Demonstration	Prototypes, Quality Assurance Potential Profit Margins
5. Production	Profits

commercial success, i.e., to become a product which can be manufactured and sold in the marketplace with a reasonable return on investment. Each technology transfer path has a timeline, which is governed by the serial sequence of steps indicated in Fig. 40.1.

Although a specific length of time is indicated for the steps shown for each path in Fig. 40.1, in reality there will be a distribution of times for each step unique for a given technology, product and organization. The timelines shown in Fig. 40.1 tend to be towards the short end of the distribution and thus can be used as a measure of effectiveness of a tech transfer program for an organization. If time increments are much longer than those depicted there is likely to be a problem somewhere in the plan, organization or technology and completion of a program may be delayed or perhaps never completed.

In practice, the total length of time shown for each of the five paths in Fig. 40.1 is close to being optimal. It is seldom possible to decrease the time required to complete the research, patent protection, market assessment or technology demonstration phases of a new product, assuming that the product involves substantially new technology. Incremental improvements in previously-existing processing methods or products take perhaps a third less time in the technology demonstration phase because the pilot plant facilities are already in existence. However, the timelines for R&D and patent protection are nearly invariant regardless of the level of innovation being pursued. Experience shows that it is seldom possible to short-circuit any of the individual steps in Fig. 40.1 without suffering expensive delays later.

Figure 40.1 shows technology transfer as five parallel paths. It is optimal to pursue all five paths in parallel as illustrated, rather than in sequence, for several reasons: shorter cumulative time to complete the overall program; feedback of information between paths; maintenance of momentum; more efficient use of personnel and physical resources; and lower total cost.

If it is possible to pursue the five tech transfer paths in parallel, as shown in Fig. 40.1, the cumulative time for a successful technology transfer process is approximately eight years.

However, if it is necessary to complete each path prior to commencing the next, the cumulative time is nearly doubled to 14 years! Often this is the case because the costs associated with patent protection and especially technology demonstration leading to regulatory approvals are usually considerably larger than research costs and require extensive capital investment, which is often delayed until patent protection is secured. Consequently, new layers of management and investors become involved in the decision-making process as investment becomes larger and the program moves from path 1–4. Typically, the number of decision makers increases two-fold for each step, as described in Hench.[4]

Because the project costs of paths 2–5 are substantially higher than usually budgeted for university programs, the time required to evaluate the project, as

well as the number of people require to evaluate, go up proportionally. The probability of approval goes down proportionally, as described in Hench.[4] Often a combination of factors leads to an excessively lengthy serial technology transfer process. This is often due to the major impedance step in the serial process of transfer from path 3 and 4. The level of financial commitment goes up by a factor of ten at least at this juncture, as shown in Fig. 40.1. However, cost is not the only barrier in moving from path 3–4; additional personnel, management and facilities are equally important factors that must be located and funded.

40.3. RESOURCES REQUIRED

In order to show that a new technology has production potential (path 4), it is necessary to create an organization composed of at least the following personnel and capabilities: representative of the researchers who originated the discovery that led to path 1; engineers capable of scaling-up the technology and experienced in designing the requisite equipment and processes; person(s) with experience in establishing and monitoring quality assurance programs; technical staff dedicated to making the process work reliably; management to oversee timelines and budget; financial planners; sufficient space to locate and run the scale-up operations; and sufficient financial resources to complete the project. The experience, skills, attitudes, responsibilities and temperaments differ greatly among such a team. Consequently, there is usually considerable time invested in achieving an acceptable, workable schedule, plan of action, budget and commitment to "make it work" before path 4 can be activated.

Often the technology will not work in the demonstration scale-up, path 4, without a number of trials. Therefore, efficient feedback of information from the technology demonstration team to the research team and vice versa; i.e., path 1–4–1, is essential. However, by this time, creative scientific personnel will typically have moved onto other interests and are seldom enthused about returning to an "old" project when problems arise. This means new personnel must be recruited and trained. The net effect is lengthening of path 4 and increasing expenditures. These difficulties are most frequent when the tech transfer effort is occurring within a university or between the university with an "arm's length" licensing agreement between the university and a corporation.

In most cases the funds to pursue path 4, a technology demonstration project, will not be approved without first completing a marketing and business study, path 3. The marketing and business analysis will attempt to estimate many items necessary to predict the eventual profitability of the technology and potential payout for the investors. The items that need to be addressed in path 3 include: cost/benefit

ratios of the healthcare products; capital required; size of market; time to reach market; percentage of market penetration as a function of time; lead times over competition; nature of competition and their market share; competitive position of the new technology over the competition; potential profit margins; effect on existing corporate products, if any; risks and potential liability issues of the new technology; and method and projected costs of distribution of the eventual products.

Most university science and engineering departments do not have the staff or experience to make the analysis listed above. Most universities also do not have licensing personnel capable of doing such studies. Consequently, a licensing agreement must be in place to move from path 2–3, with funds being made available to hire a team to do path 3. Delays often occur because funds seldom are available to negotiate and initiate path 3 until patents are issued and intellectual property rights are assured, the end point of path 2, and license agreements with rights to the intellectual property assigned.

40.4. ANTICIPATION OF EARLY DIFFICULTIES

A problem and limitation that must be faced is the fact that the greater the advance of the new technology, the more difficult it is to make marketing and business assessments. Therefore, the greater the potential of the new technology, the greater the risk and the longer the time required to pass judgment that it should be supported to enter path 4 and become a technology demonstration project. Unfortunately, a management mode of dealing with a high risk decision is to postpone it until more information becomes available. The effect is to lengthen the initiation of path 4 and the overall tech transfer timeline. Only a licensee committed to rapid product development with sufficient resources to deal with the risks and necessity of feedback between paths 1–4 can assure that this transition from 2–4 is not delayed. In order to avoid this delay, it is essential that the science and engineering team involved in paths 1 and 2 provide a cost/risk/reward assessment early on to their licensing officers in a university or to company management in a corporation. This often is a difficulty in a university setting because faculty and students do not have the experience to conduct the analysis listed above and resent being asked to do it as it is outside their scope of interest and they can see no benefit from their time invested. This is especially true for young faculty and students, whose careers depend upon completing peer-reviewed publications and submitting grant applications and not tech transfer projects which are usually not publishable.

Thus, there are two primary difficulties in pursuing paths 2, 3 and 4 entirely in parallel: the 5x to 10x increase in cost of moving from making

laboratory-scale prototypes to pilot-scale operations and the need to complete market and business assessments before large budgets can be approved and funds secured. Consequently, the staggered parallel paths 2 and 4 shown in Fig. 40.1 are required by economic realities and are the most efficient.

40.5. LATER STAGE BARRIERS

The scale-up from pilot plant to production (paths 4–5) requires even more capital and market assessment. It is critical to know the size of the production facility to achieve projected profit margins. However, production rates must be targeted towards realistic sales projections. Cash flow to establish and maintain operations must be projected and be available until sales income is sufficient to cover all costs. Failures of companies are typically due to not meeting unrealistic sales projections in the early years.

Thus, identification of profitable niche markets in the first years of scale-up are key requirements for projecting the profit/risk ratio for the new technology. Large corporations have the expertise for making these assessments, but their large overheads inflate the required margins of profits to be a successful business and limit willingness to pursue new technologies with uncertain times for pay-back of investment. Small start-ups, conversely, have low overheads but often lack the ability to assess accurately the multiple factors involved during the transition from paths 4–5 and steps required in path 5. Input from universities and their inventors is seldom judged to have much value by corporate personnel, often for good reason. Thus, the inventor team offers little help and the inventors must wait patiently for years to pass before royalty returns become a reality, if ever. This fact often is a driver for negotiating up-front license fees. The disadvantage of up-front fees is that all incentives for feedback assistance from the research team in path 1 to the technology development team in path 4 are largely eliminated. In reality, by the time path 5 is reached, student and faculty input has been bypassed by licensee technology and the original creative drive responsible for path 1 no longer exists.

40.6. THE EFFECT OF BARRIERS ON TECH TRANSFER TIMELINES

The cumulative time for a staggered parallel tech transfer program, such as depicted in Fig. 40.1, is approximately eight years. For a serial technology transfer program, where each path is completed before the next is approved,

funded and started, it is approximately 14 years. It requires a very high level of organizational efficiency and substantially greater risk and capital to reduce these figures to shorter times. It is all too easy for the timelines to lengthen to 16–18 years. Table 40.2, the timeline for technology transfer of the Bioglass® discovery to eventual commercialization, illustrates this conclusion. The initial discovery of the 45S5 Bioglass® composition bonding to bone was in 1969.[1–3] The first product cleared by the FDA for open market sale to hospitals was the ossicular chain prostheses (MEP®) for replacement of diseased or damaged bones of the middle ear, discussed in Chapter 7, which occurred in 1985 through the 510(k) regulatory process, see Chapters 38 and 39.[2,3] That is a 16-year timeline. The reasons for this lengthy process are described above. The second approved product, the endosseous ridge maintenance implant (ERMI®) followed just three years later in 1988.[2] The much shorter timeline was due to the fact that documentation of safety was already established in the prior submission for the MEP® devices, based upon numerous *in vitro* and *in vivo* trials.[5] Only efficacy in human trials at the dental clinics at the University of Florida were needed to be established prior to the FDA 510(k) submission for clearance of the ERMI®. Subsequent Bioglass® clinical products have also been cleared with much shorter timelines, for similar reasons.[2,3]

40.7. OPTIONS FOR COMMERICIALIZATION

There are numerous options for pursuing the five pathways in the tech transfer process. Risks and rewards to the inventors differ considerably for these alternatives. When technology is created within a corporation there is usually a management structure in place to make the decisions and provide financing for paths 2–5. Milestones and timelines are imposed as part of the job requirements of the teams involved. In contrast, when the technology is created within a university or a government laboratory there is seldom a management structure or budget available to fund the pursuit of paths 3 and 4. The approach to technology transfer is typically a license agreement with a company. There are five alternatives for licensing arrangements, as depicted in Fig. 40.2. Each option shown in Fig. 40.2 has a different degree of risk, time and personal capital investment associated with it. The height of the bar shown in Fig. 40.1 is proportional to these factors. The potential reward to the inventors also differs for each alternative shown in Fig. 40.2. The width of the bar represents potential payoff; the greater the risk the greater the potential payoff when commercialization is completed. It is important to remember that is always *potential payoff*. High risk means a high probability of *no payoff*.

Table 40.2. Timeline for Development of Clinical Products Based Upon 45S5 Bioglass®.

1969	Discovery of bone bonding to 45S5 Bioglass®
1971	First peer reviewed publication[1]
1972	Bonding of Bioglass® bone segments and coated femoral stems in monkeys
1975	Bioglass® coated alumina bone bonding to sheep hip implants
1975	Bioglass® dental implants bonded in baboons
1977	Bonding of Bioglass® implant in guinea pig middle ear
1977	Bioglass® coating patent applications filed
1981	Discovery of soft connective tissue bonding to 45S5 Bioglass®
1981	Toxicology and biocompatibility studies (20 *in vitro* and *in vivo*) published to establish safety for FDA clearance of Bioglass® products
1985	First medical product (Bioglass® Ossicular Reconstruction Prosthesis (MEP®)) cleared by FDA via the 510(k) process
1987	Discovery of osteoproduction (osteostimulation) in use of Bioglass® particulate in repair of periodontal defects (monkey model)
1988	Bioglass® Endosseous Ridge Maintenance Implant (ERMI®) cleared by FDA via the 510(k) process
1991	Development of sol-gel processing method for making bioactive gel-glasses
1993	Bioglass® particulate for use in bone grafting to restore bone loss from periodontal disease in infrabony defects (PerioGlas®) cleared by FDA via the 510(k) process
1995	PerioGlas® obtained CE Mark in Europe
1996	Use of PerioGlas® for bone grafts in tooth extraction sites and alveolar ridge augmentation cleared by FDA via the 510(k) process
1999	European use of 45S5 particulate for orthopedic bone grafting (NovaBone®)
2000	FDA clearance for use of NovaBone® in general orthopedic bone grafting in non-load-bearing sites
2004	FDA clearance of 45S5 particulate for use in dentinal hypersensitivity treatment (NovaMin)
2005	Development of various dental maintenance products (NovaMin)
2009	Anniversary of 1 million doses of NovaBone® bone graft product and 1 million tubes of NovaMin toothpaste
2010	Sale of NovaMin Technologies to Glaxo-Smith-Kline to market as Sensodyne Repair and Protect toothpaste as over the counter product for prevention of dentinal hypersensitivity. Evidence accumulates to also show inhibition of gingivitis.

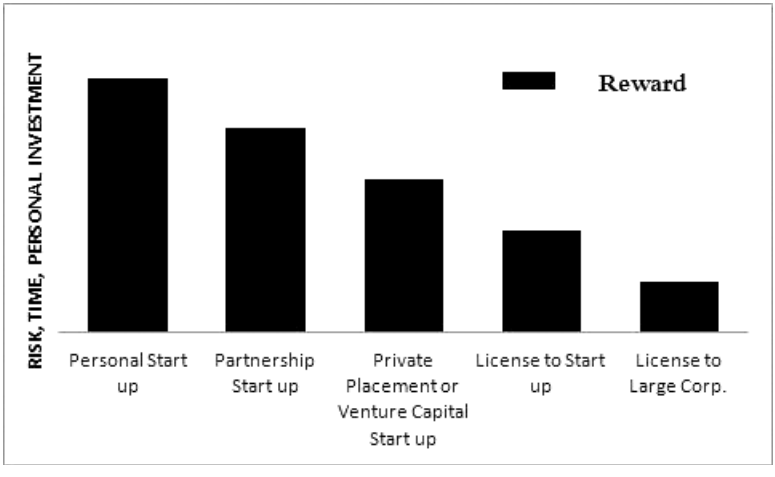

Figure 40.2. Optional routes to achieve technology transfer.

The five options are:

1) **Personal Start-Up** where the researcher raises the capital and maintains control of the first paths 1–3 of tech transfer.
2) **Partnership Start-Up** where a team is formed that shares the cost and effort required to make it through paths 1–3.
3) **Private Placement or Venture Capital Start-Up** where money is raised by the inventor team by releasing a portion of ownership and control to an equity partner that funds paths 2–4.
4) **License to Start-Up** where the inventor team and institution license the technology to another company that may or may not have participation by the inventors and the company takes the responsibility of raising the capital and teams to pursue paths 2–5.
5) **License to Large Corporation** where financing and control is taken over by the corporation and the institution is paid a royalty when the commercialization is successful. Up-front payments are often negotiated to minimize risk to the institution and prevent a lack of corporate investment in the technology.

Details of the pros and cons of each of these five options are presented in Hench.[4]

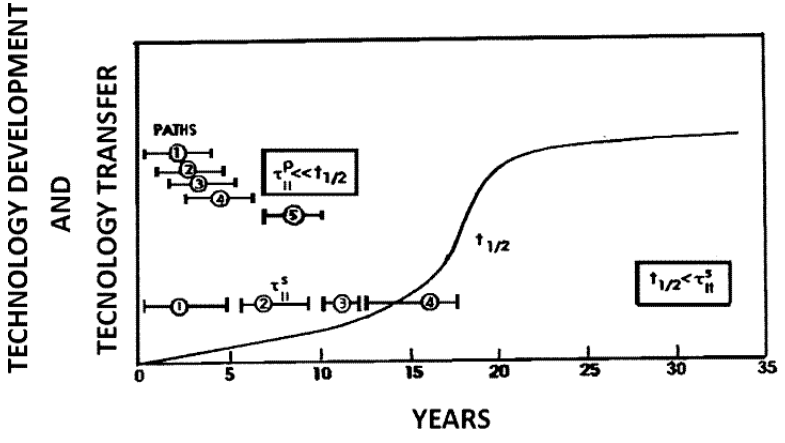

Figure 40.3. Comparison of staggered parallel versus serial technology transfer paths with technological development curve.

40.8. NEED FOR RAPID TECHNOLOGY TRANSFER

Figure 40.3 shows a typical technology development curve for a product, including medical products. For a few years there is slow growth. Growth expands rapidly as market acceptance is achieved and eventually growth slows and continues at the rate of growth of a commodity, with rates of 3–5% per year. The technological half-life is at the midpoint of the growth curve. This technological half-life is shrinking in the global economy, as discussed in Hench.[4]

40.9. UNDERSTANDING THE IMPORTANCE OF TRANSLATION

The importance and the difficulty to translate a laboratory concept to patient care has been underlined in 2001 by the Institute of Medicine (IOM)[7] and two years later by the National Institutes of Health (NIH) Roadmap that defined the translation process as a key factor for health care improvement.[8] The same institution in 2005 established the Clinical and Translation Science Awards (CTSAs) with the aim to encourage and sustain new scientific knowledge during the pathways towards a public health impact. The time required to deliver onto the market a scientific innovation is one of the first variables in the translation process that must be controlled carefully.[9] In this regard, any delays in the delivery of a

product must be avoided in order to prevent the requirement of further capital input and the concurrence on the market of similar competitive products. The optimization of the whole translation process should be based also on the ability of the system to be flexible and able to adapt itself to unexpected or poorly planned conditions.[10] Moreover, the different professional figures involved on the project should be able to show good communication skills in order to avoid dispersion of information and lack of feedback relating to the evolution of the process. Young scientists should be educated at the beginning of their research activity on the difficulty involved in translating an experiment carried out in their laboratory to the benefit of public health. This concept assumes extreme importance considering that their research activity should represent, in large part, the future of public health. Unfortunately, today, although translation has been discussed for more than 30 years,[11] different terms are used to define this concept,[12] creating confusion. Most importantly, there has yet to be delineated general and solid criteria to follow, in order to minimize the risk of failure of the translation process.

40.10. CONCLUSION

If a new concept and innovative technology enters into a tech transfer process that takes too long, i.e., is a serial process, as illustrated in Fig. 40.3, then it may never enter into the marketplace with significant impact because other new technologies with faster tech transfer times will "beat it" to market share. This competition is illustrated in Fig. 40.3 and is the primary reason that efficient tech transfer processes are now essential. Staggered parallel paths shown in Fig. 40.3 are optimal. The decision as to which option of commercialization is best to take, Fig. 40.2, needs to be made with this contest of world-wide competition in mind. Fast technology transfer is essential to achieve clinical success and profitability.

REFERENCES

1. Hench, L.L., Splinter, R.J., Allen, W.C. *et al.* (1971). Bonding Mechanisms at the Interface of Ceramic Prosthetic Materials, *J. Biomed. Maters. Res*., **2**, 117–141.
2. Hench, L.L., Hench, J.W. and Greenspan, D.C. (2004). Bioglass: A Short History and Bibliography, *J. Aust. Ceram. Soc.*, **40**, 1–42.
3. Hench, L.L. (1991). Bioceramics: From Concept to Clinic, *J. Am. Ceram. Soc.*, **74**, 1487–1510.

4. Hench, L.L. (1998). *Sol-Gel Silica: Properties, Processing and Technology Transfer*, Noyes Publications, Westwood, NJ, pp. 133–149.
5. Wilson, J., Pigott, G.H., Schoen, F.J. *et al.* (1981). Toxicology and Biocompatibility of Bioglass, *J. Biomed. Mater. Res.*, **15**, 805–817.
6. Hench, L.L. (1990). From Concept to Commerce: The Challenge of Technology Transfer in Materials, *MRS Bulletin XV*, **8**, 49–53.
7. Committee on Quality of Health Care in America IoM (2001). *Crossing the Quality Chasm: A New Health System for the 21st Century*, National Academies Press, Washington, DC.
8. Zerhouni, E. (2003). Medicine, The NIH Roadmap, *Science*, **302**, 63–72.
9. Bella, S., Morseb, S. (2005). Delivering Sustainability Therapy in Sustainable Development Projects, *J. Environ. Manage*., **75**, 37–35.
10. Cohen, D.J., Crabtree, B.F., Etz, R.S. (2008). Fidelity Versus Flexibility Translating Evidence-Based Research into Practice, *Am. J. Prev. Med.,* **35**, 381–389.
11. Graham, I.D., Logan, J., Harrison, M.B. *et al.* (2006). Lost in Knowledge Translation: Time for a Map? *J. Contin. Educ. Health Prof.*, **26**, 13–24.
12. Wolf, S. (1974). Editorial: The Real Gap between Bench and Bedside, *New England J. Med.*, **290**, 802–803.

Chapter 41

ETHICAL ISSUES

Larry L. Hench

41.1. INTRODUCTION

Millions of people currently have implants and their number is increasing rapidly.[1] It is important to examine the ethical issues associated with the increased use of artificial, non-living materials to repair, restore, or augment living tissues.

In part, the large increase in use of implants is because ethical concerns are less for artificial materials than use of living transplants.[2–4] Implants do not require donors. Thus, donor consent is not needed for an implant. However, many moral and social issues are as important for implants as for transplants. These issues include: informed patient consent, patient risk/benefit ratios, cost/benefit ratios, availability, reliability, and incidence of revision surgery. The number of implants far exceeds the number of transplants annually and it is important that these issues be addressed and boundaries for the use of implants be established that take into consideration complex ethical concerns.

41.2. THE THEORETICAL PROBLEM

The science of biomaterials and implant design and performance is based upon well-established scientific principles of physics, chemistry, biology, and physiology. The theoretical foundations of these historic disciplines are well developed and have been proven through centuries of experimental trial and error. There is little uncertainty that if the stem of a femoral head replacement is too small or the thickness of the femoral bone is too thin that fracture will result, i.e. the mechanics of the system can be calculated and the result predicted with a high level of confidence. Devices are designed using these biomechanical principles and reasonably high reliability has been achieved.

In contrast, there is conflict and uncertainty in the theoretical foundation for analyzing ethical issues.[3] Two main schools of ethics exist, with major differences in their approach to achieving a moral judgment. They are: the utilitarianism view developed by the English philosopher, John Stuart Mill and his successors, whose position is that an action is “right” if it leads to the greatest possible good or least possible bad consequences, i.e. “right is relative”; in contrast, the deontological

(binding obligation) approach of the German philosopher Immanuel Kant and successors, such as W.D. Ross, argues that moral standards exist independent of utilitarian ends and that a moral life should not be conceived in terms of means and ends but that an act is "right" because it satisfies the demands of some overriding principle of obligation. We should act as if our action was about to become a law of nature and all men were to hereafter act in the same way, i.e. "right is revealed".

Many modified versions of both Kant's and Mill's philosophies have been developed; but the fundamental differences remain, at present, unreconcilable.[3] This is in part because the principles underlying human moral behavior cannot ethically be tested by using designed experiments, as can physical principles. Tests would violate the ethical principles being tested. Thus, there appears to be an ethical uncertainty principle which limits the ability to describe a universally-acceptable moral behavior for individual humans. This is a parallel to the Heisenberg uncertainty principle which establishes bounds upon the knowledge obtainable for discrete particles in physical systems.[4] The uncertainty in ethical theory makes it difficult to reconcile differences of opinions as to the relative importance of three general principles for making ethical decisions.[4]

41.3. THREE GENERAL PRINCIPLES FOR MAKING ETHICAL DECISIONS

Moral philosophers generally agree that three general principles exist for making ethical decisions (Table 41.1).[3] The first principle is respect for autonomy. This is the concept that each person has the right to decide what is best for them. Respect for autonomy generally ranks highest in the hierarchy of ethical principles. This principle usually takes precedence in a medical situation and should seldom be violated in decision making.[3–5] However, this principle assumes that an individual is both capable of making a rational decision and desires to make such a decision. Difficulties arise when it is unclear as to whether an individual is capable of making rational decisions, as may be the case with the very young, the very old, in medical emergencies involving trauma or coma, or when an individual does not want to make a decision. Often, individuals do not have the ability to understand the consequences of their decision and prefer to abdicate this right to their physician. The moral dilemma of when to "pull the plug" for a terminally ill patient in an intensive care unit is a consequence of the conflict of this principle and the principle of beneficence.[2,6]

The principle of beneficence (first, do no harm) is at the core of the Hippocratic Oath.[2] There is seldom conflict over the importance of this principle.

Table 41.1. Three General Principles for Making Ethical Decisions.

RESPECT FOR AUTONOMY
The concept of personal self-governance. The principle of a person's right to choose. It assumes that individuals have an intrinsic value and have the right to determine their own destiny. It is the opposite of slavery.
THE PRINCIPLE OF BENEFICENCE
The concept that an action or decision should not inflict harm on another, should prevent or remove harm, or promote good to another.
THE PRINCIPLE OF JUSTICE
The concept that like cases should be treated alike. This principle is difficult to use because individuals are not alike and often do not desire to be treated alike.

However, there can be conflict between it and the respect for autonomy, as cited above. For example, a woman may desire to have an implant for breast enlargement even though there is evidence that doing so involves risk, i.e. it "may not be harmless". The burden of informing the person of the extent of risk is shared by the manufacturer and the surgeon. Each may assess the potential for "harm or risk" quite differently. Quantification of risk for an individual is difficult since risk is a statistical concept.[5] Conflicts can and do occur in such situations.

The principle of justice leads to the most uncertainty and conflict.[4] This principle maintains that like problems should be treated alike. The theoretical ideal of complete equality is impossible to achieve because individuals are *not* alike. Also, people may choose, for reasons such as taste or religion, to be treated differently. Respect for autonomy requires that preferences be honored. Problems arise when the autonomous rights of an individual or group limit the implementation of justice to others. Problems also arise when individuals believe falsely that their problem is equivalent to another, when in fact it is different.

Since the concept of ideal justice cannot be achieved in a real world, the formal principle of justice is usually implemented in terms of what are called "the material principles of justice". Table 41.2, based on Beauchamp and Walters[3] and Hench,[4] summarizes alternatives for making decisions regarding distribution of material goods or health care. Most countries have evolved a complicated mixture of these alternatives. For example, the availability of certain implants to a deaf person, such as intracochlear multichannel electrical stimulation, often depends upon family wealth because of the high cost of the device and the lack of insurance for such devices. In developing countries, even simple implants may not be available to the majority of the population due to cost and lack of surgical

Table 41.2. Material Principles of Justice[3,4]

Which include as alternatives:
1) To each person an equal share.
2) To each person according to individual need.
3) To each person according to acquisition in a free market.
4) To each person according to individual effort.
5) To each person according to societal contribution.
6) To each person according to merit.
7) To each person according to age.
8) To each person according to status (nobility).
9) To each person according to gender.
10) To each person according to race.
11) To each person according to religion.
12) To each person according to ethnicity.

facilities. The rapidly-accelerating cost of health care in all countries may eventually lead to governmental restrictions for many implants, with distribution based more and more on personal resources.[4–6]

Such restrictions create conflicts between all three ethical principles with little basis for resolving the conflicts. Prejudice can then affect decisions rather than moral judgments.

41.4. CONSEQUENCE OF THE THEORETICAL PROBLEM

Beauchamp and Walters summarize the biggest problem facing ethicists and moral philosophers at the present time as: *"The problem of how to value or weigh different moral principles remains unresolved in contemporary moral theory."*[3]

This means that when the principle of respect for autonomy is in conflict with either the principle of beneficence or principle of justice there is no agreement on acceptable means of resolving the conflict.

The most important, practical consequence of this theoretical problem is that it leads to uncertainty in assessing an ethical response in individual cases.[4] Guidelines of ethical behavior can be developed for large population groups but they may not be accepted by individuals within the group. Individuals often consider general guidelines or restrictions to be unjust if they are excluded. Thus, uncertainty in the relative importance of the three ethical principles leads to conflict between individuals and between individuals and the group.

For example, consider the situation when an implant fails. Conflict may arise between the patient and the surgeon, hospital, manufacturer, or all three. Why is there conflict? The patient chose to have the implant, risks were reviewed, and informed consent was obtained; thus the patient's autonomy was respected. The individual case history indicated to the surgeon that the implant and procedure selected had a high probability of success, thereby fulfilling the principle of beneficence. Conflict results, however, when a patient perceives that the principle of justice has been violated. The patient expects not only equal treatment, but also *equal results*. The patient and his/her family do not care about statistics and that 85 or 95% of similar cases treated the same way succeeded. They care only that *their* case failed.

41.5. SOURCE OF CONFLICT

The conflict is due to an unjustified expectation of equal *consequences* of an act instead of equal *performance* of the act. The principle of justice specifies only that "like cases be treated alike". However, because individuals are different results can be different, even when treatment is the same. The difference in results versus expectations can be perceived, wrongly, as unjust.

What are the reasons for unjustified expectations of implant success? Three factors, at least, are involved: human nature, technology, and greed. It is human nature to want the same things as others. This expectation feeds our market-driven economy.[6] The same is true for implants. People do not desire to live with pain as they become older. This is reasonable. They learn from the media or friends that certain implants eliminate pain, therefore, they want an implant if they have painful joints. They do not hear, or are unwilling to accept, that there is a finite risk associated with the surgery and a finite probability of failure of the implant. It is human nature to hear only what you want to hear. This results in unjustified expectations and a conclusion of having received unjust treatment if difficulties arise.

Technology amplifies the problem. New developments in implants are promoted as superior even when long-term data for large populations of patients are not available. We live in a technological age where most people want and expect the "latest", be it electronics, cars, or implants. Along with the "latest" comes the expectation that the latest is best. This is often unjustified but the perception still exists.

Rapid changes in technology also lead to a proliferation of choices. The surgeon and patient no longer are limited to one decision, "should a hip joint

be replaced with a prosthesis?" Instead, a series of decisions must be made with regard to type of stem, type of cup, type of fixation, etc. The statistical basis for risk assessment and beneficence becomes progressively more uncertain the greater the options.[4,5] The patient may well equate more options with greater expectations of success. This is often false. In fact, the reverse may be the case, i.e. success in a large population decreases as the number of options increases.

Greed can feed on the above factors.[4] As more people want and receive implants the potential for profit increases proportionally. As more options become available it is more likely that products will be promoted for the sake of novelty and image rather than for well-established improvements in beneficence.

Economic pressures build to introduce new implant products with only minimal standards of testing in order to have something "new" to offer. Tests that show problems may occur are undesirable in this context and therefore are avoided unless required by regulatory pressures. Research to obtain solutions to long-term reliability problems is often not done, because to do so is to admit that long-term reliability is a problem. Thus, the implant field grows in volume but not necessarily proportionally in beneficence to the larger number of patients. One consequence is an ever-increasing escalation in health care costs, which in the United States are now 13% of the gross national product.[4]

41.6. SPECIFIC ETHICAL CONCERNS IN BIOMATERIALS

As a field we need to promote testing to avoid long-term complications and implant revisions. We need to achieve >85–90% success of all implants over 10–20 years. Failure analysis needs to be done for all implants in use or proposed for use in order to provide a statistical basis for establishing beneficence for the patient. Figure 41.1 illustrates the type of analysis needed.

Clinical results of implants can be classified as those that result in high beneficence (top curves) or low beneficence (bottom curves). Moderate beneficence lies between. The ethical principle of beneficence *requires* that an implant meet the high standard of the upper curve because otherwise the principle "first, do no harm" may be violated. In other words, any implant that performs in limited trials for 2–3 years as indicated in the lower curve should not be put into general use. Any implant that is in general use with results similar to those in the lower

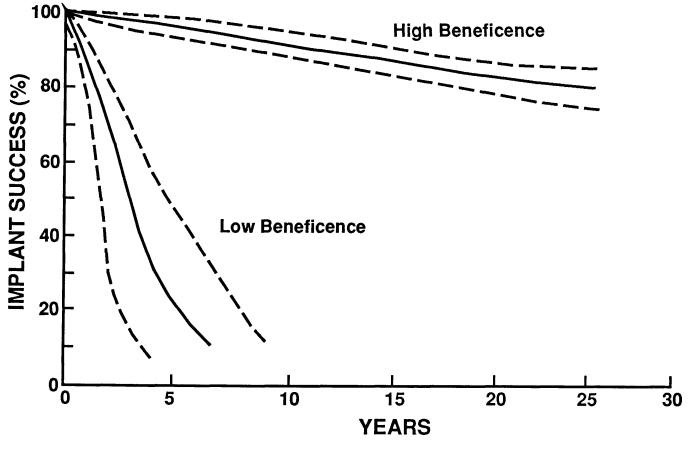

Figure 41.1. Comparison of implant failures as a function of time for high vs low beneficence to the patients.

curve should be removed from use. Implants of moderate beneficence should be subjected to regulatory monitoring to determine the reasons for failures and research funded to improve the performance until the upper curve behavior is achieved.

Figure 41.1 also illustrates that there exists a distribution of results which broadens with time. Statistical data that can be used to generate such curves needs to be compiled by the professional societies for all the prostheses now in clinical use. Patients need to be informed of their expected benefit with respect to this distribution of results. This is one of the few ways to counter false expectations of results.

Also, more controlled center testing of new products needs to be encouraged in order to produce data for plots such as Fig. 41.1. A few examples where additional controlled pre-market testing would have been desirable to avoid early failures are listed below.

- Intrauterine devices (IUD) for birth control
- Silicone injections
- PTFE powder injections for urinary incontinence
- PTFE powder for vocal cord rehabilitation
- PTFE/carbon fiber composites for TMJ repair

- Dense hydroxyapatite cones for edentulous ridge maintenance
- Porous bead coatings on orthopedic implants
- Metal on metal orthopedic total joints

41.7. SPECIFIC NEEDS TO MINIMIZE ETHICAL CONCERNS

Clinical results from a number of the implants[7] listed above produce the low beneficence curves in Fig. 41.1. To avoid this type of performance, we need standard *in vivo* and *in vitro* tests to compare alternative biomaterials under equivalent conditions.

Other areas of need to maximize beneficence are:

- Long-term predictive tests for biomechanical performance.
- Predictive *in vitro* tests to determine biochemical factors in tissue response.
- Minimization of animal testing by more effective use of *in vitro* tests, as discussed by Saha and Saha.[8]
- Avoidance of extensive "me too" development of "new" biomaterials that are only derivative in nature.
- Elimination of extensive, repetitive, short-term animal testing of unloaded, non-functional devices. This must be replaced with functional device testing under simulated clinical conditions.
- Balance the requirement of scientists to generate publications and research dollars with the desire to conduct scientific research that can improve long-term performance.
- Balance management's often short-term outlook with the long-term welfare of the patient and society.
- Balance the corporate goal of generation of profit with the need for unbiased product quality.

41.8. SUMMARY

Many researchers, clinicians, and manufacturers of implants have been exposed to the consequences of ethical conflicts which can arise when the principles of beneficence and justice are not reconciled. Many examples are discussed in Hench and results of clinical comparisons are presented.[4,7,9]

The expectations of the population with respect to implant success will continue to rise. Thus, implants must have increased long-term reliability. Failure to ensure this will result in negative consequences for individual patients. Failure

will also produce increased governmental regulations and controls. These controls will increase development costs and produce a negative spiral in which fewer manufacturers will be able to afford to produce new products and as a result will develop fewer new materials and applications. This negative scenario can be avoided by a concerted effort to improve long-term performance of all types of implants.

The over-riding principle of respect for autonomy must a concern to all of us. An individual depends on information from all sources to make crucial decisions. Such information should always be the best and most complete we have to offer and be unsullied by commercial or personal preferences. Only by these means can the best decision be made for specific clinical problems.

The new generation of bioceramics described in this book has been developed to improve beneficence for the patient. The alumina heads of total hip joints perform as indicated in the high beneficence curves of Fig. 41.1. However, as yet there is insufficient data to generate curves of beneficence (Fig. 41.1) for all types of bioceramics discussed herein.

Until the data are available, the implants must be considered developmental and be carefully monitored by the surgeon and the manufacturer.

ACKNOWLEDGEMENT

The author acknowledges Dr. Ross Mackenzie of the Chautauqua Institution, who stimulated my interest in this subject, and discussions with Dr. June Wilson Hench and Dr. David Greenspan.

REFERENCES

1. Cauwels, J.M. (1986). *The Body Shop: Bionic Revolutions in Medicine*, C.V. Mosby, St Louis, MO.
2. Hilton, B. (1991). *First Do No Harm: Wrestling with the New Medicine's Life and Death Dilemmas*, Abingdon Press, Nashville, TN.
3. Beauchamp, T.L. and Walters, L. (1989). *Contemporary Issues in BioEthics, 3rd Edition*, Wadsworth Publishing Co., Belmont, CA.
4. Hench, L.L. (2001). *Science, Faith & Ethics*, Imperial College Press, London.
5. The British Medical Association (1990). *The BMA Guide to Living with Risk,* Penguin Books, New York.

6. Callahan, D. (1990). *What Kind of Life: The Limits of Medical Progress*, Simon and Schuster, New York.
7. Hench, L.L. and Wilson, J. (1996). *Clinical Performance of Skeletal Implants*, Chapman and Hall, London.
8. Saha, P.S. and Saha, S. (1991). Ethical Issues on the Use of Animals in the Testing of Medical Implants, *J. Long-Term Eff. Med. Implants*, **1**, 127–134.
9. Hench, L.L., Jones, J.R. and Fenn, M.B. (2011). *New Materials and Technologies for Healthcare*, Imperial College Press, London.

Chapter 42

SUMMARY AND FUTURE DIRECTIONS

Larry L. Hench

42.1. OVERVIEW

One of the great challenges facing the multidisciplinary field of biomaterials is the development of a new generation of implant materials which will last as long as the lifetime of the patient. This is often 20–40 years, double or triple the expected lifetime of many spare parts in use today. The growth of bioceramics as a field during the 20 years since the first edition of this book is a response to this need. The 21 additional chapters in this second edition document the innovative approaches taken to make bioceramics one of the most dynamic and successful classes of biomaterials used clinically. The new fields of tissue engineering (TE) and regenerative medicine are only possible because of the development of a new generation of bioactive ceramic materials, as documented in this book.

However, many factors influence the long-term clinical performance of a biomaterial. This chapter presents a short summary of these factors, discusses their relative importance, and outlines future directions for research and development of bioceramics that may further improve the implant lifetimes and regeneration of tissues needed for the aging population. We begin by reviewing the elements of a "general theory of biomaterials" and discuss some of the implications of this generalization that lead to some recommendations for the future.

42.2. A GENERAL THEORY OF BIOMATERIALS

In 1975 Hench and Ethridge proposed as a general theory: *"An ideal implant material must have a dynamic surface chemistry that induces histological changes at the implant interface which would normally occur if the implant were not present."*[1]

This theory is supported by the behavior of bioactive ceramics discussed in many chapters of this book. Bone-bonding bioactive ceramics create an environment compatible with osteogenesis, with the mineralizing interface developing as a natural bonding junction between living and non-living materials. Implants that form a hydroxycarbonate apatite (HCA) layer very rapidly

incorporate collagen fibrils within the growing HCA agglomerates and thereby create a natural collagenous bonding junction between the implant and both hard and soft tissues. Bioactive glass particulates stimulate osteogenesis and new bone formation with a final "natural" result that is equivalent in morphology and biomechanical properties to autogeneous bone grafts (Chapters 3 and 9–12).

Implant materials that behave differently than is required by the above theory elicit non-adherent fibrous capsules which lead to problems in interfacial stability and eventual clinical failure.

A suitable surface chemistry is necessary, but not sufficient, to prevent the formation of non-adherent fibrous capsules at an implant–tissue interface. Table 42.1 summarizes the many factors involved in creating a stable versus unstable implant interface. The nature of the surgery, post-implantation healing, and biomechanical conditions determine not only whether a fibrous capsule will form but also its shape and thickness; all may be independent of implant surface chemistry. Continuous movement at an implant–tissue interface will always produce a capsule. The more extensive the motion and the longer the duration, the thicker the capsule. Infection, release of toxic leachables, continuous wear and release of wear particles, or uncontrolled degradation of a surface leads to a fibrous capsule that isolates the implant from normal tissues. It is futile to look for an artificial material or surface chemistry that will overcome these natural limitations of surgery, healing, and implant function.

The revised general theory that evolves from consideration of the factors listed in Table 42.1 was expressed by Hench and Ethridge in 1982 as:[2]

General Theory of Biomaterials Behavior

An ideal implant material performs as if it were equivalent to the host tissue.

Table 42.1. Factors that Influence the Histological Response to an Implant.

Non-Adherent Fibrous Capsule	**Bone Bonding**	**Soft Tissue Bonding**
Extent of tissue necrosis	Periosteal invasion	Rapid formation of HCA layer
Infection	Adherent to cells	Adherent to cells
Toxic leachables	Adherent to acellular constituents	Adherence to collagen
Wear or degradation	Tight fit	Tight fit
Movement	Vascularity	No inflammation
Inflammation	No inflammation	
	No wear debris	

Two axioms follow:

Axiom 1. The tissue at the interface should be equivalent to the normal host tissue.

Axiom 2. The response of the material to physical stimuli should be like that of the tissue it replaces.

These axioms are interdependent and are essentially the guiding principles that underlie the concept of regenerative medicine. In order for an equivalent physical response to be realized, a stable interfacial bond between tissue and implant must be achieved. Conversely, in order for a stable interface to be produced, it is necessary for physical stimuli to be controlled during the repair process. Factors that inhibit one of these relationships hinder the other as well.

Because of the critical interactions of these axioms, a focus of research and understanding of long-term performance of devices must be on creating implant–tissue interfaces which are simultaneously histologically and biomechanically stable. This is the objective of regenerative medicine. However, it is the short-term response of tissues following implantation which determines the eventual long-term response.

Many of the surface chemical features essential for formation of a stable interfacial bond with tissues have been identified. In bone, the central issue seems to be the relative competition between fibrogenesis and osteogenesis at the interface and development of a stable blood supply to the regenerated tissues, as discussed in Chapters 4 and 5. Many factors favor proliferation of fibroblasts and capsule formation, whereas very specific conditions must be satisfied for osteogenesis and angiogenesis to occur. This mimics the situation in the natural repair of bone, as implied by the general theory.

At the cellular level, fibroblasts are favored over osteoblasts if osteoblast progenitor stem cells: are not present; cannot attach; cannot differentiate; cannot divide; cannot generate bone matrix; or matrix mineralization is inhibited.

Following bone surgery it is likely that stem cells capable of becoming osteoblasts, given the right environment, will be available at the implant interface along with fibroblasts, since both types of stem cells originate from blood and tissues invaded during surgery. Damage to bone results in large changes in pH, oxygen tension gradients, local electric potentials, concentrations of chemicals, enzymes, and acellular proteins, such as bone growth factors. These local environmental changes lead to differentiation of stem cells into osteoblasts. If an implant perturbs this environment sufficiently to prevent differentiation of osteoblasts, then fibroblasts proliferate and the gap between the implant and undamaged tissue is closed with a fibrous capsule.

During the last decade, cell and molecular biology studies have established the genetic responses of osteoprogenitor cells to bioactive stimuli that lead to rapid osteogenesis and angiogenesis while inhibiting proliferation of fibroblasts through induced apoptosis of fibroblastic stem cells. This selective shift in interface cell populations favors the growth of bone at the interface of bioactive implants, as discussed in Chapter 4, with successful clinical uses documented in Chapters 6–12. Similar approaches need to be taken in the regeneration and repair of soft connective tissues and cardiovascular tissues, as indicated below.

42.3. MOLECULAR TAILORING OF SURFACE CHEMISTRY

The surface chemistry of implants needs to be optimized to meet the requirements of aged, diseased and damaged tissues. Most biomaterials in use today were developed by trial and error. There is very little understanding of the effects of disease states, such as osteoporosis or arthritis, on interfacial reactions, or the long-term biomechanical behavior of implant–tissue interfaces. Some principles have been established to guide the development of new bioceramics, as indicated above. As discussed in Chapters 3–5, the relationships between phases and compositions of bioceramics with their surface reaction kinetics have been determined. The effect of surface reactions on *in vivo* behavior is also generally known. Details of the cellular responses are established by tissue and cell culture experiments, as described in Chapter 4. Results from these studies should make it possible to modify compositions to optimize their behavior with respect to age, metabolic activity, and disease states of aging patients. At present the same materials are used in all categories of patients, regardless of the degree or type of ailment and extent of deterioration of the natural tissues to be repaired or replaced. Tailoring of surface release kinetics of bioactive stimuli for patient-specific bone regeneration should be a high research priority.

Two new directions of research hold promise for improving the scientific basis for tailoring surface reactions of bioceramics. One is the discovery that sol-gel derived glasses have a much expanded compositional range of bioactivity over glasses made by traditional melting and casting processes. The low temperatures of sol-gel processing, as illustrated in Chapter 1, make it possible to control the surface chemistry of the resulting materials with greater flexibility than high temperature melting and casting of glasses or sintering or hot pressing of ceramics. Details of the seven processing steps in making bioactive gel-glasses are discussed in Hench and West.[3] Advantages of sol-gel processing of inorganic biomaterials include: new compositions; greater homogeneity; higher levels of purity; net-shape casting of monoliths; low temperature coating of substrates

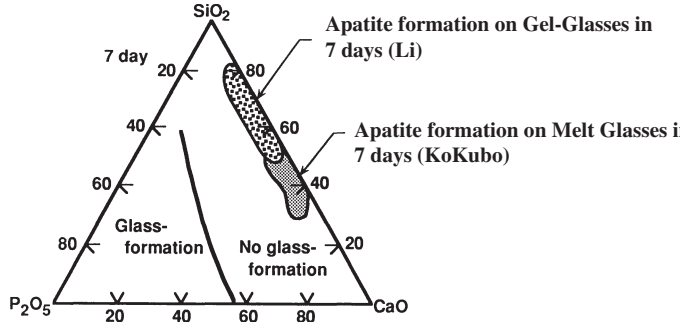

Figure 42.1. Apatite formation at seven days on gel-glasses and melt glasses.

control of powder size distribution; control of surface chemistry of the gel-glasses; expanded ranges of glass formation and control of pore networks at a nanometer scale as well as formation of interconnecting macropores. This is in addition to commercial advantages, such as lower energy consumption and nearly zero environmental impact.

Sol-gel processing and development of hybrid inorganic-organic materials are fields that show great promise, as discussed in Chapters 23, 32, and 35.

Figure 42.1 shows the extended range of compositions in the SiO_2-CaO-P_2O_5 system that are bioactive when made by alkoxide-based sol-gel processing compared with bioactive compositions made by melting and casting, from studies by Professor Kokubo's group. Gel-derived glasses with as much as 88% SiO_2 develop HCA layers, whereas the limit for melt-glasses is 60%. This is a large shift in compositional limit. Melt-glasses with >55% SiO_2 require several days to form a polycrystalline HCA layer whereas gel-glasses do so in only a few minutes. The chemical origin of these important differences appears to be the large concentration of silanols on the surface of the gels after processing temperatures of 500–800°C.

42.4. THEORETICAL MODELING OF SURFACE INTERACTIONS

Semi-empirical molecular orbital (MO) calculations, using AM-1 and extended Hückel methods, show that metastable silica clusters formed from a condensation reaction of neighboring silanols can act as heterogeneous nucleation sites for HCA crystals.[4] The metastable silica clusters can also act as preferential adsorption sites for amino acids, such as alanine.[4] These calculational

results, reviewed in Chapter 36, indicate that the surface reactions of the inorganic material can lead to biologically-specific binding sites for protein molecules. The MO calculations show differences in specific adsorption on the inorganic surface, which depend on different binding sites on the protein molecules.[4] This may lead to an understanding of the selective adsorption of proteins that act as growth factors or enzymes. Such studies may also aid in the interpretation and optimization of interactions between inorganic-biological systems and be the basis for the design of delivery systems to prevent deterioration of natural tissues.

42.5. SOFT TISSUE ENGINEERING

Much of the growth of bioceramics has been towards improving the repair of the skeletal system, as indicated by the majority of chapters in this book. However, there is great need for substantial improvement in the treatment of soft tissue-based diseases, particularly those related to diabetes, heart and cardiovascular deterioration, and the weakening of the gastrointestinal and urinary tracts in the aged. Obtaining and maintaining a blood supply in TE constructs is necessary for their long-term stability following implantation. All of these needs require enhancement of a stable capillary bed within the repairing tissues. Studies have used third-generation bioactive, resorbable composites with controlled release of bioactive stimuli to enhance vascularization of regenerated soft tissue constructs. Chapter 5 reviews these studies. Chapter 33 shows a novel method of treating chronic wounds, a highly debilitating illness. Future expansion of this new field can provide a major impact on the cost and personal suffering of a large fraction of the population.

There are important implications from these findings. Few TE constructs at present produce a stable 3D vascularization bed of tissue. Adding angiogenic stimulating particles could be an effective means to enhance vascularization *in vivo.* These findings are also relevant to a new approach to treatment of chronic wounds, which are increasing at an alarming rate due to the larger number of obese, aged, and diabetic patients. At present most treatment modalities for chronic wounds are at best palliative. There is great need for bioactive wound dressings that can counter the negative stimuli that prevent healing of chronic wounds. It should be possible to combine the anti-inflammatory characteristics of 45S5 Bioglass® particles, which also have pro-angiogenic potential at critical dosages (Chapter 5), with the nano-borosilicate fibers (Chapter 33) to create multifunctional materials for soft tissue repair.

These results also show promise for designing minimally invasive microinjectable particles for stable augmentation of soft tissues. The bioactive particles could serve to stimulate growth of soft connective tissues that can adhere to the particle surface and increase the mass and elasticity of the regenerated tissue. Such treatments are desperately needed to eliminate stress urinary incontinence in the elderly. This is a societal need and challenge to the biomaterials field that presently costs billions of dollars per year. Little research or new product development is currently pursued to solve this problem.

Another need and challenge is for innovative TE tubular constructs to replace segments of the small intestine that have been removed from cancer patients. Such constructs that possess the physiological functions of the intestine are greatly needed to improve the quality of life of this group of patients. This is a particularly difficult challenge for soft tissue engineering. All of the above are 21st century challenges of an aging population. Unfortunately, few research programs appear to be addressing these needs at present.

42.6. IMPLICATIONS FOR THE FUTURE

A genetic basis for the development of a third generation of biomaterials provides the scientific foundation for molecular design of scaffolds for TE and for *in situ* tissue regeneration and repair, using minimally invasive surgery. There are significant economic advantages to each of these new approaches, which may aid in solving the problems of care for an aging population. It should be feasible to design a new generation of gene-activating biomaterials tailored for specific patients and disease states. Perhaps of even more importance is the possibility that bioactive stimuli can be used to activate genes in a preventative treatment to maintain the health of tissues as they age. Only a few years ago this concept would have seemed impossible. We need to remember that only 40 years ago the concept of a material that would not be rejected by living tissues also seemed impossible.

42.7. CONCLUSION

Understanding the science, technology, and applications of bioceramics is an important educational need for the healthcare and engineering community. Many new developments have occurred during the last 30 years that are not discussed in standard materials science textbooks. Subjects, such as sol-gel processing of bioactive gel-glasses, genetic stimulation of osteogenesis by ionic

dissolution products of bioactive glasses, stimulation of angiogenesis, bioactive composites, hybrid bioactive materials, phosphate glasses, bioactive materials with hierarchical porosity, molecular modeling of glass structures and bioactivity mechanisms, TE, and regenerative medicine, are now important topics in the field and did not even exist as concepts in 1993 when the first edition of *An Introduction to Bioceramics* was published. Also, other important biomedical glass and glass-ceramic systems for therapeutic treatment of tumors and repair of diseased and damaged teeth are now in wide-spread use and enhancing the quality of life for millions of patients throughout the world, as documented in this second edition.

This important new edition provides a summary of all of the above topics. It provides the necessary foundation of science and technology for the reader to later explore the multitude of papers being published in this new field annually. Without a basic understanding, such as provided by this book, a person is easily confused. The reason is that the interface generated with time between a bioactive material and the body is controlled by an integrated synthesis of inorganic chemistry, physical chemistry, and biochemistry. The man-made material and the living material become as one at a molecular level. This type of "living interface" mimics that between hard and soft connective tissues in the body that have evolved over billions of years. This unique character of bioactive bonding requires a unique textbook in order to comprehend and explore these materials and their clinical use. This edition provides the fundamental level of comprehension needed. I hope it encourages the bright young creative minds of the future to enter the field and take bioceramic materials forward to the next generation of medical devices and continue to improve the quality of life of patients. For the experienced researcher the book provides a comprehensive overview of the important current topics in bioceramics, written by world-class authors. Unlike many conference proceedings, this volume is based upon carefully-selected contributors who have created much of the subject matter they discuss in their chapters and as a consequence the contents are authoritative.

To all readers, beginner or experienced: read, enjoy, and marvel at this wonderful field of bioceramics!

REFERENCES

1. Hench, L.L. and Ethridge, E.C. (1975). "Biomaterials — The Interfacial Problem", in J. Brown, H.U. and Dickson, J.F. (eds), *Advances in Biomedical Engineering*, Academic Press, New York, pp. 136–139.

2. Hench, L.L. and Ethridge, E.C. (1982). *Biomaterials: An Interfacial Approach*, Academic Press, New York.
3. Hench, L.L. and West, J.K. (1990). The Sol-Gel Process, *Chem. Rev.*, **90**, 33–72.
4. Hench, L.L. and West, J.K. (1996). Biological Applications of Bioactive Glasses, *Life Chemistry Reports*, **13**, 187–241.

INDEX